SSCL-SR-1185

SSCL-SR-1185

Summary and Presentations of the

WORKSHOP ON

VIBRATIONAL CONTROL AND DYNAMIC

ALIGNMENT ISSUES AT THE SSC

FEBRUARY 11-14, 1992

Workshop on Vibrational Control and Dynamic Alignment Issues at the SSC

February 11-14, 1992

INTRODUCTION:

Welcome
Dick Briggs (SSCL)

Overview of Collider Project and Purpose of this Workshop
Rainer Meinke (SSCL)

Overview of the SDC Detector Experimental Hall
Tim Thurston (SSCL)

Overview of the GEM Detector Experimental Hall
Mike Harris (SSCL)

Tunnel Construction and Magnet Installation

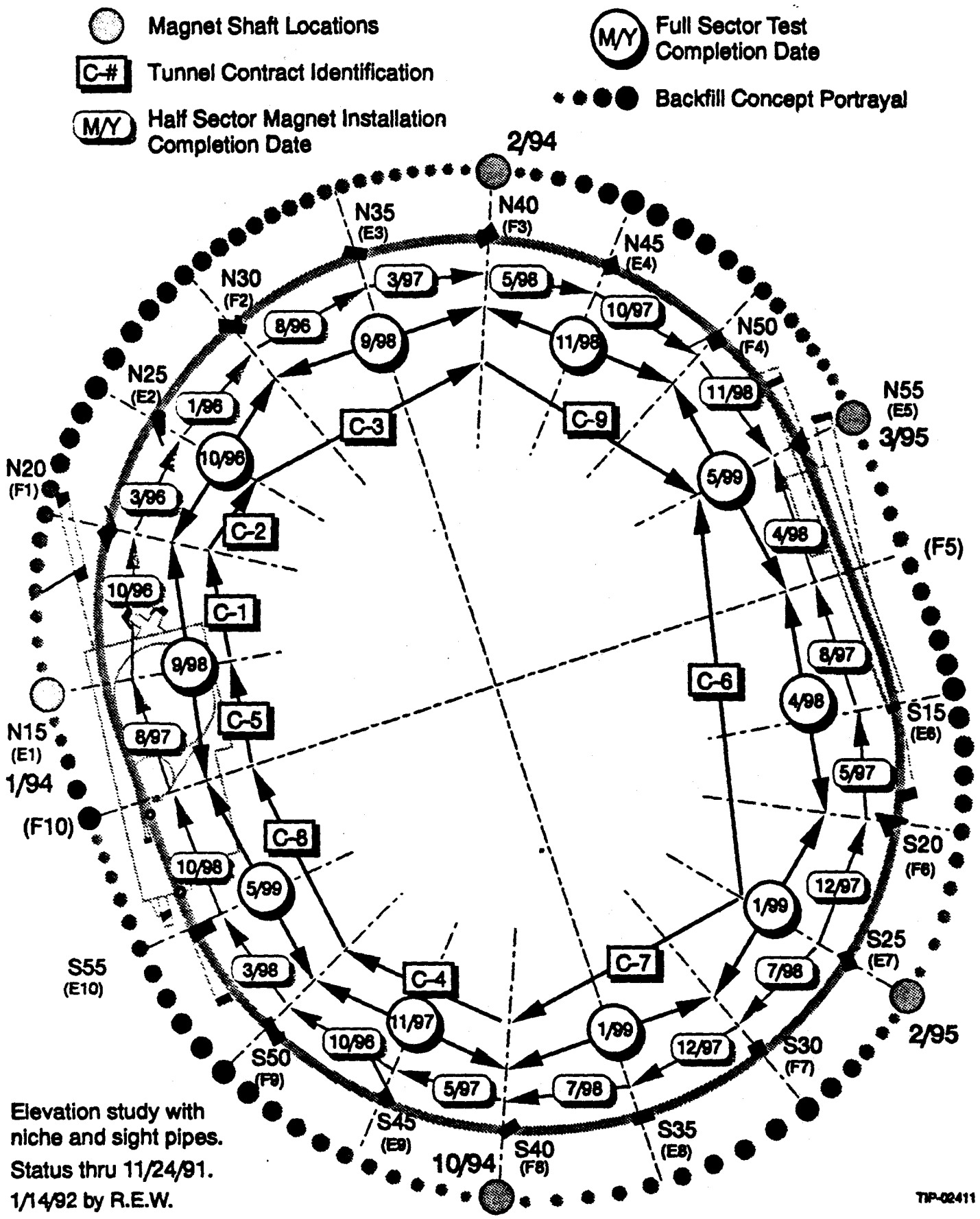

Elevation study with niche and sight pipes.
Status thru 11/24/91.
1/14/92 by R.E.W.

TIP-02411

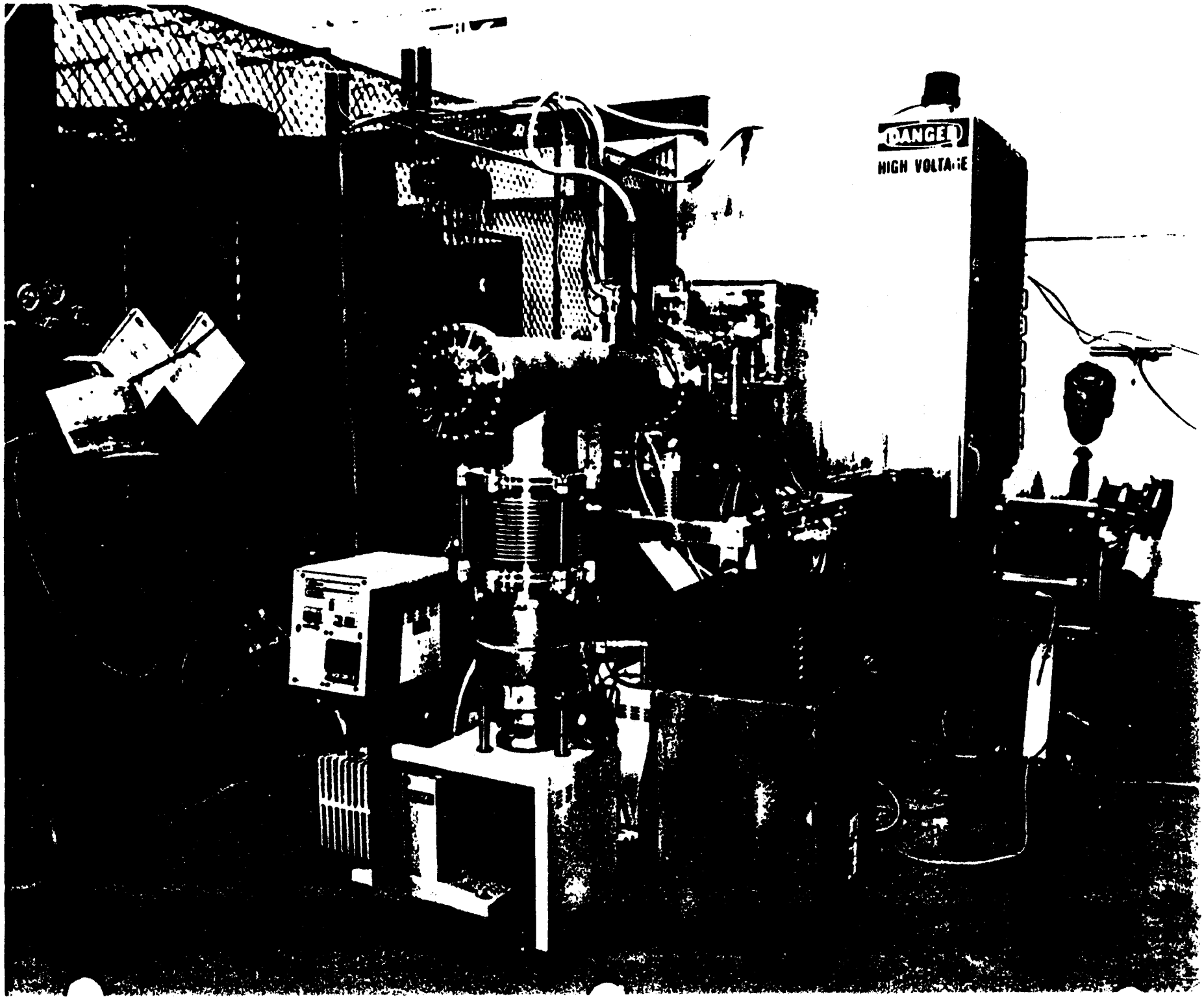
DANGER
HIGH VOLTAGE

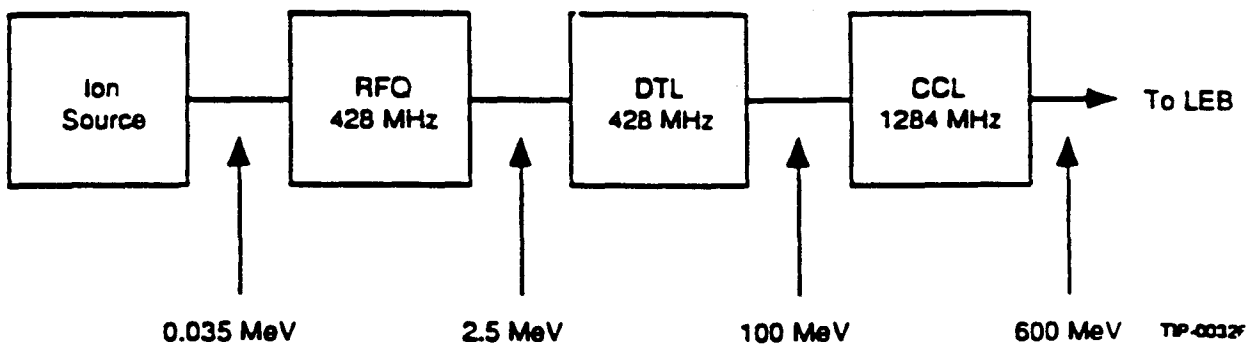

Figure 4.1.1.2-16. Linac block diagram.

Alignment Tolerances of Accel. Components

Ideal accelerator has all components in one plane with axes of magnets on design orbit.

Allowable deviations from design orbit:

<u>ARCs</u>

Dipoles:	1 mm
Quadrupoles:	0.5 mm
BPM's:	0.3 mm

<u>IRs</u>

Final focus quads: 0.001 mm

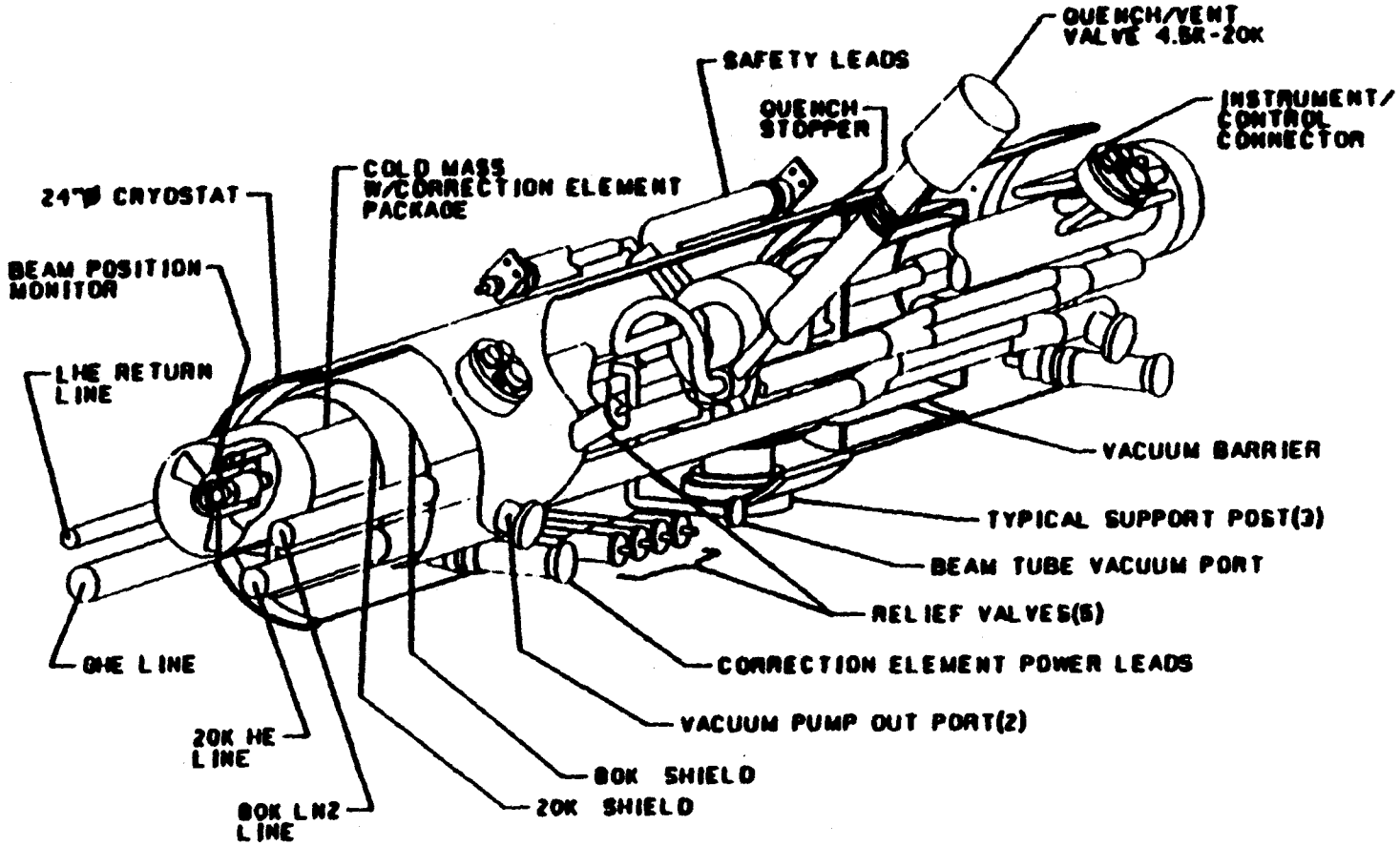
QUENCH/VENT VALVE 4.5K-20K
SAFETY LEADS
QUENCH STOPPER
INSTRUMENT/ CONTROL CONNECTOR
COLD MASS W/CORRECTION ELEMENT PACKAGE
24"Ø CRYOSTAT
BEAM POSITION MONITOR
LHE RETURN LINE
VACUUM BARRIER
TYPICAL SUPPORT POST(3)
BEAM TUBE VACUUM PORT
RELIEF VALVES(5)
CORRECTION ELEMENT POWER LEADS
GHE LINE
VACUUM PUMP OUT PORT(2)
20K HE LINE
80K SHIELD
80K LN2 LINE
20K SHIELD

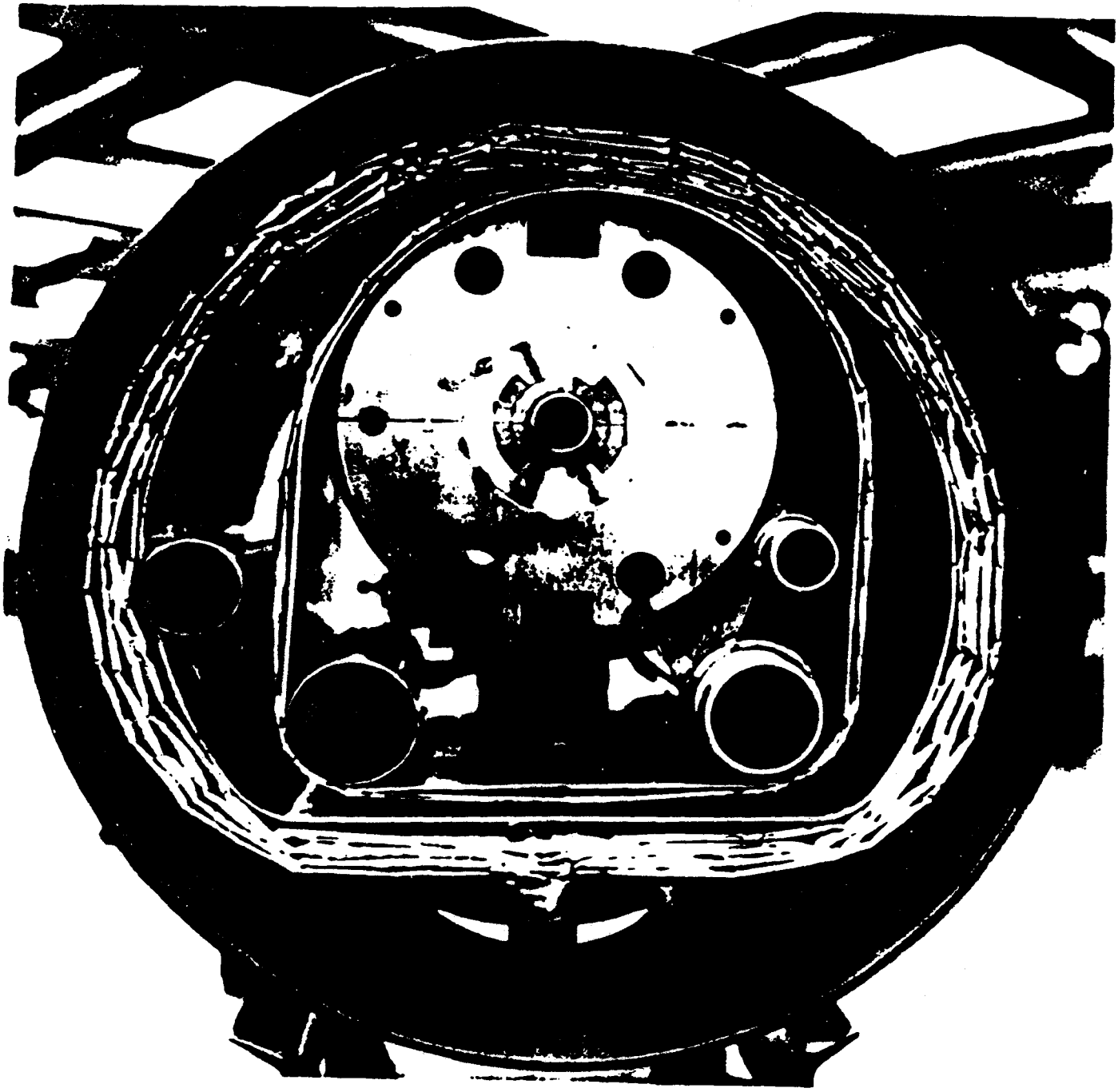

GAS
RETURN

Isometric View of LSD Detector in Hall (WBS 2.2.1.1.1)

West North Interaction Region IR1 Underground (WBS 2.2.1.1.1)

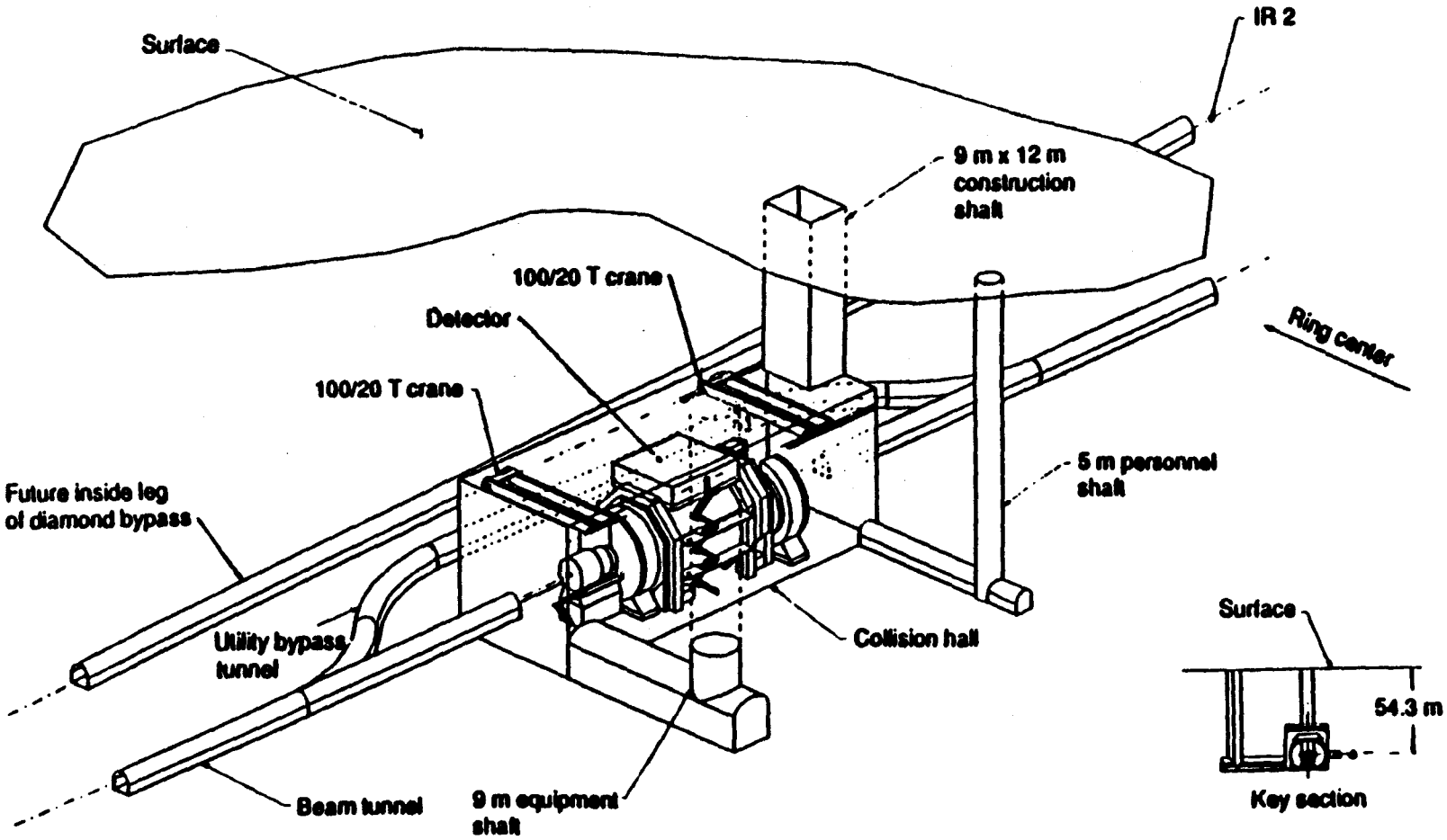

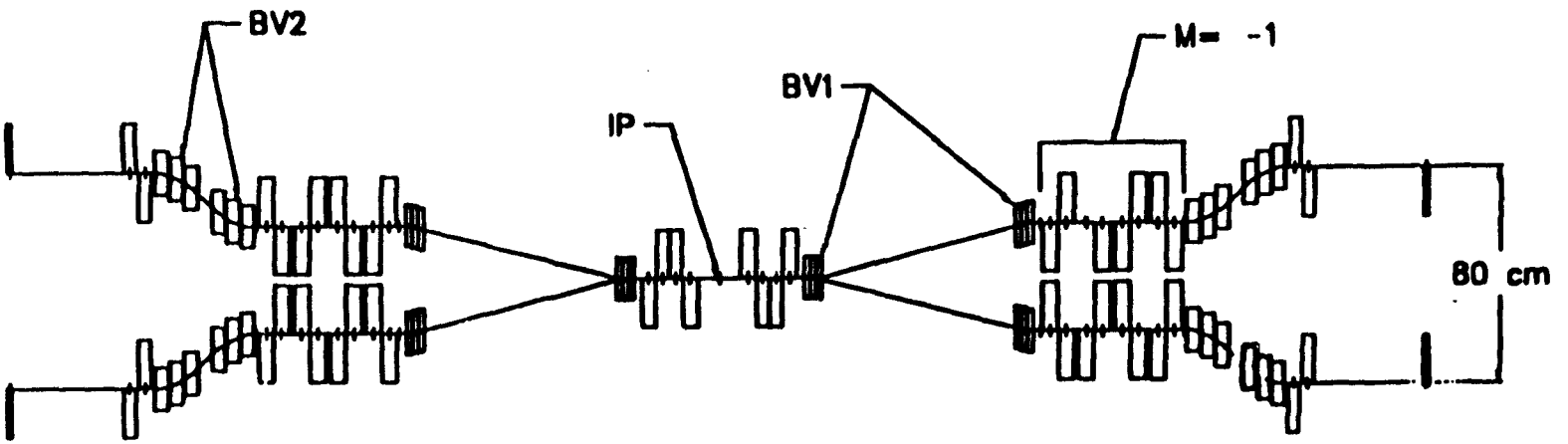
BV2
IP
BV1
M= -1
80 cm

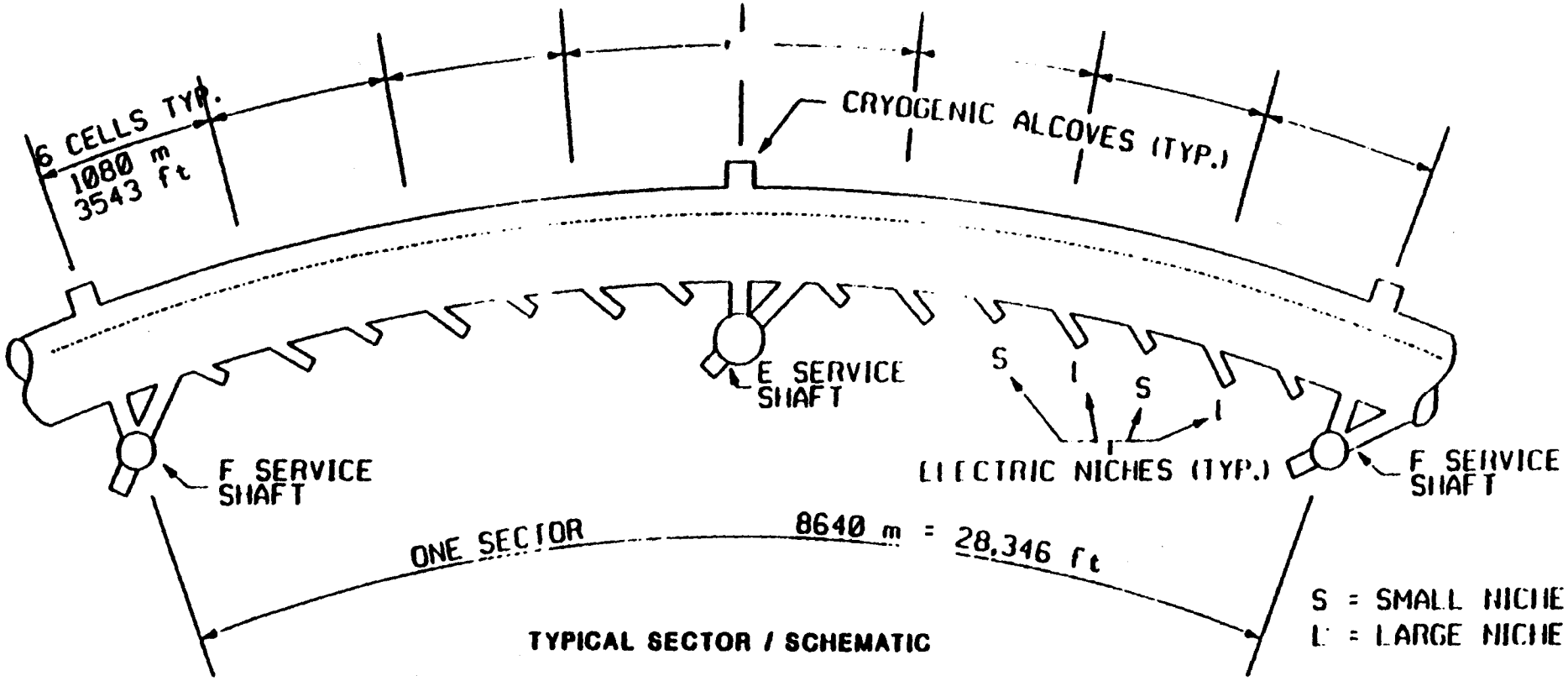

TYPICAL SECTOR / SCHEMATIC

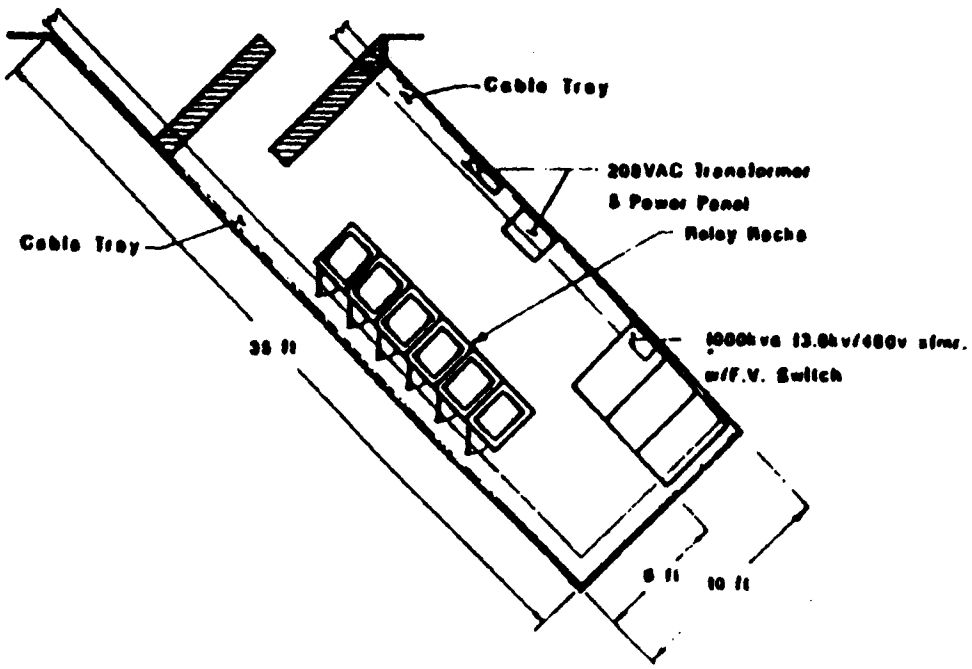

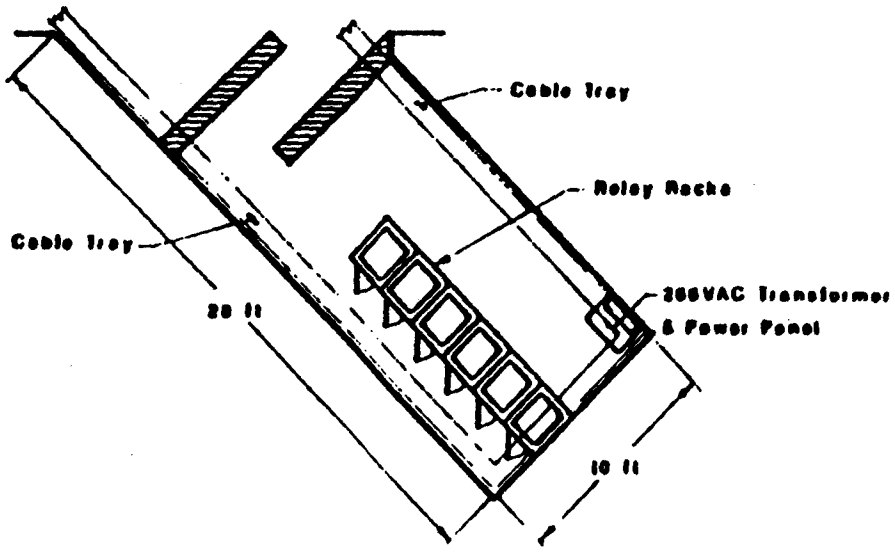

PLAN VIEW OF TYPE S NICHE

CONVENTIONAL CONSTRUCTION
BY OTHERS

Primary Corrector Magnet Strengths

B*L, T-m at r = 1.00 cm

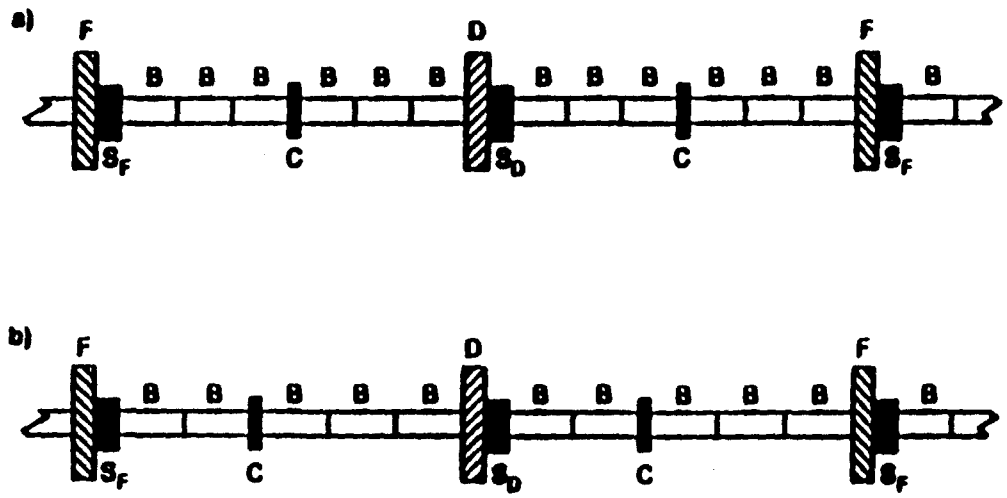

Pole	F	C	D
Dipole	2.50	—	2.50
Quadrupole	0.53	—	0.53
Sextupole	0.13	0.09	0.21
Octupole	0.007	0.016	0.007
Decapole	0.004	0.009	0.004

Alternate Dipole Layout of Footprint Configuration

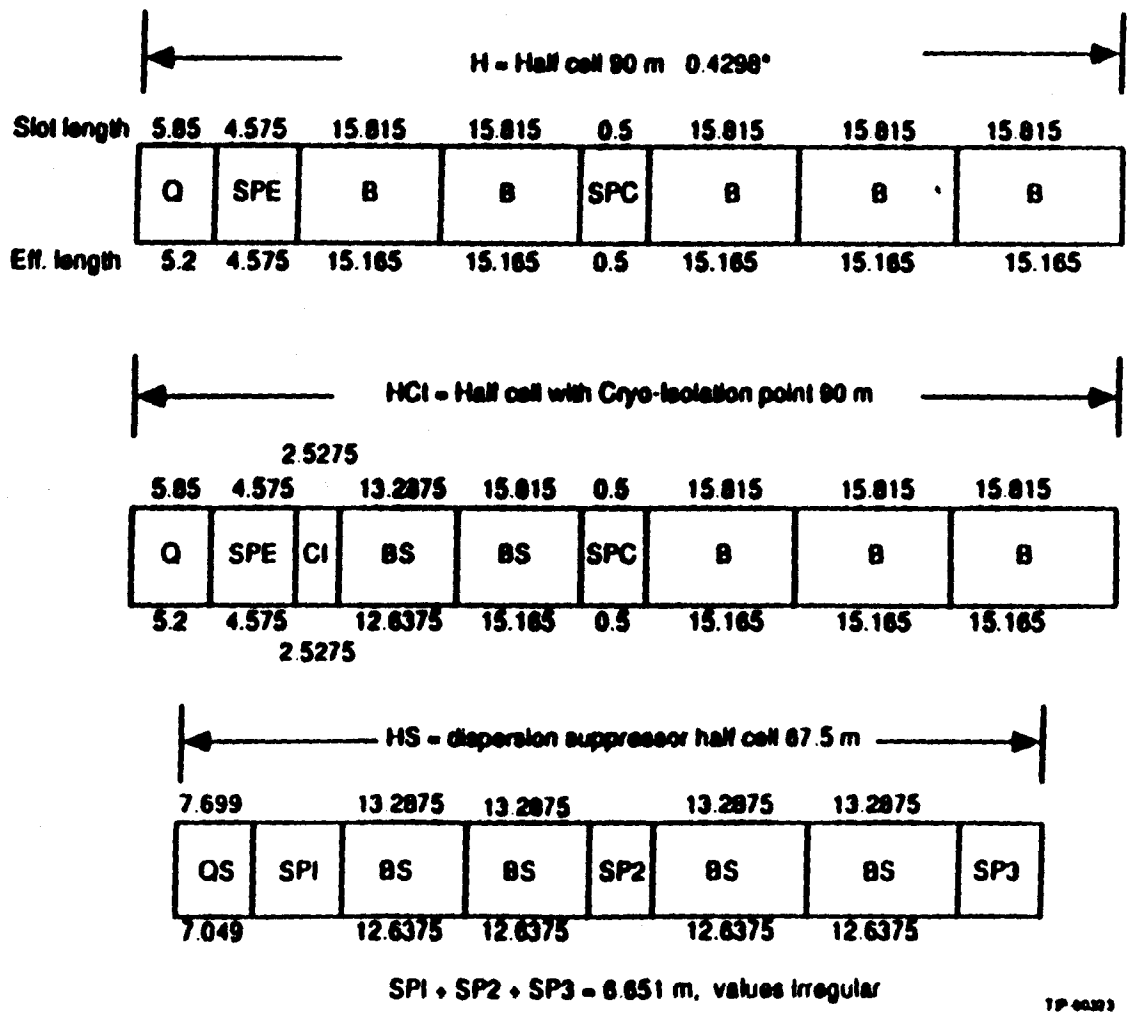

SSC Parameters

Proton Energy	20 TeV
Circumference of rings	87 KM
Protons per r.f. bunch	0.75×10^{10}
Bunch spacing	5 meters
Number of bunches/ring	17,424
Total particle energy/ring	418 megajoules
Emittance (RMS)	1π millimeter-milliradian
Interaction region focal spot size RMS radius, ($\beta^* = 0.5$ M)	5 micrometers
Proton-proton collision rate	60 MHz
Luminosity	1×10^{33} cm^{-2} sec^{-1}
Sychrotron radiation power	8.75 kilowatts/ring

TIP-01588

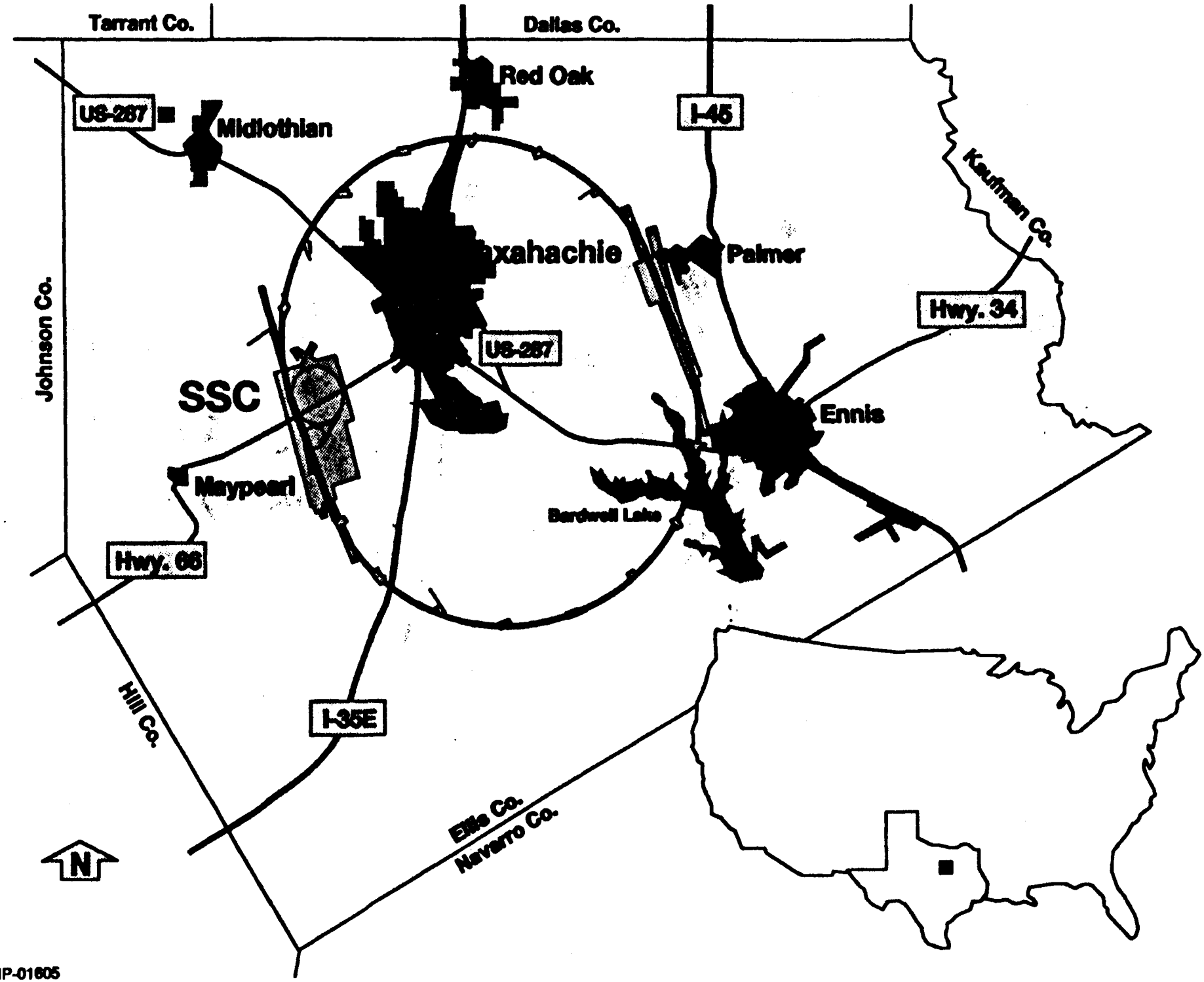
Tarrant Co.
Dallas Co.
Red Oak
US-287
Midlothian
I-45
Kaufman Co.
axahachie
Palmer
Johnson Co.
Hwy. 34
US-287
SSC
Ennis
Maypearl
Bardwell Lake
Hwy. 66
Hill Co.
I-35E
Ellis Co.
Navarro Co.
N

TIP-01605

Overall Arrangement of Collider Ring

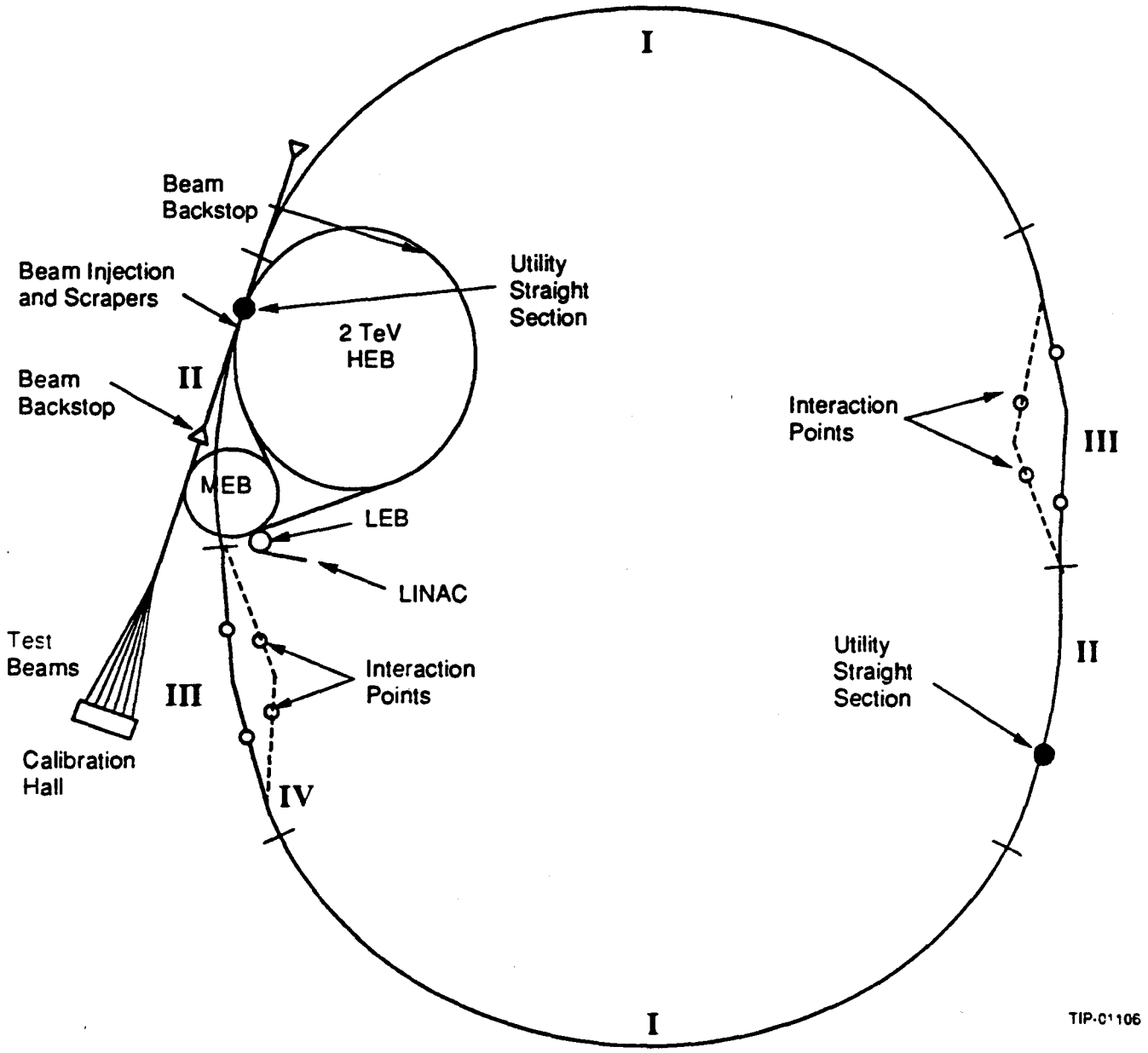

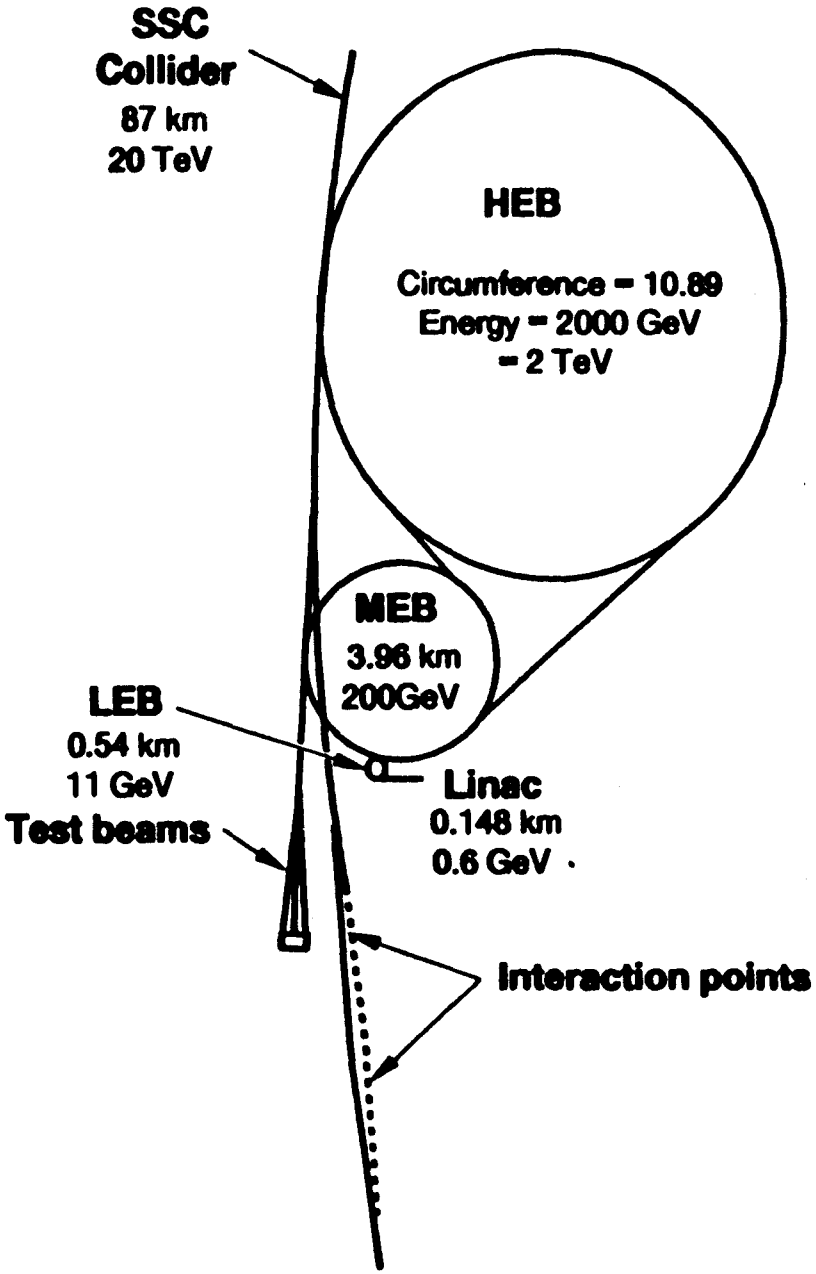

5 Stages of Acceleration	
Linac	0 – 0.6 GeV
LEB	0.6 – 11 GeV
MEB	11 – 200 GeV
HEB	200 – 2000 GeV
Collider	2 TeV – 20 TeV

Schematic layout of the injector complex, a portion of the collider ring and test beam area. The dashed line indicates a future beam bypass.

TIP-62014

#PV119
TORRANCE, CA 90503

H. Edwards, 6/90

SSC Accelerator

Scope

proton-proton collider

20 TeV x 20 TeV

$L \approx 10^{33} cm^{-2} sec^{-1}$

injectors - with energy up to 2TeV

up to four interaction regions

initial set of detectors

Laboratory & infrastructure

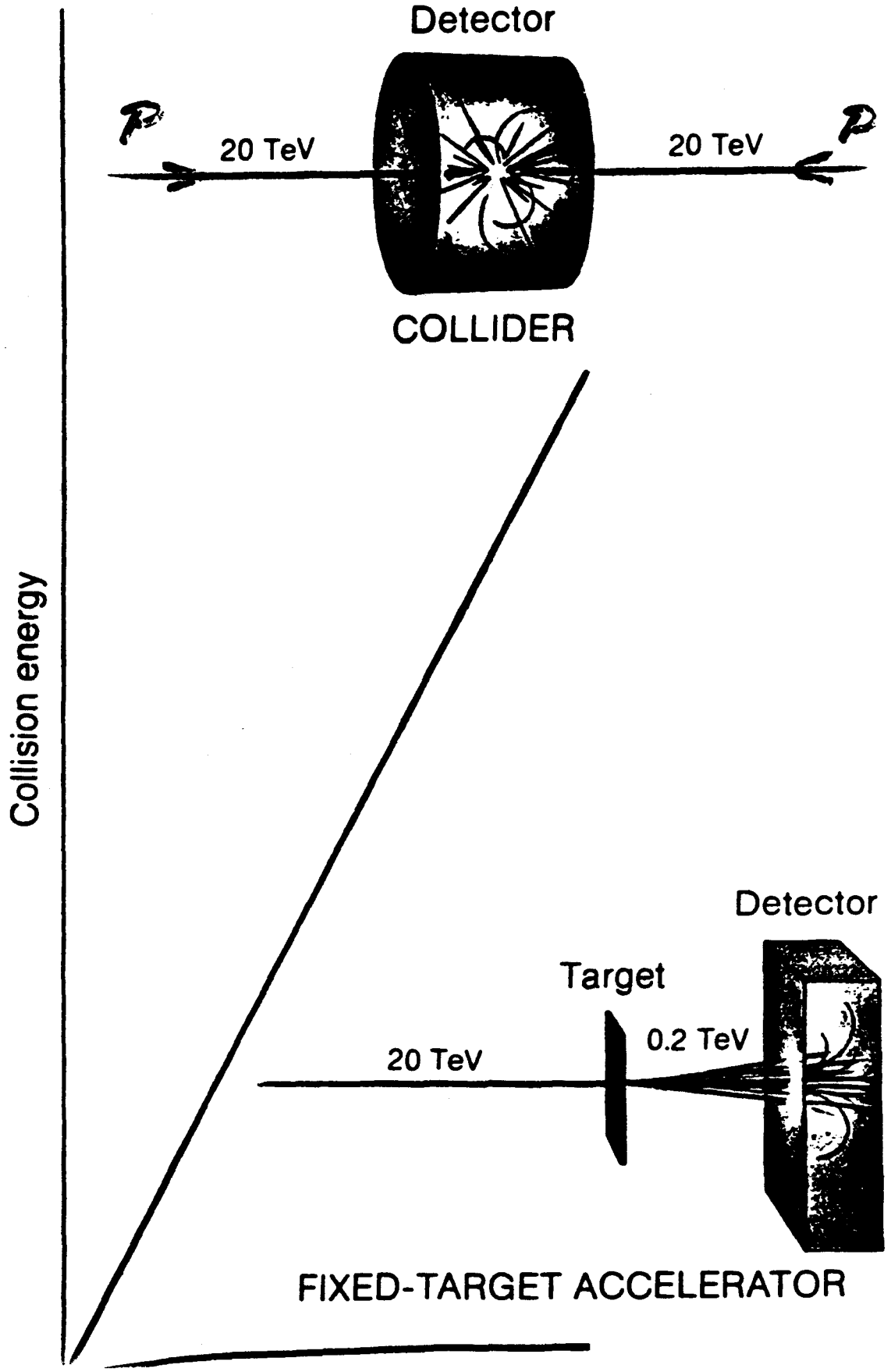
Detector
p
20 TeV
20 TeV
p
COLLIDER
Collision energy
Detector
Target
0.2 TeV
20 TeV
FIXED-TARGET ACCELERATOR

C.M. Energy:

Energy available for initiating new elementary processes, creating new particles, and probing subnuclear distances *

Luminosity:

Rate of Occurrence of Process
= Probability of Process
x Luminosity

or

Rate = Cross section x Luminosity

* For Fixed-Target Operation:

$$E_{CM} = \sqrt{2EM_P}$$

E = Beam Energy
M_P = Proton Mass ~ 0.938 GeV

For Colliding Beams:

$$E_{CM} = 2\sqrt{E_1 E_2}$$

If $E_1 = E_2 = E$

$$= 2E$$

TIP-01361

SSC Laboratory Goals

Create a premier international laboratory for high energy physics by the year 2000.

Create a major resource for science and education.

Understand the ultimate building blocks of matter and the basic forces which govern the transformation of matter and energy.

Understand electro-weak symmetry breaking.

What is the origin of mass??

SSC Laboratory Goals

Create a premier international laboratory for high energy physics by the year 2000.

Create a major resource for science and education.

Understand the ultimate building blocks of matter and the basic forces which govern the transformation of matter and energy.

Understand electro-weak symmetry breaking.

What is the origin of mass??

SDC
DETECTOR EXPERIMENTAL HALL

TIM THURSTON
SSC
11 Feb 1992

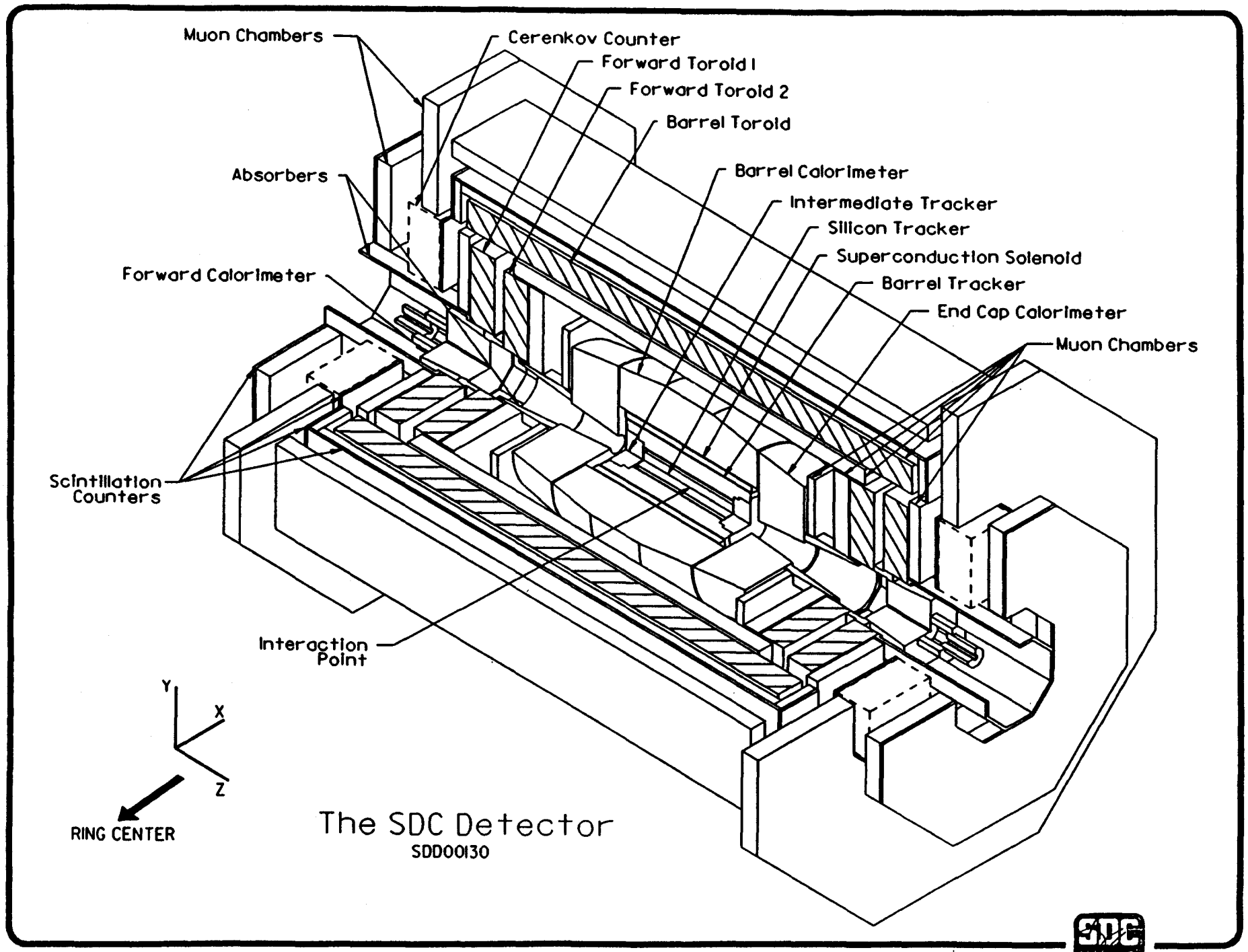

The SDC Detector
SDD00130

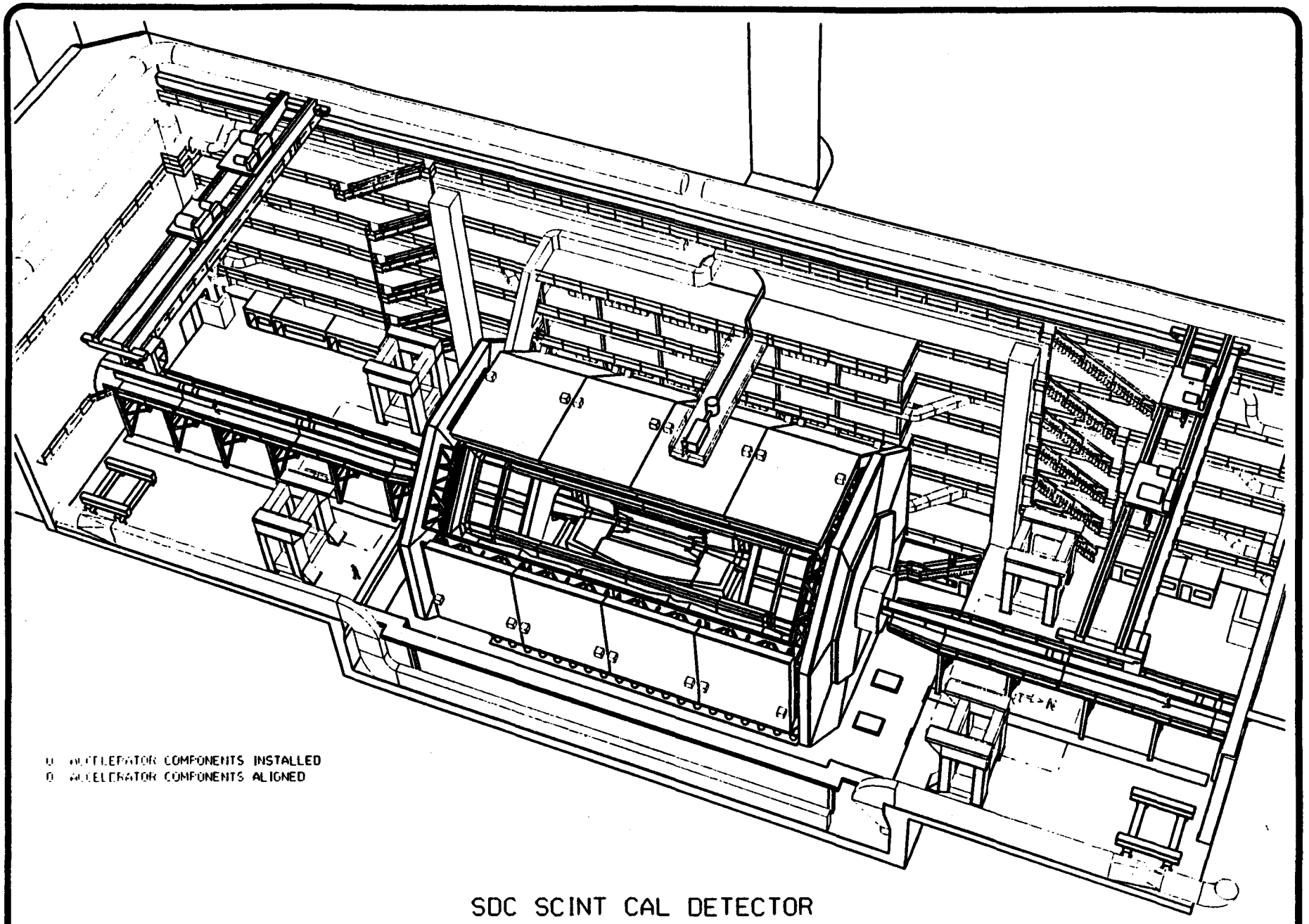

SDC SCINT CAL DETECTOR

CONSTRUCTION PROGRESS

MONTH 40

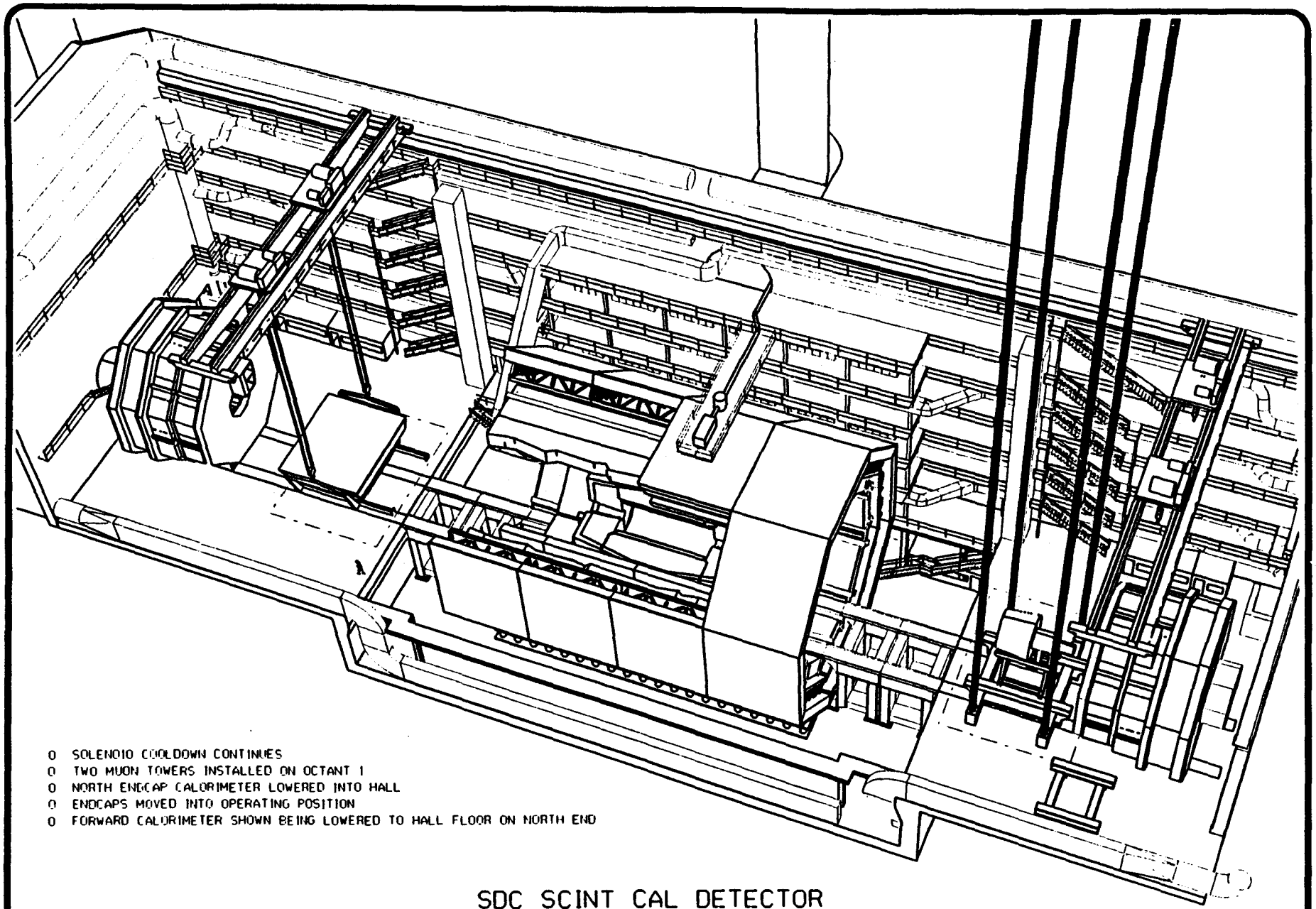

- SOLENOID COOLDOWN CONTINUES
- TWO MUON TOWERS INSTALLED ON OCTANT 1
- NORTH ENDCAP CALORIMETER LOWERED INTO HALL
- ENDCAPS MOVED INTO OPERATING POSITION
- FORWARD CALORIMETER SHOWN BEING LOWERED TO HALL FLOOR ON NORTH END

SDC SCINT CAL DETECTOR

CONSTRUCTION PROGRESS

MONTH 25

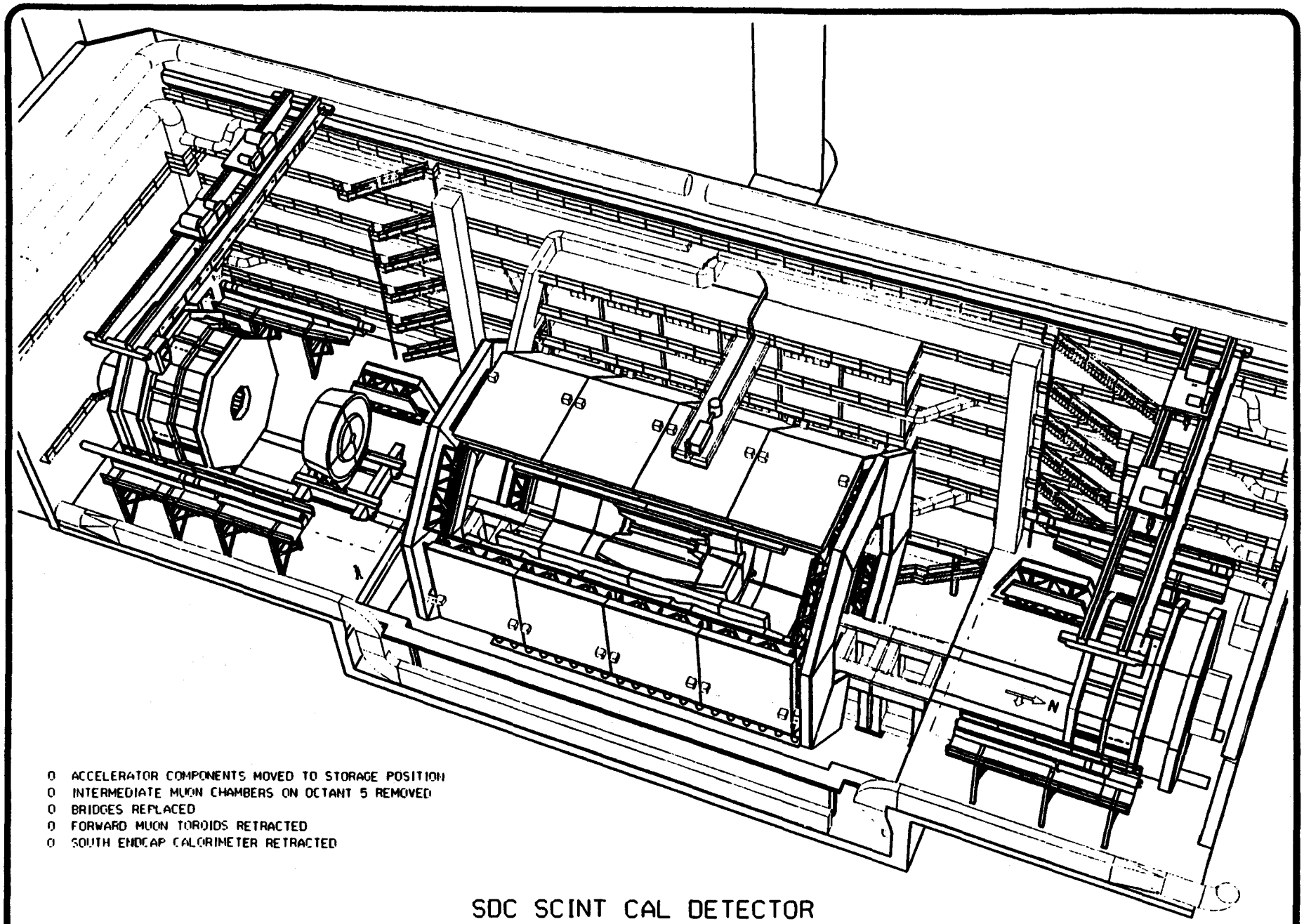

- ACCELERATOR COMPONENTS MOVED TO STORAGE POSITION
- INTERMEDIATE MUON CHAMBERS ON OCTANT 5 REMOVED
- BRIDGES REPLACED
- FORWARD MUON TOROIDS RETRACTED
- SOUTH ENDCAP CALORIMETER RETRACTED

SDC SCINT CAL DETECTOR

OPEN FOR MAJOR REPAIRS

SDC

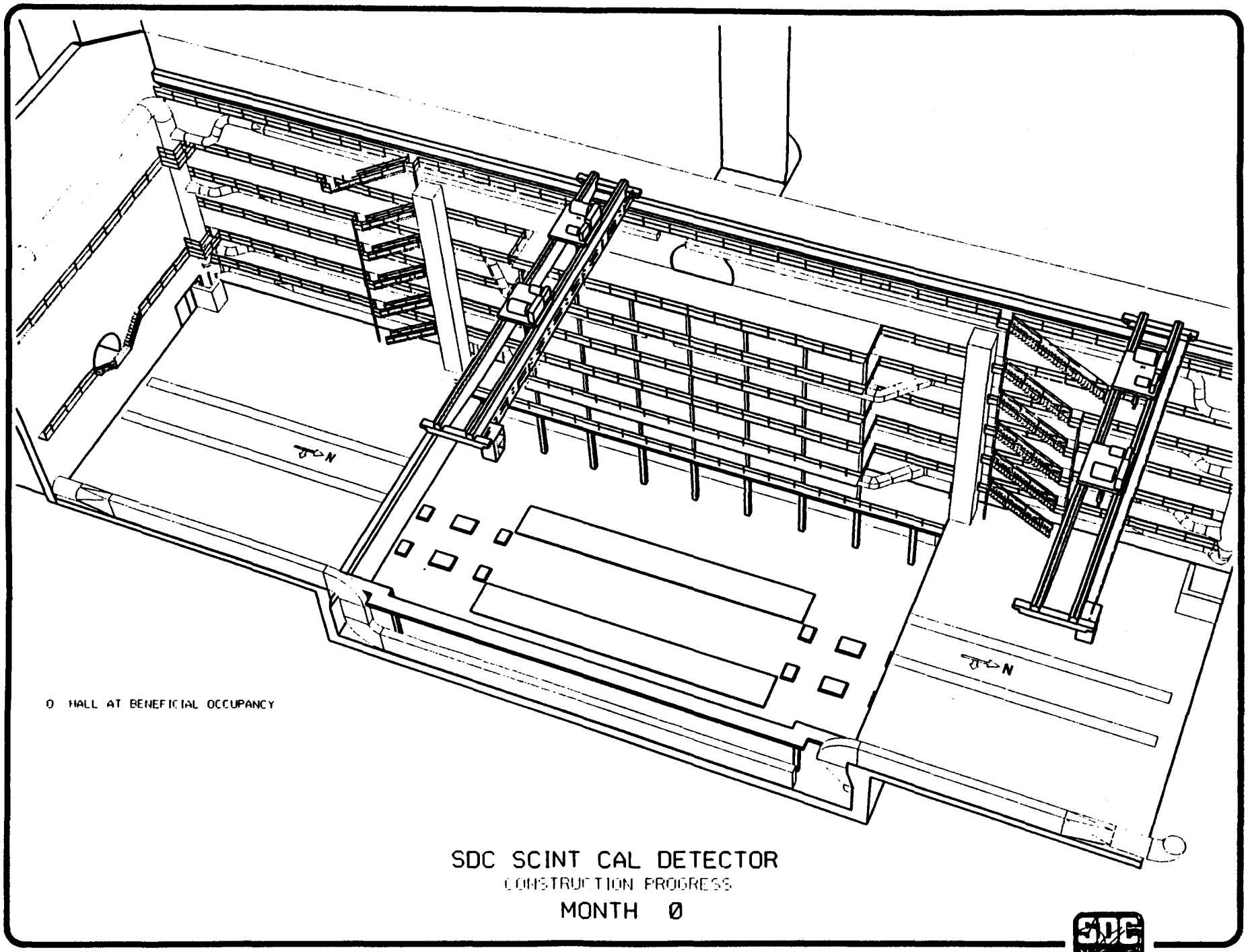

SDC SCINT CAL DETECTOR

CONSTRUCTION PROGRESS

MONTH 0

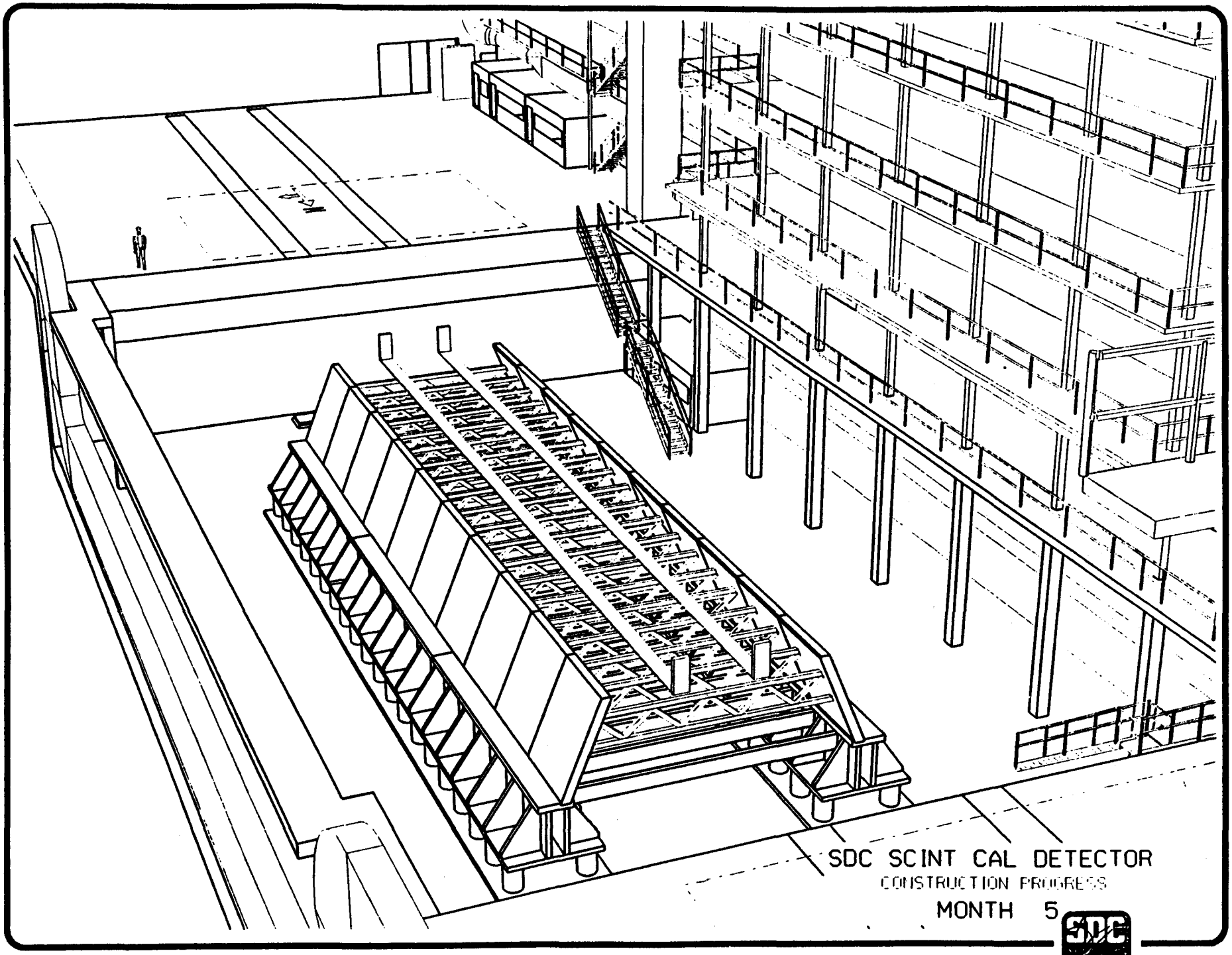
SDC SCINT CAL DETECTOR
CONSTRUCTION PROGRESS
MONTH 5
SDC

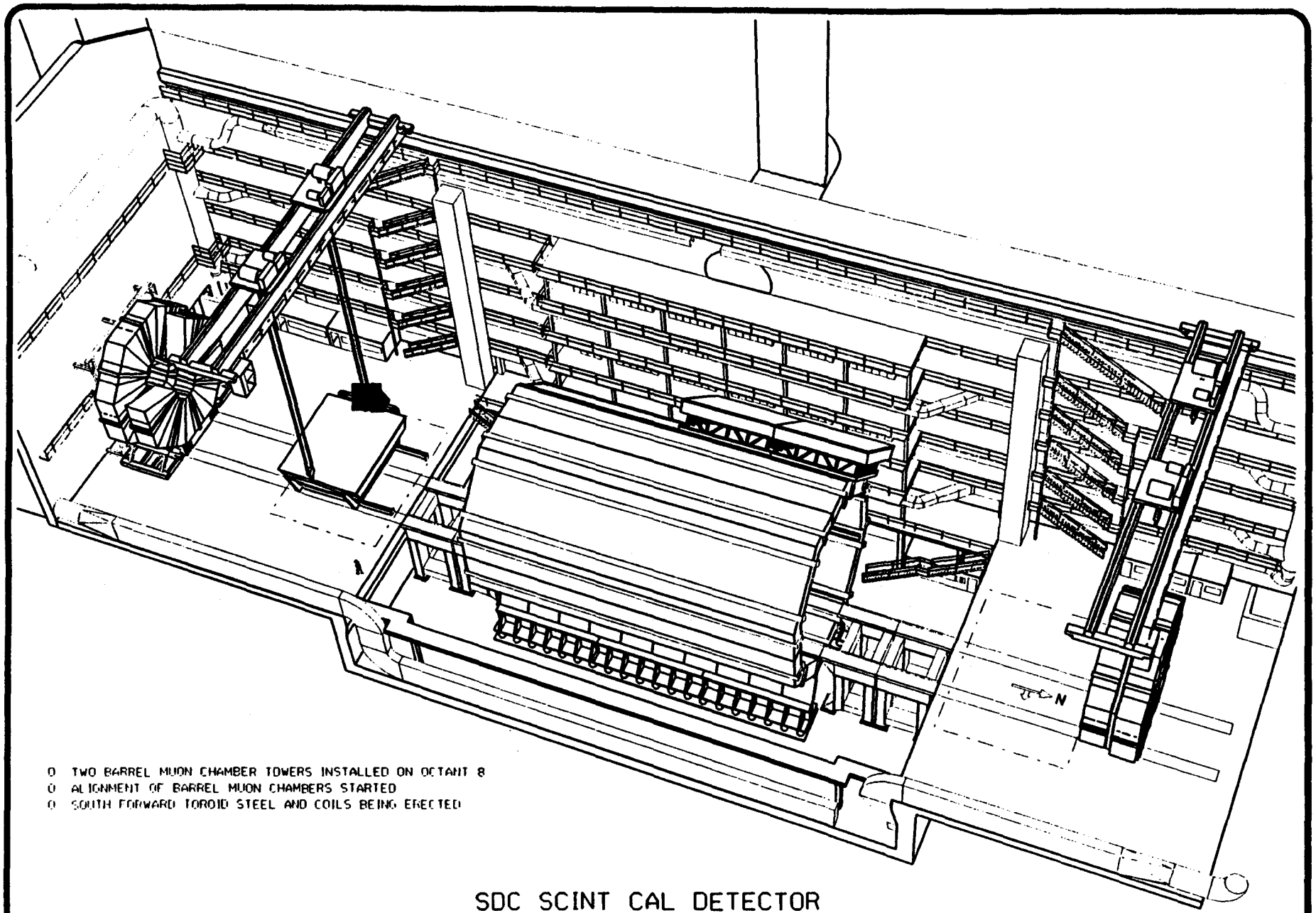

- TWO BARREL MUON CHAMBER TOWERS INSTALLED ON OCTANT 8
- ALIGNMENT OF BARREL MUON CHAMBERS STARTED
- SOUTH FORWARD TOROID STEEL AND COILS BEING ERECTED

SDC SCINT CAL DETECTOR

CONSTRUCTION PROGRESS

MONTH 14

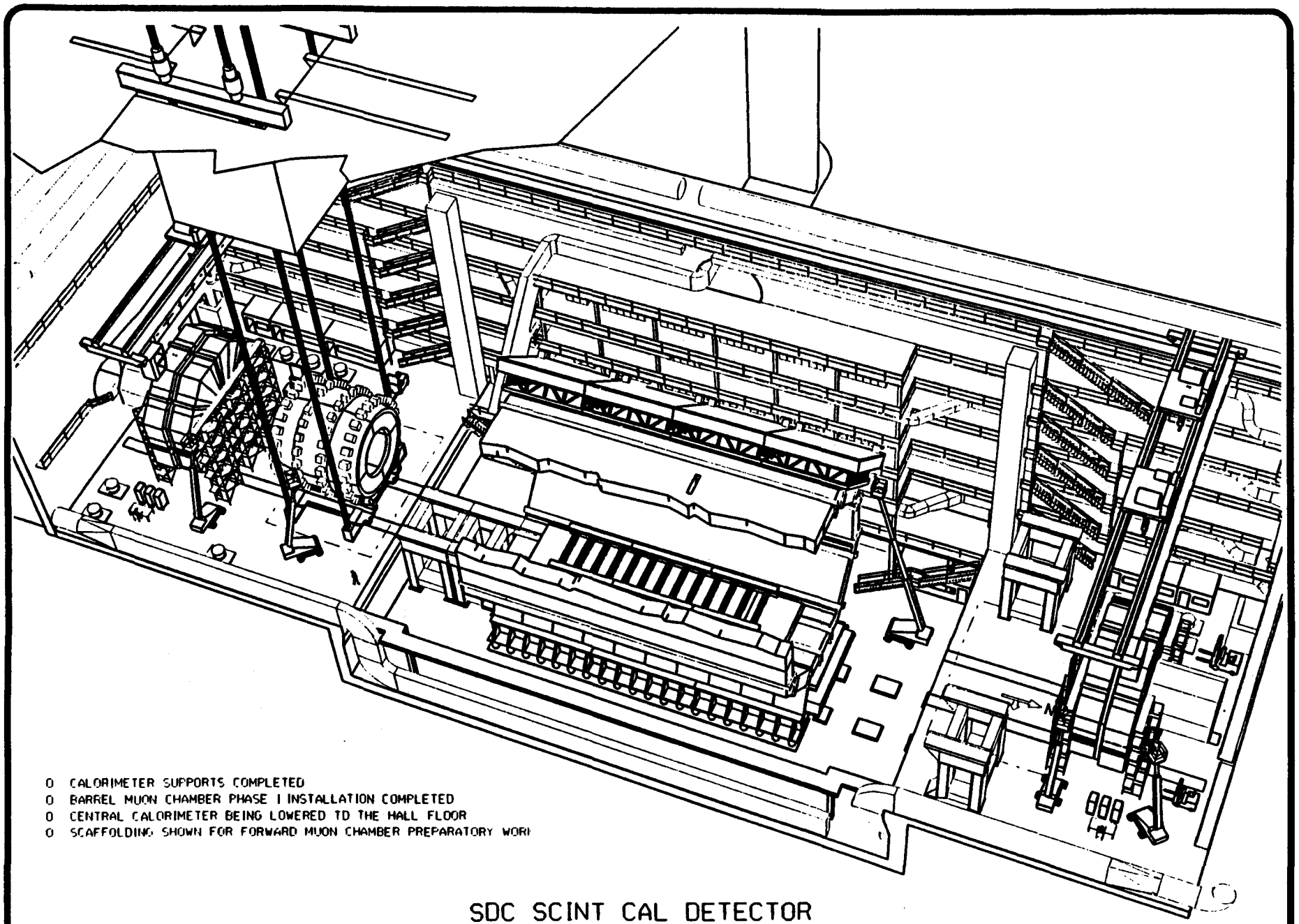

- CALORIMETER SUPPORTS COMPLETED
- BARREL MUON CHAMBER PHASE I INSTALLATION COMPLETED
- CENTRAL CALORIMETER BEING LOWERED TO THE HALL FLOOR
- SCAFFOLDING SHOWN FOR FORWARD MUON CHAMBER PREPARATORY WORK

SDC SCINT CAL DETECTOR

CONSTRUCTION PROGRESS

MONTH 18

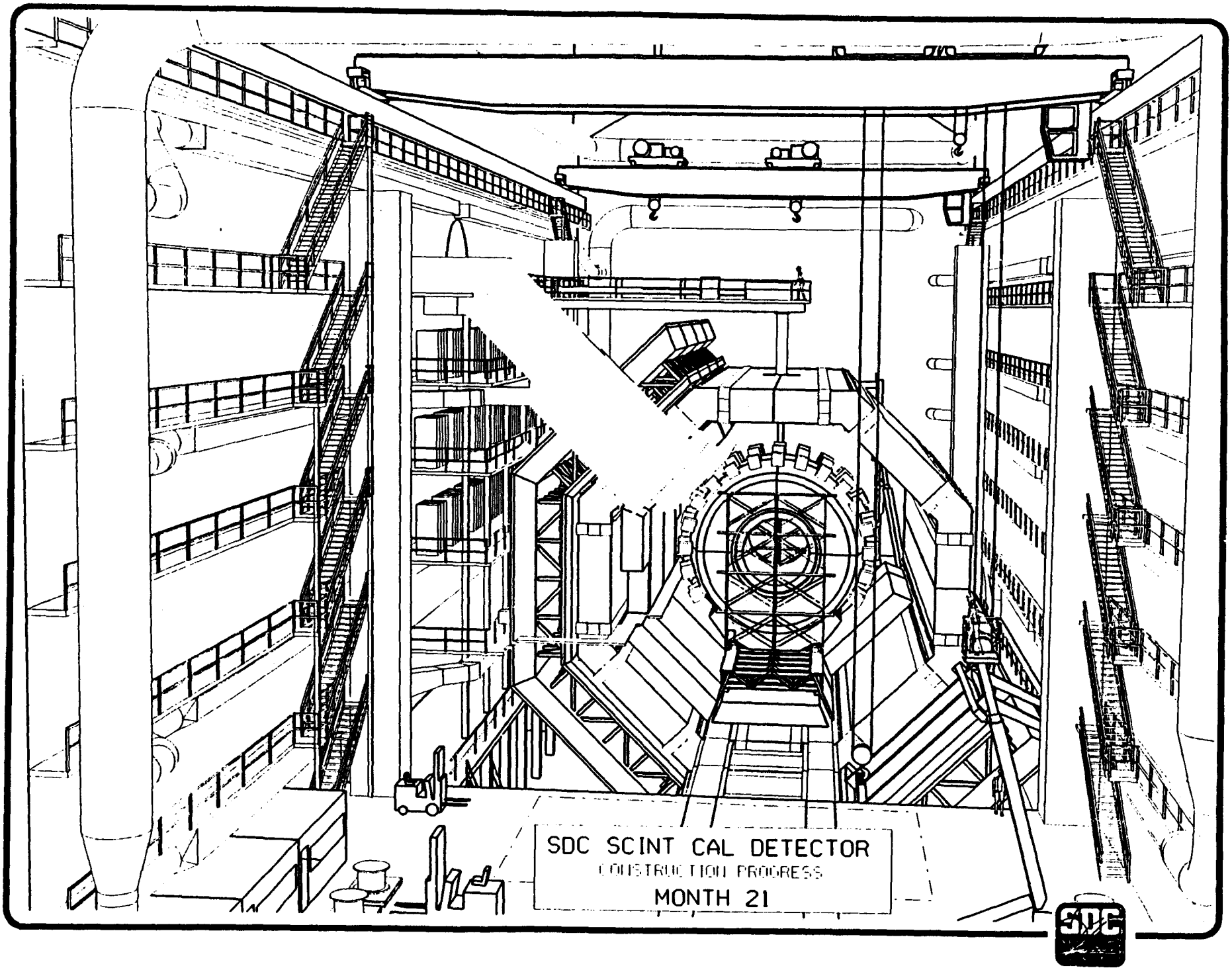
SDC SCINT CAL DETECTOR
CONSTRUCTION PROGRESS
MONTH 21
SDC

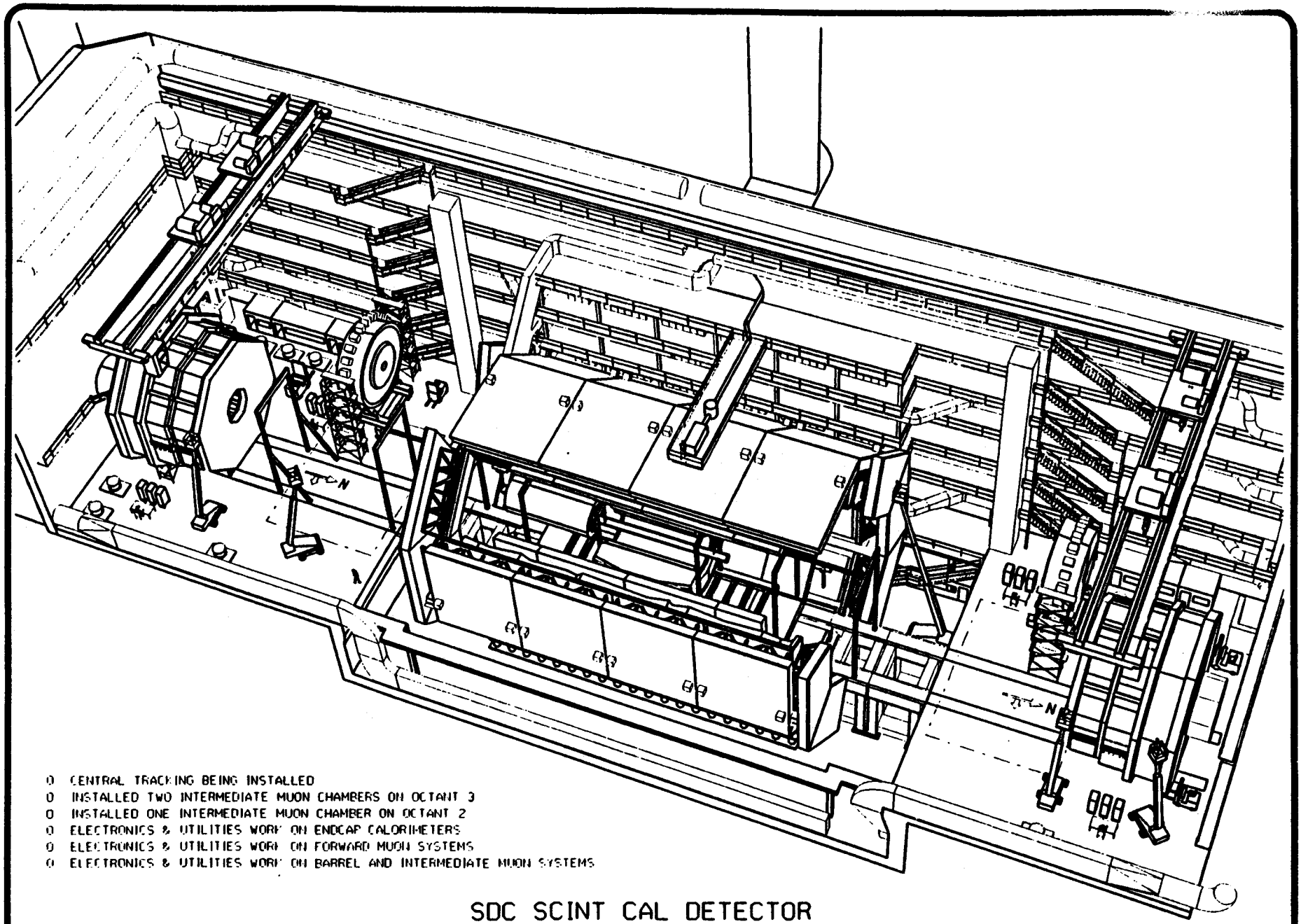

- CENTRAL TRACKING BEING INSTALLED
- INSTALLED TWO INTERMEDIATE MUON CHAMBERS ON OCTANT 3
- INSTALLED ONE INTERMEDIATE MUON CHAMBER ON OCTANT 2
- ELECTRONICS & UTILITIES WORK ON ENDCAP CALORIMETERS
- ELECTRONICS & UTILITIES WORK ON FORWARD MUON SYSTEMS
- ELECTRONICS & UTILITIES WORK ON BARREL AND INTERMEDIATE MUON SYSTEMS

SDC SCINT CAL DETECTOR

CONSTRUCTION PROGRESS

MONTH 30

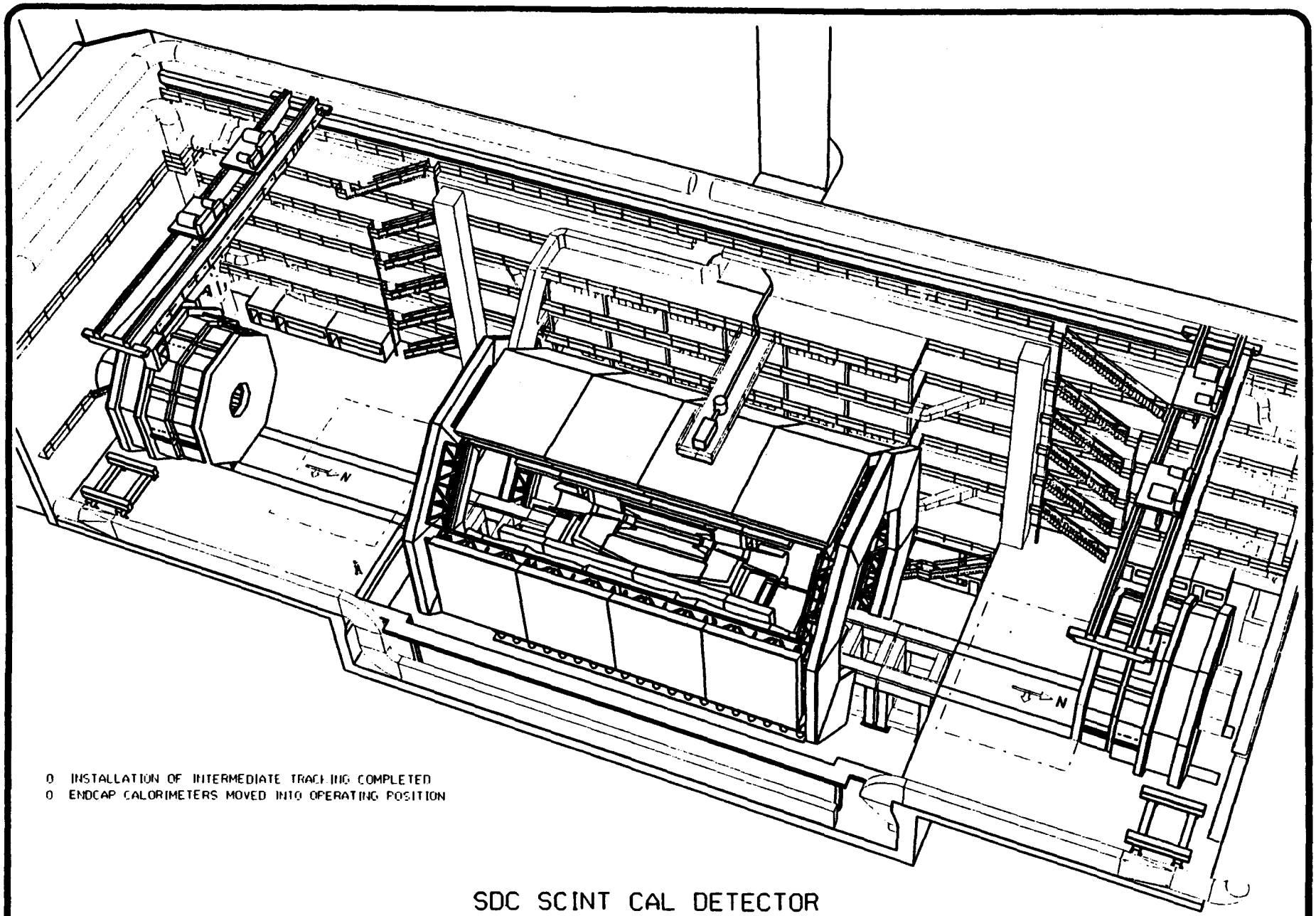

0 INSTALLATION OF INTERMEDIATE TRACKING COMPLETED
0 ENDCAP CALORIMETERS MOVED INTO OPERATING POSITION

SDC SCINT CAL DETECTOR

CONSTRUCTION PROGRESS

MONTH 36

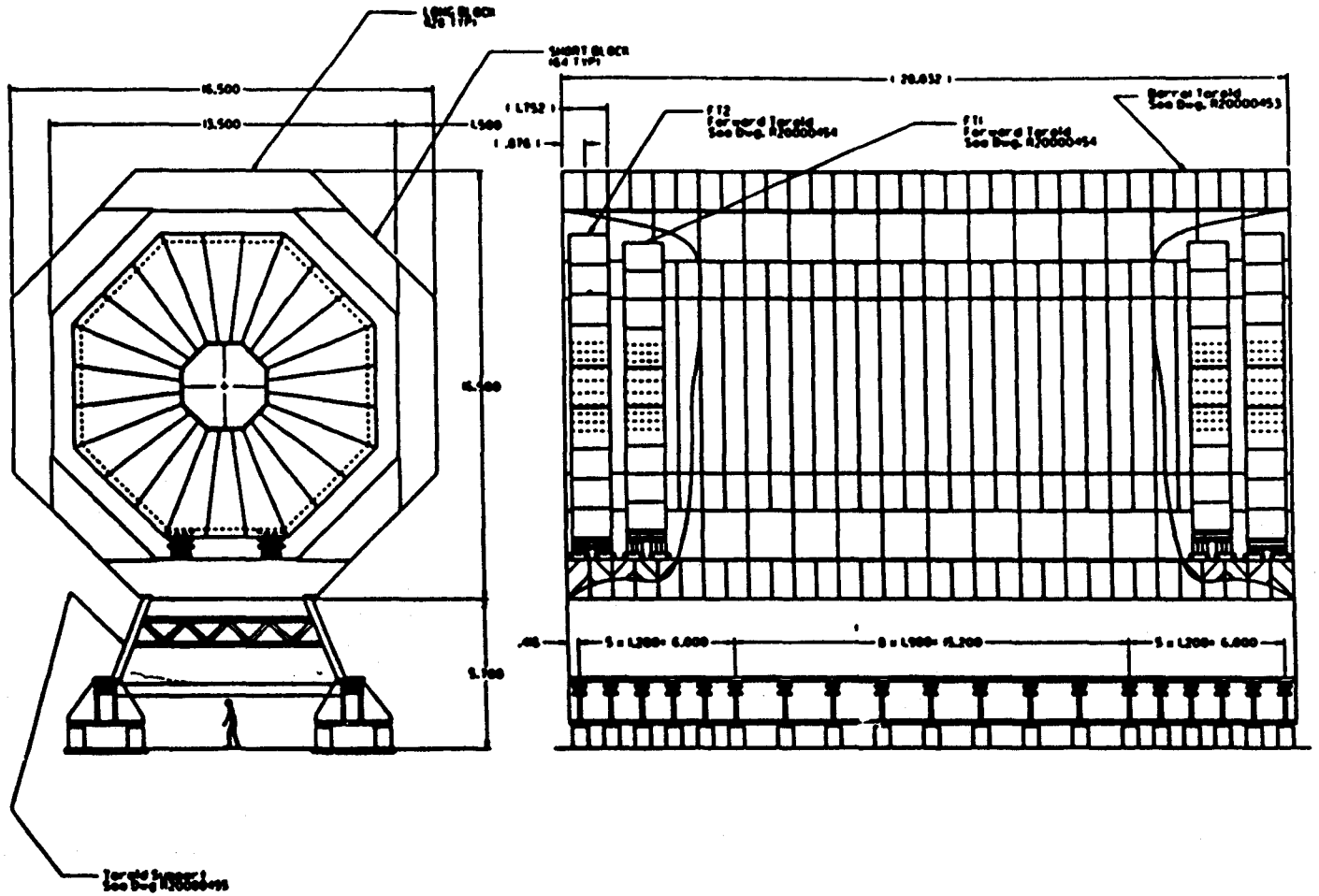

SDC MUON MAGNET ASSEMBLY
DRAWING NUMBER R20000452

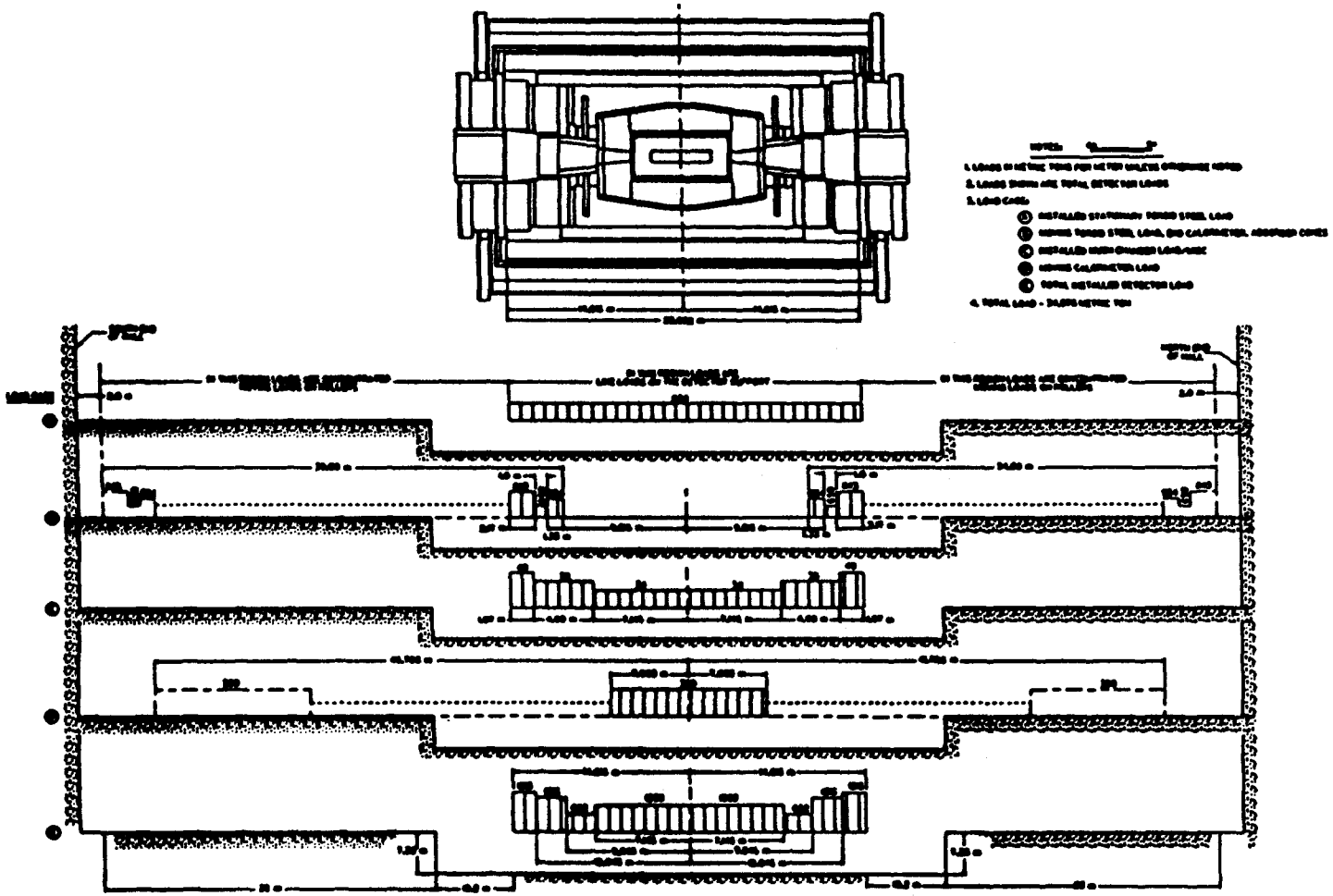

DEFLECTION DUE TO SELF WEIGHT

AUSTIN CHALK

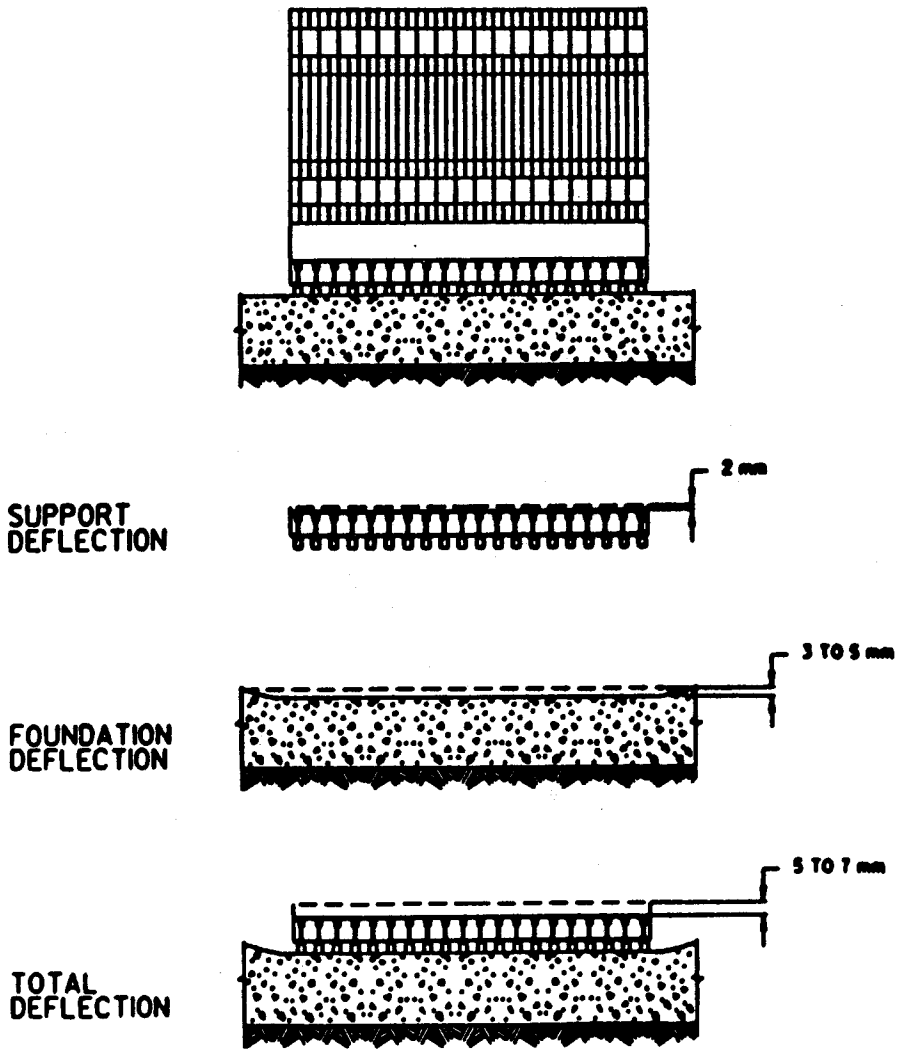

DEFLECTION DUE TO MOVING TOROID LOAD

AUSTIN CHALK

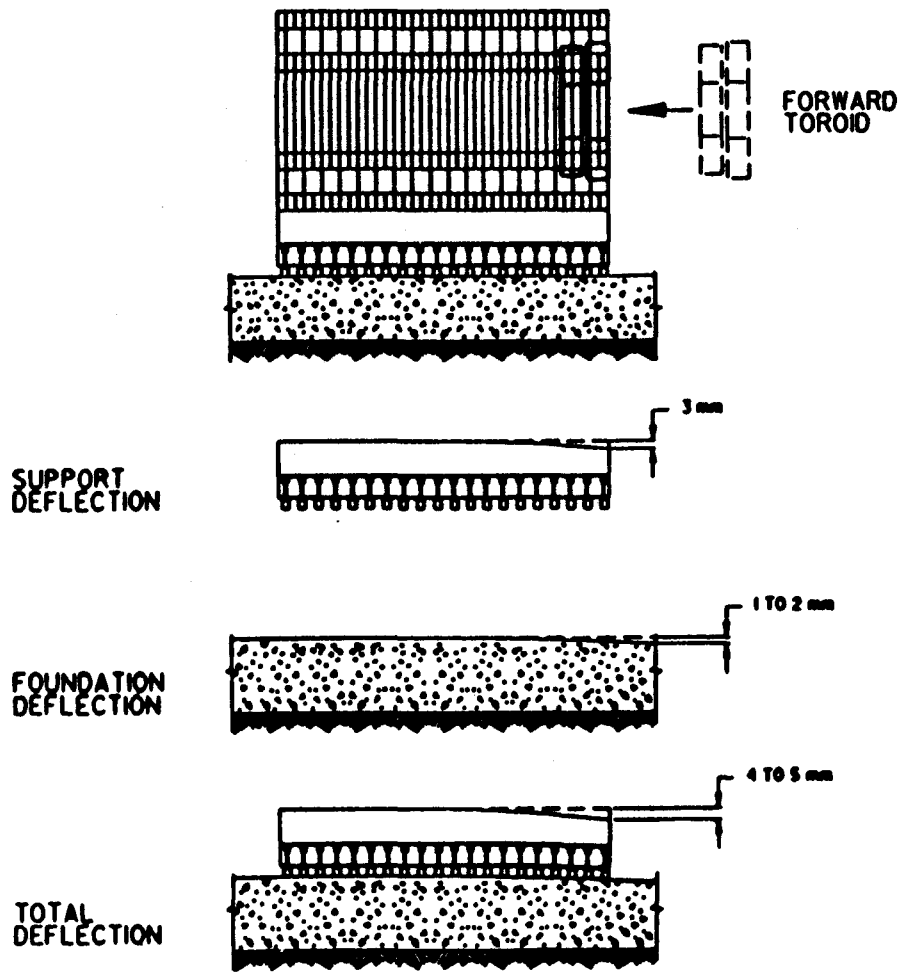

GEM DETECTOR

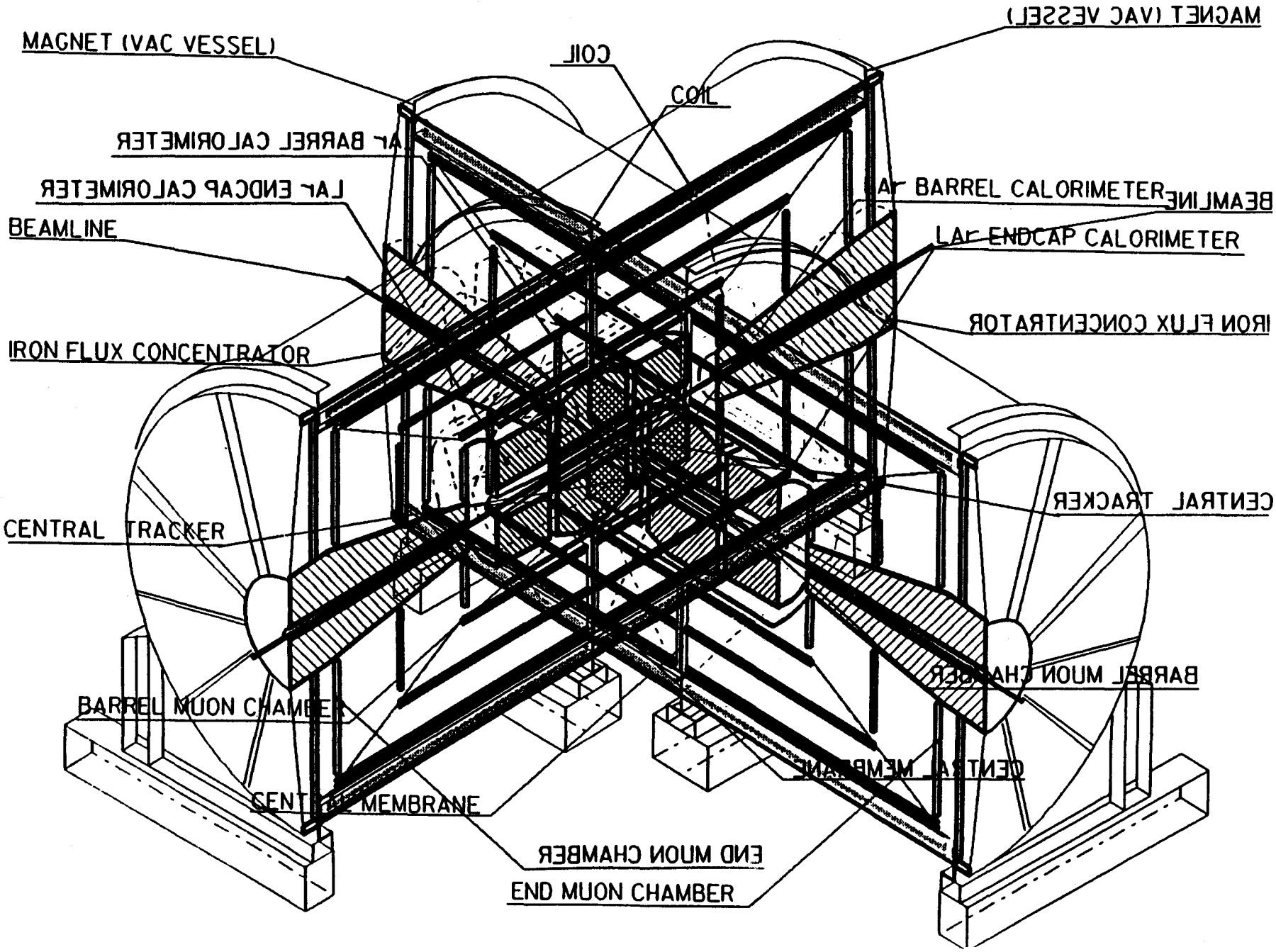

EXPERIMENTAL HALL GEM

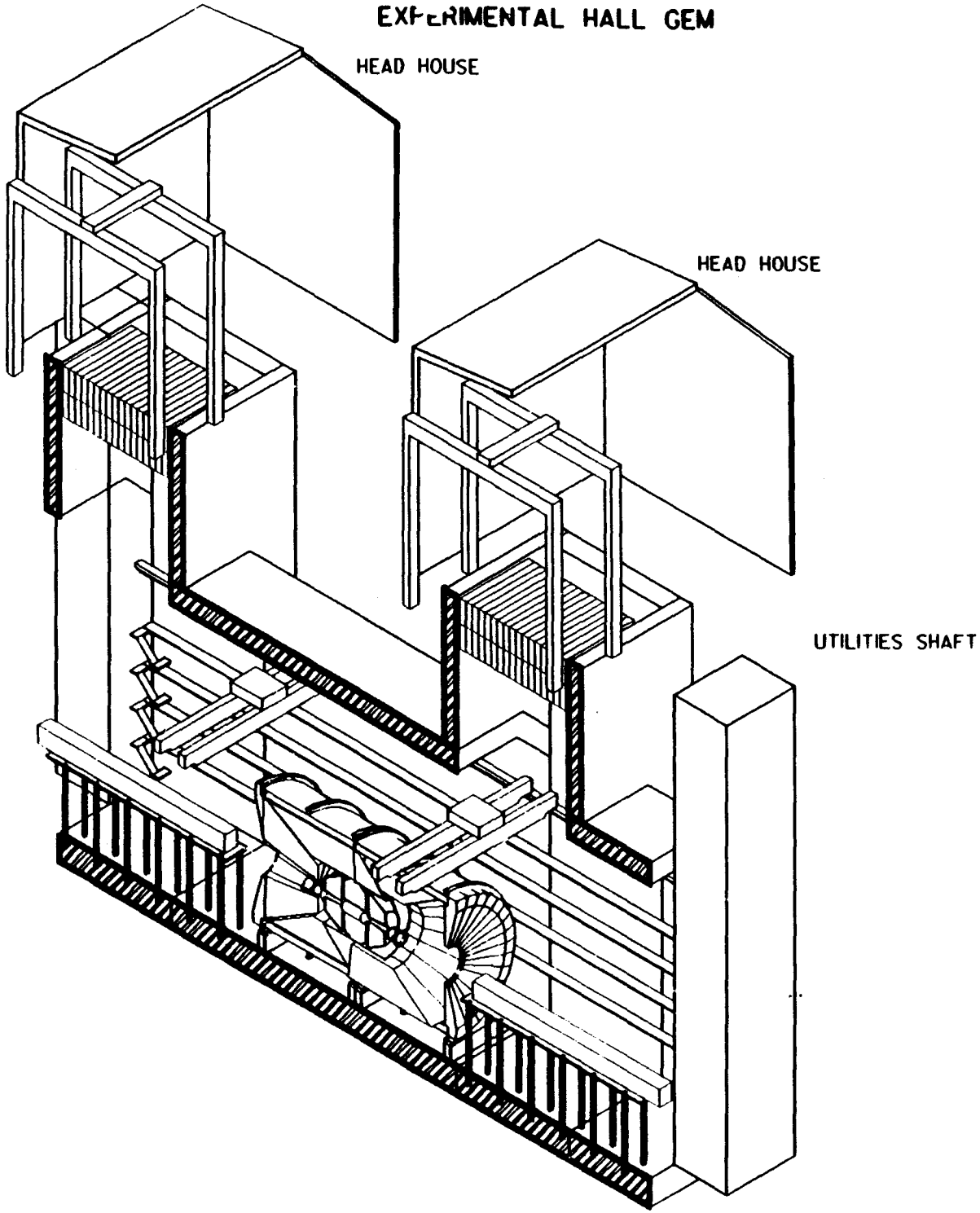

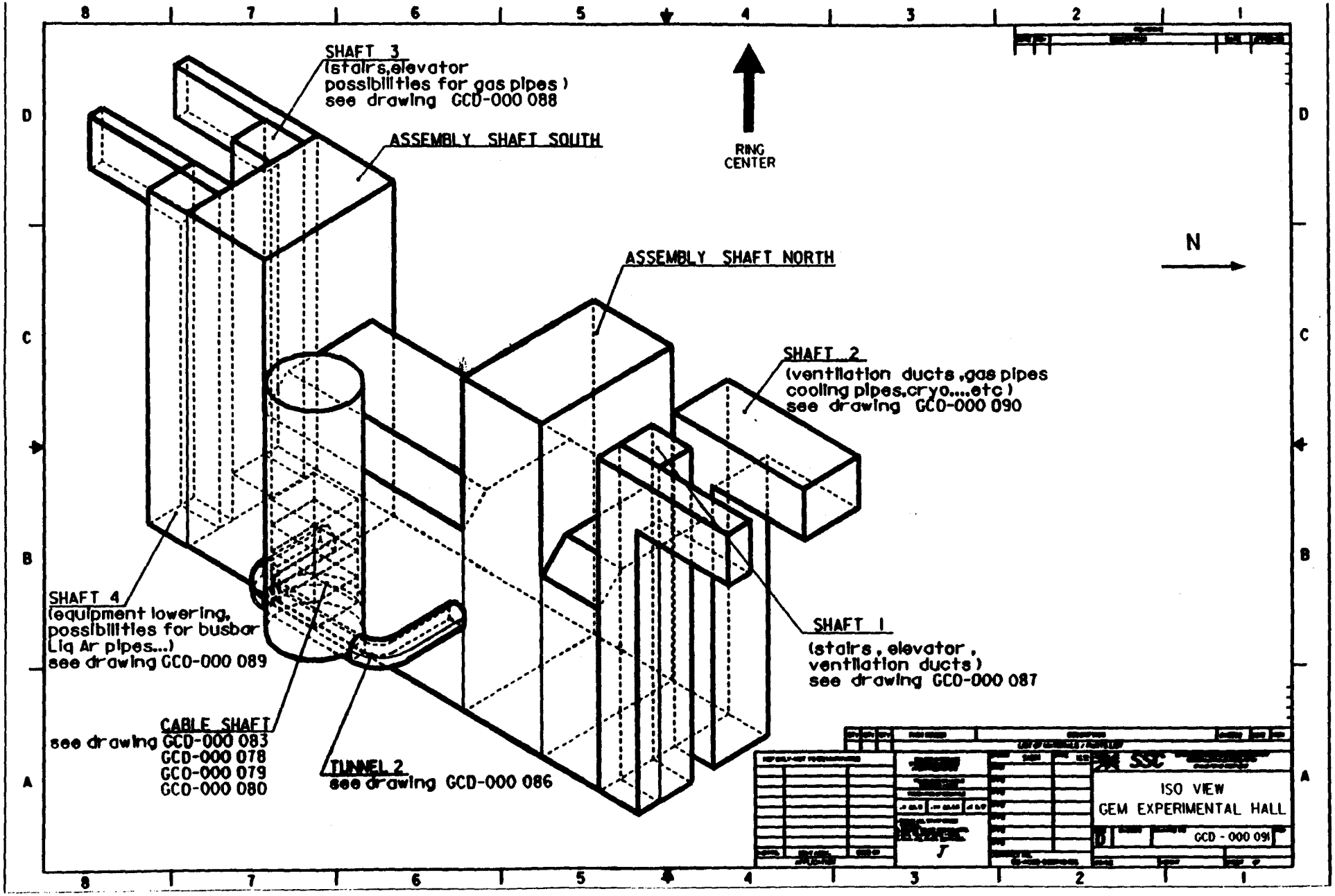
SHAFT 3
(stairs,elevator
possibilities for gas pipes)
see drawing GCD-000 088
ASSEMBLY SHAFT SOUTH
RING CENTER
N
ASSEMBLY SHAFT NORTH
SHAFT 2
(ventilation ducts,gas pipes
cooling pipes,cryo....etc)
see drawing GCD-000 090
SHAFT 4
(equipment lowering,
possibilities for busbar
Liq Ar pipes...)
see drawing GCD-000 089
SHAFT 1
(stairs, elevator,
ventilation ducts)
see drawing GCD-000 087
CABLE SHAFT
see drawing GCD-000 083
GCD-000 078
GCD-000 079
GCD-000 080
TUNNEL 2
see drawing GCD-000 086
SSC
ISO VIEW
GEM EXPERIMENTAL HALL
GCD - 000 091

OPTION 2 FIGURE 1

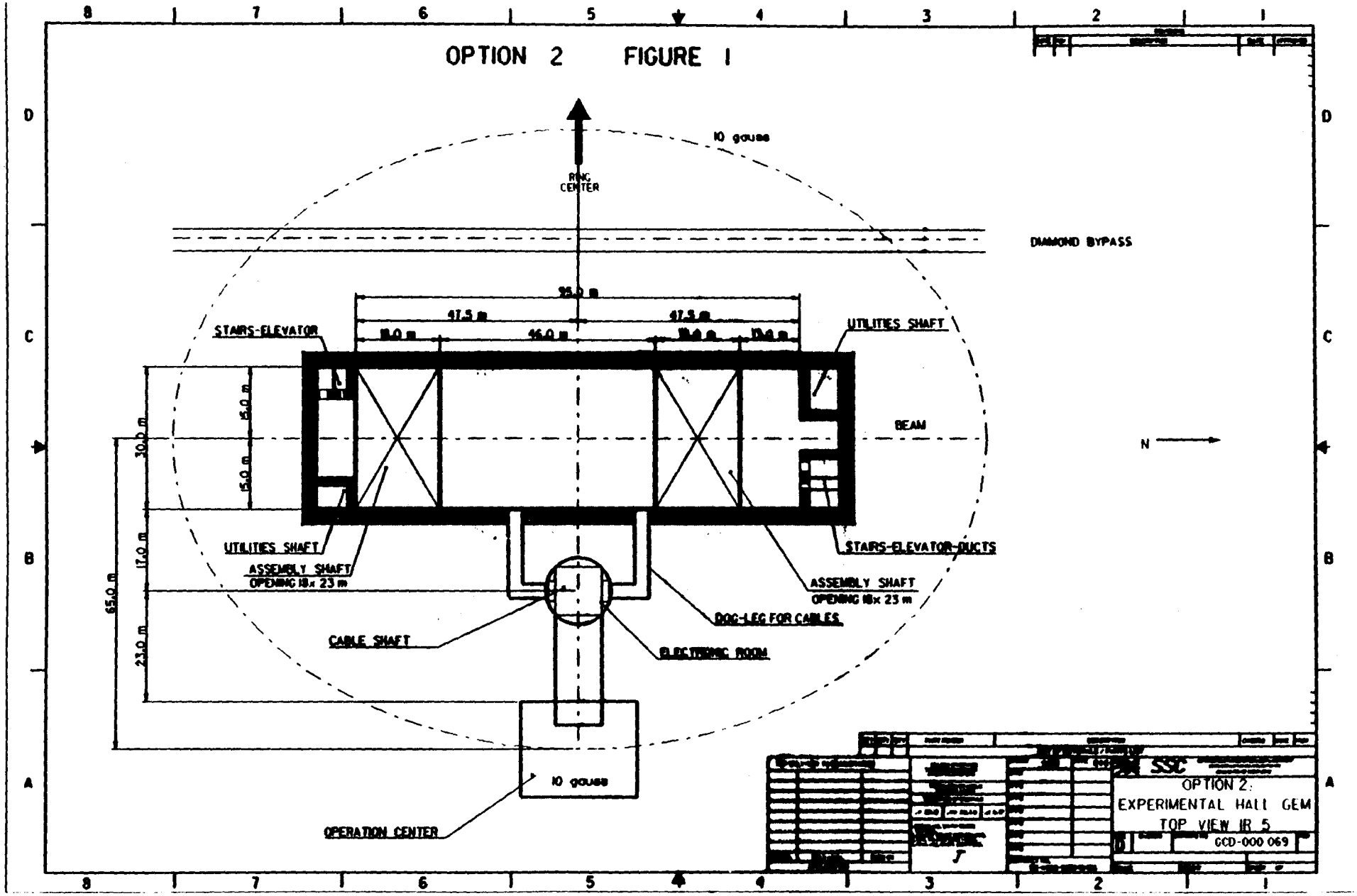

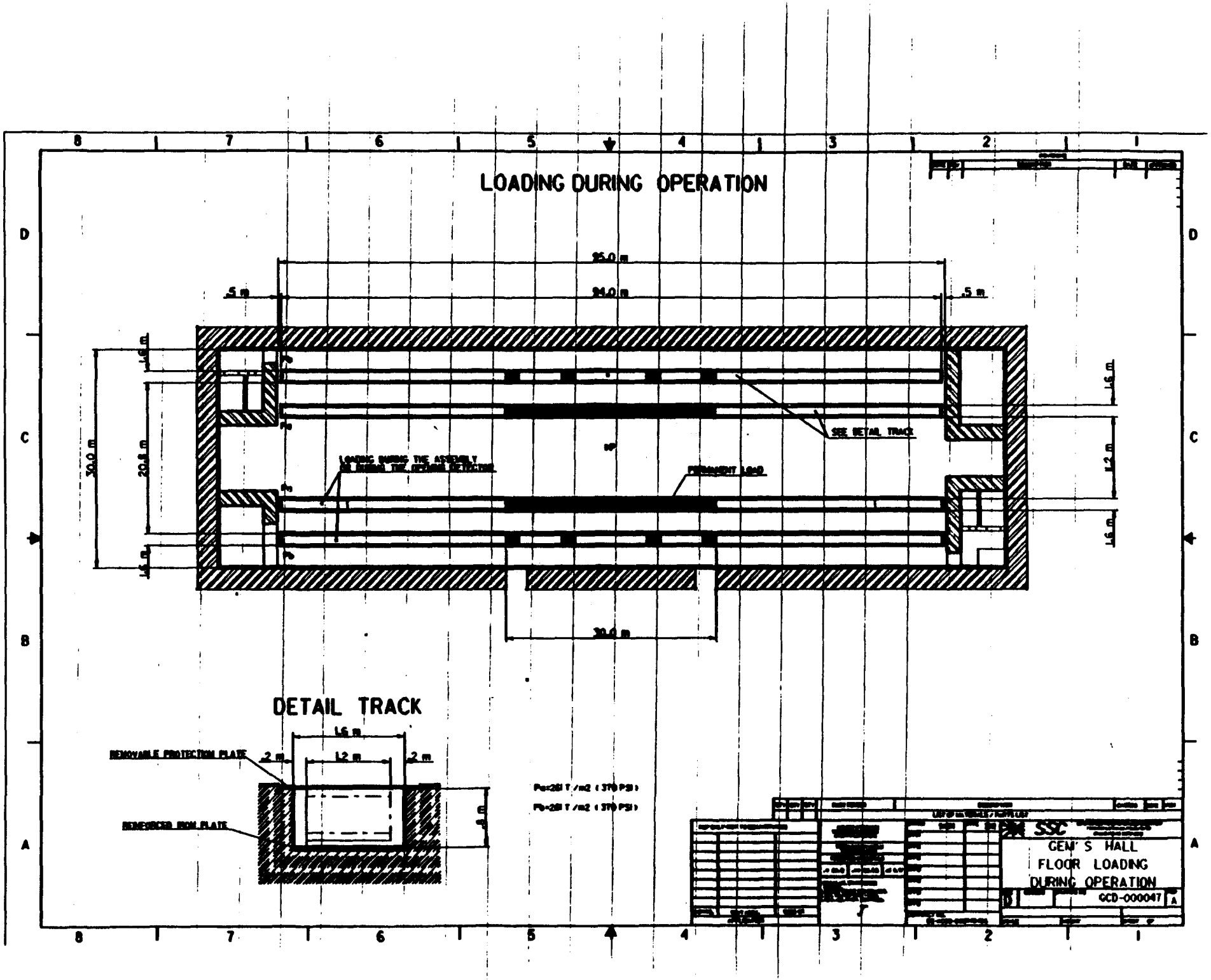
LOADING DURING OPERATION
95.0 m
.5 m
94.0 m
.5 m
30.0 m
20.8 m
1.6 m
1.6 m
1.2 m
1.6 m
1.6 m
SEE DETAIL TRACK
LOADING DURING THE ASSEMBLY OR DURING THE DETAILED INSPECTION
PERMANENT LOAD
30.0 m
DETAIL TRACK
1.6 m
1.2 m
.2 m
.2 m
REMOVABLE PROTECTION PLATE
REINFORCED IRON PLATE
.8 m
Pa=28 T/m2 (370 PSI)
Pb=28 T/m2 (370 PSI)
SSC
GEM'S HALL
FLOOR LOADING
DURING OPERATION
GCD-000047
A

FIGURE 2

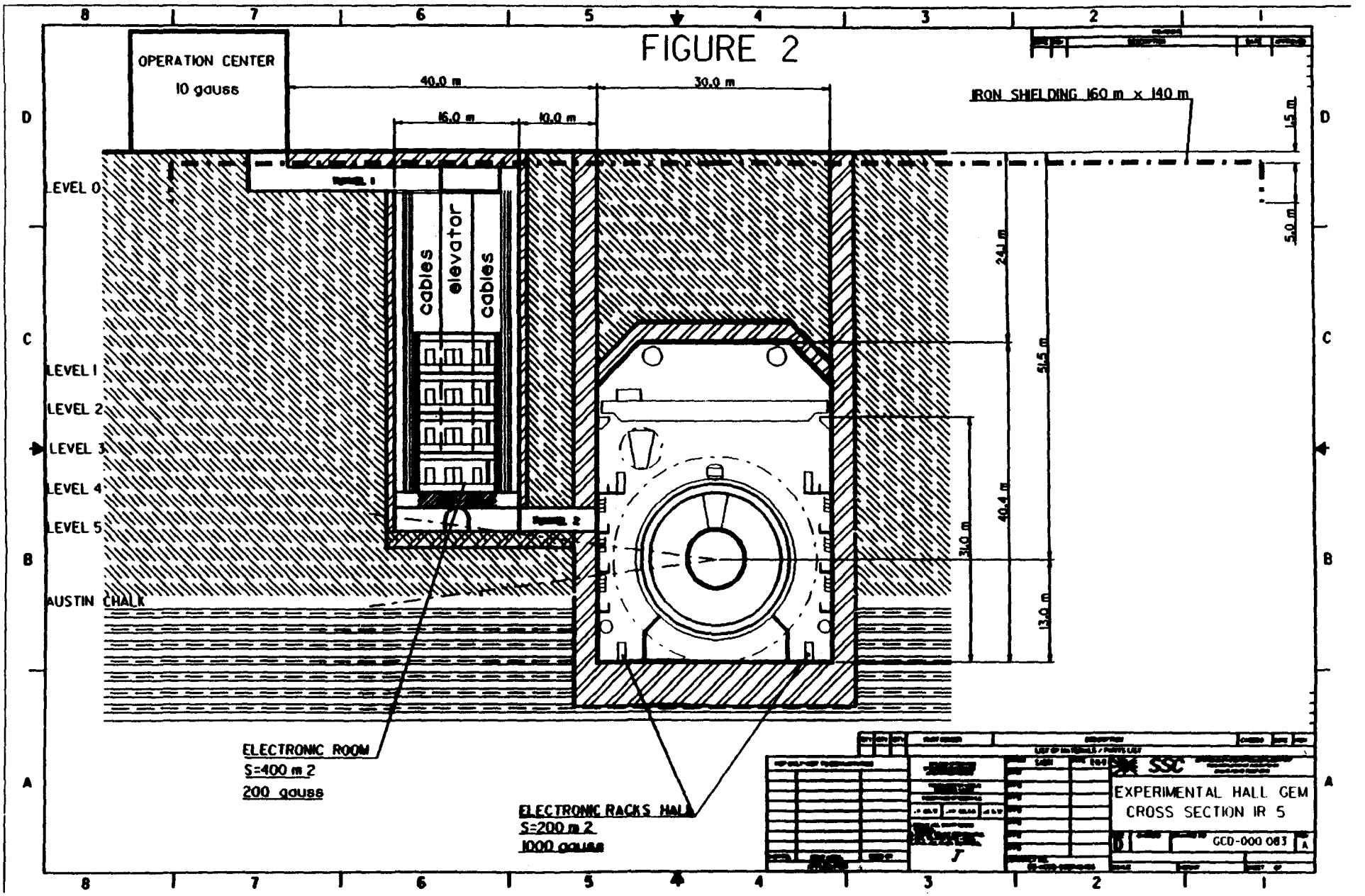
OPERATION CENTER
10 gauss
40.0 m
30.0 m
16.0 m
10.0 m
IRON SHIELDING 160 m x 140 m
1.5 m
5.0 m
24.1 m
51.5 m
40.4 m
34.0 m
13.0 m
LEVEL 0
LEVEL 1
LEVEL 2
LEVEL 3
LEVEL 4
LEVEL 5
AUSTIN CHALK
cables
elevator
cables
ELECTRONIC ROOM
S=400 m 2
200 gauss
ELECTRONIC RACKS HALL
S=200 m 2
1000 gauss
SSC
EXPERIMENTAL HALL GEM
CROSS SECTION IR 5
GCD-000 083

FIGURE 3

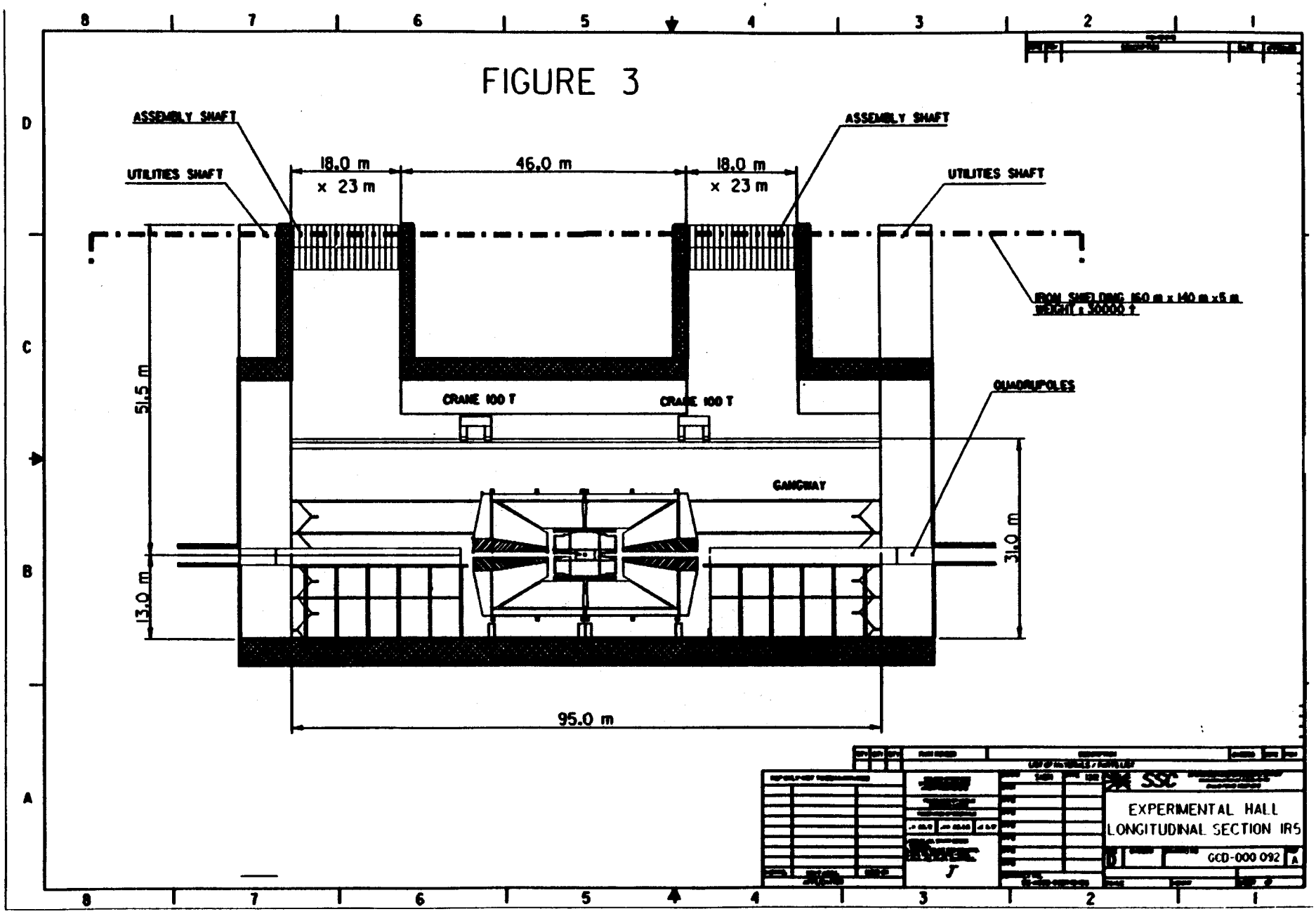
ASSEMBLY SHAFT
UTILITIES SHAFT
18.0 m
x 23 m
46.0 m
18.0 m
x 23 m
ASSEMBLY SHAFT
UTILITIES SHAFT
IRON SHIELDING 150 m x 140 m x 5 m
WEIGHT = 300000 T
CRANE 100 T
CRANE 100 T
QUADRUPOLES
GANGWAY
51.5 m
13.0 m
31.0 m
95.0 m
SSC
EXPERIMENTAL HALL
LONGITUDINAL SECTION IR5
GCD-000 092
A

(PRESENTATIONS)

VIBRATIONAL EFFECTS ON BEAM BEHAVIOR

A General Review of Ground Motion
Gerry Fischer (SLAC)

Ground Motion Spectra
Bob Murray(LNLL)

Vibrational Measurements and
Analysis of USSR Accelerator Sites
Vasili Parchomuchuk (INP/USSR)

Ground Motion Effects on the SSCL
Jack Peterson (LBL)

Excitation of Betatron Oscillations by Vibrating
Quadrupoles and Luminosity
Degradation due to Beam-Beam Interaction
Gena Stupakov (INP/SSCL)

Emittance Growth Issues
Bill Ng (FERMI)

Deterioration of Beam Quality at the SSC
Resulting from Ground Motion
Dave Ritson (SLAC)

Ground Motion Measurements at the Site
of the Advanced Photon Source (APS)
J. A. Jendrzejczyk (ANL)

GENERAL REVIEW OF GROUND MOTION ISSUES

G. E. FISCHER - SLAC
(415) 926-4198

OUTLINE

1. REVISIT SSC REPORT SSC-55 JAN. 1986

2. DESCRIBE RECENT VIBRATION POWER SPECTRAL DENSITY MEASUREMENTS ON QUIET SITES WITH RESPECT TO RECENT CONCERNS AT HIGH FREQ.

3. HIGHER LEVELS ARE DUE TO "CULTURAL" ACTIVITY

4. SHOW LONGTERM MISALIGNMENT DATA FROM EXISTING MACHINES - SURFACE MOVES WITH RESPECT TO BASE STRATA

5. POINT OUT THAT FOUNDATIONS OF EXP. HALL WILL DISTORT WITH MOVING LOADS

6. POINT OUT THAT SUSPENSIONS DO NOT NORMALLY TRANSMIT HIGH FREQ.

7. MAKE A PLEA - DO NOT SPOIL A GOOD SITE

2

3. SUMMARY OF RECOMMENDED GROUND MOTION TOLERANCES

Throughout we assume that the beam centroids should not be displaced from each other by more than 10% of 1 sigma of their beam size at the interaction point.

Below, in Table II we list our recommendations for the three cases studied: totally random motion, coherent motion in the plane wave approximation with an assumed constant wave velocity of 2.5 km/sec, and the improbable but limiting situation with an SSC demon. The tolerances given in the first column are the tolerances calculated in Section 2.1 in absence of any feedback system and neglecting any resonances in the magnet support structures. The effect of the feedback on increasing the tolerances for frequencies below 20 Hz is shown in column two. We have assumed the feedback system to be capable of suppressing the effects of noise by a factor of 10 for the frequencies below 20 Hz. For the first case of random noise, which comes from local sources, we have divided the frequency range into two bands. The resonances of the magnet support structures are assumed to all be above 3 Hz so that only the local noise will be amplified by structure resonances. It can be shown that, if the bandwidth of the noise is much larger than the width of a structure resonance, the rms amplitude of the magnet motion, Δy_m, is equal to $\sqrt{Q}$ times the rms amplitude of the ground motion, Δy_g, due to the noise from all the frequencies above the structure resonance, where Q is the quality factor. In the third column we take into account amplification of the ground motion of 10 due to resonances in the magnet support structure for the incoherent case only.

We have used the power spectrum (noisy station) given in Fig 1.1 and converted the curve into rms amplitudes in the appropriate frequency range and presented them in Table III. It should be noted that we have been reluctant to present Table III. It is feared that Table III will be misused because many of the readers may not fully appreciate that it refers to a hard rock site where no cul-

TABLE II

Recommended Ground Motion Tolerances

	no feedback rigid support	with feedback rigid support	with feedback with assumed support ampl. factor of 10
Case 1. Completely random local noise: 3 Hz $< f <$ 20 Hz	$< 0.4\ \mu m$	$< 4\ \mu m$	$< 0.4\ \mu m$
$f >$ 20 Hz	$< 0.4\ \mu m$	$< 0.4\ \mu m$	$< 0.04\ \mu m$
Case 2. Correlated by plane waves: 0.02 Hz$< f <$ 3 Hz	$< 0.1\ \mu m$	$< 1\ \mu m$	$< 1\ \mu m$
Case 3. Improbable total correlation at the betatron wavelength:	$0.02\ \mu m$	$< 0.2\ \mu m$	$< 0.2\ \mu m$

TABLE III

Expectation of rms ground amplitudes in various frequency bands on a hard rock site as given in Fig. 1.1 (No cultural noise)

Freq. Band	0.02 Hz $< f <$ 3 Hz	3 Hz$< f <$ 20 Hz	$f >$ 20 Hz
$< y >$ rms	$1\ \mu m$	$.003\ \mu m$	$3 \times 10^{-4}\ \mu m$

tural noise has been included. Nevertheless, it was felt that there might be some readers unfamiliar with the connection between the power spectrum curve and the expectation value of the amplitude, so it has been included **NOT AS A TYPICAL EXAMPLE** but as an illustrative example.

Discussion

The reader may now well ask: "What do these numbers really mean with respect to ground motions one might expect from typical sites?" We conclude that the situation is: (a) Definitely *not hopeless – an SSC can be built and operated.* (b) Unfortunately, it appears also that the problem *cannot be dismissed out of hand.* In other words one must now examine and evaluate in more detail the parameters that went into our assumptions in order to determine the most economic tradeoffs.

We believe:

- The effects of ground motion would become quite small if the lattice did not possess the focus – defocus properties of configuration $(2,4)_b$.
- Since the magnitude of ground motions are, among other things, a function of soil conditions, due care should be exercised in this matter.
- Weather and other uncontrollable natural sources and variable conditions introduce a range in the base levels of at least one order of magnitude. A feedback system ought to be able to counteract these effects.
- Care should be taken to avoid the introduction of controllable cultural noise, since this generally occurs at higher frequencies (> 3 Hz.) Motions at these frequencies are more likely to be amplified by the supports and are more difficult to suppress with a feedback system.
- The general design of components and civil structures should take into account the ground motion problem so that the recommended values of column 3 of Table II can be relaxed.

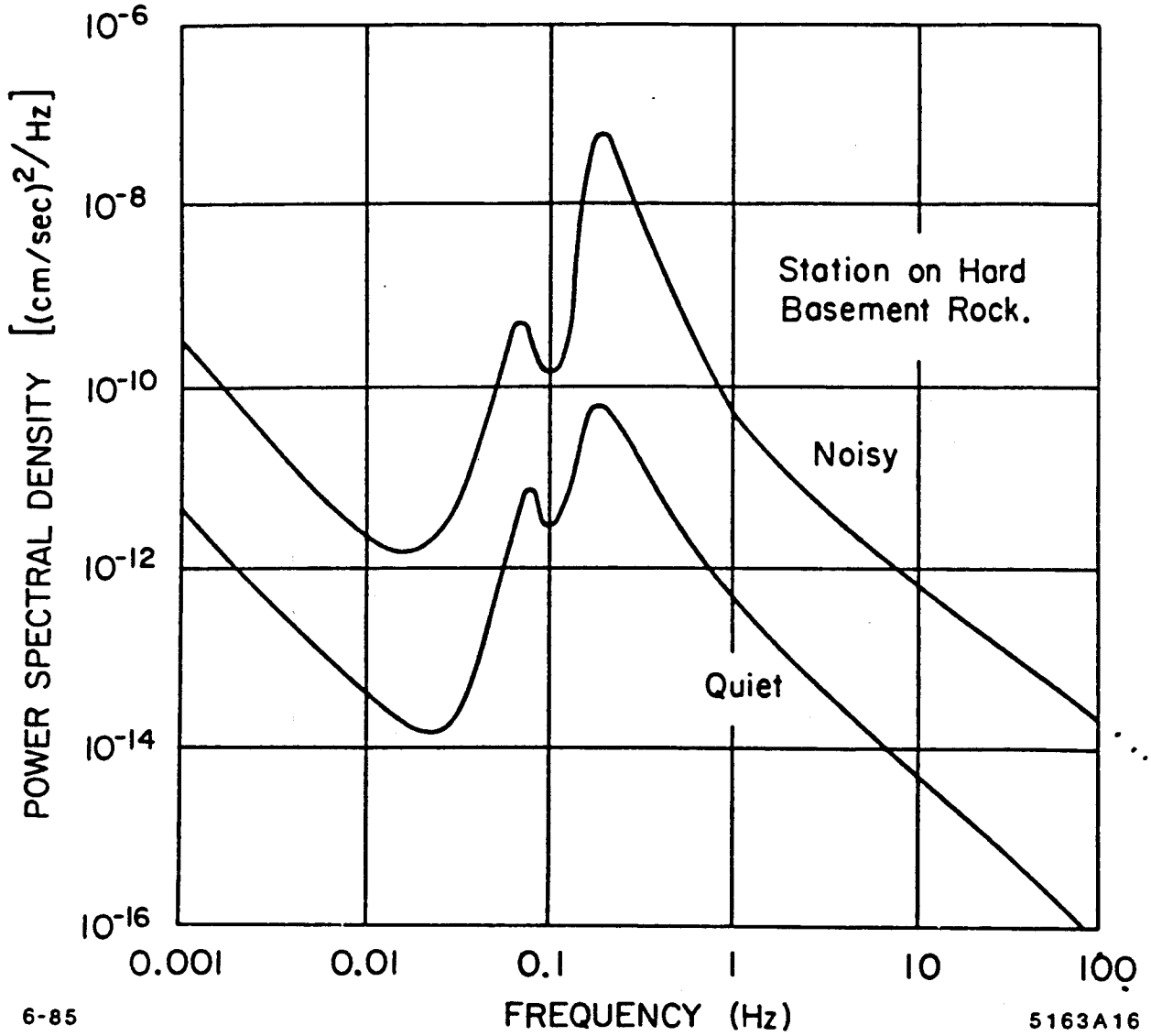

Fig. 1.1. Long Term Averaged "Maximum" and "Minimum" Noise Power Spectra (from Ref. 8).

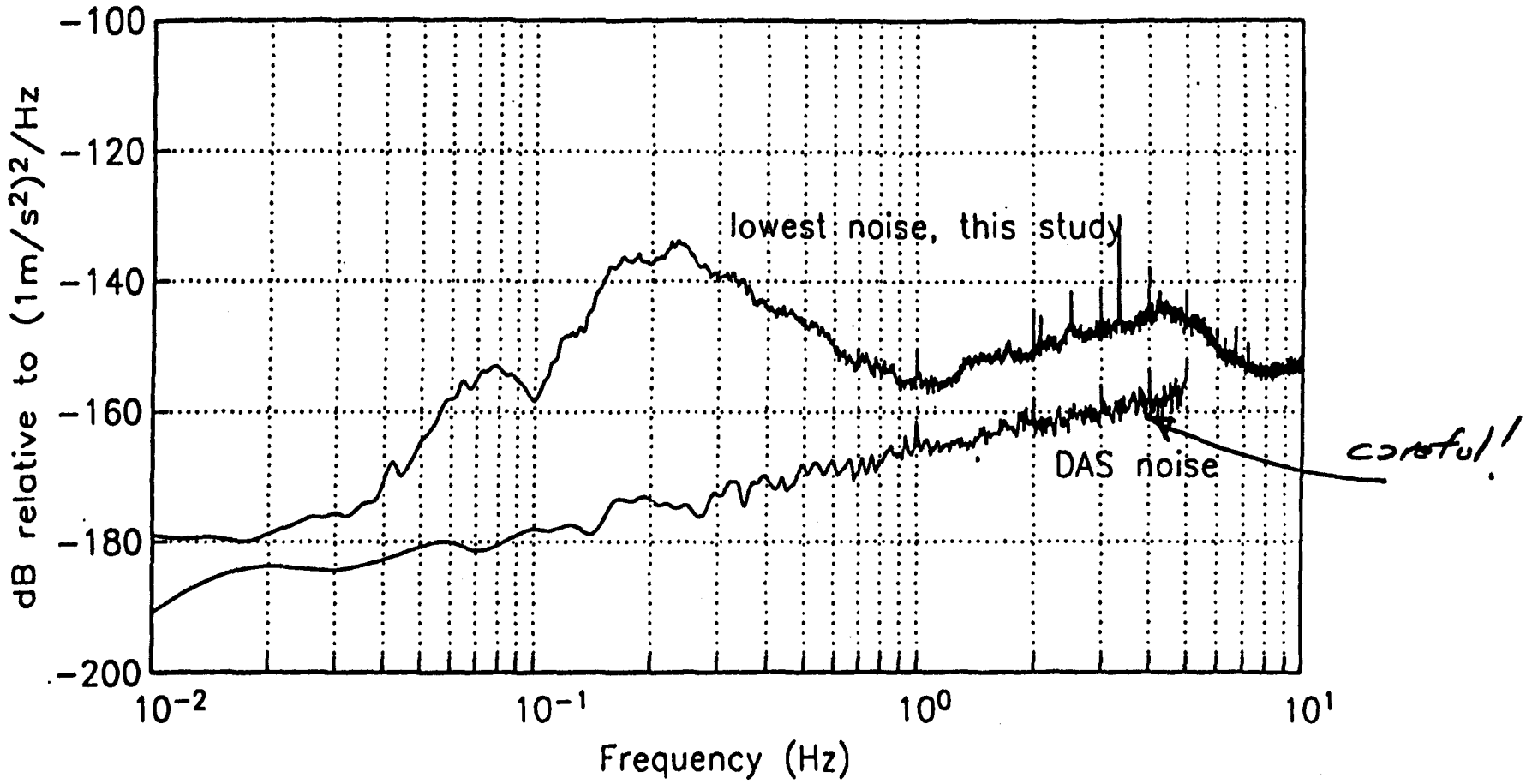

FIG. 8. Inherent noise of the electronics of the data acquisition system (DAS), which is the dominant source of system noise in the IRIS/IDA equipment. The lowest noise spectrum observed in this study, vertical-component winter night noise at GAR, is shown for comparison.

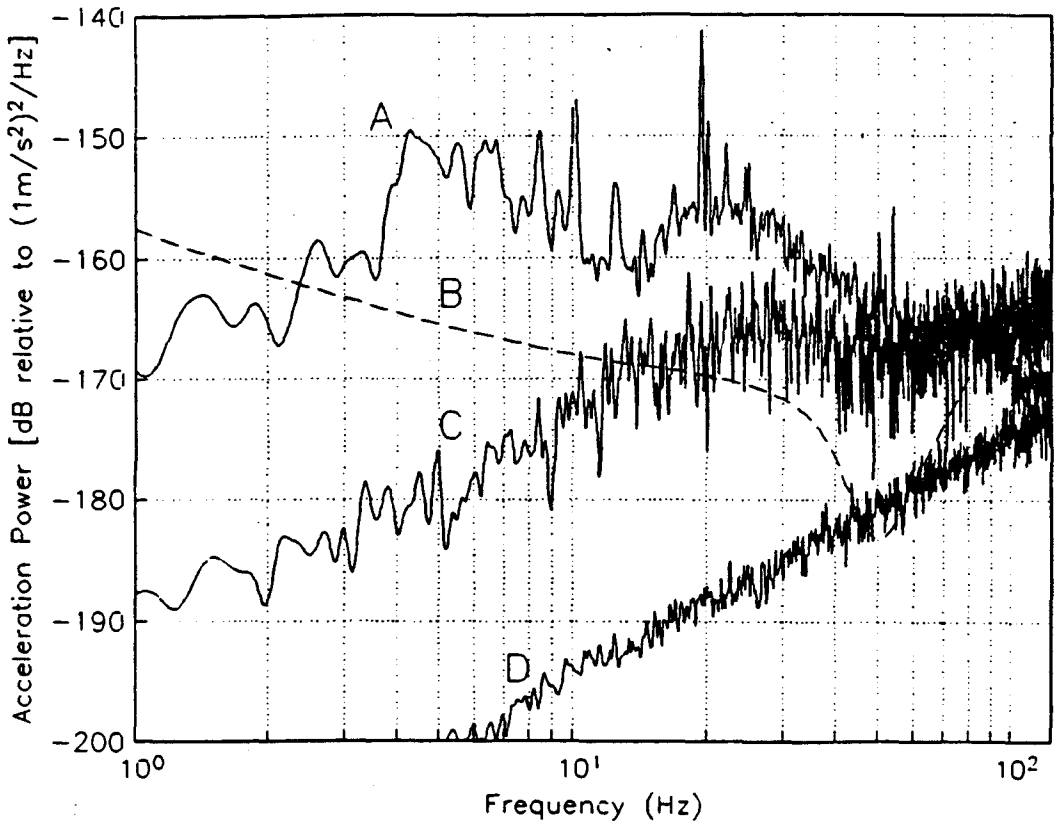

FIG. 6. System noise performance. (A) Ambient ground noise spectrum during a quiet period at BAY. From 1 to 10 Hz the measurements are taken from the surface GS-13 seismometer and from 10 to 125 Hz from the borehole seismometer. (B) Theoretical borehole seismometer noise as supplied by the manufacturer. (C) GS-13 seismometer noise with mass clamped. (D) Electronic system noise observed by replacing the seismometer with its equivalent impedance.

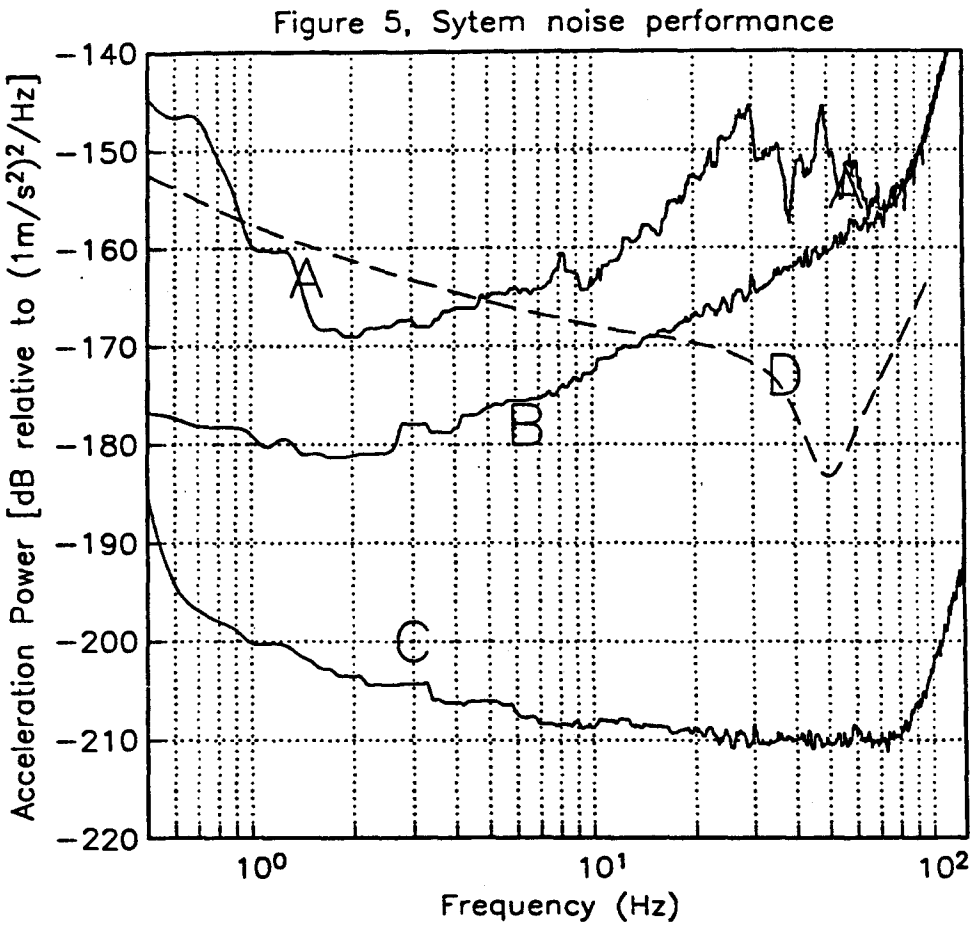

FIG. 5. Summary of system noise performance. Curve A is a power spectrum depicting low noise conditions at Deep Springs with the amplifier gain set at 48 dB. Curves B and C are the system noise tests, corrected for the surface and borehole system responses respectively, with the seismometer replaced by an equivalent resistance, and recorded at 48 dB. Curve D is the theoretical noise level of the borehole seismometers as supplied by the manufacturer, which does not include noise generated in the amplifiers and filters (Berger *et al.*, 1988).

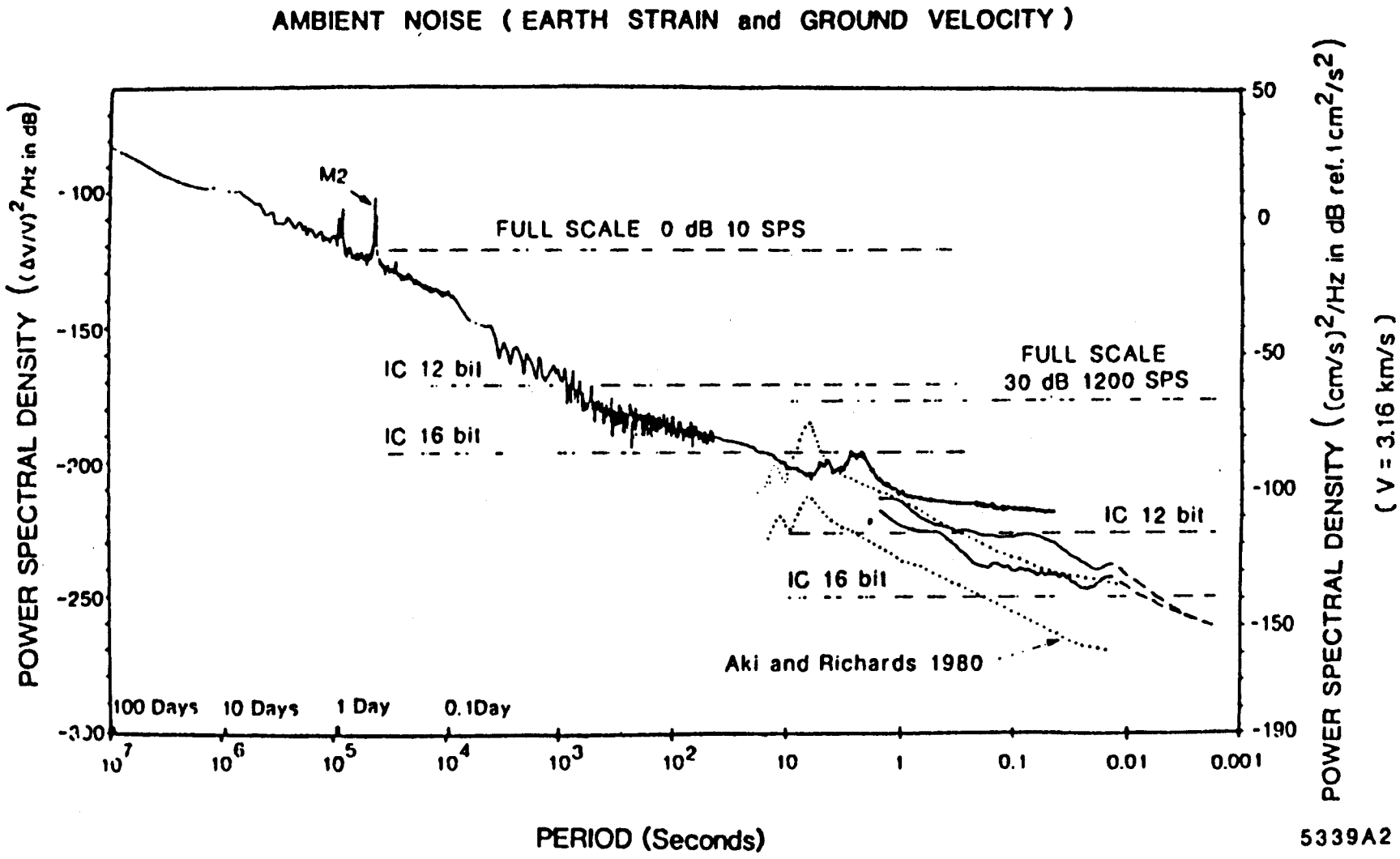

Fig. 1.2. Compilation of Ground Motion over a Wide Range of Periods (Ref. 10).

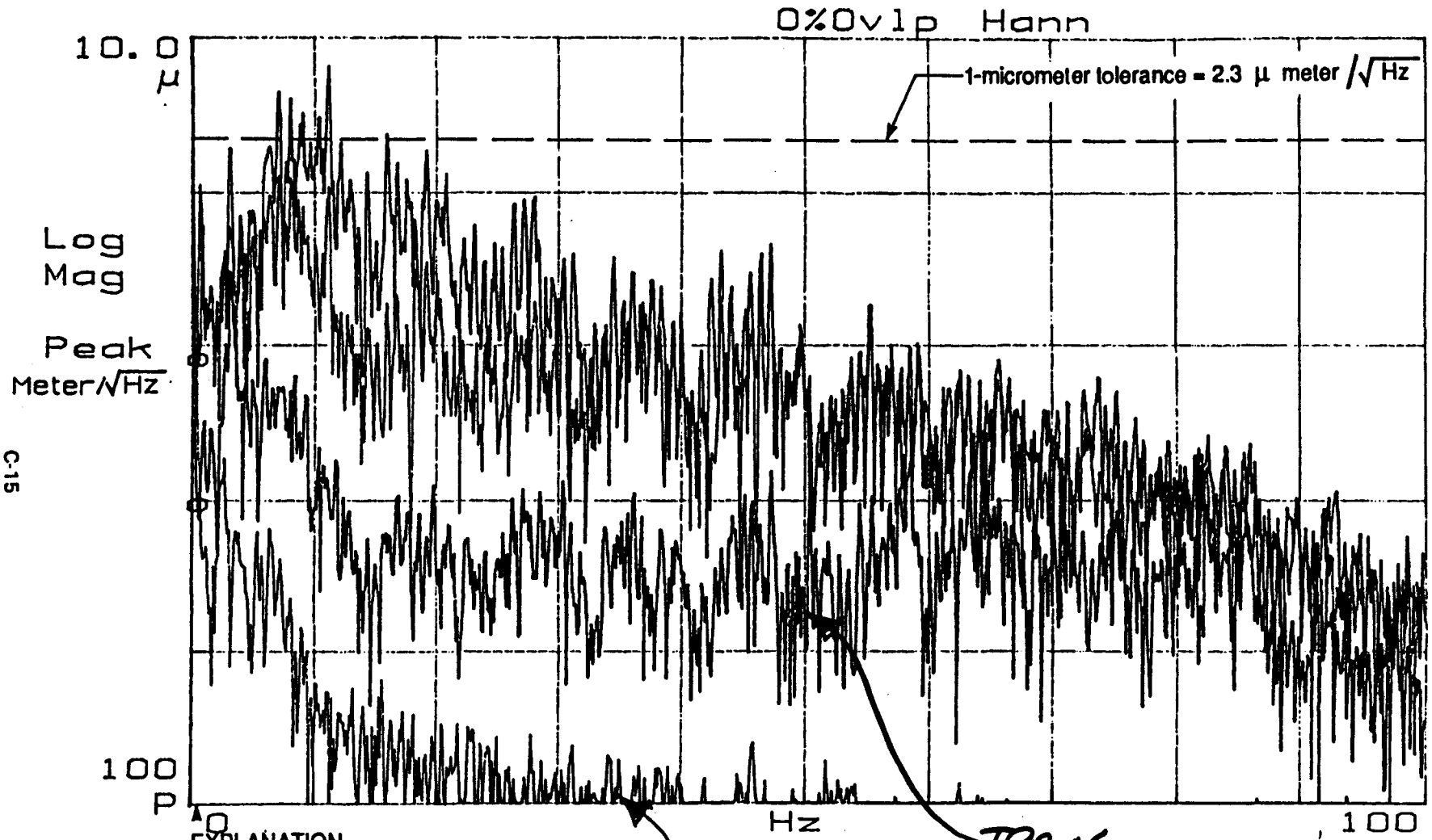

EXPLANATION
1 Hz Geophone Data
Geophone Depths in feet (meters)
Blue = Max. Vibrations Measured @ 5.0 (1.5)
Green = Max. Vibrations Measured @ 30.0 (9.1)
Red = Max. Vibrations Measured @ 261.5 (79.7)
Black = Ambient Vibrations Measured @ 261.5 (79.7)
Lower Frequency Limit of Calibration
Bandwidth = 0.187 Hz
Record made at Site VF-5.4 (Data set 2)

The Earth Technology Corporation

Project No.: 87-888-0011

RTK Joint Venture

Vibration Measurement
Composite Displacement (meters)
Linear Spectra
Example

12-89

Figure C-10

AMBIENT NOISE COMPILATION

POWER SPECTRAL DENSITY IN M^2/Hz

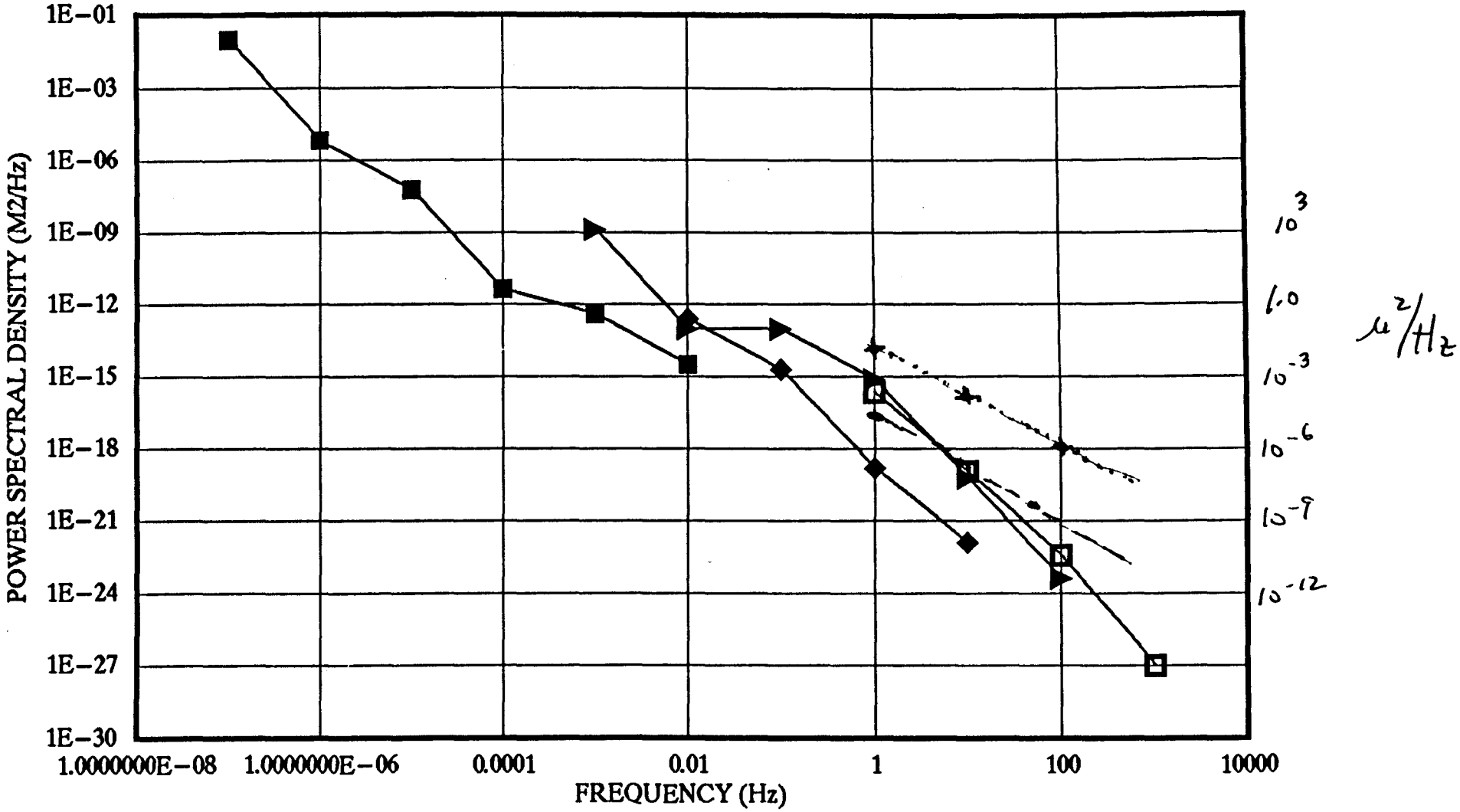

WYATT, OPTICAL ANCHOR

GIVEN, LOW NOISE

AKI, HIGH NOISE

BORCHARDT, HIGH

SSC Sd Station Tunnel Depth & Rail Crossing (notrain)

TRAIN AT SSC

behind raised daytime noise levels at KIV are not obvious, since the site is fairly well isolated from the city. Lower time-of-day variations at OBN and GAR can be attributed directly to the isolating effects of the tunnel deployments.

12

Seasonal Variations in Noise Levels

Figure 4 shows the difference in decibels between vertical acceleration power levels observed at night in winter versus summer as a function of frequency. In most cases, seasonal variations are confined to the low end of the spectra and are largest near the microseism peak due to the increase in ocean storms during winter. GAR shows the lowest seasonal variation, about 7 dB at the microseism peak,

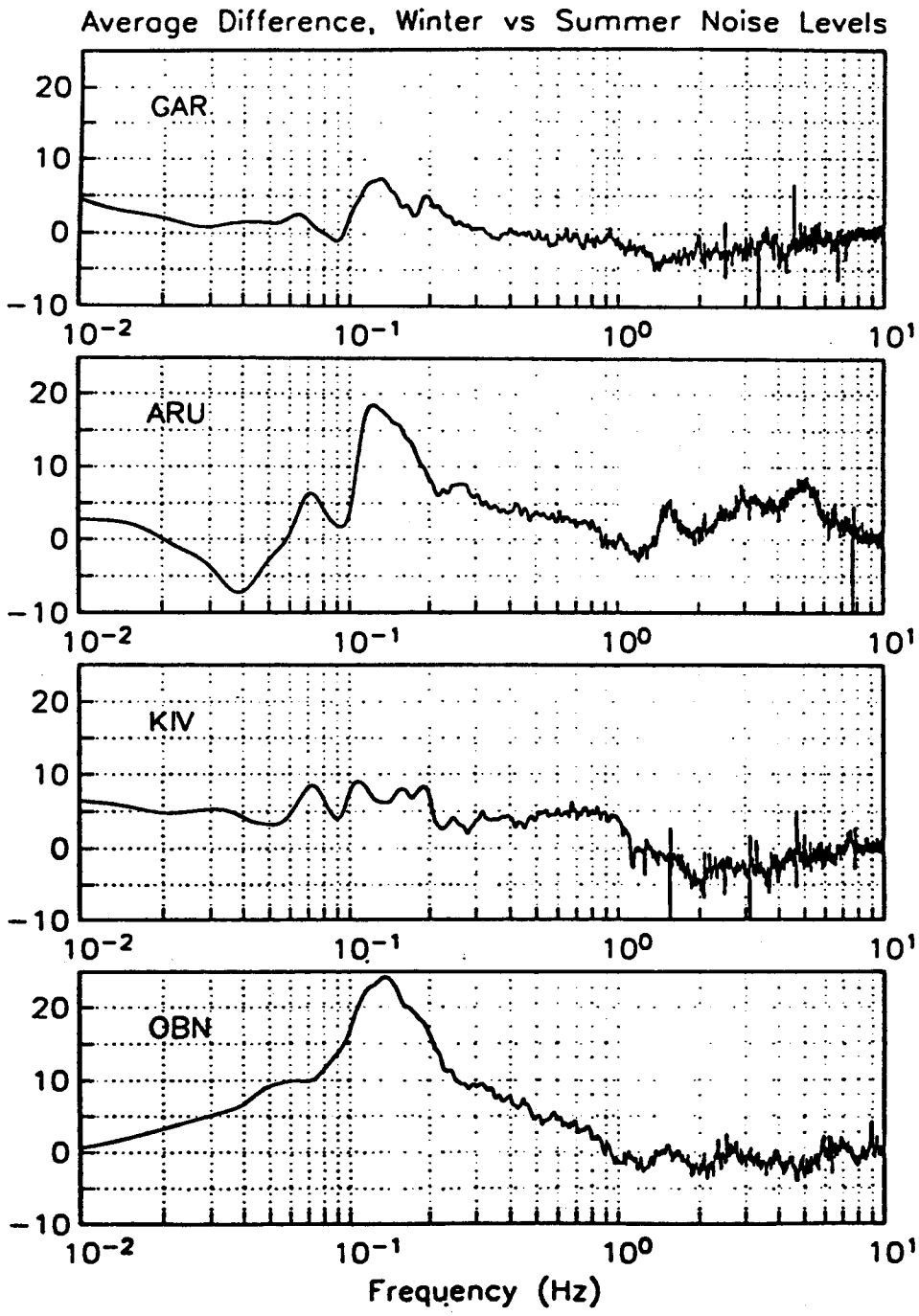

FIG. 4. Difference in decibels in averaged vertical night noise spectra observed in the winter and in summer. Large increases in noise in the microseism band are seen at ARU and OBN. GAR and KIV shows less of a seasonal variation, most likely due to their geographical locations.

Figure 3 shows the difference in decibels of the 5-day average vertical noise levels observed during the day and at night in the summer at the four IRIS/IDA sites as a function of frequency. In all cases, time-of-day variations are not significant below 0.8 Hz. OBN shows insignificant time-of-day variation below 2 Hz. Above this, the structure in the time-of-day variation occurs because the underlying spectral shape of the night noise (Fig. 2) is masked by a constant raised noise level of about −120 dB between 2 to 4 Hz during the day. GAR shows low time-of-day variation, with the increase in noise power being about 7 dB during the day above 1.5 Hz. Correspondingly, GAR also has the lowest *absolute* daytime noise levels. KIV and ARU show dramatic increases in daytime noise levels. At ARU, the increase in day

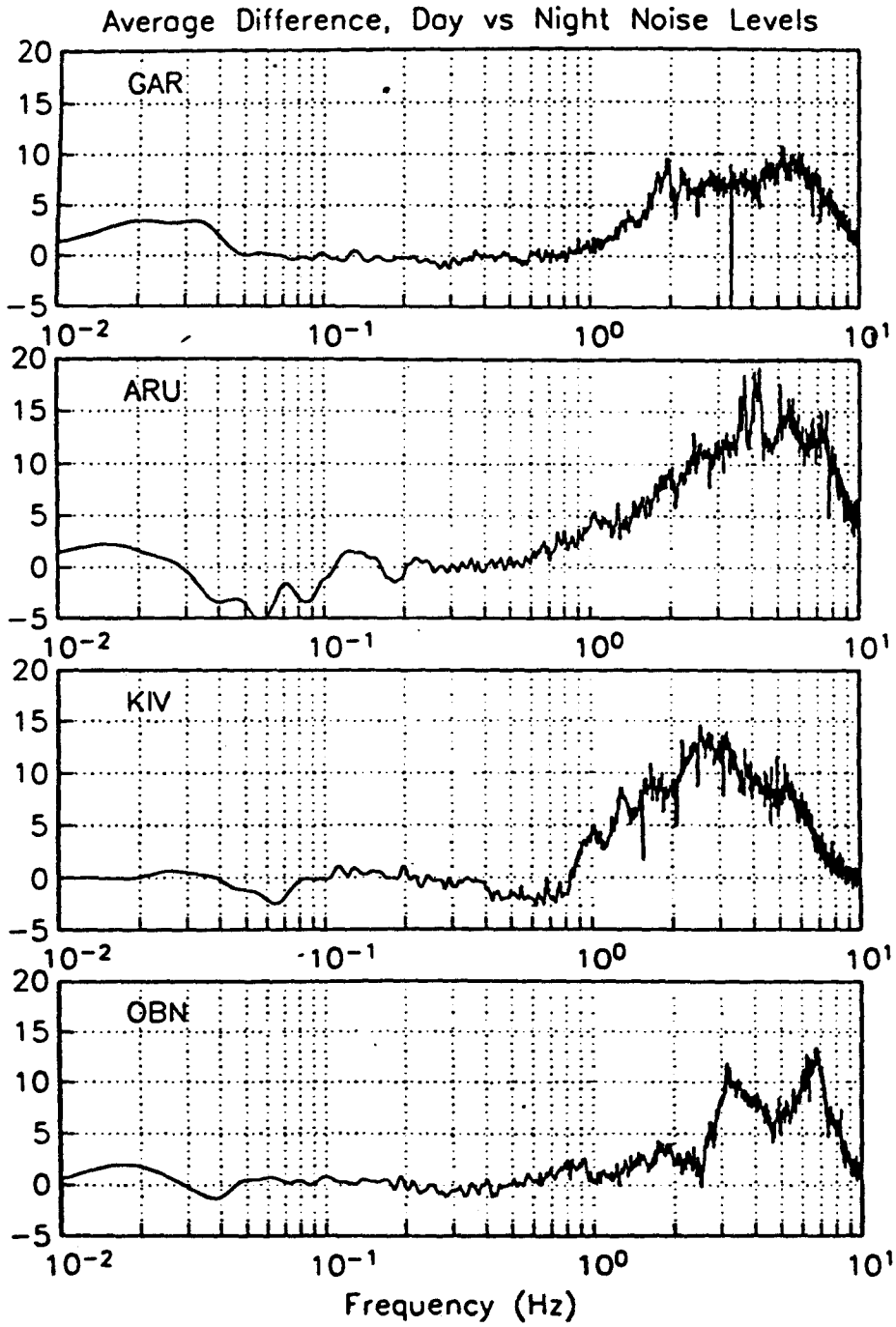

FIG. 3. Difference in decibels in averaged vertical summer noise spectra observed during the day (2 p.m. local time) and at night. Daytime noise increases are most significant at ARU and KIV, where these noises are less isolated than at GAR and OBN.

Time-of-Day Variations in High-Frequency Noise

Figure 7 shows the time-of-day variation in vertical-component high-frequency noise observed in the borehole at OBN and ARU. OBN shows a factor of 2 noise power increase during the day from about 2 to 20 Hz. ARU has a larger increase in high-frequency noise during the day, about 15 dB from 3 to 80 Hz. These results are consistent with the levels of increase during the day on the broadband instruments above 1 Hz. Note that the OBN high-frequency average contained 34 samples taken over a 2-week period, whereas only six samples were available for the ARU average (Table 3).

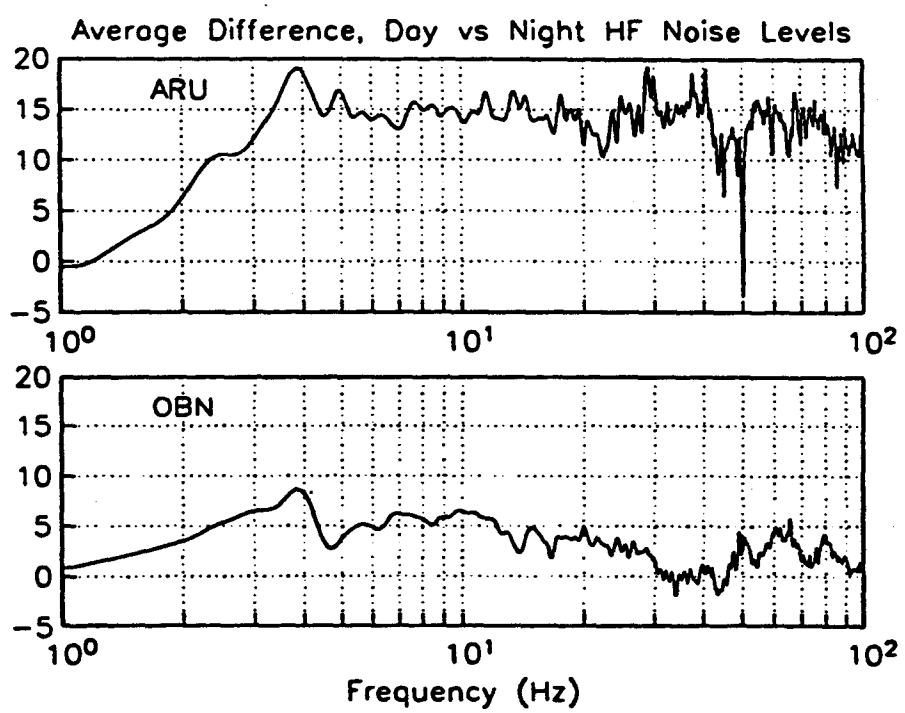

FIG. 7. Difference in decibels of averaged high-frequency noise spectra observed in the borehole during the day and at night at two stations. ARU shows an increase of 15 dB in high-frequency noise levels during the day, presumably due to its location on the outskirts of a small town. OBN shows a much smaller daytime increase, although it also is located near a town. The borehole depths at ARU and OBN are 30 and 87 m, respectively. At KIV and CHS, noise samples were not adequately distributed in time to allow a day–night comparison.

Figure 3 shows the difference in decibels of the 5-day average vertical noise levels observed during the day and at night in the summer at the four IRIS/IDA sites as a function of frequency. In all cases, time-of-day variations are not significant below 0.8 Hz. OBN shows insignificant time-of-day variation below 2 Hz. Above this, the structure in the time-of-day variation occurs because the underlying spectral shape of the night noise (Fig. 2) is masked by a constant raised noise level of about −120 dB between 2 to 4 Hz during the day. GAR shows low time-of-day variation, with the increase in noise power being about 7 dB during the day above 1.5 Hz. Correspondingly, GAR also has the lowest *absolute* daytime noise levels. KIV and ARU show dramatic increases in daytime noise levels. At ARU, the increase in day

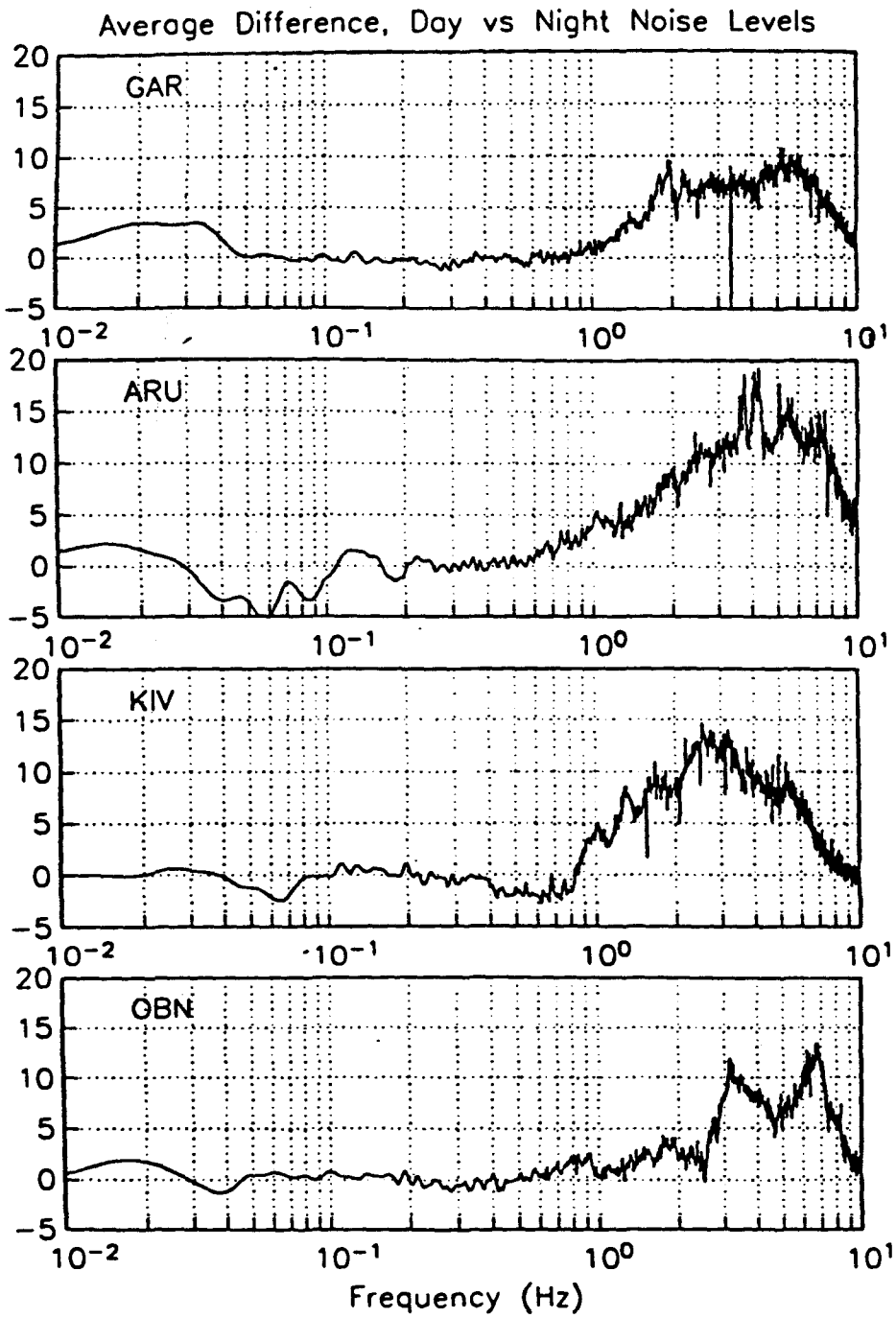

FIG. 3. Difference in decibels in averaged vertical summer noise spectra observed during the day (2 p.m. local time) and at night. Daytime noise increases are most significant at ARU and KIV, where

noise levels at higher frequencies (greater than 10 Hz) by up to 10 dB. At lower frequency (3 to 10 Hz) the superior vault construction in the Soviet Union apparently did not greatly affect this noise ratio.

CONCLUSIONS

From an analysis of several hundred surface and borehole noise samples collected in 1987 at three sites in Kazakhstan and 2000 samples collected from 1988 to 1989 at three sites in the western United States, we conclude that:

1. In general, noise levels in the 100 m deep boreholes were affected by wind conditions to a much smaller degree than were the surface emplacements.
2. Wind did not become a noticeable source of noise at the surface emplacements until a minimum wind speed was reached (typically 4 to 5 m/sec).
3. Between 3 and 10 Hz, surface and borehole noise levels are comparable, but downhole noise levels are strongly reduced at higher frequencies.
4. Between 3 and 10 Hz, surface and borehole emplacements in the western United States were generally quieter than those in Kazakhstan.
5. At high frequencies, in the 10 to 80 Hz band, surface installations in the western United States were considerably noisier than surface installations in Kazakhstan, but borehole installations in both regions yielded comparable noise levels. We suspect that the difference in surface vault quality between the two sets of stations is a significant factor. In this frequency band, borehole noise was lower than surface noise at all stations.

ACKNOWLEDGMENTS

This research was supported by the Air Force Geophysical Laboratory Grant No. F19628–88-K-0026. The seismic stations in Kazakhstan and Nevada were built and operated with support provided by the Natural Resources Defense Council and the Academy of Sciences of the Union of Soviet Socialist Republics. We thank V. Martinov and G. H. Patton for useful discussions. D. Chavez prepared the data acquisition software. We also thank our colleagues from the University of Nevada at Reno, especially Wally Nicks and Bill Honjas, as well as Larry May and James Batti from IGPP, for providing field support and maintenance for the Nevada seismic stations.

REFERENCES

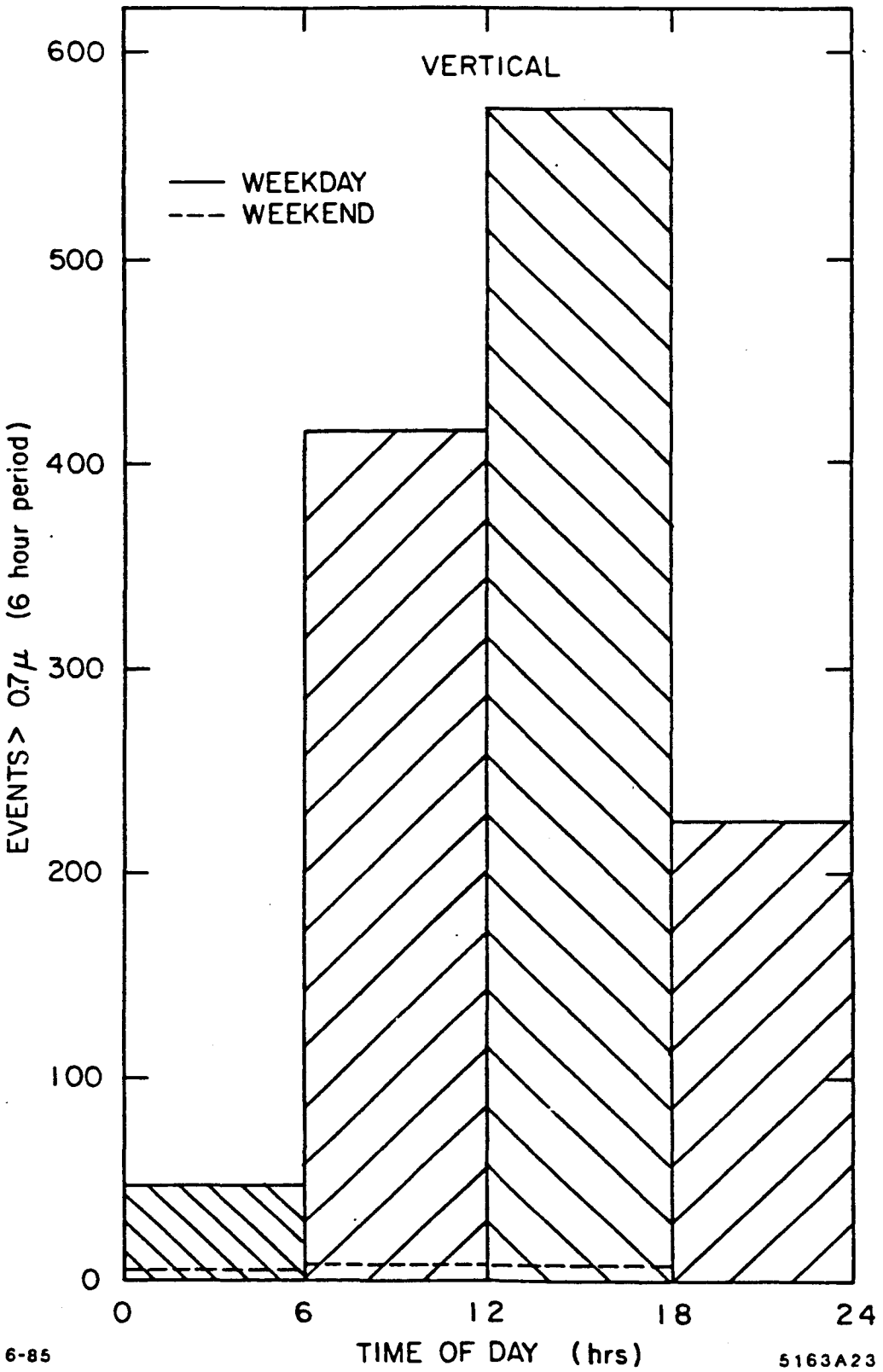

Fig. 1.3. Number of Vertical Transient Events/6 Hour Interval as a Function of Time of Day. at SLAC

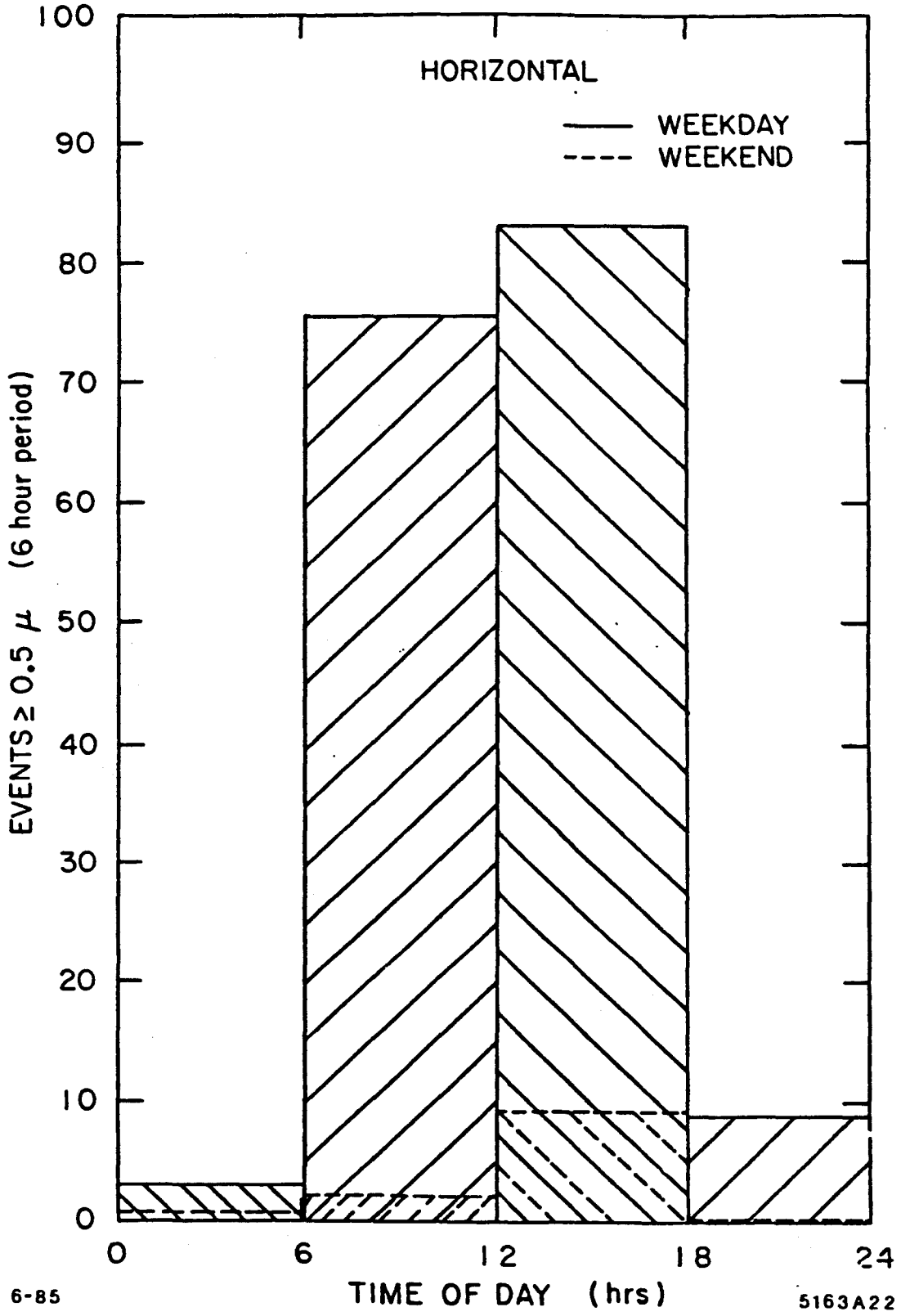

Fig. 1.4. Number of Horizontal Transient Events/6 Hour Interval as a Function of Time of Day.

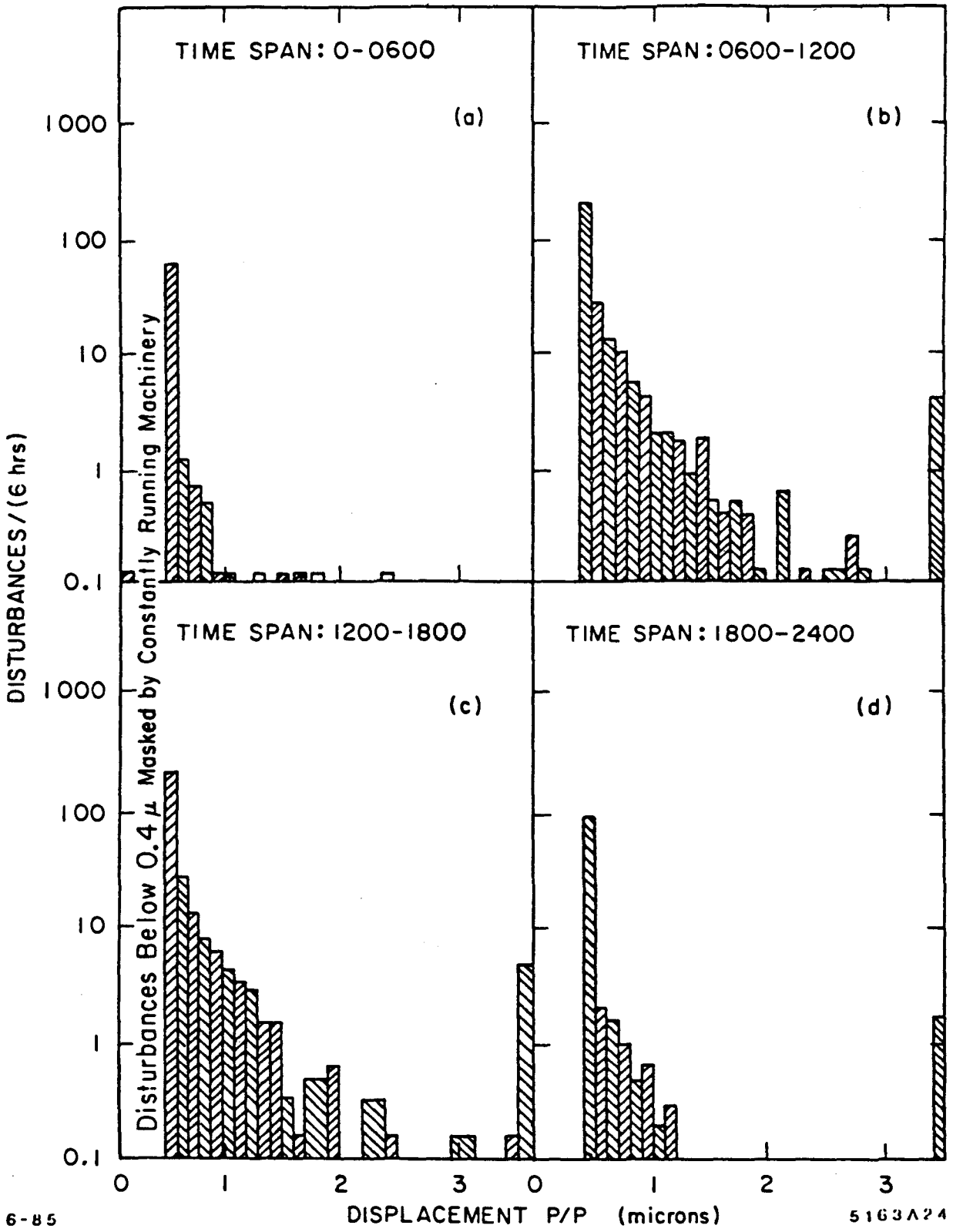

Fig. 1.5. "Amplitude Spectrum" of Transient Signals.

PEP ELEVATION

LIQUID LEVEL ELEVATION CHANGES:
JUNE 20, 1985 TO MARCH 20, 1987

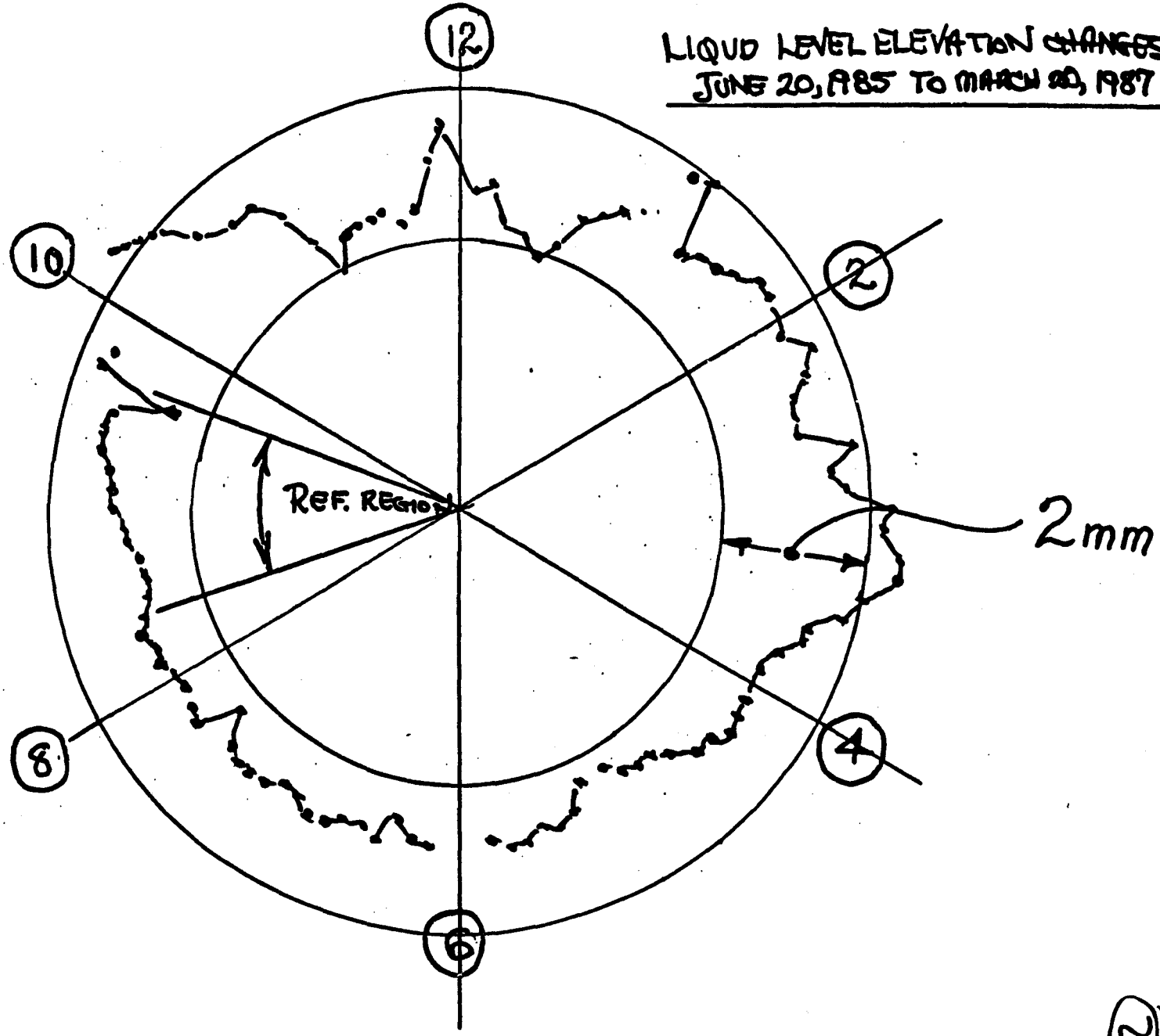

LONG TERM TUNNEL DISTORTIONS

RADIAL MONUMENT MOVEMENT: JUNE 1985 TO MARCH 1987

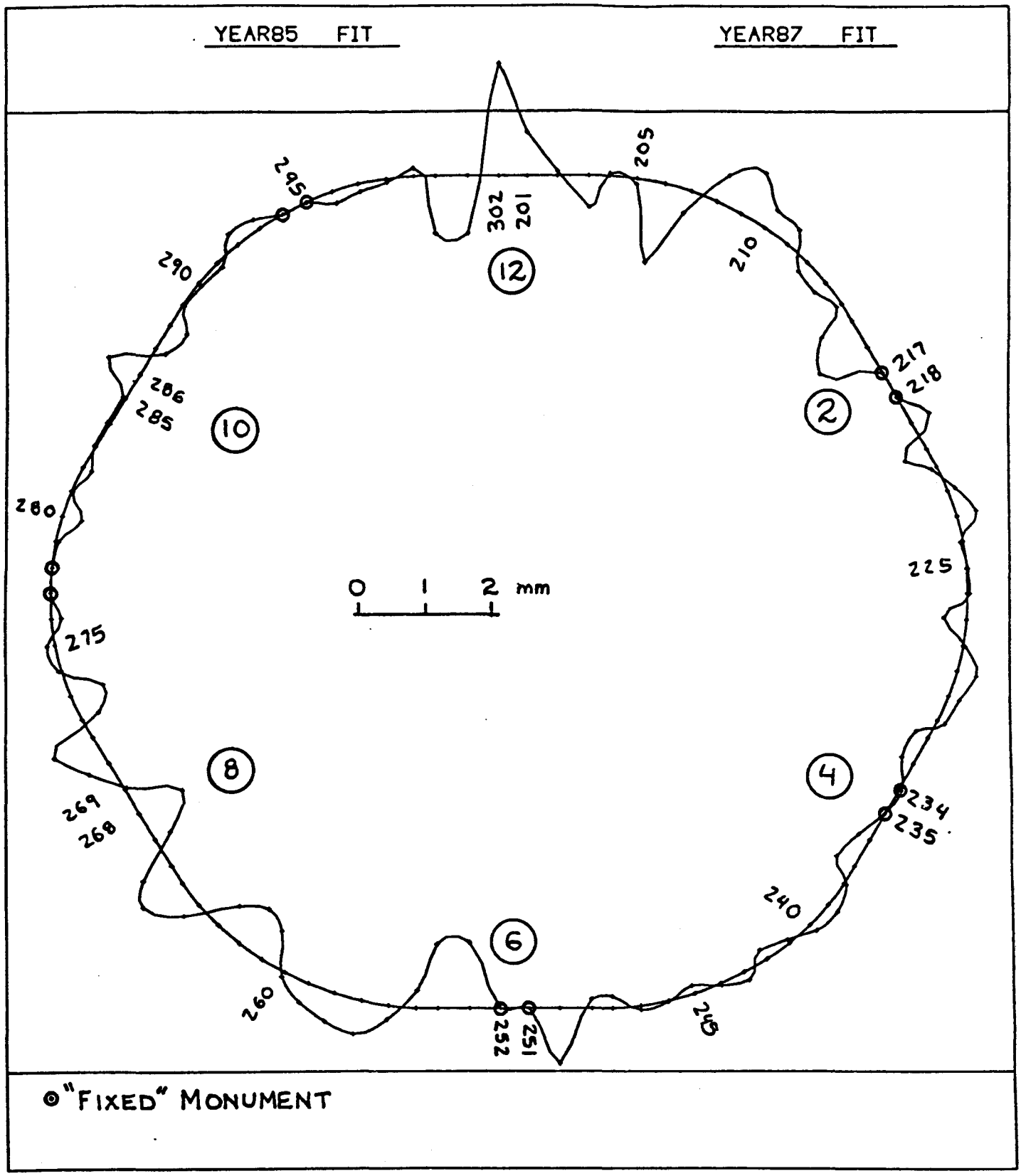

(... à revers
lumineuse montrant la
correction faite.)

SPS
1976-80
from
M. Mazoud

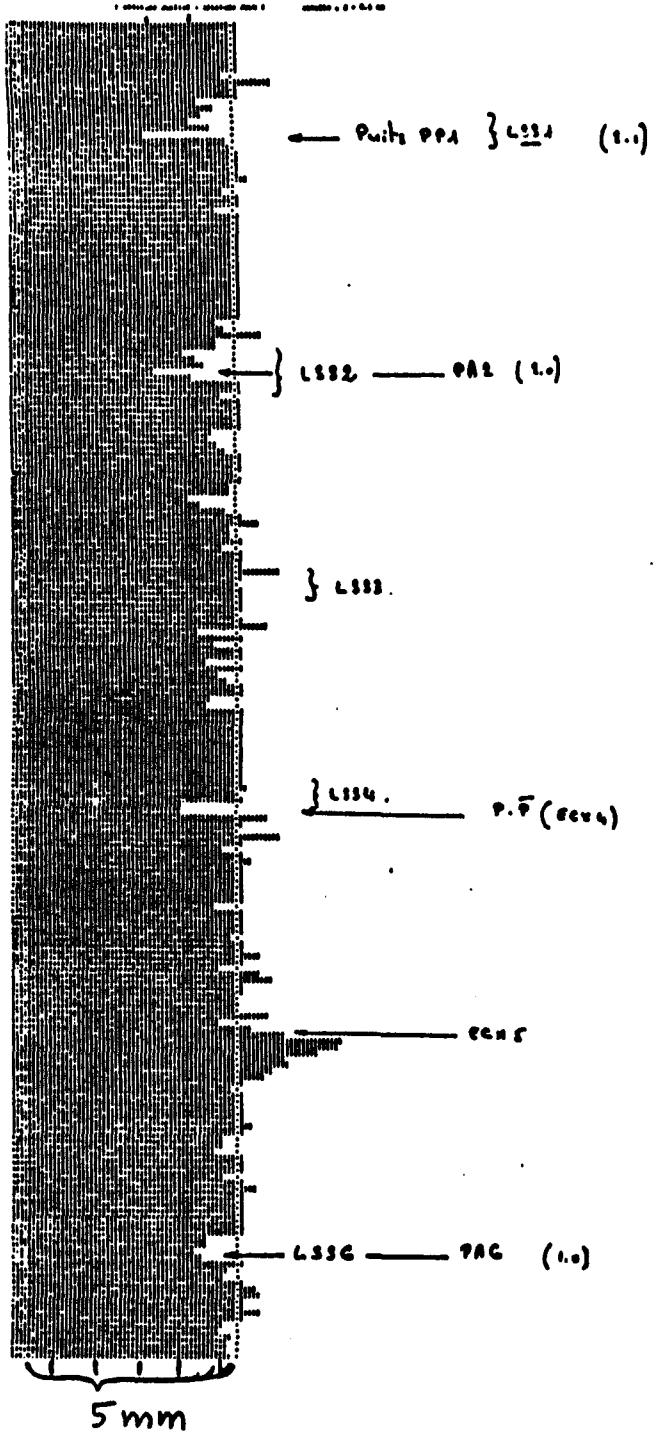

SPS
1980/

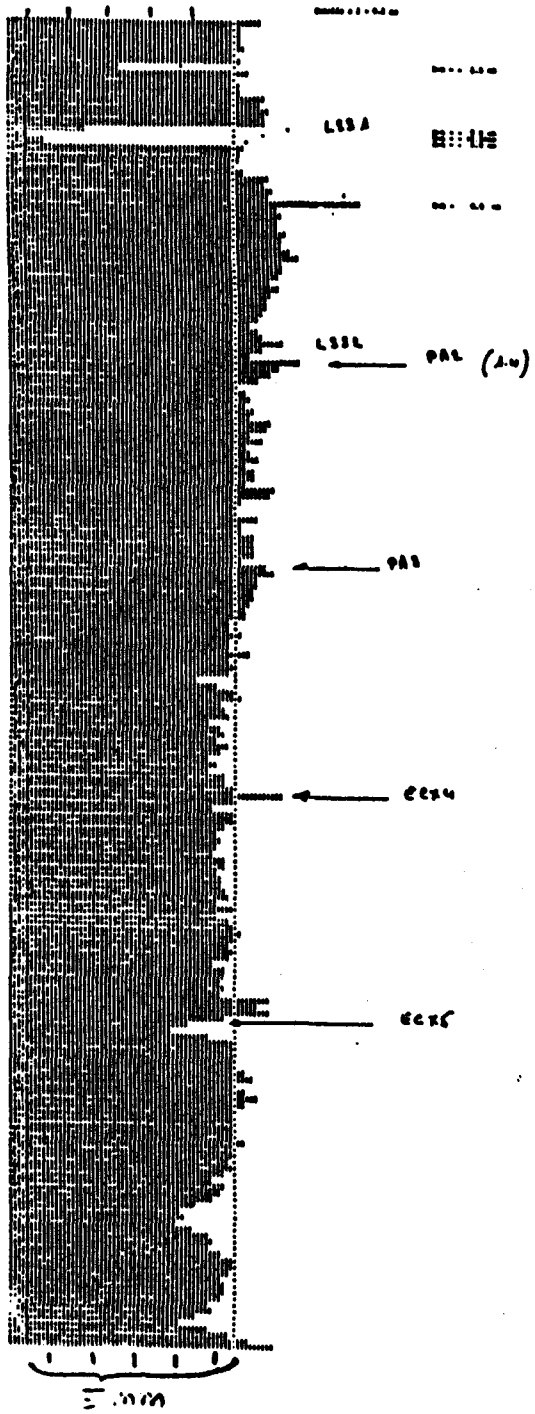

1976-1980

(2)

1985-88 (23)

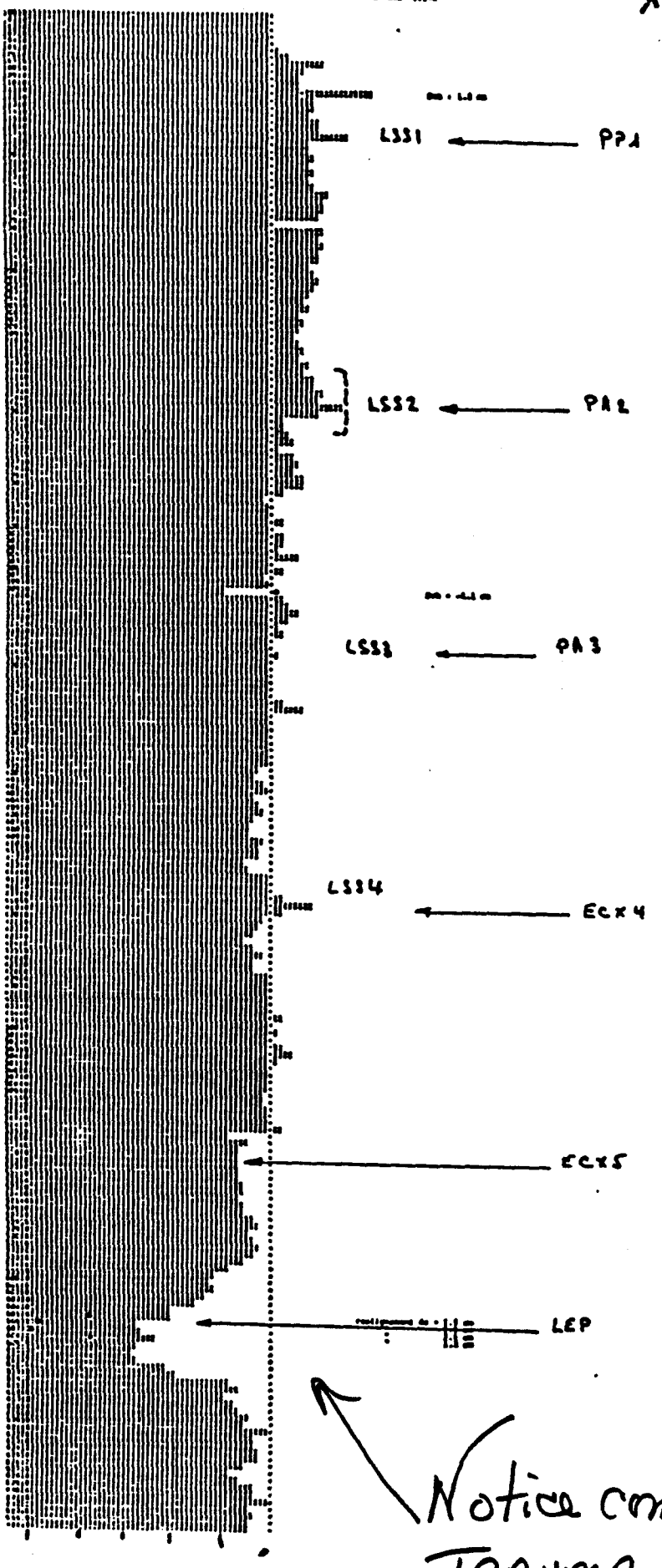

Notice construction TRAUMA from 40 meters

1985 - 1988

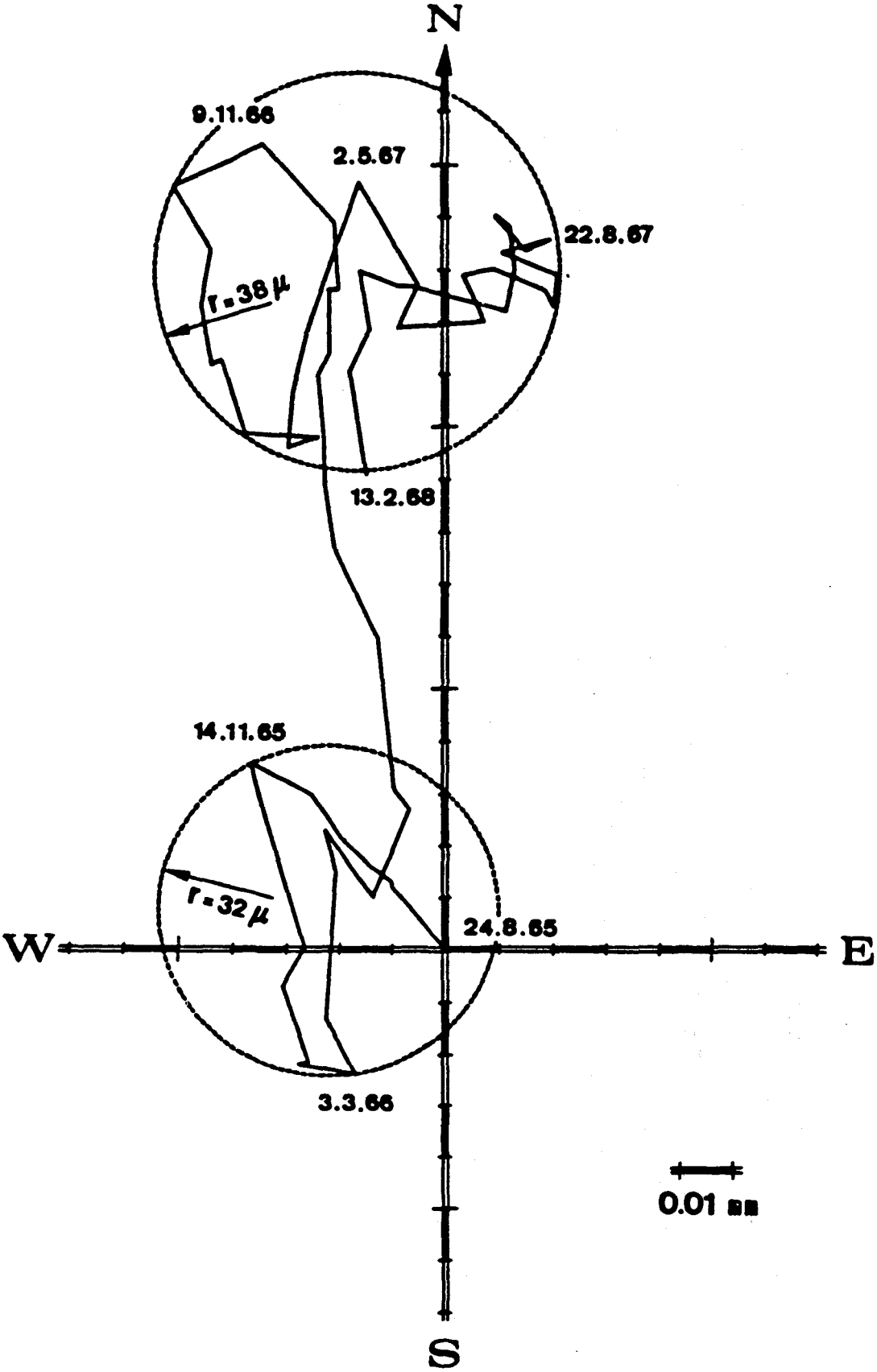

Fig. 1 Movement of the PS central pillar from 1965-68

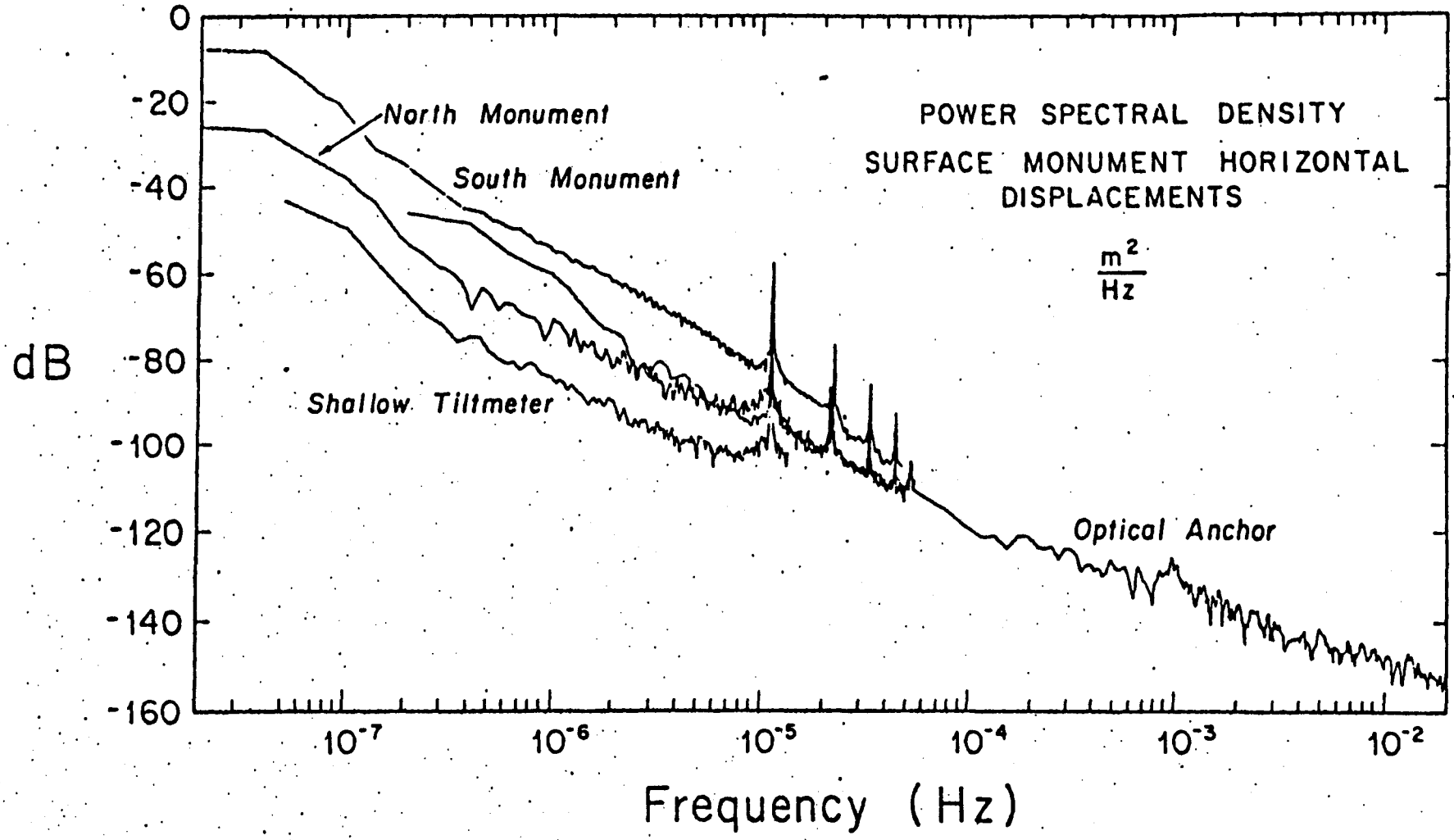

Fig. 9. Power spectral density of the near-surface horizontal displacements in weathered granodiorite. Included are the power levels recorded by the optical anchor and those inferred from the monument tiltmeter and the shallow borehole tiltmeter records.

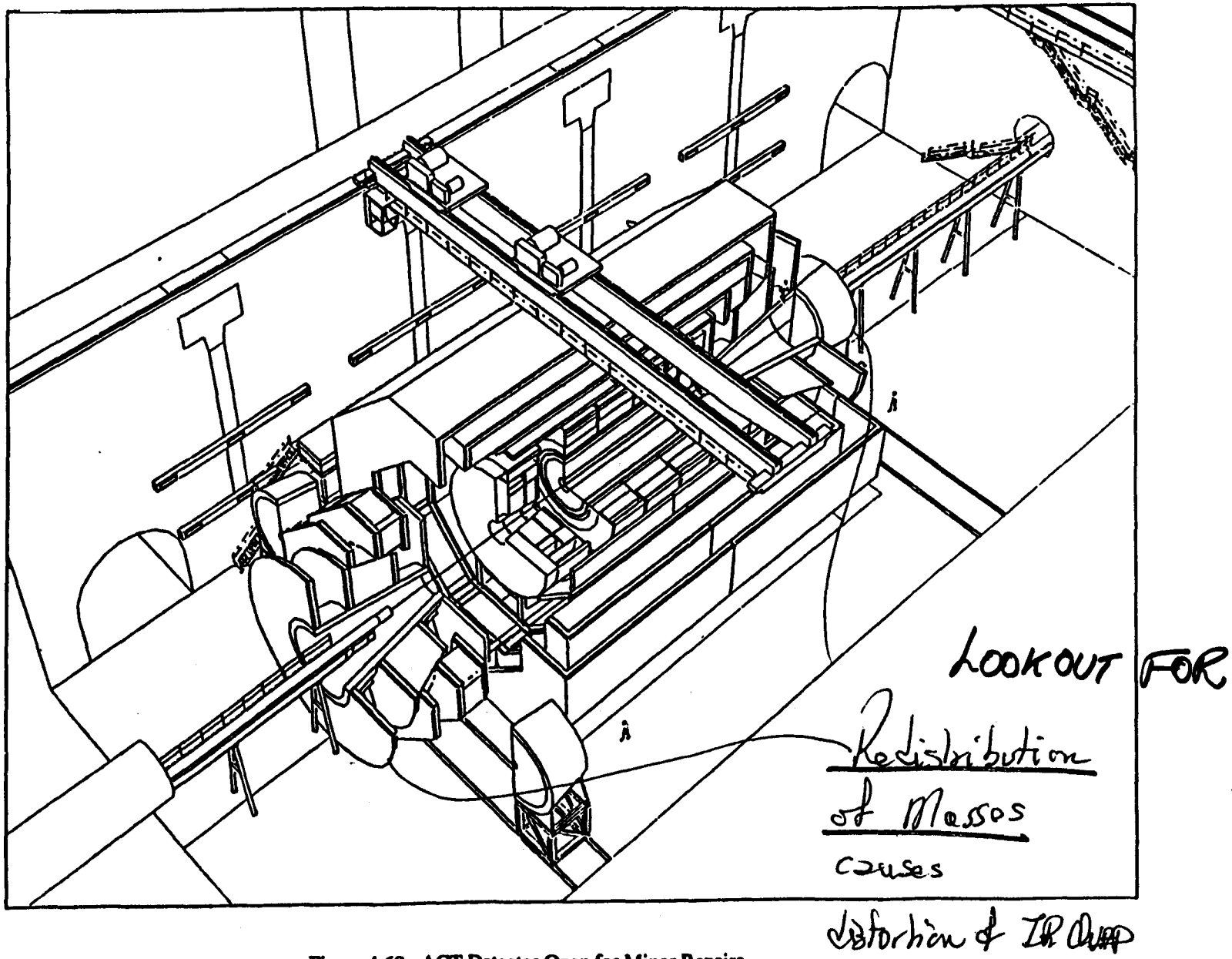

Figure 4.60. ACT Detector Open for Minor Repairs

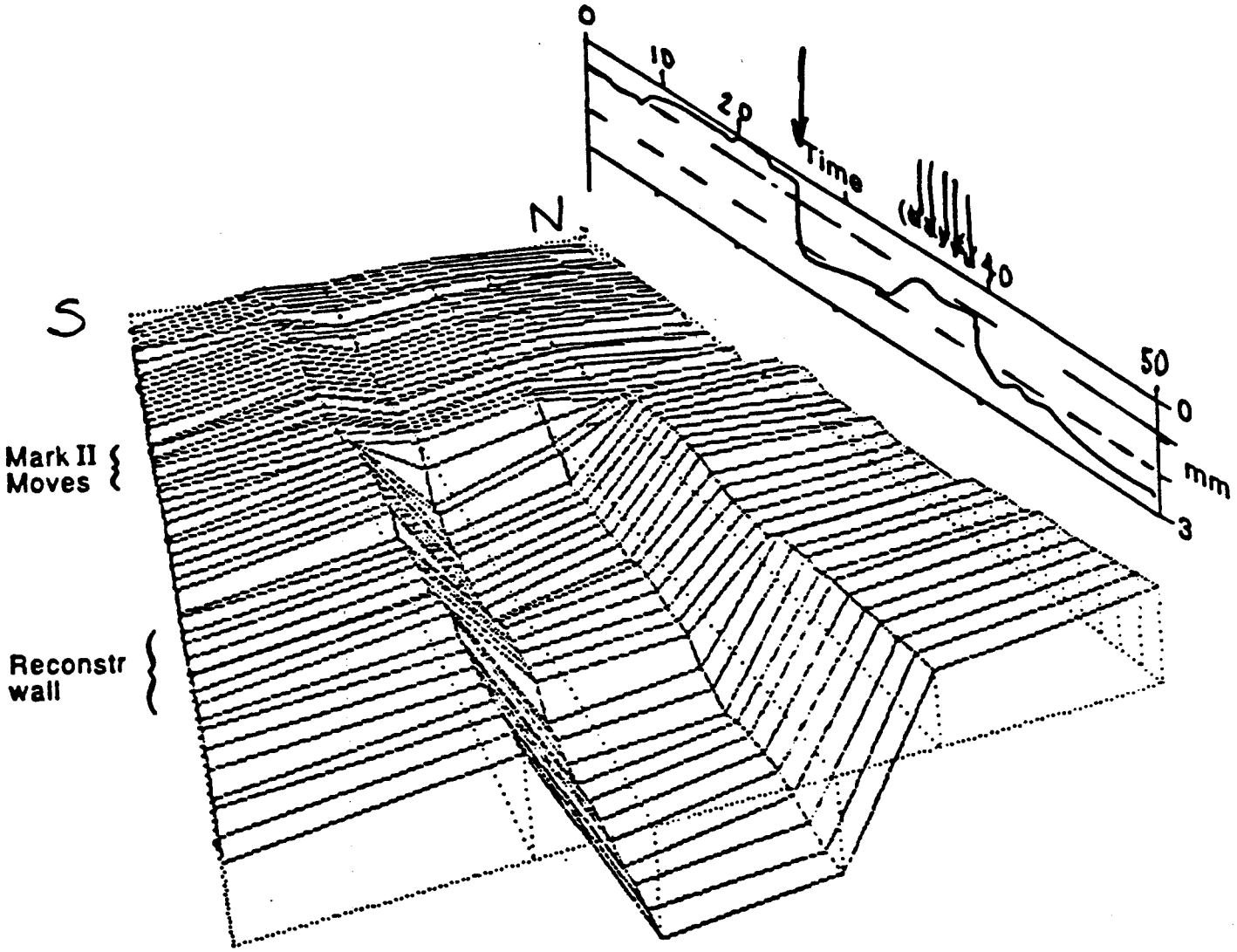

Figure 8. Isometric display of Mark II roll-in data, Oct - Nov 1987

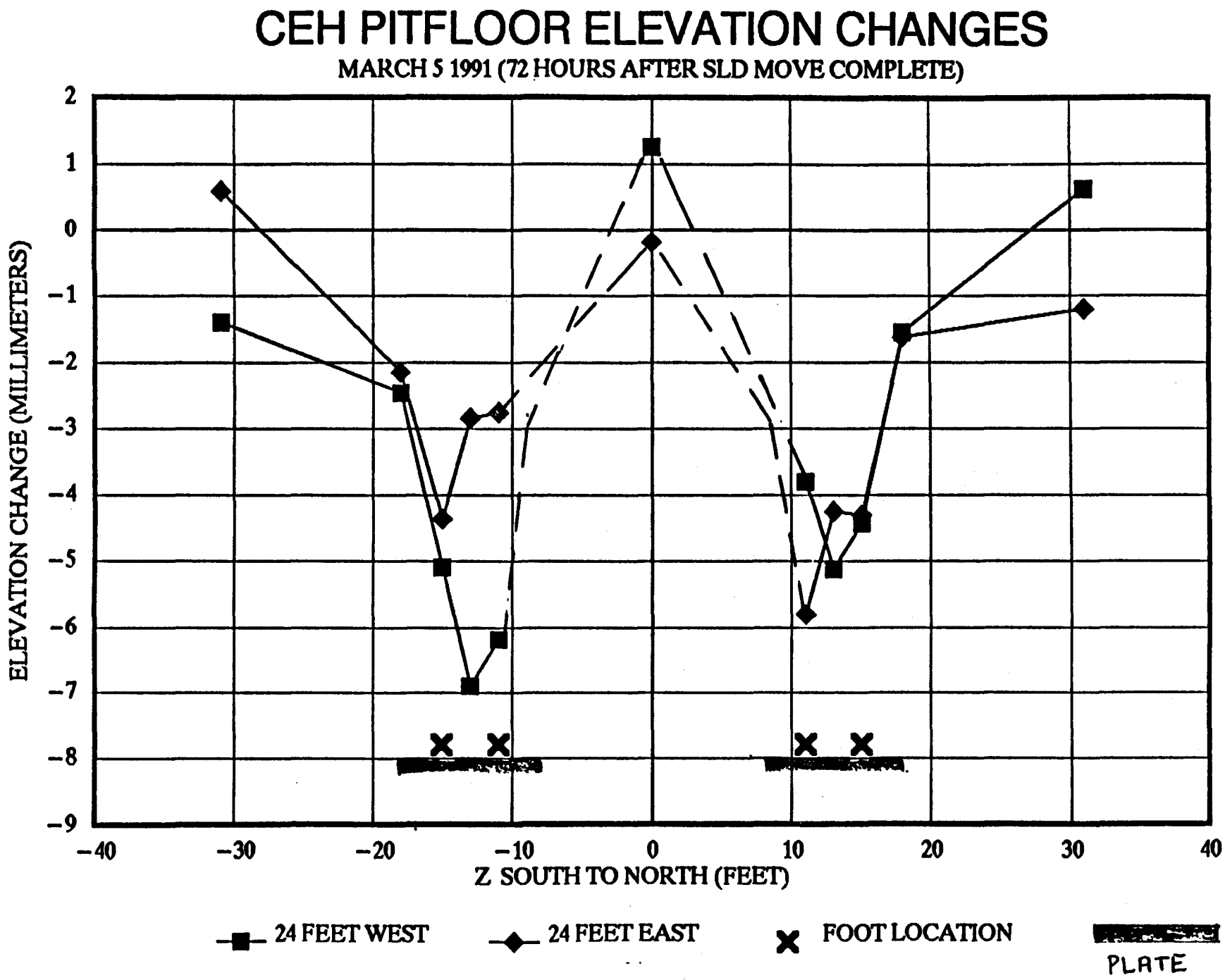

Figure 14. Plot of floor deformation around SLD "footings".

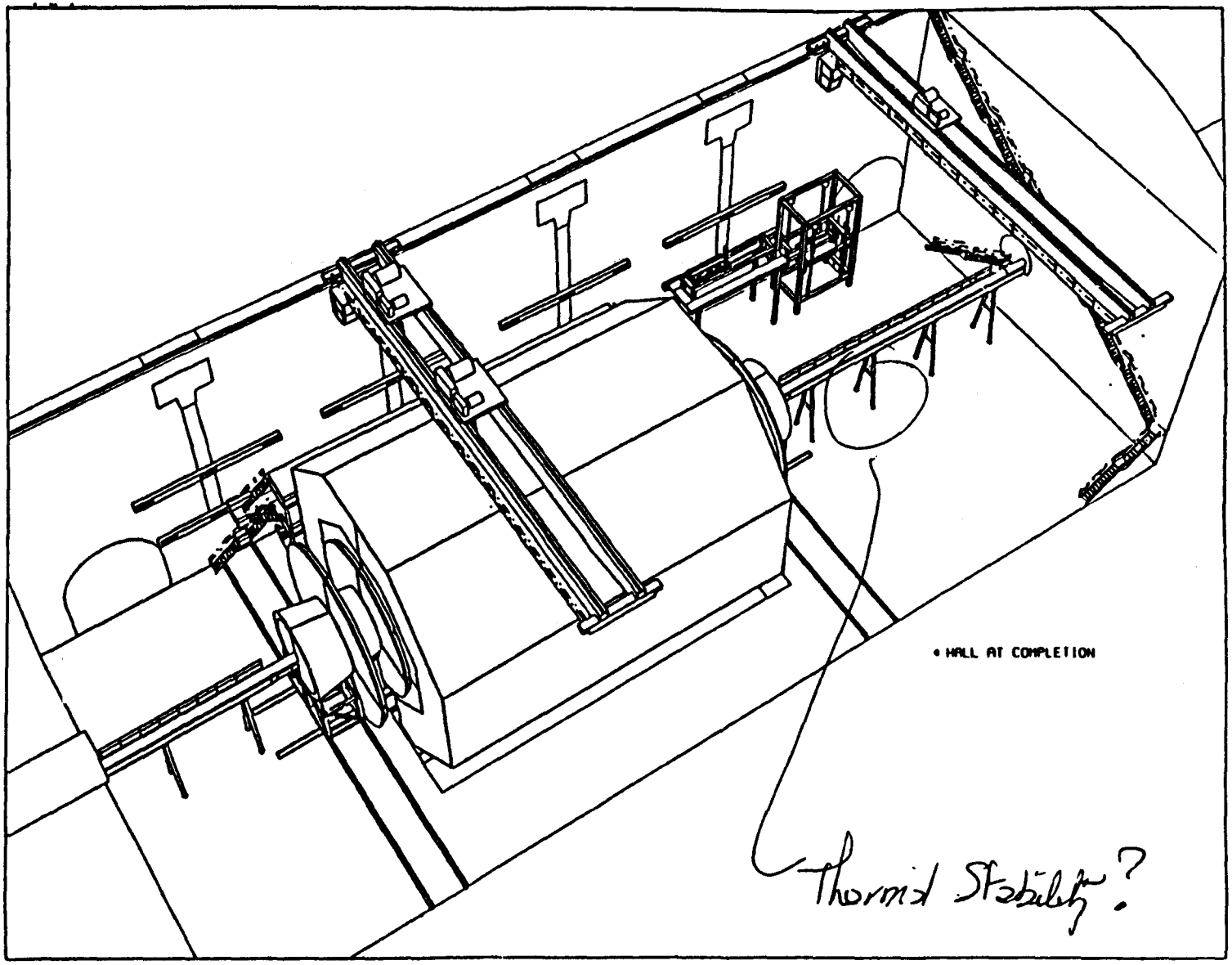

Figure 4.59. ACT Detector Construction Sequence (Month 42)

29

TRANSMISSIBILITY

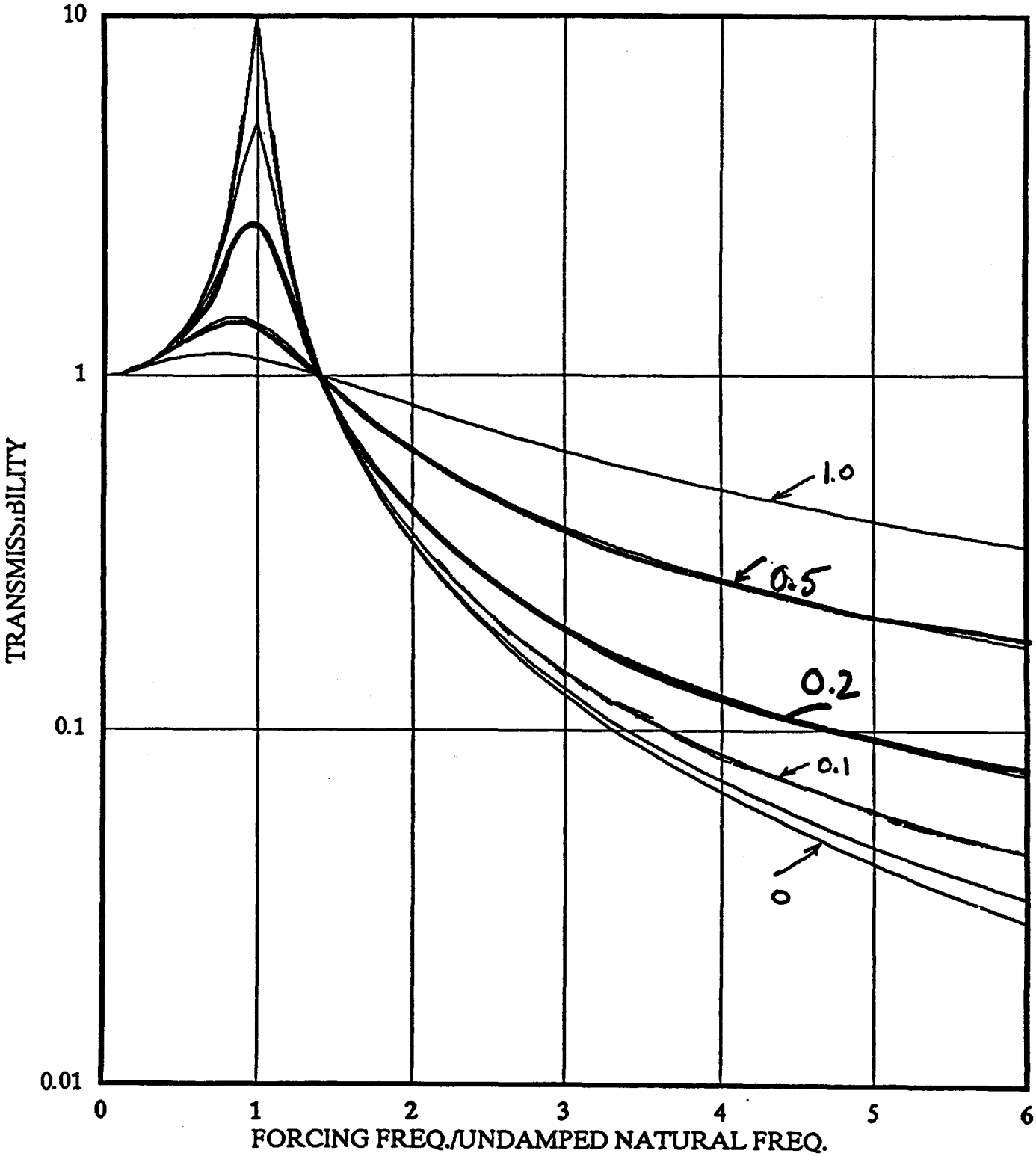

C/Cc = 0 .05 .1 .2 .5 1.0

FREQUENCY VS STATIC DEFLECTION

f = 1/2piSQRT(g/d)

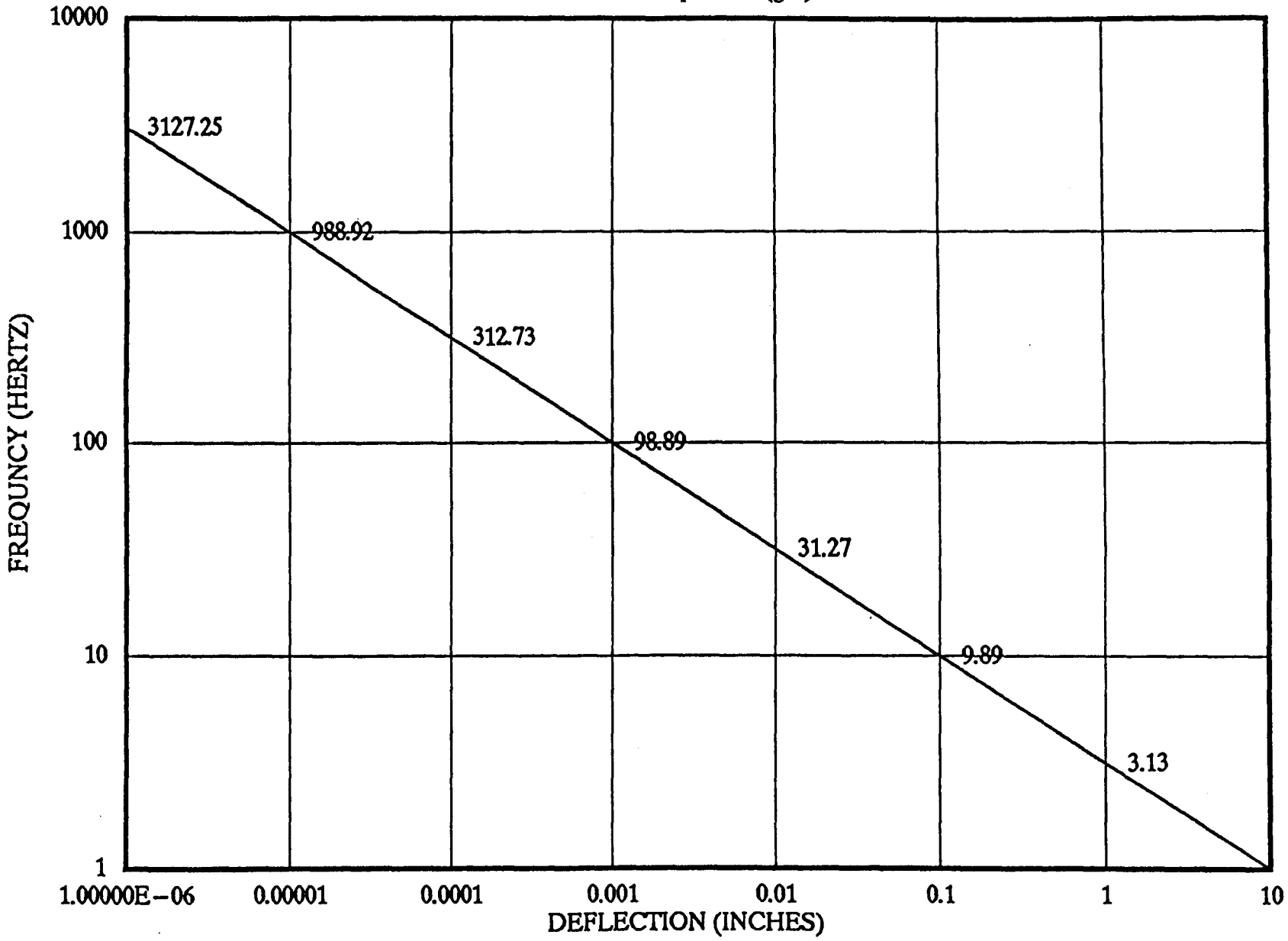

Natural Phenomena Hazard Mitigation Program for the U.S. Department of Energy

Robert C. Murray
Lawrence Livermore National Laboratory

Workshop on
Vibrational Control and Dynamic
Alignment Issues at the SSC

Superconducting Super Collider
DeSoto, Texas

February 11-14, 1992

Policy, requirements, standards and guidance

- Completed Hazards Estimates
  - earthquake (26 sites)
  - wind and tornado (26 sites)
  - flood (10 sites)
- Develop and expand UCRL-15910 Design and Evaluation Criteria for Natural Phenomena ← COPY
  - presented at international conferences
  - consulting to sites
- Develop state-of-the-practice manuals
  - seismic concepts and detailing requirements
  - wind detailing requirements
  - tie down and anchorage guidelines ← COPY
  - suspended ceiling bracing requirements
  - seismic safety guide

The Guidelines fits into the overall DOE safety plan

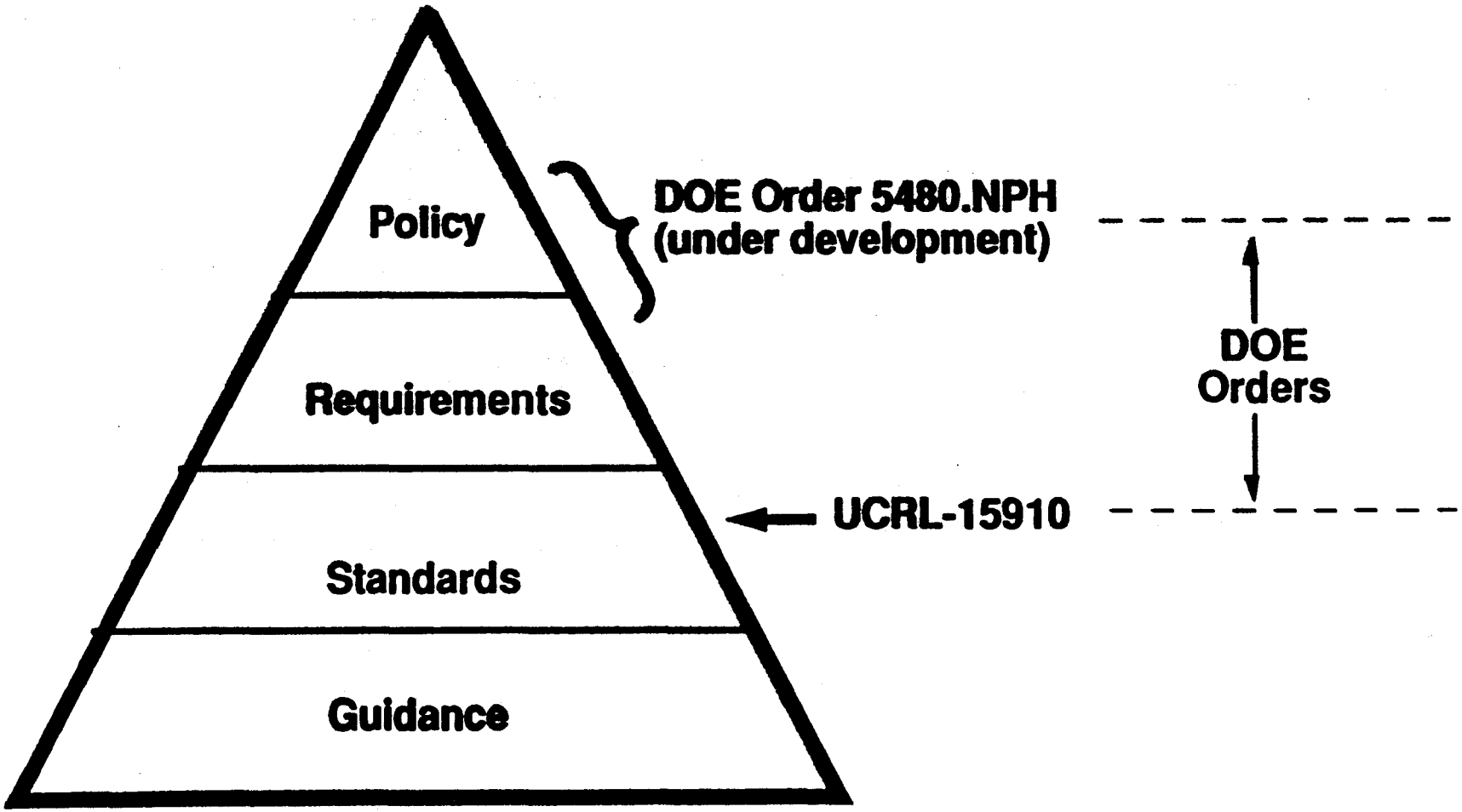

The Guidelines:

- Provide the natural phenonema design and evaluation basis for DOE facilities
  - Provide guidelines for earthquakes, winds, and floods such that specific levels of protection can be achieved
- Applies to buildings, structures, equipment, components and distribution systems
  - 4 sets of guidelines for levels of protection ranging
    - from that provided by the UBC for normal facilities
    - to near that provided by nuclear power plant criteria

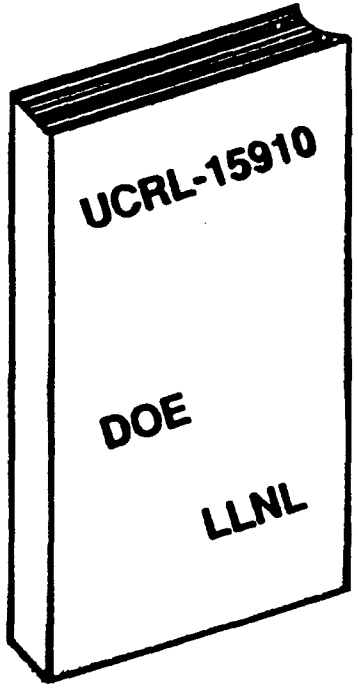

Required by GDC 6430.1A for new facilities
DOE Developing Policy for existing facilities
DOE Developing Overall NPH Order

Consistent Approach

The guidelines provide a consistent level of protection from natural phenomena

Earthquake

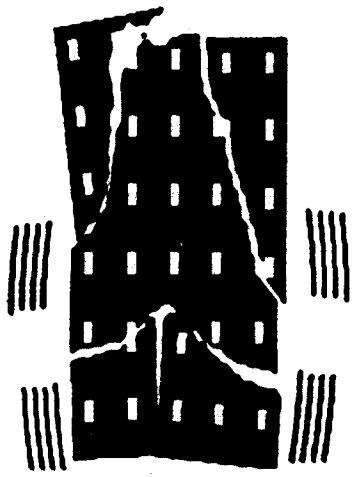

Wind

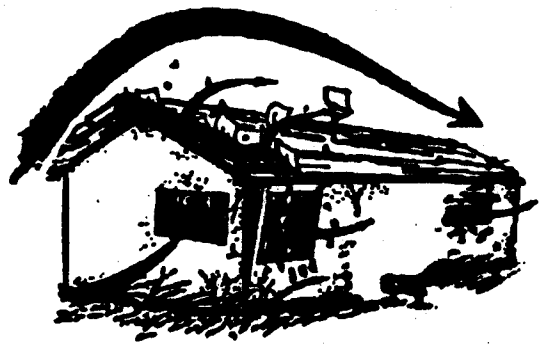

Flood

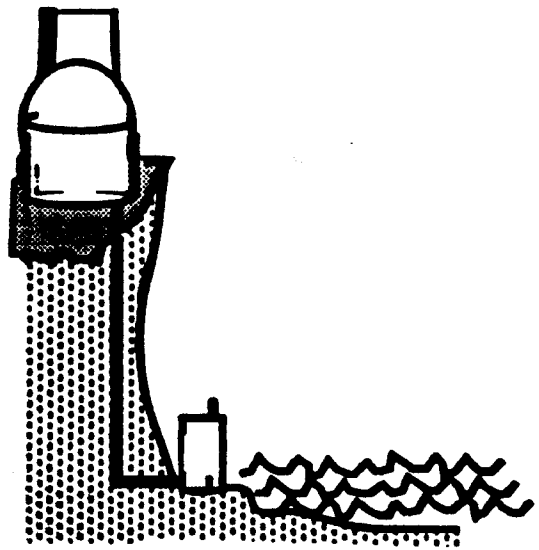

Consistent Approach

Consistent methodology is used to assess hazards for DOE sites throughout the U.S.

Most DOE facilities are existing

Variable hazards across the country

APL92-001/v-36

Simplified Approach

We have identified a wide variety of facilities we established four categories

Category	Description	Hazard-response goal
General	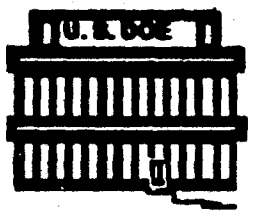	Protect personnel from death and injury
Important or low hazard		Permit functioning during and immediately after event
Moderate hazard	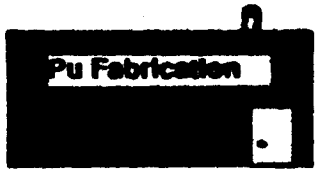	Confine contents to protect employees, the public, and the environment.
High hazard		Confine contents to protect employees, the public, and the environment. *Very high confidence of confinement.*

Simplified Approach

Facility Management must select a category based on many considerations

Considerations

- Importance
- Cost
- Mission dependence
- Impact
  - personnel
  - public
  - environment

Category	Numerical Targets	Comparability
General Use	10^{-3}	UBC normal
Important Low Hazard	5×10^{-4}	UBC essential
Moderate Hazard	10^{-4}	Intermediate
High Hazard	10^{-5}	Near NRC

Simplified Approach

Determine the hazard level for facilities being designed or evaluated (Done by Guidelines)

Hazard level (varies for each facility category)

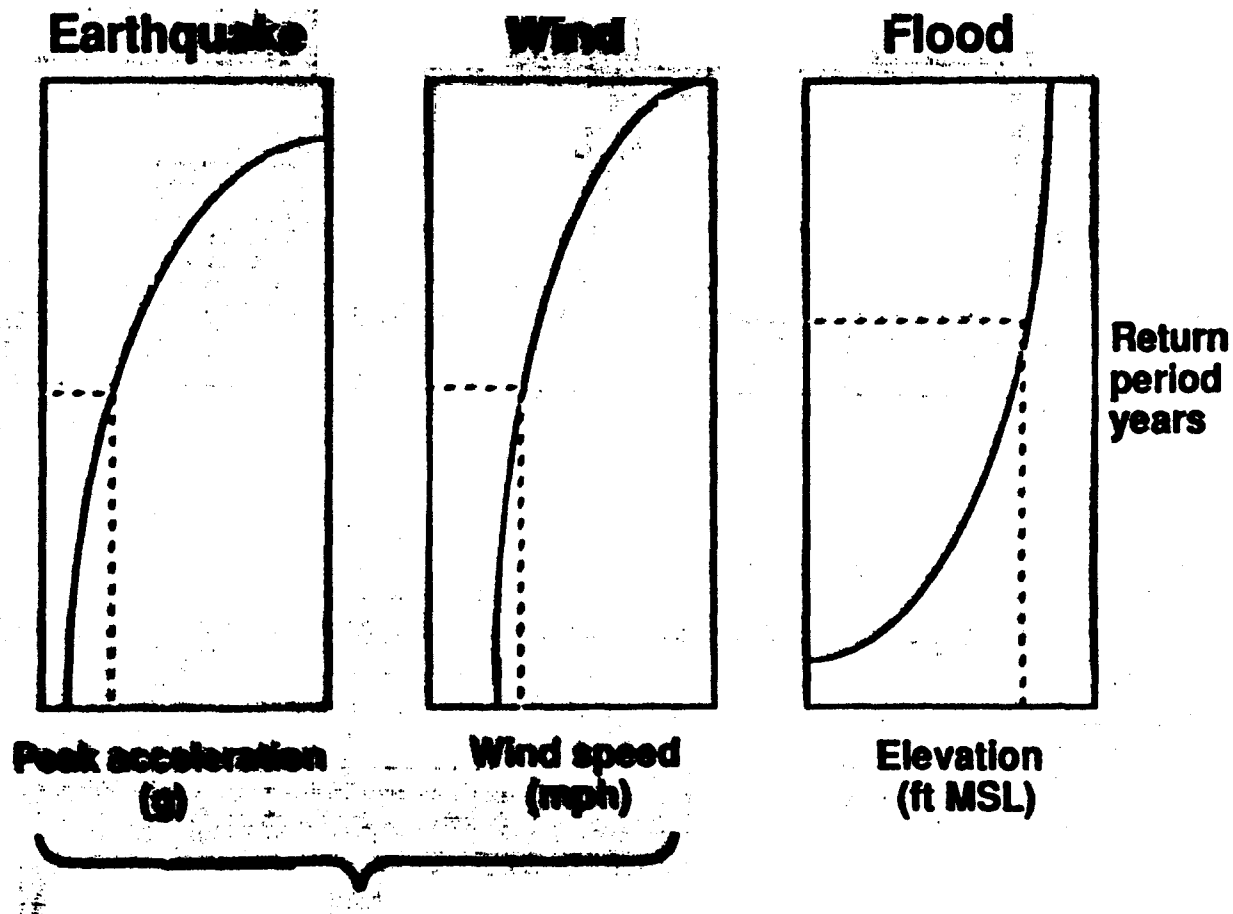

Can reduce hazard loading for existing facilities

Technical support, research and development

- Participate in earthquake damage investigations
  - Costa Rica (1991)
  - Loma Prieta (1989)
  - Whittier (1987)
  - New Zealand (1987)
  - Mexico City (1985)
  - Morgan Hill (1984)
- Conduct special studies
  - tornado missile testing
  - feasibility study on earthquake alert system
  - seismic instrumentation requirements — procure instruments (LLNL/LBL/SLAC)
  - field guide for walkdowns
  - use of experience data for NPH qualification of equipment
  - revise seismic safety guide
- Projects being formulated
  - methodology for evaluation of existing facilities
  - methodology for facility classification

Simplified Approach

Rules were developed to determine response and acceptability

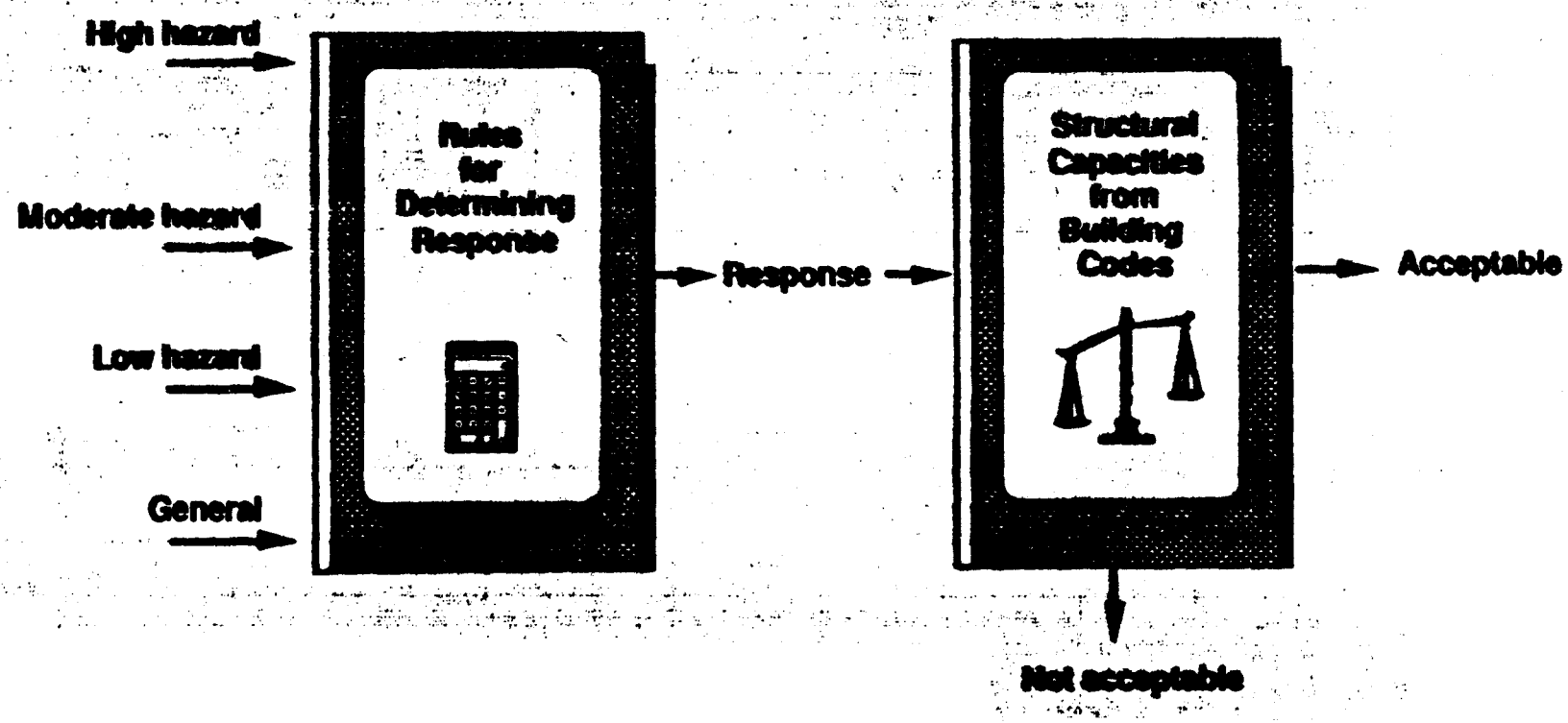

Technology transfer

- Developed and video taped six 3-hour mini courses in the Natural Phenomena area
  - seismic analysis
  - seismic design
  - wind & tornado overview
  - wind & tornado design/evaluation
  - flood overview
  - emergency preparedness
- Issue quarterly newsletter — *Phenomenal News*
- Conduct workshops on philosophy and use of UCRL-15910
- Organize conferences on Natural Phenomena Hazards Mitigation

Technology transfer (con't)

- Organize special workshops
  - how to conduct facility walkdowns
  - seismic base isolation for design and upgrade
  - volcanic hazards and issues
  - LLNL/LBL/SLAC/ETEC seismic safety seminar

- Establish Natural Phenomena Hazards Information Center

This year we are establishing the Natural Phenomena Hazards Information Center at LLNL

- Centralized source of information and reference material
- Provide resources in developing and reviewing hazard definitions and criteria development
- Evaluate lessons learned from observation of events
- Provide training and technology transfer
- Keep current on state-of-the-art

LLNL has become the Natural Phenomena Hazards Center for DOE

Vibration Measurements and Analysis of USSR Accelerator Sites.

Parkhomchuk Vasily

Workshop on Vibrational Control and Dynamic Alignment Issues at the SSC. February 11-14,1992

1. The results of measurement of vibration noise in tunnel of UNK

2. The comparison of the power spectrum in different accelerators and the estimation of situation for the SSC.

3. The estimation of the cultural noise: traffic,ventilation...

4. The slow motion and closed orbit distortion

6. Summary and recommendations for the future development

$$\tau^{1} = \frac{d\varepsilon}{\varepsilon dt} = \frac{\gamma c^{2}\mathrm{tg}(\mu/2)}{\varepsilon R l^{2}} \sum P(\omega_0(n\text{-}Q)) \approx$$

$$\approx \frac{\gamma c \delta^{2}}{\varepsilon l^{2}}$$

$\frac{c}{e} \approx 3 \cdot 10^{6}$ 1/sec

$N_Q = \frac{c}{e} \cdot \tau = 10^{11}$

$\Delta X \approx \delta \cdot \sqrt{N_Q} \approx 10^{-4} \cdot 3 \cdot 10^{5} = 30\ \mu m$

where $\gamma = E/mc^{2}$ -Lorentz factor, l - distance between lenses, c-the velocity of light, μ - phase advance in FODO structure, ε - norm. emittance, P - the spectral power of the vibrations, δ - the amplitude of vibrations at the frequency ω_0(n-Q).

Parameter	Tevatron	SSC	factor
ε, μm*rad	5.6	1	5.6
τ, hours	13.0	9.2	0.8
γ	10^3	$2.0*10^4$	20
f_0, kHz	50	3.4	
f_0(n-Q), kHz	19.3	0.76	
Appreciable lens jitter δ, μm	$2*10^{-3}$	10^{-4}	10^4**

** For the power spectrum $P = \mathrm{const}/\omega^4$

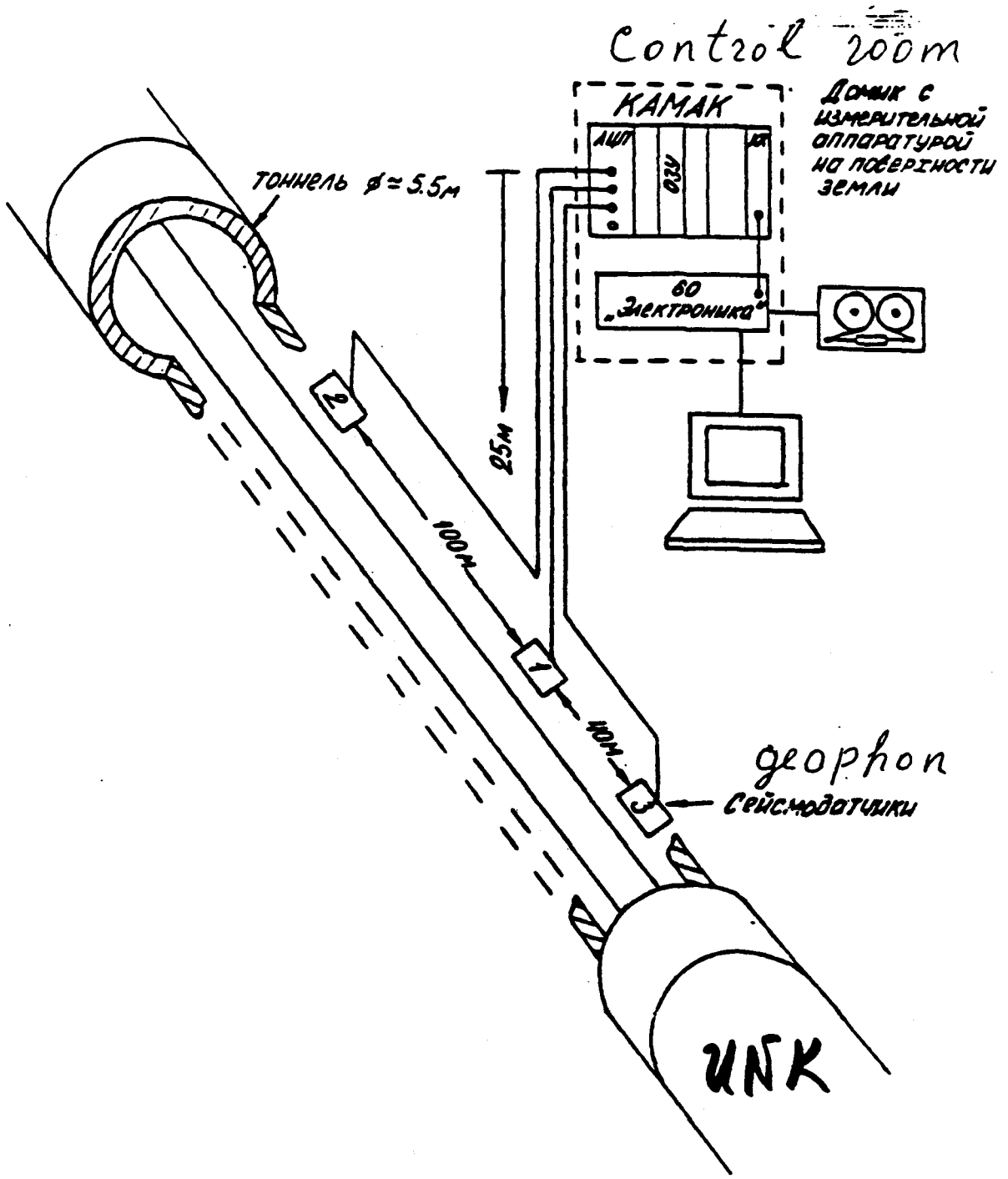

Fig. 3 Shema of undeground measurement in UNK tunnel.

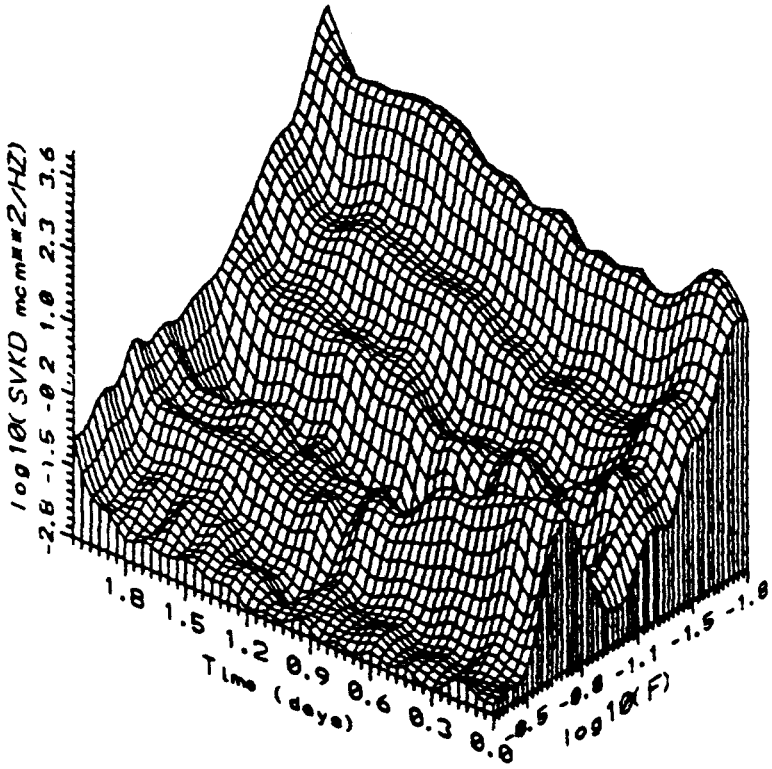

Рис. 9. Спектр мощности абсолютных колебаний в зависимости от времени в течение двух суток с 26 по 28 января 1991 года.

The Power spectrums of vibration vs. time – 2 days and frequency $1 \div 10^{-2}$ Hz

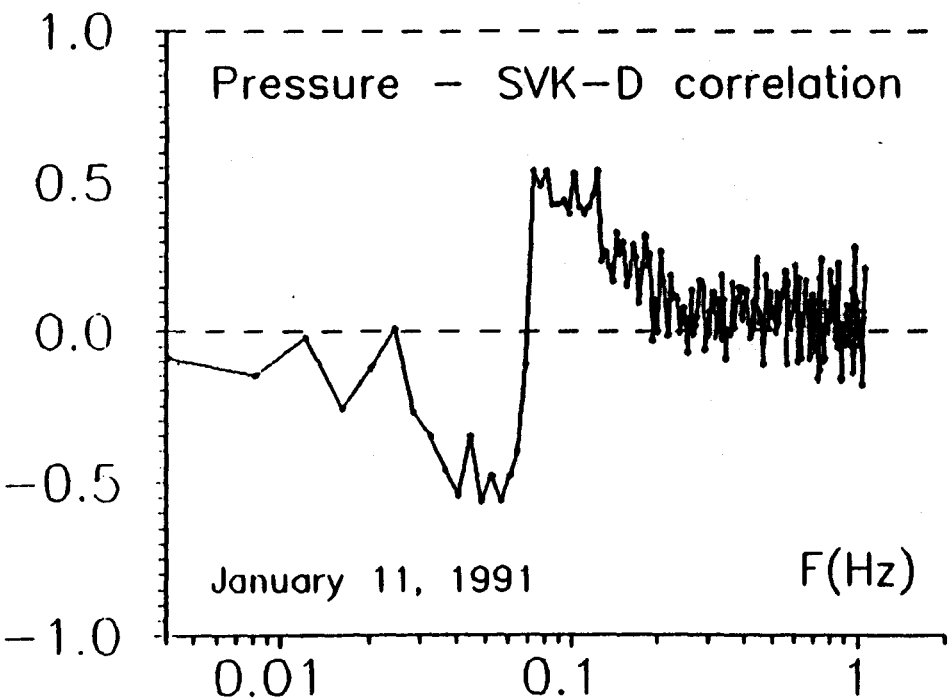

$$\frac{\langle P_\omega \cdot X_\omega \rangle}{\sqrt{\langle P_\omega^2 \rangle \cdot \langle X_\omega^2 \rangle}}$$

Fig. 25 Correlation signals of atmosferic pressure and seismometr SVK-D vs. frequence.

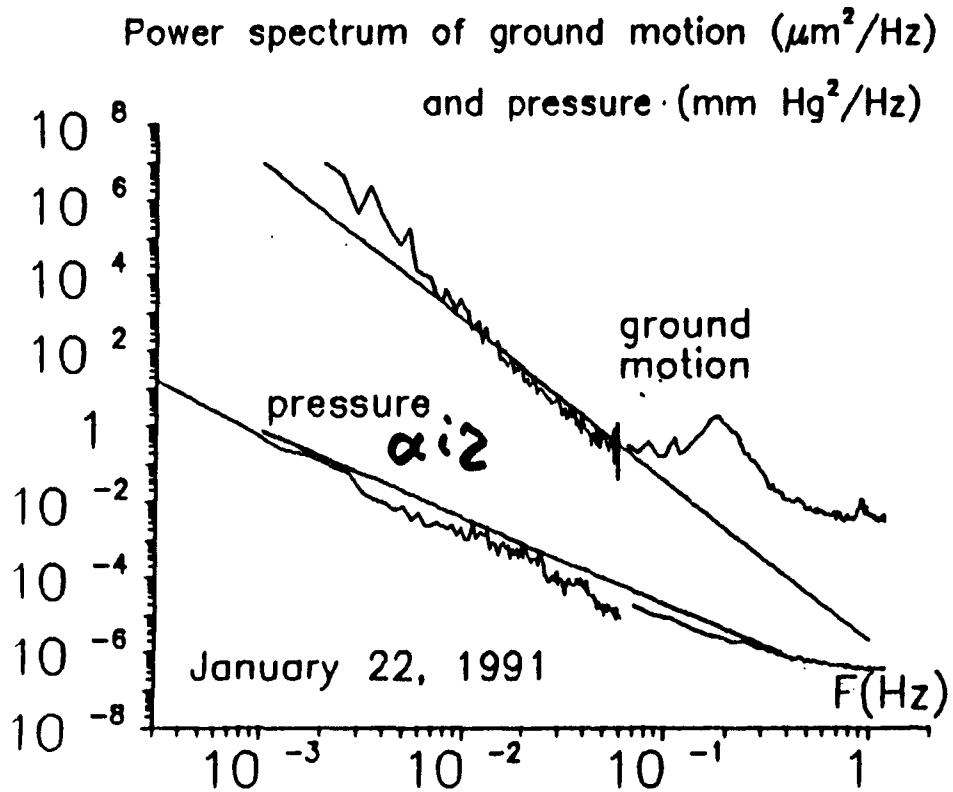

图 Power spectrums of ground and atmospheric oscilation. Strait lines calculated according to model.

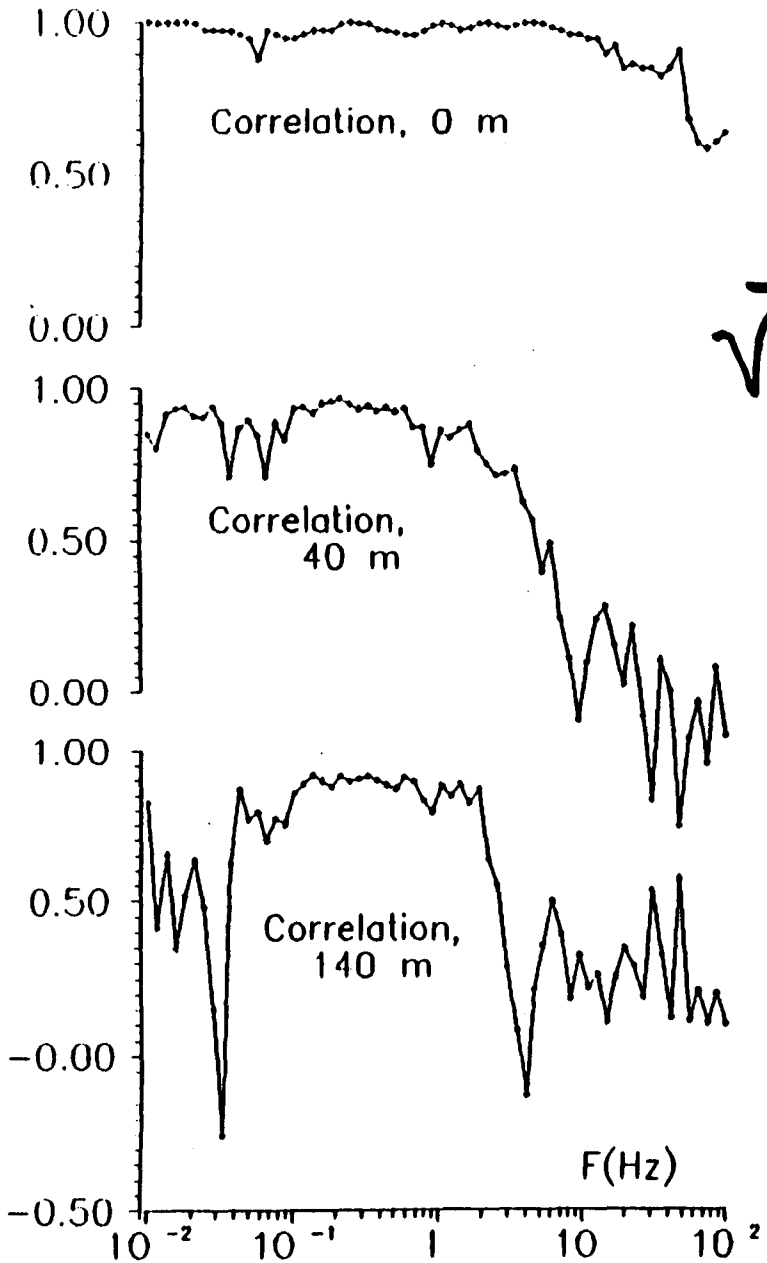

$$\frac{\langle X_{1\omega} \cdot X_{2\omega} \rangle}{\sqrt{\langle X_{1\omega}^2 \rangle \langle X_{2\omega}^2 \rangle}}$$

Fig.24 Correlation spectrums of vertical motion between two points with distances 0 m, 40 m, 140 m.

COMPARISION OF EARTHLY NOISE SPECTRUMS

Parkhomchuk Vasily

Workshop on Vibration Control and Dynamic
Alignment Issues at the SSC. 02/11-14/1992

The power spectrum of ground vibration are the basic information for calculation of the time degradation of machine luminosity and indispensable amplitude of feedback correction. The measurements of the power spectrum was made in many places and it is very interesting to have comparison of date measured in different condition. I am try to prepare this information for discussion on Workshop. In figs. was used data measured in Protvino in UNK tunnel /1,2/, in Novosibirsk at maximum quiet places- air-raid shelter, at the SSC Site /3/ and data seismostantion I am take from review G.E. Fisher-/4/.

In fig.1 is show this date together with limitation on the power of quadruple axes vibration for normal run of SSC with and without feedback for suppression transverse coherent beam oscillation /5/. The noise in high frequency band are changeable on few order of magnitude. The design of tunnel and equipment have strong influence on amplitude of high frequency vibration. So for UNK tunnel easy see increasing noise in hundreds Hz frequency band when wave length became the same order of magnitude as diameter of tunnel and wave propagate along tunnel with small attenuation.

The changing of spectrum in time are show fig.2 measured in INP (Novosibirsk) in different time.

The fig.3. show data from SSC Site. The line 3 demonstrate the noise spectrum from report E.Daly about transportation magnet at time of motion the truck.

The fig.4 show data vertical change in SSC Site. It is very interesting that the spectrum of displacement in noisy case don't depend vs. frequency up to 100 Hz. It is necessary pay attention the reason so slow decreasing with frequency spectral power for the large depth.

References

1.B.A.Baklakov,P.K.Lebedev,V.V.Parkhomchuk,B.A.Tokmakov, N.L.Trapeznikov,A.A.Seriy,V.D.Shiltsev,"Measuremet of level of ground vibration in UNK tunnel",Preprint INP 90-88, Novosibirsk,1990.

2.B.A.Baklakov,P.K.Lebedev,V.V.Parkhomchuk,A.A.Seriy,A.I.Slepcov, V.D.Shiltsev, "Exploration of correlation and spectral characteristic of oscilations of earth surfece in the UNK site"

3.K.Hennon,D.Hennon,the Earth technology corporation,"Field measurements and analyses of underground vibrations at the SSC site WAXAHACHIE,TEXAS" 1989.

4.G.E.Fisher, "Ground motion and its effects in accelerator design" SLAC-PUB-3392 Rev,1985.

5 V.A.Lebedev,V.V.Parkhomchuk,V.D.Shiltsev,A.N.Skrinsky, "Suppression of emittance growth caused by mechanical vibrations of magnetic elements in the presence of beam-beam effects in the SSC.",preprint ,INP,1992.

Fig.2 demonstrate maximum spectral power [illegible]
moved was near boring with geophones. The estimation calculated with parameters $m=500$ kG, $M=50$ T, $n=0.05$, $\omega_0=2\pi*10$ Hz, $\lambda=0.5\omega_0$, $\delta x_1=1$mm, $l_1=1$m, $h=100$m, $S=0.01$, $\rho=2000$ kG/m^3, $c=3000$ m/sec, $v=90$ km/sec.
As easy see the estimations look close to real measurements.

The next step in improvement this model should be take in acaunt more realistic model of ground wave with attenuation on high frequency. For this necessary have detail information about distribution velocity of wave in depth.

Fig. 2. Spectrum of vibration

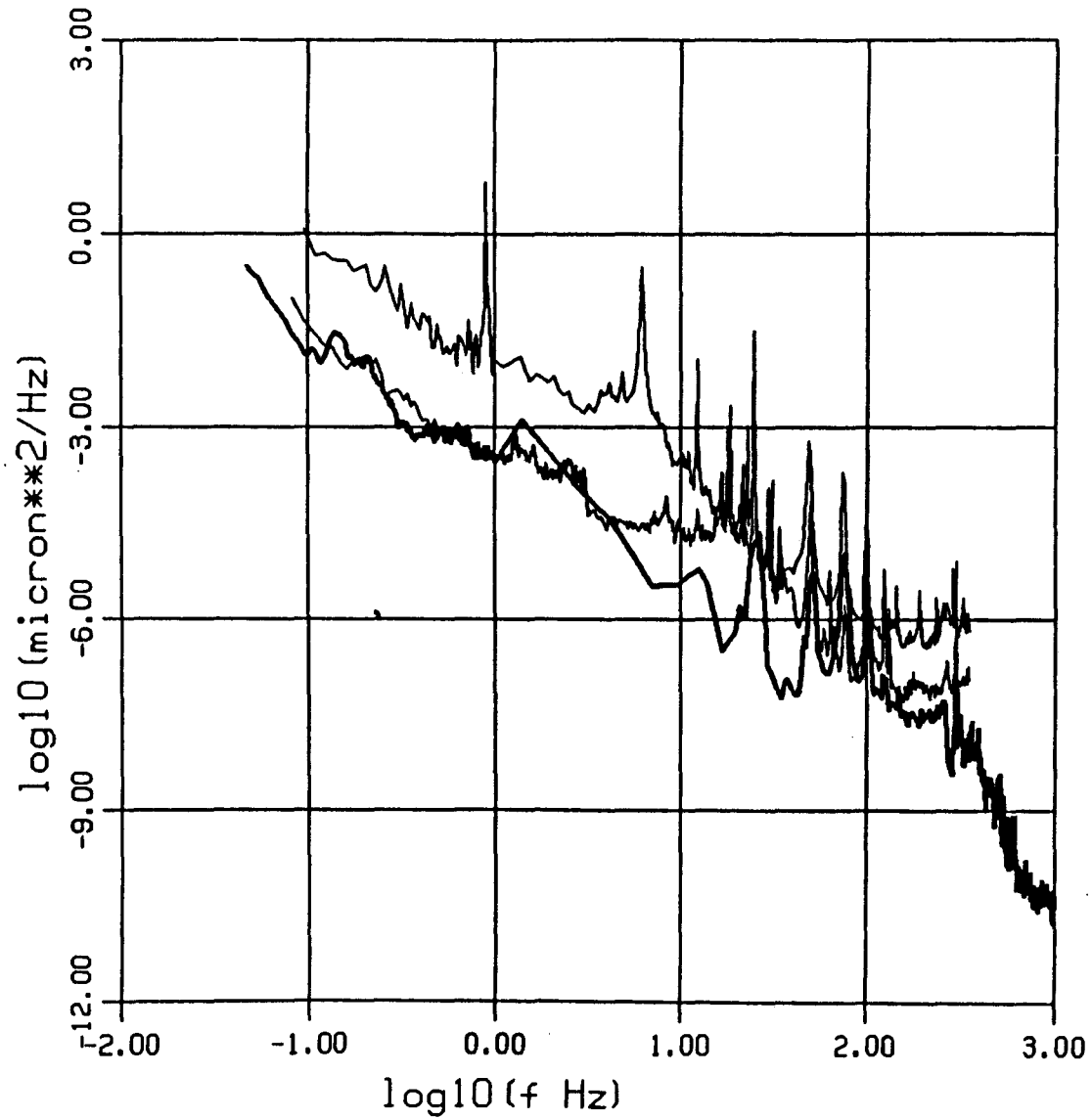

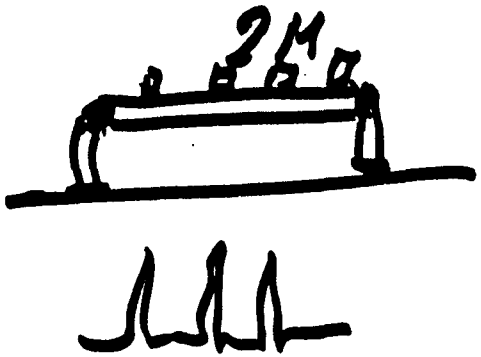

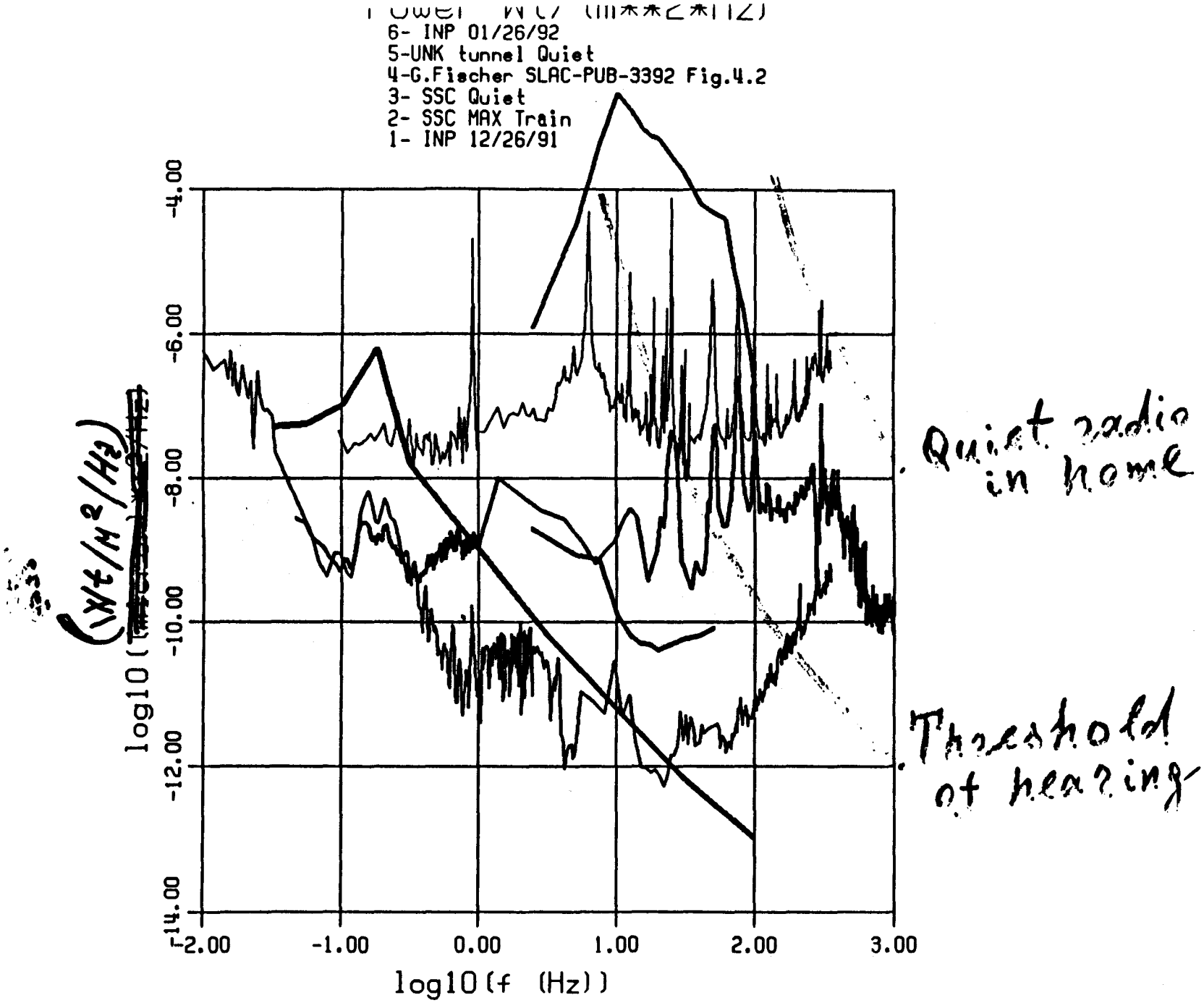
6- INP 01/26/92
5-UNK tunnel Quiet
4-G.Fischer SLAC-PUB-3392 Fig.4.2
3- SSC Quiet
2- SSC MAX Train
1- INP 12/26/91
-4.00
-6.00
-8.00
-10.00
-12.00
-14.00
-2.00
-1.00
0.00
1.00
2.00
3.00
log10(f (Hz))
(Wt/H²/Hz)
Quiet radio in home
Threshold of hearing

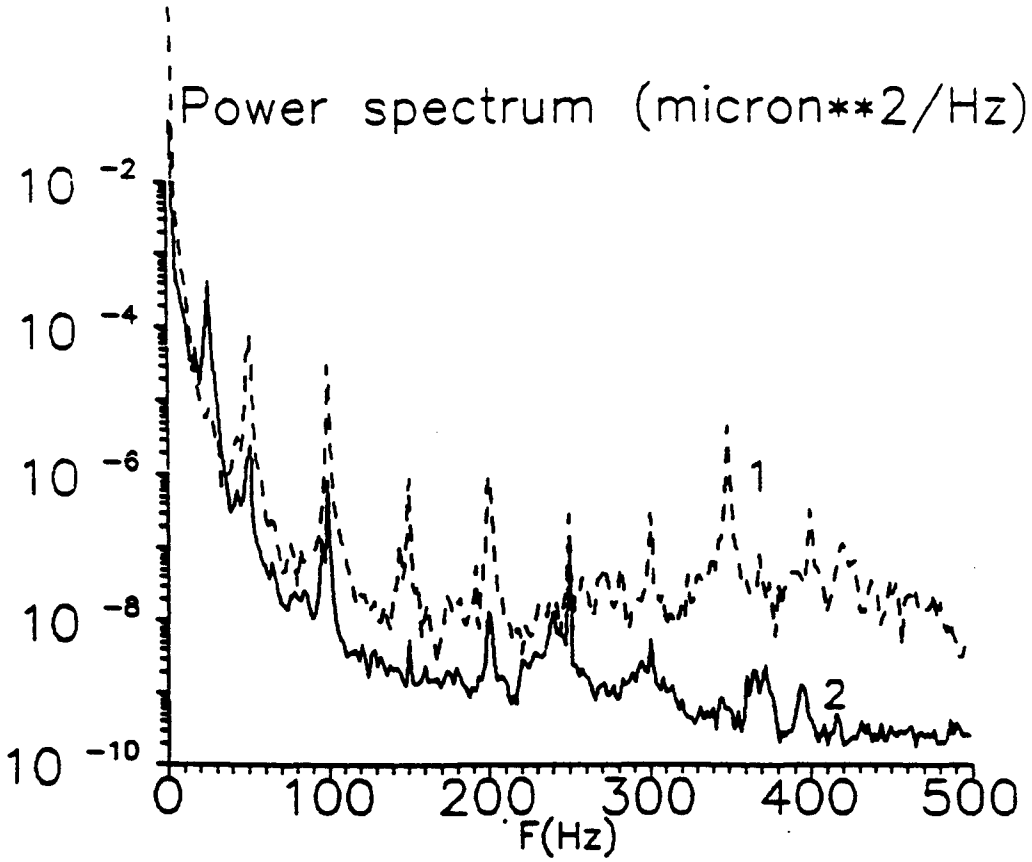

Vibration spectra of ground-1
and lense FFTB-2

Fig. 1 Spectrum of vibration

6- INP 01/26/92
5-UNK tunnel Quiet
4-G.Fischer SLAC-PUB-3392 Fig.4.2
3- SSC Quiet
2- SSC MAX Train
1- INP 12/26/91

limitation
● without (off) feedback
✖ with (on)

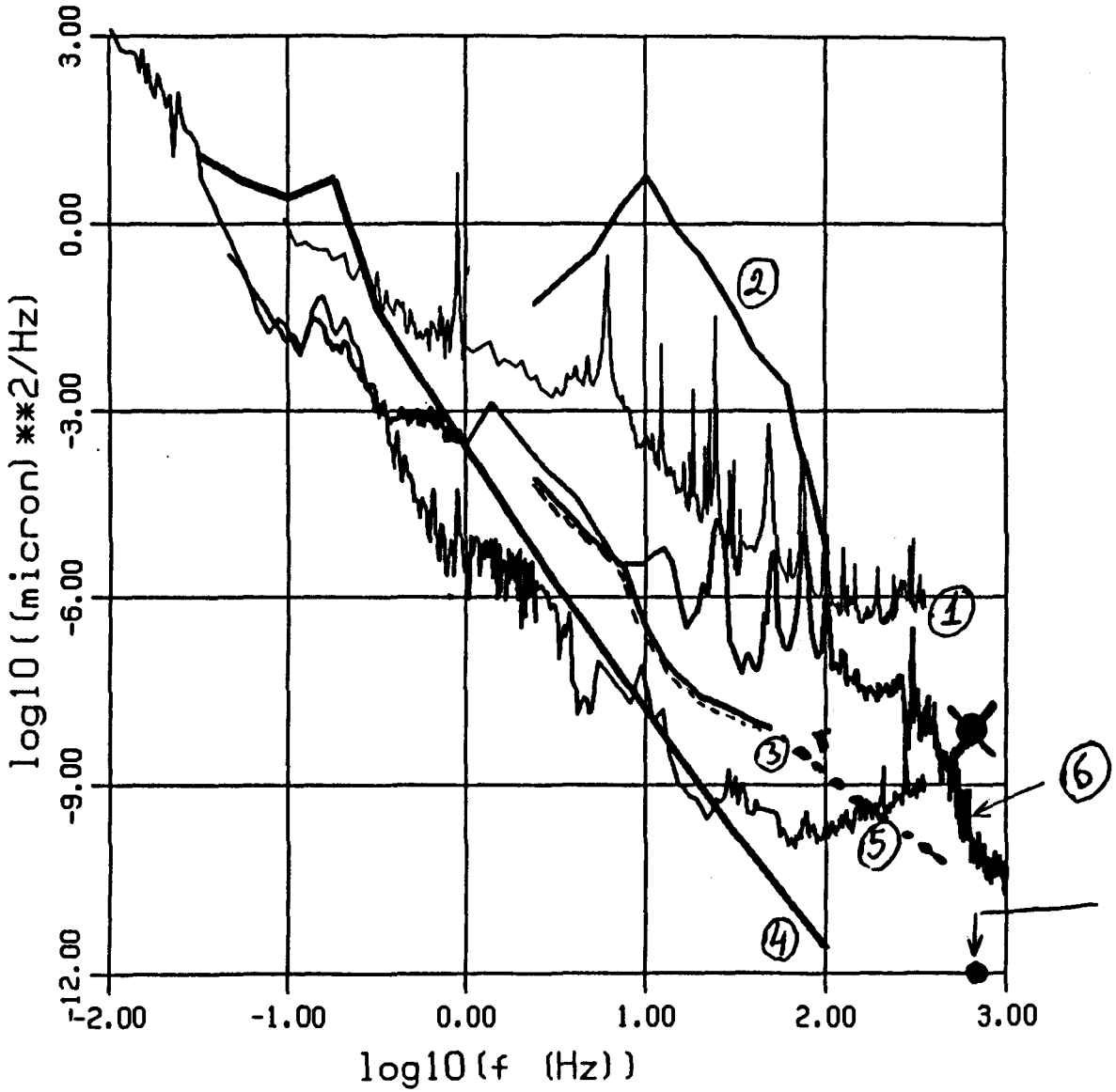

$S \approx 10^{-8} \frac{\mu m^2}{Hz}$

$S(760\,Hz) \leq 10^{-12} \frac{\mu m^2}{Hz}$

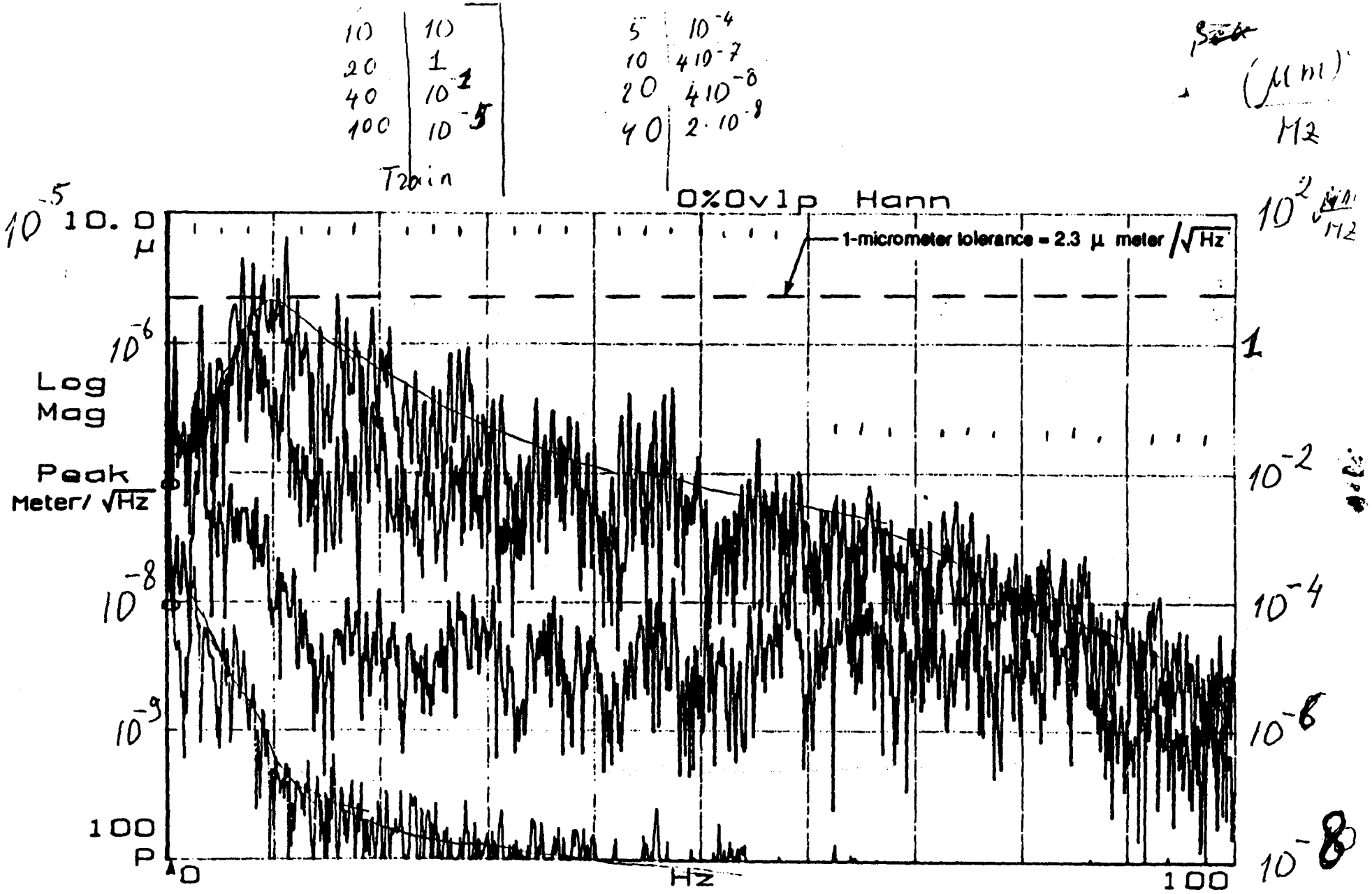

EXPLANATION

1 Hz Geophone Data
Blue = Max. Train Vibrations Measured @ 5.0 feet (1.5 meters)
Green = Max. Train Vibrations Measured @ 30.0 feet (9.1 meters)
Red = Max. Train Vibrations Measured @ 261.5 feet (79.7 meters)
Black = Ambient Vibrations Measured @ 261.5 feet (79.7 meters)

Lower Frequency Limit of Calibration
Bandwidth = 0.187 Hz

The Earth Technology Corporation

Project No.: 87-888-001

RTK Joint Venture

Composite Displacement Linear Spectrum
Showing Vertical Change
Data Set 2

CLOSE ORBIT DISTORTION

Pakhomchuk Vasili 1/23/1992 (SSCL)

Beside the oscillation type of motion earth surfer has another one like diffusion due to tension drops inside the bulk. Random character of that jumps leads to continues diffusion in all surface points. The measurements of relative motions two points show that dispersion of transve position are equaled:

$$\langle x^2 \rangle = A*t*l$$

Where t-time, l-distance, A-empirical constant in our measurement are equaled 0.75-1.5 10^{-4} $\mu m^2/(sec*m)$.

Using of this model permit to calculate slow motion of quadruples
produce a close orbit distortion. This estimation can predict strength of correction dipoles (B*l) for control proton orbit.

The fist of all calculate the position of quadruples the next way. The random displacing of neighboring quadruples are equaled:

$$x1=0$$
$$xi=x(i-1)+sqrt(A*t*l)*xrnd \quad (1<i\le N)$$

where l-distance between quadruples, xrnd-random value with dispersion equaled 1. Continue this calculation along circumference of ring we produce model of displacement of lenses. For closing circumference it is necessary subtract linear dependence the next way:

$$xi=xi-xN*(i-1)/(N-1)$$

In this way we build surfer of displacement that can be used for calculation of close orbit distortion. In figs 1-4 are show this way calculation of displacement in time 1 sec, 1 hour, 1 year and finally for 30 millions years together with today sunsurfer along circumference of SSC tunnel.

The motion of quadruples and orbit distortion can estimate as :

$$\delta x^2 = AtC$$

t-time period, C-circumference of SSC. For control orbit the strength of correction dipoles near quadruples should be equaled:

$$P=(\Delta Bc*lc)=Gl*ll*\delta x=Bo*Q*(AtC)^{1/2}/(2\pi)$$

Bo-average magnetic field of SSC, ΔBc, lc-magnetic field and length of dipole correct. For successful activity in time period of 1 year without mechanical correction of quadruple positions it is necessary to have magnetic correction (ΔB=1 T) with length :

$$lc=\frac{Gl\,ll(AtC)^{1/2}}{\Delta Bc} = \frac{BoQ(AtC)^{1/2}}{\Delta Bc}$$

For Gl=206T/m, ll=5.85 m, Bo=5T, ΔBc=1T, Q=123.78, C=90 km, t=1year=3 10^7 sec, A=10^{-16} m/sec, the length of corrector lc=10-17m.

It seems too large!!! In Conceptual Design (1990) Table 4.2.1.1-23 strength of dipole correction are given 2.5 T*m. If estimation for A is correct, the time for saturation of correctors will be less them 1 month.

The time of correction we can estimate take limitation on possible disalignment in interaction point 0.01σ=0.05 μm. It means that in main ring it is the acceptable distortion of close orbit δx=2 μm. The time of feedback for close orbit control should be equal:

$$\tau=\delta x^2/(AC)=0.4 \text{ sec.}$$

far
noise
small
eathquake

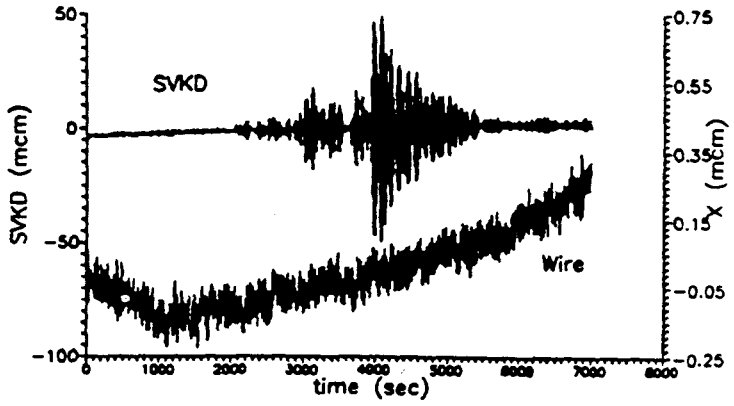

Рис. 2. Абсолютное и относительное положение платформ в зависимости от времени. Возмущение (микроземлетрясение) возникло далеко от места измерения.

local
noise

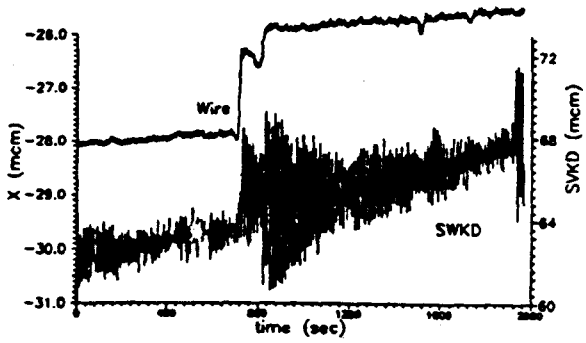

Рис. 3. Абсолютное и относительное положение платформ в зависимости от времени. Возмущение возникло вблизи от места измерения.

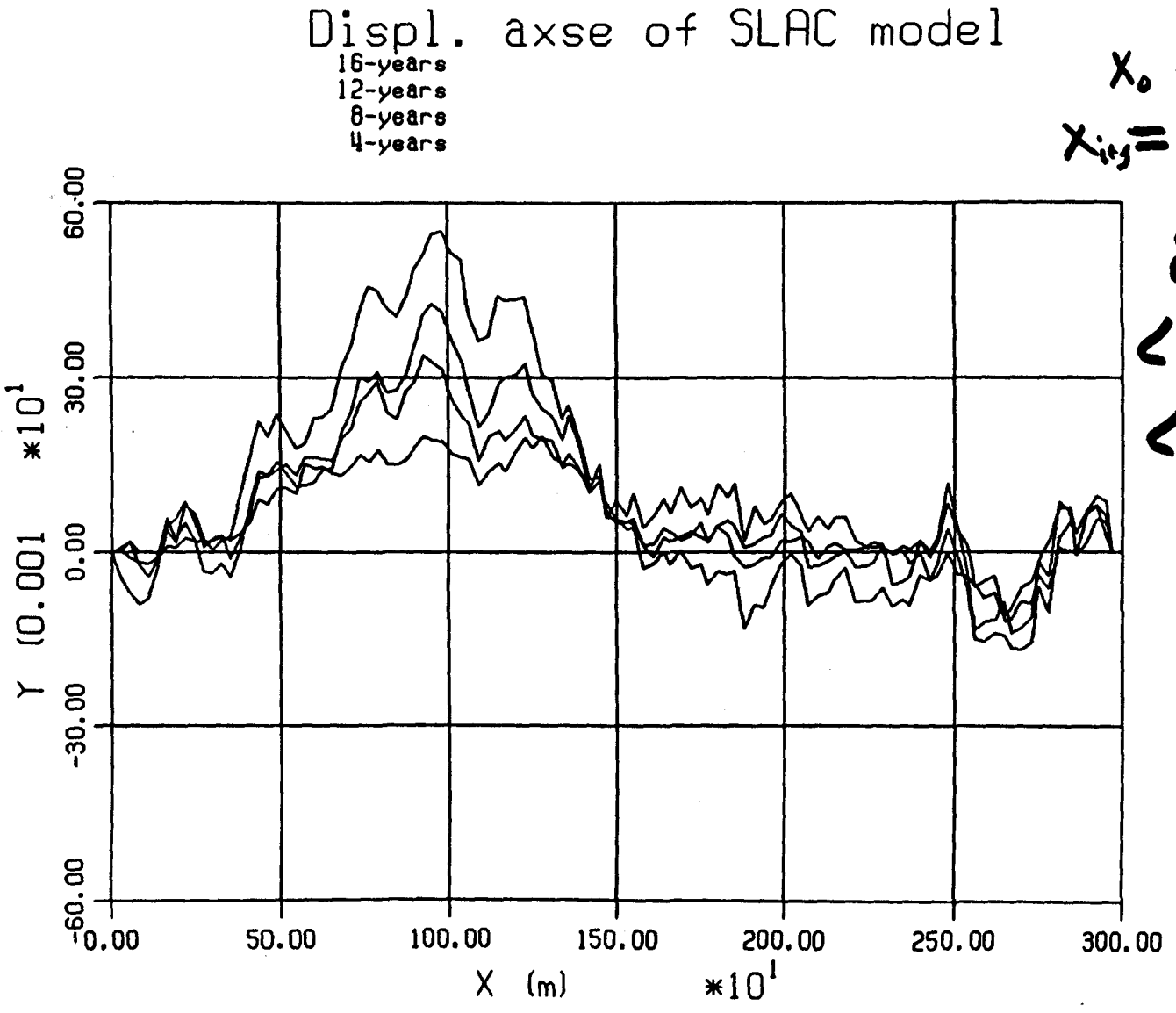

$x_0 = 0$

$x_{i+j} = x_i + A \cdot \tau \, \ell_{i+j,i} \, \delta x_2$

δx_2 - random

$\langle \delta x_2 \rangle = 0$

$\langle \delta x_2^2 \rangle = 1.$

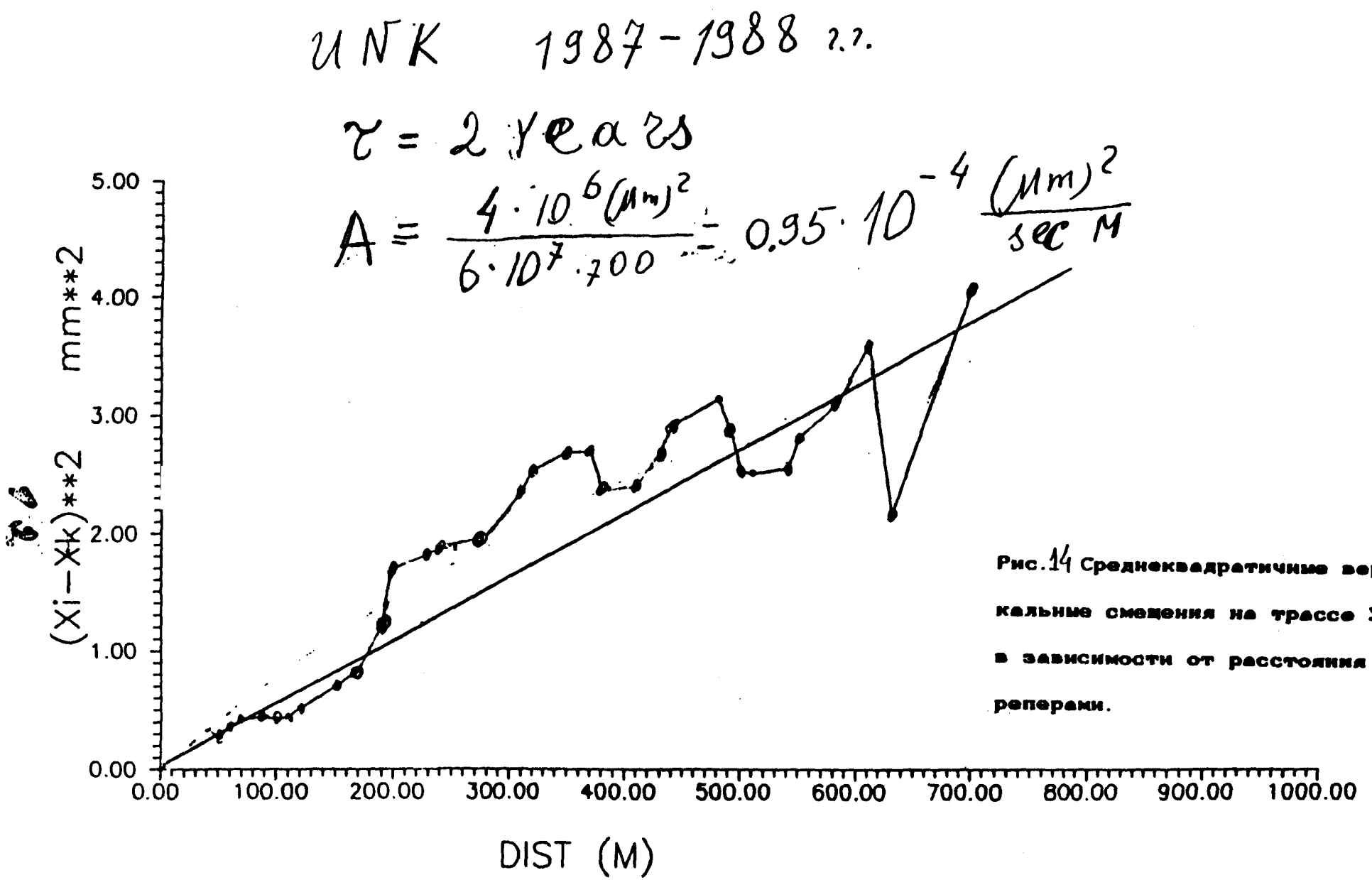

Рис.14 Среднеквадратичные вертикальные смещения на трассе УНК в зависимости от расстояния мех реперами.

2.1 GROUND SETTLEMENT

Seasonal variations in the local ground water table, water content of the soil, further compaction of even well engineered fill or rebound of the ground under cuts etc., all tend to push the tunnel out of its original shape.

For example, the SLAC linac *"cut and cover"* tunnel is 10,000 feet long and has built into it a laser alignment system capable of a transverse resolution of about .001 inches.[4] Figures 2.2(a,b), show the cumulative displacements of some 240 targets along the line, in the horizontal and vertical directions – summed over the 17 years 1966 to 1983. Although the motions were faster just after initial construction, recent yearly surveys still indicate motions in certain regions of the order 1/2 mm/year. Generally speaking, the wavelengths of the distortions are comparable or larger than the betatron wavelength of the focussing structure and, therefore, less dangerous. Needless to say, the accelerator waveguide is readjusted once a year.

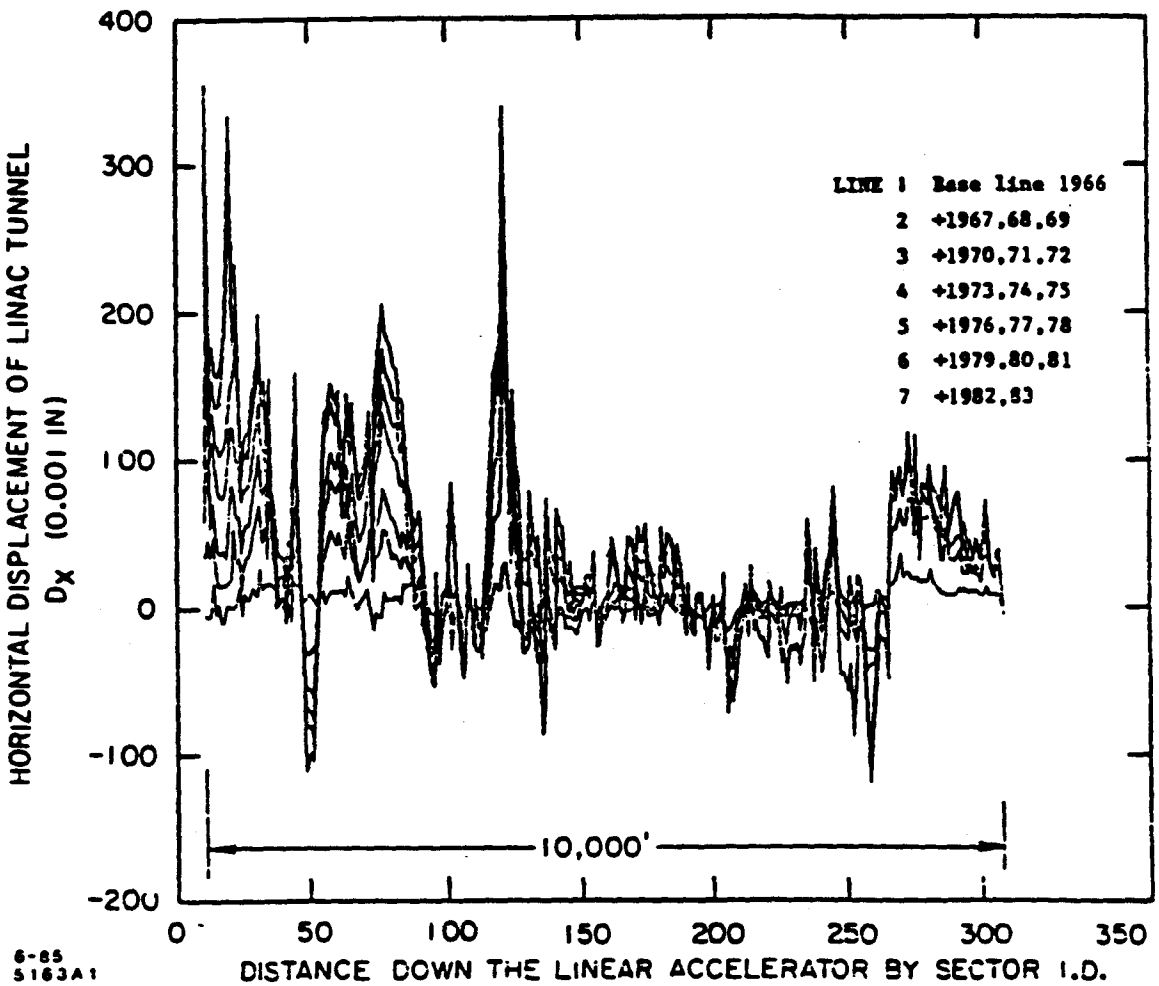

Fig. 2.2(a). Displacement of the SLAC Linac Tunnel – Horizontal.

Fig 1 Dispasment at time=1 sec

dashed - x
solid - cod

COD close Orbit Distortion

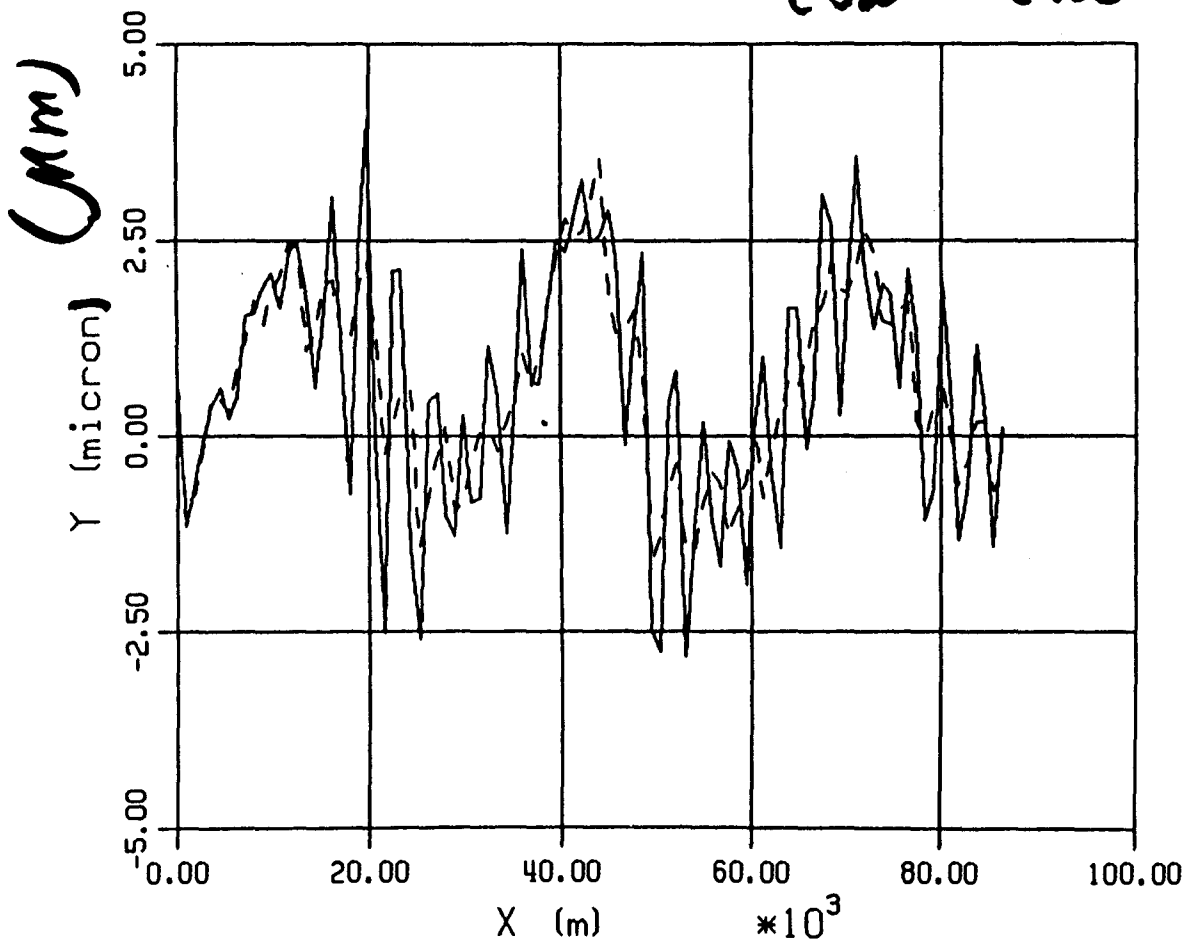

$\Delta X \sim 2\,\mu m$

Fig 2 Displasment at 1 hour

dashed - x
solid - cod

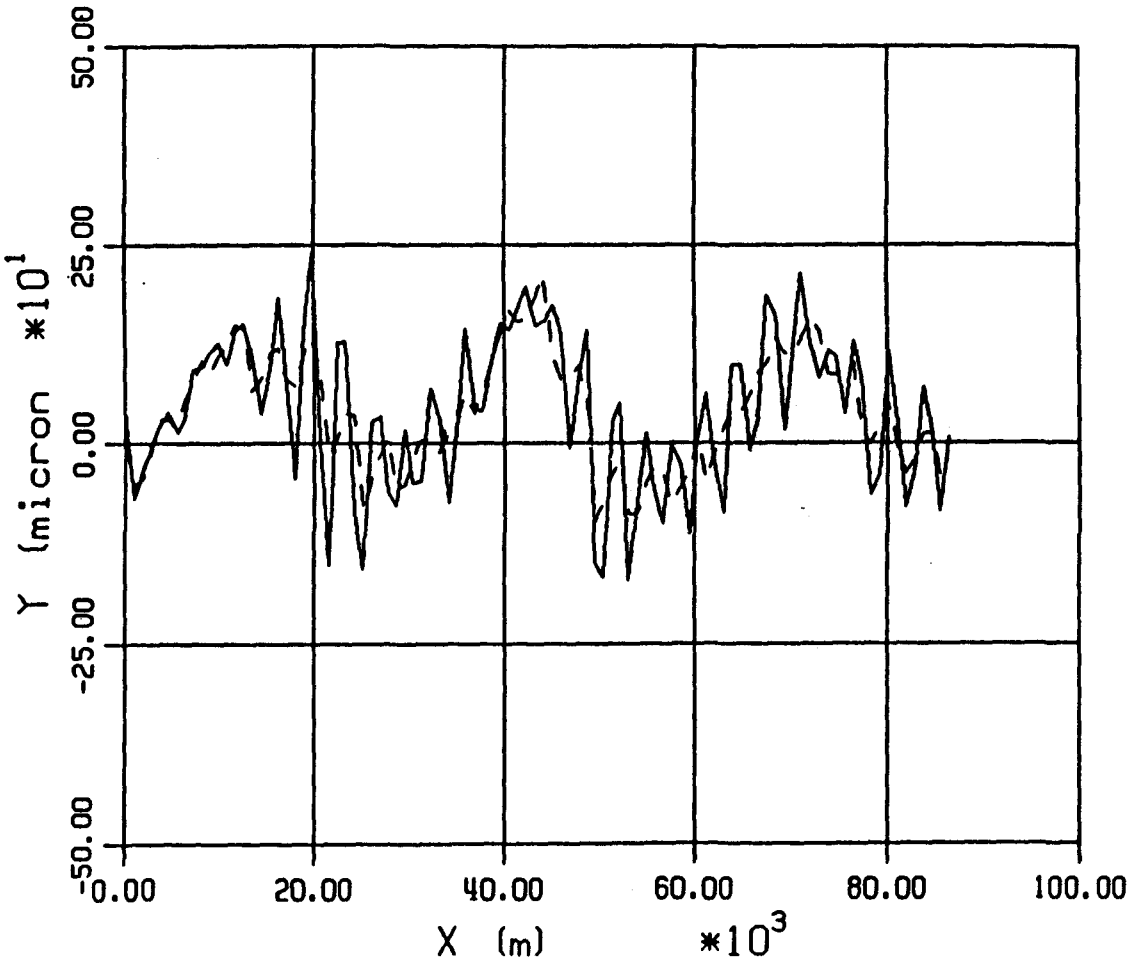

$\Delta X \sim 200\ \mu m$

Fig 4. Vertic profile (model)

dashed - SSC sunsurfer
solid - model t=30 Myears

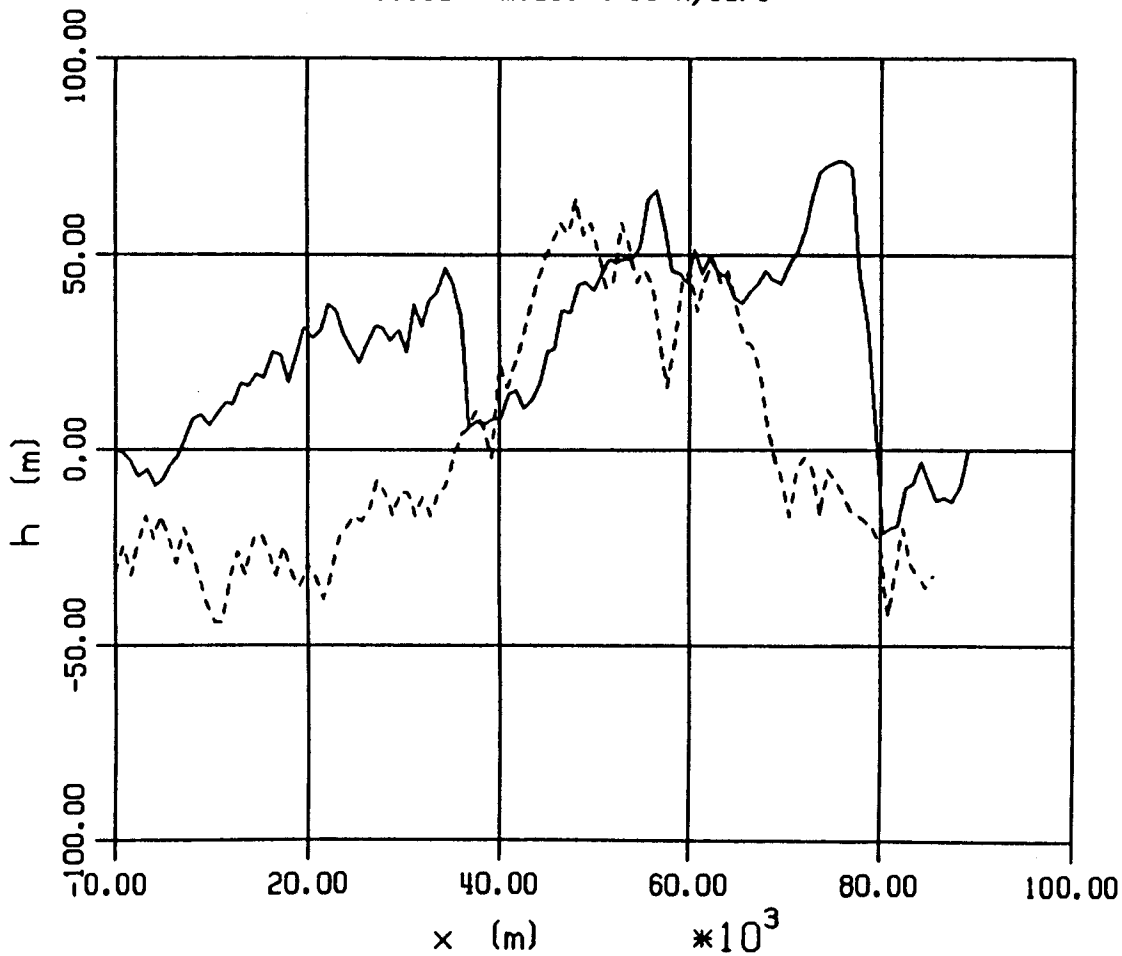

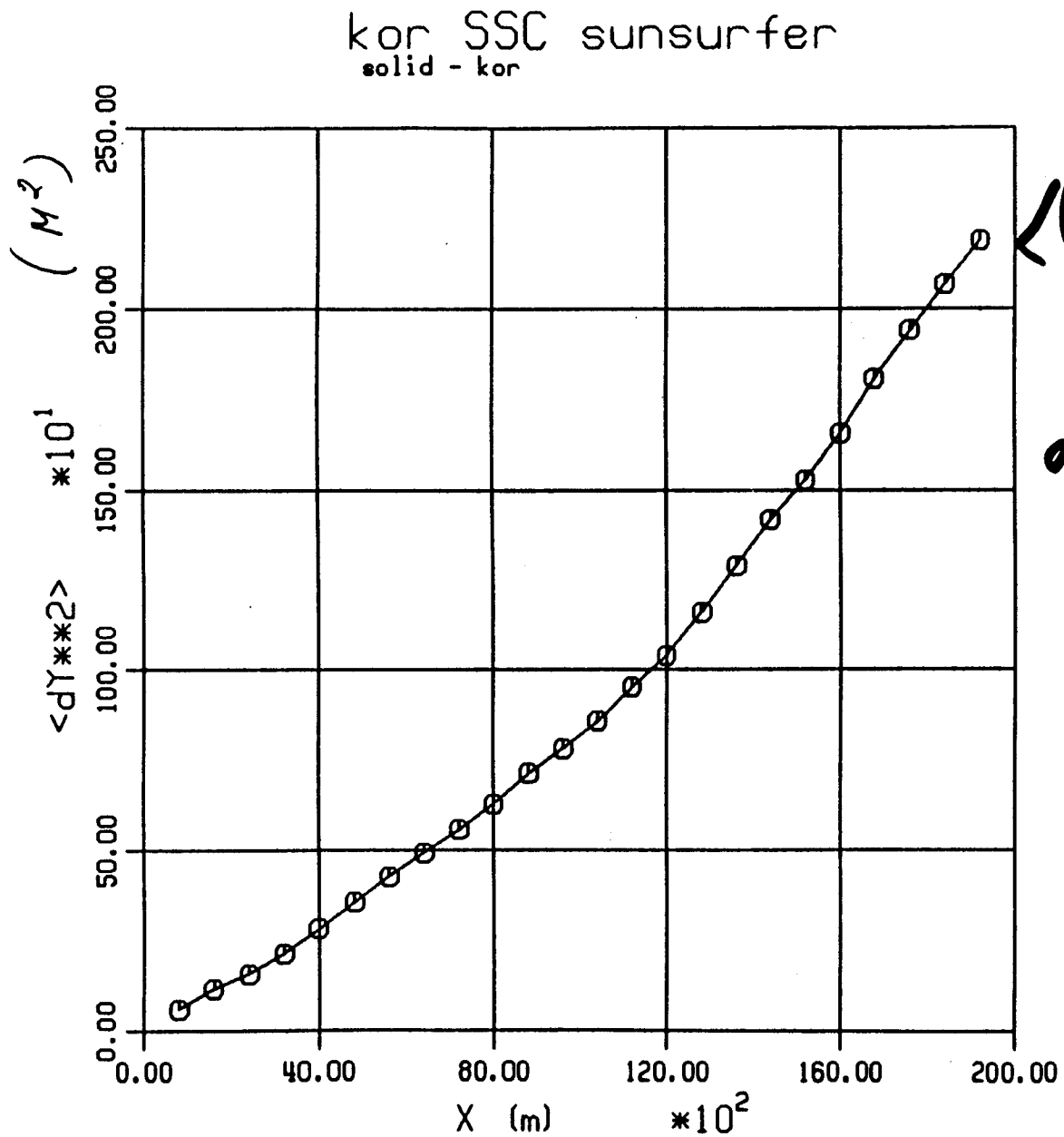

$\langle (h_i - h_k)^2 \rangle$ vs distance $(i-k)$

VIBRATION CONNECTED WITH TRAFFIC

Parkhomchuk Vasili 1/30/1992

For calculation of amplitude of vibration exit of motion of cars it is necessary to have model of car. Choice very simple model that car consist of mass M on spring witch contact with ground across wheel mass m. In this case equation of vertical motion car we can write in next view:

$$\frac{d^2 x_c}{dt^2}+\lambda\frac{dx_c}{dt} + \omega_o^2 x_c=\omega_o^2 x \qquad (1)$$

x_c-vertical coordinate of car, λ,ω_o-decrement and frequency of car oscillation, x(t)-the vertical position of road surfer.
The force act on road are equal:

$$F(t)=m\frac{d^2 x}{dt^2}+M\frac{d^2 x_c}{dt^2} \qquad (2)$$

The pressure on ground are equal :

$$\Delta p=\frac{F}{S} \qquad (3)$$

S-squire of wheel contact with ground.

For oscillation on frequency ω amplitude of excitation flat wave A are equal :

$$A\omega=v=\Delta p/(\rho c) \qquad (4)$$

ρ-density of ground, c-velocity of wave
and power of excitation are equal :

$$W=v*F=F^2/(\rho c S) \qquad (5)$$

If all this power propagate as cylindrical wave in surfer layer with depth h the amplitude of vibration on distance R are equal:

$$x_g^2=W/(\rho c\omega^2 2\pi Rh)=\frac{F^2}{(\rho c\omega)^2 2\pi RhS} \qquad (6)$$

If density of car per length of road is n full energy of oscillation
are equal:

$$x_g^2=\frac{F^2}{(\rho c\omega)^2}\frac{n}{hS}*\frac{\ln(L/R)}{2\pi}\approx\frac{F^2}{hS(\rho c\omega)^2}\frac{n}{2} \qquad (7)$$

If choose model of the road as random triangle with height δx_1 and length l_1 we can write power of space garmonic as:

$$x_k^2=\delta x_1^2/(l_1 k^2) \qquad (8)$$

where k-space vector $(x_g=\delta x*\sin(k*z))$ .The frequency of oscillation
depend of velocity of car $\omega=k*v_c$. For spectral power force we can write equation:

$$F_\omega^2=\frac{|m+M*\omega_o^2/(\omega_o^2-\omega^2+i\lambda\omega)|^2\,\delta x_1\omega\, v}{l_1} \qquad (9)$$

Finally we can write the estimation for spectral power of vibration connected with traffic in view:

$$X_\omega^2=\frac{|m+M\omega_o^2/(\omega_o^2-\omega^2+i\lambda\omega)|^2\,\delta x_1 vn}{l_1 hS(\rho c)^2} \qquad (10)$$

For low frequency effective mass M and for high frequency m .
Fig 1 demonstrate spectral power of oscillation witch was measure in UNK tunnel in working day together with estimation (10) with parameters: m=10 kG, M=1000 kG, $\omega_o=2\pi*5$Hz, $\lambda=0.5\omega_o$, δx_1=1mm, l_1=1m, h=100 m, S=0.01 m^2, ρ=2000 kG, c=1000 m/sec., v=90 km/hour, n=0.01/m.

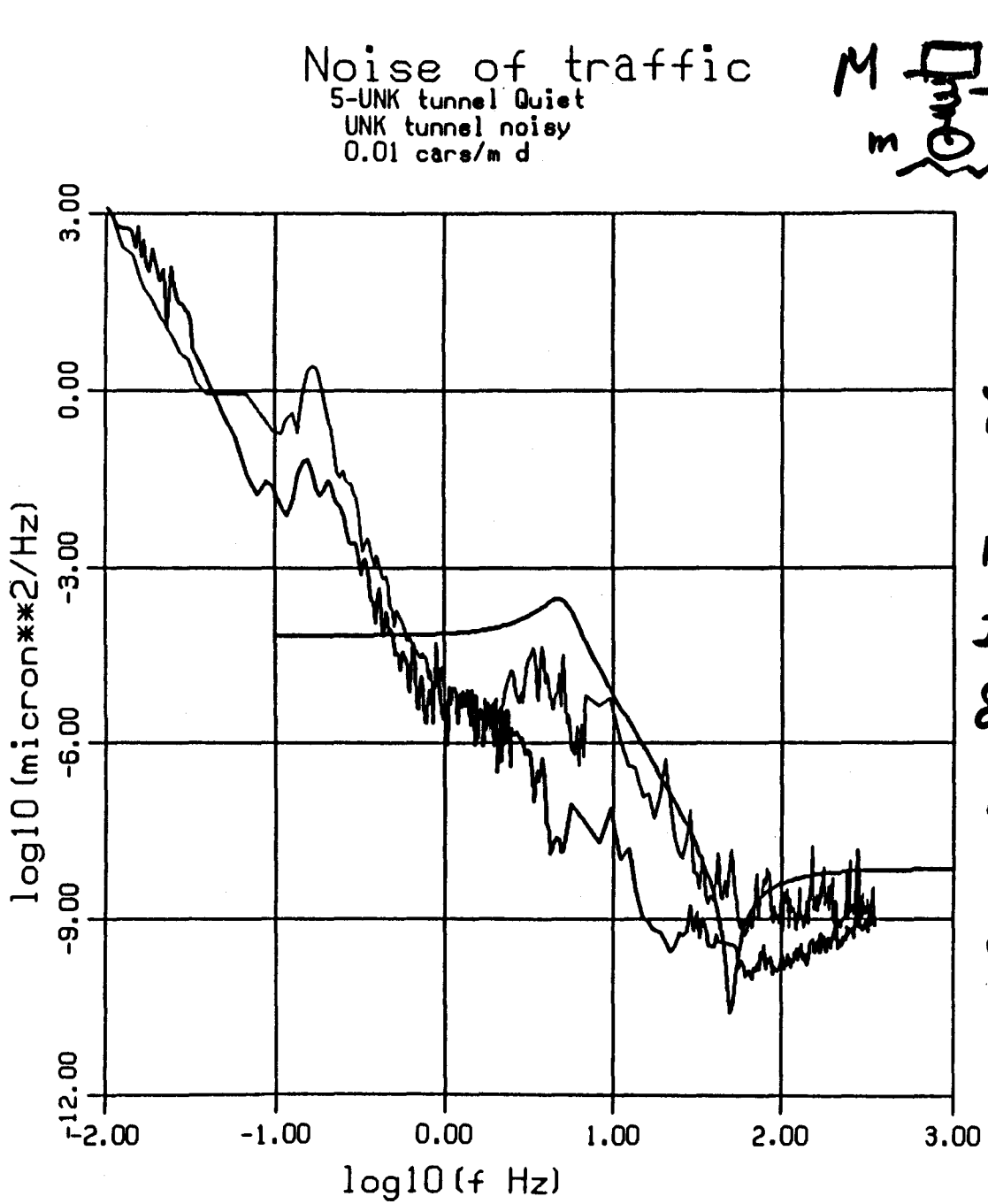

$$X_N^2 = \frac{\vartheta \left| m + \frac{M\omega_0^2}{(\omega_0^2-\omega^2)+i\lambda\omega} \right|^2 \delta X_i^2}{\ell_i \, h \, S (\rho c)^2}$$

$m = 10\,kG$, $M = 1\,T$

$f_0 = 5\,Hz$, $\lambda = 0.5\,\omega_0$

$\delta X_i = 1\,mm$, $\ell_i = 1\,m$

$h = 100\,m$

$S = 0.01\,m^2$

$\rho = 2\,T/m^3$

$c = 1\,km/sec$

$\vartheta = 90\,km/h$

$n = 0.01\,cars/m$

Noise of train

3- SSC MAX Train
50 T, 500 kG

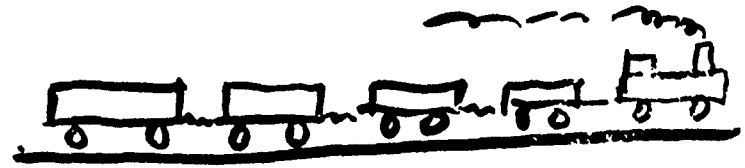

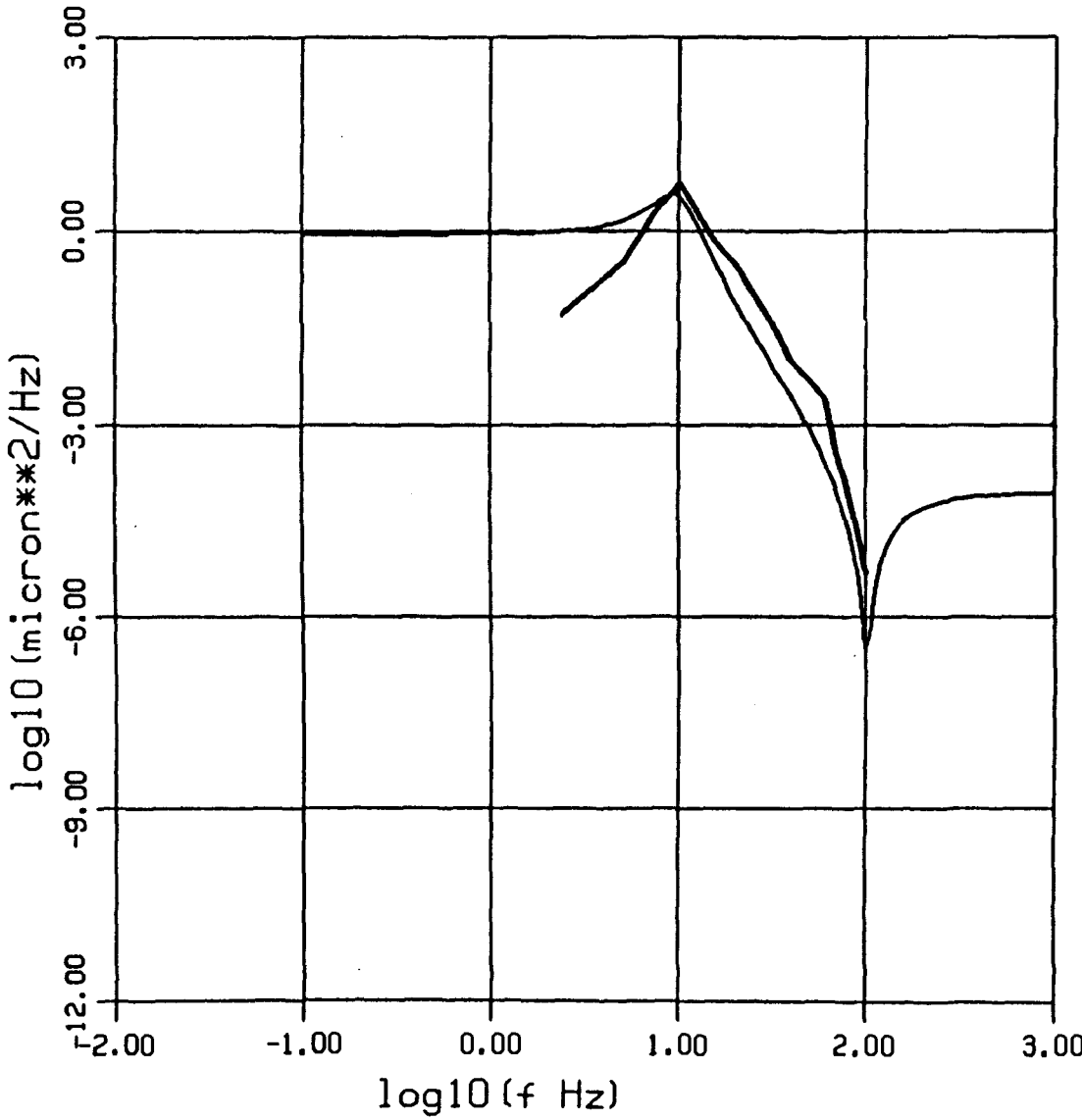

$m = 500\,kG$

$M = 50\,T$

$n = 0.05 \frac{\text{carriage}}{m}$

$f_0 = 10\,Hz$

$\delta x_i = 1\,mm \,/\, l_i = 1\,m$

$h = 100\,m$

$S = 0.01\,m^2$

$\rho = 2\,T/m^3$

$c = 3\,km/sec$

$V = 90\,km/sec.$

$$P(f) = \frac{1}{Kz}$$

VIBRATION ASSOCIATED WITH VENTILATION IN THE SSC TUNNEL

Vasily Parkhomchuk

The air flowing along the tunnel usually has high power of turbulence. For estimation of the spectral power of fluctuations of pressure one can use the formula [1,2] :

$$P_f^2 = \rho^2 U^{16/3}/(4\ R^{4/3}\ f^{7/3}),$$

where, ρ-air density, U-average velocity of air, R-radius of the tunnel, f - frequency of fluctuation.

The amplitude of oscillation of the wall of a tunnel is equal:

$$\delta x = \delta P/(\rho c \omega) = \delta P/(2\pi \rho_g c_g f)$$

where, ρ_g-ground density, c_g-velocity of longitudinal wave.

As a result, the estimation of the spectral power of vibration of the wall of a tunnel is equal:

$$\delta x_f^2 = \rho^2 U^{16/3}/((4\pi \rho_g c_g)^2 R^{4/3} f^{13/3})$$

$$f > f_c = U/R \quad \text{- cut off frequency}$$

Table 1. Spectral power of vibration of hard wall of a tunnel μm^2/Hz for different velocities of ventilation.

Spectral power of vibration of inside surface of a tube with flowing liquid		(μ^2/Hz)
Tube radius	(m)	2
flow density	(kg/m^3)	1.3
tube material density	(kg/m^3)	2000
wave velocity in tube material	(m/sec)	1000

f(Hz)	U=1.00	U=3.16	U=10.00	(m/sec)
.50E+00	.21E-01	.68E-01	.21E+00	
.11E+01	.77E-03	.68E-01	.21E+00	
.23E+01	.28E-04	.13E-01	.21E+00	
.50E+01	.99E-06	.46E-03	.21E+00	
.11E+02	.36E-07	.17E-04	.77E-02	
.23E+02	.13E-08	.60E-06	.28E-03	
.50E+02	.46E-10	.21E-07	.99E-05	
.11E+03	.17E-11	.77E-09	.36E-06	
.23E+03	.60E-13	.28E-10	.13E-07	
.50E+03	.21E-14	.99E-12	.46E-09	

As it can be easily seen, when the velocity of ventilation increases to 3 m/sec the vibration becomes too large.

The vibration of the elements of structure inside a tunnel can be even larger if there are resonance frequencies near 100-500 Hz.

The next question is vibration excitation caused by temperature ripple. The air cooling of equipment generates large temperature ripples in the turbulent air flow. Sharp change of the temperature of magnet surface generates mechanical kicks. These kicks are especially dangerous for long magnets. The estimation of transversal displacement of a tube with length l is the following:

$$\delta x = \frac{l^2}{8\,a\,\Delta}\,\delta_s\, k\delta T$$

$$\delta_s = (k_t/(2\rho c\omega))^{1/2}$$

$k=10^{-5}$ temperature expansion
δT-temperature ripple
a-radius of a tube
Δ-thickness of a wall
δ_s-thickness of temperature skin
k_t-heat conductivity
ρc-temperature capacities
ω-frequency

for $l=4$ m, $a=0.2$ m, $\Delta=10^{-2}$m, $\delta_s=10^{-3}$ m, $\delta T=1\ C^0$

$$\delta x = 2\ \mu m \qquad (!!!)$$

This type of vibration excitation is very dangerous in conditions when equipment-to-air heat exchange exists. In this conditions the temperature ripple is associated with the turbulent motion of air with different temperatures. For an estimation, one can write the spectral power of vibration associated with this effect :

$$\delta x_f^2 = \frac{l^4 \delta_s^2 k^2}{(8a\Delta)^2} * \frac{\Delta T^2}{f} * (U/(Rf)^{2/3} \qquad f > U/R$$

where, ΔT - the temperature difference between air and cooled equipment.

If $\Delta T = 10\ C^0$, noise on frequency near 1 kHz becomes too large. To decrease the excitation of vibration caused by this mechanism it is necessary to cover the quadruple with thermal shield to avoid its contact with air.

Yet another source of vibration is associated with flow of liquid in various tubes of the equipment cooling system. For its estimation let's try to calculate the vibration of a tube with very thick wall and water flowing inside.

Spectral power of vibration of inside surface of a tube with flowing liquid (μ^2/Hz)

Radius of a tube	(m)	0.01
flow density	(kg/m^3)	1000
density of tube material	(kg/m^3)	7000
wave velocity in tube material	(m/s)	3000

f(Hz)	U=.10 (m/s)	U=.32 (m/s)	U=1.00 (m/s)
10.0	.14E-05	.45E-05	.14E-04
19.9	.72E-07	.45E-05	.14E-04
39.8	.36E-08	.17E-05	.14E-04
79.4	.18E-09	.84E-07	.14E-04
158.3	.91E-11	.42E-08	.20E-05
315.8	.46E-12	.21E-09	.98E-07
630.0	.23E-13	.11E-10	.49E-08
1256.6	.12E-14	.53E-12	.25E-09
2506.6	.58E-16	.27E-13	.12E-10
5000.0	.29E-17	.13E-14	.62E-12

Amplitude of waves with frequency 100 Hz can increase by 0.03 micron for velocity of water 1 m/sec for a tube with very thick wall. For a thin wall tube this amplitude may increase as ratio R/Δ (Δ-thickness of a wall).

Vibration by act of ventilation

3-V=10.00
2-V= 3.16
1-V= 1 m/sec

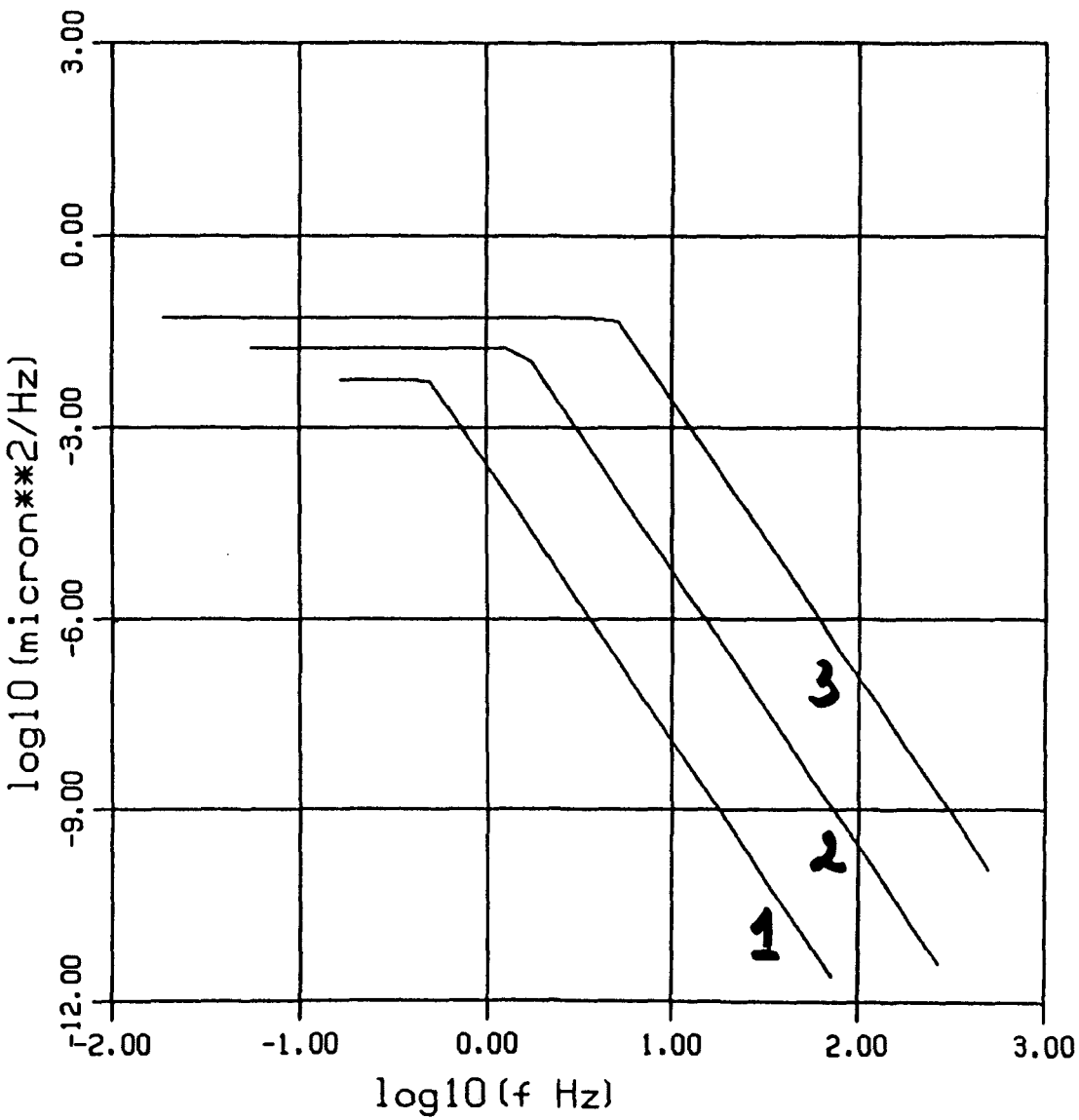

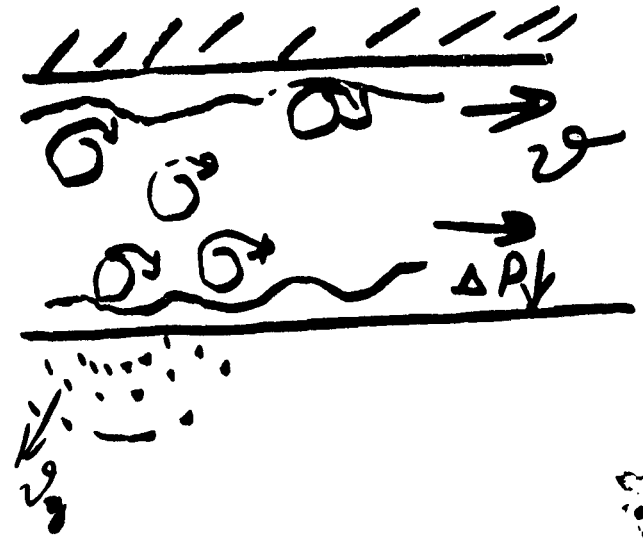

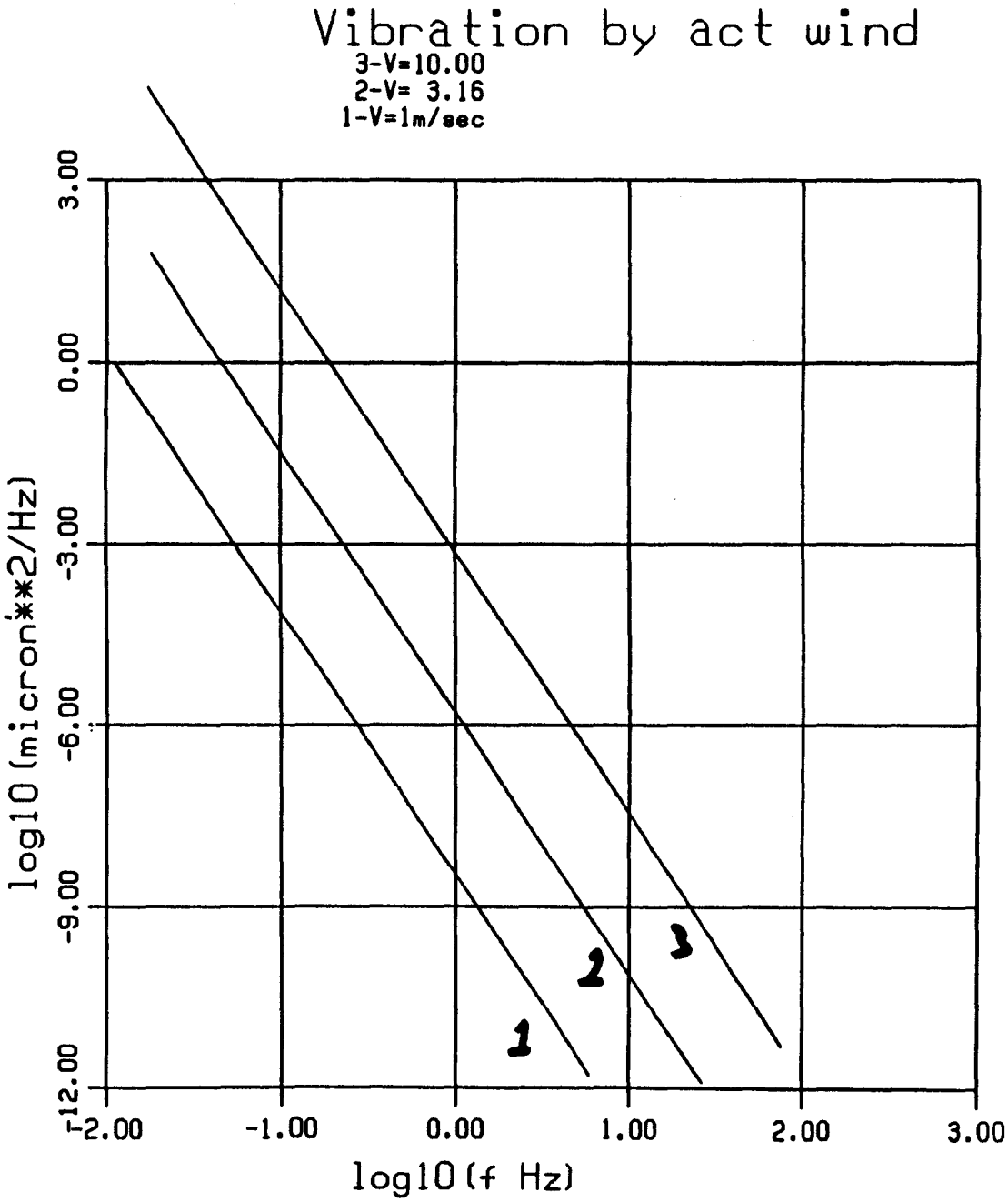
Vibration by act wind
3-V=10.00
2-V= 3.16
1-V=1m/sec
3.00
0.00
-3.00
-6.00
-9.00
-12.00
log10(micron**2/Hz)
-2.00
-1.00
0.00
1.00
2.00
3.00
log10(f Hz)
1
2
3

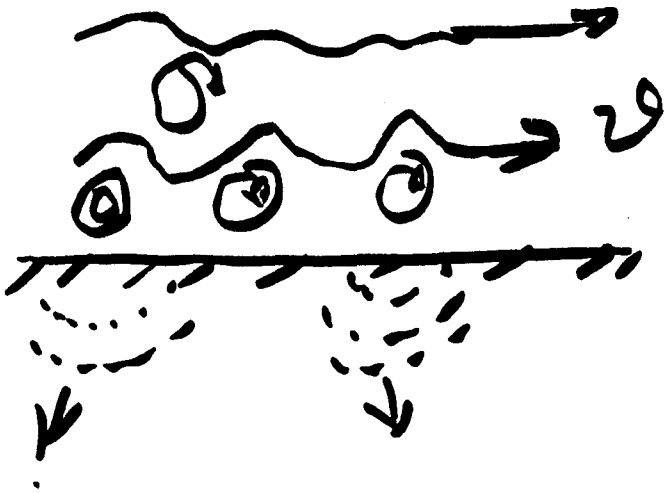

Axit. of vibr. by temp. ripple

2-dT=10 gr. C
1-dT=0

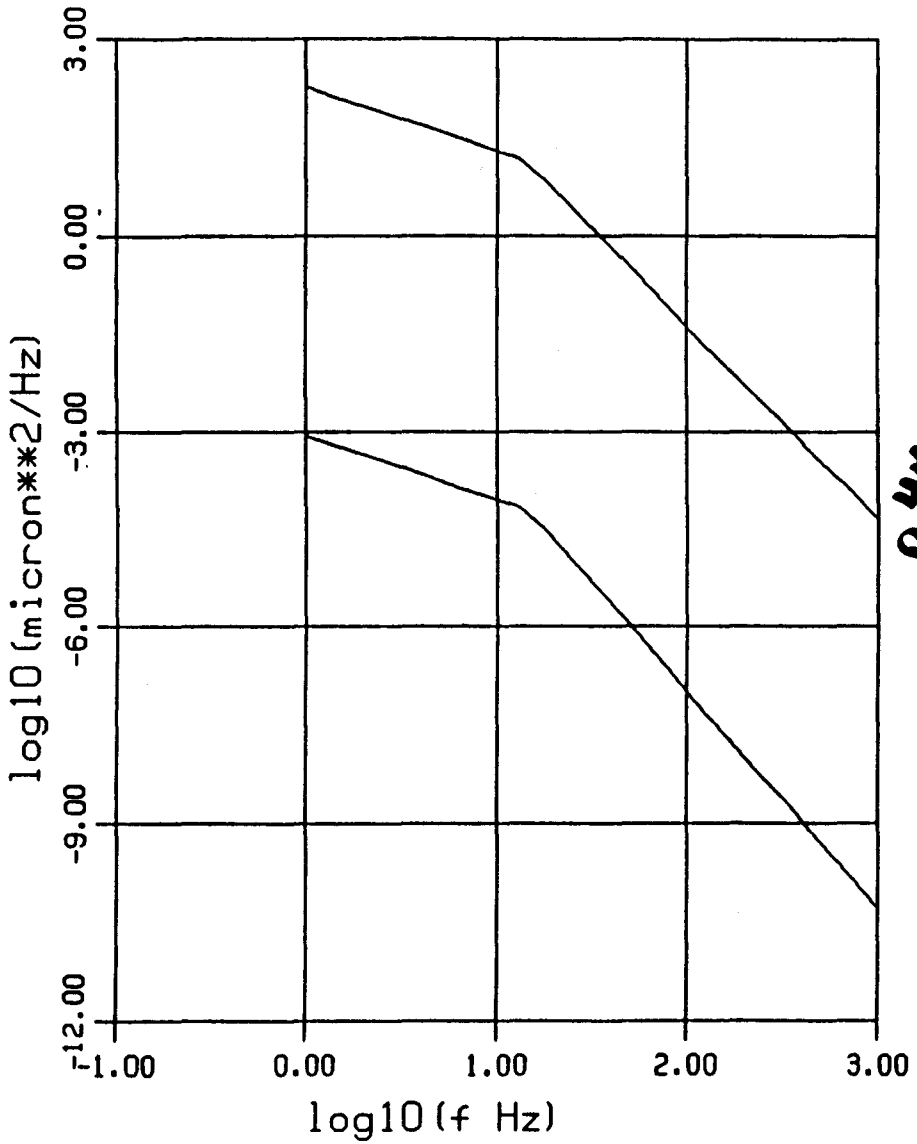

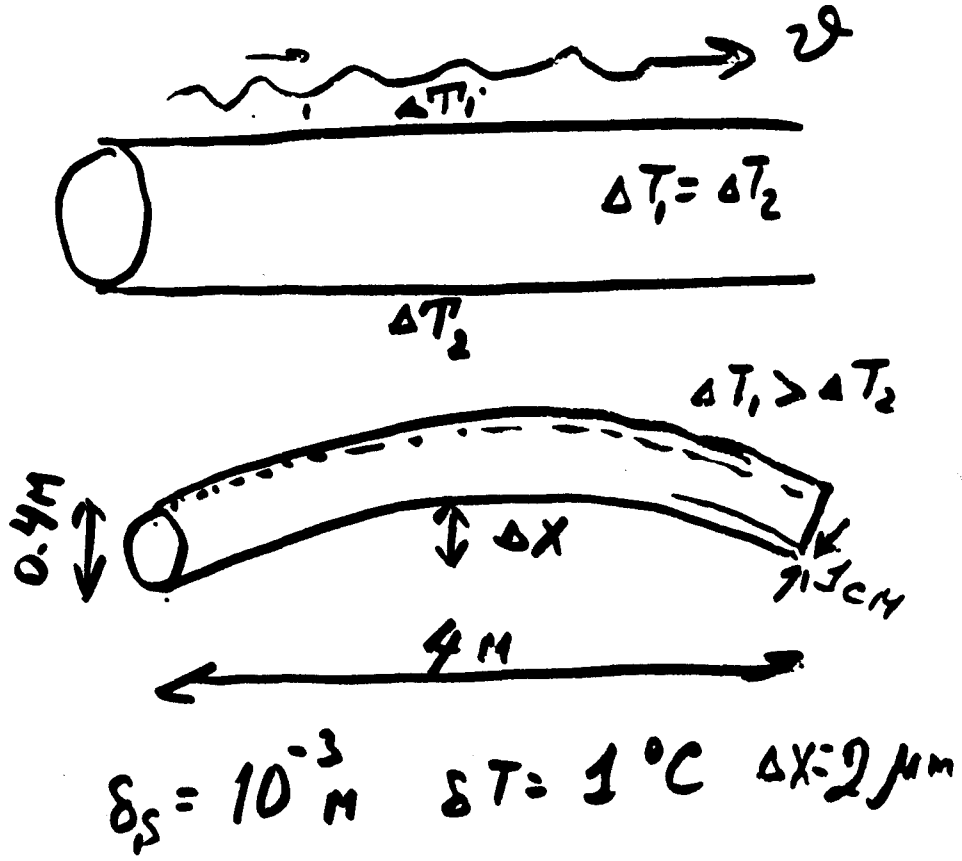

RECOMMENDATIONS

1. To make real measurements of the power spectrum and correlation functions along circumference of the SSC. To this end, it is necessary to simultaneously measure the signal of 6-10 geophons distributed along the ring. This will give a possibility to directly calculate the beam degradation.

2. To investigate the mechanical response of magnets and quadruples to vibrations at high-frequency band.

3. To investigate the cultural sources of noise: ventilation, compressors, cooling, traffic.

4. To study the low-frequency noise and high order resonances of proton beam. The requirement on fast feedback and the control of closed orbit systems

5. To measure slow relative ground motion of the points at the SSC site at the distance 20-100 km for direct estimate of orbit distortion .

SUMMARY

1. The level of ambient vibrations at quite conditions can influence the life time of the luminosity for running the SSC collider without feedback. (10^{-12} μm^2 /Hz at resonant frequency of betatron oscillation)

2. A powerful feedback system with dumping time 3 msec increase the tolerable level of vibration to 10^{-8} μm^2 /Hz.

3. The measurements show that cultural noise (ventilation, traffic, cooling flows of water, liquid nitrogen) can produce vibration at high frequency band (500-1000 Hz) of the order of magnitude 10^{-9} - 10^{-6} μm^2 /Hz.

4. The extrapolation of slow motion data from measured data from different sites for the SSC predicts too large displacements of quadrupoles -1 cm/1 year and 5 cm /25 years.

BEAM EFFECTS CAUSED BY GROUND MOTION AND VIBRATIONS

J M Peterson
SSC 11 Feb '92

A. INTRODUCTION

TWO BEAM EFFECTS PRODUCED BY GROUND MOTION AND OTHER VIBRATIONS:

1) DISTORTION OF THE CLOSED ORBITS OF THE TWO RINGS SO THAT THE TWO BEAMS DO NOT QUITE MEET HEAD-ON AT THE COLLISION POINTS

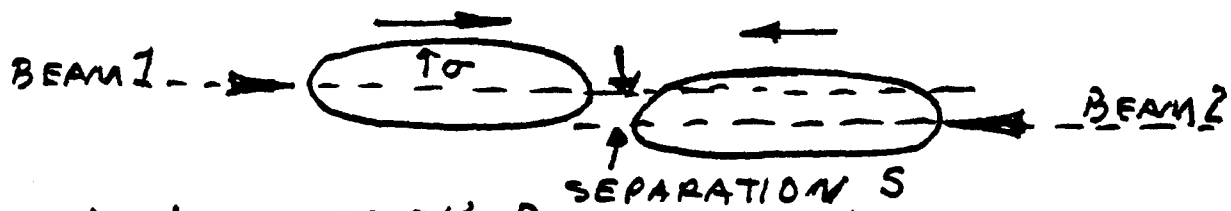

⇒ LUMINOSITY REDUCTION

$$\mathcal{L} = \mathcal{L}_0 \, e^{-\left(\frac{s}{2\sigma}\right)^2}$$

2) EMITTANCE GROWTH

$\Rightarrow$ LUMINOSITY REDUCTION

$$\mathcal{L} = \frac{N_B^2 f_{coll}}{4\pi\beta^* \epsilon}$$

WE SHALL REVIEW HOW THESE TWO BEAM EFFECTS ARE PRODUCED AND POINT OUT WHICH FACTORS ARE IMPORTANT.

B. CLOSED-ORBIT EFFECT

B1. EFFECT OF MOVING ONE QUADRUPOLE

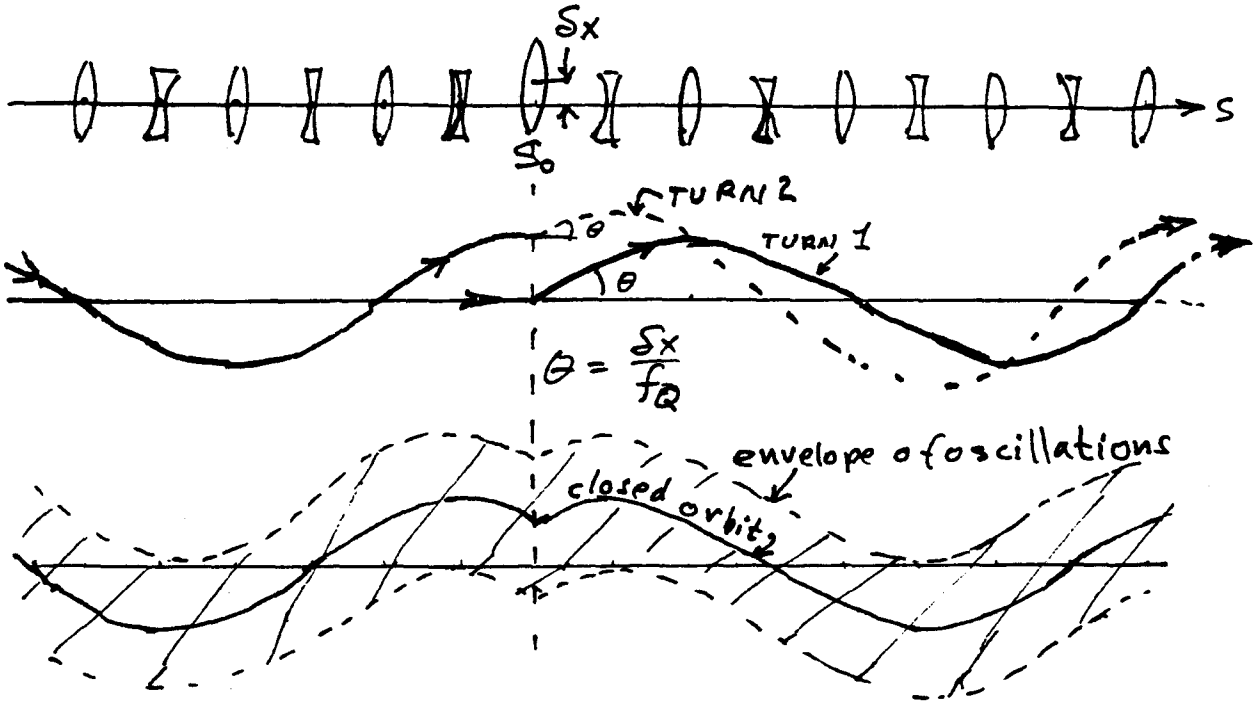

"CLOSED ORBIT" IS THE UNIQUE ORBIT THAT CLOSES ON ITSELF. BETATRON OSCILLATIONS ARE WITH RESPECT TO THE CLOSED ORBIT.

$$X_{c.o.}(s) = \frac{\delta x \sqrt{\beta_0 \beta_s}}{2 f_Q \sin \pi \nu} \cos(\phi_s - \pi \nu)$$

CONCEPT OF CLOSED ORBIT

-- COMPLETELY VALID FOR STATIC ARRAY OF QUADS.

-- A GOOD APPROXIMATION IF QUAD MOTION IS SLOW WITH RESPECT TO REVOLUTION FREQUENCY.

i.e., $f_{modulation} << f_0$ (= 3.44 KHz SSC)

THEN ALL BEAM BUNCHES SEE APPROXIMATELY THE SAME QUAD CONFIGURATION ON EACH TURN, & THUS THE SAME CLOSED ORBIT.

... <u>NOT</u> PERTINENT IF QUAD-MOTION FREQUENCY IS COMPARABLE TO REVOLUTION FREQUENCY,

BECAUSE THEN DIFFERENT BUNCHES SEE DIFFERENT QUAD CONFIGURATIONS.

MORE ON THIS WHEN CONSIDERING EMITTANCE GROWTH.

FACTORS AFFECTING THE CLOSED-ORBIT:

$$X_{c.o.}(s) = \frac{\delta x \sqrt{\beta_0 \beta_s} \cos(\phi_s - \pi\nu)}{2 f_Q \sin \pi\nu}$$

β_0 = 305m at F-QUAD ARC
53 m at D-QUAD ARC
8,000 m at Q2/Q3
Low-β TRIPLETS

f_Q = 64 m Q_F + Q_D ARC
~ 20 m Q1, Q2, Q3
Low-β TRIPLET

THUS A TRIPLET QUAD IS
ABOUT 20 TIMES MORE EFFECTIVE
IN PRODUCING CLOSED-ORBIT
AMPLITUDE.
BUT, THERE A LOT MORE ARC QUADS
THAN IR. QUADS

MORE ON THIS POINT LATER.

THE $\cos(\phi_s - \pi\nu)$ TERM SHOWS THAT A QUAD ON THE <u>FAR</u> SIDE OF THE RING CAN HAVE AS LARGE A CLOSED-ORBIT EFFECT AT A BEAM CROSSING AS A <u>NEARBY</u> QUAD. <u>ALL THE QUADS IN THE RING HAVE TO BE CONSIDERED.</u>

THE COS ( ) TERM INDICATES ALSO THAT INTERFERENCE AND RESONANCE EFFECTS ARE LIKELY WHEN MANY QUADS ARE VIBRATING, AND WHEN λ_G AND λ_β ARE RELATED BY INTEGERS.

IN PRESENT SSC LATTICE

$$\lambda_\beta = 720\ m$$

For $\lambda_G = \lambda_\beta$,

$$f_G = \frac{v_G}{\lambda_G} \approx \frac{1500\ m/s}{720\ m}$$

$$\approx 2\ Hz$$

B2. EFFECTS OF MOVING MANY QUADS

TOTAL CLOSED-ORBIT RESPONSE IS SIMPLE SUM:

$$\text{TOTAL C.O.}(s,t) = \sum_{\substack{i \\ \text{ALL} \\ \text{QUADS}}} \frac{\delta X_i(t)\sqrt{\beta_{0i}\,\beta_s}}{2 f_{Qi} \sin \pi\nu} \cos(\phi_{si} - \pi\nu)$$

ROSSBACH (DESY) CALCULATED CLOSED-ORBIT AMPLITUDE DUE TO PLANE GROUND WAVES TRAVERSING A ROUND FODO-LATTICE STORAGE RING

NOTE: THE POSSIBLE AMPLIFICATION OR ATTENUATION OF THE GROUND MOTION BY THE MAGNET SUPPORT STRUCTURES WAS NOT INCLUDED HERE.

QUAD MOTION = GROUND MOTION ASSUMED.

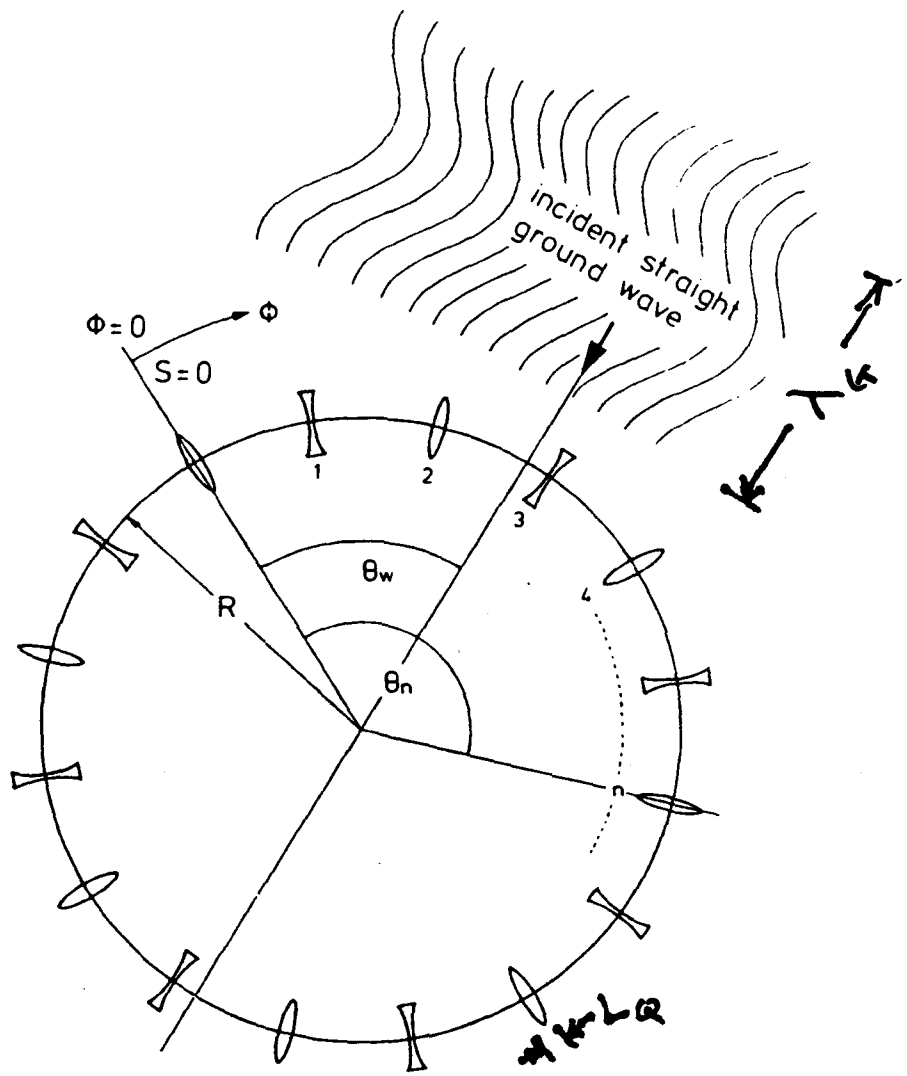

FIGURE 2 Sketch of geometry

POINT QUADRUPOLES ASSUMED IN CALCULATIONS.
i.e. $L_Q << \lambda_G$

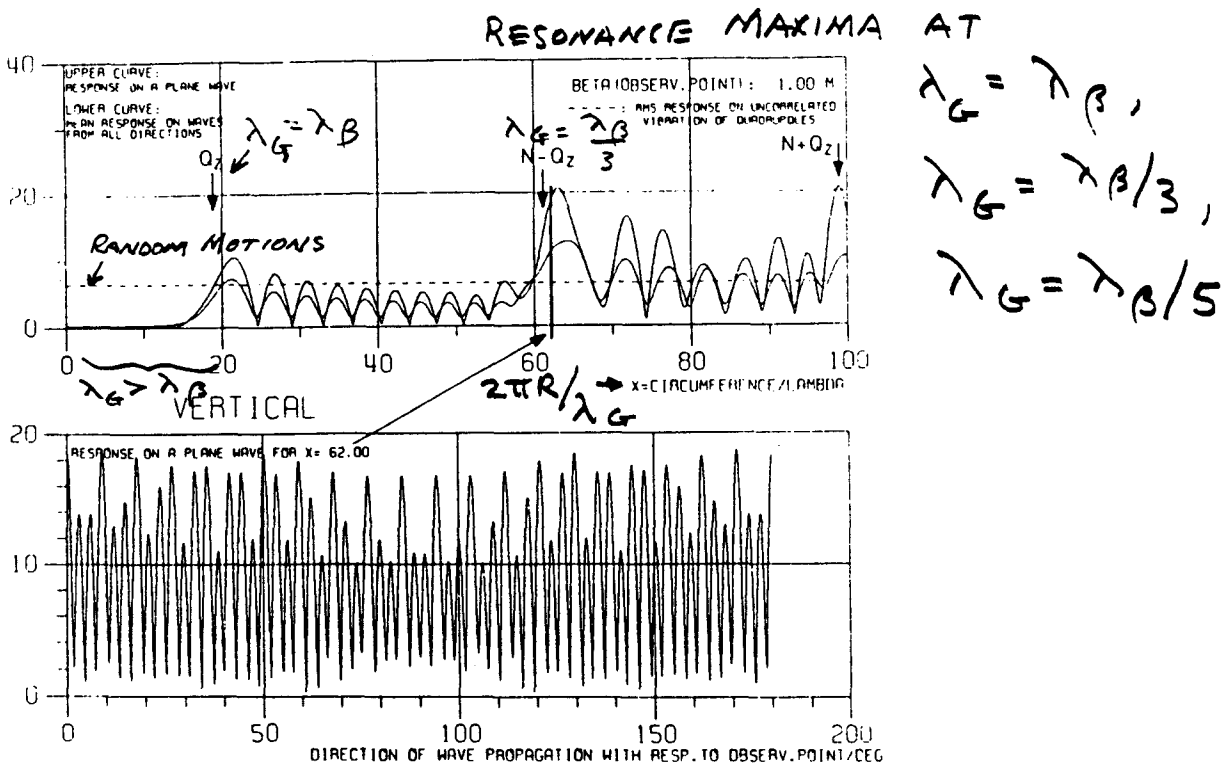

FIGURE 3 As an example for the vertical response to ground waves, parameters of the European Synchrotron Radiation Facility ESRF have been adopted: $C = 850$ m, $Q_z = 19.2$, $N = 80$. The upper plot shows R_z and R_z^{rms} as a function of C/λ for $\theta_w = 0$. It shows that the response increases whenever C/λ increases through the values Q_z, $N - Q_z$, $N + Q_z$, . . . , see Eq. (12). The lower plot shows that, for C/λ fixed, R_z depends on θ_w in a complicated way.

NOTE (1) ZERO RESPONSE FOR $\lambda_G > \lambda_\beta$
(IF WAVES ARE COHERENT).
(2) C.O. RESPONSE FOR RANDOM QUAD MOTION
≈ RESPONSE FOR COHERENT QUAD MOTION

BILLING (FERMILAB/SSC) HAS DONE SIMILAR CALCULATIONS FOR THE SSC LATTICE, INCLUDING THE IR REGIONS (1989 LATTICE), WITH SIMILAR RESULTS

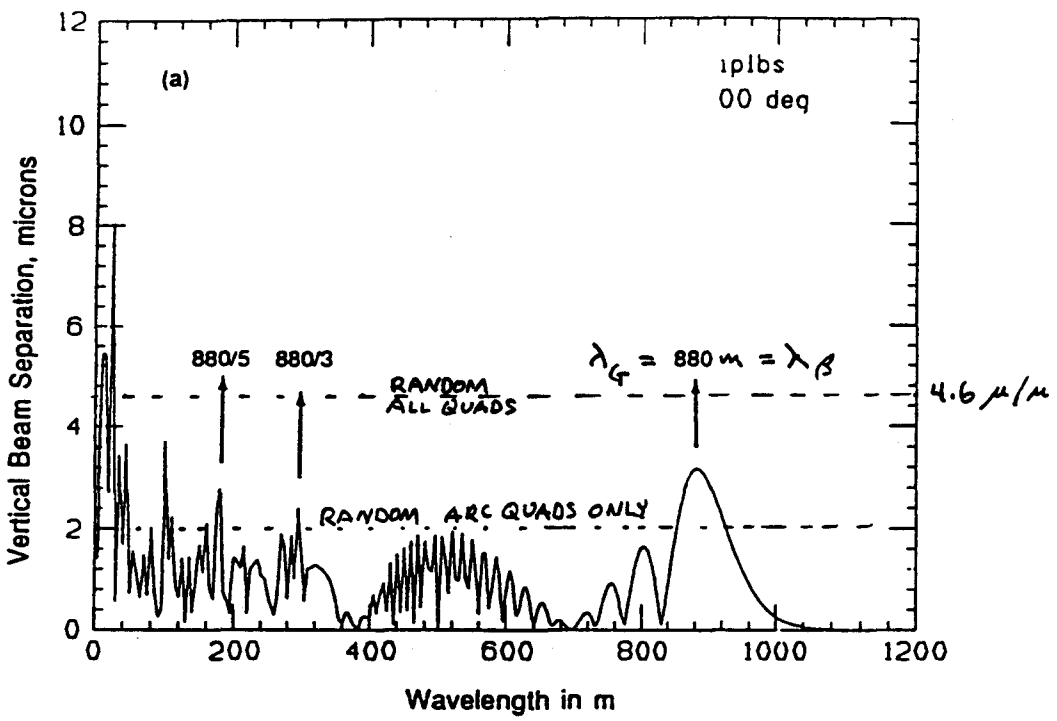

Fig. 5a. Vertical beam separation at a low-beta crossing caused by plane waves in the east/west direction (for the SSC ring long axis in the north/south direction). The ground waves have a 1-micron vertical displacement at each wavelength.

NOTE THAT IN THE SSC CASE, THE CLOSED-ORBIT EFFECT FOR RANDOM QUAD MOTION IS APPRECIABLY LARGER THAN FOR COHERENT PLANE GROUND WAVES OF SAME AMPLITUDE — DUE TO IR QUADS

NOTE THAT FOR RANDOM VIBRATIONS OF ANY FREQUENCY, THE RESULTANT RMS SEPARATION OF THE TWO BEAMS IN THE SSC AT A LOW-BETA INTERACTION POINT IS 4.6 MICRON PER MICRON OF QUAD MOTION.

SINCE $\mathcal{L} = \mathcal{L}_0 \; ^{-\left(\frac{S}{2\sigma}\right)^2}$

AND $\sigma = 5\,\mu$,

THE TOLERANCE ON QUAD MOTION IS <u>SUB-MICRON</u>, IF CORRECTION METHODS ARE NOT IMPLEMENTED.

THE OPTICS OF THE TWO SSC RINGS ARE ANTI-SYMMETRIC. THUS, WHERE EVER ONE BEAM SEES A FOCUSING QUAD, THE OTHER BEAM SEES A DEFOCUSING QUAD. THUS, EVEN IF THE TWO QUADS OF A VERTICAL PAIR MOVE IDENTICALLY, THEIR CLOSED ORBIT CONTRIBUTIONS ARE DIFFERENT DUE TO THE f_Q FACTORS

$$f_{QF} = -f_{QD}$$

AND THE $\sqrt{\beta_0}$ FACTORS

$$\beta_{0F} = 305 \text{ m (arc)}$$
$$\beta_{0D} = 53 \text{ m (arc)}$$

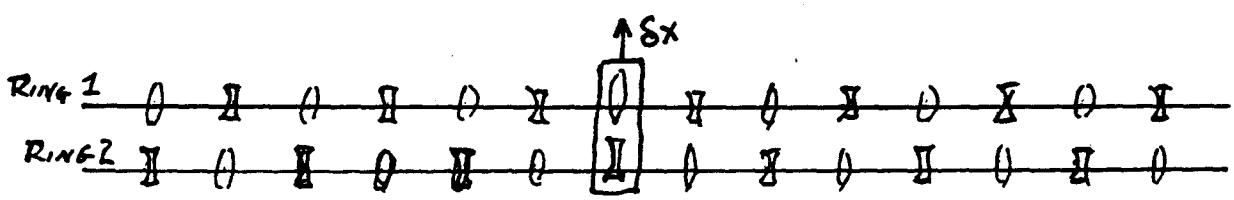

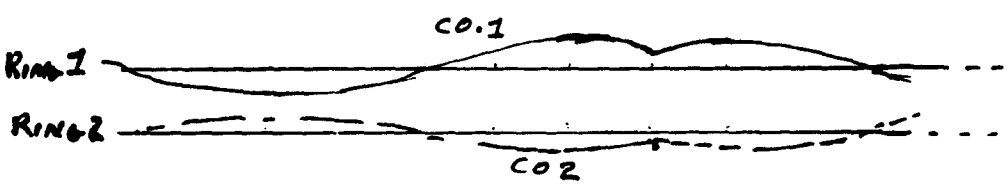

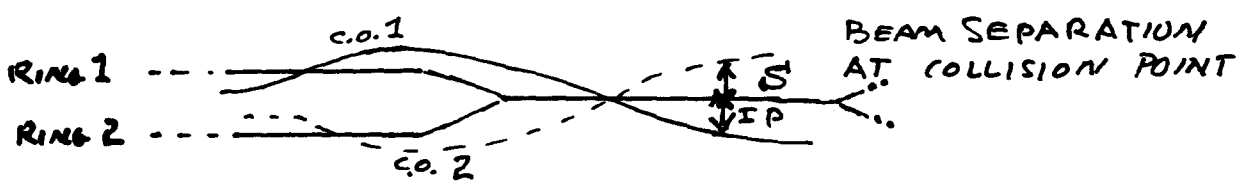

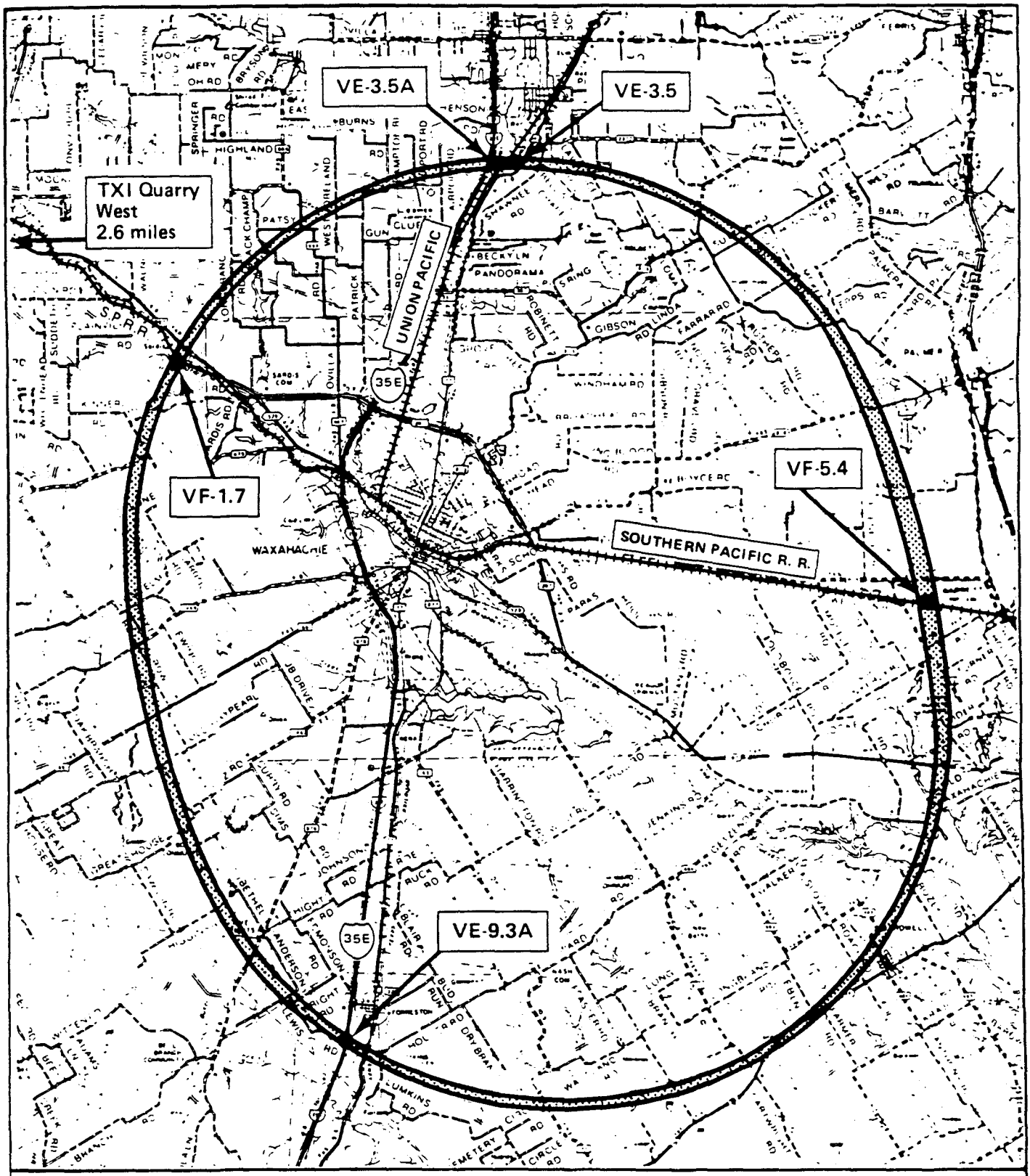

Scale (miles)

0 1 2 3 4

EXPLANATION

PROPOSED COLLIDER RING ALIGNMENT USED DURING FOOTPRINT VALIDATION

The Earth Technology Corporation

PROJECT NO. 87-888-0011

RTK Joint Venture

SSC Base Map
Showing Vibration Meaurement Locations

12-89

Figure 1-1

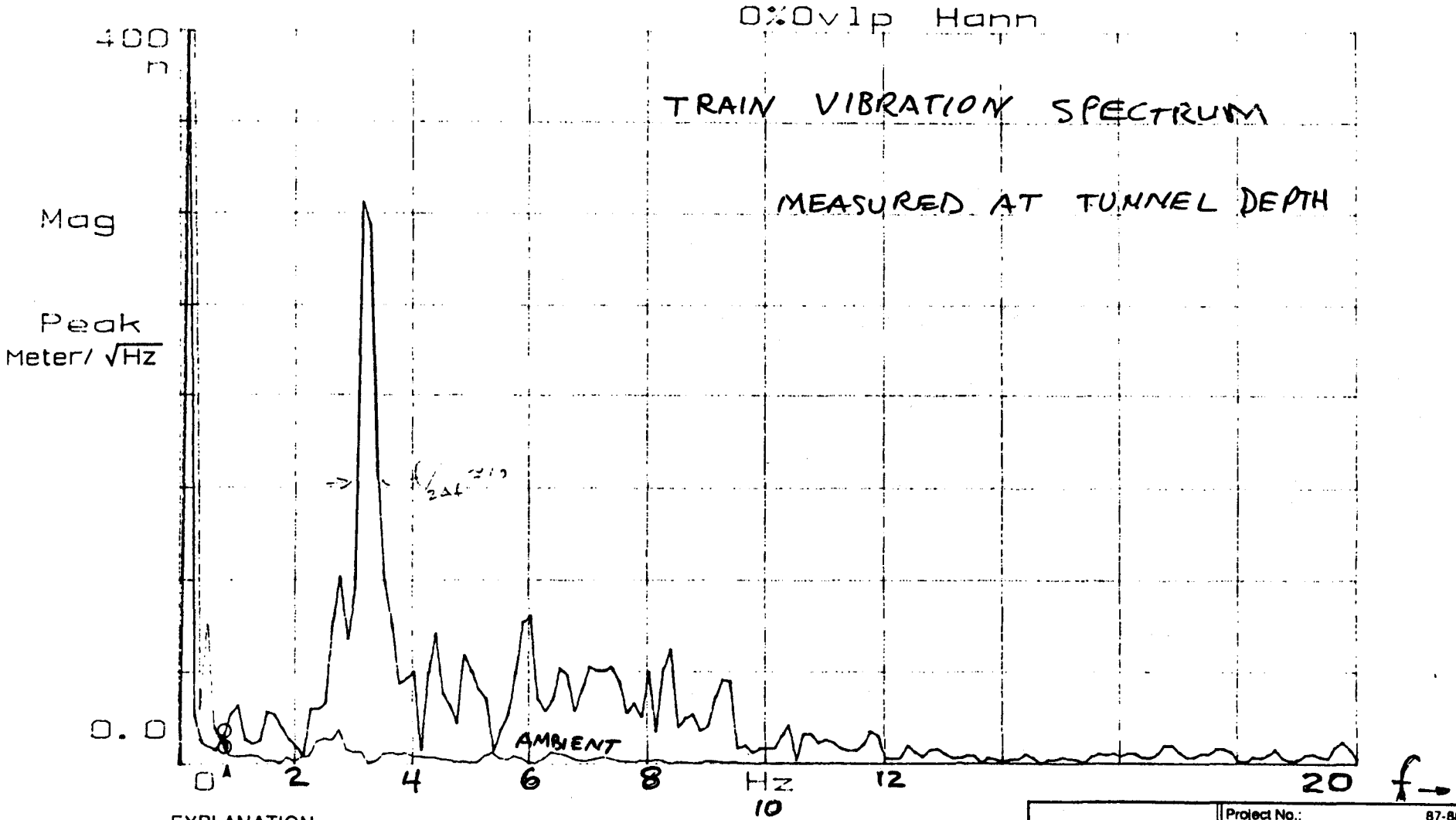

EXPLANATION

1 Hz Geophone Data

Red = Max. Train Vibrations Measured @ 261.5 feet (79.7 meters)

Black = Ambient Vibrations Measured @ 261.5 feet (79.7 meters)

Lower Frequency Limit of Calibration

The Earth Technology Corporation	Project No.: 87-888-0011
	RTK Joint Venture
Displacement Linear Spectrum Data Set 2	

GROUND VIBRATION SPECTRUM FROM QUARRY BLAST

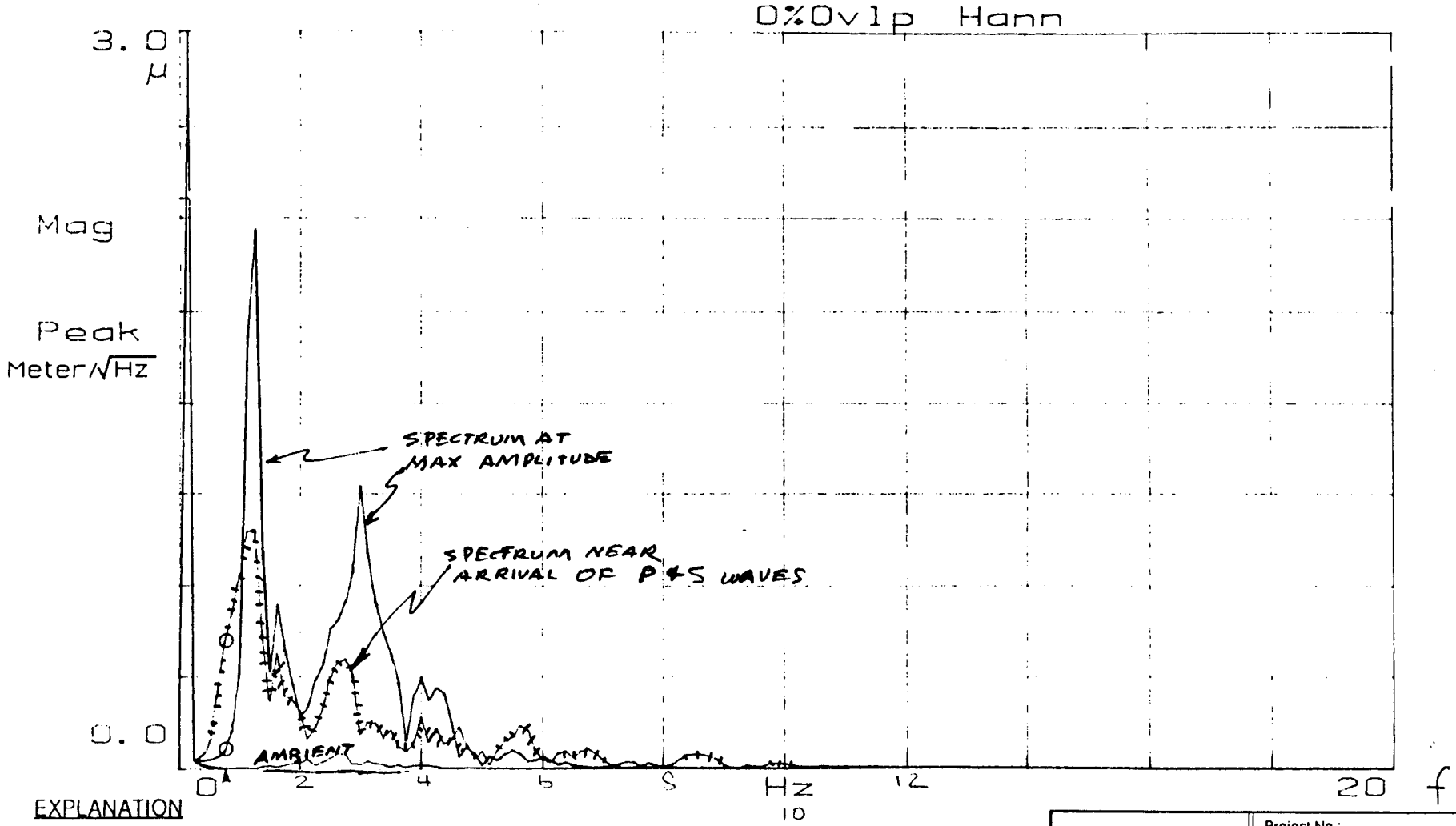

EXPLANATION

Geophone Depth in feet (meters)
1 Hz Geophone 4106 @ 62.0 (18.9)
Blue = Max. Amplitude Wave generated by Blast
Green = P & S Wave generated by Blast
Black = Ambient Vibration
Lower Frequency Limit of Calibration
Bandwidth = 0.187 Hz
(Compare with VE-3.5)

The Earth Technology Corporation

Project No.: 87-888-0011

RTK Joint Venture

Displacement Linear Spectrum
Site VF-1.7

12-89

Figure J 3

ANALYSIS OF MEASURED TRAIN DATA
(WORST CASE)

$$\Rightarrow S_{max_{TRAIN}} = 0.17\mu \quad (= .035\,\sigma)$$

EVEN WITH AMPLIFICATION OF 5X
DUE TO MAGNET SUPPORTS

$$\Rightarrow \Delta\mathcal{L}/\mathcal{L} < 1\%$$

MEASURED QUARRY-BLAST DATA
(WORST CASE)

$$\Rightarrow S_{max_{TRAIN}} = 2\mu \quad (= 0.4\,\sigma)$$

IF AMPLIFIED BY 5X DUE
TO MAGNET SUPPORTS

$$\Rightarrow \frac{\Delta\mathcal{L}}{\mathcal{L}} \cong 67\%$$

2-3 BLASTS PER WEEK

"DIFFUSION" MOTION OF QUADRUPOLES

PARCHOMCHUK HAS DESCRIBED A DIFFUSION-LIKE GROUND MOTION THAT SUGGESTS THAT RELATIVE QUAD MOTIONS ON THE ORDER OF 1 MICRON ARE POSSIBLE FOR THE SSC WITHIN SECONDS!

IF THIS MODEL APPLIES TO THE SSC, THIS WILL BE A VERY SERIOUS EFFECT AND WILL REQUIRE CORRECTIONS.

THIS WILL BE A SUBJECT FOR DISCUSSION IN OUR WORKING GROUP.

EMITTANCE GROWTH

OCCURS WHEN A BUNCH UNDERGOES A COLLECTIVE OSCILLATION, DUE TO SMEARING CAUSED BY A SPREAD IN THE BETATRON FREQUENCY.

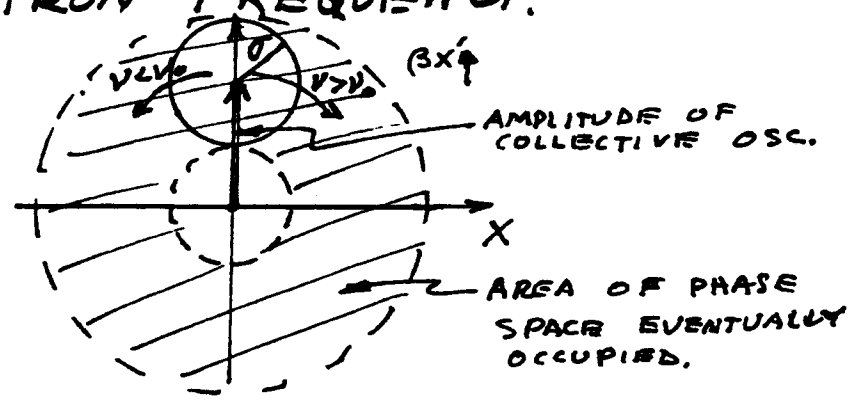

FOR A MORE MODEST AMPLITUDE OF COLLECTIVE OSCILLATION $(a < \sigma)$

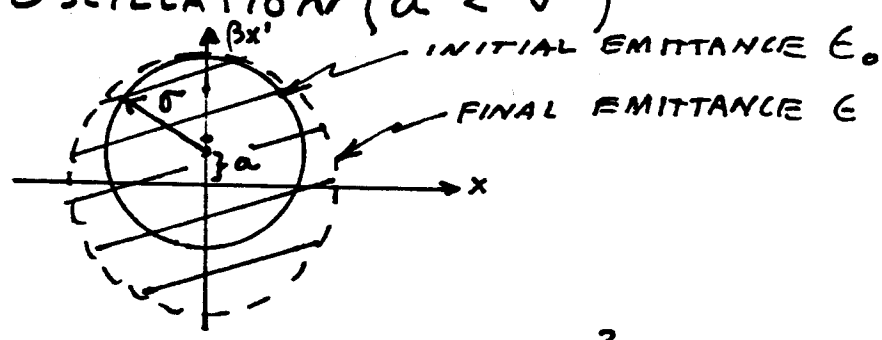

$$\frac{\varepsilon}{\varepsilon_0} \cong 1 + \frac{1}{2}\left(\frac{a}{\sigma}\right)^2$$

THIS EMITTANCE GROWTH HAS BEEN CALCULATED FOR 4 CASES:

THE COLLECTIVE-OSCILLATION AMPLITUDE HAS BEEN FOLLOWED FOR THE 3 TYPES OF GROUND-MOTION SPECTRA MEASURED AT THE SSC SITE:

1. TRAIN CROSSING (120 seconds)
   RESULT $\Delta\varepsilon/\varepsilon < 1\%$

2. QUARRY BLAST (30 seconds)
   RESULT $\Delta\varepsilon/\varepsilon < 1\%$

3. AMBIENT, LOW FREQUENCY, ~3 Hz (12 hr)
   RESULT $\Delta\varepsilon/\varepsilon < 1\%$

THE MOST INTERESTING CASE IS THAT POINTED OUT BY PARCHOMCHUK, STUPAKOV, SKRINSKY, ET AL - THE RESONANT TYPE GROWTH FROM AMBIENT VIBRATIONS WHICH MATCH THE BETATRON FREQUENCIES OF THE BEAM.

QUAD-VIBRATION FREQUENCIES THAT CAN RESONATE WITH THE BETATRON MOTION:

$$f_{RES} = [\nu] f_0 \,,\ (1-[\nu]) f_0 \,,\ (1+[\nu]) f_0 \,,\ (2-[\nu]) f_0 \,, \cdots$$

$$\nu = 123.28$$
$$[\nu] = 0.28$$
$$f_0 = 3.44\,\text{kHz}$$

$$f_{RES} = 960\,;\ 2{,}480\,;\ 4{,}400\,;\ 5{,}920\,;\ \ldots\ \text{Hz}$$

AT THESE FREQUENCIES THERE IS NO UNIQUE CLOSED ORBIT, DIFFERENT GROUPS OF BUNCHES OSCILLATE ABOUT DIFFERENT CENTRAL ORBITS.

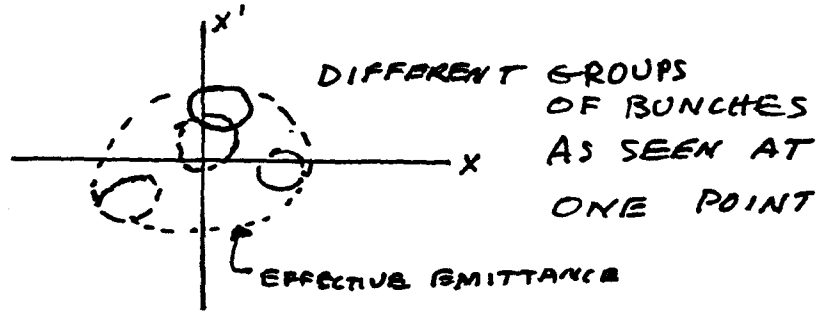

RESULT:

USING VIBRATION SPECTRA MEASURED IN THE UNK TUNNEL (PROTVINO), THE EMITTANCE DOUBLING TIME IS ~ 1 MINUTE!!

FURTHER CONSIDERATIONS

1. WHAT WILL BE NOISE LEVEL NEAR 1 kHz IN SSC TUNNEL?
   a) "QUIET" TUNNELS CAN BE LESS NOISY AT 100 Hz BY FACTOR 10^5.
   b) ALL PLUMBING AND MACHINERY ON SSC SITE MUST BE EXAMINED FOR VIBRATION LEVELS.

2. RESPONSE OF MAGNET SUPPORTS NEAR 1 KHz MUST BE INCLUDED IN ANALYSIS.

3. WAVELENGTH IN AUSTIN CHALK AT 1 KHz $\approx$ 1.5 meters < QUAD LENGTH (5-14m). POINT-QUADRUPOLE APPROXIMATION MUST BE RE-EXAMINED.

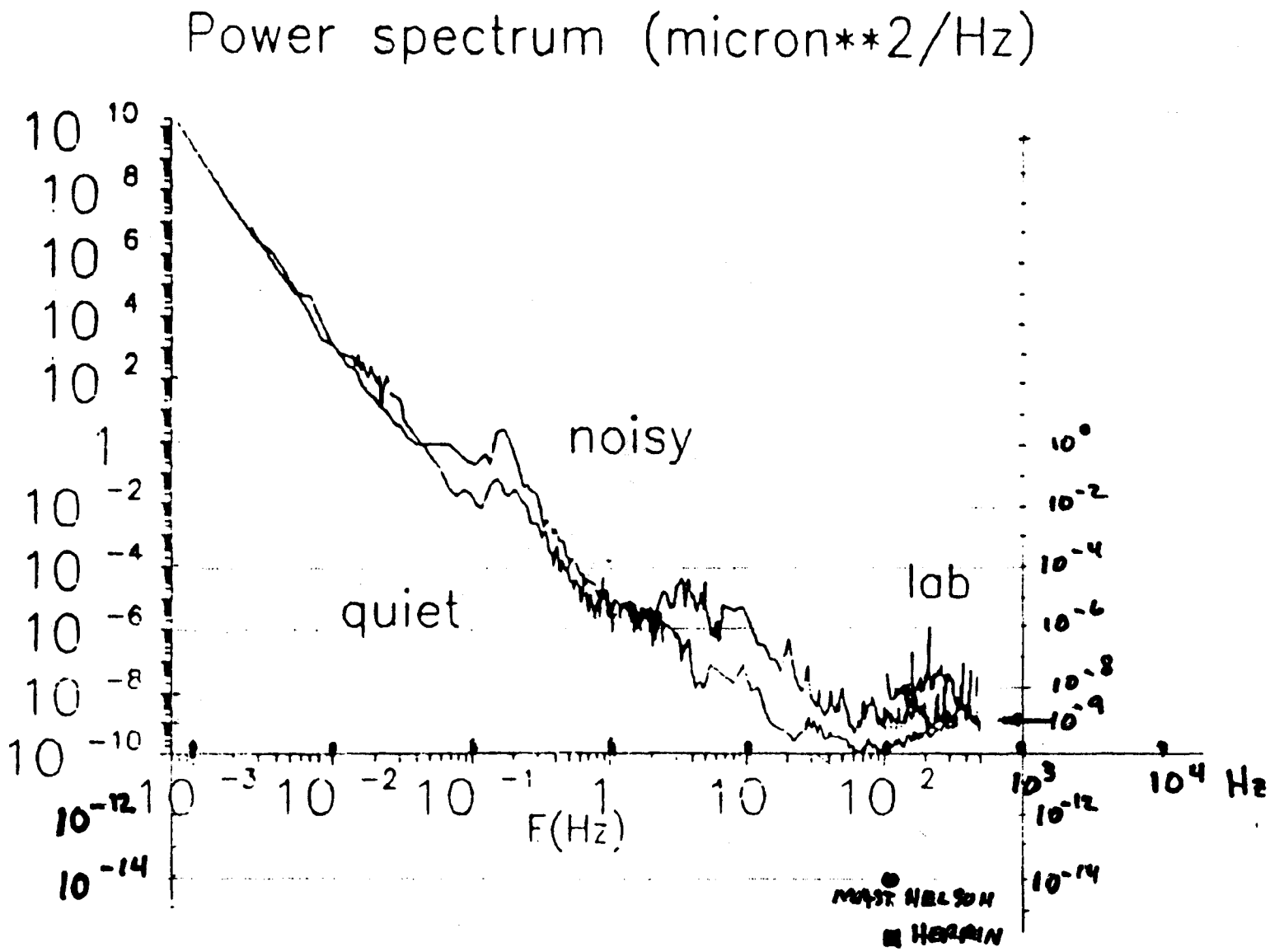
Power spectrum (micron**2/Hz)
noisy
quiet
lab
F(Hz)
Hz
MUST NELSON
HERMIN

4. FEEDBACK TO REDUCE AMPLITUDE OF COLLECTIVE OSCILLATION.

DAMPING TIME MUST BE LESS THAN TIME FOR DECOHERENCE (SMEARING).

DECOHERENCE OCCURS IN $(\sigma_\nu)^{-1}$ TURNS

RMS TUNE SPREAD $\sigma_\nu \approx 0.2\,\Delta\nu_{bb}$ TOTAL

$\approx 7.7\times10^{-4}$ (SSC)

$\therefore \tau_{DECOH} \approx 1.3\times10^{3}$ TURNS

$= 0.4$ sec

REQUIRES HIGH PICKUP SENSITIVITY.

OUR WORKING GROUP (BEAM BEHAVIOR) NEEDS HELP FROM FEEDBACK WORKING GROUP ON THIS PROBLEM.

EXCITATION OF BETATRON OSCILLATIONS AND EMITTANCE GROWTH DUE TO GROUND MOTION

GENNADY V. STUPAKOV
SSCL

Permanent address: Institute of Nuclear Physics,
Novosibirsk, Russia

Outline of the talk

- Introduction
- Resonant excitation of the betatron oscillations by a vibrating quadrupole
- Random offset beam-beam interaction
- Nonresonant emittance growth due to low-frequency noise
- Conclusion

HIGH VERSUS LOW FREQUENCIES

- Measured spectra of ground motions show vibrations in a wide range of frequencies with a spectral density decreasing with f.

- Beams respond differently on high and low frequency perturbations.

$$\text{Resonant frequency} = 0.22 \cdot 3.44 \text{ kHz} \approx$$

$$\approx 760 \text{ Hz}$$

Low frequency ~ few Hz or tens of Hz

High frequency ~ kHz

Resonant excitation of the betatron oscillations due to quadrupole vibrations

- One-dimensional linear model
- A thin quadrupole

x - position offset of a particle

$\eta = x/\sqrt{\beta(s)}$

$$\frac{d^2\eta}{dt^2} + \nu^2\Omega^2\eta =$$

$$= \nu\Omega\beta_0^{1/2}\frac{\Delta(t)}{f_q}\sum_{m=-\infty}^{\infty}\delta(t - mT)$$

$\Delta(t)$ - displacement of the quadrupole

f_q - focal length

Ω - revolution frequency $T = 2\pi/\Omega$

• An evident effect of low-frequency noise is the distortion of the closed orbit (Ng & Peterson).

• High-frequency noise resonantly excites coherent betatron oscillations of the beam (Parkhomchuk et al., Stupakov). This effect accumulates in time.

• Oscillations decohere due to nonlinear dependence of ν on the amplitude causing the growth of emittance.

• Nonlinearity of the betatron oscillations is mainly due to beam-beam interaction

$$\Delta\nu \approx \xi \approx 10^{-3}$$

Decoherence time

$$t_{\text{decoh.}} = \frac{T}{\Delta\nu} = 0.3s$$

Assume for a moment that $\Delta(t)$ is a harmonic function with the frequency ω

$$\sum_{m=-\infty}^{\infty} \delta(t - mT) = \frac{1}{2\pi} \sum_{n=-\infty}^{\infty} e^{in\Omega t}$$

The resonance occurs at

$$\omega + n\Omega = \pm\nu\Omega$$

The minimum ω is

$$\omega = (n - \nu)\Omega = 0.22 \cdot 3.44 \text{ kHz} = 760 \text{ Hz}$$

The averaged square of the amplitude of the betatron oscillations linearly grows with time

$$\langle x^2 \rangle = \frac{\pi \beta \beta_0 t f^2}{2 f_q^2} \sum_{n=-\infty}^{\infty} S(\Omega(\nu - n))$$

where the spectral density $S(\omega)$ is related to autocorrelation function $K(\tau)$

$$K(\tau) = \langle \Delta(t) \Delta(t-\tau) \rangle$$

$$S(\omega) = \frac{1}{\pi} \int_{-\infty}^{\infty} K(\tau) \cos(\omega \tau) d\tau$$

$$\langle \Delta^2 \rangle = \int_0^{\infty} S(\omega) d\omega$$

Implementations for the SSC

Low-β IR, $\beta = 0.5$m, $\sigma = 5\mu$m, $t = 10$ hours
The constraint

$$\sqrt{\langle x^2(t)\rangle} < 0.5\sigma$$

1. IR quadrupoles contribution

$\beta_0 \approx 8000$m, $f_q \approx 20$m

$$S(760\text{Hz}) < 10^{-12}\mu\text{m}^2/\text{Hz}$$

2. Lattice quadrupoles, N=800

$\beta_0 \approx 200$m, $f_q \approx 60$m

$$S(760\text{Hz}) < 0.8\cdot 10^{-12}\mu\text{m}^2/\text{Hz}$$

• There is an uncertainty factor in these estimations related with the support and magnet body response to the vibrations.

Random offset beam-beam interaction

- Assume that with the use of a feedback technique the betatron oscillations driven by magnet vibrations are stabilized at some level.

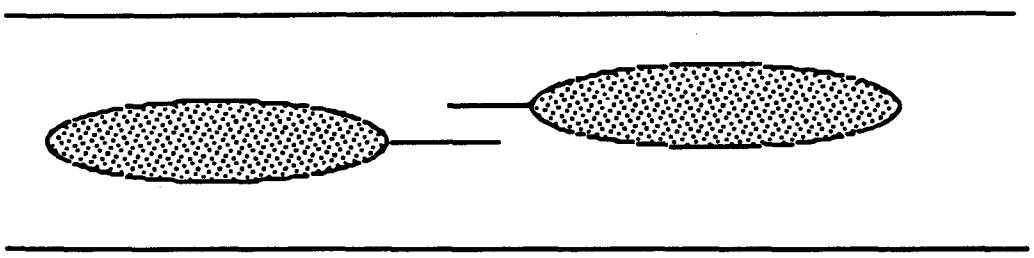

$\zeta(t) = x_1(t) - x_2(t)$ - is a random function of time

A MODEL

- One - dimension, x, p
- Strong - weak interaction
- Small displacements, $\zeta \ll \sigma$

Initial density profile of the bunches

$$n_0(x) = \frac{N_B}{\sqrt{2\pi} l d \sigma} e^{-x^2/\sigma^2}$$

l - length of the bunch
d - width of the bunch

The potential energy of interaction (in dimensionless units)

$$V(x,t) = 2T\xi h(x-\zeta(t)) \sum_{m=-\infty}^{\infty} \delta(t-mT)$$

$$h(x) = \int_0^x dy \int_0^y dz e^{-z^2}$$

$$\xi = \frac{N_B r_p \beta^*}{\sqrt{2\pi} d \sigma \gamma}$$

J - is the action variable

$$x = \sigma\sqrt{2J\beta/\beta^*}\,\sin\varphi,$$

$F(J)$ - is particle's distribution function

$$\frac{\partial\langle F\rangle}{\partial t} = \frac{1}{2}\frac{\partial}{\partial J}\langle(\Delta\dot{J})^2\rangle\frac{\partial\langle F\rangle}{\partial J}$$

$$\langle(\Delta\dot{J})^2\rangle = \frac{16\pi^3}{T}\xi^2 J\, e^{-J}\sum_{k=0}^{\infty}[I_k(J/2)+I_{k+1}(J/2)]^2\times$$

$$\times\sum_{m=o}^{\infty}[S(\omega_{km}^{(1)}) + S(\omega_{km}^{(2)})]$$

$$\omega_{km}^{(1)} = \Omega(\{\nu(2k+1)\} + m),$$

$$\omega_{km}^{(2)} = \Omega(\{1-\nu(2k+1)\} + m),$$

$$S(\omega) = \frac{1}{\pi}\int_{-\infty}^{\infty} K(\tau)\cos(\omega\tau)d\tau$$

$$K(\tau) = \langle\zeta(t)\zeta(t-\tau)\rangle$$

Luminosity dilution

$$\frac{\Delta\dot{\mathcal{L}}}{\mathcal{L}_0} = -39.1\frac{\xi^2}{T^2}S(\Omega\Delta\nu)$$

Low-β IR, $\sigma = 5\mu m$, $t = 10$ hours, $\Delta\mathcal{L} < 0.5$

$$S(760\text{Hz}) < 7.5\cdot10^{-7}\mu m^2/\text{Hz}$$

Defining displacement at the resonant frequency $\Omega\Delta\nu$ by

$$\delta x^2 = \Omega\Delta\nu\, S(\Omega\Delta\nu)$$

$$\delta x < 1.1\cdot10^{-2}\sigma = 5.5\cdot10^{-2}\mu m$$

Nonresonant effects of the low frequency noise

$$\frac{d^2\eta}{dt^2} + \nu^2\Omega^2\eta =$$

$$= \nu\Omega\beta_0^{1/2}\frac{\Delta(t)}{f_q}\sum_{m=-\infty}^{\infty}\delta(t - mT)$$

$\Delta(t)$ - is a slow function with characteristic frequency $\omega_{\text{noise}} \ll \Omega$.

$$z = \frac{1}{\sqrt{\beta_0}}(\eta - i\dot{\eta})$$

$$z_{\text{closed orbit}} = \frac{1}{2}\Delta(TN)\frac{e^{i\nu\Omega t - i(\mu N + \pi\nu)}}{f_q \sin \pi\nu}$$

$$N = \{\frac{\Omega t}{2\pi}\}$$

N is the number of the last kick at the moment t, TN is the moment of the last kick.

$$\Delta z(t) = z(t) - z_{closed\ orbit} =$$

$$= \frac{iTe^{i(\nu\Omega t-\mu N)}}{4f_q \sin^2 \pi\nu} \frac{d\Delta}{dt}(TN) + II$$

$$\frac{I}{z_{closed\ orbit}} \sim \frac{\omega_{noise}}{\Omega}$$

$$\frac{II}{z_{closed\ orbit}} \sim \left(\frac{\omega_{noise}}{\Omega}\right)^{n+1}$$

n is the number of the first nonzero derivative of $\Delta(t)$ at $t=0$.
For a smooth start, III is negligible.

A rough estimate of the emittance growth rate (Parkhomchuk et al.)

$$\frac{d\langle x^2\rangle}{dt} = \Delta z^2 \Delta\nu^2 \frac{\beta\beta_0}{T}$$

For $\Delta = 0.1\mu\text{m}$, $\Delta\nu = 10^{-3}$, $\omega_{noise} = 2\pi\times 1\text{Hz}$, $t = 10$ hours, $\beta_0 = 200\text{m}$

$$\langle \Delta x^2 \rangle = 2.4\times 10^{-2}\sigma$$

CONCLUSIONS

1. High-frequency ground motion (760Hz) will resonantly excite betatron oscillations in SSC to untolerable level. Due to nonlinear tune spread coherent oscillations would translate to increased emittance. Further studies are needed to clarify the role of magnets and supports mechanical response to ground motion. A sort of feedback is required to suppress the betatron oscillations.

2. Random setoff beam-beam interaction causes emittance growth of the beams. A tolerable level of beam displacements at the IR is about $5\times10^{-2}\mu m$ (at the frequency 760 Hz)

3. Nonresonant effect of the low-frequency ground motion mainly results in closed orbit distortion. However, further studies are necessary of nonlinear resonant interactions that can deteriorate the beam performance.

Emittance Growth Issues

K. Y. Ng

February 11, 1992

When the beam is kicked by

1. ground motion
2. Jestlein's beam centering scheme

the transverse emittance & longitudinal emittance may grow.

The mechanisms are smearing due to:

1. chromaticity & momentum spread
2. tune dependence on oscillation amplitude

We emphasize here on perturbation with "long" correlation time, not <u>random</u> perturbation

Train

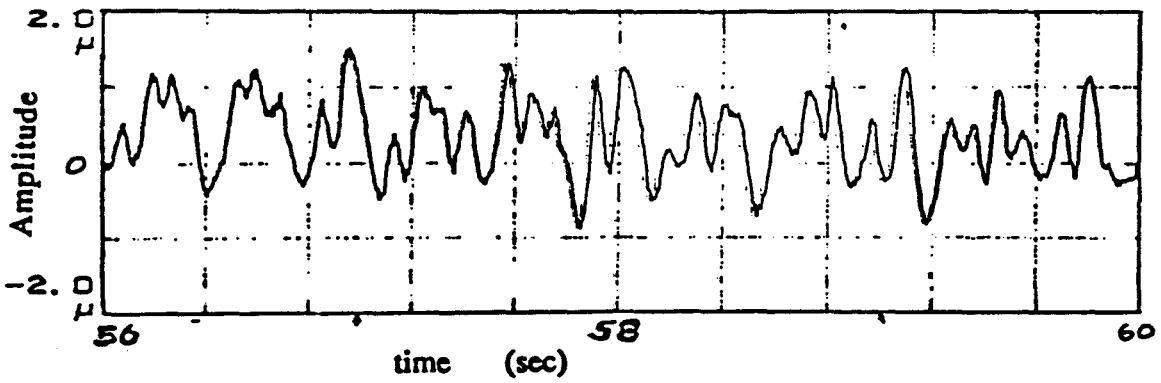

Figure 6. The Approximate Displacement Waveform Obtained by Integrating the Geophone Signal of Figure 2 and Applying the Average Geophone Calibration Constant.

Quarry blasts

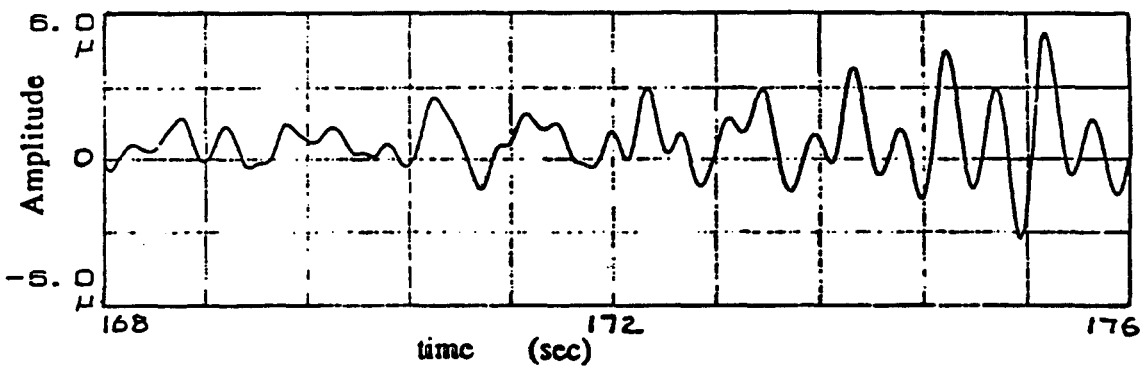

Figure 7. The Approximate Displacement Waveform Obtained by Integrating the Geophone Signal of Figure 4 and Applying the Average Geophone Calibration Constant.

Train

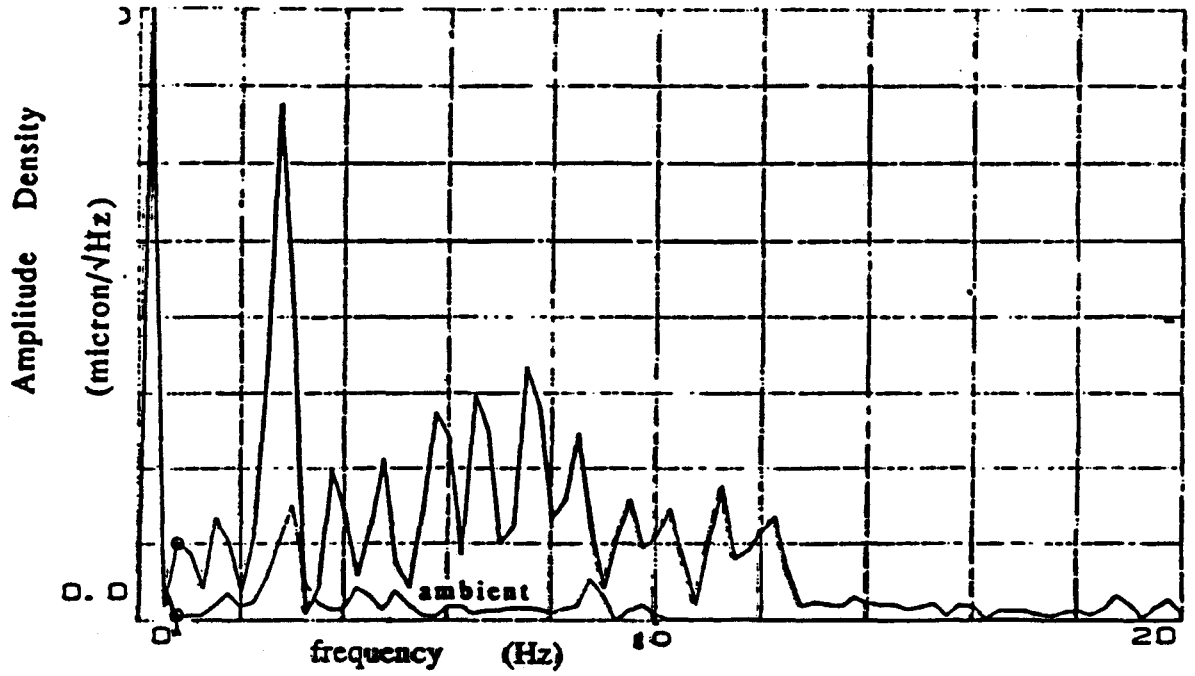

Figure 3. The Vibration Amplitude Spectrum Obtained by a Fast Fourier Transform of the Signal in Figure 2, Application of the Measured Geophone Calibration Curve, and Time-integration to Convert the Velocity Spectrum to a Displacement Spectrum. The units ($m/\sqrt{Hz}$) are due to the power-spectrum analysis that was employed—i.e., the square of the geophone signal was frequency analyzed.

Quarry blast

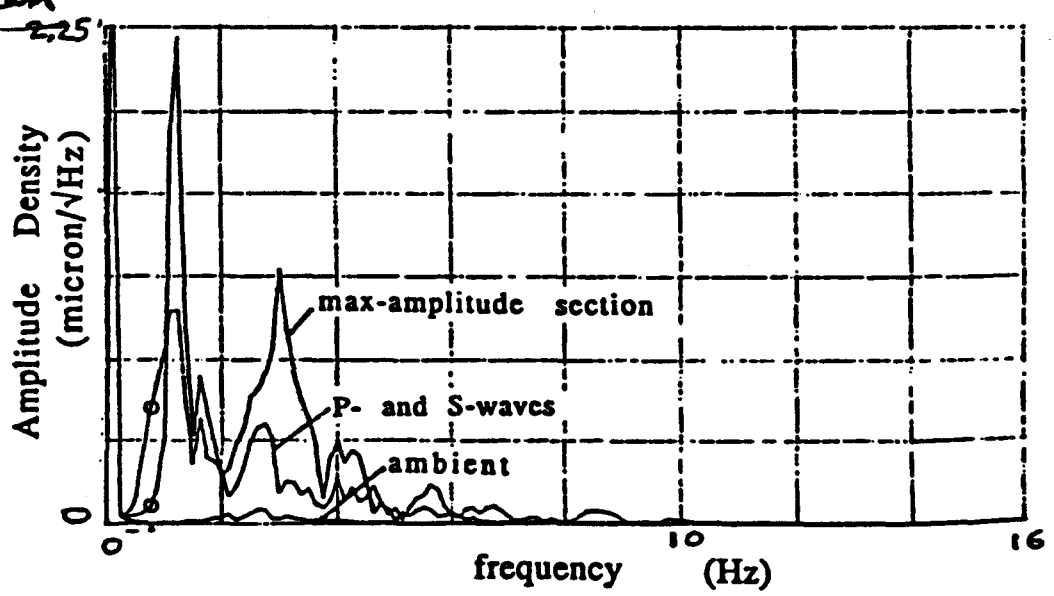

Figure 5. The Amplitude Spectrum Corresponding to the Geophone Signal in Figure 4.

Originally particle at $A_0 = |A_0| e^{i\phi_0}$

After first turn, it is kicked by $i a \sin 2\pi\nu_m$

beam displacement

$$\therefore \quad A_1 = A_0 e^{i2\pi\nu_0} + i a \sin 2\pi\nu_m$$

After N turns

$$\vec{X}_N = A_N = A_0 e^{i2\pi\sum_{j=1}^{N}\nu_j} + \sum_{j=1}^{N} i a \sin 2\pi\nu_m j \, e^{i2\pi\sum_{k=j+1}^{N}\nu_k}$$

1. Chromaticity Effects

$$\nu_k = \nu_0 + \Delta E \xi \sin\left(2\pi\nu_s k + \varphi_s\right)$$

here we neglect time dependence on amplitude

Can sum exactly. This is a breathing mode

Subtract center, then get max. breathing amplitude

$$\left|\vec{\hat{X}}_N\right| = \frac{b_m \beta_0}{f_Q} \frac{\pi \nu_m \xi \delta}{\nu_s \sin^2 \pi \nu_0} \qquad \text{max. at } \varphi_s = 0$$

$\downarrow$

a in above (beam displacement)

b_m quadrupole displacement

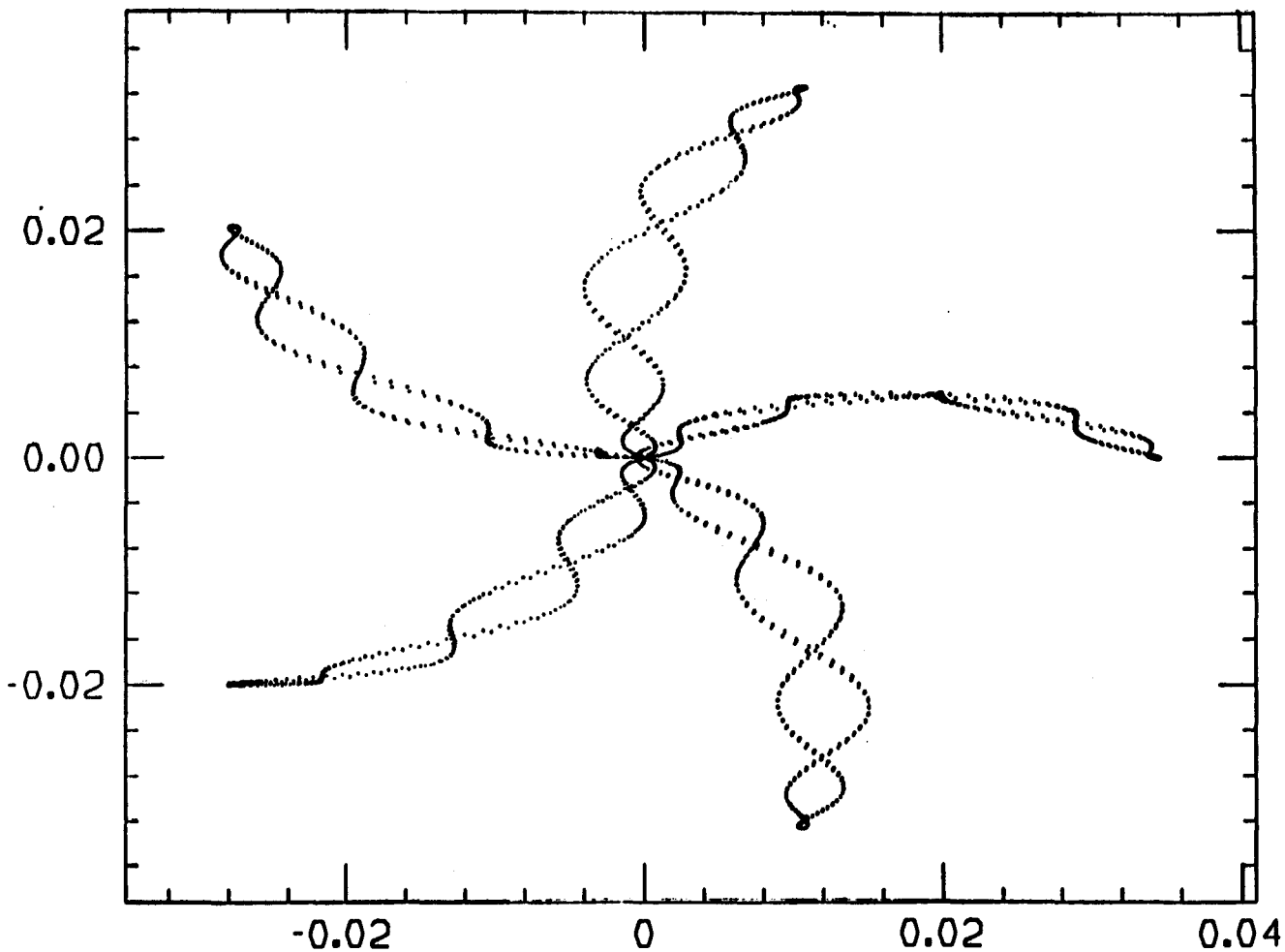

turn no. 1720, syn phase 0.000, rev freq 3440.00
pert freq 22.000, syn freq 4.000, tune 0.200, chrom 5.000

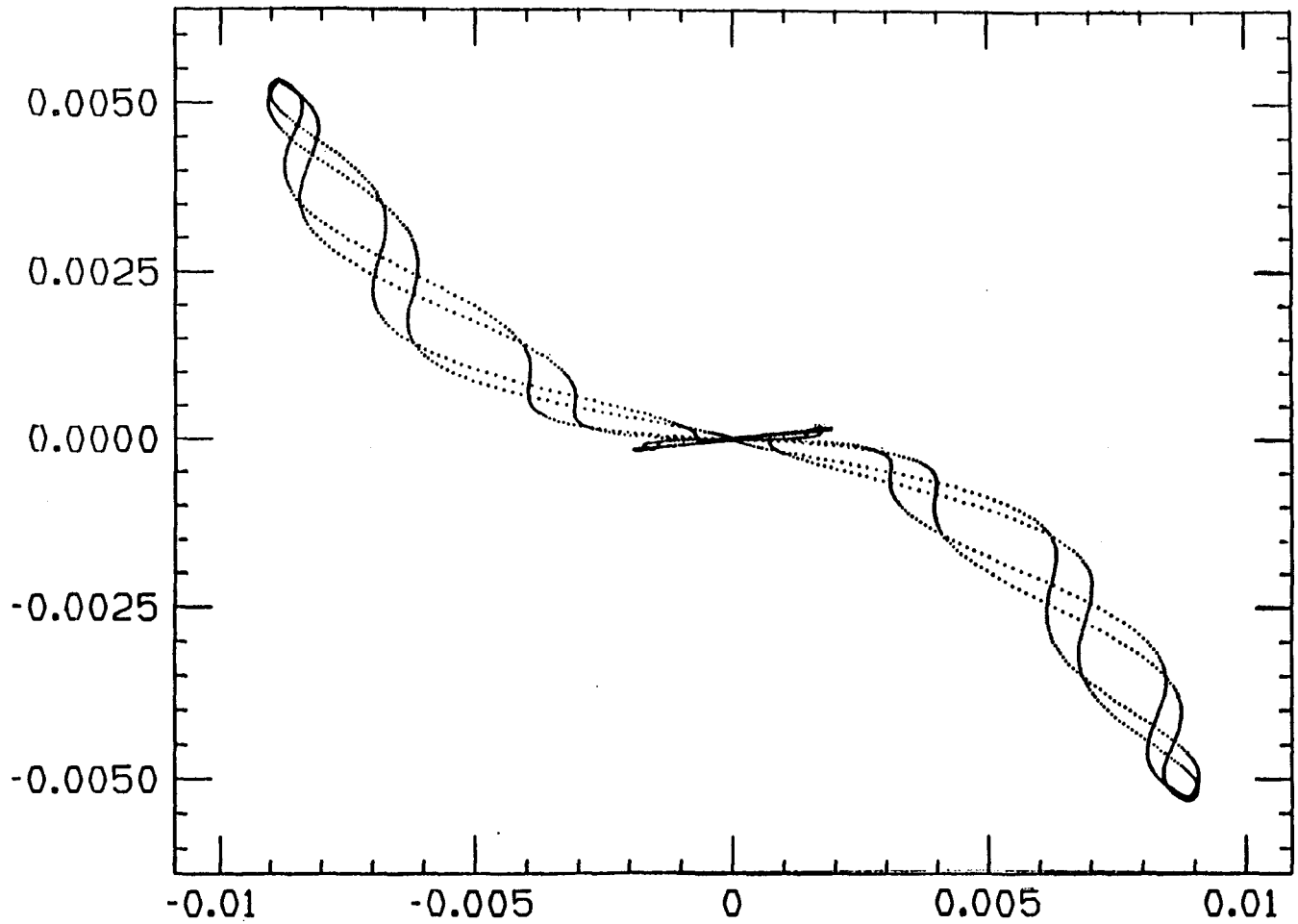

turn no. 1720, syn phase 0.250, rev freq 3440.00
pert freq 22.000, syn freq 4.000, tune 0.500, chrom 5.000

Jostlein's Beam Centering

Chromaticity $\xi = 5$

momentum spread $\delta = 6 \times \sqrt{6} \times 10^{-5}$

perturbed freq. $f_m = 20\,Hz$ beam rotation freq.

sym. freq. $f_s = 4\,Hz$

$$\beta_0 = 0.5\,m$$

beam-beam tune shift $\Delta\nu_{bb} = 0.004 \Rightarrow f_Q = 10\,m$

betatron tune $\nu_0 \approx 123.6$

then $$|\vec{\hat{x}}_N| = \frac{b_m \beta_0}{f_Q} \frac{\pi \nu_m \xi \delta}{\nu_s \sin^2 \pi\nu_0} = 5.77 \times 10^{-4}\, b_m$$

Since the perturbed amplitude is << σ of beam this breathing of emittance is negligible.

Ground Motion

Quarry Blast $b_m \sim .14\mu$ $.01\mu$ (horizontal)

$f_m \sim 1\,Hz$ $3\,Hz$

at F quad $\beta = 390\,m$ $f_Q = 80.8\,m$

For 1000 quads

$$|\vec{\hat{x}}| = \begin{cases} 0.097\, b_m & 1\,Hz \\ 0.292\, b_m & 3\,Hz \end{cases}$$

Train

b_m:	0.055μ	0.058μ	horizontal
f_m	3 Hz	7 Hz	

Here, assume only 20 neighboring quads are affected

$$|\vec{x}| = \begin{cases} 0.041\, b_m & 3\ Hz \\ 0.096\, b_m & 7\ Hz \end{cases}$$

Tune Dependence on Amplitude

Hamiltonian

$$H = \frac{p^2}{2} + \nu_\beta^2 \frac{x^2}{2} - x\,F(\theta) \qquad F(\theta) = a\nu_\beta \sin \nu_m \theta \sum_n \delta(\theta - 2\pi n)$$

Go to action-angle variables with $F_1(x,\phi) = -\frac{1}{2}\nu_\beta x^2 \tan^2\phi$

Then $\quad x = \sqrt{\frac{2J}{\nu_\beta}} \cos\phi$

$$H = \nu_\beta J - \sqrt{\frac{2J}{\nu_\beta}} \cos\phi\, F(\theta)$$

ν_β depends on J in general

Hamiltonian is integrable ?? [I believe so if $\Delta\nu_\beta \ll 1$, so there are no resonances]

$\therefore$ we can solve for an approximate constant trajecto.

$$\frac{d\phi}{d\theta} = \frac{\partial H}{\partial J} \cong \nu_{\beta_0} - 2b\left(\frac{2J}{\nu_{\beta_0}}\right) \qquad \text{if } \nu_\beta = \nu_{\beta_0} - b\left(\frac{2J}{\nu_{\beta_0}}\right)$$

$$\approx \nu_{\beta_0} \quad \text{if tune spread} \ll 1$$

$$\therefore \quad \phi = \phi_0 + \nu_\beta \theta$$

$$\frac{dJ}{d\theta} = -\frac{\partial H}{\partial \phi} = -\sqrt{\frac{2J}{\nu_\beta}} \sin\phi\, F(\theta)$$

[Dropping the "o" in ν_{β_0}]

Look every perturbation period

$\therefore$ final $\theta = 2\pi N = 2\pi \dfrac{n_0}{\nu_m}$ $\qquad$ n_0 an integer

$$\Delta \sqrt{\frac{2J}{\nu_\beta}} = \frac{a}{2} \sum_{n=0}^{N} \left[\cos(\phi_0 + 2\pi \nu_- n) - \cos(\phi_0 - 2\pi \nu_+ n) \right]$$

$$\nu_\pm = \nu_\beta \pm \nu_m$$

$$A = \sqrt{\frac{2J}{\nu_\beta}}$$

$$\Delta A_N(\phi) = \frac{a \sin 2\pi \nu_m}{4 \sin \pi \nu_- \sin \pi \nu_+} \left[\sin \phi - \sin \phi_0 \right]$$

$$\phi - \phi_0 \simeq 2\pi \nu_\beta N$$

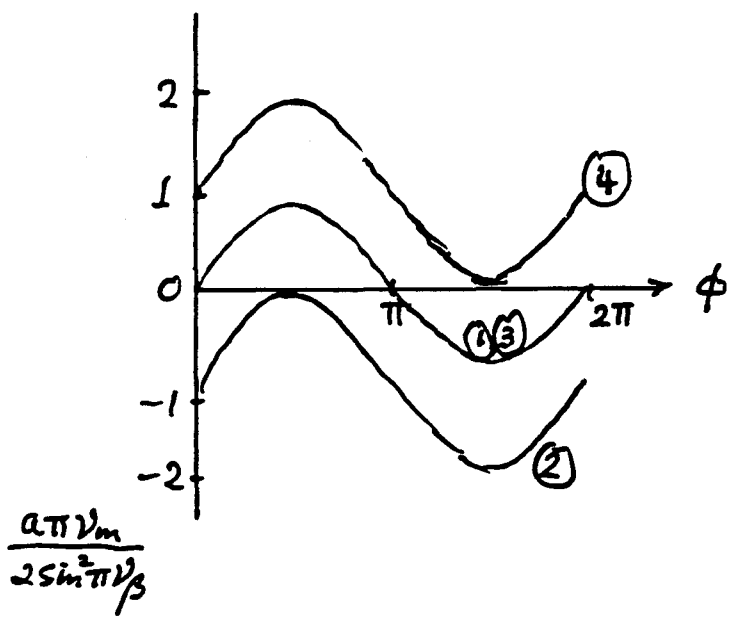

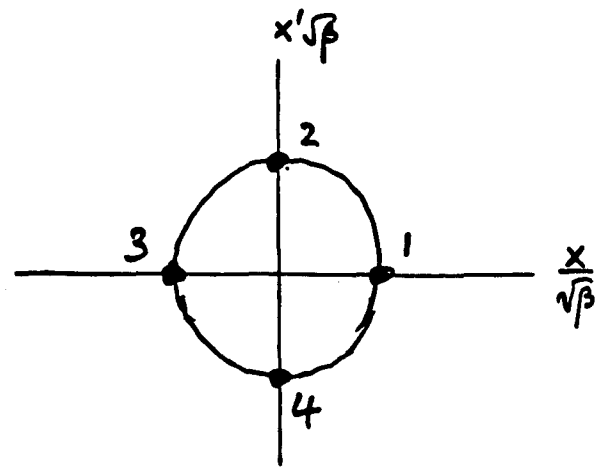

Amplitude vs phase
showing invariant curves which are almost independent of detuning

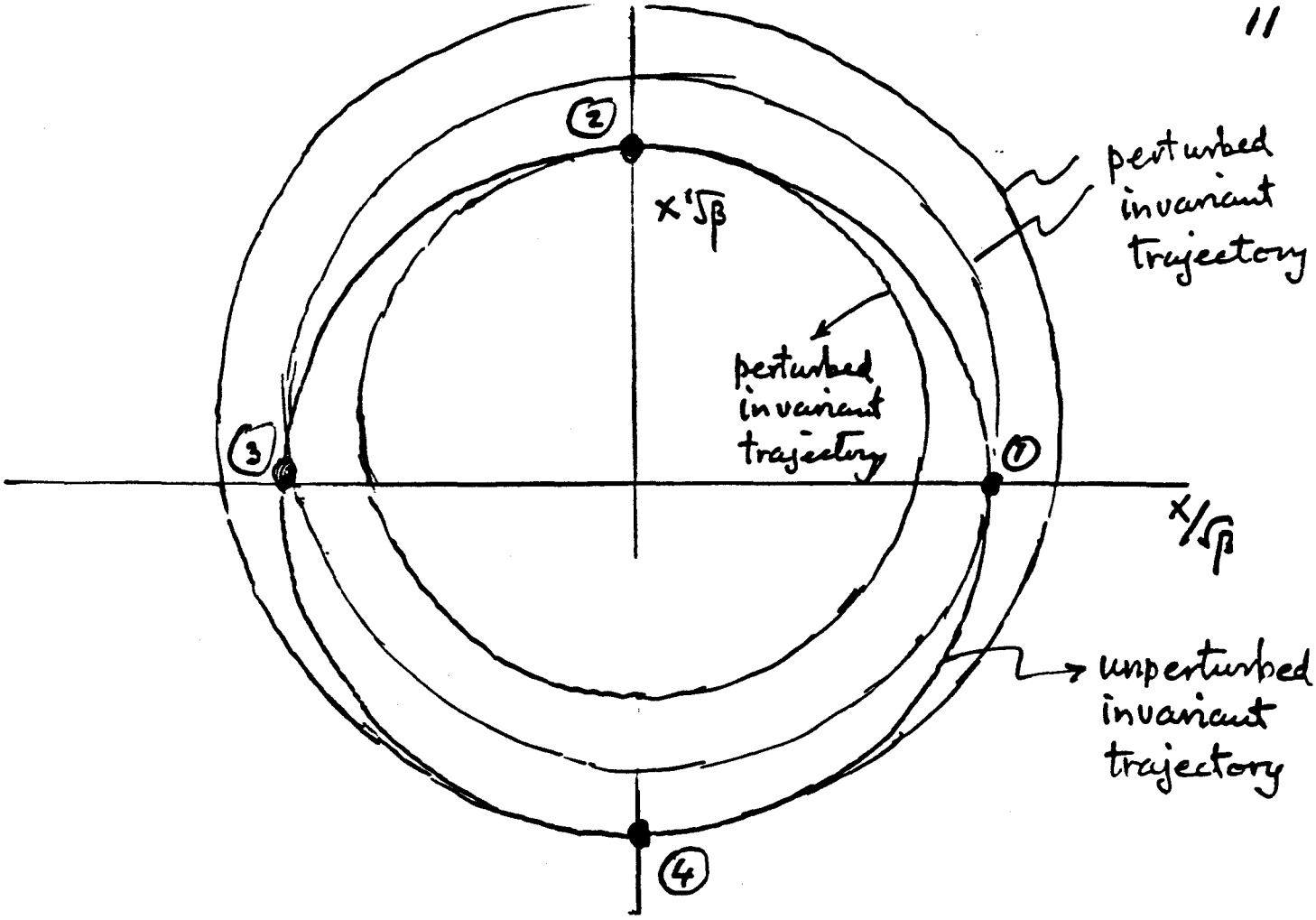

If ν_β is constant there is no growth in emittance

If ν_β depends on amplitude, phase difference between ③ & ④ will be less & less, & emittance increases ∴ final emittance is the area of big "circle"

$$\boxed{\frac{\Delta \varepsilon}{\varepsilon_0} = \frac{a \pi \nu_m}{A_0 \sin^2 \pi \nu_\beta}}$$

Note: $\frac{a \pi \nu_m}{2}$ = average increment kick per turn

Example: initial amp. $A_0 = 1$
kick amp. $a = 0.2$
perturbing tune $\nu_m = 1/172$

$\Delta\varepsilon/\varepsilon_0 = 0.004$
Time to reach ½ growth limit can be estimated

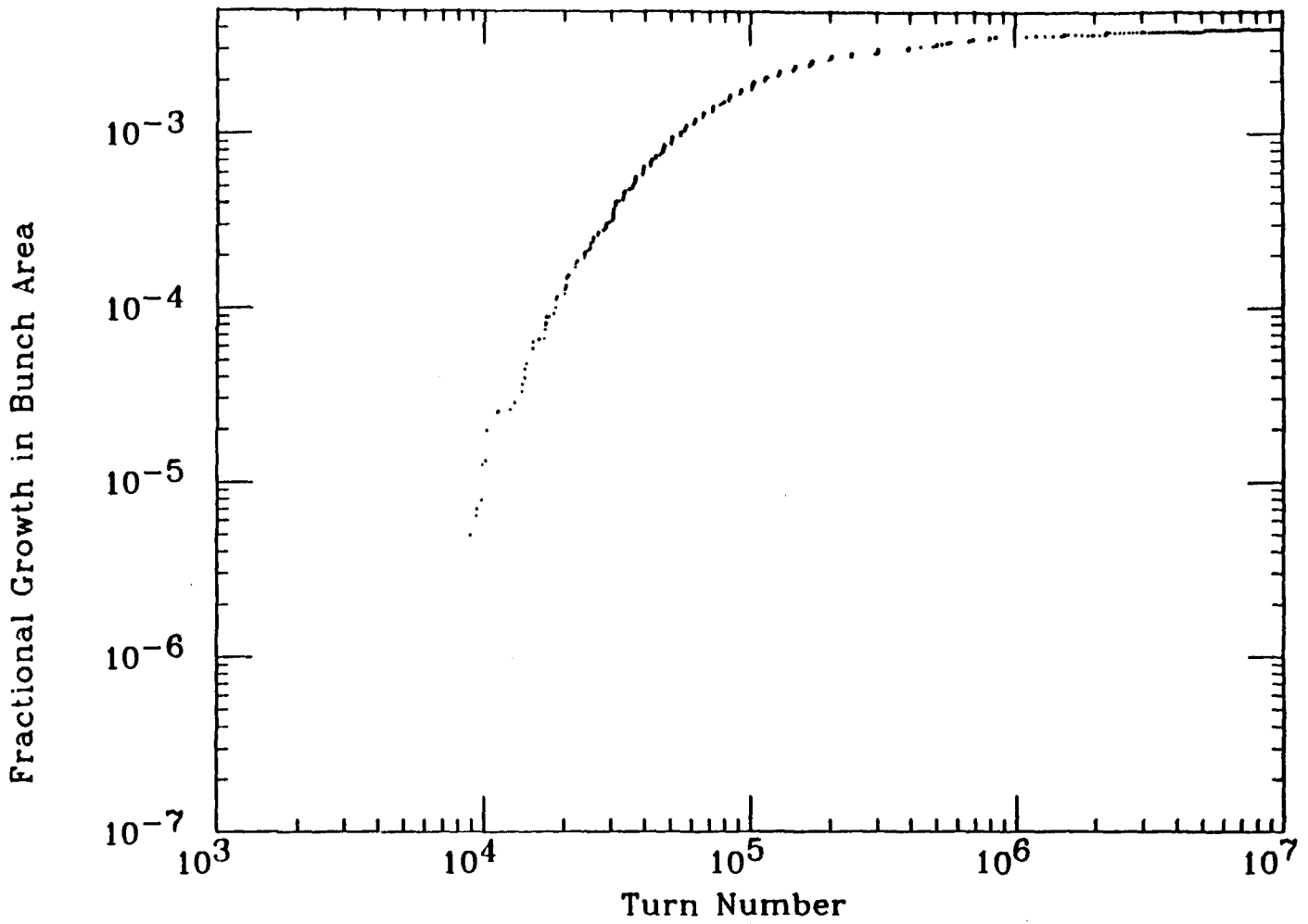

No. of particles 201, tune 0.400, detuning 0.00100, kick 0.2000, f_m 20.00 Hz

Jostlein's Beam centering scheme

$$a_m = \frac{b_m \sqrt{\beta_0}}{f_Q}$$

b_m = rotation amplitude

f_Q = focal length of equivalent quad.

$f_m \sim 20$ Hz (rotational freq)

then $$\frac{\Delta\epsilon}{\epsilon} = \frac{b_m}{x_{max}} \frac{\beta_0}{2 f_Q} \frac{\sin 2\pi\nu_m}{\sin^2 \pi\nu_0} = 0.001 \frac{b_m}{x_{max}}$$

Sometimes the modulation stops at a time when the amplitude is largest. Decoherence gives

$$\frac{\Delta\epsilon}{\epsilon} = \frac{b_m}{x_{max}} \frac{\beta_0}{f_Q} \frac{1}{\sin \pi\nu_0} = 0.026 \frac{b_m}{x_{max}}$$

Detuning from simulation by Yan

$$\nu_\beta = \nu_0 - \alpha A_0^2 \qquad \alpha = 1.87 \times 10^4 \, m^{-1}$$

$x_{rms} = 0.12$ mm at F quad $\Rightarrow$ $A_0 = 6.07 \times 10^{-6} \, m^{\frac{1}{2}}$

$$\text{Half growth time} = \begin{cases} 58 \left(\frac{x_{max}}{b_m}\right) \text{ hours} \\ 9 \left(\frac{x_{max}}{b_m}\right) \text{ hours} \end{cases}$$

Quarry blast

The growth is small & slow for the quarry blast wave

However, at the end of the wave, the beam may be kicked off-center.

Average off set $\langle \Delta A \rangle = \langle \frac{X}{\sqrt{\beta}} \rangle = \sum \frac{a_m}{\pi \sin \pi \nu_0} \cdot \sqrt{1000}$

$= 6.50 \times 10^{-6} m^{\frac{1}{2}}$

~ original size of bunch

But decoherence time ~ 140 sec.

Crossing train

fractional emittance growth ~ 0.0033

$\frac{1}{2}$ growth time ~ 25 hours

But train crossing time ~ a few minutes only

Longitudinal Emittance Growth

Horizontal kick on quad. $a_m \sin 2\pi\nu_m j$ (j^{th} turn)

angular kick on beam $\theta_j = \frac{a_m}{f} \sin 2\pi\nu_m j$

Incremental kick from $(j-1)^{th}$ to j^{th} turn is

$$\Delta\theta_j = \theta_j - \theta_{j-1}$$

Change in orbit length for j^{th} turn

$$\Delta C_j = \Delta\theta_j D \qquad D = \text{dispersion at quad}$$

Synchronous particle will arrive at rf cavity late by rf angle

$$\Delta\phi_j = 2\pi \frac{\Delta C_j}{\lambda_{rf}} = \frac{2\pi h D}{C} \Delta\theta_j$$

If this late arrival accumulates, the bunch area will increase & eventually go out of the rf bucket.

Equations of motion

$$\begin{cases} \dfrac{d\phi_j}{dn} = 2\pi\eta h \delta_j + \psi_j \\[2ex] \dfrac{d\delta_j}{dn} = -\dfrac{eV}{E}\phi_j \end{cases}$$

Assumption: constant synchrotron tune

$$\psi_j = \sum_{i=1}^{j} \Delta\psi_j = \frac{2\pi h D}{C}\theta_j$$

Effect of a constant kick

That is θ_j is the same every turn

$\therefore$ the new closed orbit has an extra length $\Delta C = \theta D$

For each turn, there is an increase of phase lag

$$\psi = \frac{2\pi h D}{C}\theta$$

Will the phase lag for each turn accumulate so as to throw the particle (or bunch) out of the bucket ?

Answer: No

~~Constant kick~~

There is just a change in synchronous center to a lower energy so as to accomodate a shorter orbit length.

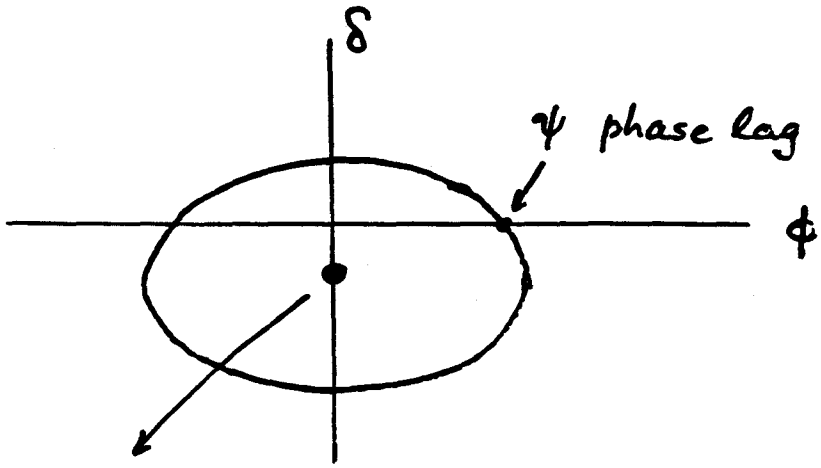

new synchronous center $\delta_c = -\frac{\psi}{2\pi\eta h}$

Periodic kick

$$\begin{cases} \dfrac{d\phi}{dt} = \eta h \omega_0 \delta + \dfrac{\omega_0 h D a_m}{Cf} \sin \omega_m t \\[2ex] \dfrac{d\delta}{dt} = -\dfrac{eV\omega_0}{2\pi E}\phi \end{cases}$$

Initial conditions: $\phi = \phi_0$, $\delta = \delta_0$

Want solution with ω_m close to ω_s

Let $\Phi = \dfrac{\nu_s}{\eta h}\phi$ so that elliptical trajectory becomes circular

Solution:

$$(\Phi, \delta) = a_0 e^{-i 2\pi \nu_s N}$$ ← initial condition

$$+ \frac{i \nu_\Omega^2}{\nu_s} \frac{\sin \pi(\nu_m - \nu_s)N}{\nu_m - \nu_s} e^{-i 2\pi \nu_s N}$$ ← synchronous oscillation with big amplitude

$$- \frac{i \nu_\Omega^2}{\nu_s} \frac{\cos \pi(\nu_m - \nu_s)N}{2\nu_s} \sin 2\pi \nu_s N$$ ← synchronous center shifted

$$\nu_\Omega^2 = \frac{2\pi \nu_s^2 D a_m}{\eta C f}$$

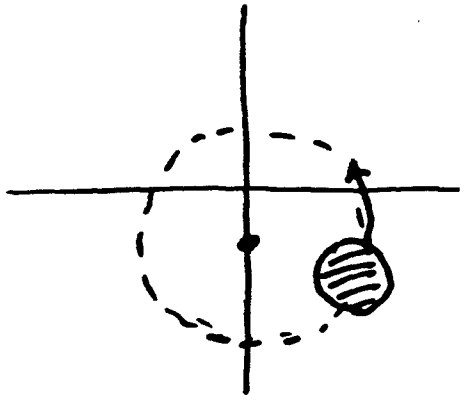

The small denominator in second term can give very big amplitude. Synclotron tune dependence on amplitude will smear out the bunch leading to increase in bunch area

Estimation

$$\Delta\delta = \frac{2\pi a_m}{f}\frac{f_s}{|f_m - f_s|} = 1.56\times10^{-7}$$

$$\Delta\phi = \frac{\eta h}{\nu_s}\Delta\delta = 1.54\times10^{-3}\ \text{rad}$$

with $a_m = 0.05\mu$ $\quad f = 80.8\ m$

$f_s = 4\ Hz \quad |f_m - f_s| = 0.1\ Hz$

$\eta = 1.1\times10^{-4}$

$h = 1.05\times10^{5}$

For 1000 quads multiply by $\sqrt{1000}$

D. RITSON
Feb 11 '92

SEISMIC PROBLEMS(?) AND SOLUTIONS?

Will use results from previous speakers. The G.Stupakov, Skrinsky et al power spectrum formulation is very convenient. I agree with the CDR (G.Fischer, P.Morton) results.

THE "ADIABATIC" REGIMES

— Long term ground or support subsidence (months)

When resteering no longer works send in the surveyors.

— Short term changes (minutes)

Operators manually or with feedback resteer machine.

— Few Herz disturbances from ground vibration.

CDR proposed the Gostlein scheme for keeping beams centered.

Does this do more harm than good? Simulation results will be discussed.

— The movement is unimportant for 20 to few hundred Herz.

(1) unless the perturbing frequency is exactly the same as synclotron freq. & lock on to it exactly, there will not be much problem.

(2) With f_s dependence on amplitude, story may be different

(3) Perturbation is a continuum covering the synclotron freq.

$$\int_0^\infty \mu(\omega_m)\, d\omega_m = 1$$

$\mu(\omega_m)$ centers at ω_s & is narrow

$$(\bar{\Phi}, \delta) \approx i \frac{\pi \nu_r^2 \omega_0^2}{2\omega_s} \mu(\omega_s)\, e^{-i 2\pi \nu_s N}$$

$\therefore$ no resonance

(4) If the perturbation is random, there will be a resonance.

EMITTANCE GROWTH FROM POWER SPECTRUM IN KILOHERZ DOMAIN.

— The "train" quarry shot problem.

— The external (sources outside of the magnet supports) problem.

— The INTERNAL to the magnet problem from cooling flow or whatever.

Better engineer it so that this doesn't happen

— Mild safety net from feedback.

SEISMIC PROBLEMS(?) AND SOLUTIONS?

Will use results from previous speakers. The G.Stupakov, Skrinsky et al power spectrum formulation is very convenient. I agree with the CDR (G.Fischer, P.Morton) results.

THE "ADIABATIC" REGIMES

— Long term ground or support subsidence (months)

When resteering no longer works send in the surveyors.

— Short term changes (minutes)

Operators manually or with feedback resteer machine.

— Few Herz disturbances from ground vibration.

CDR proposed the Jostlein scheme for keeping beams centered.

Does this do more harm than good? Simulation results will be discussed.

— The movement is unimportant for 20 to few hundred Herz.

DOES THE JOSTLEIN MODULATED SIGNAL CAUSE EMITTANCE GROWTH?

— What is feared are non-linear beam beam effects.

— I did extensive beam beam simulation over a wide range of frequencies and amplitudes. Basically it leaves the beam-beam limit unchanged.

(Example figures compare beam-beam limits with and without a Jostlein sweep of 2 micron amplitude at 40 Hz).

— It is an "EPSILON effect" compared to the synchrotron motion modulation which typically moves the beam by $\pm$ 1.4 microns at a frequency of $\sim$10 Hz.

JOSTLEIN FEEDBACK FOR < FEW HZ MOTION.

— Well described in CDR. Objective is to assure beam centering to

than 0.1 σ.

—One of the beams at the IR is circularly rotated. And a phase locked luminosity signal is used for feed back to maintain centering.

—Because the IPs throw hundreds of watts of highly collimated hadronic debris instantaneous relative luminosities can be measured to a better than 0.1%. (10^8 interactions per sec).

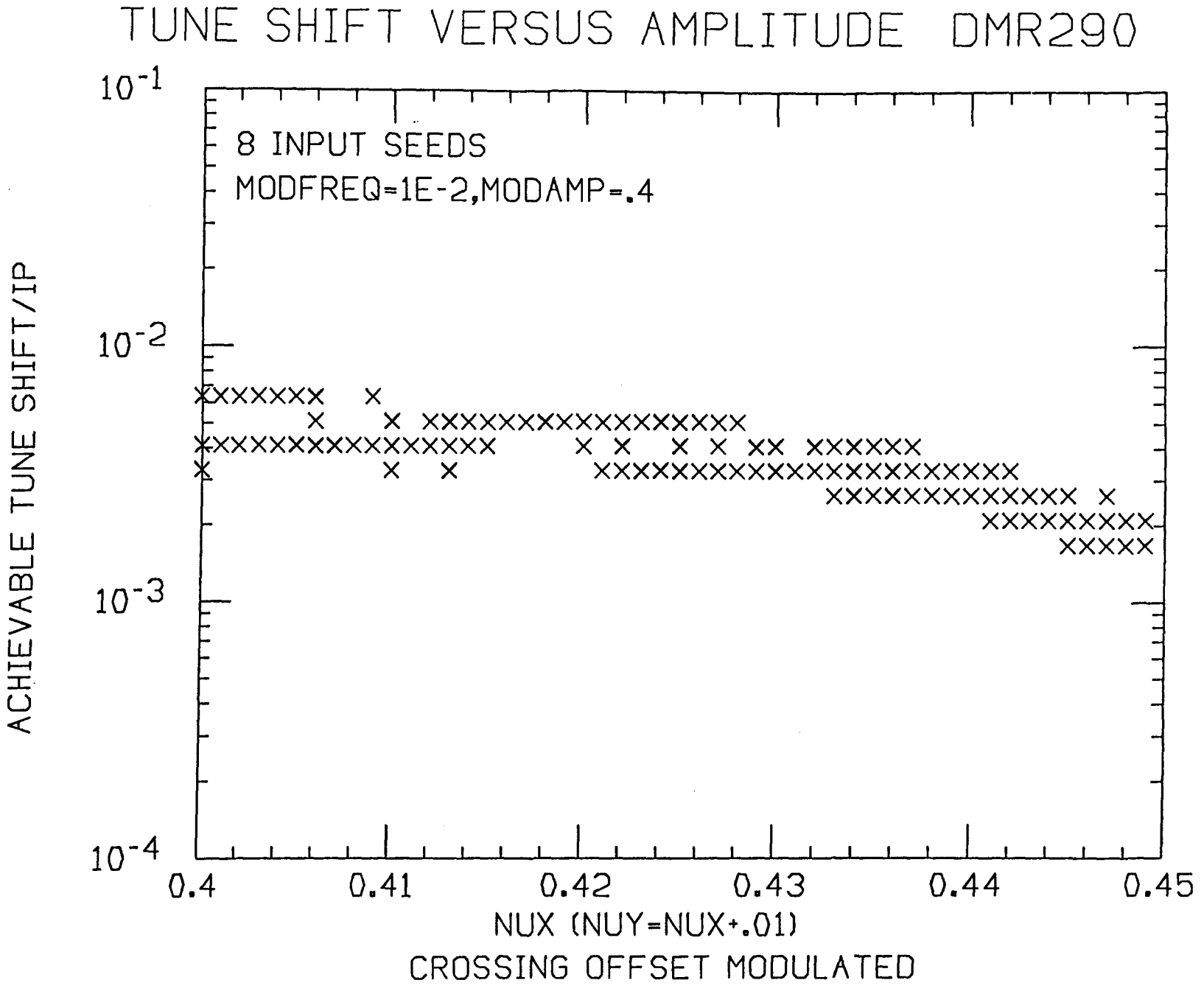
TUNE SHIFT VERSUS AMPLITUDE DMR290
8 INPUT SEEDS
MODFREQ=1E-2,MODAMP=.4
ACHIEVABLE TUNE SHIFT/IP
10^-1
10^-2
10^-3
10^-4
0.4
0.41
0.42
0.43
0.44
0.45
NUX (NUY=NUX+.01)
CROSSING OFFSET MODULATED

TRAIN AND QUARRY SHOTS.

Ng and Jack Peterson have gone over this.

EVEN if they were too OPTIMISTIC

— These are disturbances at predictable times of a few minutes in the day.

— The beams could be separated prior to a shot or train passage.

— Without the beam beam interaction decoherence times are long and a modest (probably already existing) feedback system could remove the induced coherent signal.

500 TO KILOHZ NOISE PROBLEMS.

— Gerry Fischer has discussed this.

— Only "cultural noise sources" can cause such effects.

— Typically magnet mounts resonate in the tens of Hz range not kiloHz range.

The input power spectrum $P(\omega)$ must be multiplied by a response function $Z(\omega)$ to give the noise power at the magnet.

$$J^{-1} \propto P(\omega_r)\,|Z(\omega)|^2$$

with $$|Z(\omega)|^2 = \frac{(\omega_0^4 + \Gamma^2)}{(\omega^2 - \omega_0^2)^2 + \Gamma^2}$$

ω_0 is res frequency

Therefore even if the INP results were correct at the SSC the power spectrum would be attenuated in the kiloHZ range (with reasonable design) by factors

For $\omega \gg \omega_0$ $\quad |Z(\omega)|^2 \approx \left(\frac{\omega_0}{\omega}\right)^4$

ie for $\omega_0 \sim 50$ Hz attenuation factors of 10^{-4} should be possible

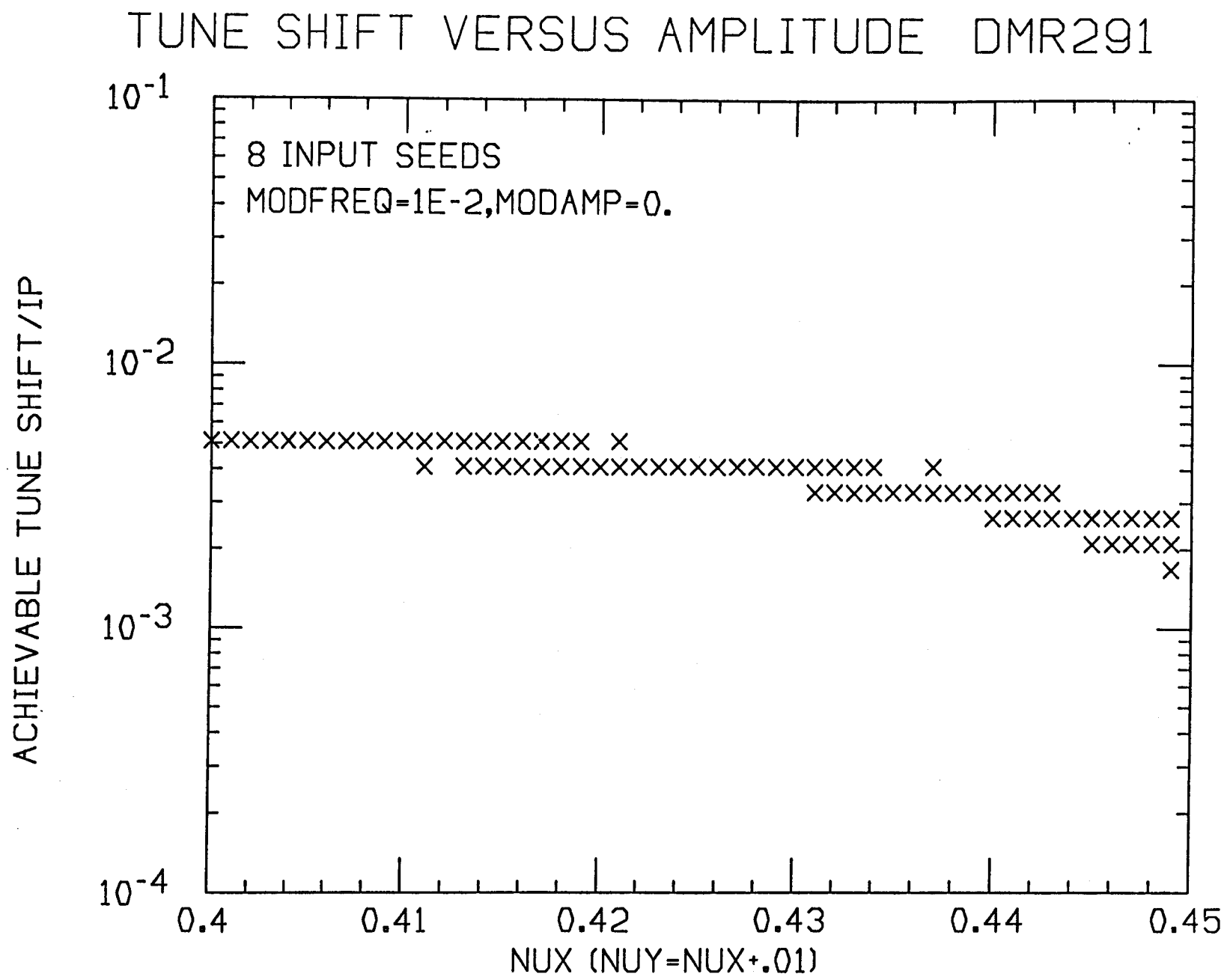
TUNE SHIFT VERSUS AMPLITUDE DMR291
8 INPUT SEEDS
MODFREQ=1E-2,MODAMP=0.
ACHIEVABLE TUNE SHIFT/IP
10-1
10-2
10-3
10-4
0.4
0.41
0.42
0.43
0.44
0.45
NUX (NUY=NUX+.01)

Ground Motion Measurements at the Site of the Advanced Photon Source (APS)

Joe Jendrzejczyk and Marty Wambsganss

Argonne National Laboratory
Argonne, IL 60439

Workshop on Vibrational Control and
Dynamic Alignment Issues at the SSC

February 11–14, 1992

WHAT REMAINS?

KiloHZ noise power generated directly within the magnets could be a problem???

Obviously must be measured.

APS Facility

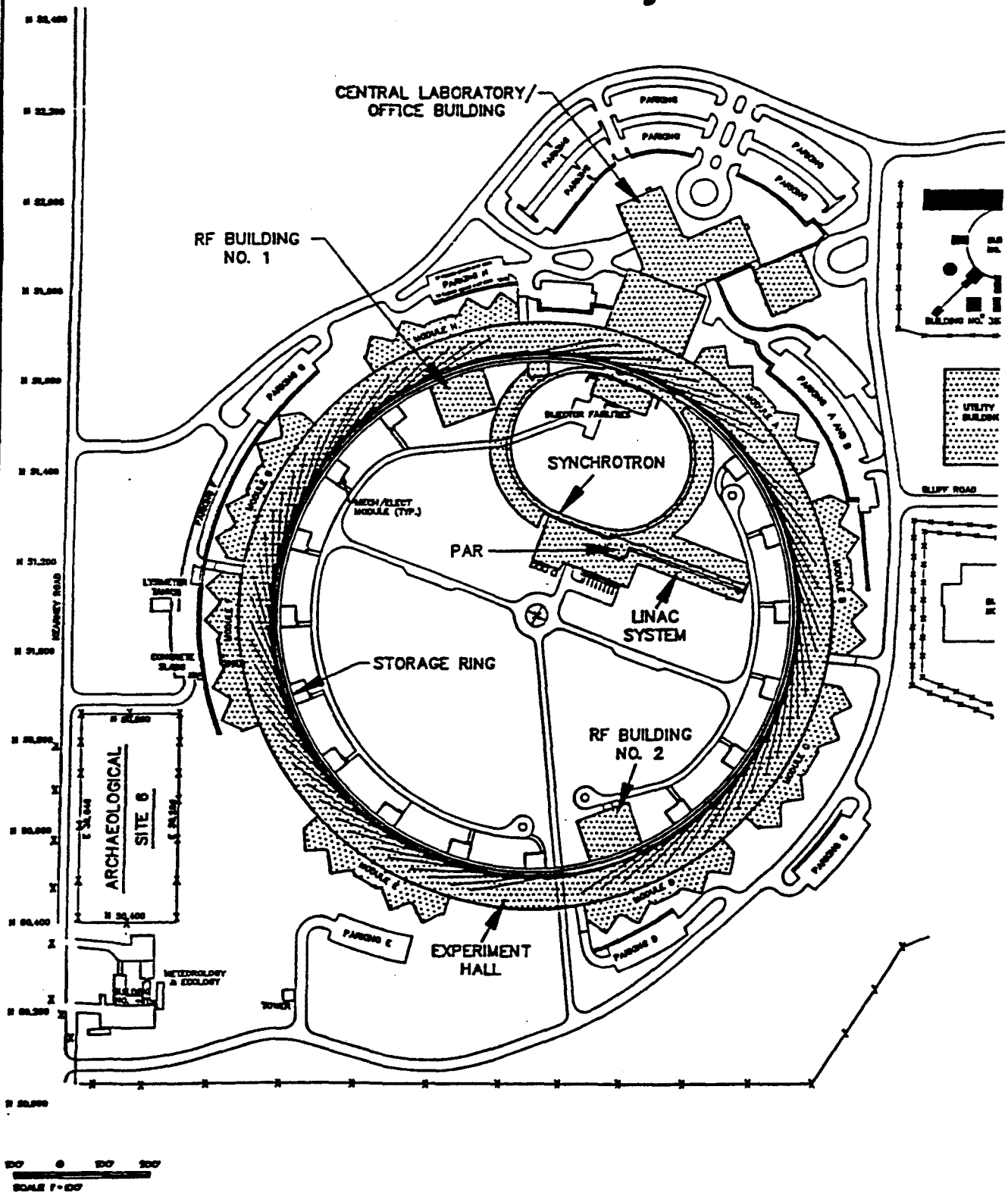

Outline

- Background information
- Ambient ground motion at APS site, May 1988
- Surveillance of 18 Hz and 60 Hz components of ground motion at APS site – July 1988–January 1990
- Vibration response of the APS Linac floor slab to ambient ground motion October 10, 1991

Geotechnical Investigation

- Soil profile
- Ground water level
- Bedrock continuity
- Crosshole seismic testing

Vibration Criteria

Maximum Allowable Vibration Amplitudes

Vibration Type	Displacement (μm) (peak) Horizontal	Vertical
Single Quadrupole	2.2	1.29
Random (all quadrupoles)	0.34	0.12
Plane Wave (v = 306 m/s; f in Hz)		
$f < 2.2$	16.1	4.4
$2.2 < f < 4.6$	16.1	4.4–0.28
$4.6 < f < 7.7$	16.1	0.28
$7.7 < f < 13.5$	16.1–0.90	0.28
$f > 13.5$	0.90	0.28

Ambient Ground Motion, May 1988

- Near–field sources generated within the site – generally can be controlled
- Far–field sources generated external to the site – may or may not be controllable

Measurement Locations

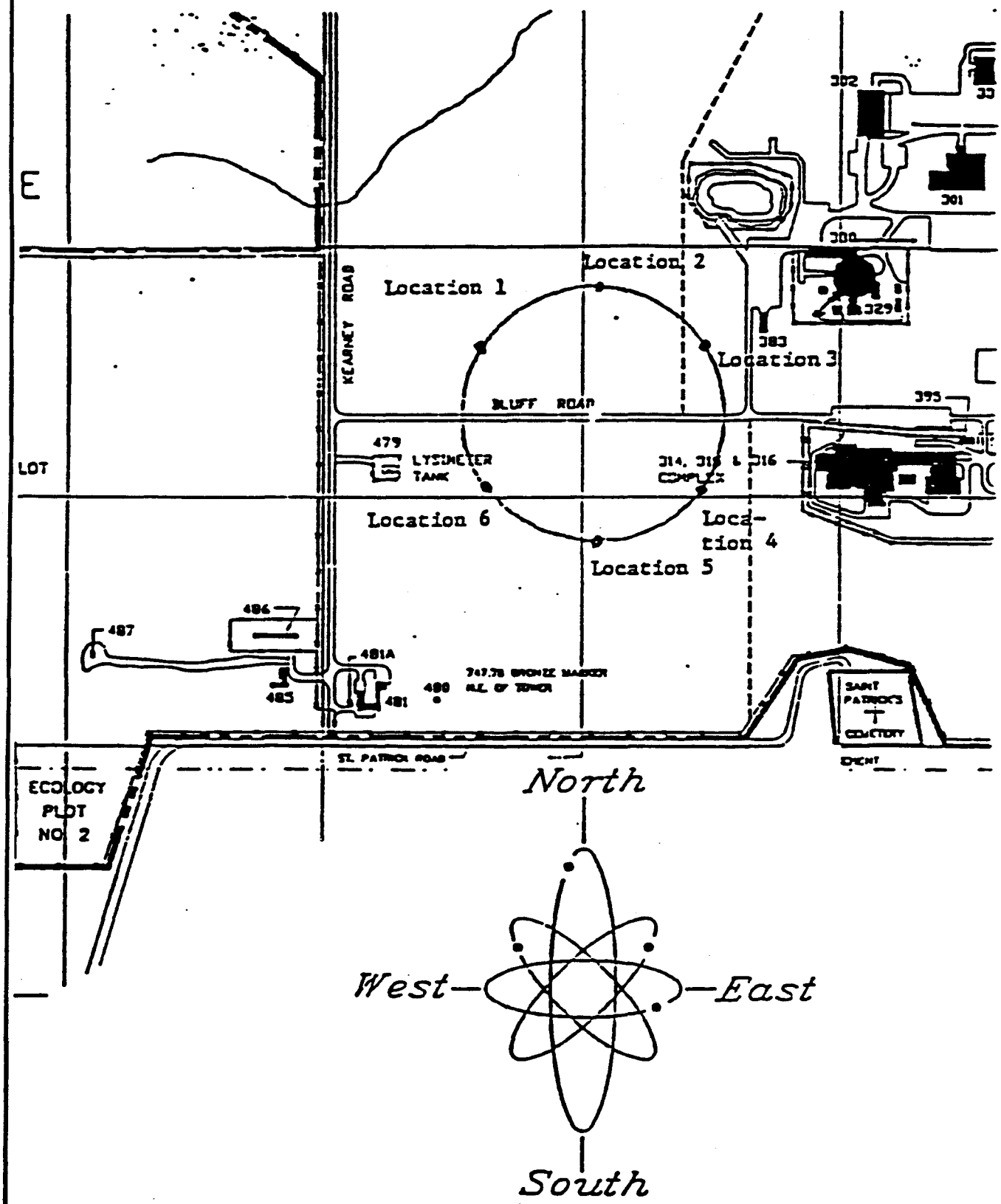

Total Displacement in Microns for Locations 1 and 2

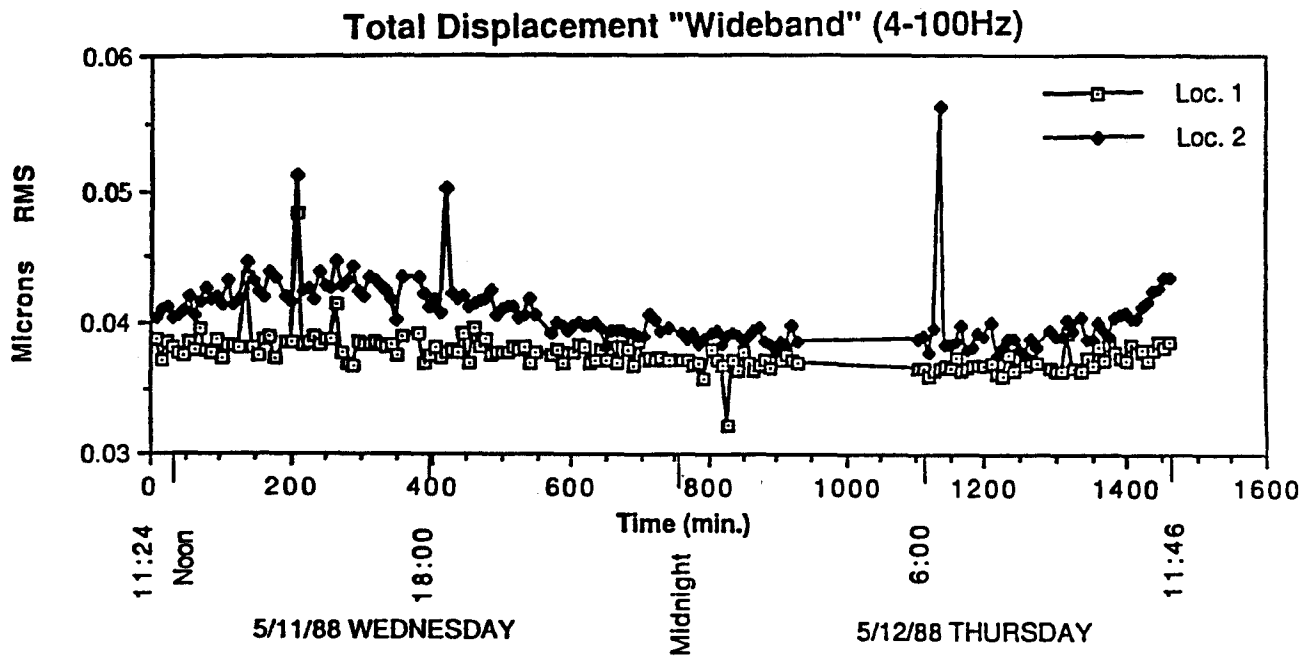

Measurement Technique

- At six locations along proposed storage ring perimeter
- Accelerometers mounted on 2 ft long stakes driven into soil
- Vertical direction only
- Accelerometer signals double integrated to obtain displacements
- Displacements averaged over 4–minute time interval

Total Displacement in Microns for Locations 3 and 4

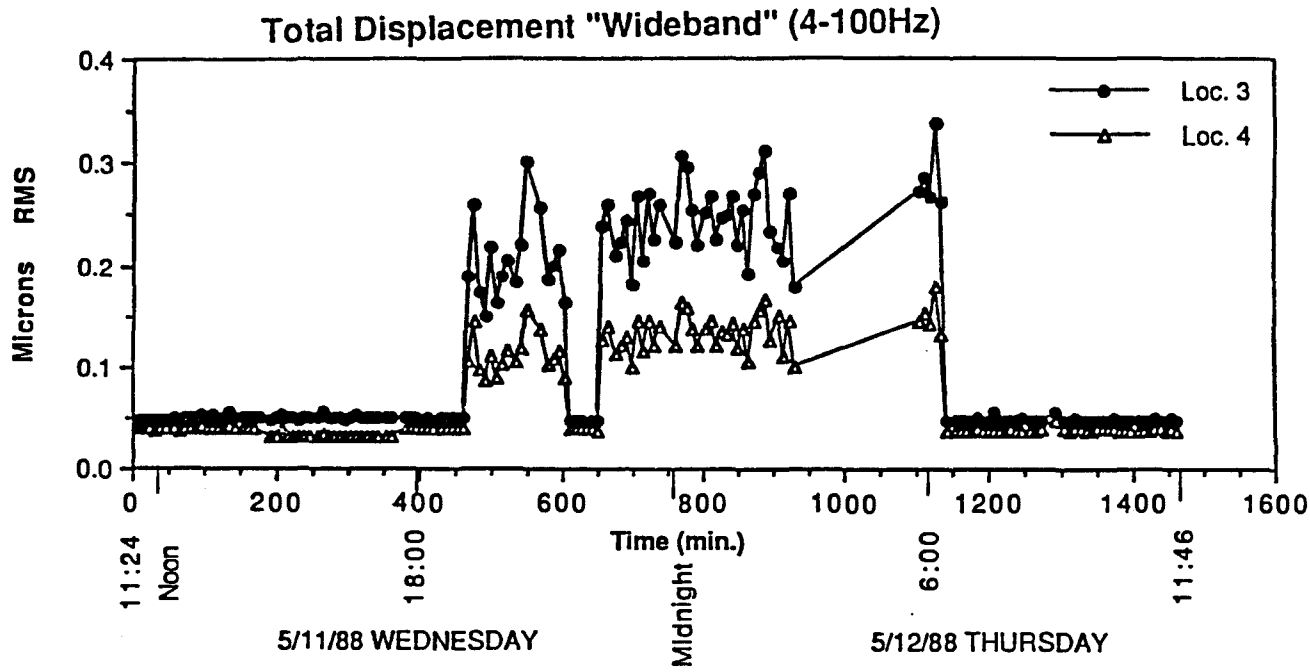

Ground Motion Survey – Transients

Three types of transients were observed:

- Local low energy, observed on only one transducer.
- Near–field, medium energy observed at all locations with a velocity of 1,100 ft/s.
- Far–field, high energy, observed at all locations with a velocity of 18,000 ft/s.

Measured displacement values were high – up to 1.2 microns peak–to–peak.

Surveillance Results

- Only one positive occurrence on July 28, 1988
- Has not been observed after July 1988

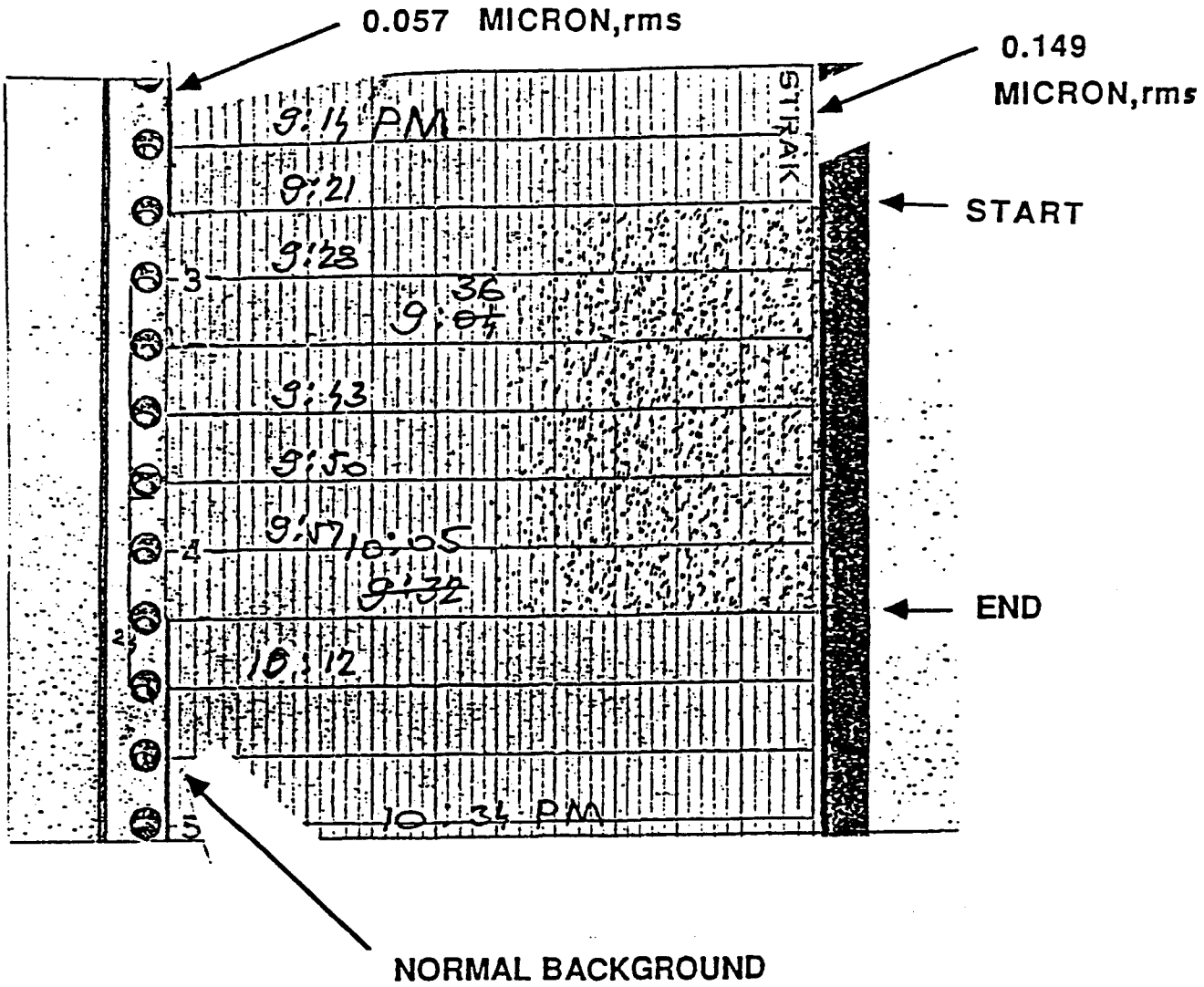

Actual 60 Hz measurement on July 28, 88

Surveillance of 18 Hz and 60 Hz component of Ground Motion at APS Site, July 1988–January 1990

- Location 3 monitored
- Continuous monitoring system used

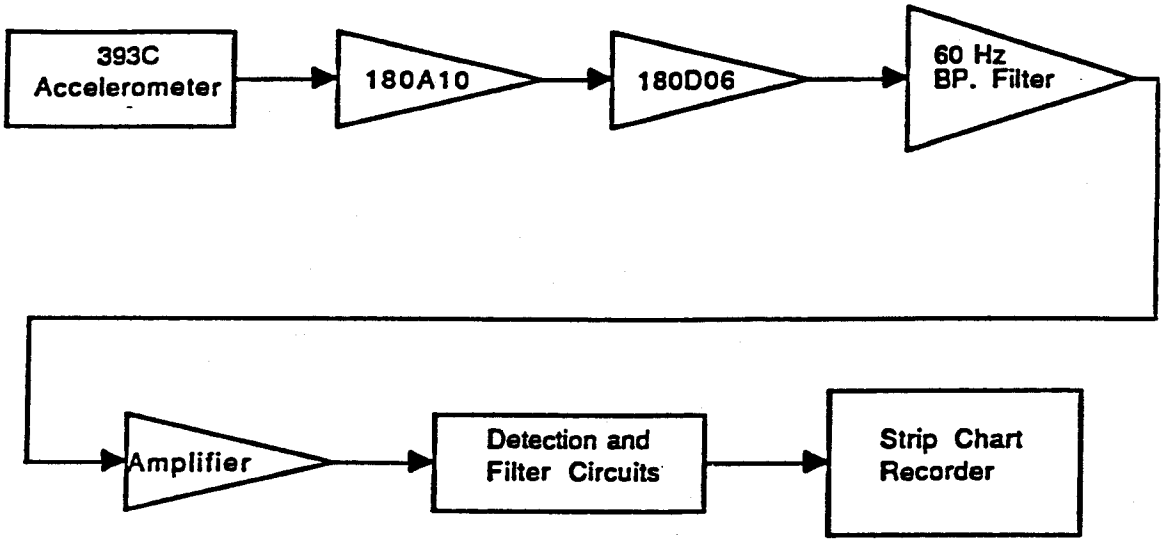

Ambient Ground Motion/Linac Slab Response

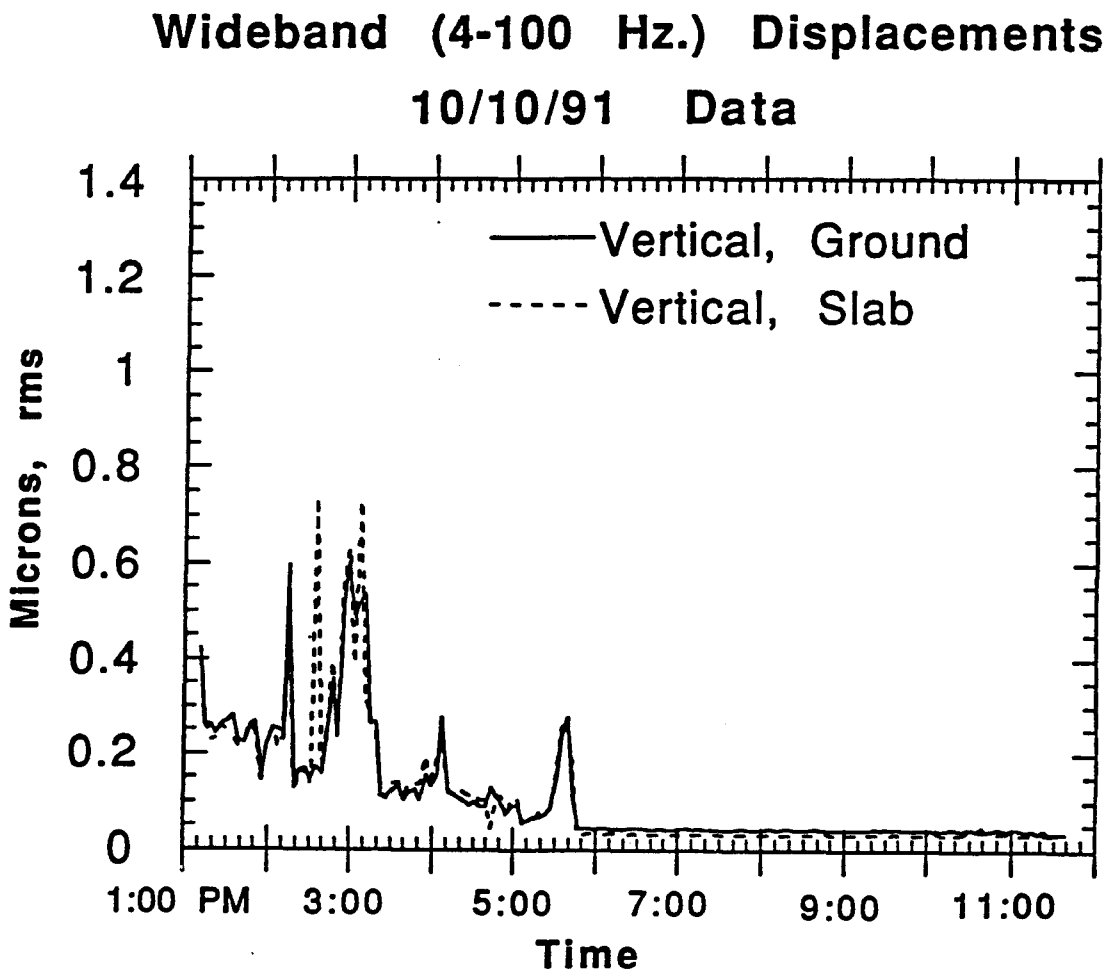

Vibration Response of the APS Linac Floor Slab to Ambient Ground Motion, October 10, 1991

- Three axis measurements on Linac floor slab and adjacent soil
- Same data reduction techniques as previously noted
- Measurements made during high activity time (construction) and low activity time

Ambient Ground Motion/Linac Slab Response, Horizontal, East

Wideband (4–100 Hz) Displacements

10/10/91 Data

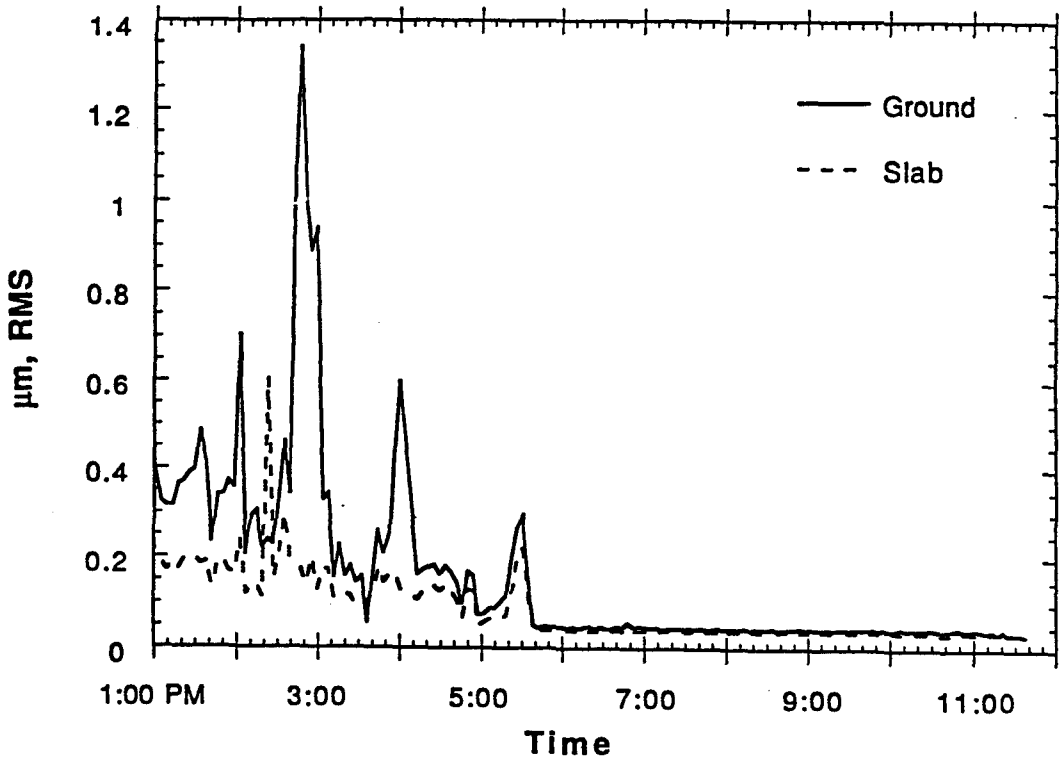

Ambient Ground Motion/Linac Slab Response, Horizontal, North

Wideband (4–100 Hz) Displacements

10/10/91 Data

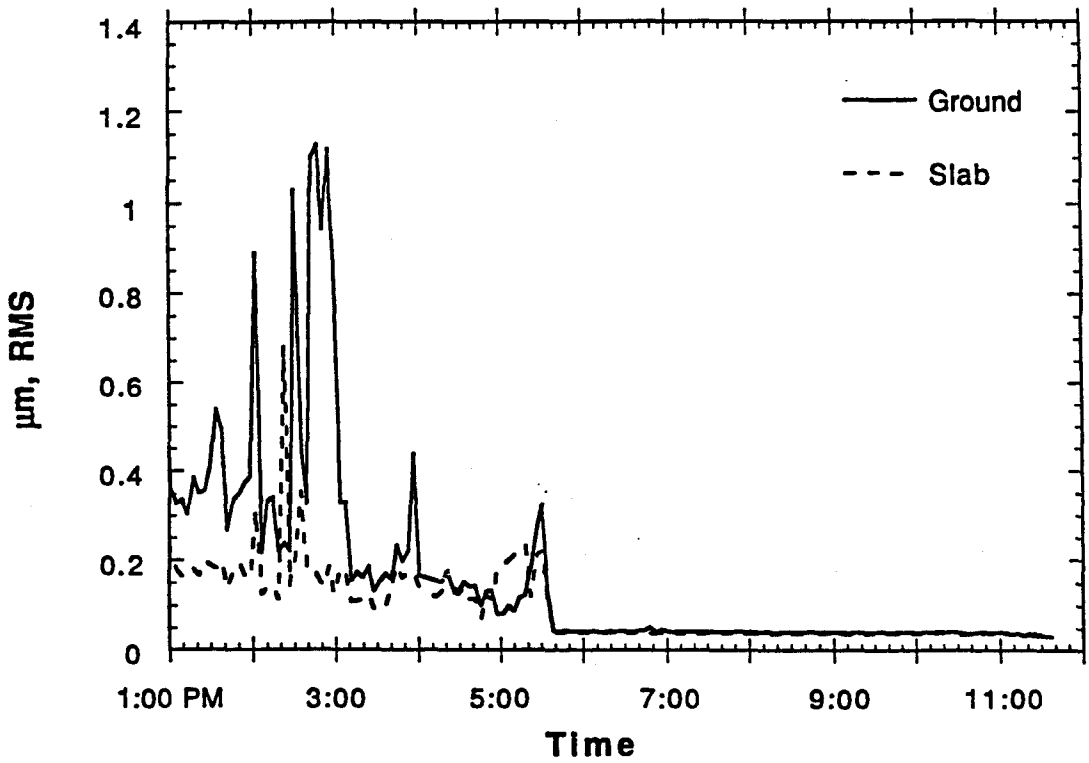

Vertical Ground Spectra for High Activity Time

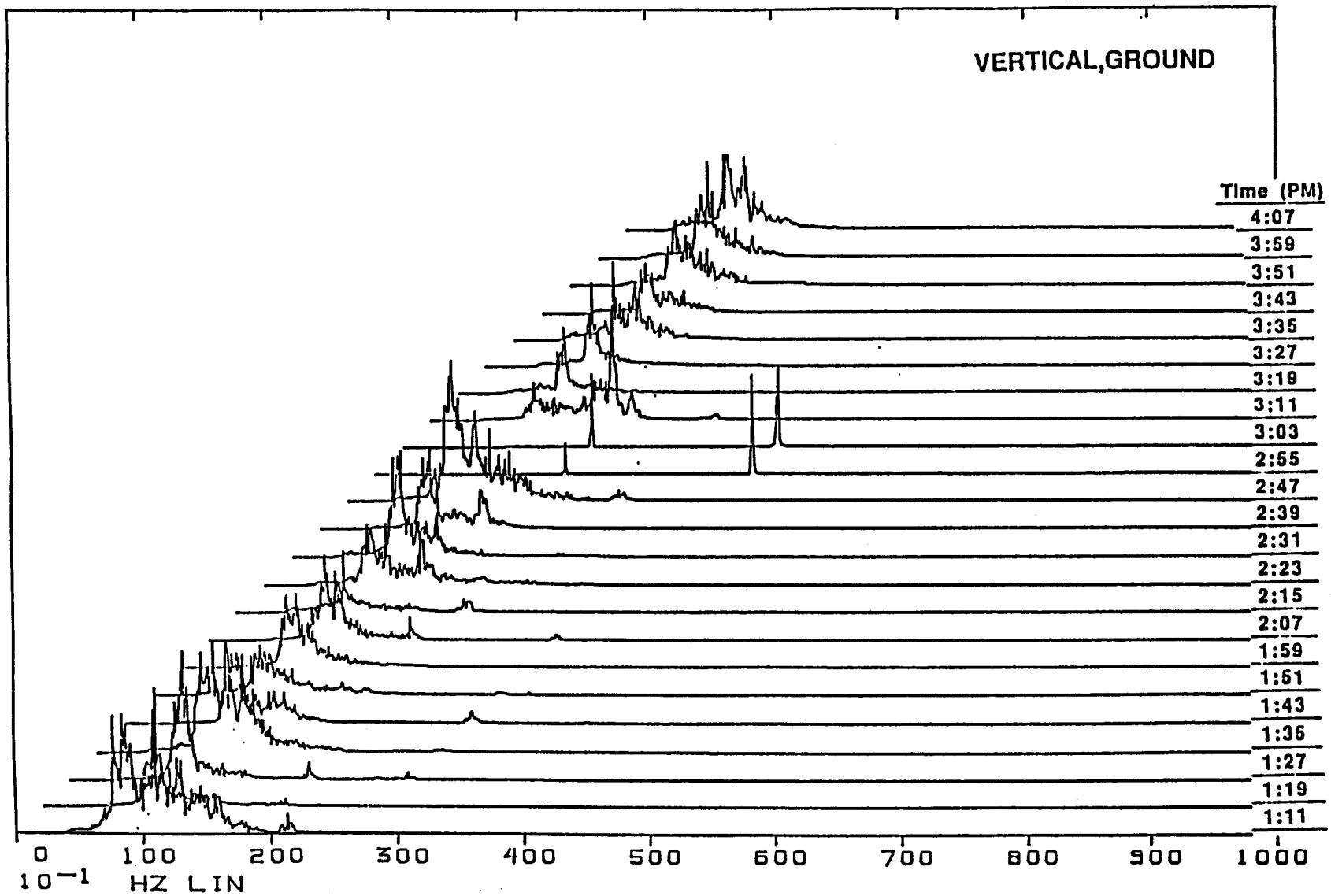

Vertical Ground Spectra for Low Activity Time

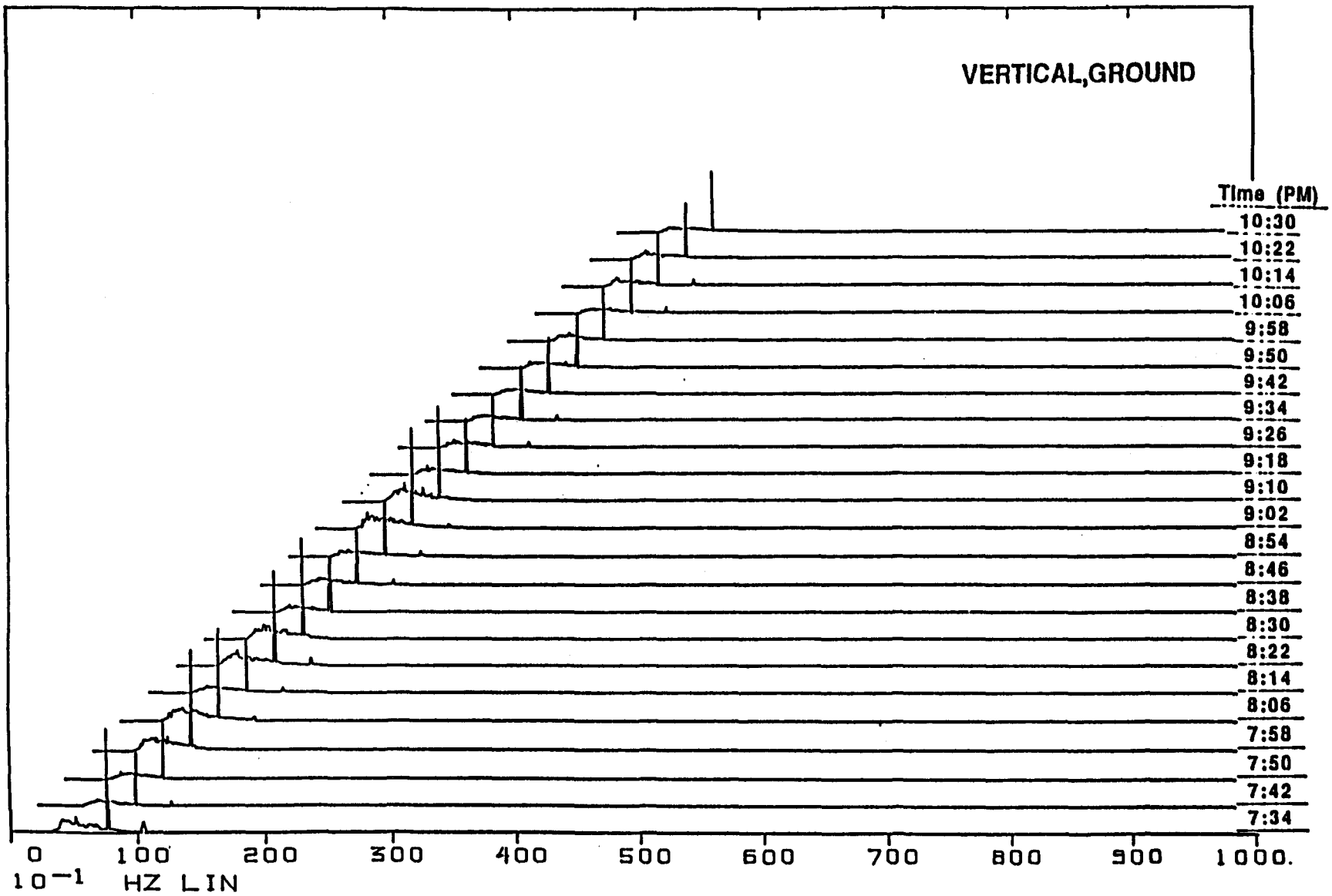

Ambient Ground Motion/Linac Slab Response

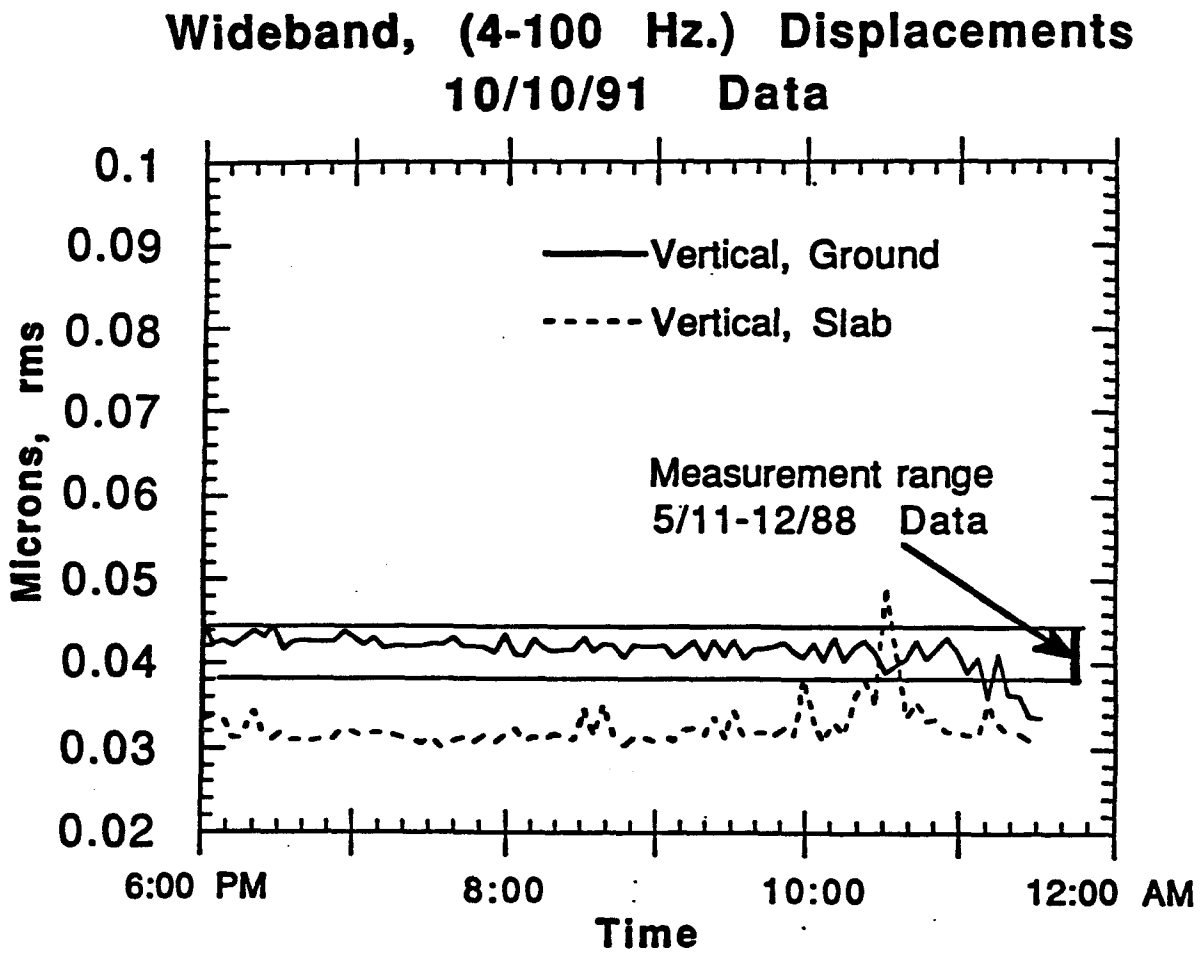

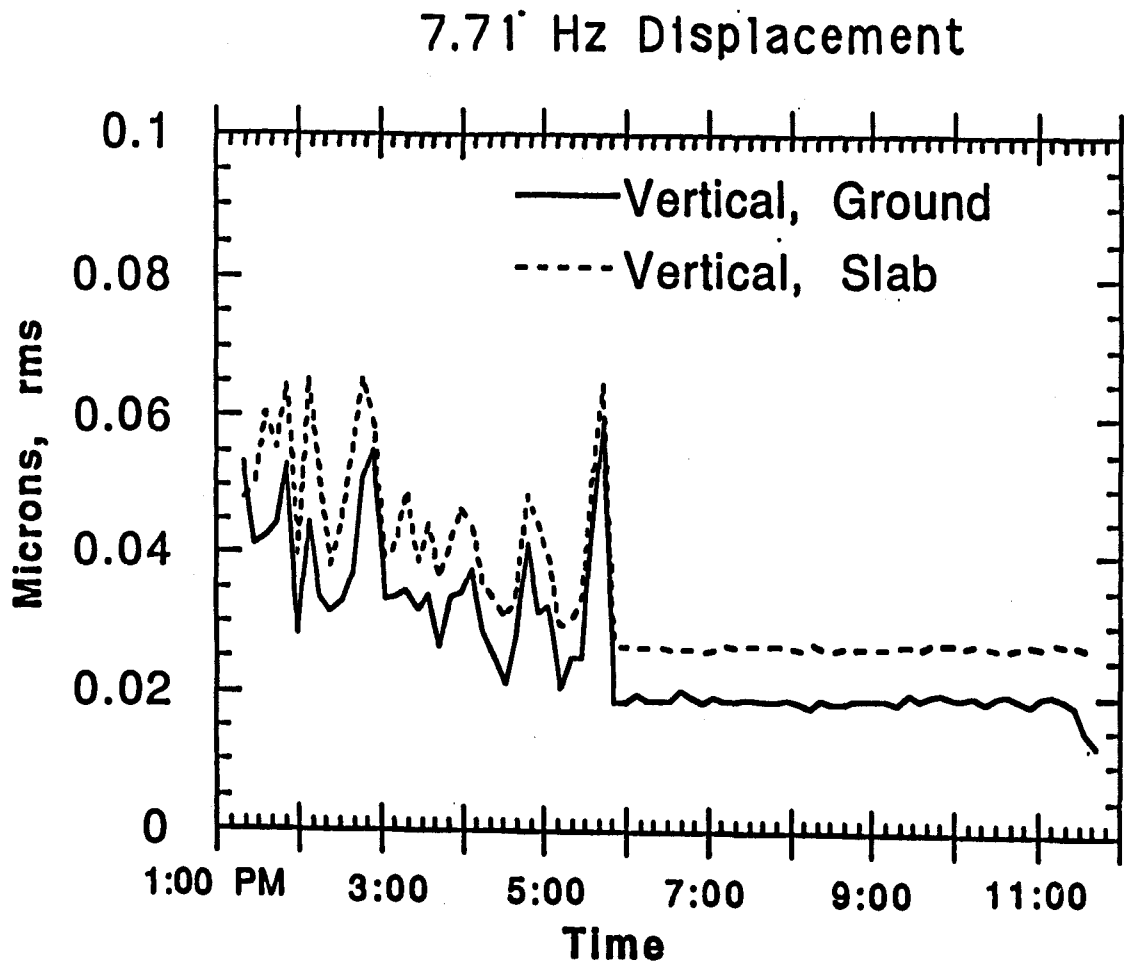
7.71 Hz Displacement
0.1
0.08
0.06
0.04
0.02
0
Microns, rms
Vertical, Ground
Vertical, Slab
1:00 PM
3:00
5:00
7:00
9:00
11:00
Time

References

"Subsurface Exploration and Geotechnical Engineering Evaluation for Proposed 7-GeV Advanced Photon Source," *STS Consultants, Northbrook, IL, Final Report, STS Project No. 25229,* May 20, 1988.

"Title II - Subsurface Exploration and Geotechnical Engineering Evaluation for Proposed 7-GeV Advanced Photon Source (APS)," *STS Consultants, Northbrook, IL, Final Report, STS Project No. 25229-B,* April 30, 1990.

J. A. Jendrzejczyk and M. W. Wambsganss, "Surface Measurements of Shear Wave Velocity at the 7-GeV APS Site," *Argonne National Laboratory Report LS-129,* Dec. 1987.

J. A. Jendrzejczyk and R. K. Smith, "Building-Soil Vibration Coupling," *Argonne National Laboratory Report LS-79,* Jan. 1987.

J. A. Jendrzejczyk, M. W. Wambsganss, and R. K. Smith, "Ambient Ground Motion Measurements at Argonne National Laboratory over Extended Time Periods," *Argonne National Laboratory Report LS-111,* March 1988.

J. A. Jendrzejczyk, Z. Nagy, and R. K. Smith, "Ambient Ground Motion at the 7-GeV APS Site at Argonne National Laboratory over Extended Time Periods," *Argonne National Laboratory Report LS-136,* Dec. 1988.

J. A. Jendrzejczyk, M. W. Wambsganss, and R. K. Smith, "Surveillance of 18 Hz and 60 Hz Components of Ground Motion at the APS Site," *Argonne National Laboratory Report APS/IN/VIB/90-1,* March 1990.

H. Amick and C. G. Gordon, "Site Vibration Survey - Advanced Photon Source - Argonne National Laboratory," *Acentech Inc., Report No. 18,* Aug. 1989.

J. A. Jendrzejczyk and M. W. Wambsganss, "Vibration considerations in the design of the Advanced Photon Source at Argonne National Laboratory," to be published in *Proceedings of Conf. on Vibration Control in Microelectronics, Optics, and Metrology,* 1991 Symp. on Optical Science and Engineering, San Jose, CA, Nov. 1991.

J. A Jendrzejczyk, M. W. Wambsganss, and R. K. Smith, "Vibration Response of the APS Linac Floor Slab to Ambient Ground Motion," *Argonne National Laboratory Report APS/IN/VIB/92–1,* November 1991.

Conclusions

- With the exception of the 18 Hz–60 Hz vibration, the site is quiet
- The ground vibration measurements of May 1988 and October 1991 are in excellent agreement
- The Linac floor slab generally follows the ground motion
- The Linac floor slab acts as a filter at all frequencies except its soil/structure resonances
- Construction activity greatly increases ambient ground motion

DESIGN AND ANALYSIS OF STRUCTURES

Lessons learned from the
NOVA Laser Spaceframe Design
Chuck Hurley (LLNL)

Finite Element Analysis of Large Structures
Dave McCallen (LLNL)Presented by Bob Murray

Structural Dynamic Testing and
Systems Identification
J. P. Lauffer (SNL)

Dynamic (Modal) Analysis of SSC
Dipole/Quadrupole Magnets
Bob Viola (SSCL)

A Six Strut Support and
Alignment System
Ted Lauritzen (LBL)

Dynamic Analysis of Six Strut System
Brad Burdick (LLNL)

Vibrational Testing of the Advanced Proton Source (APS)
Storage Ring Girder/Support Assembly
Marty Wambsganss (ANL)

Lessons Learned From the Nova Laser Spaceframe Design

C. A. Hurley

LLNL

Presented at the *Workshop on Vibrational Control and Dynamic Alignment Issues* at the Superconducting Super Collider

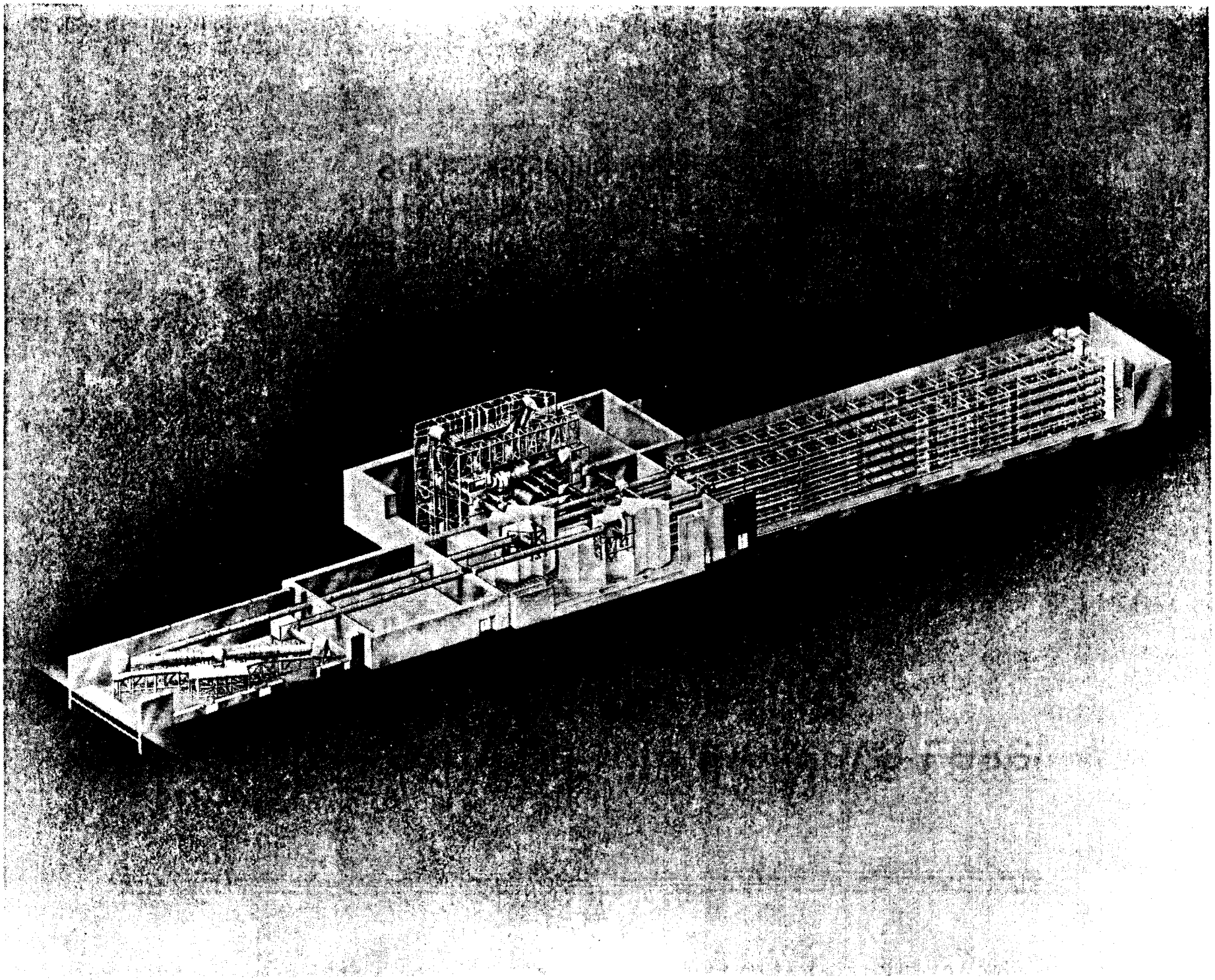

The Nova Laser is a large, accurate, stable optical system

- **Engineering Elements of Nova**
  - **Stability as a target shooter**
  - **Specifications**
  - **Alignment system**
  - **Design approach**
- **Nova is the sixth in a series of lasers built at LLNL within a period of 12 years**
- **Basic lessons learned**
  - **How to design a large system to be stable and very accurate**
  - **Provides a good baseline to design new projects**

Nova was completed in 1985 at a cost of $176 M

- 120 kilojoules for periods of 300 ps to 3 ns
- Ten 74 cm diameter beams travel 280 m
- Arrive simultaneously and irridiate target
  (focused spot on target is 20 μm)
- Travels through 600 major opitcal components
- Automatic alignment System
  - Total system aligned in 20 minutes
  - Requires 300 alignment loops to close for a target shot
- Two target chambers
  - Six shots per day
- Housed in 1 million cubic foot clean room

Design approach for a stable Nova

- For a cost effective system—used a combination of strict specifications of manufacturing tolerances with computer controlled automatic alignment
  - Alignment system
  - Thermal and vibrational stability
  - Strict specification of mechanical and structural design
  - Manufacturing and installation control

Alignment system

- Alignment system includes
  - centering (parallel translation)
  - pointing (angular rotation)
  - focusing

- Computers analyze images from video sensors to locate beam references for automatic alignment

- Each component has removable cross-hairs which are compared to insertable cross-hairs as a fixed permanent reference

  - Shadows are cast from the insertable cross-hairs to the video sensors

  - Information is digitized, analyzed

  - Closed loop adjusts the motor driven mirror gimbals

Closed loop alignment through image processing

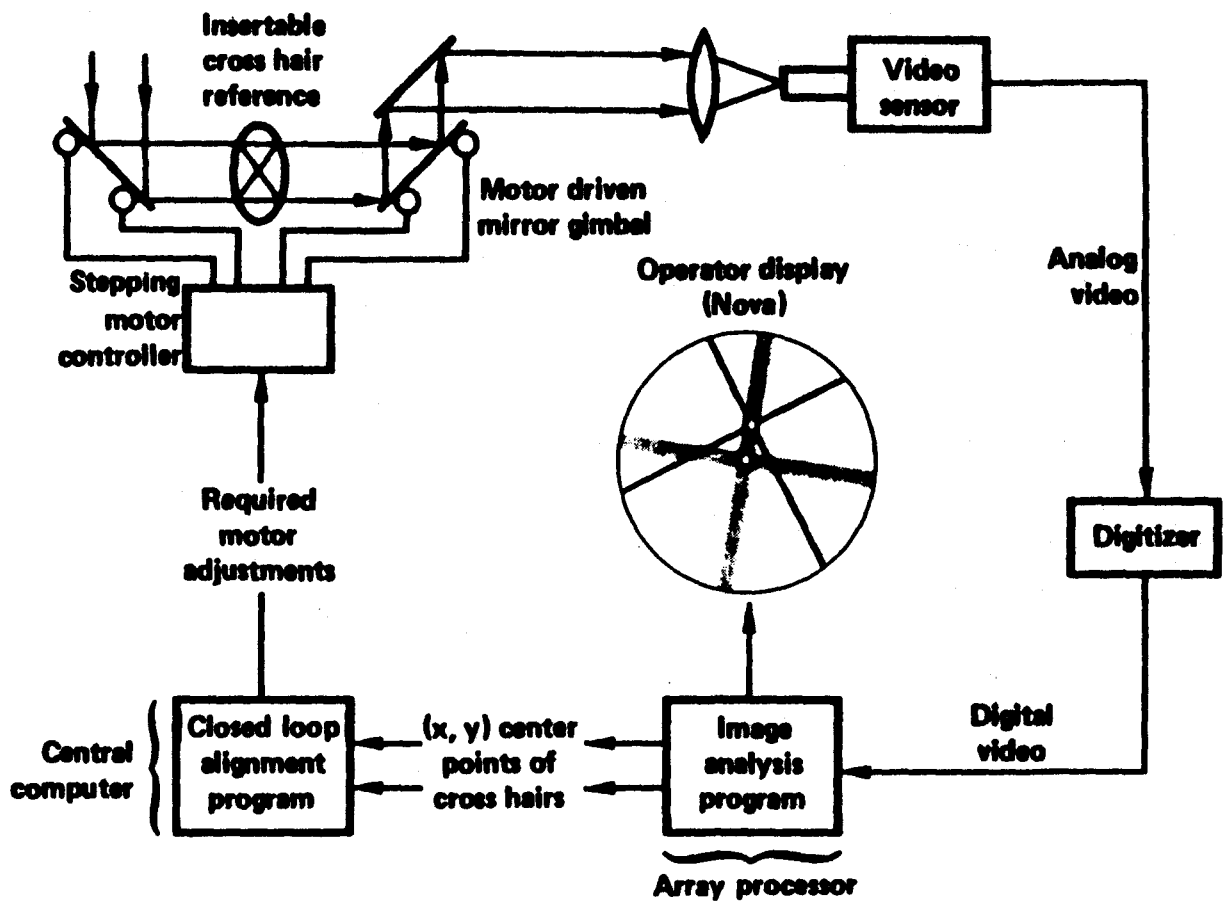

Alignment system features

- Automatic remote with manual adjustment capability
- Uses 1000 stepper motors and acutators
- Eight insertable cross-hairs permanently mounted on the space frame
- Video sensors—permanently mounted on space frame in 3 places: Input, mid-chain, and output.
- Sensors examine near-field image of beam in plane of each cross-hair
- Beam positioning is compared to the insertable crosshair using an alignment beam.
- Pointing is controlled by bringing the beam to focus on a sensor. Offsets are proportional to changes in pointing angle.
- Sensors also give images of spatial filter pinholes or of the target

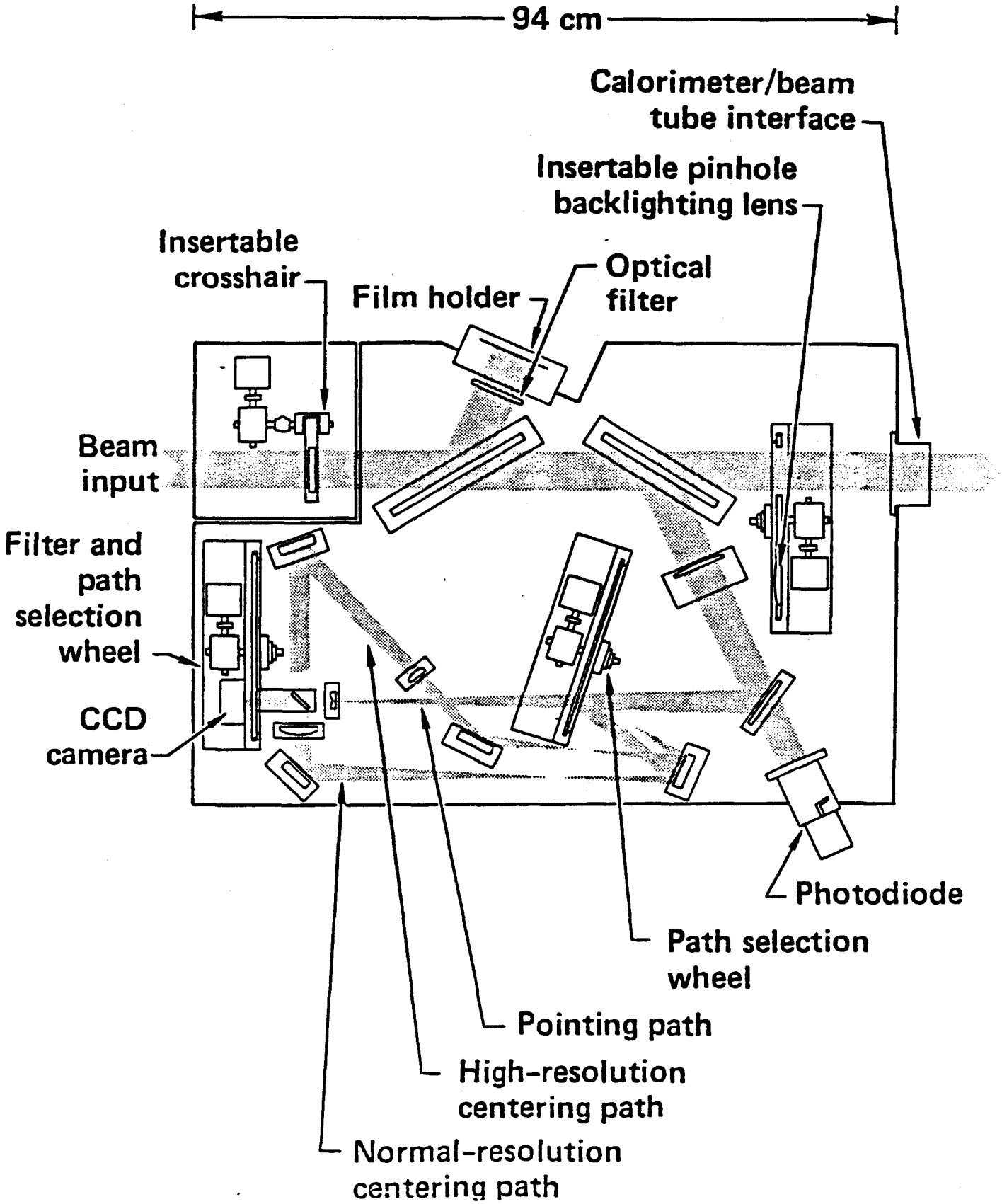

Input Sensor Package

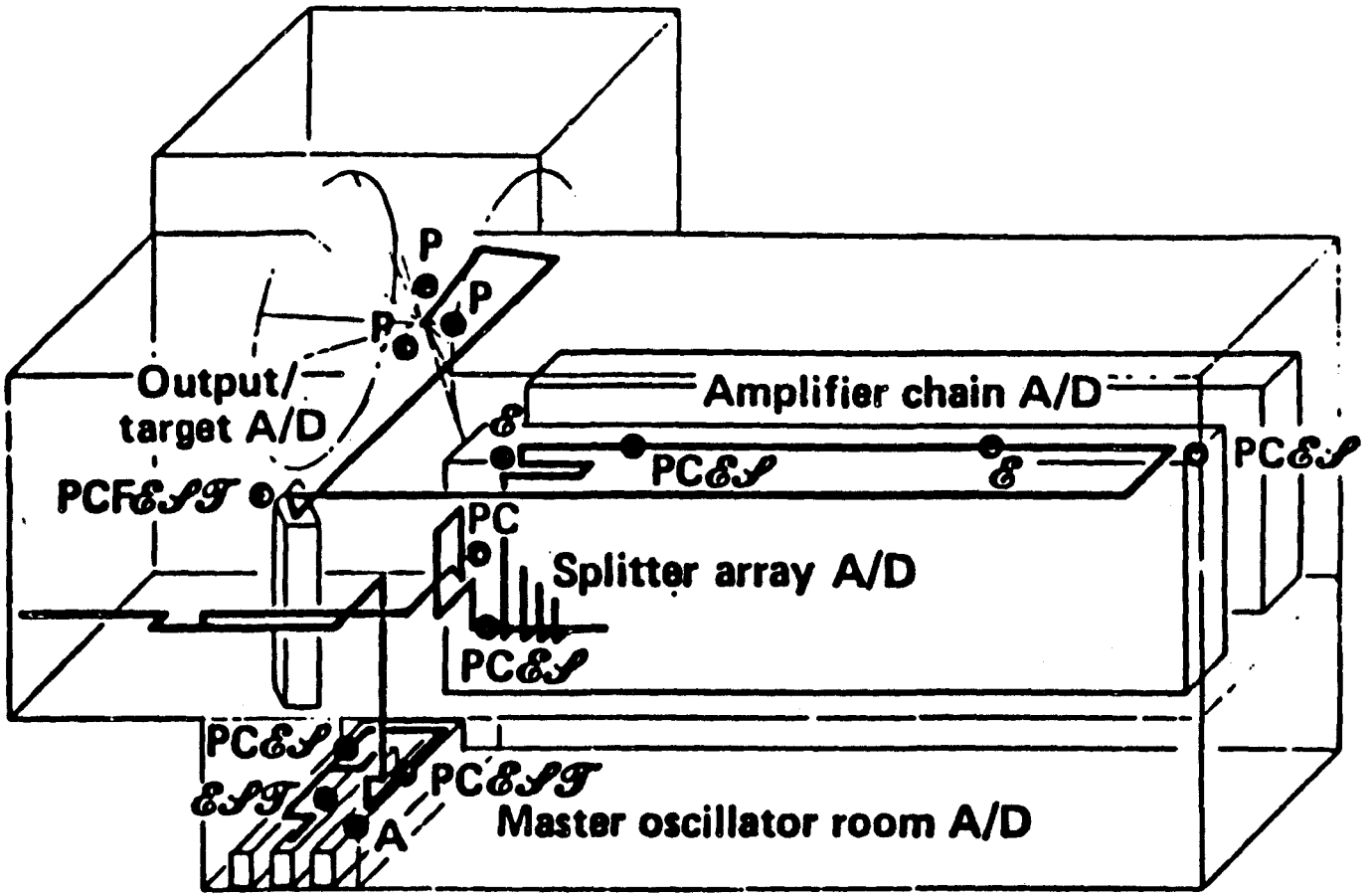

Alignment functions

- A – Pulse arrival synchronization
- P – Beam pointing/target or pinhole viewing
- C – Beam centering/near field viewing
- F – Beam focusing

Diagnostic functions

- $\mathcal{E}$ – Calorimetry
- $\mathcal{S}$ – Spatial profile measurement
- $\mathcal{T}$ – Temporal profile measurement

ALIGNMENT SENSOR LOCATIONS FOR A SINGLE BEAM

OUTPUT POINTING WITH THE PFC SENSOR

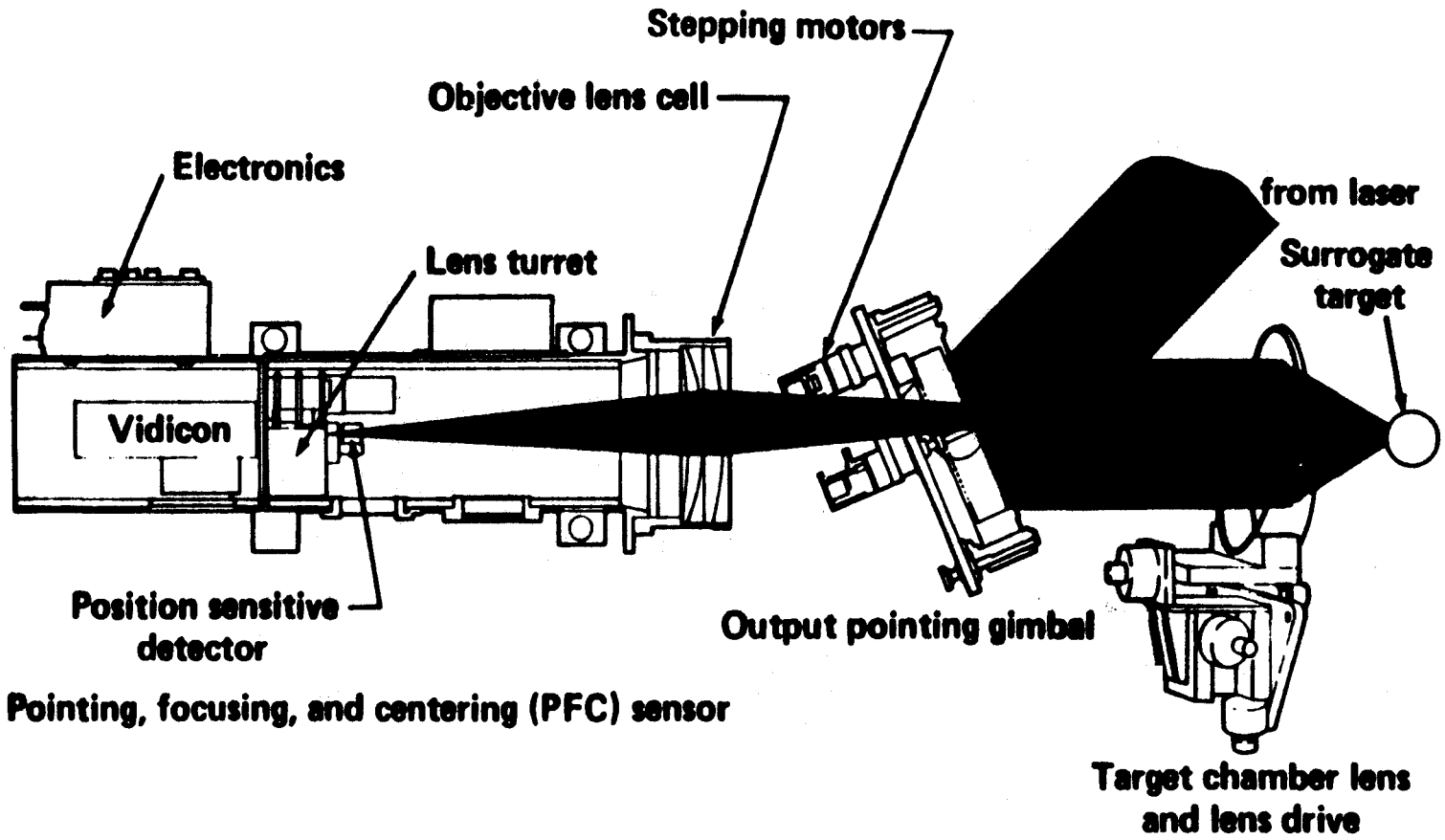

Pointing, focusing, and centering (PFC) sensor

Alignment error tolerances

- **Input beam, 2 cm diameter**
  - **Maintain ± 4 μ rad pointing & 0.5 mm translation for more than 100 sec**

- **Output beam, 74 cm diameter**
  - **Maintain ± 4 μ rad pointing and 8 mm translation**

- **Total error**
  - **21 μm on target**

- **Arrival time at target**
  - **Within 5 picoseconds**

Structural system stability

- **Dominant stability considerations**
  - **Thermal**
    - **thermal stability is controlled by strict specification of facility air conditioning**
  - **Vibrational**
    - **vibrational stability is controlled by sizing elements for low weight & maximum stiffness to keep resonant frequencies high**
  - **Seismic**
    - **seismic stability is secondary to thermal & vibration stability**
      - **they are not necessarily compatible—one ensures stable operation & one ensures survival (i.e. system is mounted on rollers with a seismic anchor)**

Nova stability

- **Thermal stability**
  - **temperature control ± 1/2° C (no gradients)**

- **Zone air system**
  - **clean room—change every 30 seconds**

- **Thermal inertia of space frame is several hours**

- **Space frame mounted on rollers w/single seismic restraint**
  - **prevents structural damage**
  - **tested on a hot day**

LATERAL THERMAL DISPLACEMENTS OF NOVA SPACE FRAME

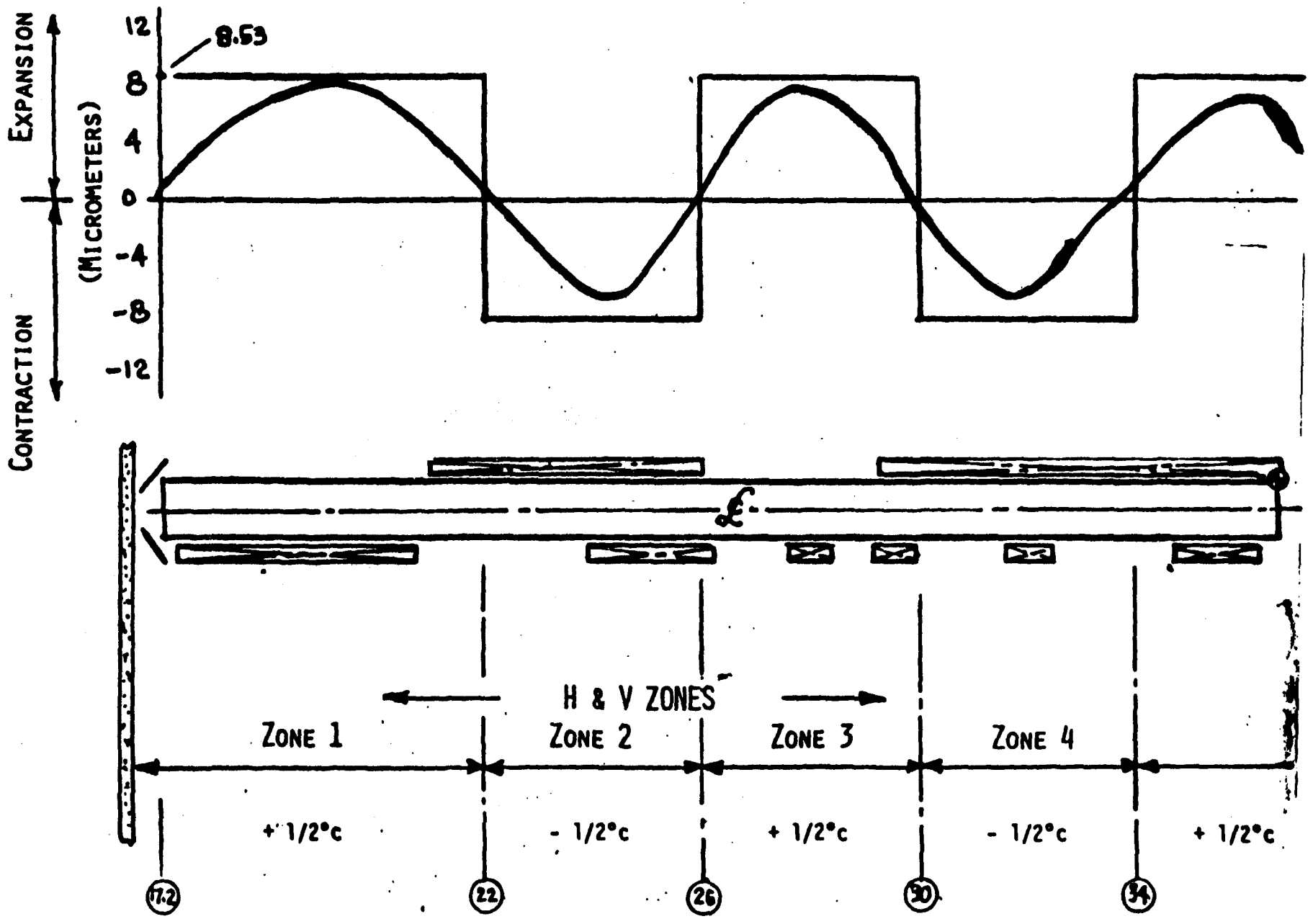

Design approach for vibration stability

- **Measurement of site input forces**

- **Determine type of construction**
  - **consider damping (welded steel 2%)**
  - **design for low-weight and high stiffness**

- **Design for seismic events**

- **Perform dynamic analysis of design** (finite element model to find modal frequencies [SAP IV])

- **Adjust design accordingly**
  - **iterate the model to find desired frequencies & amplitude**

- **Determine pointing accuracy of system**
  - **ray tracing to develop an error budget**

- **Construction & deployment**

- **Perform dynamic testing**
  - **experimental modal analysis to verify finite element analysis**

NOVA LASER FRAME

- Dynamic analysis — first mode shape

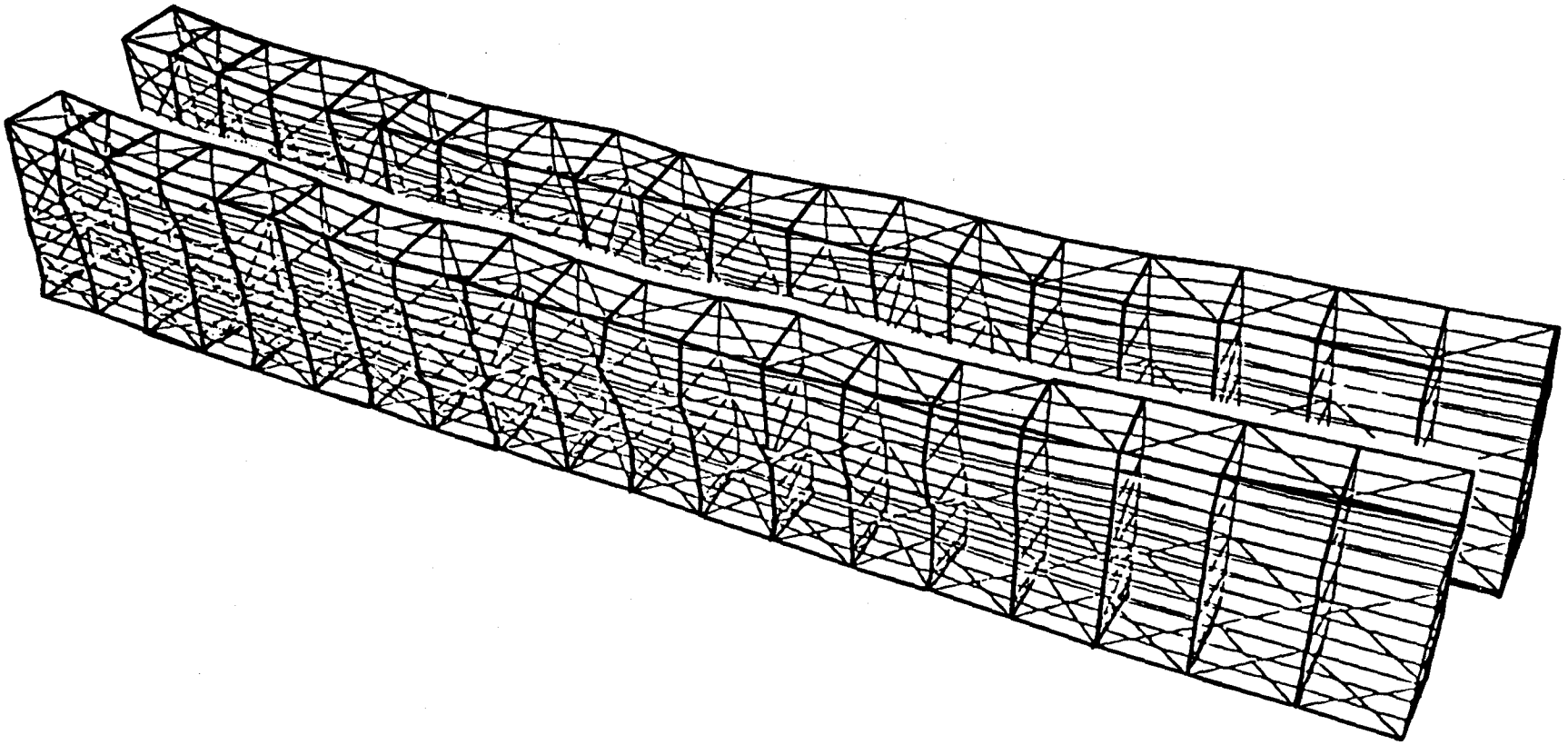

02-31-0931-3087

Mode 2 8.500 hz.

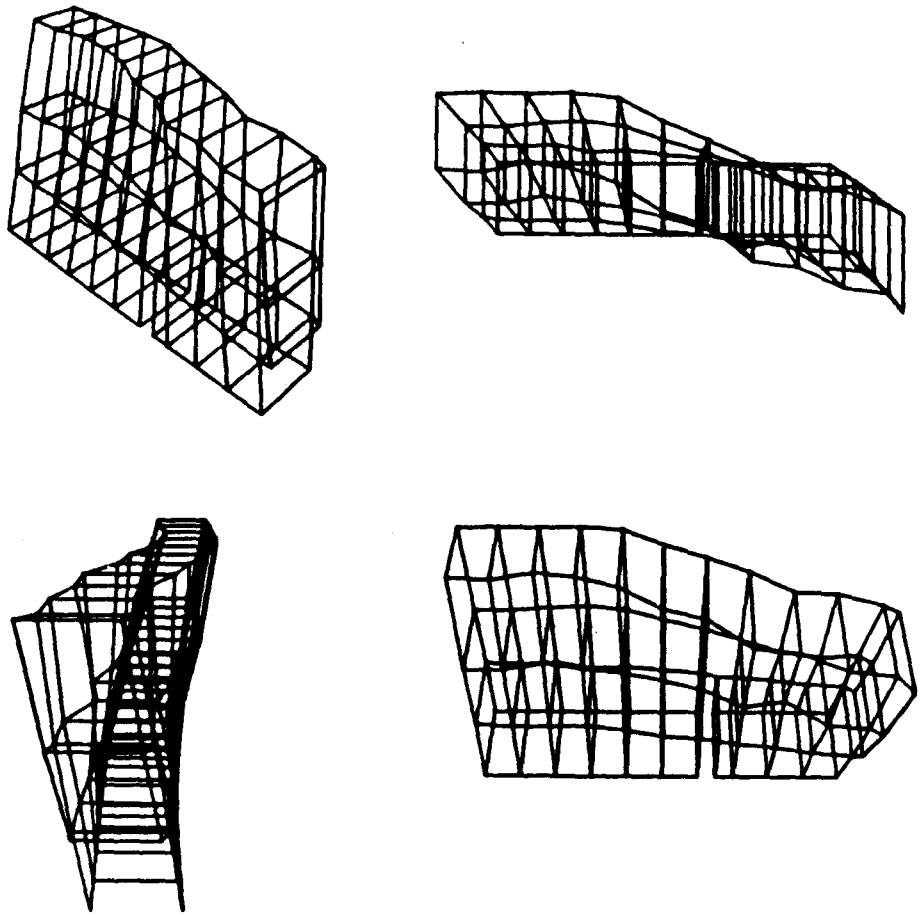

Nova stability

Laser bay frames

Mode	Calculated frequency (Hz)	Measured frequency (Hz)
1	9.95	8.27
2	10.08	8.45
3	11.32	8.72
4	12.11	9.57
5	13.61	11.25

Switchyard frames

Mode	Calculated frequency (Hz)	Measured frequency (Hz)
1	6.66	5.5
2	7.06	6.3
3	8.25	8.6
4	15.56	19.1
5	16.13	21.4

Target frame

Mode	Calculated frequency (Hz)	Measured frequency (Hz)
1	4.15	5.6
2	5.45	5.9
3	5.72	6.3
4	5.91	6.5
5	6.56	7.5

Translation ± 5 μm
Rotation ± 0.7 μ rad

Mechanical & structural design

- Space frames designed as an optical bench
- Installed to within 1/8" in 225 ft.
- 1/8" tolerance is <u>not</u> adequate for a machined optical bench
- System of shimplates clamped to frame generates vertical & horizontal planes to within 1 mm
  - Installed using installation tool and an alignment laser
  - C omponent cradles are located and fixed to these plates
  - Tool mounted on cradle accurately locates each component. Cradle is locked and bolted in place & tool is removed leaving no knobs
- Each conponent is accurately positioned in the V-block cradle allowing interchangeability of components and easy change with no realignment

NOVA COMPONENT CRADLE & INSTALLATION ALIGNMENT FIXTURE

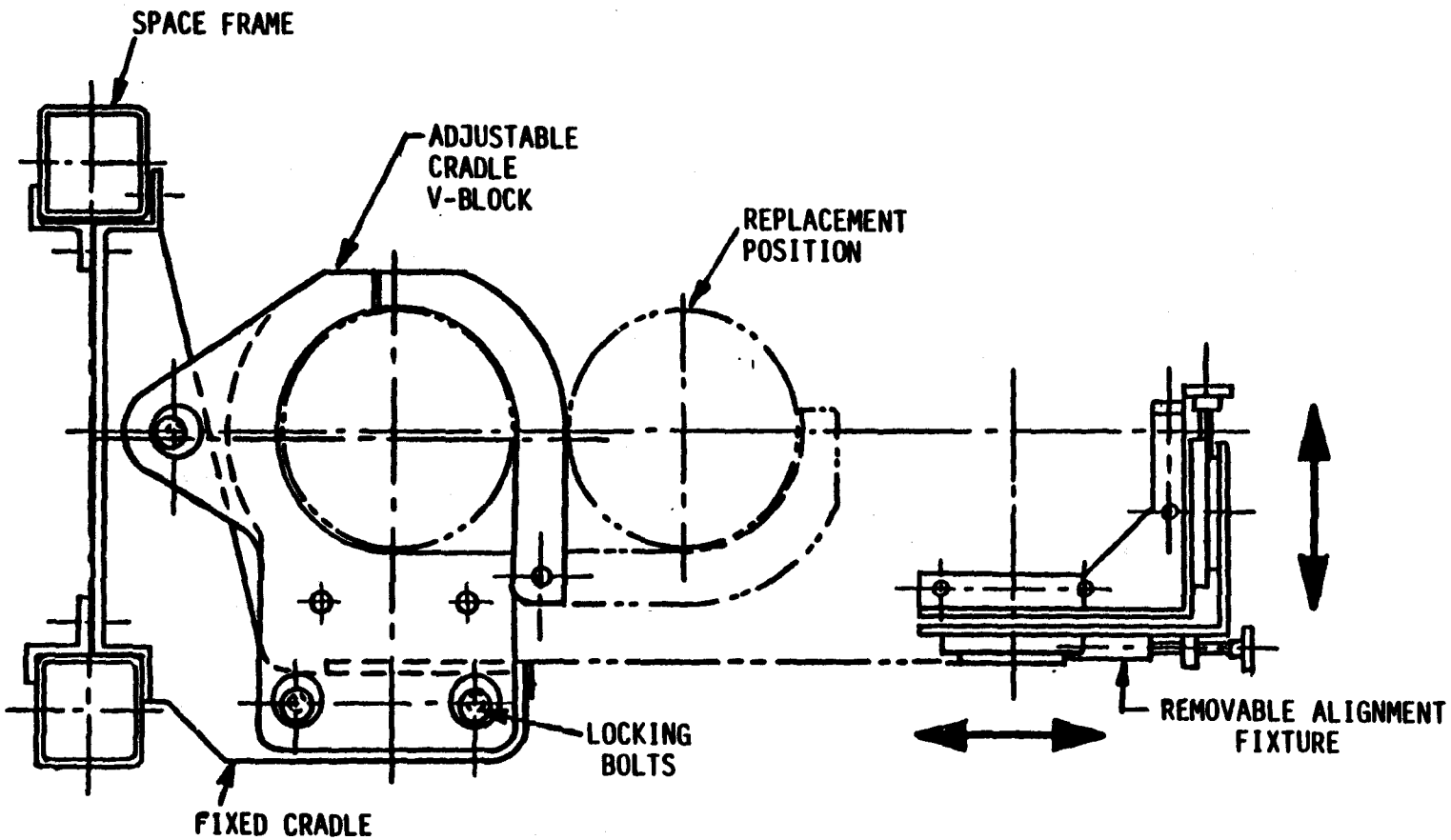

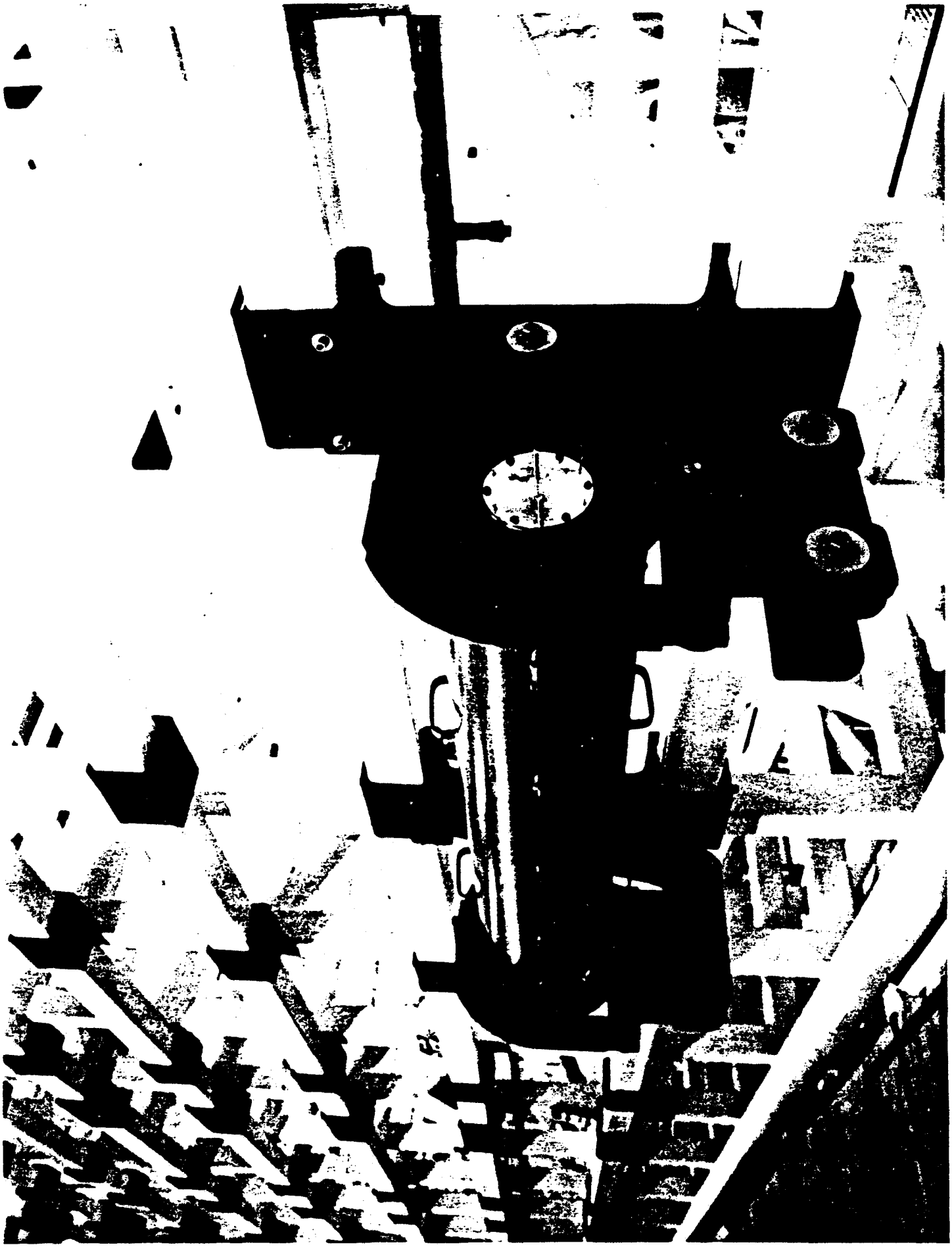

Nova stability
Cost effective steel structure

- **Nova space frame—a cost effective steel structure**
  - **800,00 lbs @ $2.28 per lb**
  - **Designed for shop fabrication using tooling & fixtures to control dimensiions & distortions**
  - **Machined and welded joints**
  - **6 x 6 square structural tubing**
    - **flat surfaces for mounting**
    - **simple joints**
    - **moment of inertia is the same in all directions**
  - **Shop-fabricated maximum size units to minimize field welds**
    - **size limited only by transport, load limits, doorways & cranes**
  - **Erected using engineered alignment procedures**

High bay of Nova laser with laser glass amplifier assemblies

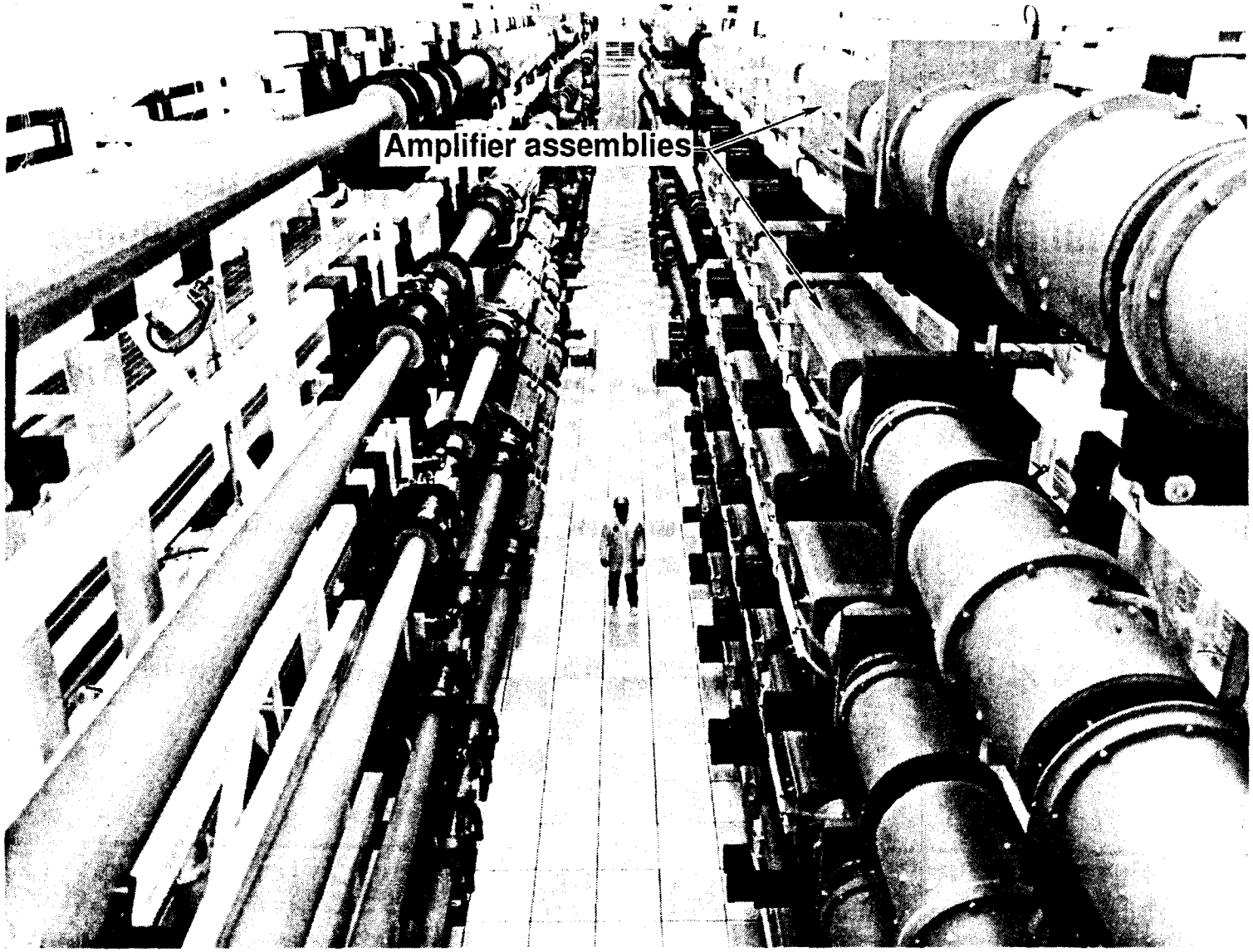

02-31-0585-2377C

4/87

Nova target chamber construction

- 16 ft. spherical aluminum vacuum chamber, 4 in. thick wall
- Alignment possible only when evacuated
- Target and optics mounted on vacuum wall
- Recommendation: if possible, separate sensitive alignment equipment from vacuum wall.

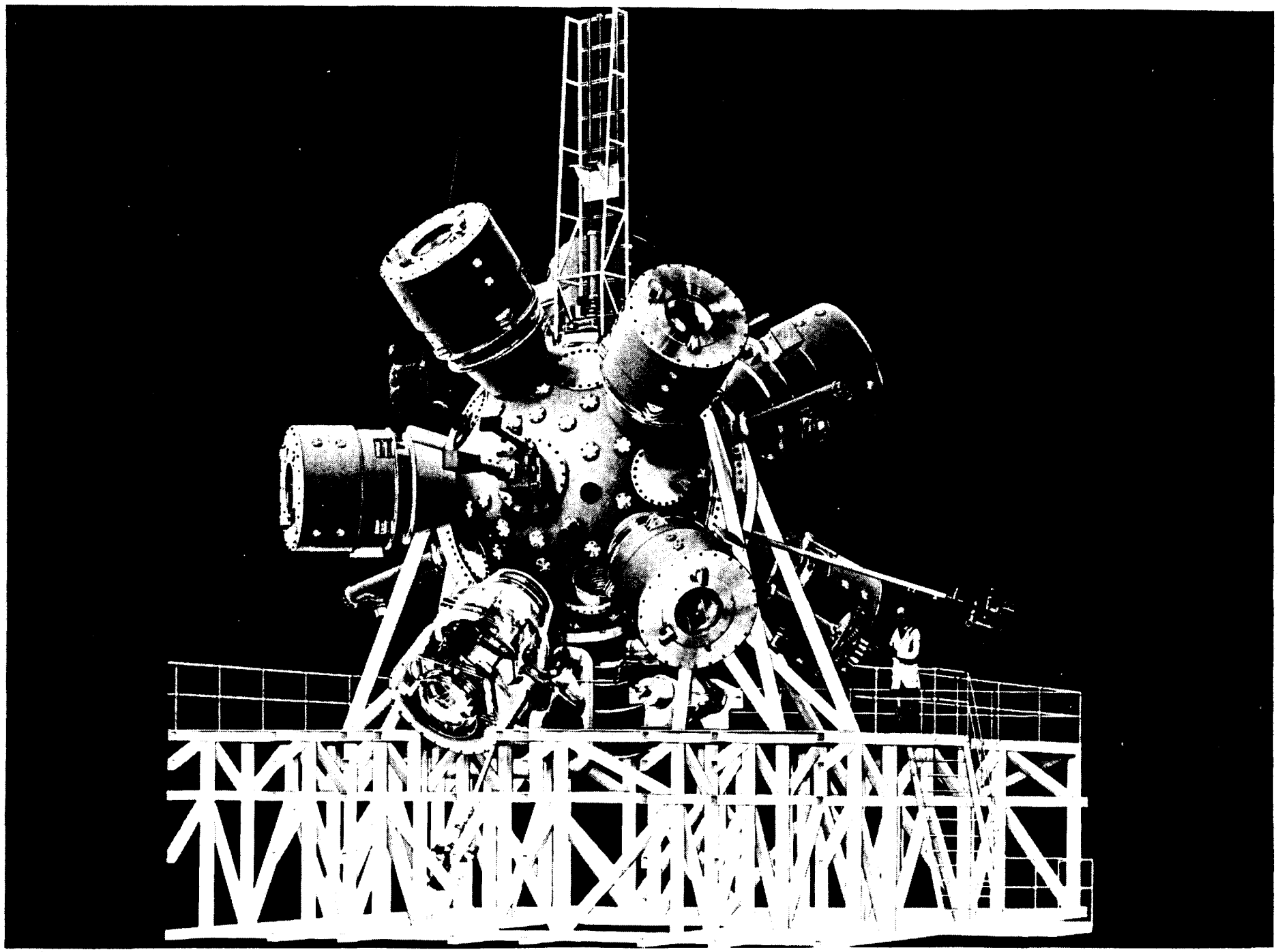

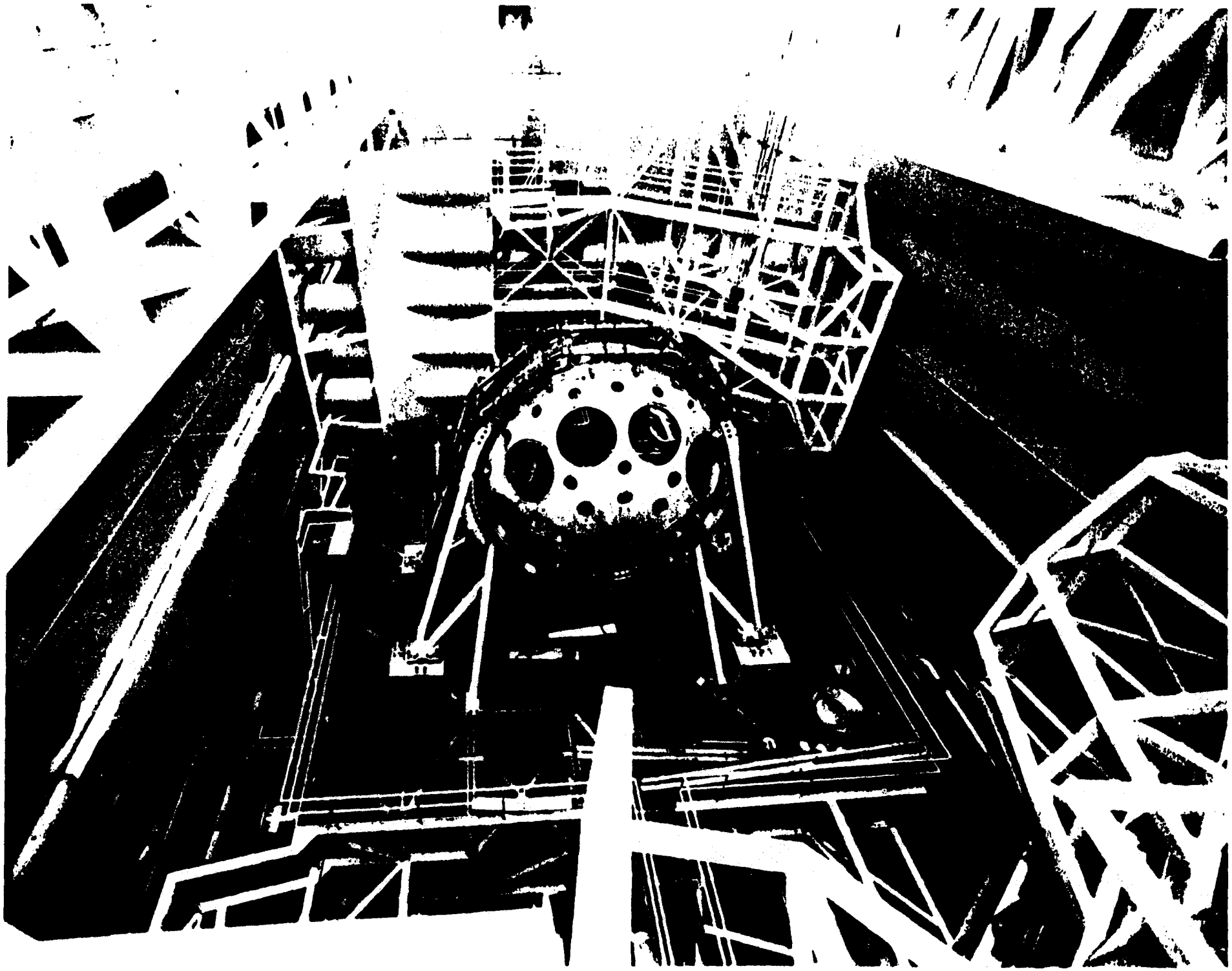

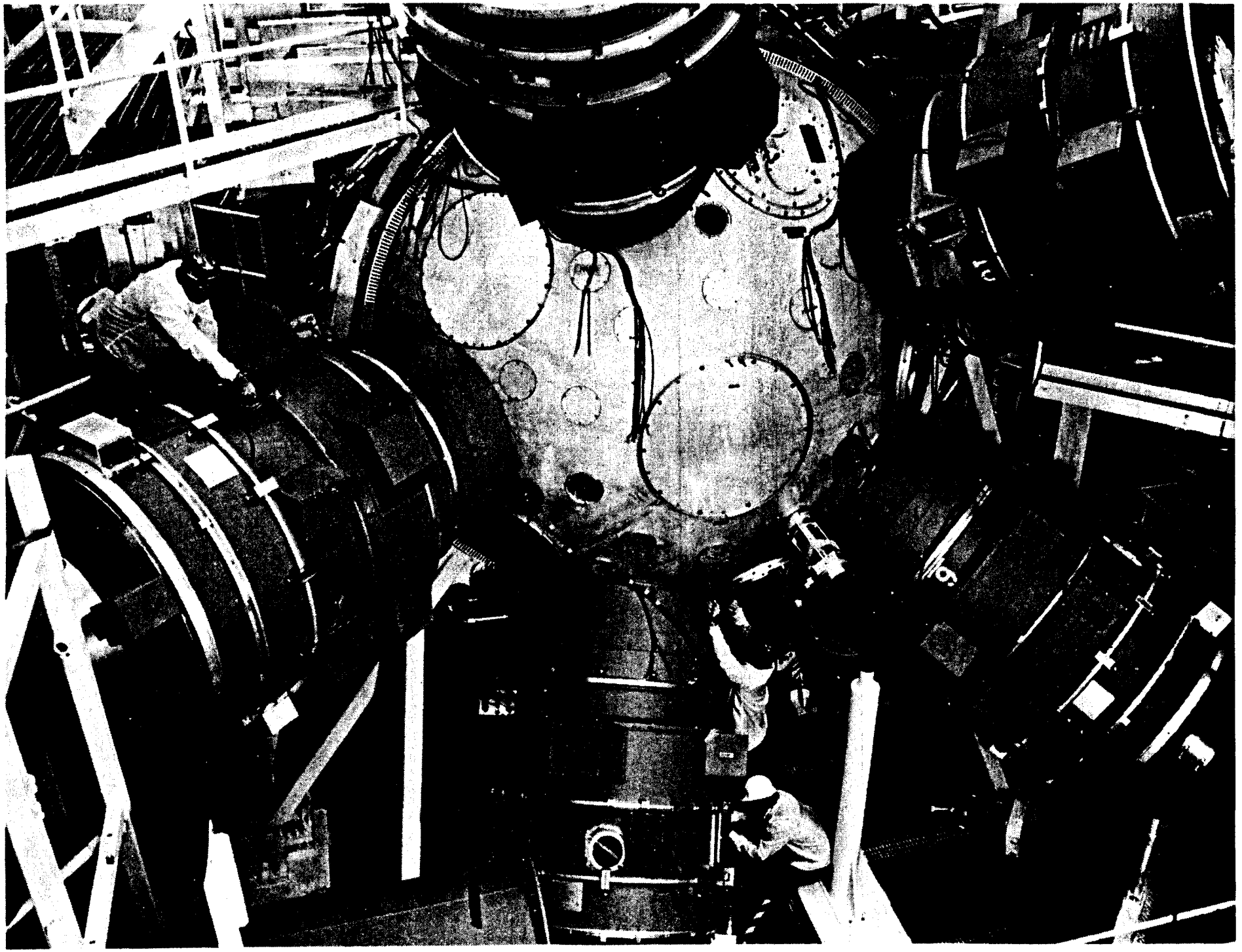

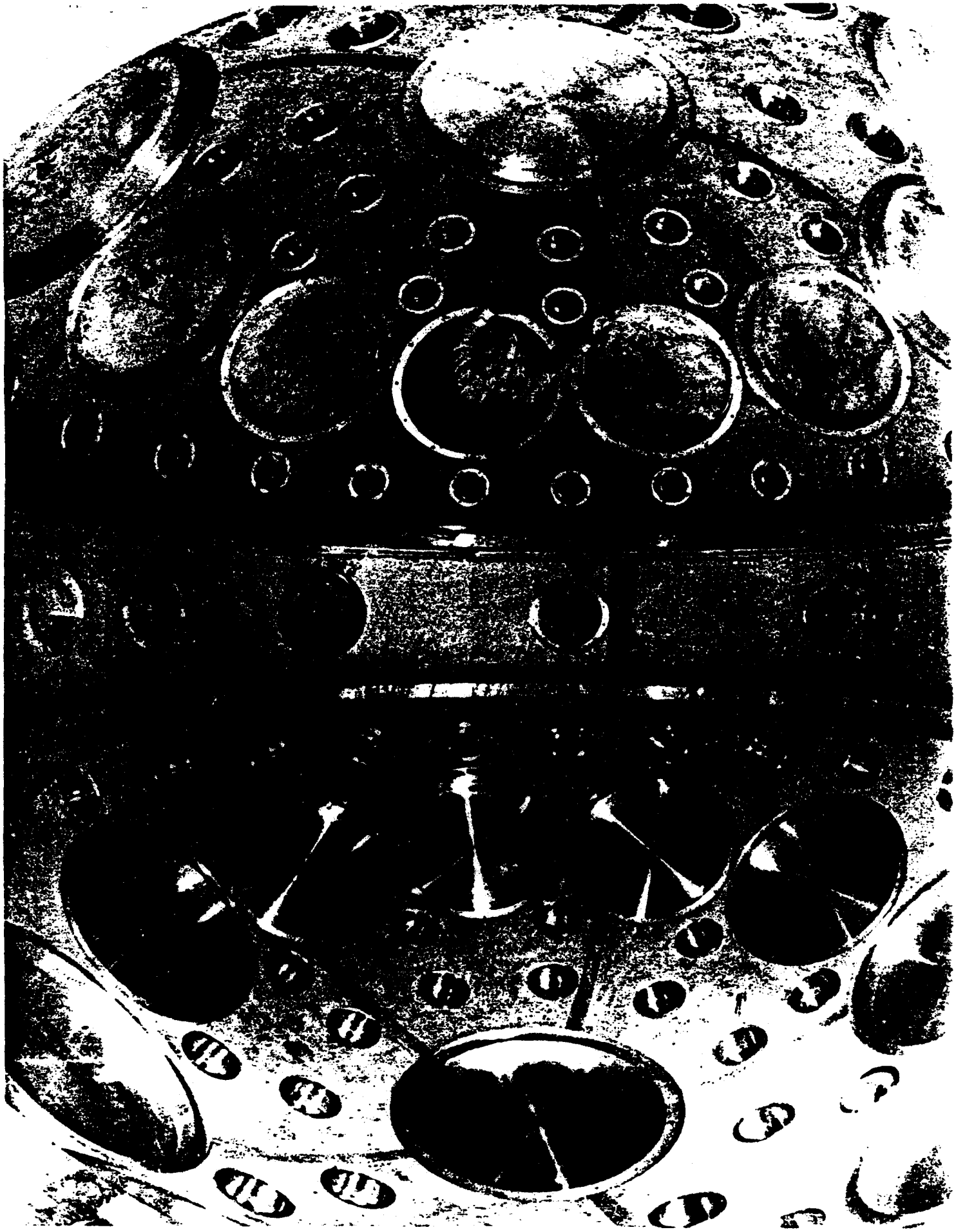

Nova stability—other comments

- Major equipment gravity loads must be on stable foundations (i.e. thick, concrete slabs or footings)
- Springs such as cantilevers must be avoided
- When mounting to concrete, consider thermal cracks & continuous chemical change.
- Design successfully used by four other systems
  - Shiva, LLNL
  - Novette, LLNL
  - Phebus, France
  - Gekko XII, Japan

Summary

- **We used a combination of structural stability and automatic alignment to successfully build an accurate and cost-effective target shooter.**

Finite Element Analysis of Large Structures

David B. McCallen*

Robert C. Murray**
(Presenter)

SSC Workshop

February 11, 1992

* Structural Mechanics Engineer, Structural Mechanics Group, LLNL (510) 423-1219

** Associate Program Leader, Nuclear Systems Safety Program, LLNL (510) 422-0308

Three topics relative to large scale finite element computations will be briefly discussed

- Hardware available to structural analysis engineers and how recent hardware changes have increased productivity

- Subset of LLNL developed computer software most pertinent to structural and solid mechanics problems

- Examples of large scale finite element computations (with a focus on dynamics problems)

  - Alignment sensitive structures
  - Current work on modeling a large bridge structure (integration of *CAD* in analysis process)
  - Illustration of a computer generated movie

Hardware Available to LLNL Structural Analysts

Sun Workstation

Structural Analysts Office

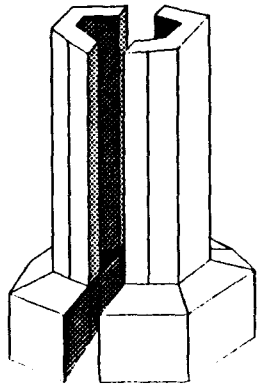

Supercomputers (Cray YMP)

CPU intensive tasks
(i.e. number crunching)

-Finite Element Analysis of *Large* Systems

- Post Processing of *Large* Analysis Results

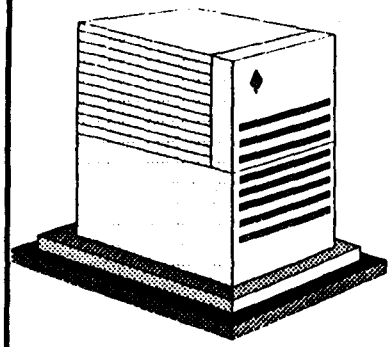

Workstation File Server

IO intensive tasks
(require user interactivity)

-Mesh Generation

-Small and Intermediate Analyses

LLNL has a "complete package" including the latest technological developments in both hardware and software

- All of the LLNL developed programs are continuously maintained and updated

- All three legs of a modeling effort are available with programs that communicate
  - mesh generators
  - analysis programs
  - post processors

- Access to developers of large codes allows speedy implementation of special features

LLNL has a suite of computer codes which are utilized for structural and solid mechanics problems

- SLIC/INGRID - Mesh generating routines for interactive definition of model geometry (Cray/Sun/Vax versions)
- GEMINI - General purpose linear elastic program for structural analysis, essentially an updated and modernized version of SAPIV (Cray version only)
- Category 1 Problems: DYNA3D/DYNA2D - General purpose nonlinear program for analysis of solids and structures (Cray/Sun/Vax versions)
- Category 2 Problems: NIKE3D/NIKE2D - General purpose nonlinear program for analysis of solids and structures (Cray/Sun/Vax versions)
- TAURUS/ORION - Post processing routines for above analysis codes (Cray/Sun/Vax versions)

Structural dynamics problems at LLNL fall into one of two categories: 1) high frequency-short duration loading, 2) low frequency-long duration loading

Category 1) example....

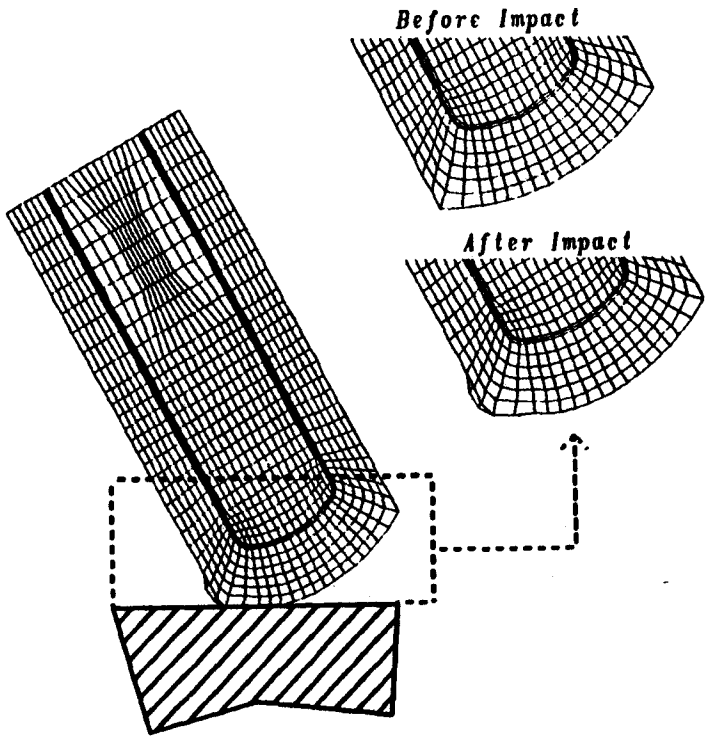

(e.g. Impact Analysis)

Category 2) example....

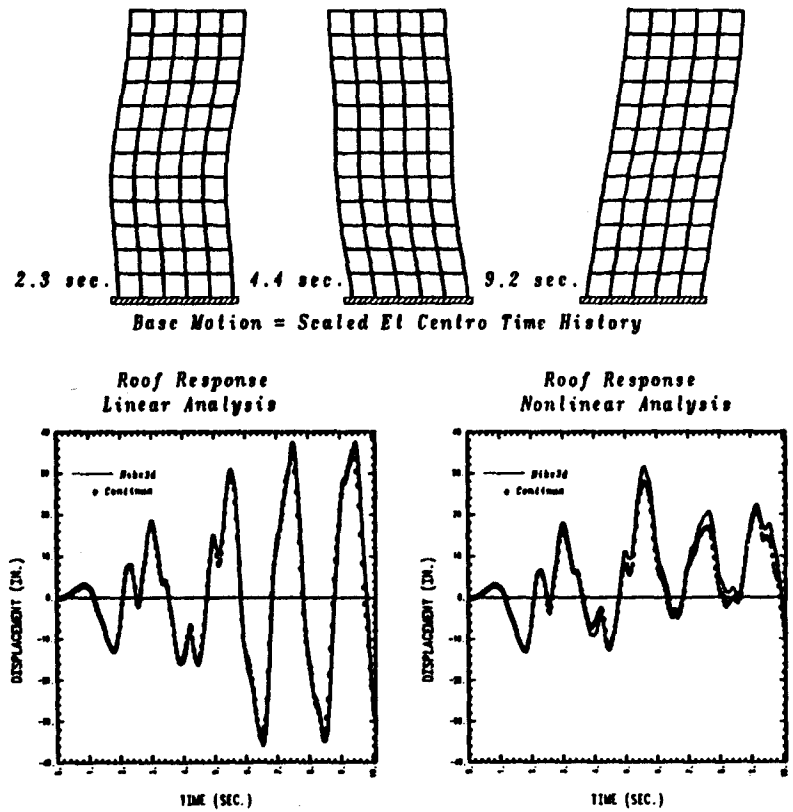

(e.g. Weak and Strong Ground Motion)

Mesh generating capabilites allow us to generate very detailed models of complex structural systems

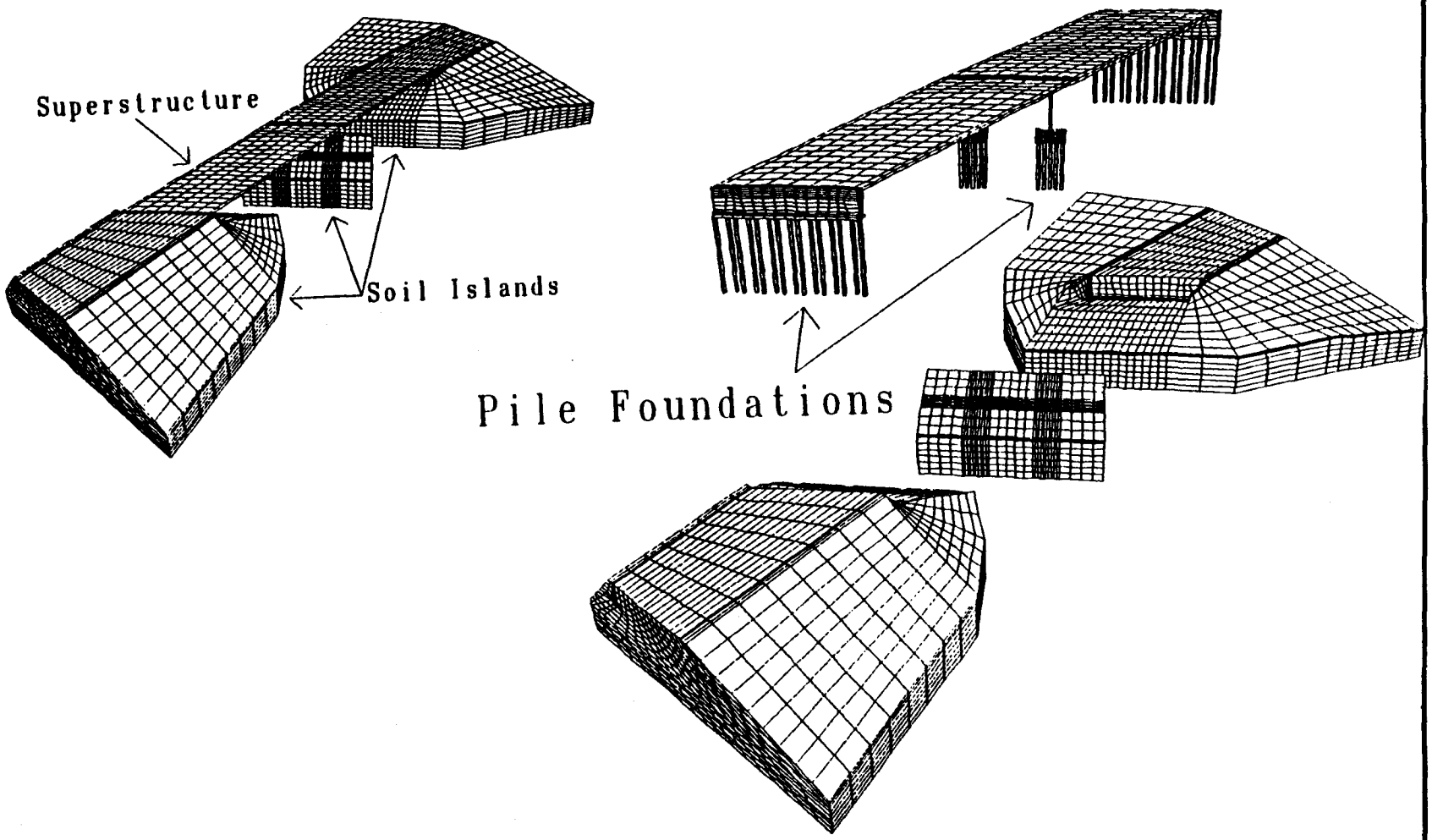

Supercomputer capabilites plus efficient software allow us to perform large scale numerical computations in an efficient manner

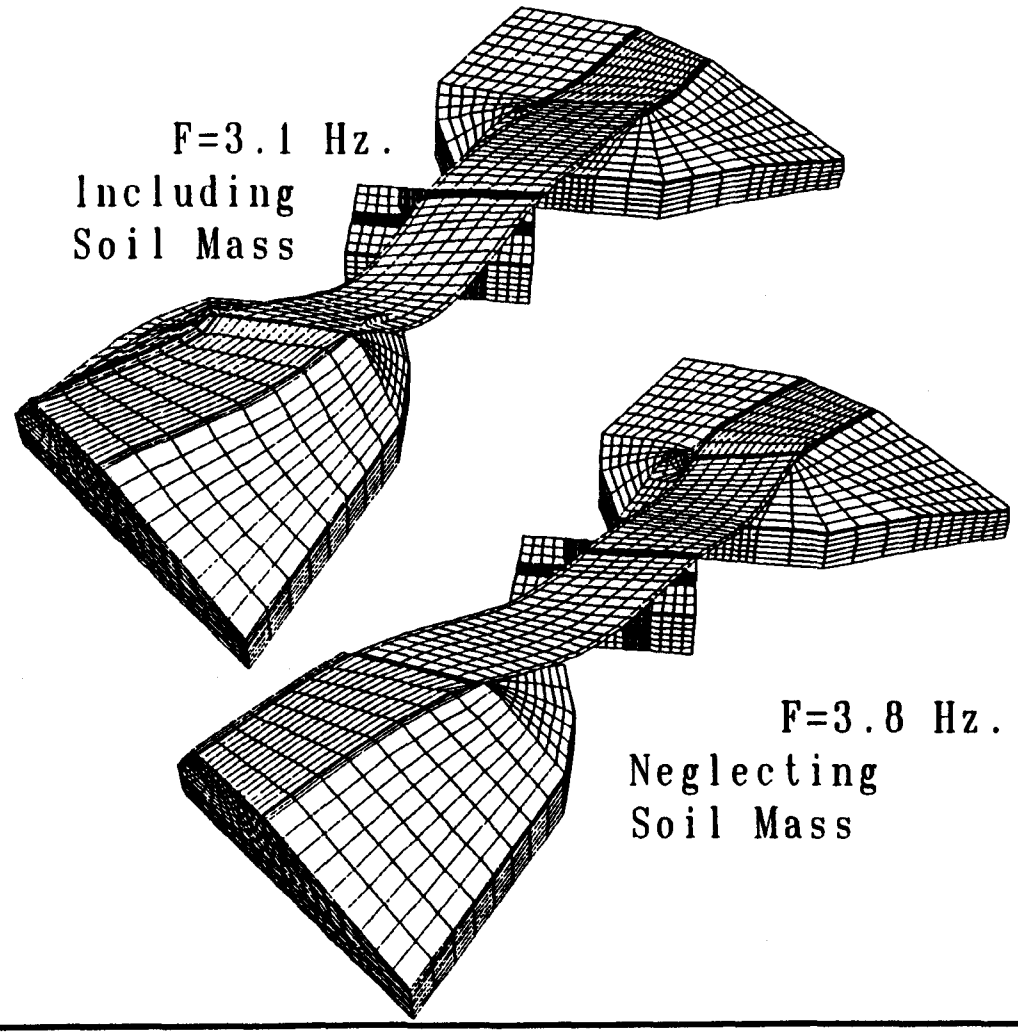

Example of large scale analysis of an alignment sensitive structure; *Nova Space Frame*

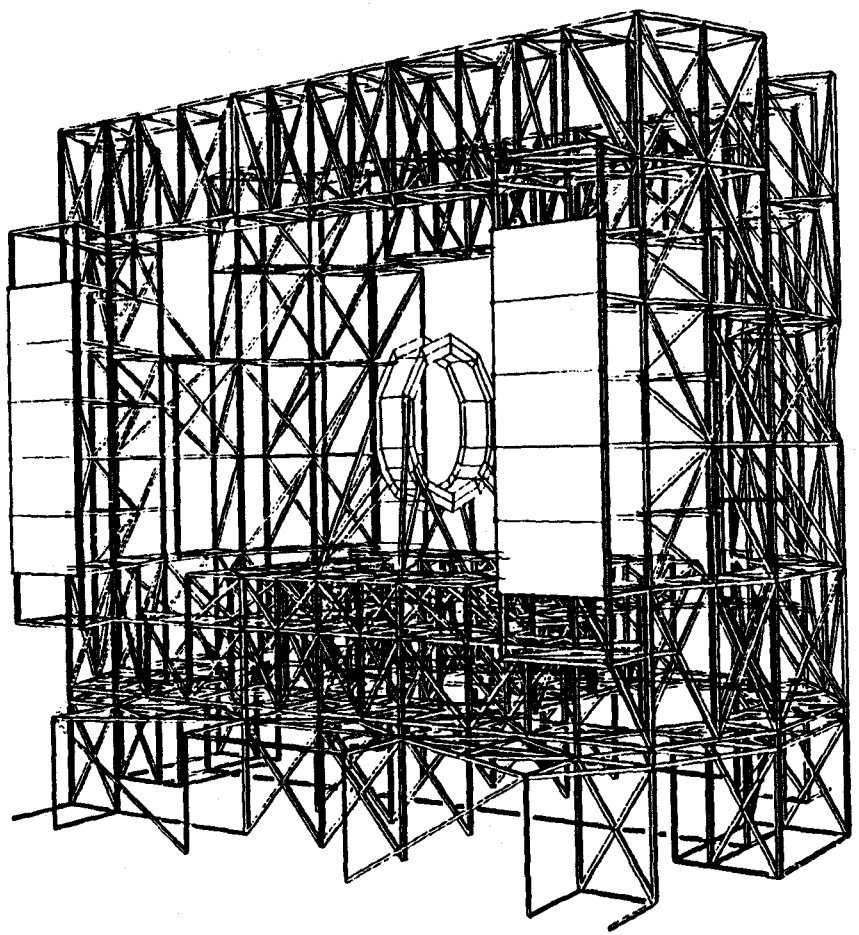

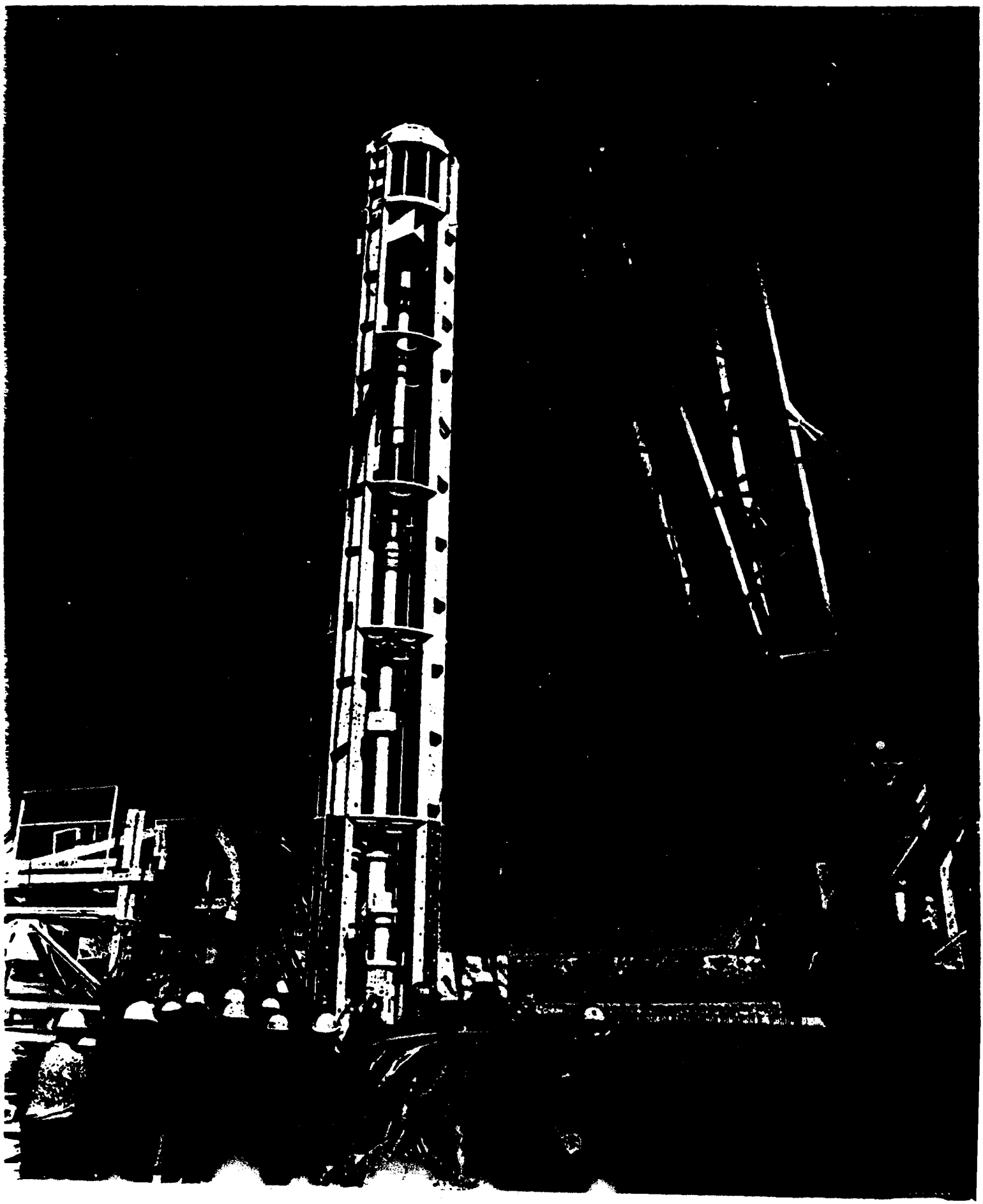

Example of large scale analysis of an alignment sensitive structure; *Nuclear Test Canisters*

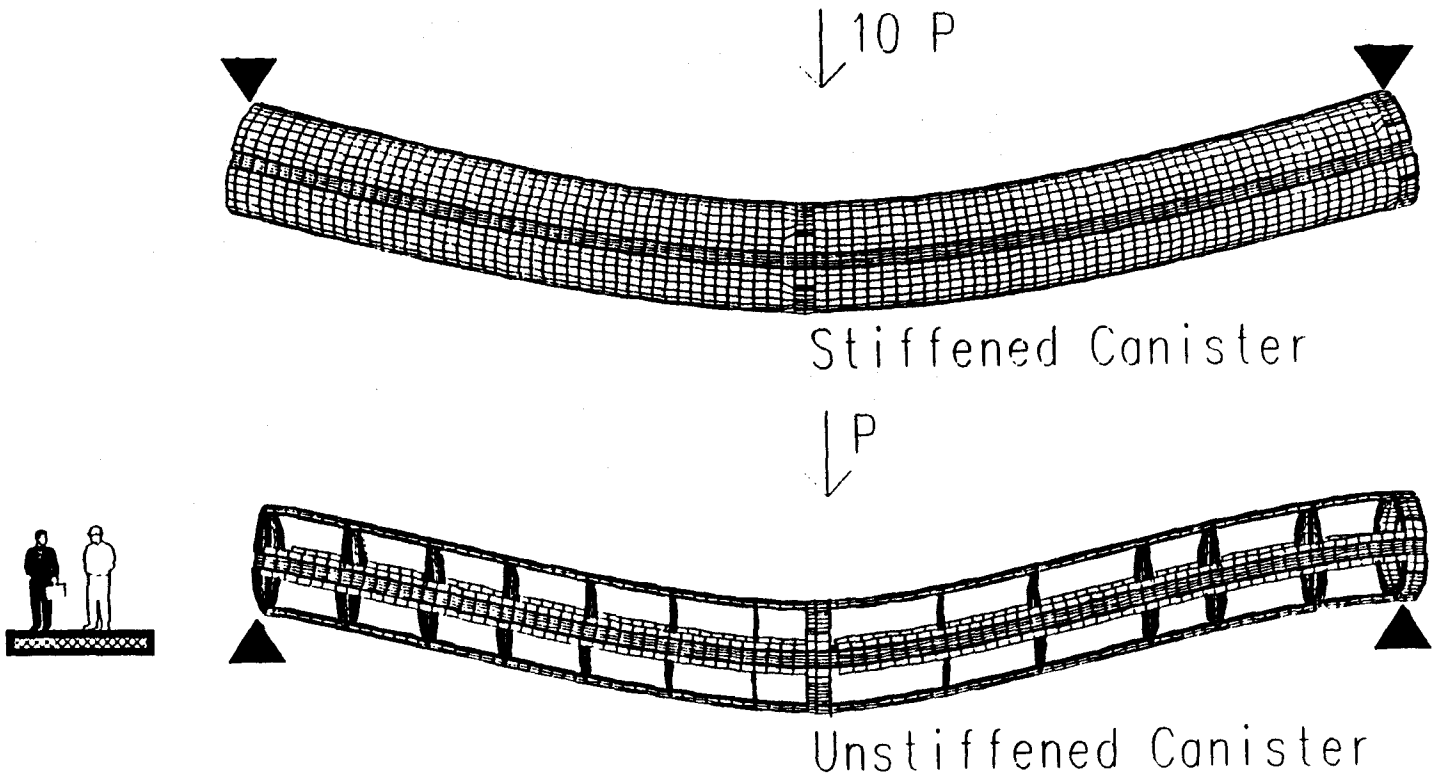

→ Finite element analysis provided guidance on cost and weight effective and weight minimizing stiffening schemes

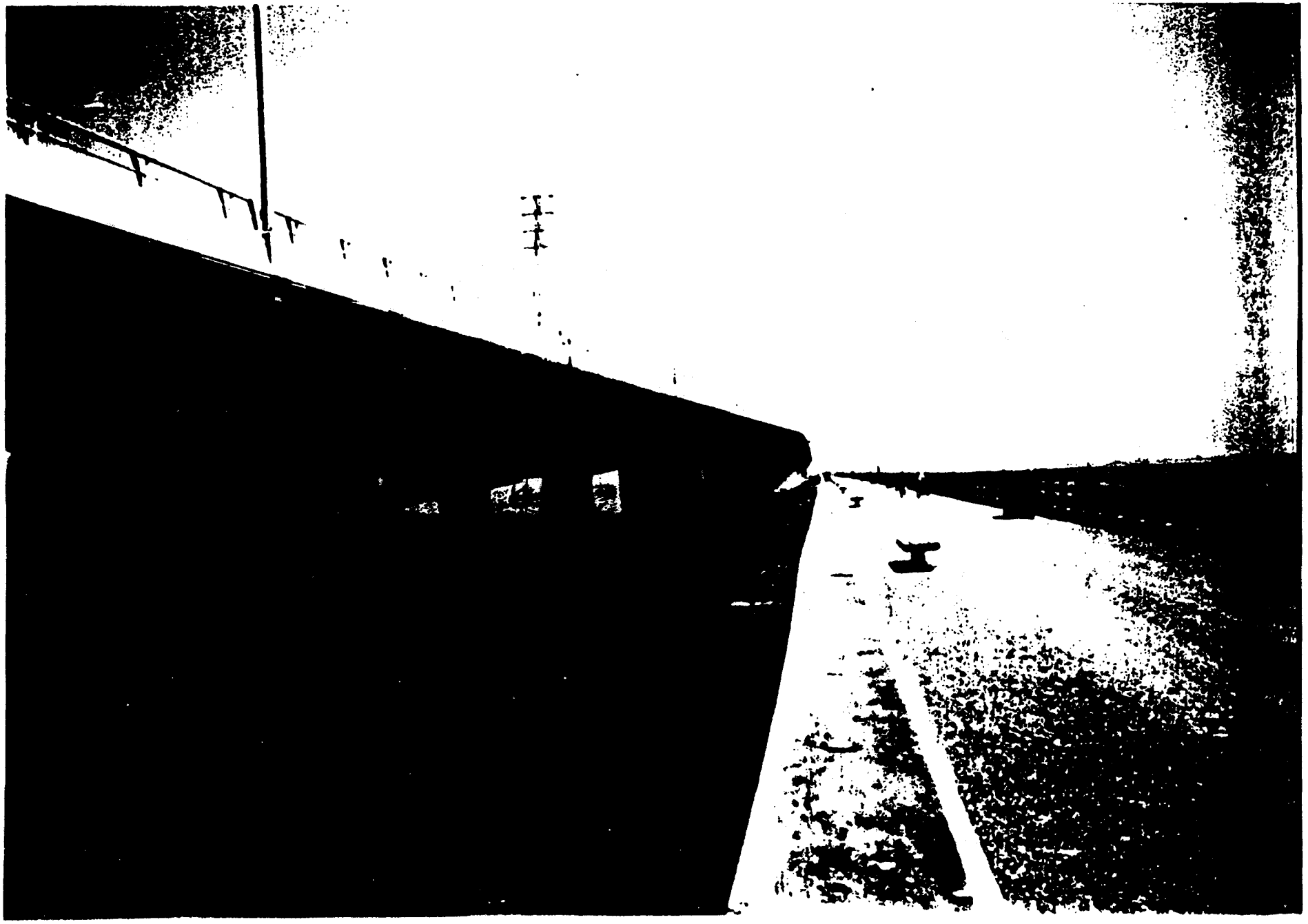

Example of large scale analysis currently being performed; *The Dumbarton Bridge*

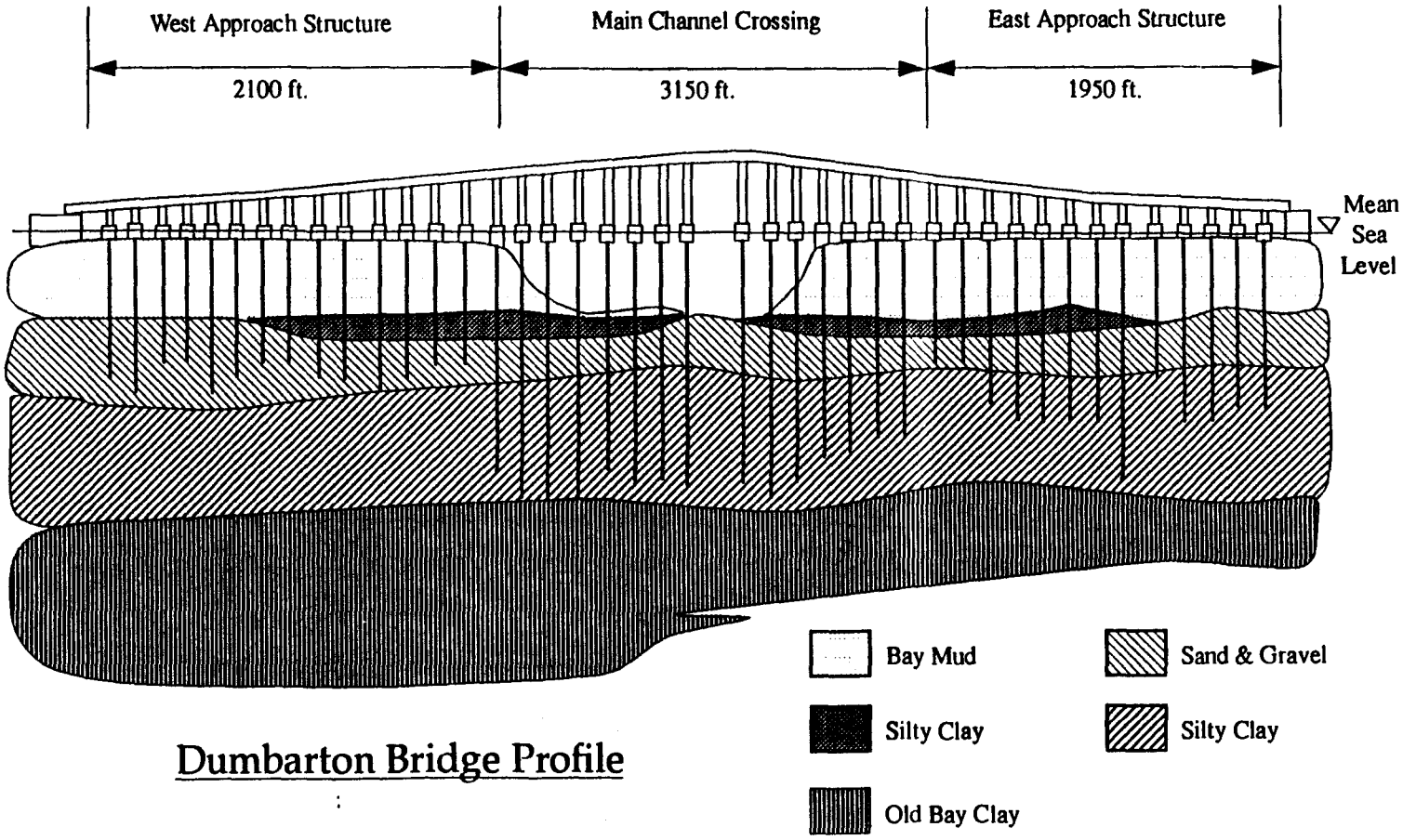

Dumbarton Bridge Profile

Varying structural connectivity between the deck and piers and the existence of numerous expansion joints significantly complicates the overall bridge response

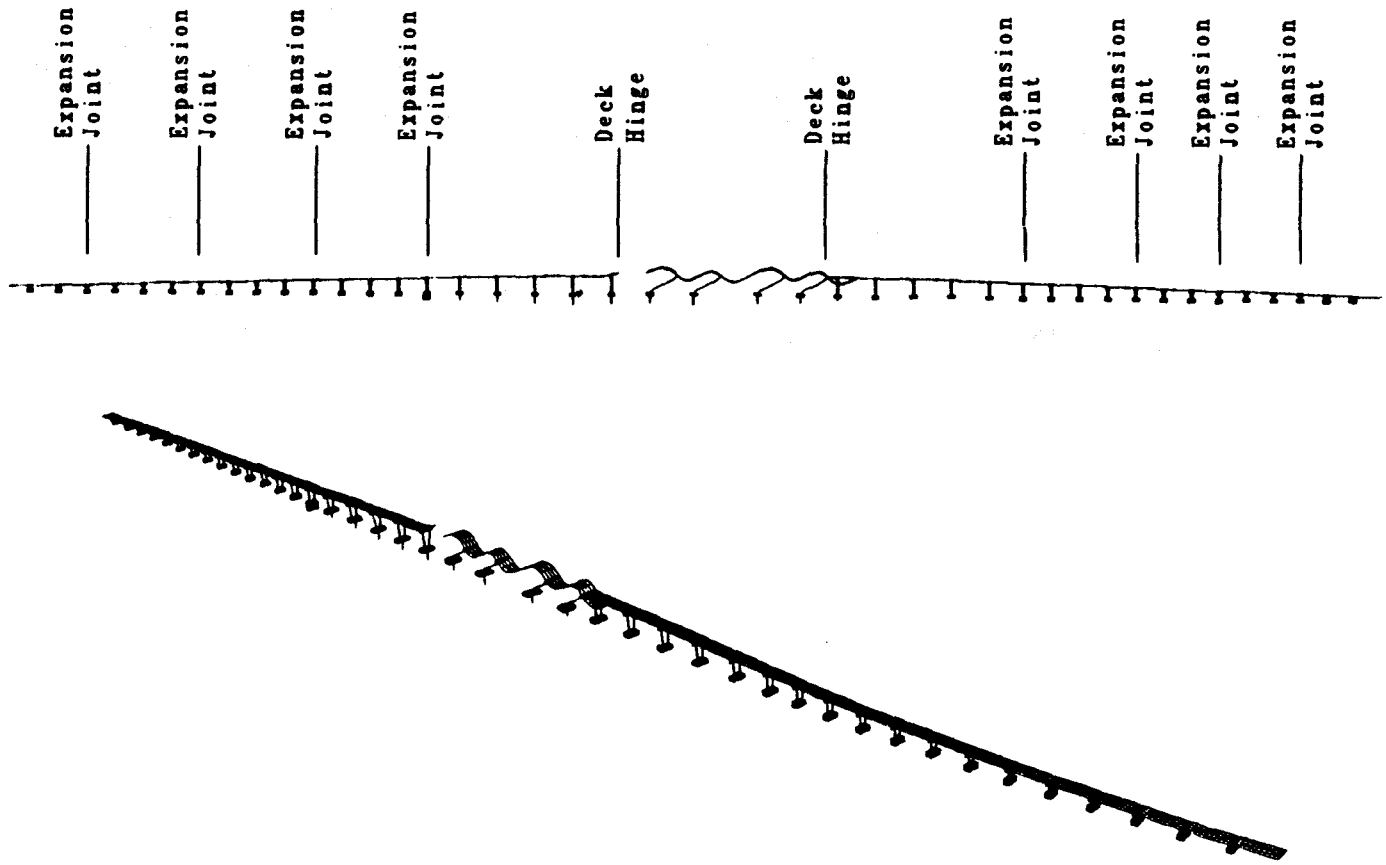

Dumbarton bridge mode #1; Axial vibration between deck hinges

The response of the Dumbarton bridge for the "maximum credible" earthquake will be predicted utilizing our large scale global model

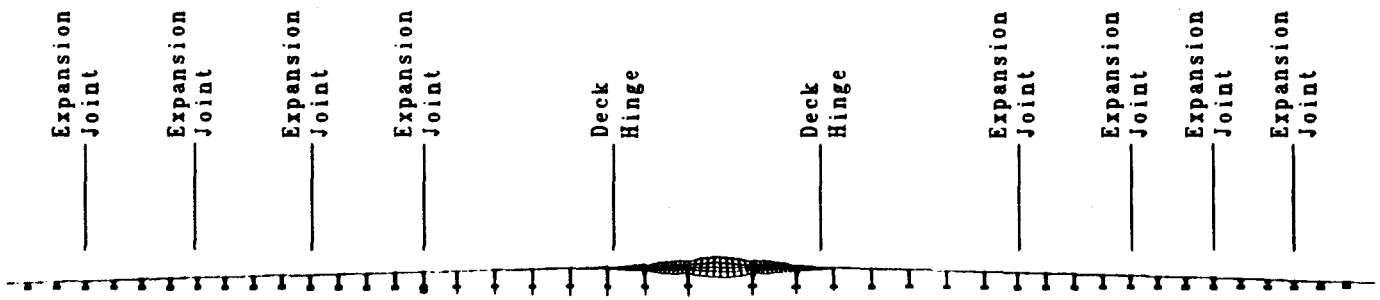

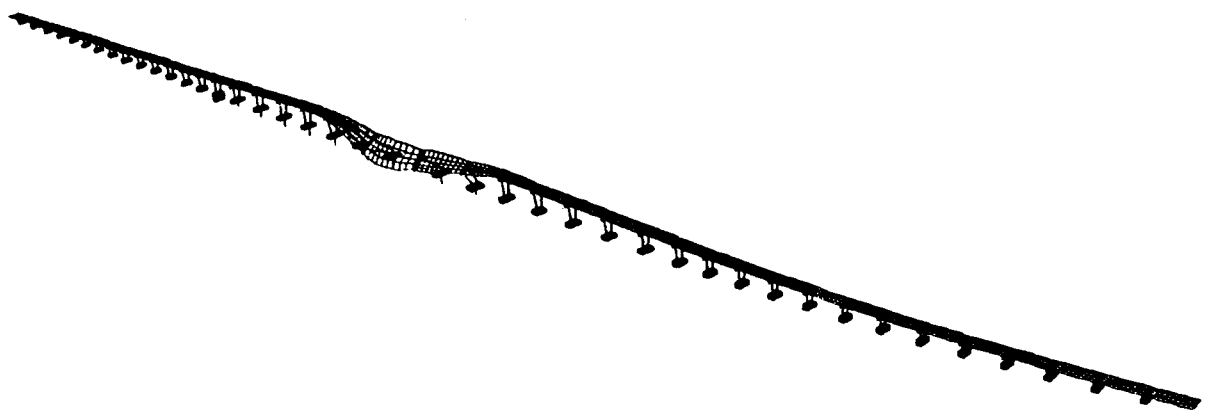

Dumbarton bridge mode #3; Transverse vibration of center span

Computer generated movies allow visualization of complex phenomenon

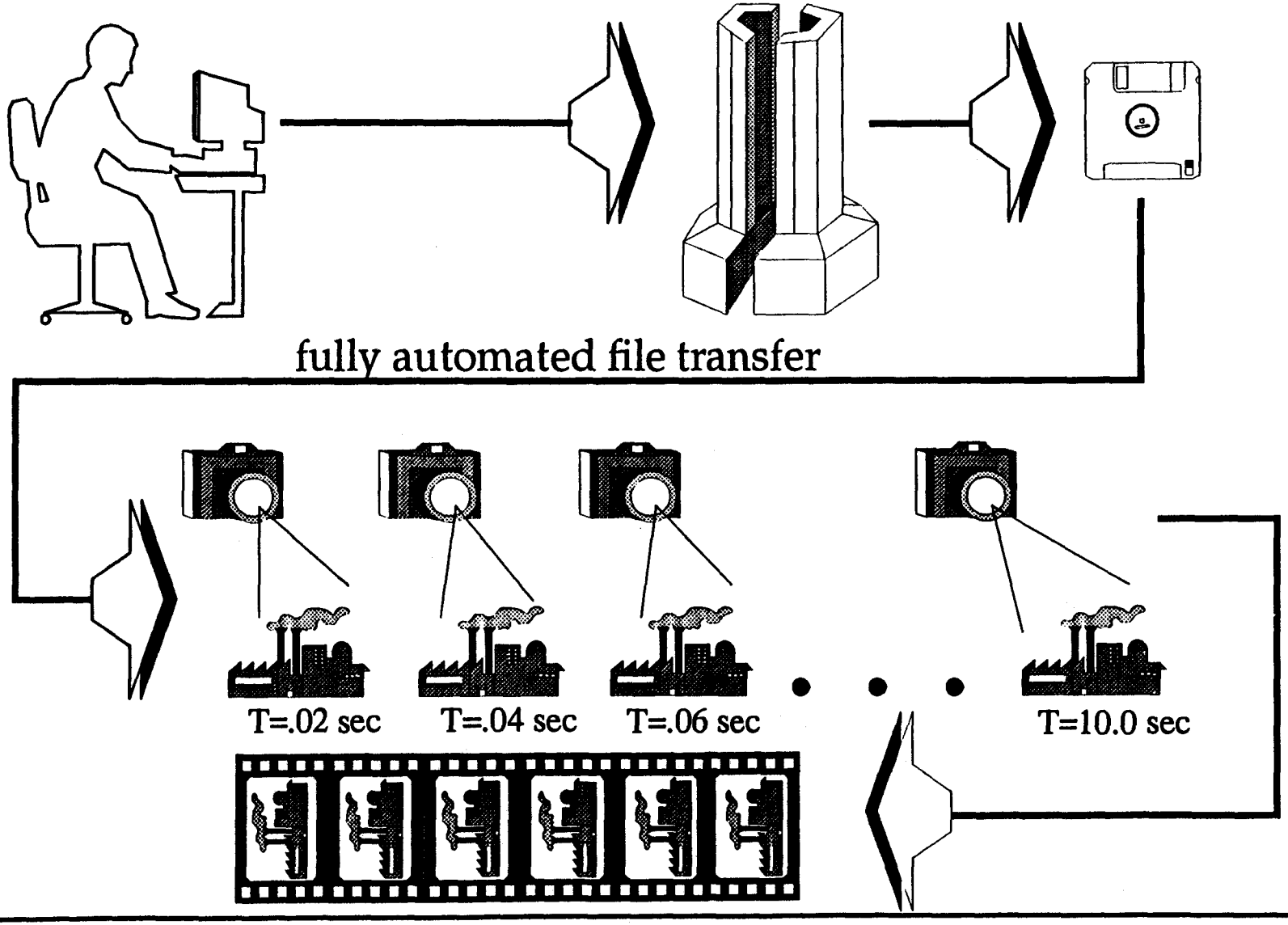

The movie will visually illustrate the dynamic response of some large structural systems

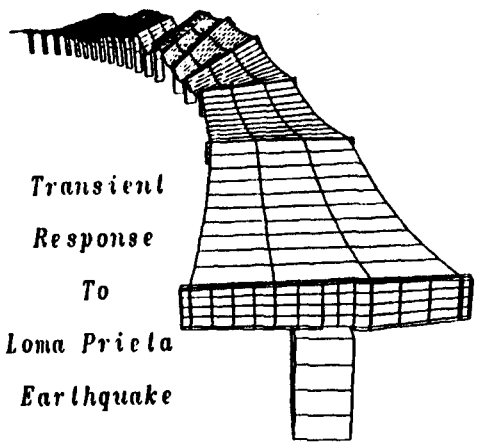

1) Bridge Structure

2) 3D Building

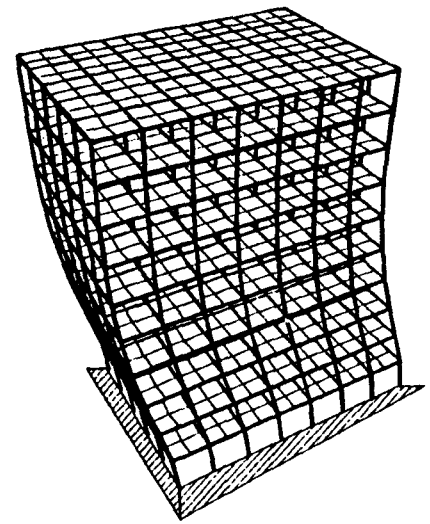

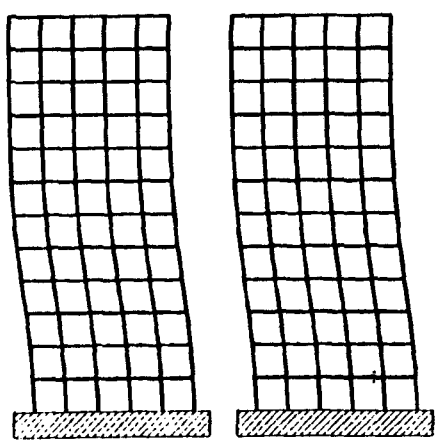

3) Linear vs. Nonlinear Analysis

4) Model Verification

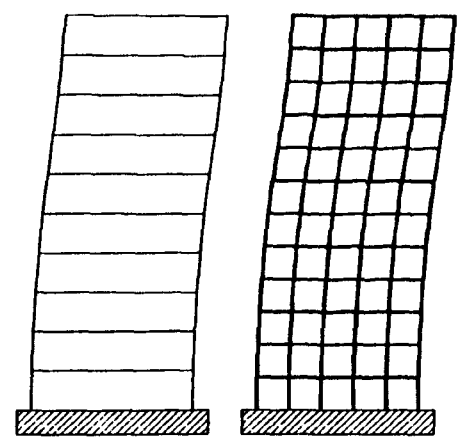

In summary, LLNL has all of the necessary ingredients to perform large scale finite element analysis

- Supercomputers readily available for large scale number crunching

- State-of-the-art LLNL developed software for *all three* steps of the analysis process

  - model generation
  - finite element analysis
  - post processing

- Experienced structural analysts capable of efficiently and correctly utilizing the hardware and software available

Structural Dynamic Testing and System Identification

Jim Lauffer
Sandia National Laboratories
Albuquerque, NM 87185

Workshop on Vibrational Control and
Dynamic Alignment Issues at the SSC
February 11, 1992

ilename:SNLA_2743_02_HD:FrameMaker 3.0:JPLauffer_Documents:scsi_Feb:scsi_presentation

Sandia is active in the area of MIMO structural control design

1) internal research and development program, 87 -89

2) DoD program, 89 to present

3) internal research and development program, 91 to 92

Filename:SNL A 2743_02_HD:FrameMaker 3.0:JPLauffer_Documents:scsi_Feb:scsi_presentation

An actively controlled structure consists of several components

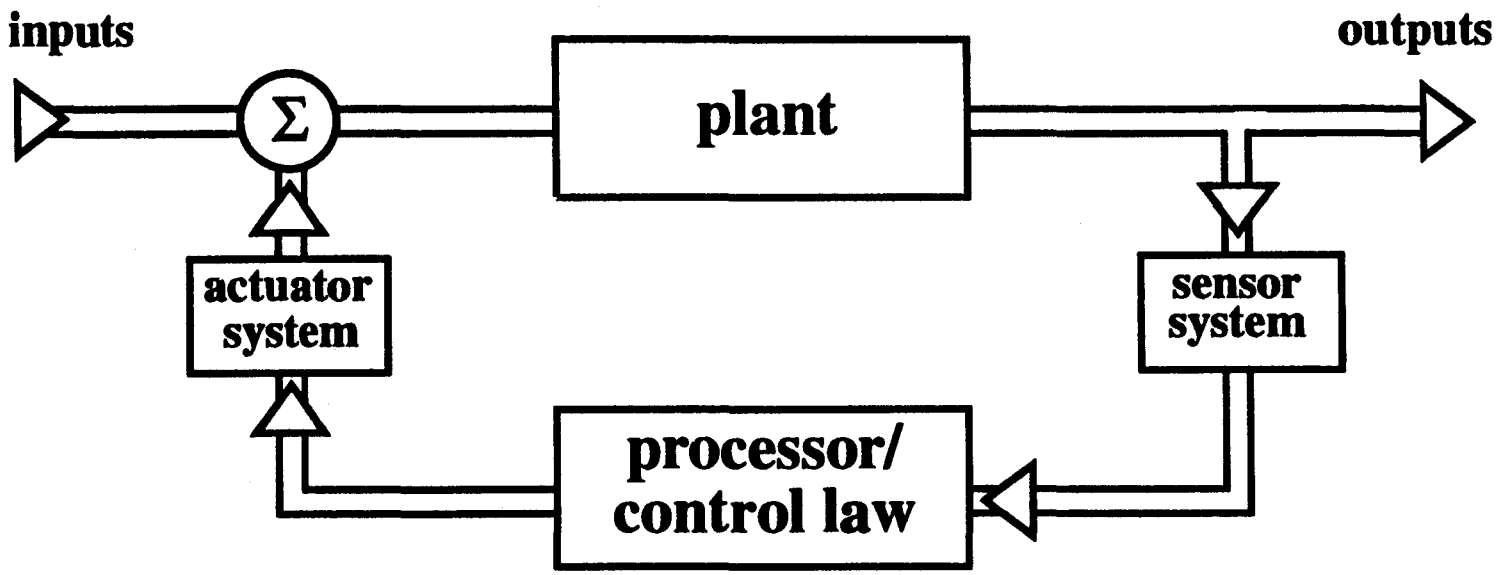

Each system can be represented by a state space equation

$$\dot{X}=AX + BU$$
$$Y=CX + DU$$

Filename:SNLA_2743_02_HD:FrameMaker 3.0:JPLauffer_Documents:scsi_Feb:scsi_presentation

We can divide active control into four core technologies

Active control of structures

Structural Analysis

1) preliminary design and analysis
2) plant modeling

Structural testing

1) disturbance requirements
2) plant model identification
3) component testing
4) implementation

Control design

1) design methods
2) implementation

Components

1) sensors
2) actuators
3) processors

Filename:SNLA_2743_02_HD:FrameMaker 3.0:JPLauffer_Documents:scsi_Feb:scsi_presentation

Structural control design is an iterative process

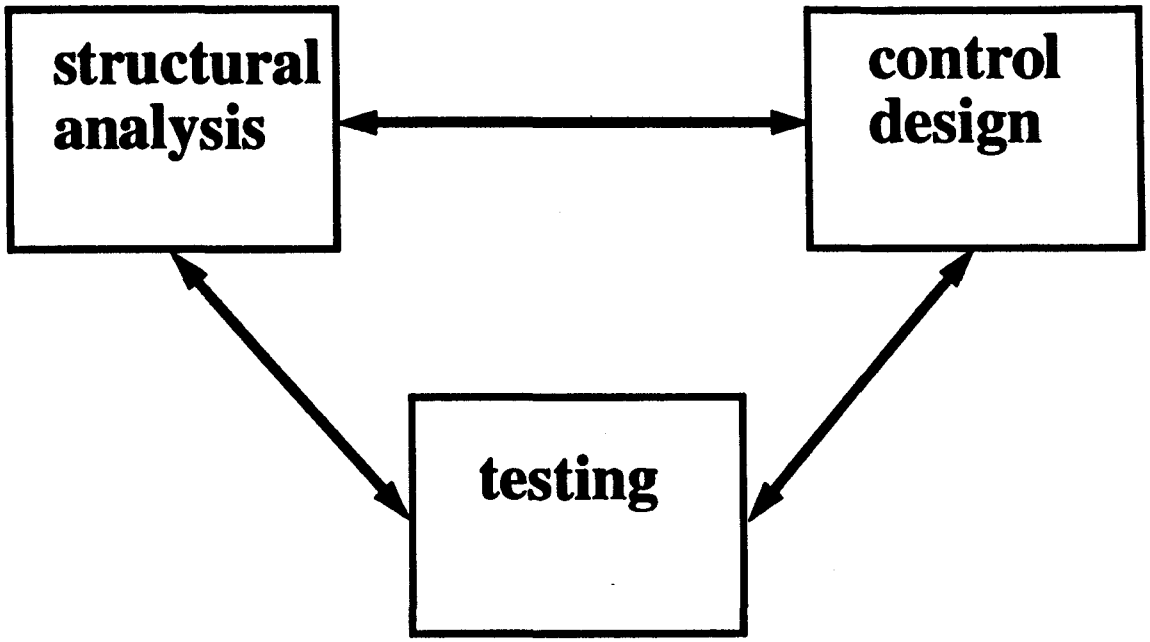

We define structural system identification as:

1) determination of a math model of a structure directly from test data

2) updating a finite element to agree with test data

Filename:SNLA 2743 02 HD:FrameMaker 3.0:JPLauffer_Documents:scsi_Feb:scsi_presentation

We perform modal testing for three reasons:

1) troubleshooting

2) updating finite element models

3) identification of a stand alone math model

⇨ **Developing a math model from test data is the most ambitious use of modal testing**

Filename:SNLA_2743_02_HD:FrameMaker 3.0:JPLauffer_Documents:scsi_Feb:scsi_presentation

Modal testing is difficult for real systems

1) nonlinearities
2) unknown order
3) time variant
4) modal density
5) damping
6) non-ideal sensors/actuators
7) boundary conditions

Modal testing consists of four steps

Excitation → **measurement** → **data processing** → **model estimation**

Excitation
1) transient
2) random
3) continuous wave

measurement
1) transducers
2) force
3) ADC/DAC
4) filtering
5) noise
6) sampling
7) block size
8) windowing
9) multiple inputs

data processing
1) FRF
2) IRF
3) correlation
4) spectral analysis
5) coherence

model estimation
1) ERA
2) poly-ref
3) Q-Markov
4) ITD
5) ARMA
6) CMIF
7) MIF
8) SVD
9) SDOF
10) resynthesis
11) error estimation

⇨ **Each step is important in performing system ID**

Current system identification techniques yield state space models

$$X = AX + BU$$

$$Y = CX + DU$$

performing an eigensolution yields

$$\eta = \left[\frac{1}{(s-p)} \right] \Psi U$$

$$Y = \Phi\eta + DU$$

Ψ is the modal participation matrix
Φ is the mode shape matrix
p is a complex pole of the system, $-\zeta\omega \mp \omega\sqrt{1-\zeta^2}$
ω is the natural frequency
ζ is the damping ratio

Filename:SNLA_2743_02_HD:FrameMaker 3.0:JPLauffer_Documents:scsi_Feb:scsi_presentation

Sandia personnel have tested a wide variety of structures including:

1) Eol'e wind turbine 111m
2) piezoelectric motor
3) polaris missile
4) optical systems
5) trucks
6) missile components
7) electron microscopes
8) naval system
9) lithography machines

Filename:SNLA_2743_02_HD:FrameMaker 3.0:JPLauffer_Documents:scsi_Feb:scsi_presentation

The modal survey of the Eol'e wind turbine was the most difficult.

1) size - (111 m)
2) environment
3) ambient disturbance
4) instrumentation
5) field test - (Quebec)
6) excitation level

lename:SNLA_2743_02_HD:FrameMaker 3.0:JPLauffer_Documents:scsi_Feb:scsi_presentation

We compared frequency response functions

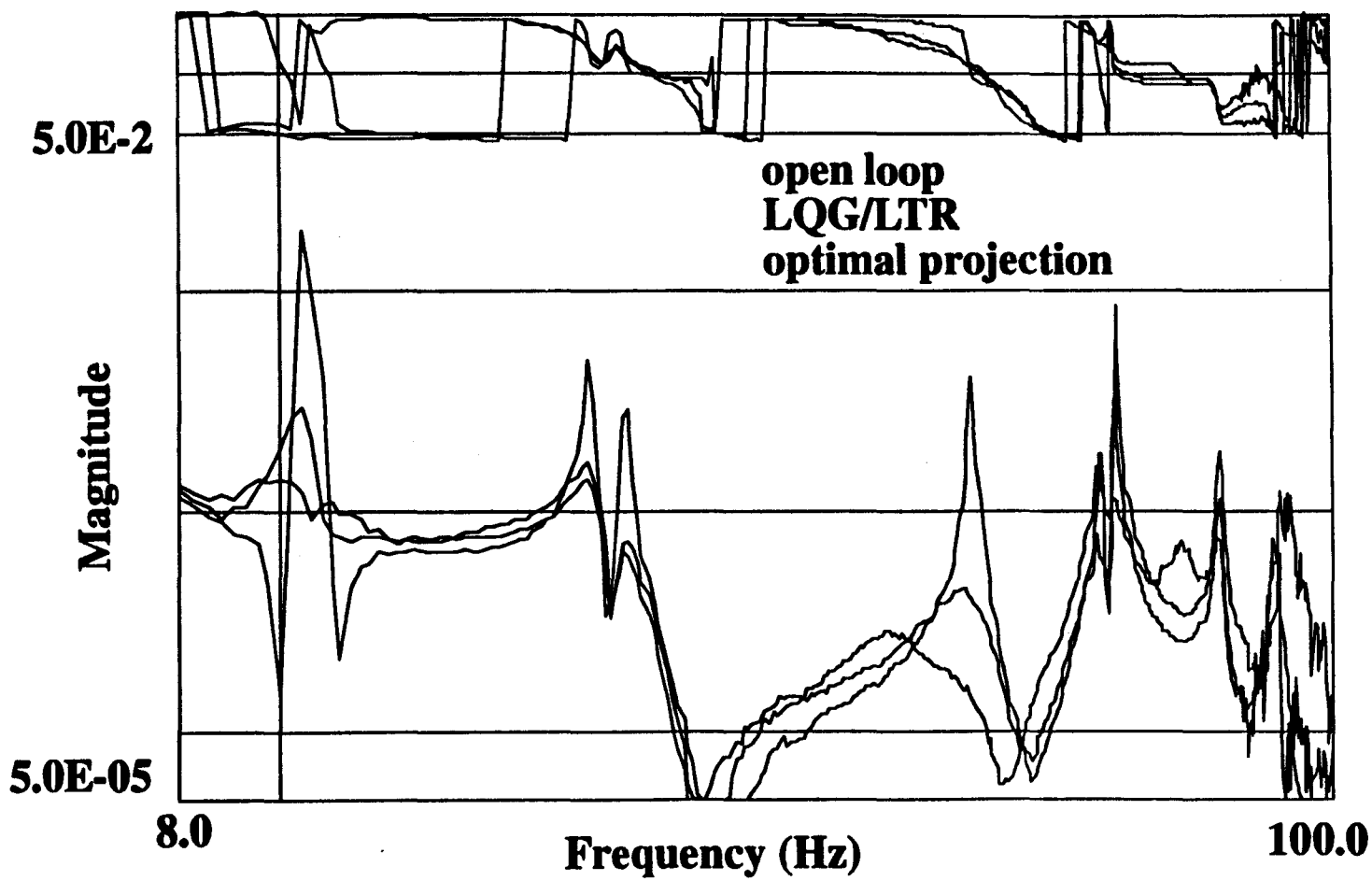

Sandia National Laboratories

We compared impulse response functions

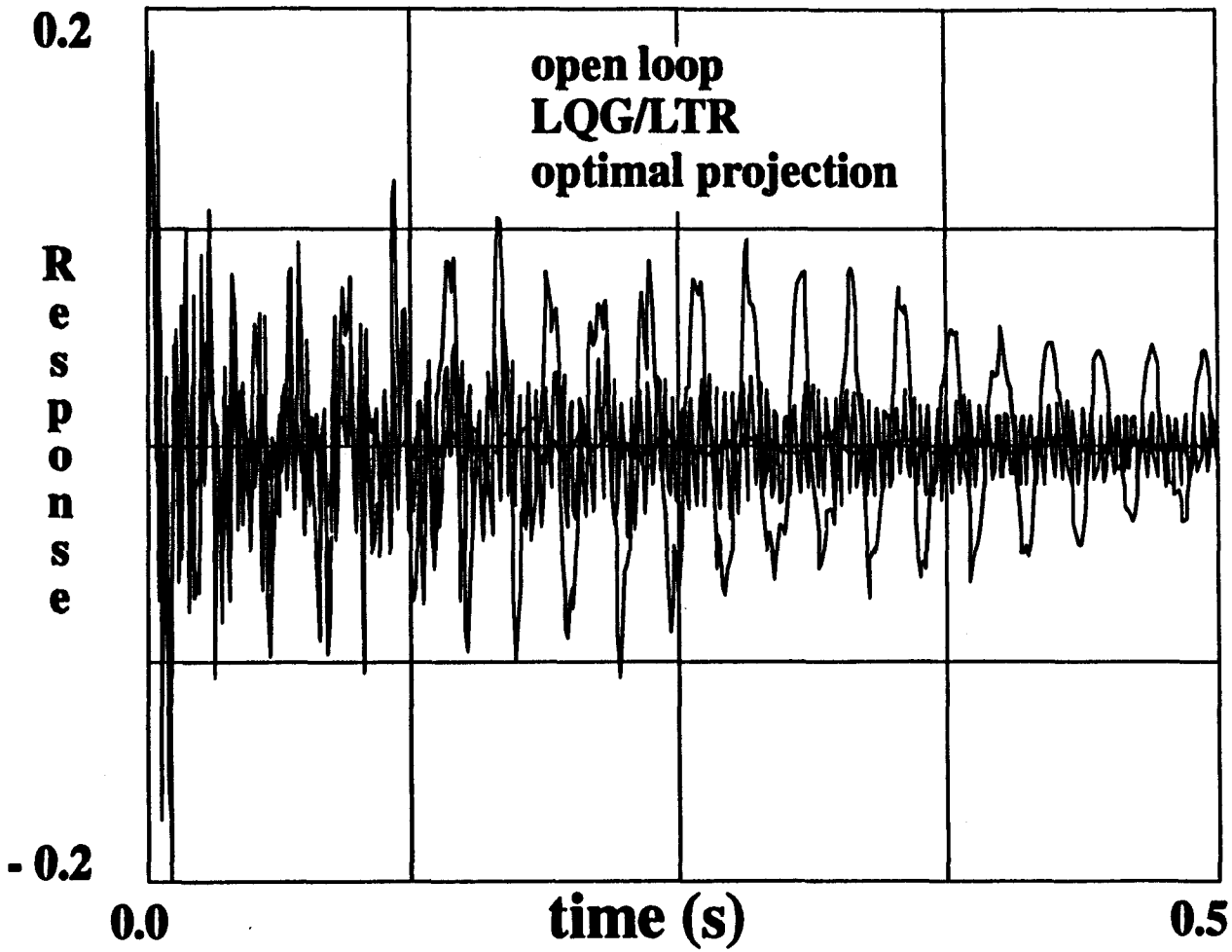

Resources of the modal testing group

- 6 engineers, 3 Phd's and 3 MS
- 2 technicians, 2 BS
- 3 laboratories
- variety of instrumentation
- extensive computer resources
- controls testbed

Active areas of research

- structural control
- system identification
- force reconstruction
- large scale modal testing techniques
- natural excitation testing
- sensor actuator evaluation
- nonlinear systems

Filename:SNLA_2743_02_HD:FrameMaker 3.0:JPLauffer_Documents:scsi_Feb:scsi_presentation

Dynamic Characteristics of the SSC Dipole Magnet

February 11, 1992

Robert Viola

Vibration and Transportation Studies

Objectives:

* Develop and verify dynamic finite element models for both the dipole and quadrupole.

* Use these magnet models in combination with those of the support stands in order to predict the magnet displacements which will result from tunnel floor motion.

* Use the results of these studies to modify the design of the magnet suspension system and support structures as required to minimize vibrational response.

* Measure the vibration levels that the magnets are subjected to during shipping.

* Measure any loss of alignment or other changes to the magnets that occur during transportation. Correlate these changes to the shipping environment.

* Develop support hardware and shipping procedures which will ensure that the magnets can be transported safely.

Numerical Models

Finite element models written in ANSYS

ANSYS capabilities include:

* Frequencies and mode shapes
* Transient response
* Forced response

Models constructed using substructures

Status:

* All major components built and verified
* Complete 40mm dipole model assembled
* Verification in process

The 40mm ANSYS Dipole Model

Originally used a symmetric boundary condition to take advantage of the magnet's bilateral symmetry.

Newer model is complete

Vacuum Vessel constructed of Stif63 thin shell elements. Stif43 thick shell elements were used at the reinforcing rings and the feet.

The cold mass skin was represented using thin shell elements.
A series of massive partitions were added to give the cold mass the proper weight.

Post model was developed by Fermilab and also uses shell elements.

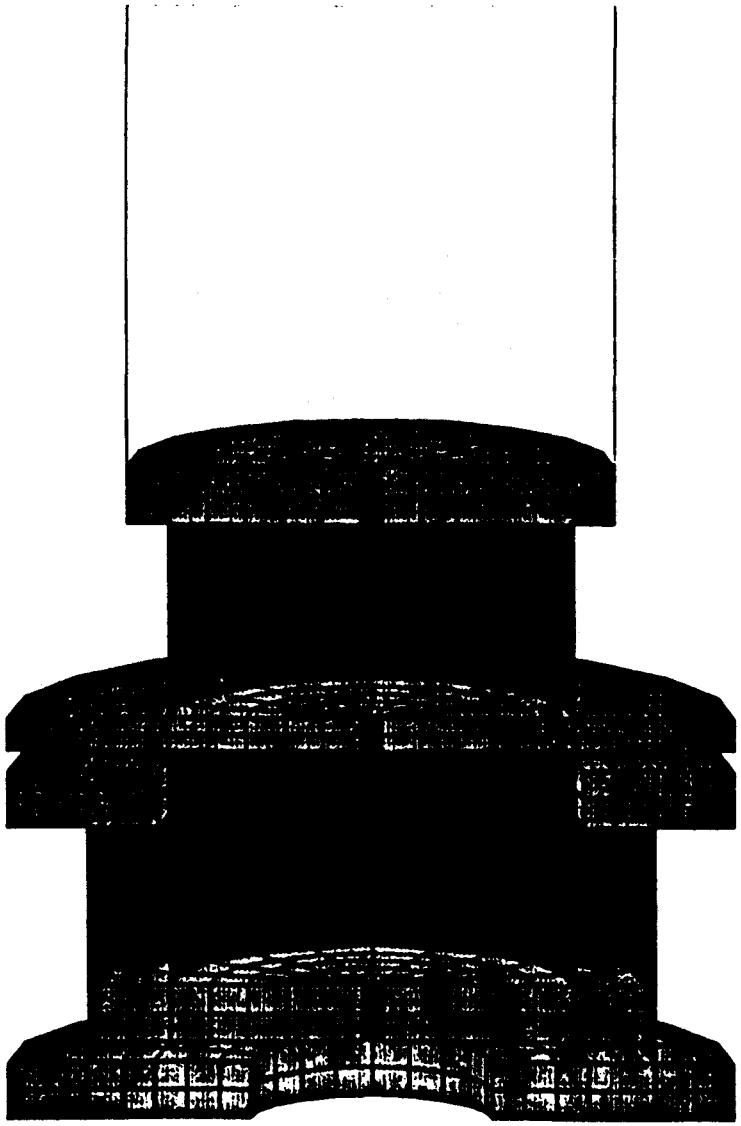

ANSYS 4.4
JUN 25 1990
17:29:42
POST1 ELEMENTS
TYPE NUM

YV =0.2
ZV =1
DIST=8.137
YF =7.094
ZF =-2.25
CENTROID HIDDEN

550 4cm Post Design Br...05-18-1989

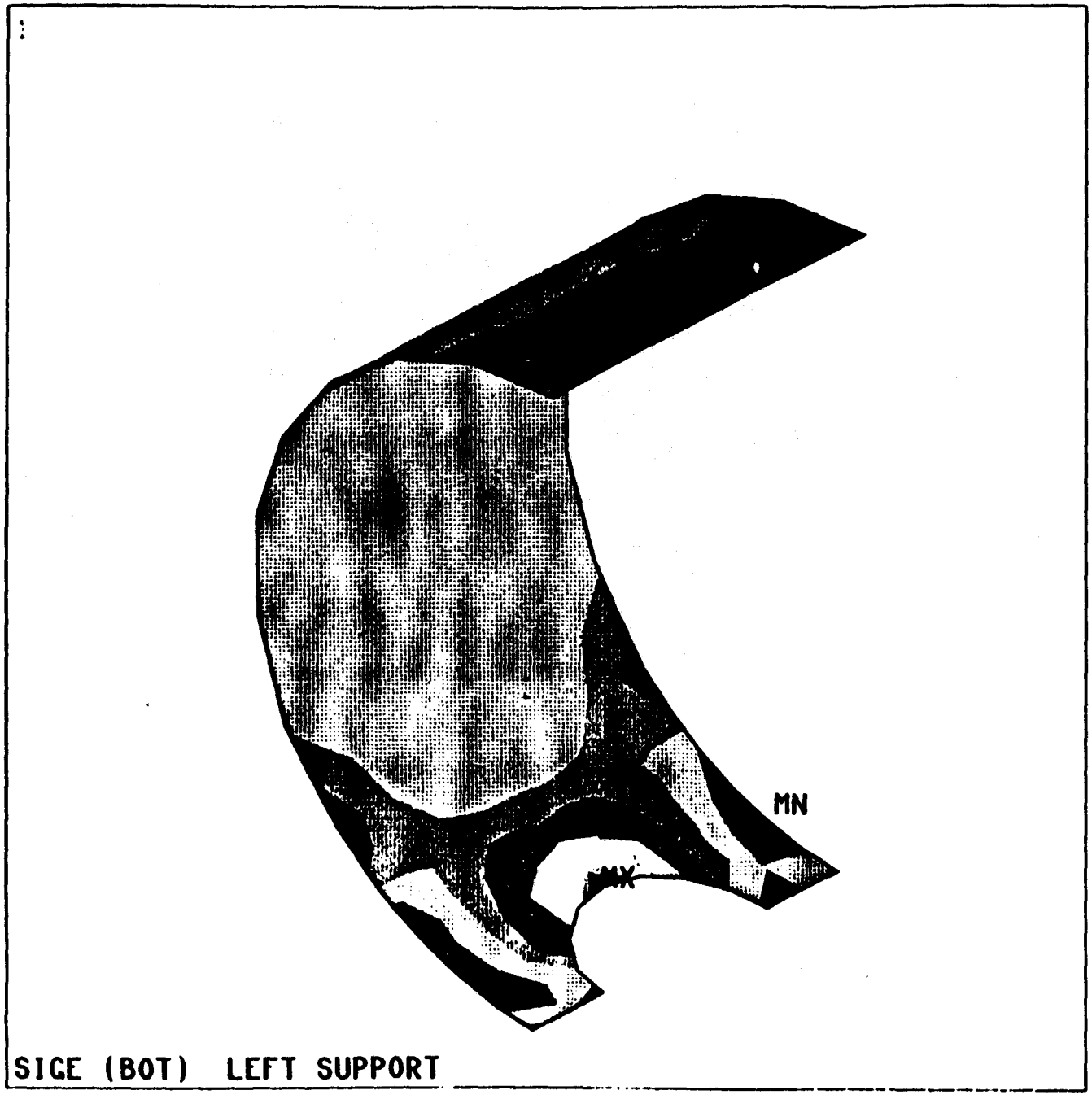

ANSYS 4.4A
AUG 27 1990
11:31:52
PLOT NO. 8
POST1 STRESS
STEP=1
ITER=1
SICE (AVG)
BOTTOM
DMX =0.059925
SMN =980.909
SMX =12558
SMXB=17419

XV =1
YV =1
ZV =1
DIST=16.028
XF =-5.816
ZF =177.63
EDGE

980.909
2267
3554
4840
6127
7413
8699
9986
11272
12558

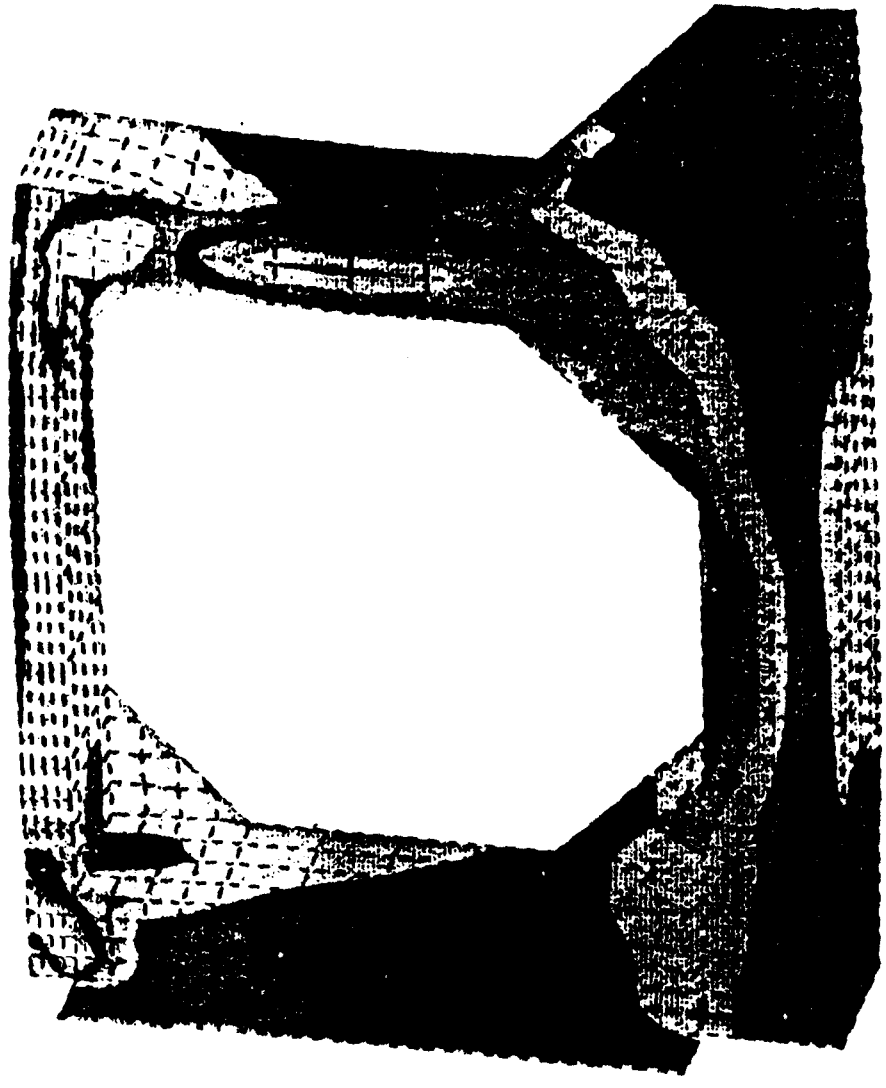

ANSYS 4.4
JUN 25 1990
17:38:52
POST1 STRESS
STEP 1
ITER 1
SUB 1000
MIDDLE
DMX 0.011966
SMX =3083

XV 0.2
YV 0.5
ZV =1
DIST=22.989
XF =17.6
YF =22.2
ZF 4
CENTROID MIDDLE

	0
	342.555
	685.111
	1028
	1370
	1713
	2055
	2398
	2740
	3083

Supported Stand

Model Validation

Vibration measurements made using a Hewlett-Packard spectrum analyzer

Mode shapes, frequencies and associated damping determined using structural analysis software supplied by SMS, Inc.

Numerical model variables adjusted to agree with experiment.

40mm Cold Mass/Vertical

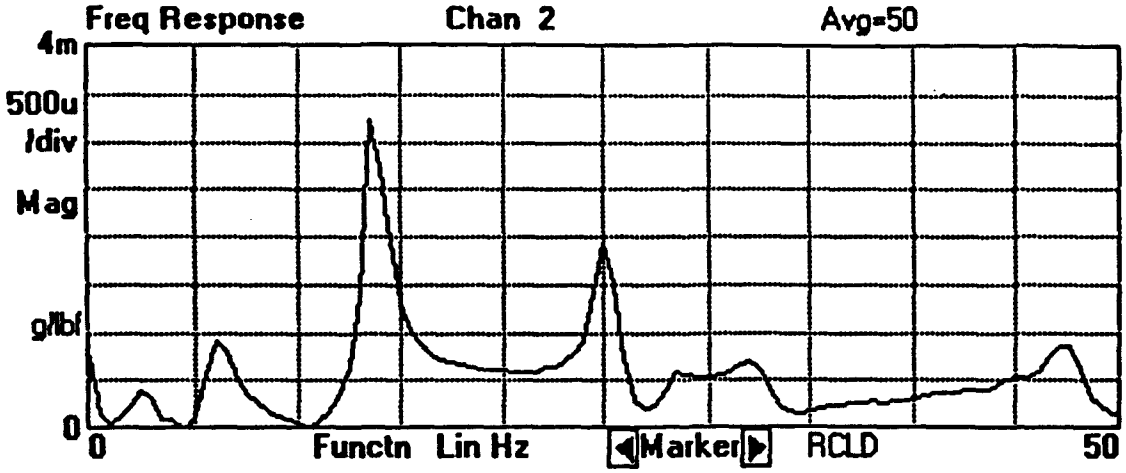

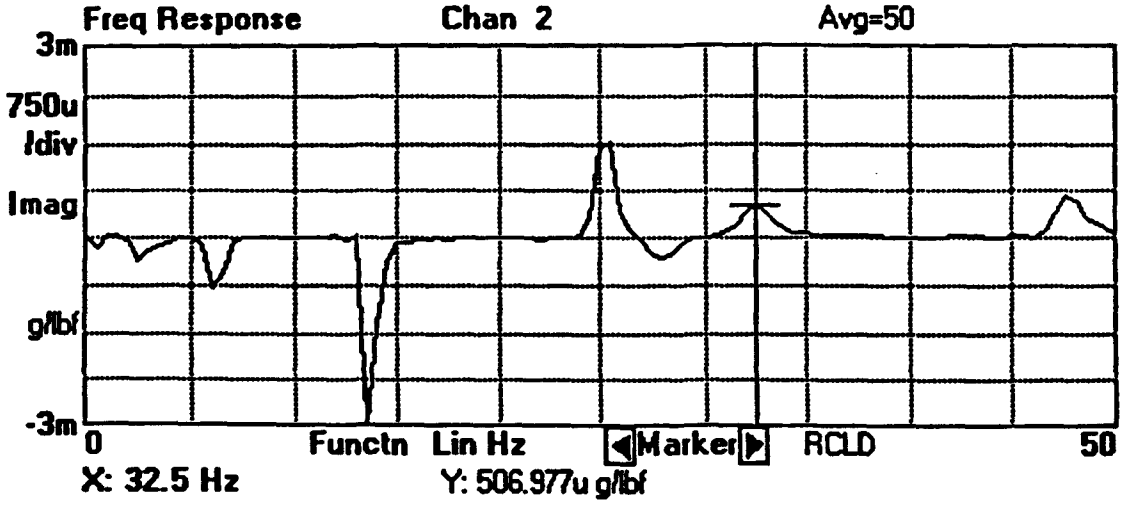

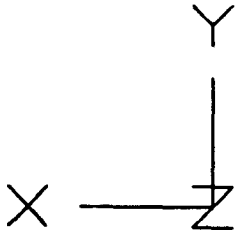

Comparison of Finite Element and Experimental Results
40 mm Dipole Cold Mass

Mode #	Freq. (exp.) (Hz)	Freq. (FEA) (Hz)
1	2.50	2.50
2	3.50	2.71
3	5.95	6.37
4	13.71	15.75
5	25.25	26.12
6	27.98	28.11
7	32.43	35.27
8	47.44	47.75

Table 2. Experimental vs. FEA Frequencies/Complete Magnet.

Mode #	Freq (Expt) (Hz)	Freq (FEA) (Hz)
1	6.5	5.7
2	7.5	6.6
3	15.5	15.6
4	16.5	16.4
5	-	17.8
6	20.5	25.8
7	-	29.6
8	37.5	39.4
9	39.0	41.6
10	44.0	45.1

Schedule of Work

* Modify model geometry to reflect the 50mm dipole

* Predict forced dynamic response of dipole/stand system

* Model and verify quadrupole

Longer term...

* Magnet dynamic response at operating temperature

* Measure vibration induced by cryogen flow

* Modification of the stand to include vibration isolation

SSC LABORATORY
SIX STRUT SUPPORT & ALIGNMENT SYSTEM

Dallas, Texas
Tuesday, February 11, 1992
Ted Lauritzen

INTRODUCTION

VIEW GRAPH 1 (My Name,M.E., LBL, etc.)

Ted Lauritzen, Mechanical Engineering staff with the Advanced Light Source (ALS)

Responsible for Survey & Alignment of the accelerator and its beam lines. Also responsible for the Stands & Supports for position sensitive items, mainly magnets.

VIEW GRAPH 2 (Talk Outline)

Outline of talk

- What is the Advanced Light Source (ALS)?
- Where Is It Located
- Supports - Alignment
- ALS Design Criteria
- Six Strut System
- Different Types Of Struts
- How The Struts Are Used
- Advanced Light Source Applications

VIEW GRAPH 3 (ALS Plan View)

The ALS is a 1 to 2 GeV light source consisting of:

- Linear Accelerator
- Booster Ring about 22m in diameter
- Storage Ring about 60m in diameter
- Transfer Lines that connect everything together

VIEW GRAPH 4 (184" Building Photo)

The ALS is being constructed under the dome of what used to be LBL's 184-inch cyclotron. This is a view of the project site before the start of ALS construction.

VIEW GRAPH 5 (What Are Supports?)

- *Supports Hold Things* as we all know, and usually against gravity loading. Since most of the position sensitive items in our accelerator that need holding up are magnets, I'll concentrate on them. You start with various sizes of magnets, sometimes many tons. Magnets are very carefully designed and put together to maintain a specific magnetic field and you just can't grab onto them in any old fashion. Magnets do not like to be bent or twisted, but you do have to support them and your supports must maintain position.

VIEW GRAPH 6 (What Is Alignment?)

- *Alignment Puts Magnets In A Predetermined Location*. Magnets want to be located at a special place in space, that you can't see or touch, and usually with very high positional tolerances.

VIEW GRAPH 7 (Alignment Tolerances - Best You Can Do)

Have you ever seen this tolerance requirement before?

Engineers like to get their tolerances in a little different format, so, for the ALS this is what it looks like.

VIEW GRAPH 8 (Alignment Tolerances ALS)

(Go over view graph)

VIEW GRAPH 9 (Fussy Individual)

REVIEW
We Now Have A Fussy Individual (Magnet)
That Worries About How You Hold It
Worries About Its Shape
And Its Place In The World

Sound Familiar? (Sounds Like My Wife)

CAN WE GET THERE FROM HERE

SURE WE CAN

VIEW GRAPH 10 (ALS Design Criteria)

- **Magnets, Supports, Survey & Alignment, *A System***

  First thing to understand is that Magnets, Supports, Survey, and Alignment must go hand in hand. If you design a magnet without supports in mind you can find it next to impossible to find a place to grab onto (we have come close to this). If you have no fiducials or targets on your magnets, or you put them in the wrong place, you can't survey the magnet's location. If you build a support system that just holds the magnets up and you need a ten pound hammer to align them you will never make it. Magnets, supports, survey, and alignment should be designed as a **system**.

- **Do Not Over Constrain**

  First on our list was to support the magnets in such a way as to **not over constrain** them. We did not want the support system to change the shape of the magnets.

- **Position To High Tolerances**

  The support system must allow us to position our magnets to high tolerances. We wanted a system that was clean and simple to use, yet alignable to microns.

- **Generic Design**

  We wanted a design that could be used on small magnets, 100 pounds or so, and large magnets up to 7500 pounds, beamline equipment that require stable accurate placement as well as withstanding vacuum loading, and used on support structures that held many magnets that could weigh up to 60,000 pounds.

- **Small Footprint**

  Our accelerator design requires the magnets to be very close to each other so the support system must not take up a lot of room.

- **Motion Coupling**

  Most adjustable support systems have some coupling between motions in different planes, but we wanted to minimize this if we could. We have chosen to align our magnets with real-time position feedback so a little coupling doesn't hurt us.

SO WHAT'S THE MAGIC SYSTEM?

THE SIX STRUT SYSTEM

Not so magic. This type of support has been around, maybe not in this exact arrangement, but it isn't new.

VIEW GRAPH 11 (6 Strut Sys. Strut)

Our definition of a strut is a rigid member with spherical joints at each end. It will only support an axial load in compression or tension and because of the spherical joints at either end it will never see loads in any other direction.

VIEW GRAPH 12 (6 Strut Sys. 3 Struts)

We all know that 3 vertical legs are the fewest you can have to support something, but with spherical joints on each end of our struts the object can still fall over. Soooo.

VIEW GRAPH 13 (6 Strut Sys. 5 Struts)

We add two more struts, parallel to each other, 90° to the vertical struts, to keep it from moving in the "X" direction. Again, since the struts have spherical joints at their ends, our object can still fall over.

VIEW GRAPH 14 (6 Strut Sys. 6 Struts)

With the addition of this last strut we now have the object supported and held in a specific spot in space. Remember, and this is very important, you remove any one of the struts and it will fall down.

Now we have a support system that doesn't over-constrain, but as yet won't allow alignment. If you make all of the struts adjustable in length you now have a system that allows you to change position of the object in all 6 degrees of freedom. If you keep all of the struts at right angles to each other you keep the coupling down, but you still get coupling.

WHAT DO OUR STRUTS LOOK LIKE

VIEW GRAPH 15 (LTB Transfer Line Quad. Magnets)

This shows a couple of small quadrupole magnets and a dipole in our Linac-To-Booster-Transfer Line. Note all six struts. This is our smallest strut. The strut is made up with two male rod end bearings and a female threaded tube joining the rod end bearings.

- The rod end bearings are especially made to our specifications. Normal stock off-the-shelf rod end bearings have loose balls.

- The rod end bearings are all right hand threads with one a course thread and the other a fine thread. **These are not turn-buckles.** These struts are differentially threaded devices and this is where we get the high precision. One turn of the tube changes the length of the strut a little less than 1 mm.

- At each end of the tube you will notice a shaft collar. The shaft collars will squeeze the female thread against the male thread of the rod ends to remove any backlash in the threads.

VIEW GRAPH 16 (5 Ton Strut)

This strut is a machine screw jack rated at 5 tons. Notice we again use rod end bearings.

Next is our largest strut.

VIEW GRAPH 17 (20 Ton Strut)

This strut is a machine screw jack rated at 20 tons.

VIEW GRAPH 18 (20 Ton Strut With Bearing Cross Section)

The bearings on the ends are spherical with split outer races separated by a peelable shim stack. You can taylor the brake-away torque of the ball with respect to the outer races by adding or removing shims.

Lets put this all together with some photos of actual magnets and girders.

VIEW GRAPH 19 (Booster Girder With Dipole Magnet Struts)

This gray table, we call a girder, is designed to support several magnets. Note that the girder is supported form the floor with six 5 ton machine screw jack struts. On top of the girder you see six struts waiting for a magnet. Note that the magnet gets bolted into place with only six bolts.

Lets see what magnets bolted (strutted) to a girder looks like.

VIEW GRAPH 20 (Booster Girders In Tunnel)

This is what it looks like in our Booster Ring. The largest booster ring girder with its magnets installed weights in at over 20,000 pounds.

VIEW GRAPH 21 (LTB Transfer Line Quad. Magnets Cantilevered)

These small quads had to be close to the booster ring magnets with no room to support them from underneath. This is a cantilevered configuration.

Lets take a look at where the big struts go.

VIEW GRAPH 22 (Storage Ring Girder Mounting)

This picture shows how we use the 20 ton struts.

VIEW GRAPH 23 (Storage Ring Girder Installation)

When these girders are in place with all their magnets attached, the entire system can weight up to 30 tons.

VIEW GRAPH 24 (Storage Ring Girder With Magnets)

See what I mean about being close together.

To give you an idea on other applications and how the six strut system has worked for smaller items lets take a look at the ALS prototype Spherical Grating Monochromator installed at SSRL, SLAC.

VIEW GRAPH 25 (SGM At SSRL)

Note six strut system holding up the grating chamber.

VIEW GRAPH 26 (Ted Adjusting A Grating)

To give you some scale, you can see the size of things with me in the picture. I am adjusting one of three water cooled defraction gratings mounted with the six strut system. Now lets see one of the gratings up close.

VIEW GRAPH 27 (SGM Grating)

These are the defraction gratings before being polished and ruled. They weigh about 10 pounds each and are adjustable to 0.5 micro-radians with a screwdriver.

THAT'S IT

Ted Lauritzen
Mechanical Engineering
Lawrence Berkeley Laboratory

Advanced Light Source

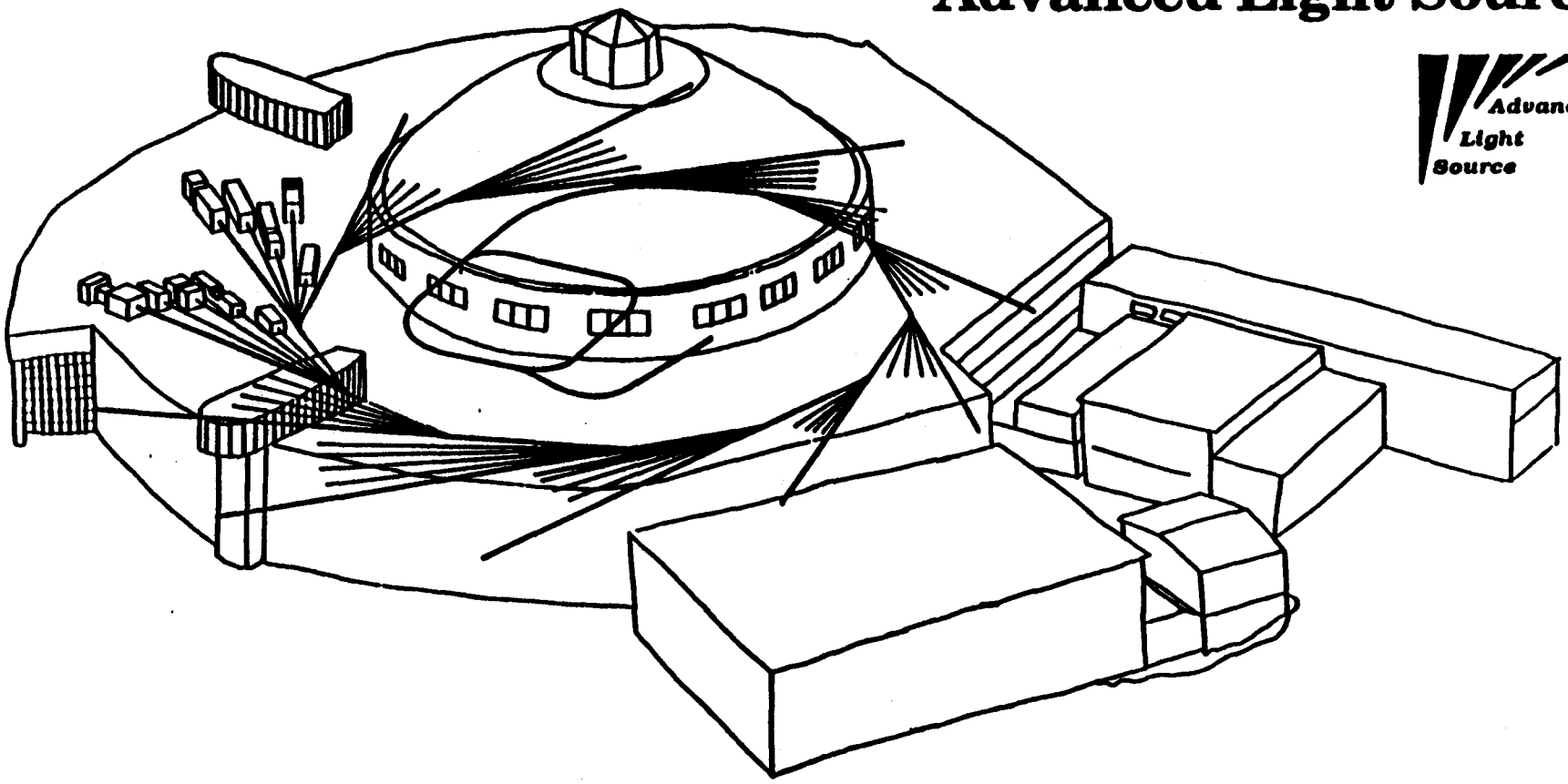

OUTLINE

- What Is The Advanced Light Source (ALS)
- Where Is It Located
- Supports - Alignment
- ALS Design Criteria
- Six Strut System
- Different Types Of Struts
- How The Struts Are Used
- Advanced Light Source Applications

ALS Building Layout

Advanced Light Source

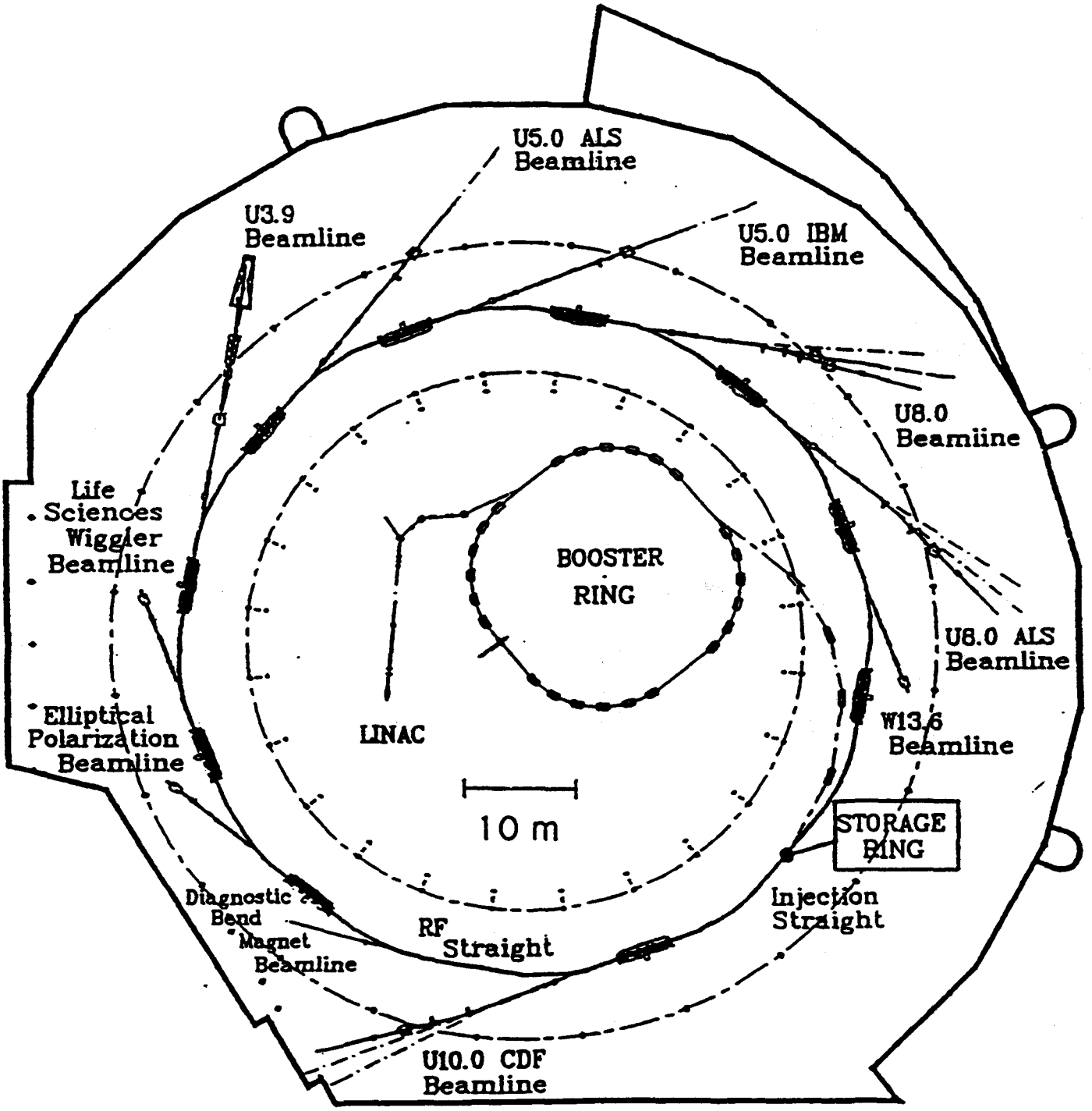

WHAT ARE SUPPORTS ?

WHAT IS ALIGNMENT ?

Alignment Tolerances

Advanced Light Source

THE VERY BEST

THAT CAN BE

DONE !

ALS Alignment Tolerances

Advanced Light Source

Storage Ring
(Magnet to Magnet)

Degree Of Freedom			Dipole	Quadrupole	Sextupole
X	(Radial)	mm	± 0.15	± 0.15	± 0.15
Y	(Up)	mm	± 0.15	± 0.15	± 0.15
Z	(Beam Direction)	mm	± 0.25	± 0.25	± 0.25
θ_X	(Pitch)	mrad	± 0.50	± 0.50	± 1.00
θ_Y	(Yaw)	mrad	± 0.50	± 0.50	± 1.00
θ_Z	(Roll)	mrad	± 0.25	± 0.50	± 0.50

Global 1.0 mm

REVIEW

We Now Have A Fussy Individual (Magnet)

That Worries About How You Hold It

Worries About Its Shape

And

Its Place In The World

Sound Familiar?

(Sounds Like My Wife)

ALS Design Criteria

Advanced Light Source

- Magnets, Supports, Survey & Alignment, *A System*
- Do Not Over Constrain
- Position To High Tolerances
- Generic Design
- Small Footprint
- Motion Coupling

Six Strut Mounting System - Strut

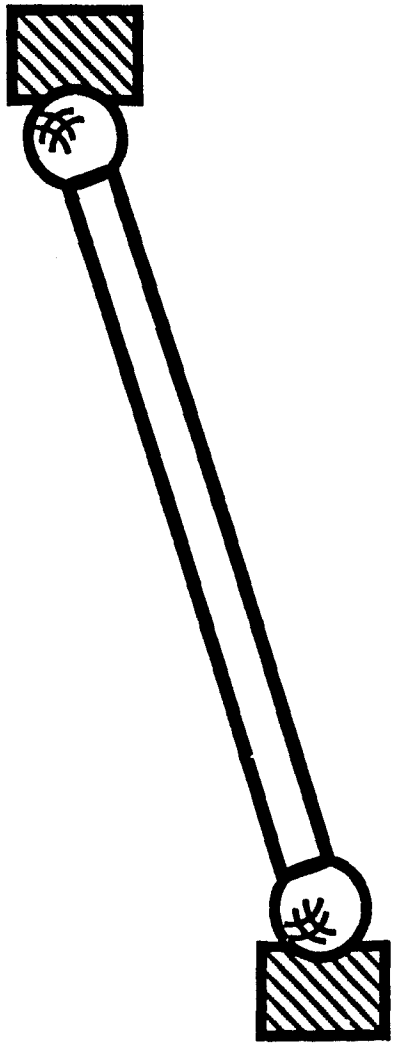

STRUT IS ALLOWED TO SWIVEL

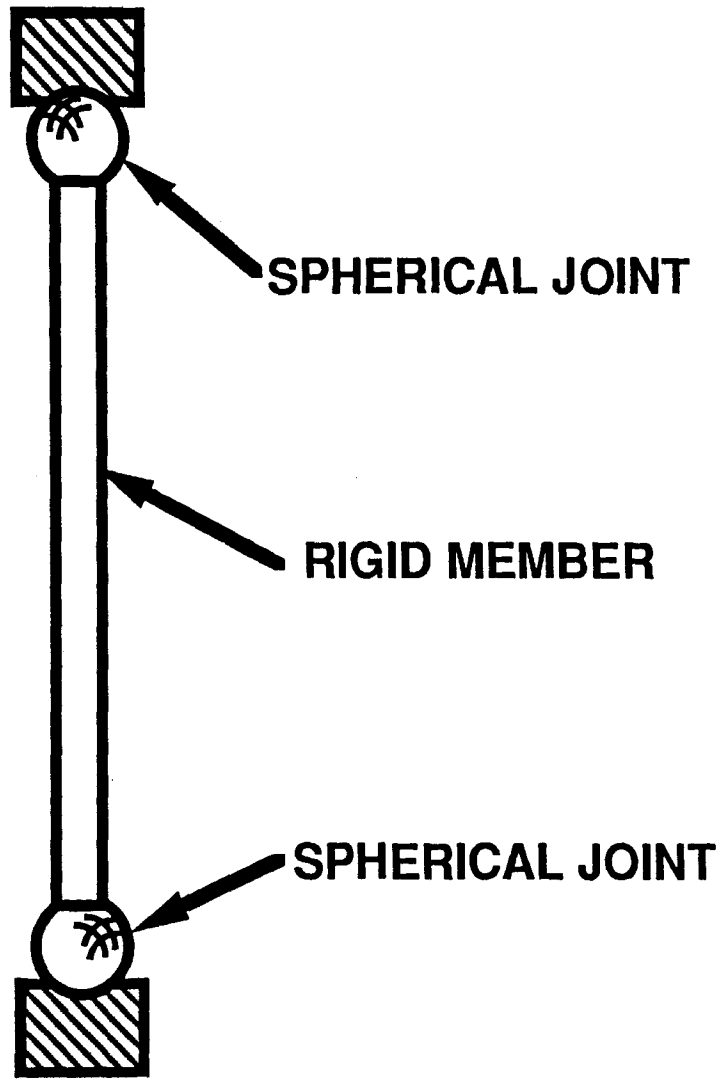

Six Strut Mounting / Three Struts

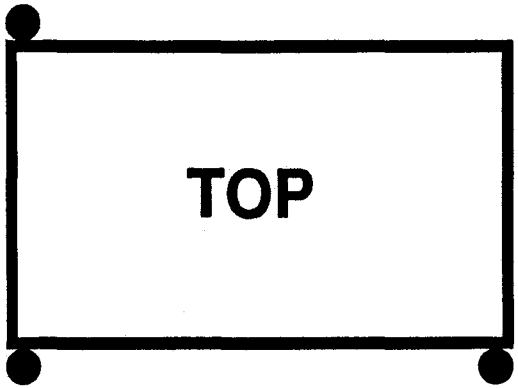

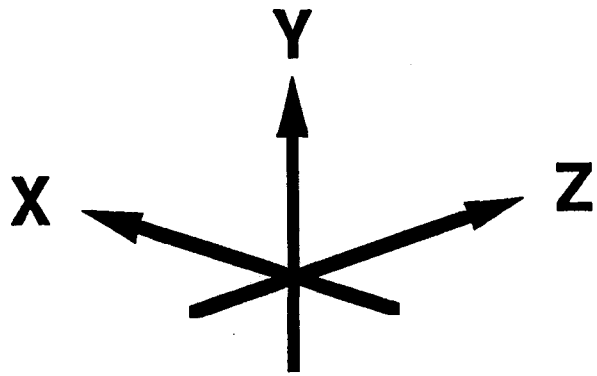

3 (Y) VERTICAL STRUTS

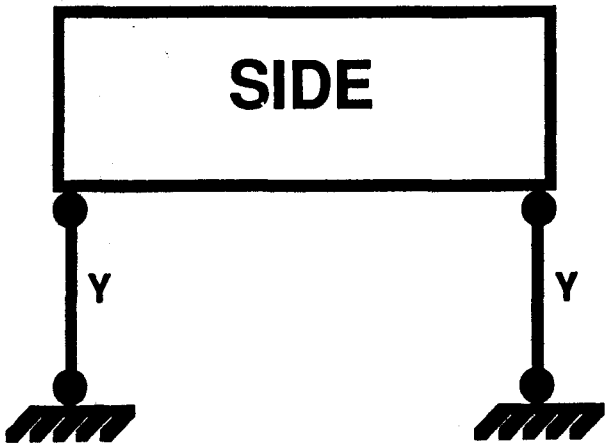

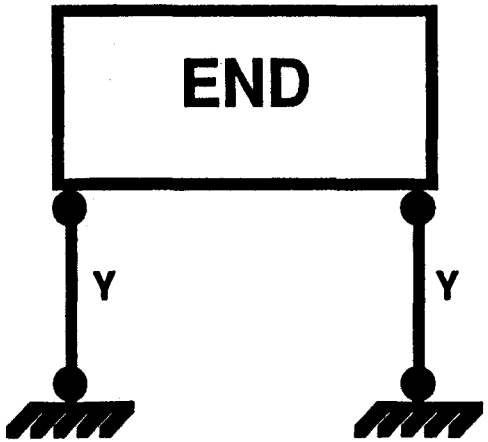

Six Strut Mounting / Five Struts

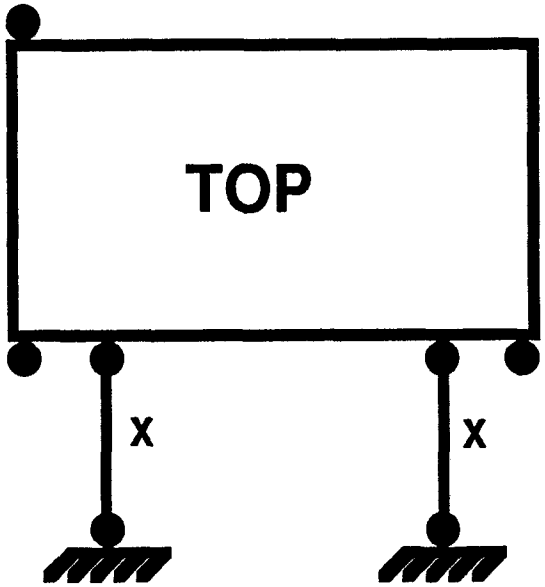

3 (Y) VERTICAL STRUTS

2 (X) LATERAL STRUTS

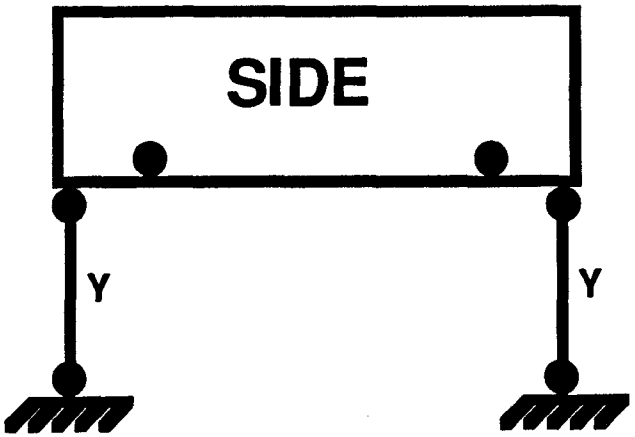

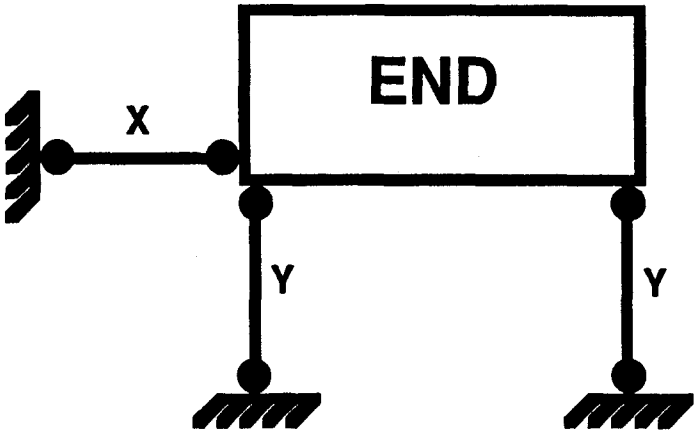

Six Strut Mounting / Six Struts

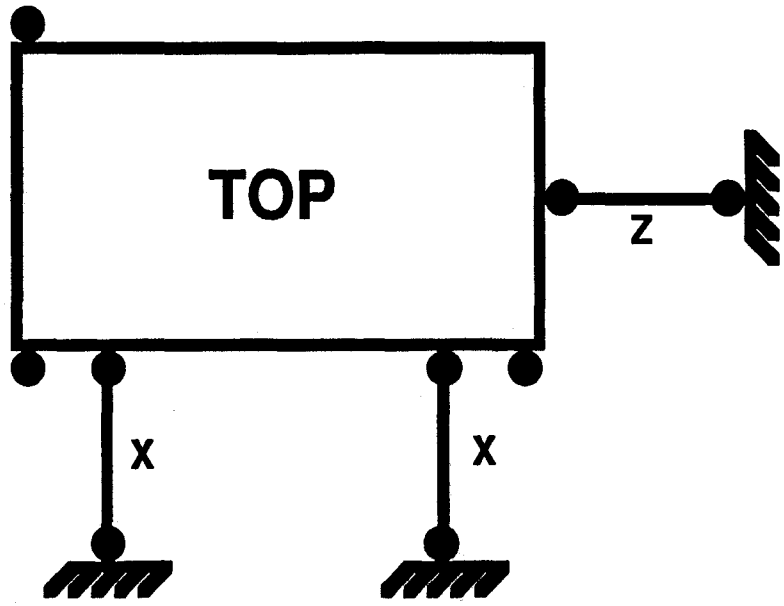

3 (Y) VERTICAL STRUTS

2 (X) LATERAL STRUTS

1 (Z) LATERAL STRUT

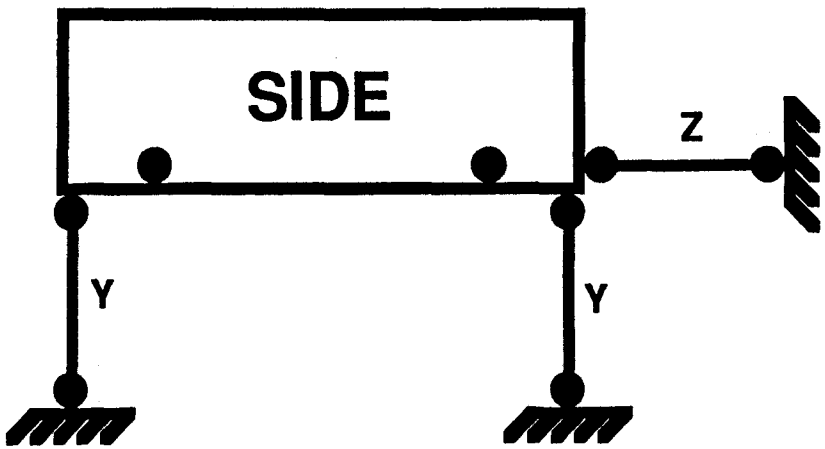

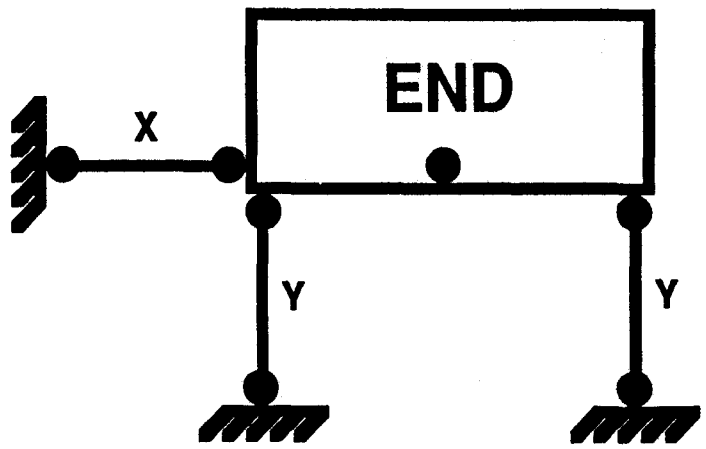

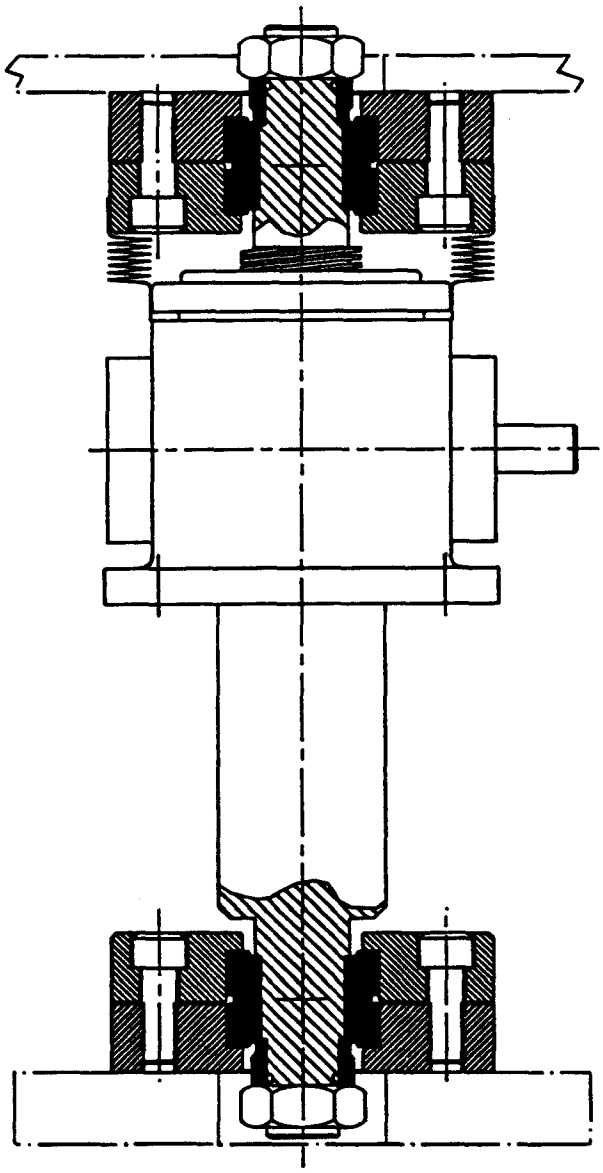

STORAGE RING Y-STRUT

(MACHINE SCREW JACK, 20 TON CAPACITY)

Dynamic Analysis of a Six Strut System

R. Bradley Burdick
Patricia A. Manning

Engineering Measurements and Analysis
Engineering Sciences Division

Presentation to:

Workshop on Vibrational Control and Dynamic Alignment Issues at the Superconducting Super Collider
Waxahachie, Texas

February 11 - 14, 1992

Background

- Important to understand the dynamic behavior of the strut system
- Struts are the "first line" dynamic link between ambient / operating vibrations and the alignment system
- Need to fully understand how vibrations are transmitted through the struts into the alignment system

Work Overview

- Characterize struts in various config.
  - Horizontal / Vertical
  - Unloaded / Loaded
  - 20 ton / 5 ton / others
- Develop analytical / experimental models as a platform for future predictions
  - Finite Element Analysis
  - Forced Response
  - Transmissibilty

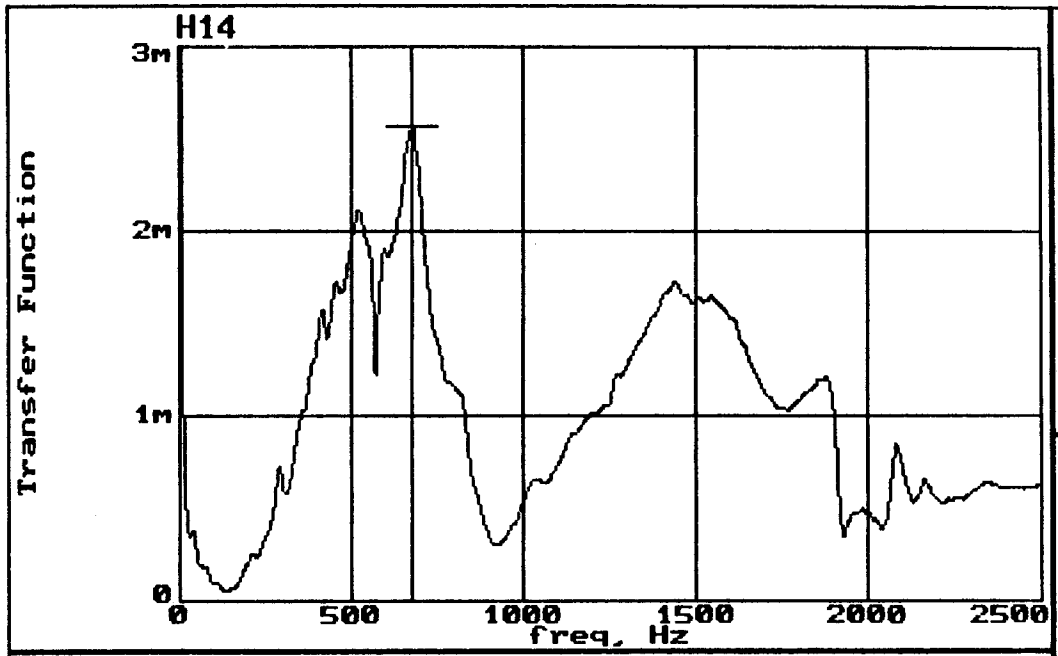

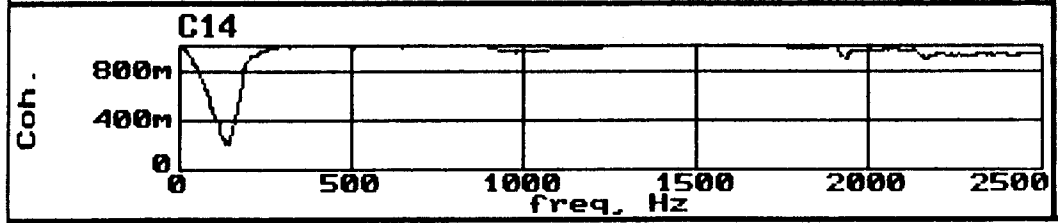

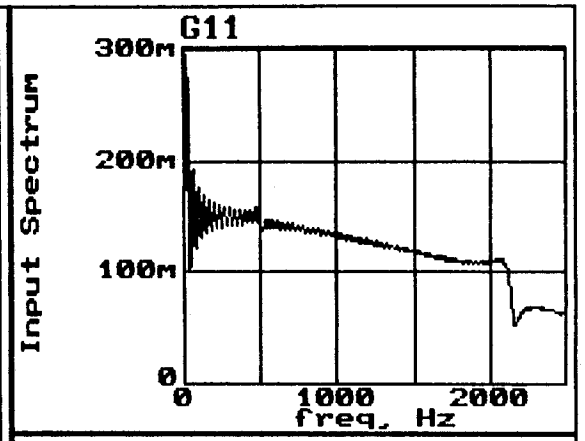

LBL 20-ton STRUT

Excitation:	Base Vertical
Measurement:	Load End Vertical
Strut Config:	Unloaded Vertical

J=268 H= 6.815E+02 V= 2.572E-03

Date: 2/8/1992 Time: 21:20:33

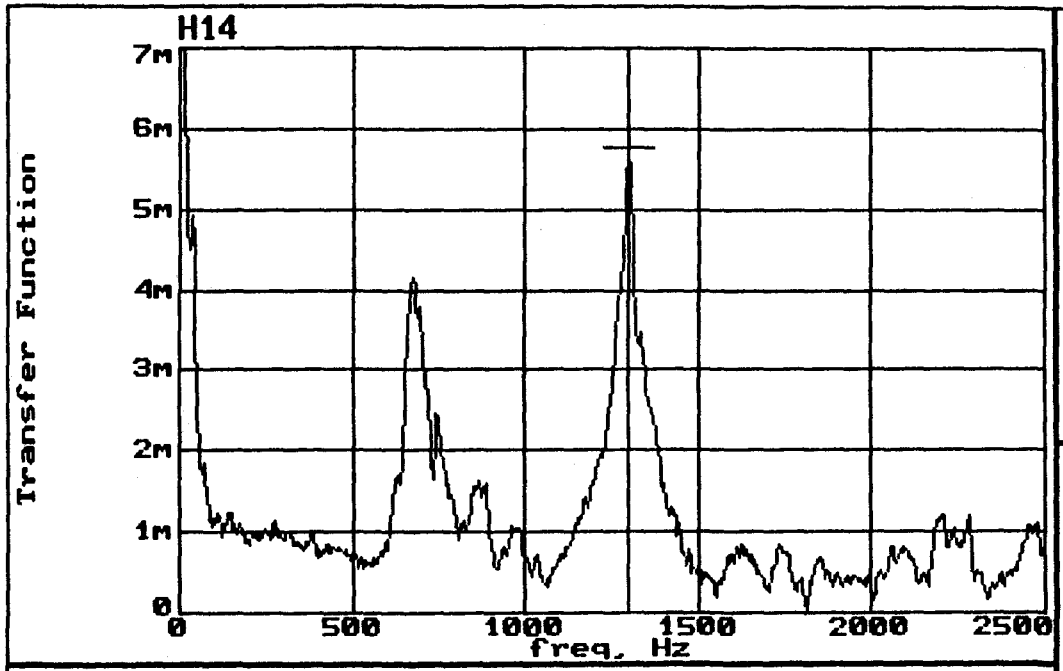

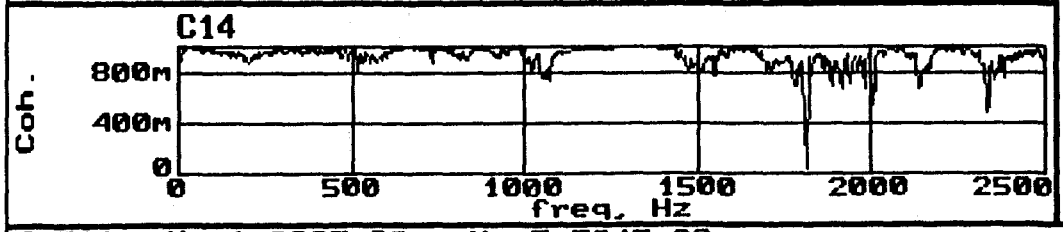

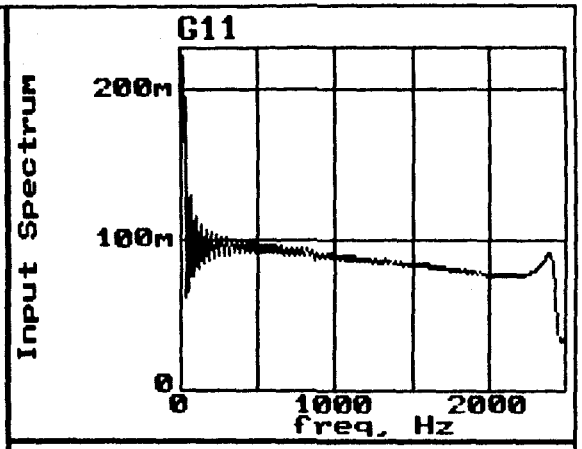

LBL 20-ton STRUT

Excitation:	Base Vertical
Measurement:	Load End Vertical
Strut Config:	Loaded Vertical

J=511 H= 1.299E+03 V= 5.764E-03

Date: 2/8/1992 Time: 22:15:17

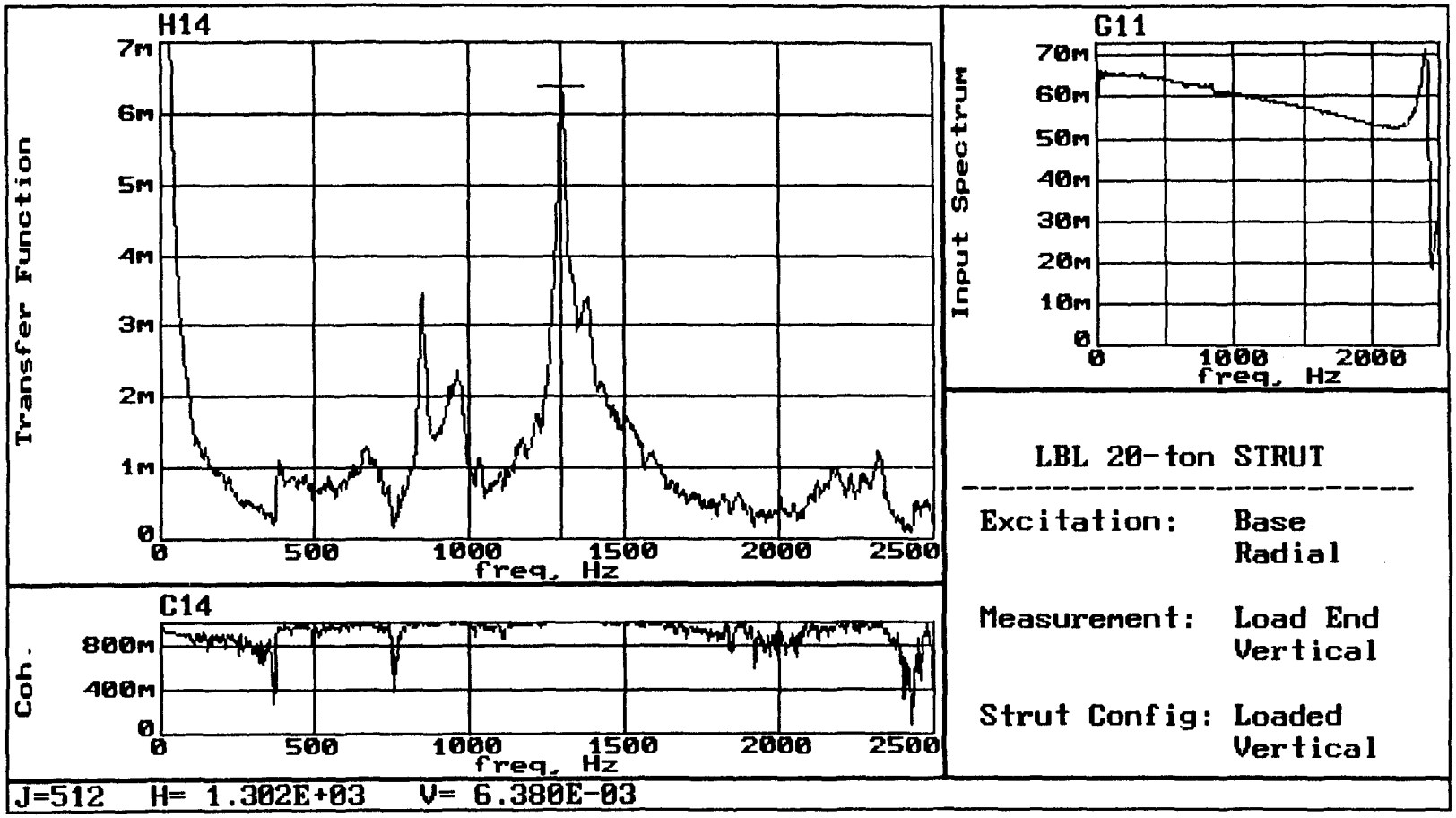

Date: 2/8/1992 Time: 22:38:11

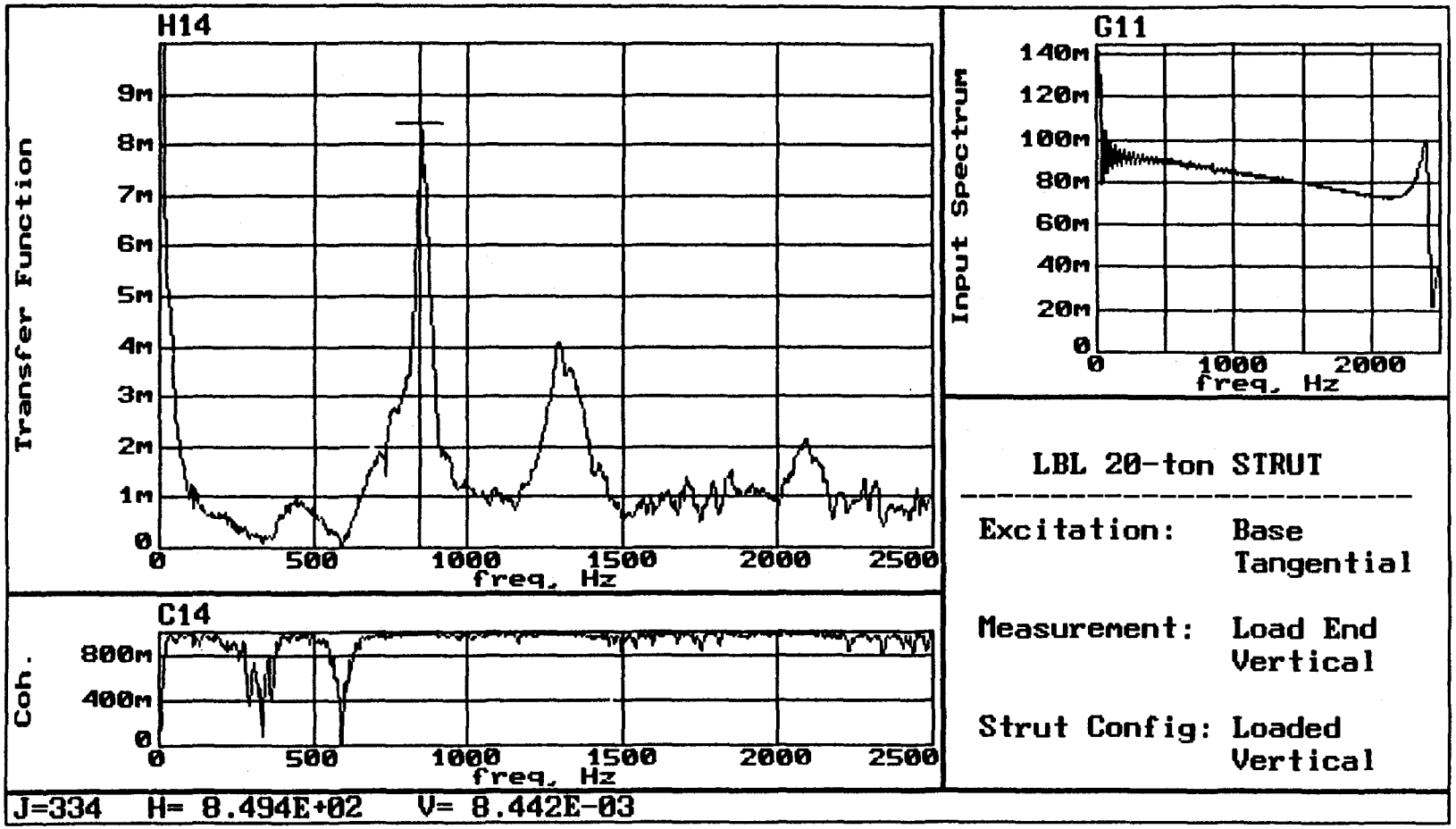

Date: 2/8/1992 Time: 22:49:28

Summary of Progress

- Significant differences between the unloaded and loaded cases
- Many peaks throughout the analysis bandwidth indicate struts may be active in frequency ranges of concern
- Further analysis necessary to understand the spatial contribution of each peak

Future Work

- Complete testing on other strut configurations
- Develop modal analysis model to assist in evaluating interaction of strut with alignment system
- Incorporate effects of ambient / operating vibrations as well as alignment concerns into analysis

VIBRATION TESTING OF THE ADVANCED PHOTON SOURCE (APS) STORAGE RING MAGNET GIRDER/SUPPORT ASSEMBLIES

Marty Wambsganss
Joe Jendrzejczyk
S.S. Chen
Tony Passi
Danny Mangra

Argonne National Laboratory
Argonne, IL 60439

Workshop on Vibrational Control and
Dynamic Alignment Issues at the SSC

February 11-14, 1992

Outline

- Background
- Vibration criteria
- Technical approach
- Vibration analysis - Exp. hall floor
- Design goals/approach
- Vibration tests
- Summary/Conclusions

Background

- APS is synchrotron radiation facility under construction at Argonne National Laboratory - scheduled completion date is 1996.
- Positrons circulate in a storage ring that is 1104 m in circumference; photon beams are extracted.
- 40 identical sectors in storage ring lattice.
- 5 magnet groupings (sections) within a sector; 200 sections in total.
- Storage ring and experimental photon beam lines are housed in experimental hall.
- Magnets mounted on girders which are supported off of the experimental hall floor.
- Girders also support vacuum chamber, beam position monitors, and vacuum pumps.
- Unprecedented precision and stability in aligning the storage ring magnets are required.

APS Facility

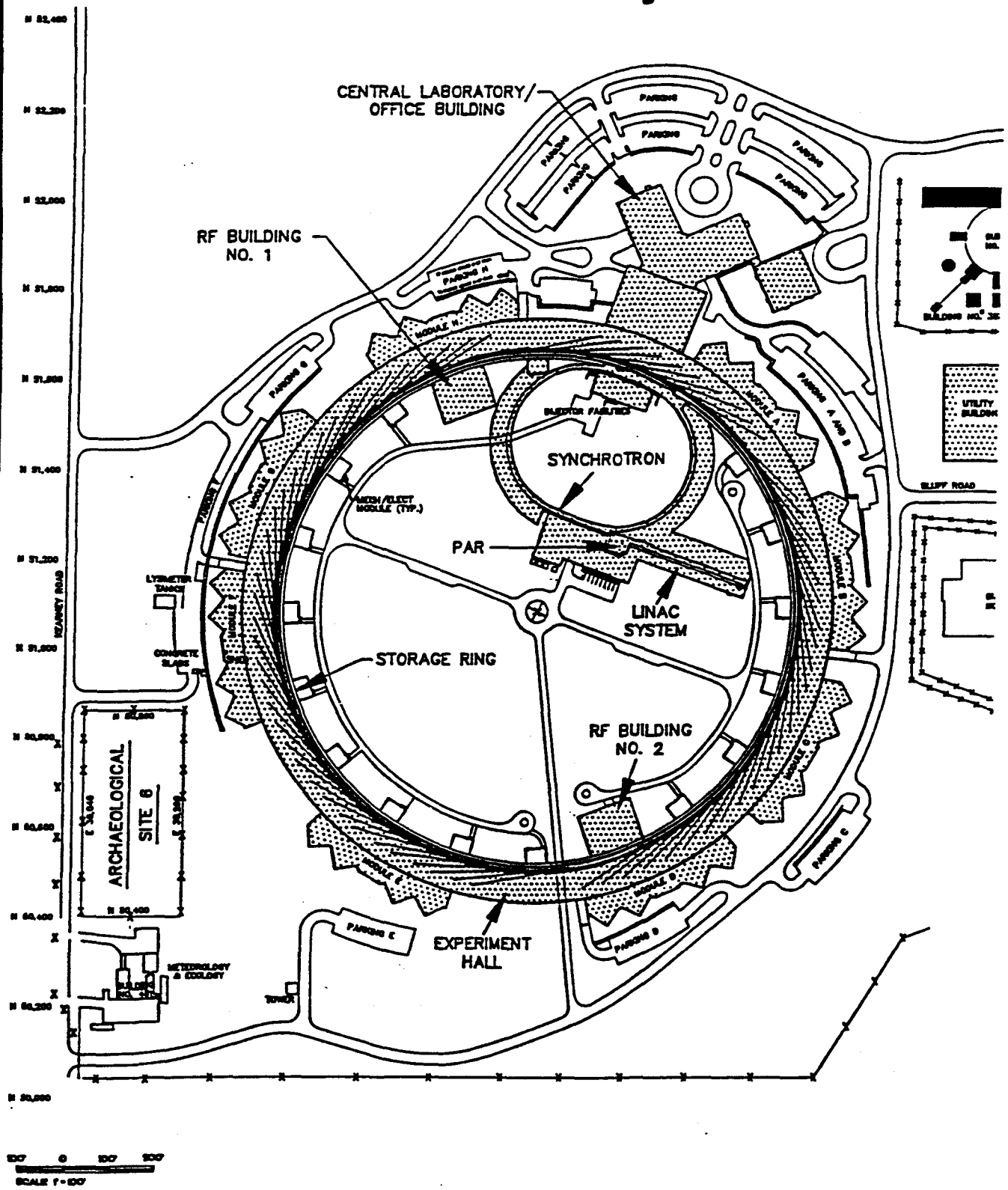

Typical Storage Beamline Sector

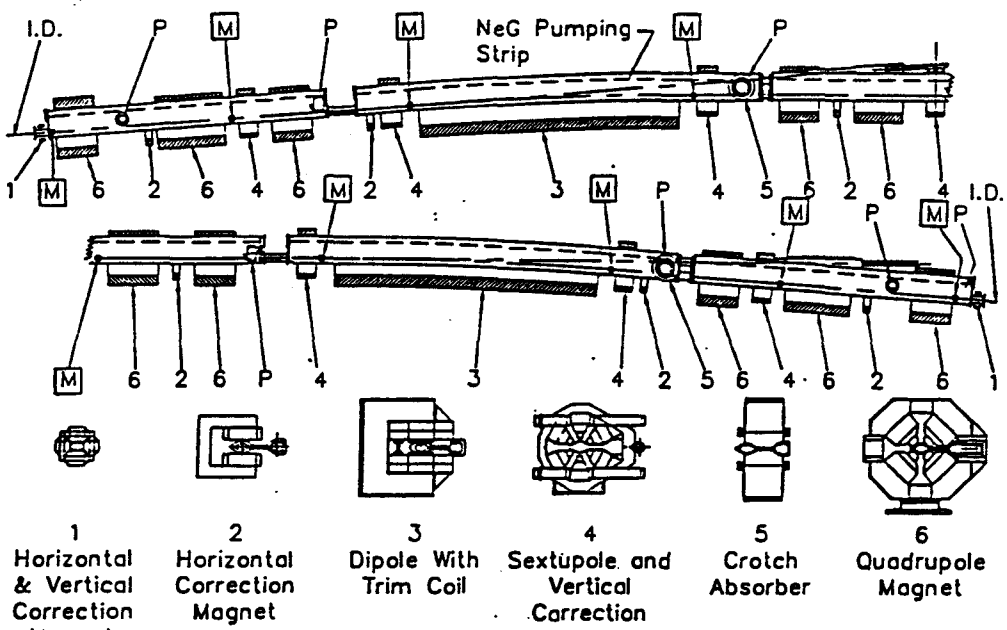

M = Beam Position Monitor
P = Lumped Ion and Neg Vacuum Pump

EXPERIMENT HALL SECTION

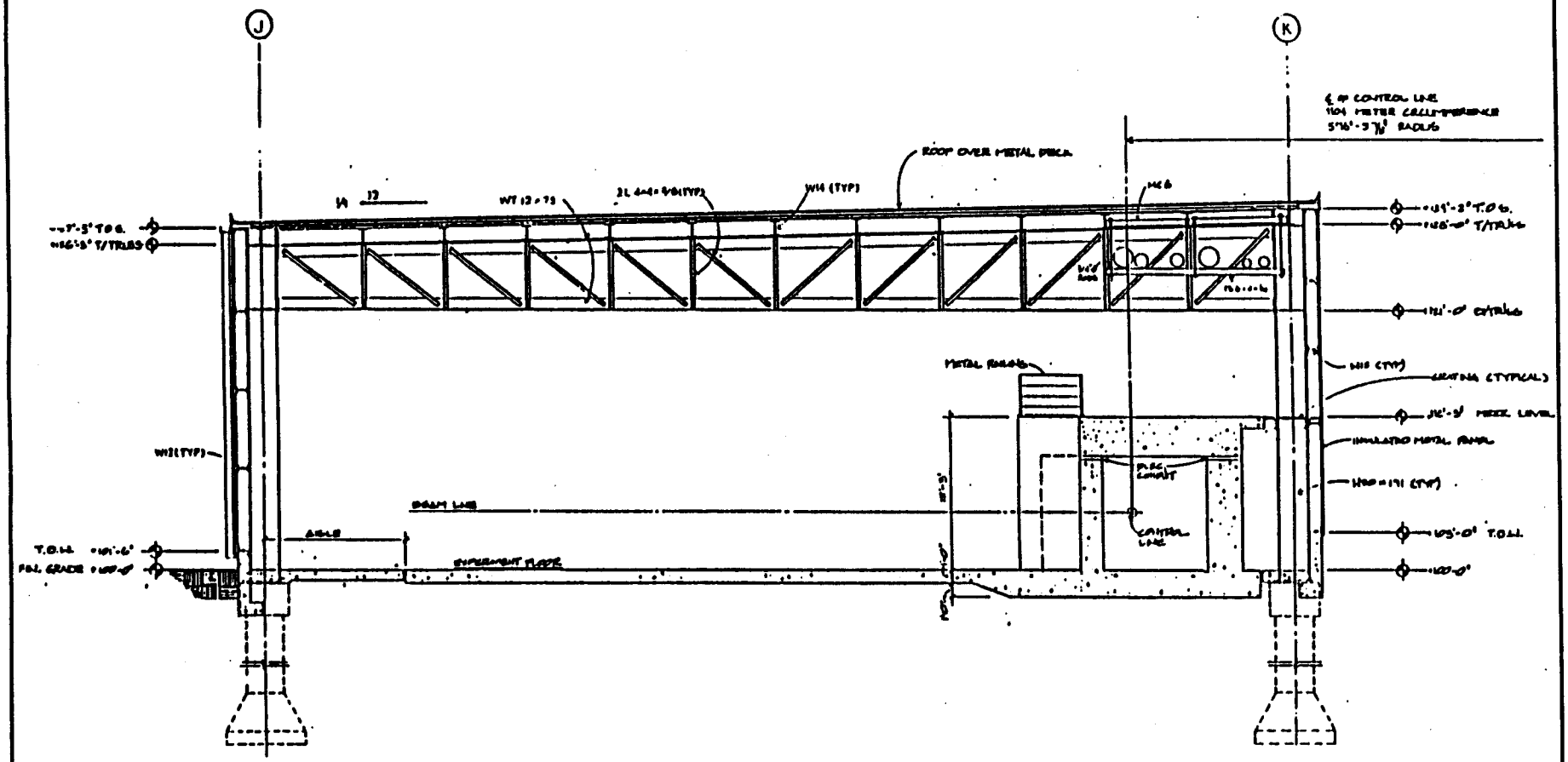

Prototypic APS Storage Ring Magnet Support Assembly

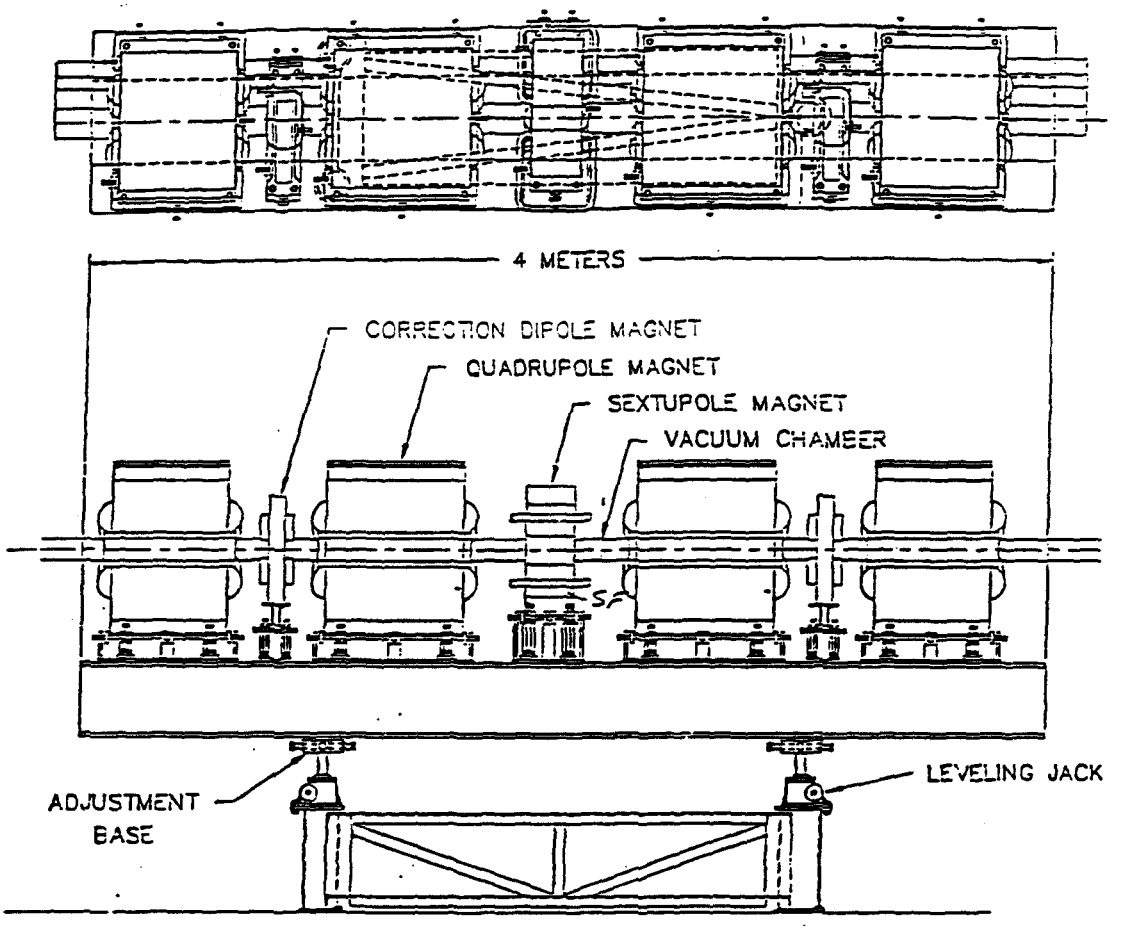

APS Storage Ring Magnet Support Assembly

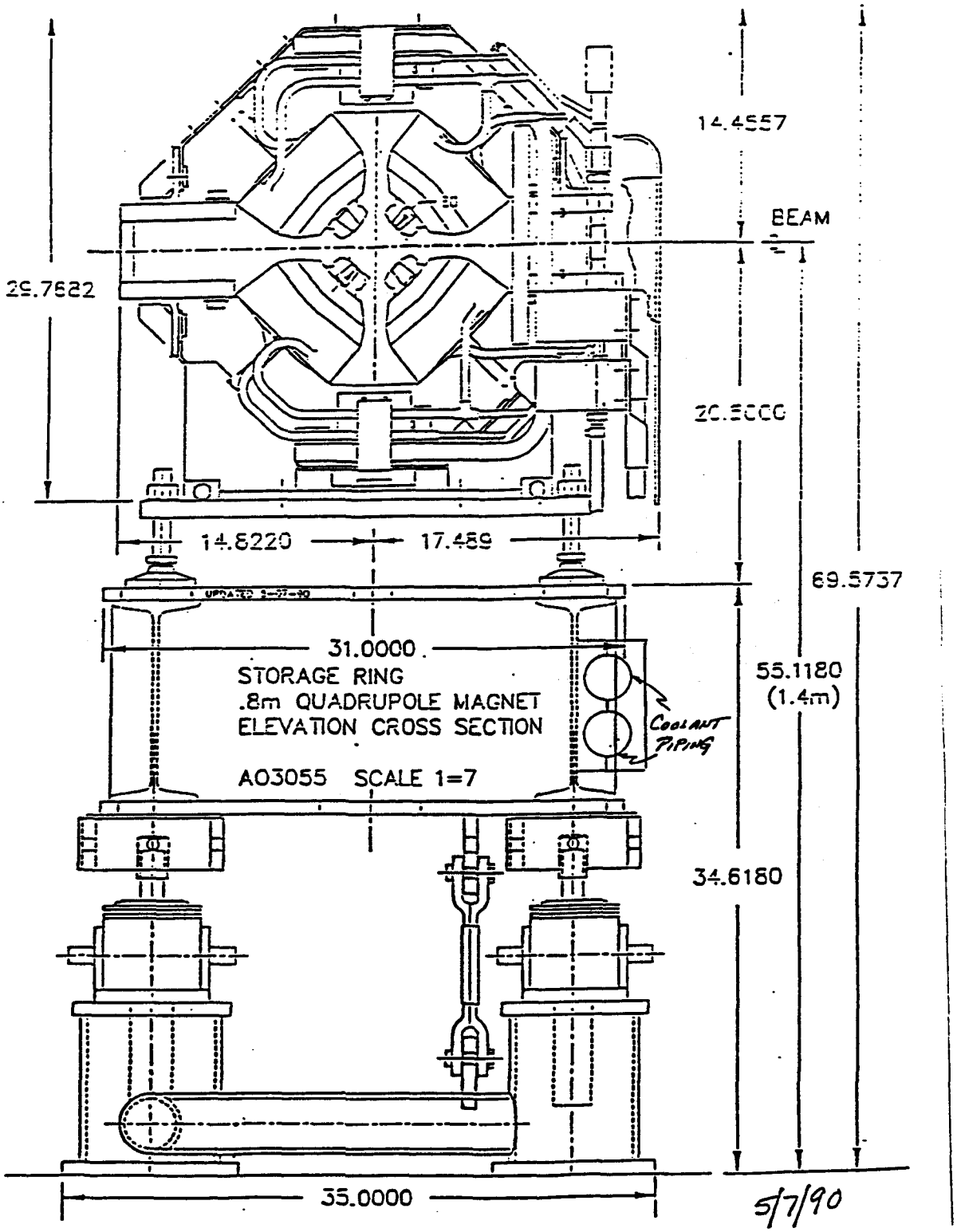

Vibration Criteria

- Based on requirement that emittance growth be limited to 10 per cent.
- Quadrupoles most sensitive relative to orbit distortion and emittance growth.
- Three different scenarios considered; maximum allowable vibration amplitudes are as follow:

Vibration Type	δ_H, μm	δ_V, μm
Single Quadrupole	2.20	1.29
Random (all quads)	0.34	0.12
Plane Wave (V=306 m/s, f in Hz)		
$f < 2.2$	16.1	4.4
$2.2 < f < 4.6$	16.1	4.4-0.28
$4.6 < f < 7.7$	16.1	0.28
$7.7 < f < 13.5$	16.1-0.90	0.28
$13.5 < f$	0.90	0.28

δ_H and δ_V are peak horizontal and vertical components, respectively, of magnet vibration.

Vibration Criteria (cont'd)

- Low frequency vibration (< 10-20 Hz) can be corrected with feedback systems using steering magnets; amplitudes must still be within dynamic range of feedback controls.

- High frequency vibrations (>10-20 Hz) must satisfy the vibration criteria.

- Criteria for random motion of all quadrupoles are most stringent and are assumed as the vibration criteria to be met for the APS.

- In terms of RMS displacement, for a Gaussian random motion, the APS criteria for maximum allowable vibration of the storage ring quadrupoles are

$$\delta_H < 0.11\ \mu m,$$

$$\delta_V < 0.04\ \mu m.$$

[Thickness of a sheet of paper is ~ 50 - 100 μm]

Technical Approach

VIBRATION STUDIES IN SUPPORT OF 7-GeV APS

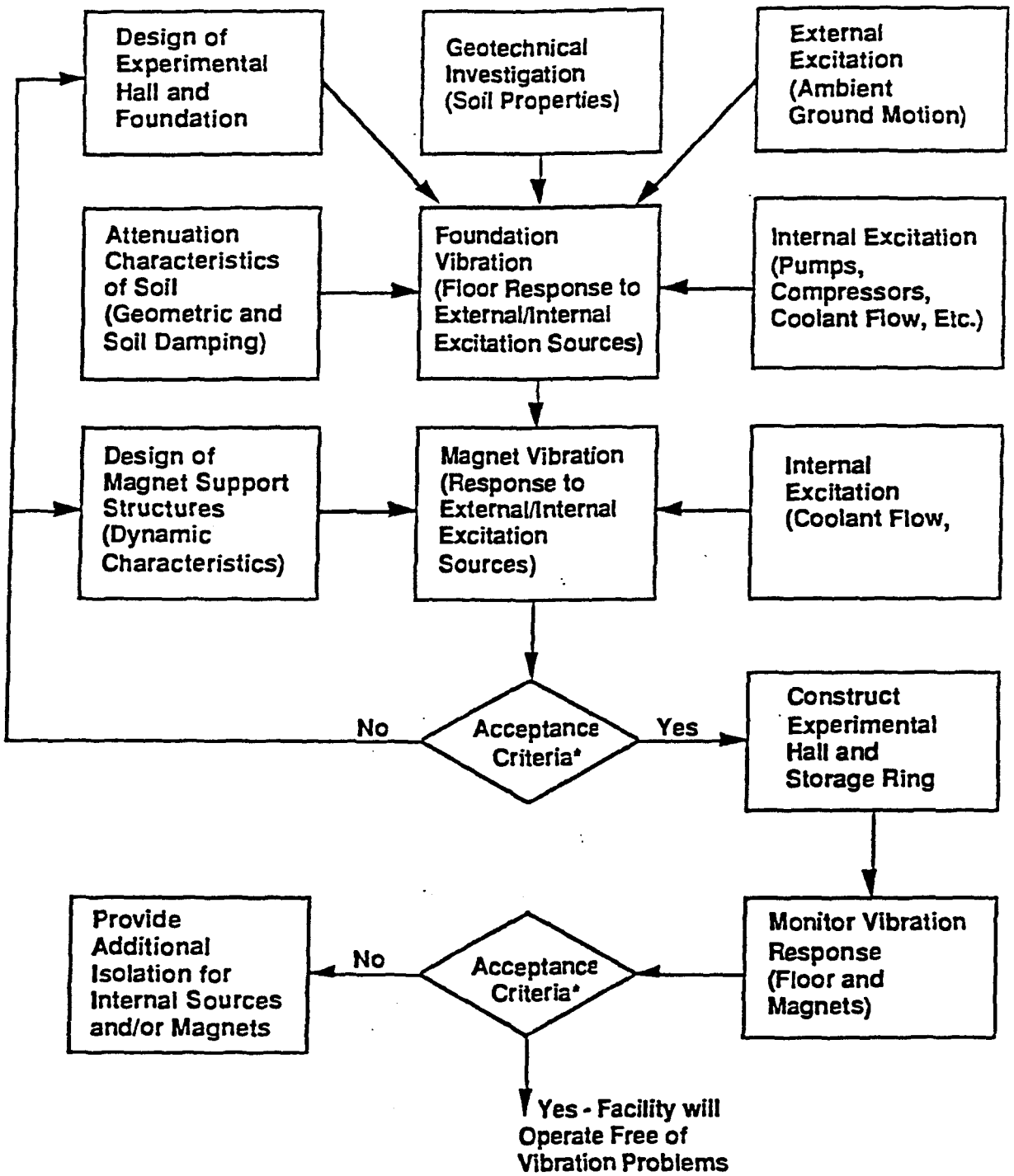

*Vibration acceptance criteria: for f > 10-20 Hz; peak vertical amplitude < 0.12 μm, peak horizontal amplitude < 0.34 μm

Vibration Analysis
Experimental Hall Floor

- Equivalent lumped parameter modelling based on elastic half-space theory.

  Example - vertical mode:

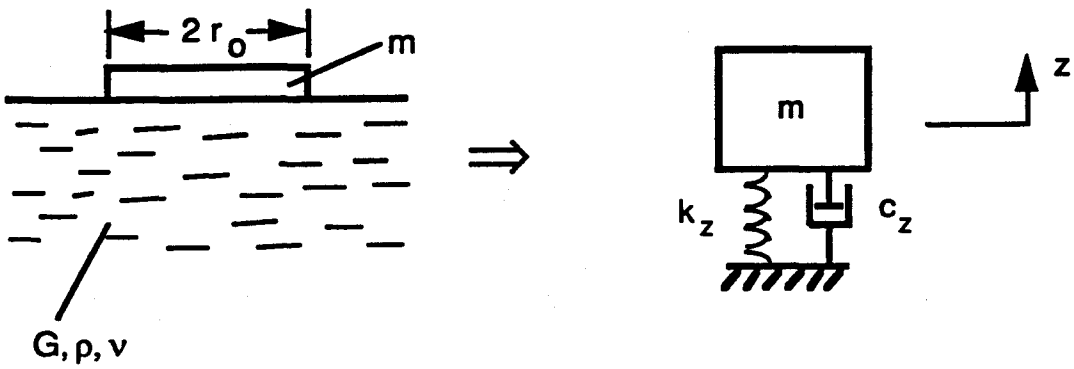

$$G = \rho V_s^2 \qquad k_z = \frac{4Gr_0}{1-\nu}$$

$$r_0 = \left(\frac{bL}{\pi}\right)^{1/2} \qquad c_z = \frac{3.4\,r_0^2}{1-\nu}\sqrt{\rho G}$$

- Large plan dimensions ⇒ large damping ⇒ magnification factor small.
- Support floor slab on grade.
- Can expect floor slab to follow ground motion with little or no magnification; "waveform averaging"suggests response will be less.

Design Goals

- Avoid the potential for magnification of floor motion.
- Minimize response to internal excitation sources such as flow in coolant water flow headers.

Approach

- Iterative procedure involving design, analysis, and testing.
- Scoping analyses based on both simple lumped parameter models and finite element models.
- Vibration tests with and without magnets simulated.

Vibration Tests

- Determined vibrational characteristics (natural frequencies, modes, and damping) of girder/support assemblies; with and without magnets simulated.
- Evaluated two different support arrangements.
- Measured response of girder/support assemblies to ambient floor motion.
- Evaluated effects of coolant water flow.
- Evaluated vacuum chamber supports and dynamic coupling with girder/support assemblies.
- Determined response of individual magnet/support assemblies and coupling with girder/support assemblies.

Theoretical and Experimental Frequencies: A Comparison

Table 5. Natural frequencies (Hz) Test D: configuration B - without magnets

Out-of-Plane Mode		In-Plane Mode		Axial Mode	
Theory	Experiment	Theory	Experiment	Theory	Experiment
12.6	12.6	49.6	63.5	14.8	
18.3	22.7	71.2		666.5	
64.0		138.3	132.0		
212.7	212.7	355.9	358.0		
419.9		656.6			
521.6	393.0				
833.0					
907.3					

Table 6. Natural frequencies (Hz) Test E: configuration B - with magnets

Out-of-Plane Mode		In-Plane Mode		Axial Mode	
Theory	Experiment	Theory	Experiment	Theory	Experiment
5.7	5.0	21.2		6.1	
7.8	8.3	29.6	36.8	284.8	
62.4	53.6	67.0	87.6		
103.2		165.5			
241.5	361	396.2			
419.5		485.8			
539.6					

Support Configurations Evaluated

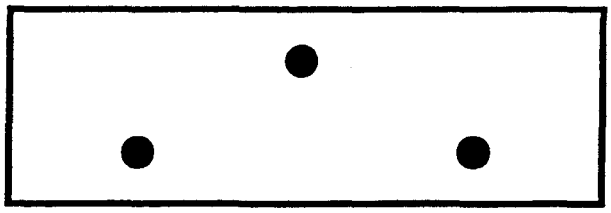

Configuration A

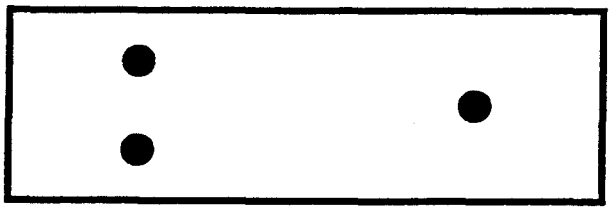

Configuration B

Response to Ambient Floor Motion

Table 10. Response (μm RMS) to ambient floor motion (10 - 100 Hz range)

	Horizontal	Vertical
Floor	0.012	0.018
Girder*	0.032	0.034

* Horizontal displacement is measured at node 11; vertical displacement is measured at node 1

Table 4. Displacement Response for Ambient Excitation (Wideband, Test 3)

Measurement Position	Displacement,microns,rms
X,Magnet	0.114
Y,Magnet	0.526
Z,Magnet	0.0871
X,Floor	0.0711
Y,Floor	0.0529
Z,Floor	0.0319

Table 5. Displacement Response for Ambient Excitation (7.62 Hz, Test 3)

Measurement Position	Displacement,microns,rms
X,Magnet	0.0368
Y,Magnet	0.5
Z,Magnet	0.0282
X,Floor	0.0428
Y,Floor	0.0392
Z,Floor	0.000428

Summary/Conclusions

- Storage ring girder/support assemblies represent a complex system from structural dynamics standpoint: second order effects are important (e.g., clearances and component interfaces) - many degrees of freedom - large mass (> 6,800 kg) with a high center of gravity - interest is in extremely small motions (on the order of 0.1 μm).

- Girder bending/torsional modes are high (typically > 100 Hz) ⇒ for lower modes of interest, flexibilities of the pedestal supports are controlling ⇒ can consider girder and magnets as rigid body.

- Analytical modeling useful for preliminary design - vibration testing of prototypic hardware under prototypic conditions is required.

- For the two support arrangements tested, the results were comparable.

- Coolant flow through headers attached to the girder has measurable, but small, effect on response.

Summary/Conclusions (cont'd)

- Design with jack-screws-on-pedestals is marginal: frequencies in range of concern (10 -80 Hz) - inherent uncertainties in alignment of jackshaft/screw assembly can lead to variable/unacceptable response.

- Stiffer, more predictable, support assemblies recommended - concrete pillars suggested (rigid, massive, low damping) - project determined not practical.

- Support assembly redesigned with goal to keep $f_n > 80$ Hz: jack-screws replaced with sliding-wedge jacks; stiffened I-beam structure.

- Vibration tests of redesigned system recently completed - results are being analyzed.

- Reasonable to expect girder to follow floor motion in vertical direction with an overall RMS amplification factor of approximately 2 in the horizontal directions.

References

M. W. Wambsganss, "Dynamic Analysis of the 7-GeV APS Experimental Hall Foundation Based on Equivalent Lumped Parameter Modeling," *Argonne National Laboratory Report APS/IN/VIB/89-1,* Jan. 1989.

J. A. Jendrzejczyk, R. K. Smith, and M. W. Wambsganss, "Vibration Survey of IPNS Beam Line Magnets and Experimental Hall," *Argonne National Laboratory Report LS-89,* April 1987.

M. W. Wambsganss, "Preliminary Dynamic Analysis of Conceptual Design of Magnet/Support System for the APS Storage Ring," *Argonne National Laboratory Report, APS/IN/VIB/89-2,* June 1988 (Rev. May 1989).

S. S. Chen and M. W. Wambsganss, "Vibration Analysis of APS Magnet/Support Systems Based on the Finite Element Method," *Argonne National Laboratory Report APS/IN/VIB/89-3,* March 1989.

M. W. Wambsganss, J. A. Jendrzejczyk, and S. S. Chen, "Vibration Study of the APS Magnet Support Assemblies," *Argonne National Laboratory Report APS/IN/VIB/90-3,* Nov. 1990.

J. A. Jendrzejczyk, M. W. Wambsganss, and R. K. Smith, "Vibration Study of the APS Storage Ring Vacuum-Chamber/Girder Assembly," *Argonne National Laboratory Report APS/IN/VIB/91-1,* Feb. 1991.

J. A. Jendrzejczyk, M. W. Wambsganss, and R. K. Smith, "Vibration Study of the APS Storage Ring 0.8 Meter Quadrupole/Girder Assembly," *Argonne National Laboratory Report APS/IN/VIB/91-2,* May 1991.

J. A. Jendrzejczyk, M. W. Wambsganss, and R. K. Smith, "Vibration Study of the APS Storage Ring 0.8 Meter Quadrupole Magnet/Magnet Support Assembly," *Argonne National Laboratory Report APS/IN/VIB/91-3,* June 1991.

J. A. Jendrzejczyk and M. W. Wambsganss, "Vibration considerations in the design of the Advanced Photon Source at Argonne National Laboratory," to be published in *Proceedings of Conf. on Vibration Control in Microelectronics, Optics, and Metrology,* 1991 Symp. on Optical Science and Engineering, San Jose, CA, Nov. 1991.

ALIGNMENT OF FINAL FOCUS LENSES

Overview of Alignment Concerns and Requirements for Low Beta Magnets
David Veal (SSCL)

Prognosis for an Automated Alignment System
Robert Ruland (SLAC)

On-Line 3D Control of LHC Low Beta Quadrupoles: Preliminary Approach of Possible Solutions
Michel Mayoud (CERN)

Kinematic Cam Positioning Mounds
Gordon Bowden (SLAC)

***ILSE* Active Alignment with a Stretched Wire Reference**
Lee Griffith (LLNL)

Hz Modulation of Accelerator Components due to Mechanical Vibration
Craig Moore (FERMI)

DV 10 Feb

Presentation to Workshop on Vibrational Control and Dynamic Alignment Issues at the SSC

3 months before commissioning at the moment of the alignment of final focus quadrupoles from a survey point of view will be 3 axis

1) machine north of experiment
2) machine south of experiment
3) experiment installation axis (established ~3 years ago)

Aim - render 1&2 collinear/smooth (no dogs-legs) and as close to 3 (<3mm) as is possible without distorting geometry of machine

Link between two segments of machine

1) survey passage through experiment - not acceptable physics
2) survey passage through vacuum chamber
3) around experiment - inevitable loss of precision

Present option - optical measurements by vacuum chamber

Will require

1) removable sections of vacuum chamber near low beta quad to allow insertion alignment telescope, human head
2) observations through vacuum to avoid refraction, optically flat window on vacuum chamber, adjustable to render perpendicular to line of sight of alignment telescope
   - minimum diameter of beam pipe
3) stable support for alignment telescope!!!!! (must be dissociated from movements of operator, others on bridge)
4) time!!!! (several days)

Will yield tenths of mm

Problem

1) non-redundant method on a crucial measurement

Maintenance - reestablishing alignment after shut-down

1) optical methods with human operator may not be possible after commissioning because of residual radiation
2) relative measurements using interferometer from "fixed" stations on cavern walls to re-establish position machine had just before the shut-down
   - but convention of cavern walls, temperature effects

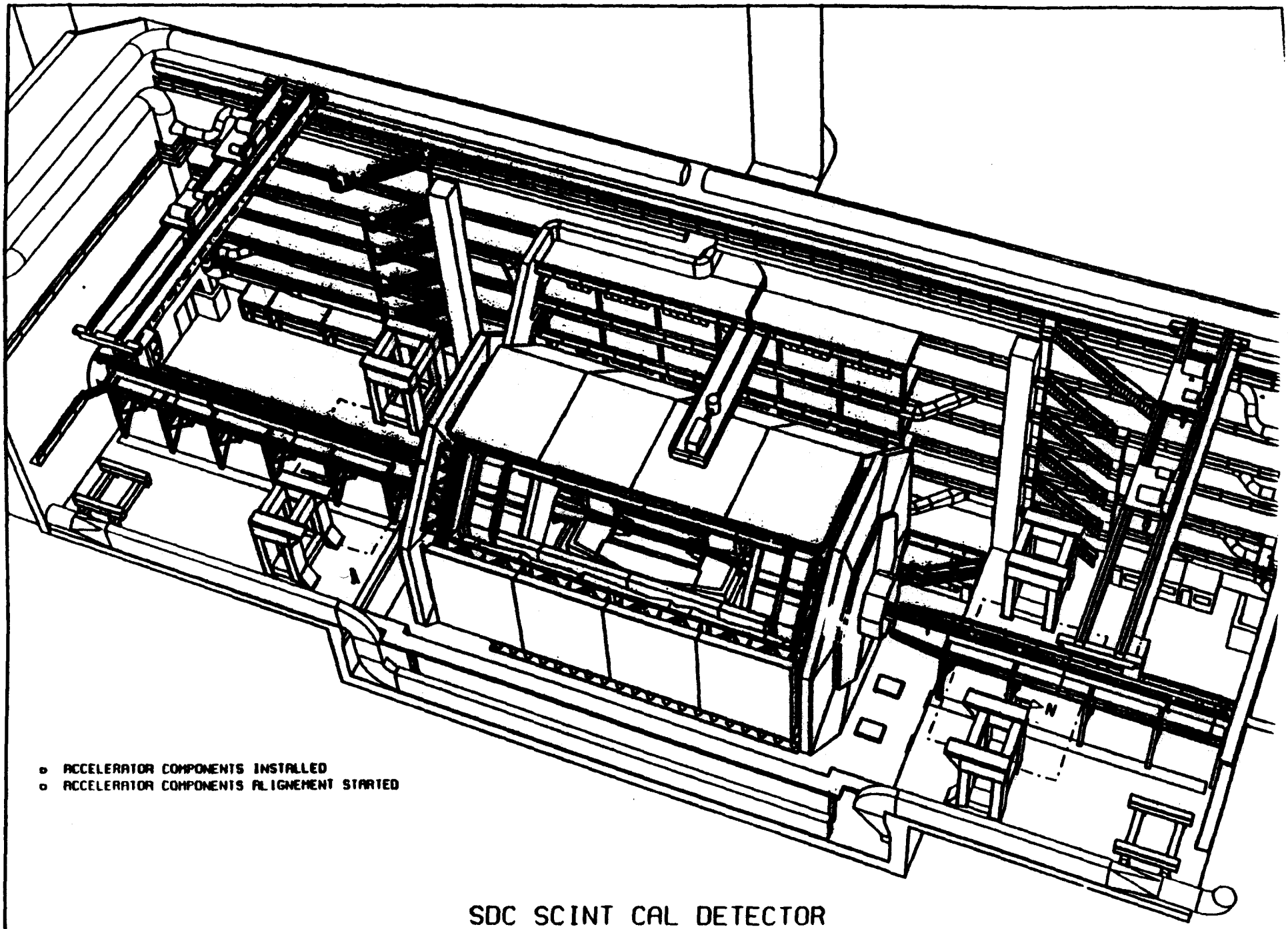

- ACCELERATOR COMPONENTS INSTALLED
- ACCELERATOR COMPONENTS ALIGNEMENT STARTED

SDC SCINT CAL DETECTOR

CONSTRUCTION PROGRESS

MONTH 40

ICF KAISER ENGINEERS 9-18-91 MODEL 523M0045.DGN MONTH40 HI

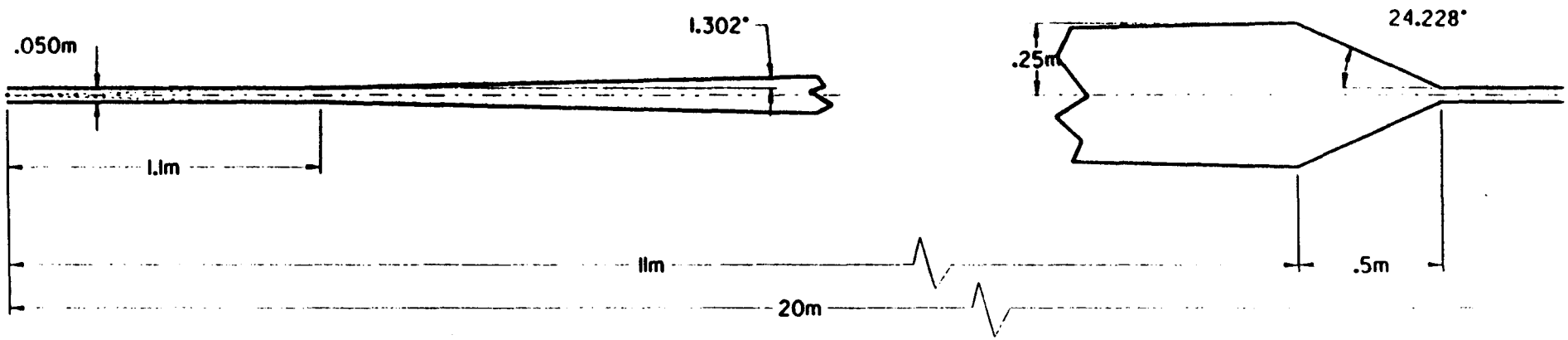
.050m
1.302°
1.1m
11m
20m
.25m
24.228°
.5m

Prognosis for an Automated Alignment System

Robert E. Ruland

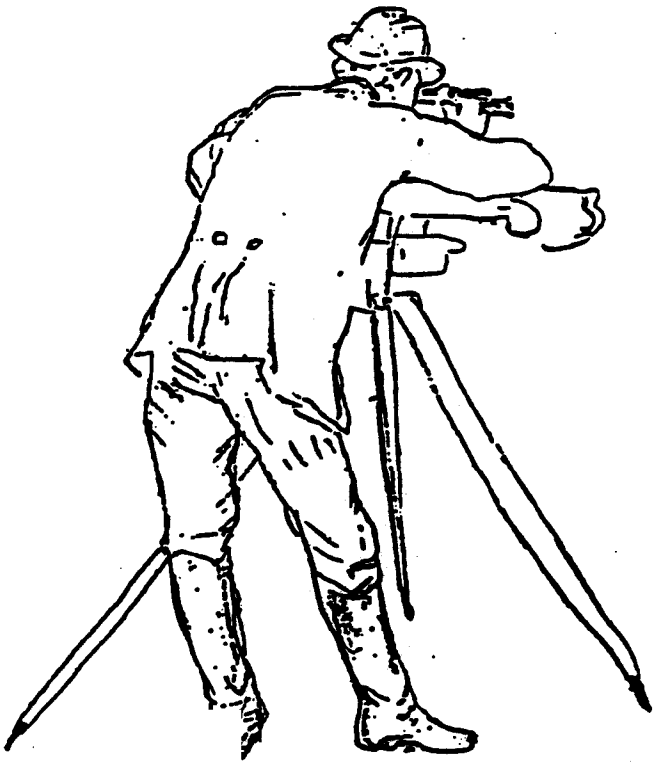

Stanford Linear Accelerator Center
Survey and Alignment Department
Jan 29, 1992

Fig. 1

(a) Straight Sections

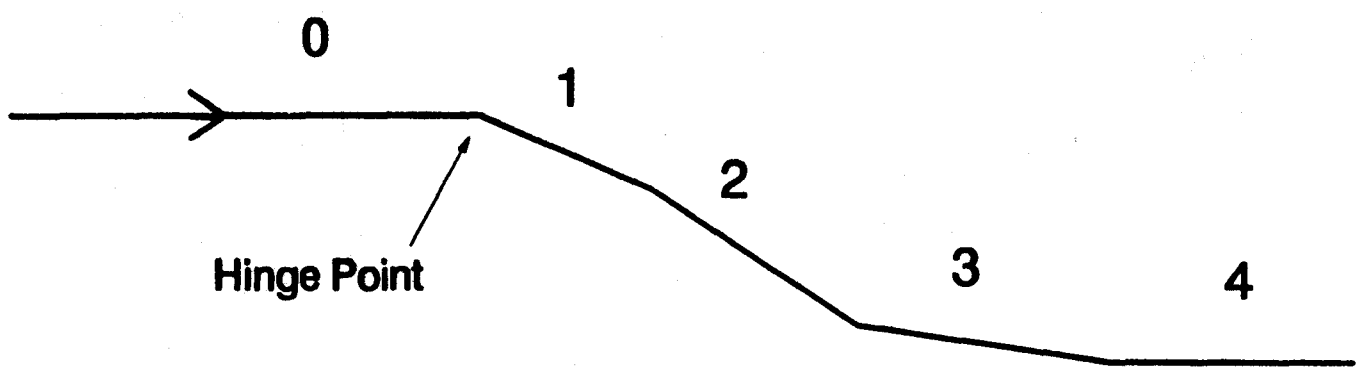

Stanford Linear Accelerator Center
Survey and Alignment Group
January 29, 1992

FFTB Alignment

3 Goals:

- Initial Alignment
- On-line Monitoring
- Reconfiguration

Stanford Linear Accelerator Center
Survey and Alignment Department
Jan 29, 1992

Initial Positioning

☞ Global Position of Hinge Points

$X < 2000\ \mu m$

$Y < 200\ \mu m$

☞ Relative Position of Straight Sections

Required

$X < 100\ \mu m$

$Y < 30\ \mu m$

Desired

$X < 30\ \mu m$

$Y < 10\ \mu m$

On Line Monitoring

- Minute to Minute

  $X < 2\,\mu m$

  $Y < 2\,\mu m$

- 20 Minute Basis

  $X < 10\,\mu m$

  $Y < 5\,\mu m$

Stanford Linear Accelerator Center
Survey and Alignment Group
January 29, 1992

Reconfiguration

(Weekly Basis)

- **Required**

  X < 100 μm

  Y < 30 μm

- **Desired**

  X < 30 μm

  Y < 10 μm

Stanford Linear Accelerator Center
Survey and Alignment Group
January 29, 1992

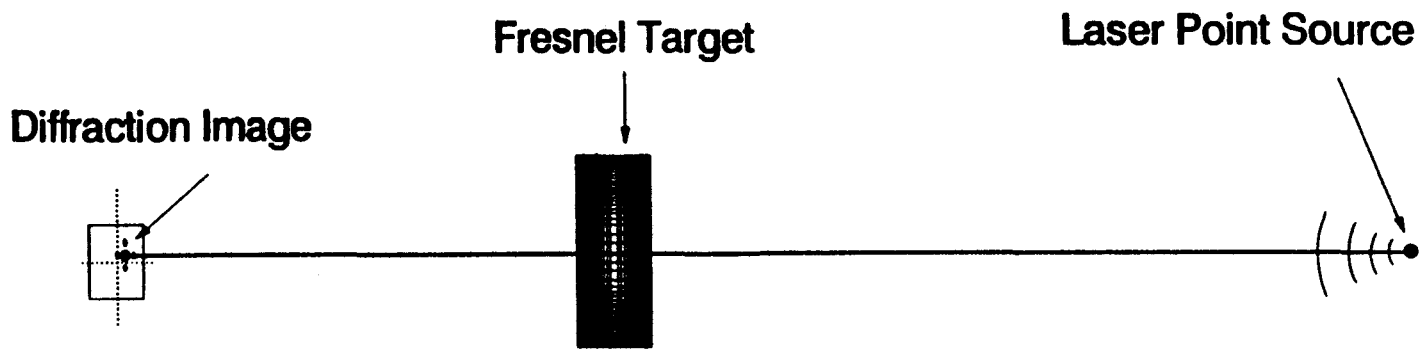

Stanford Linear Accelerator Center
Survey and Alignment Group
January 29, 1992

Geometry of Laser Reference System

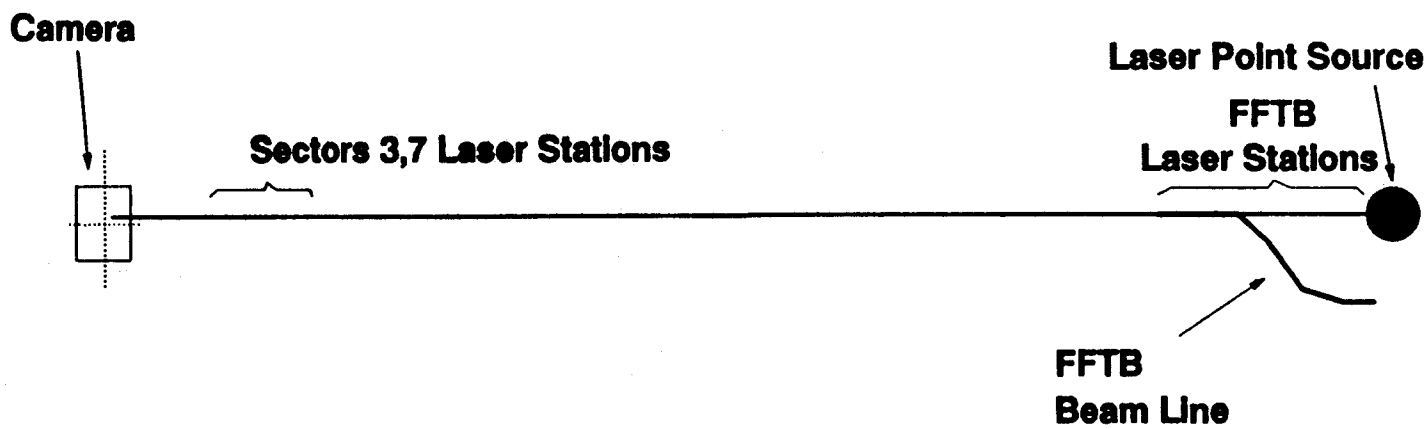

Stanford Linear Accelerator Center
Survey and Alignment Group
January 29, 1992

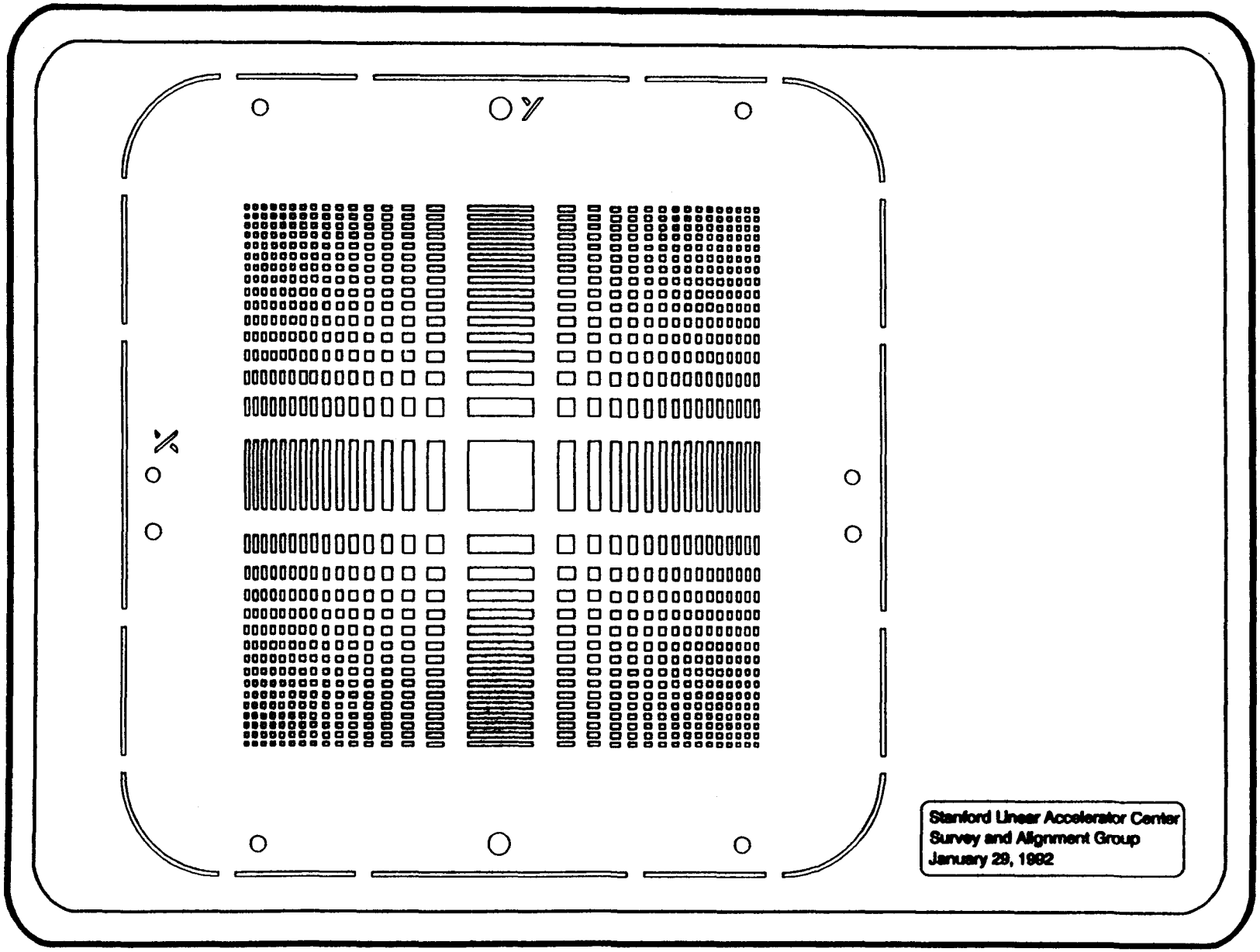
Y
X
Stanford Linear Accelerator Center
Survey and Alignment Group
January 29, 1992

(b) Layout of Beam, Monuments, Laser Stations

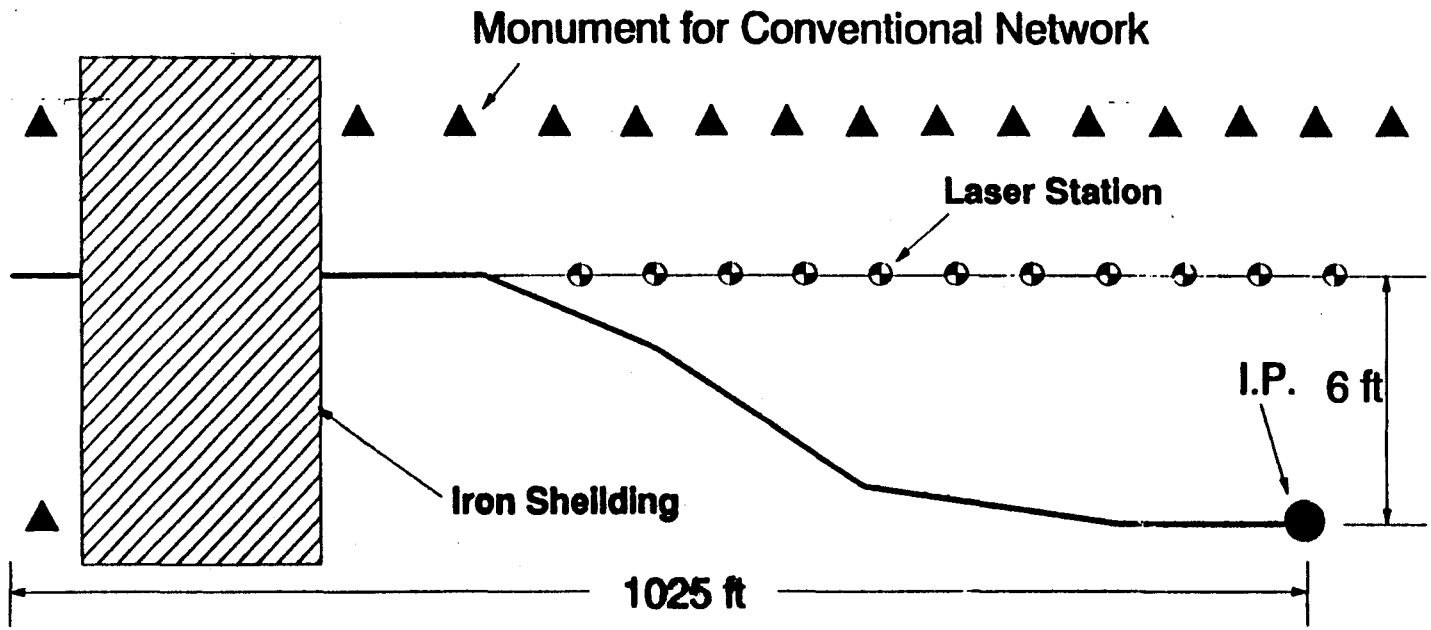

Slope 5 mradians

Stanford Linear Accelerator Center
Survey and Alignment Group
January 29, 1992

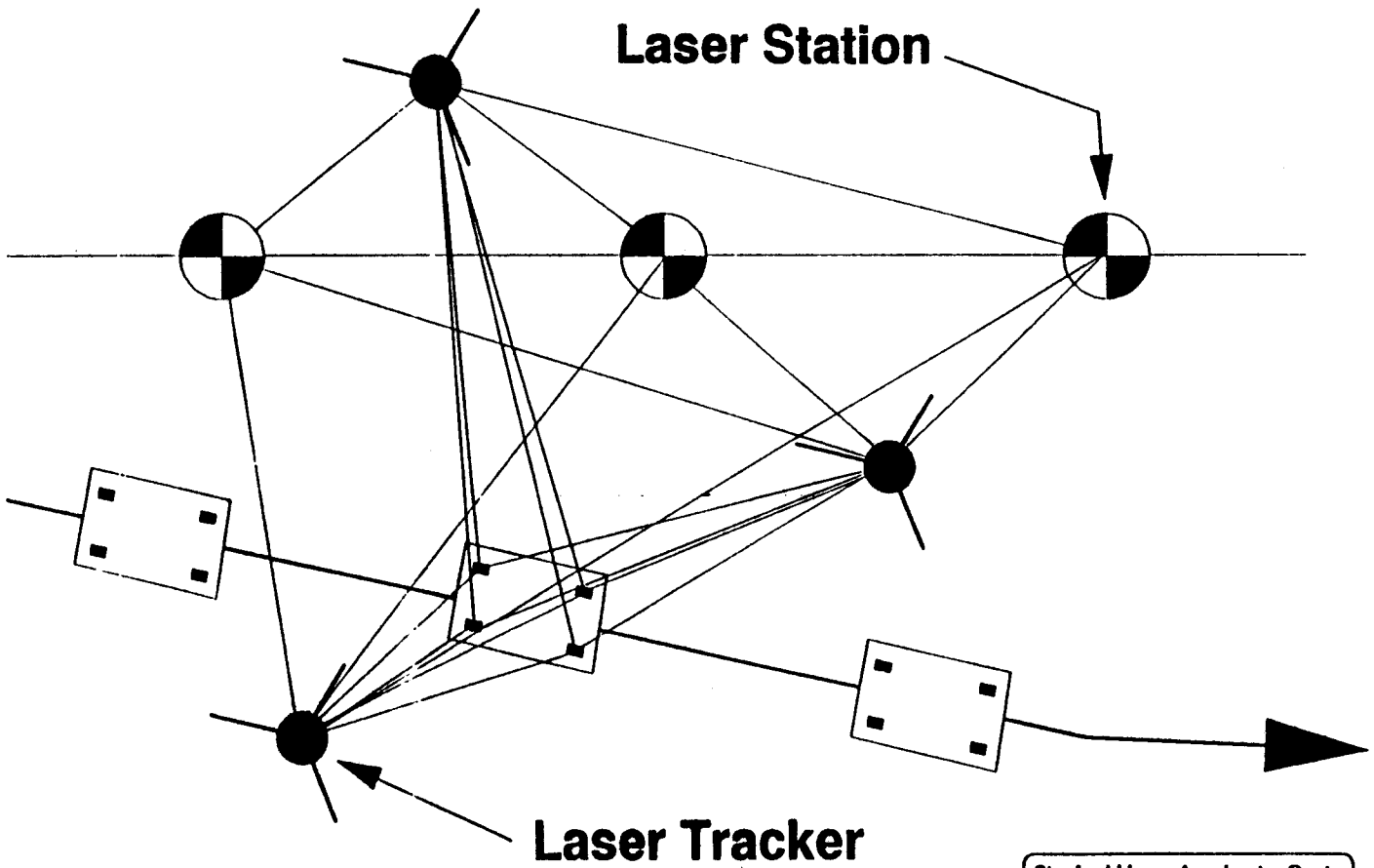

Stanford Linear Accelerator Center
Survey and Alignment Group
January 29, 1992

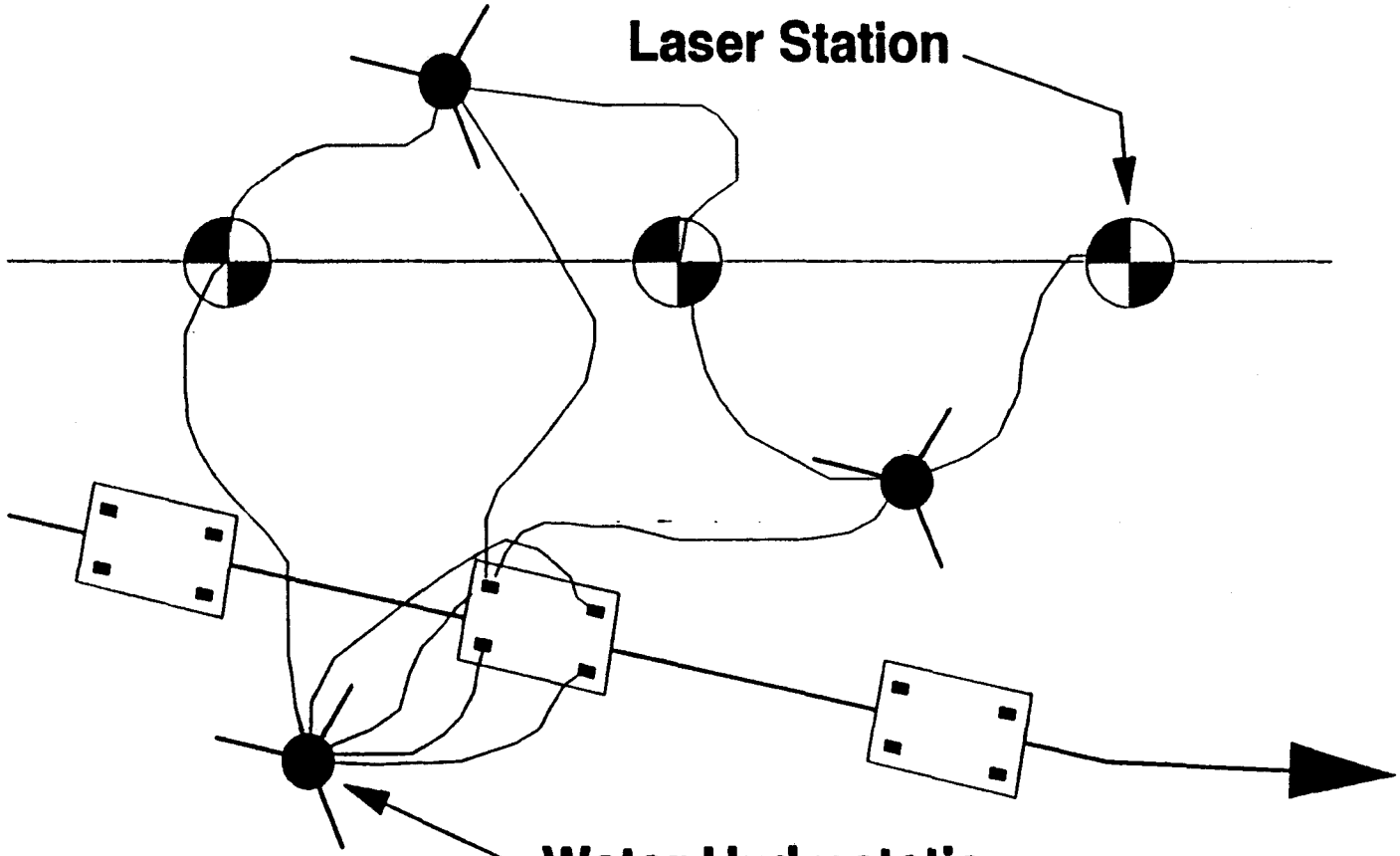

Stanford Linear Accelerator Center
Survey and Alignment Group
January 29, 1992

FFTB Alignment Error Budget: 12/5/91

Initial Alignment

Item	Contribution to error in microns	
Change in position of magnetic center:	2	4
Node finding wire to magnetic center:	2	4
Node finding wire to microscope fiducial:	3	9
Microscope fiducial to tooling frame fiducial:	12	144
Tooling frame fiducial to laser station fiducial:	10	100
Laser station fiducial to Fresnel target fiducial:	10	100
Target fiducial to optical center of target:	2	4
Detection of image:	2	4
Actuator non repeatability:	4	16
Z position of laser stations:	2	4
Movement of laser over one cycle:	7	49

Quadrature Sum:	21
Required:	30 Y-axis
Desired:	10 Y-axis

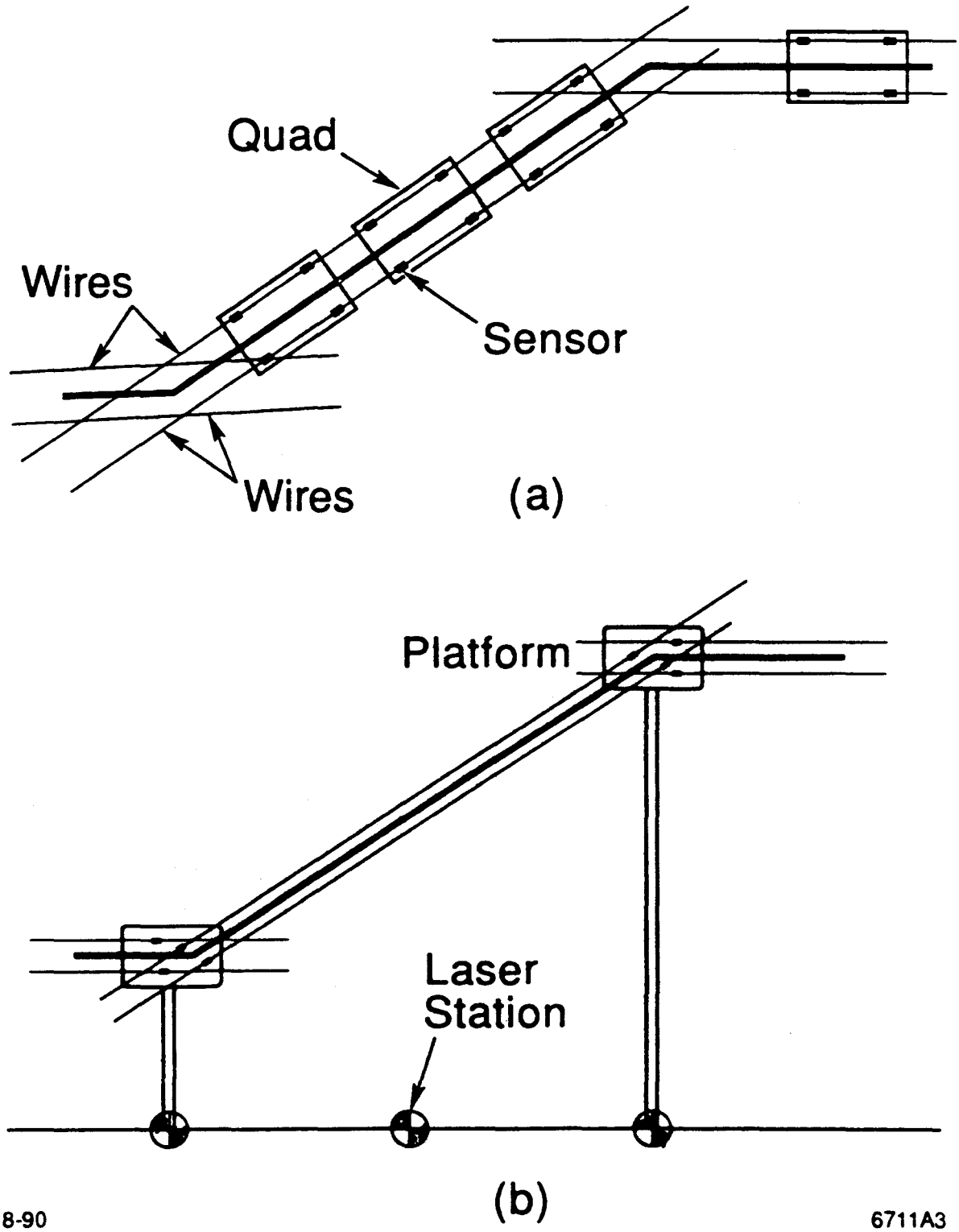

8-90

6711A3

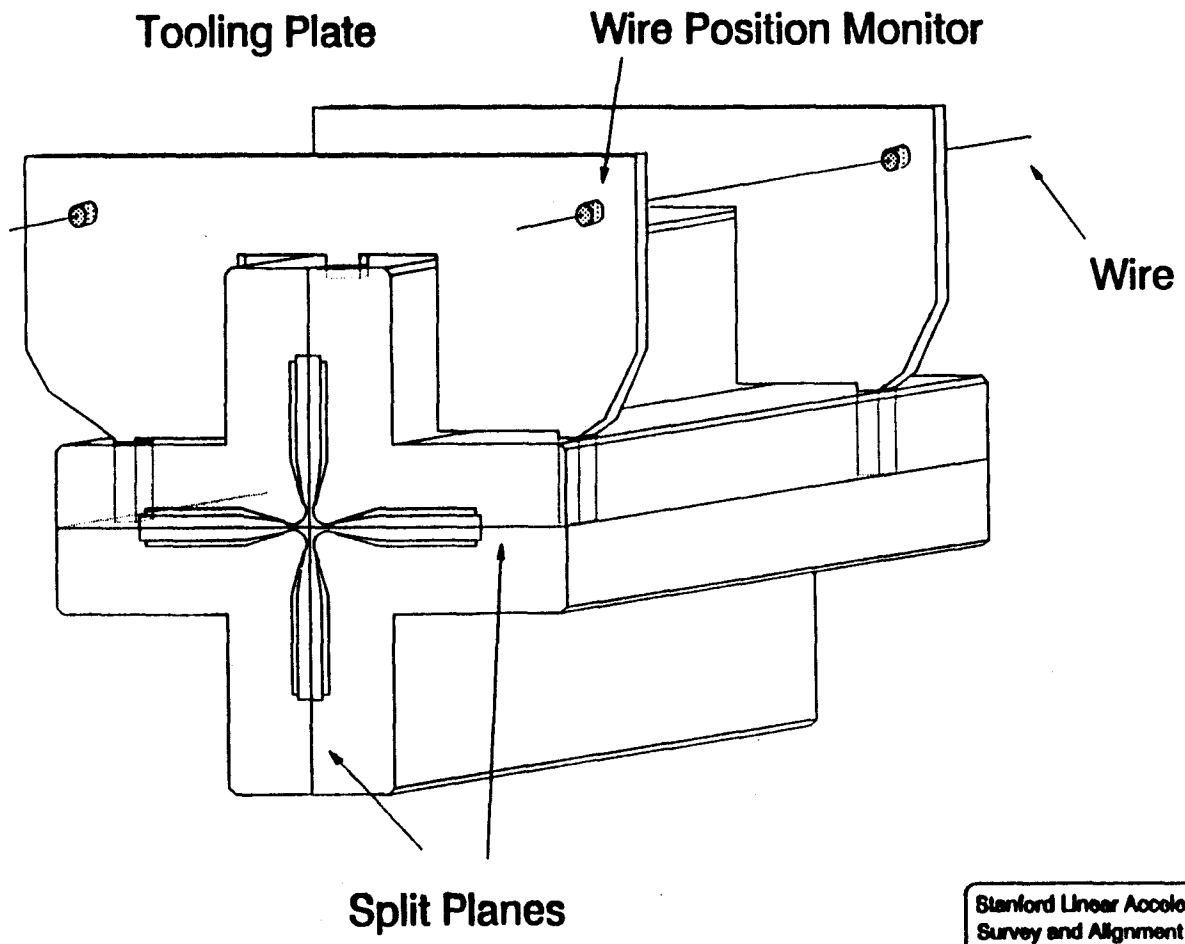

Stanford Linear Accelerator Center
Survey and Alignment Group
April 10, 1991

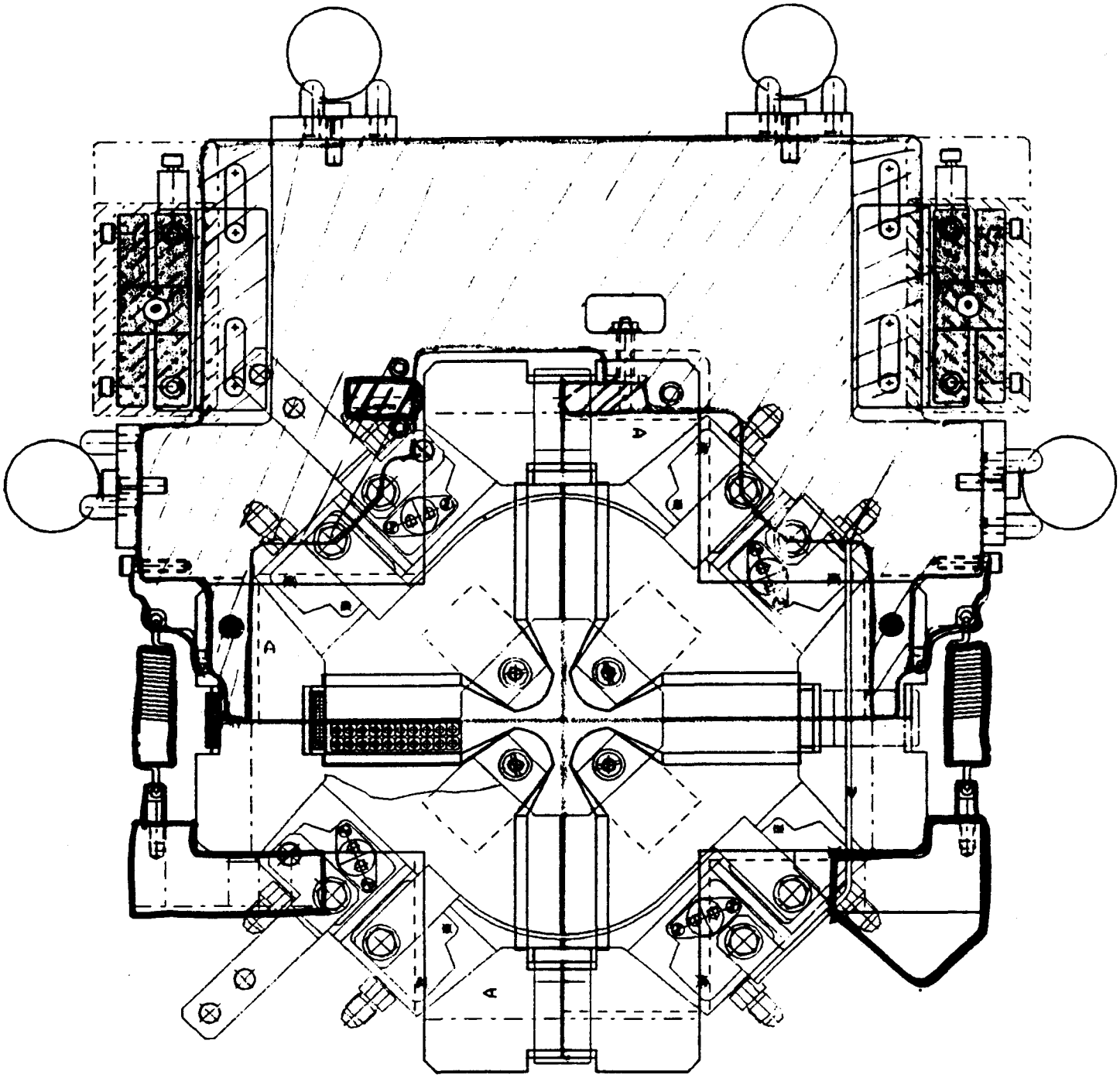

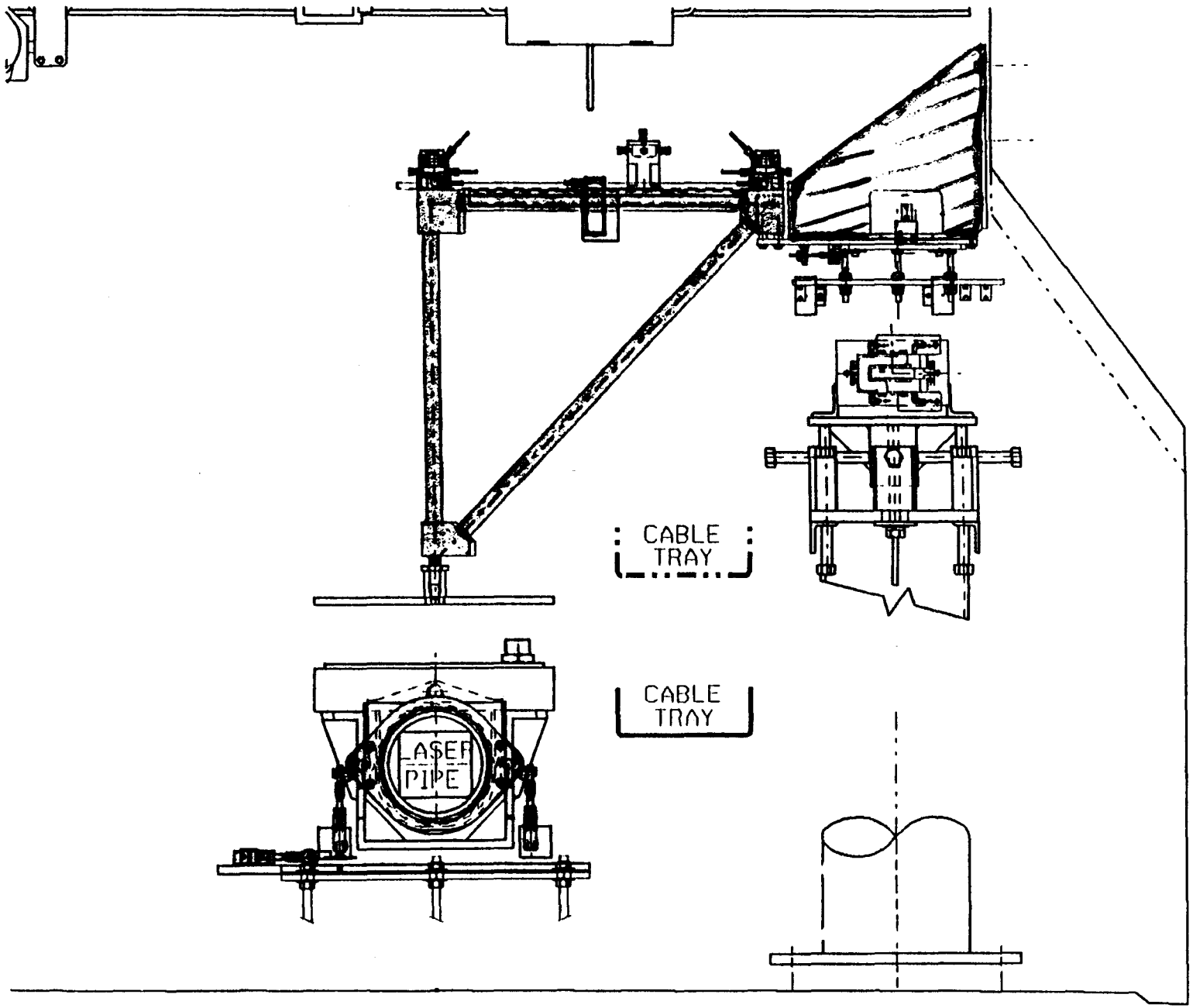

LSX4 STA 10817.400'

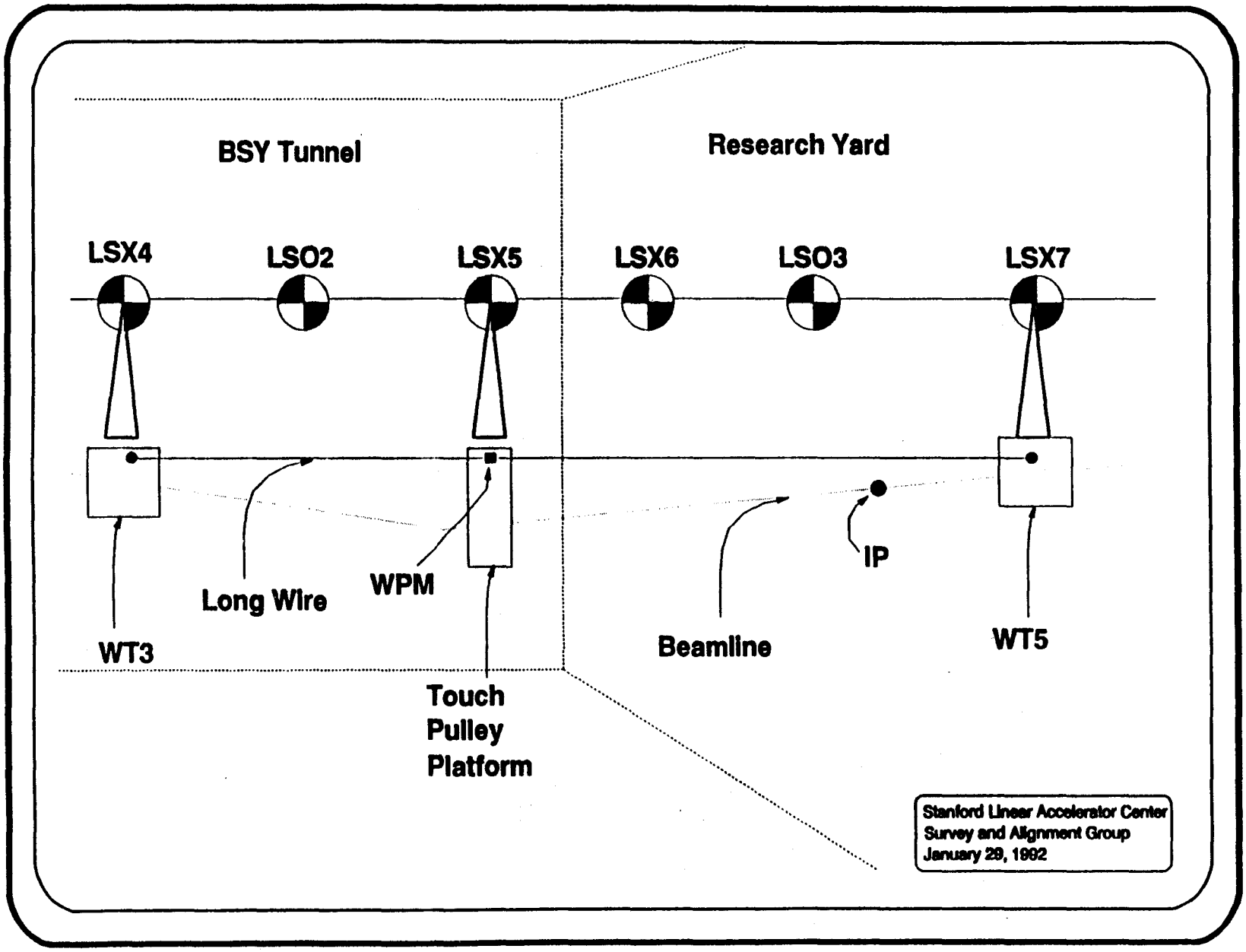
BSY Tunnel
Research Yard
LSX4
LSO2
LSX5
LSX6
LSO3
LSX7
WT3
Long Wire
WPM
Touch
Pulley
Platform
Beamline
IP
WT5
Stanford Linear Accelerator Center
Survey and Alignment Group
January 29, 1992

Error Budget:

On-line Monitoring (minute to minute)

Item	Contribution to error in microns
Change in position of magnetic center:	<1
Non systematic motion / distortion of wires:	1
Wire position monitor resolution:	<1
Thermal gradients in tooling frame:	<1
Response time of the control system:	<1
Quadrature sum:	<2
Goal:	<2

On-line Monitoring (twenty minute) additional items:

Roll, yaw of wire terminator (20 min):	<1
Drift of bridge sensors (20 min):	<1
Roll of actuator (20 min):	<1
Actuator non repeatability:	4
Detection of image:	2
Laser Ref line instability	1
Quadrature sum:	<5
Goal:	<5

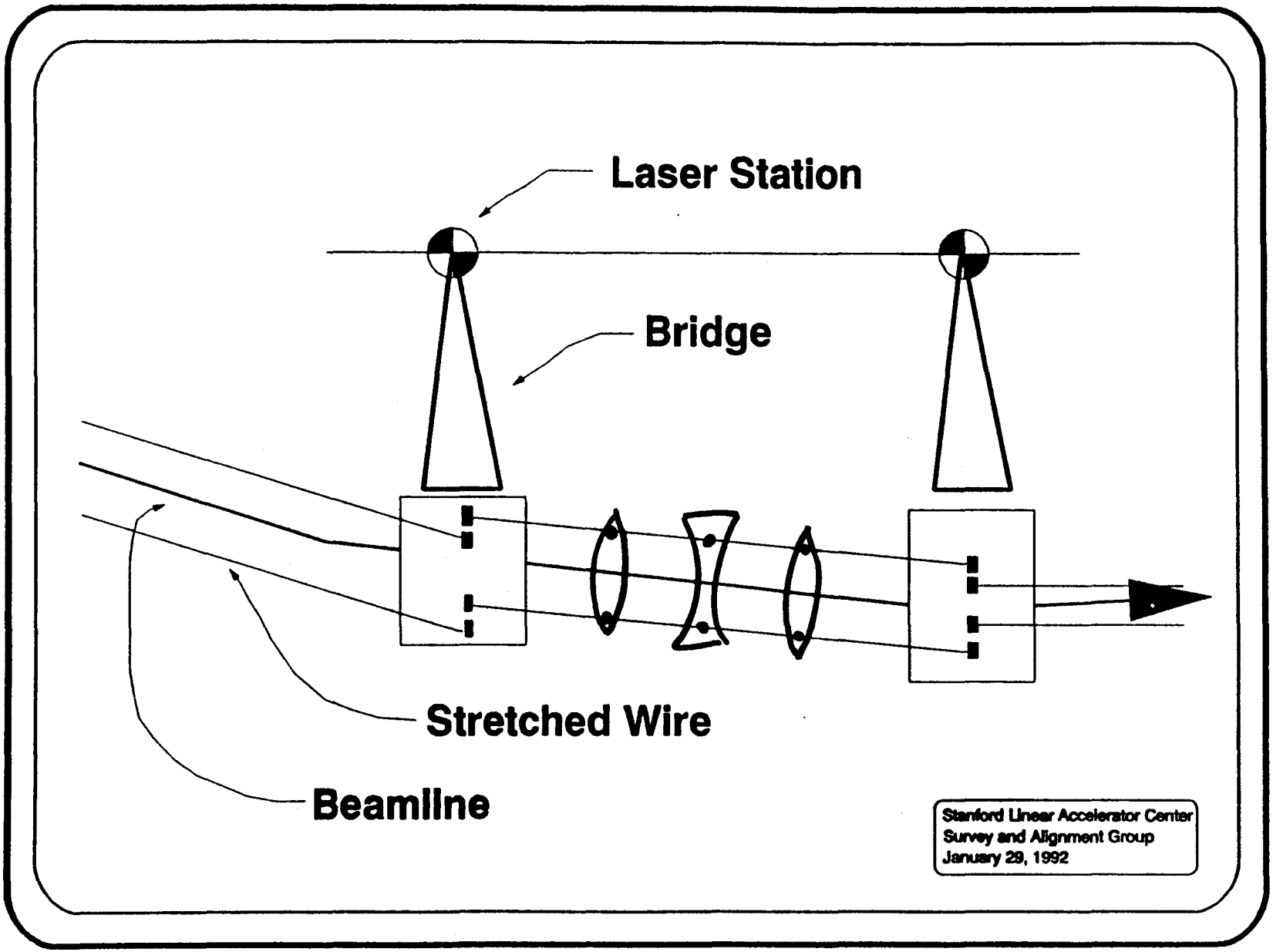
Laser Station
Bridge
Stretched Wire
Beamline
Stanford Linear Accelerator Center
Survey and Alignment Group
January 29, 1992

Error Budget:

Reconfiguration (weekly)

Item	Contribution to error in microns	
Change in position of magnetic center:	5	25
Change in position of tooling frame (weekly):	3	9
Wire position monitor drift (weekly):	10	100
Non systematic motion / distortion of wires (weekly):	3	9
Roll, yaw of wire terminator (weekly):	3	9
Drift of bridge sensors (weekly):	2	4
Roll of actuator (weekly):	3	9
Actuator non repeatability:	5	25
Movement of laser over one cycle:	7	49

Quadrature sum:	16
Required:	30 Y-axis
Desired:	10 Y-axis

ON-LINE GEOMETRICAL CONTROL OF LHC LOW-β QUADRUPOLES

PRELIMINARY APPROACH OF POSSIBLE SOLUTIONS

Michel MAYOUD & Jean-Pierre QUESNEL
with contributions from Williame Coosemans
CERN - Geneva

1 - Quick review of past or present situations in ISR, SPS and LEP

2 - Recent developments or trends for new instruments and methods

3 - Possible schemes of measurement

1 - Quick review of past or present situations

- **ISR and SPS**

Alignment of low-β sections using CERN techniques, pushed to their best...

Typically , $s_r = s_z \leq 0{,}08$ mm as relative transverse errors (rms) after smoothing.

In the ISR, (tentative) remote control of the alignment, using motorized jacks.

- **LEP**

Again a "classical " refinement of radial and orthogonal positions, derived from a careful smoothing scheme of measurements in the low-β area.....BUT.....in two points, the experiment has been settled before the low-β magnets ==> half-blind alignment ==> the resulting colinearity depends on how good the reference network is...

One shut-down later, it proved to be not so bad !

In addition, along the last (overhanging) girders, hydrostatic levels and movers have been installed for the on-line Z control of some superconducting Quads.

2 - Recent developments and trends...

CLIC is a very demanding project, regarding alignment too. CERN "Survey Group" is working more and more deeply in that new field o investigation, running after fractions of microns with various actuator: and sensors.

The consideration of CLIC and LHC alignment problems has le to develop (or implement) a new family of instruments and methods

- Optical systems : RASNYK (from NYKHEF, Netherlands)
  UVAS (Under Vacuum Alignment System)
- Off-set device : CBOS (Capacitive Bi-axial Off-set System)
- Hydrostatic system : HAC (Hydrostatic Alti-Clinometer)

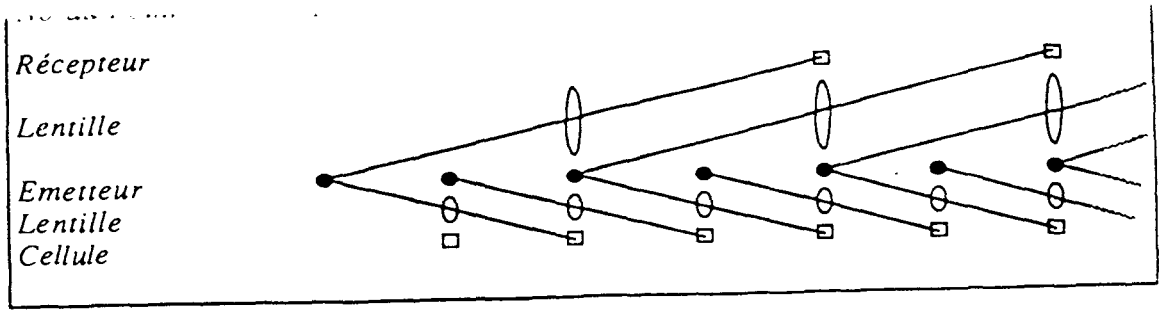

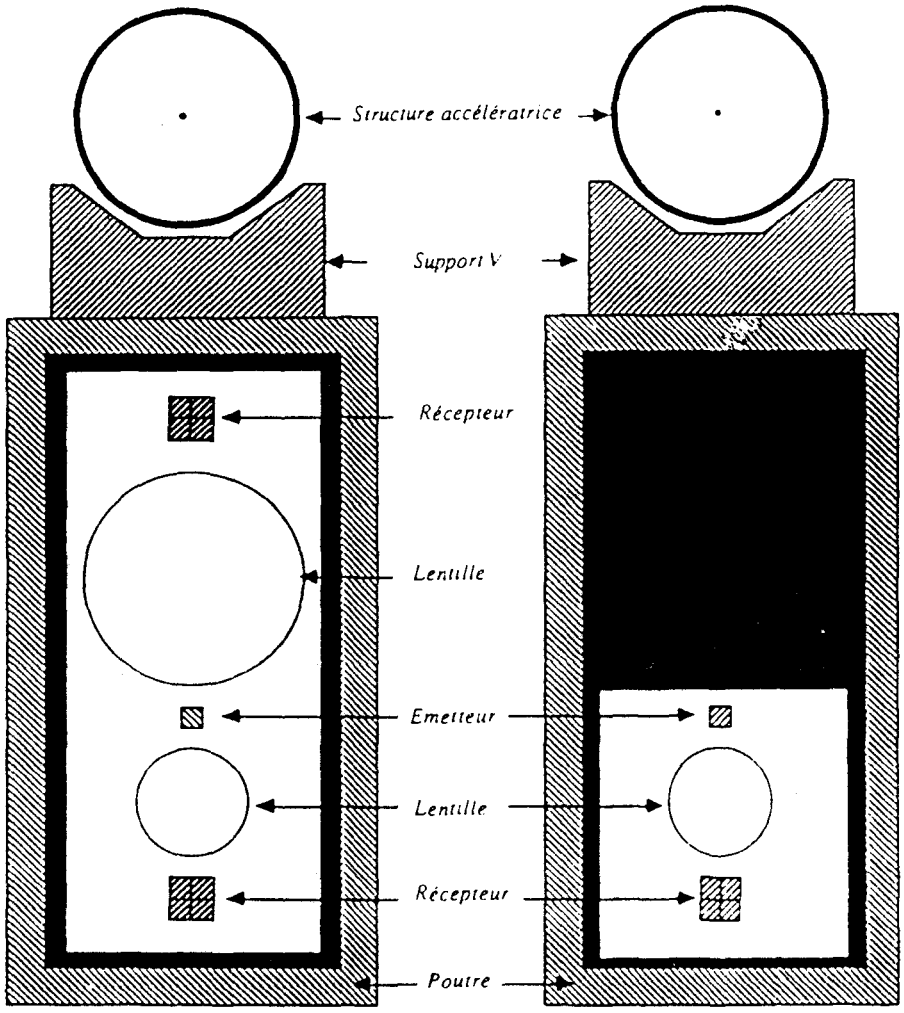

Point 5 Point 6

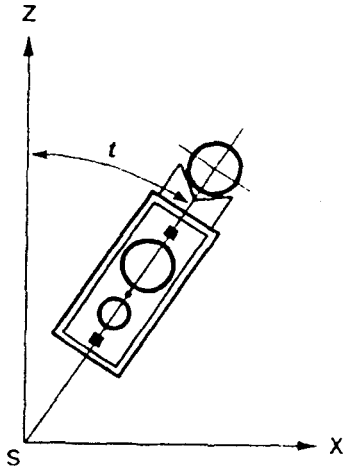

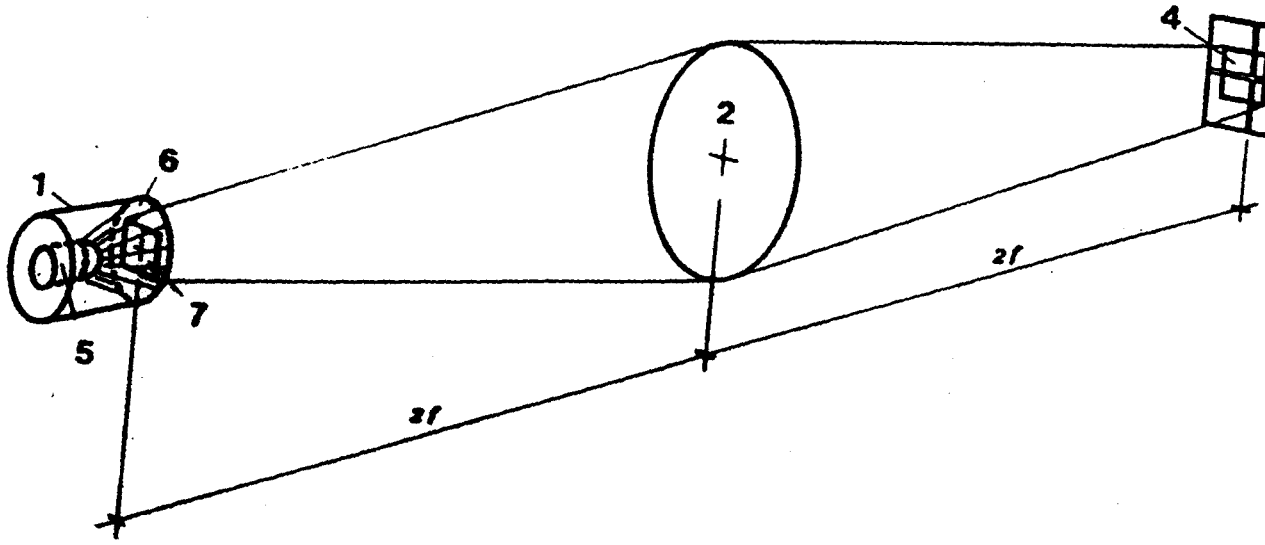

1 Emetteur
- *5* Source de lumière
- *6* Verre dépoli plus cache
- *7* Objet lumineux

2 Lentille

3 Récepteur
4 Image

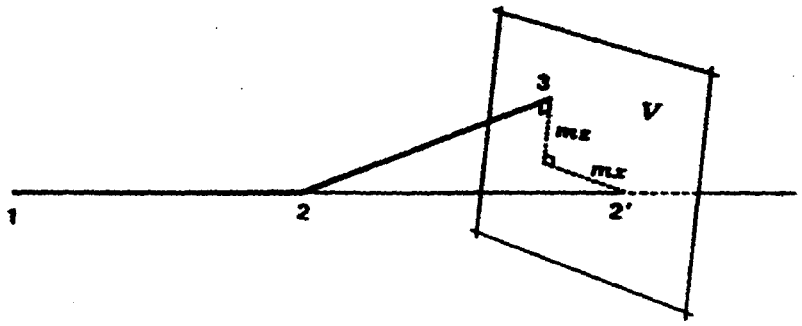

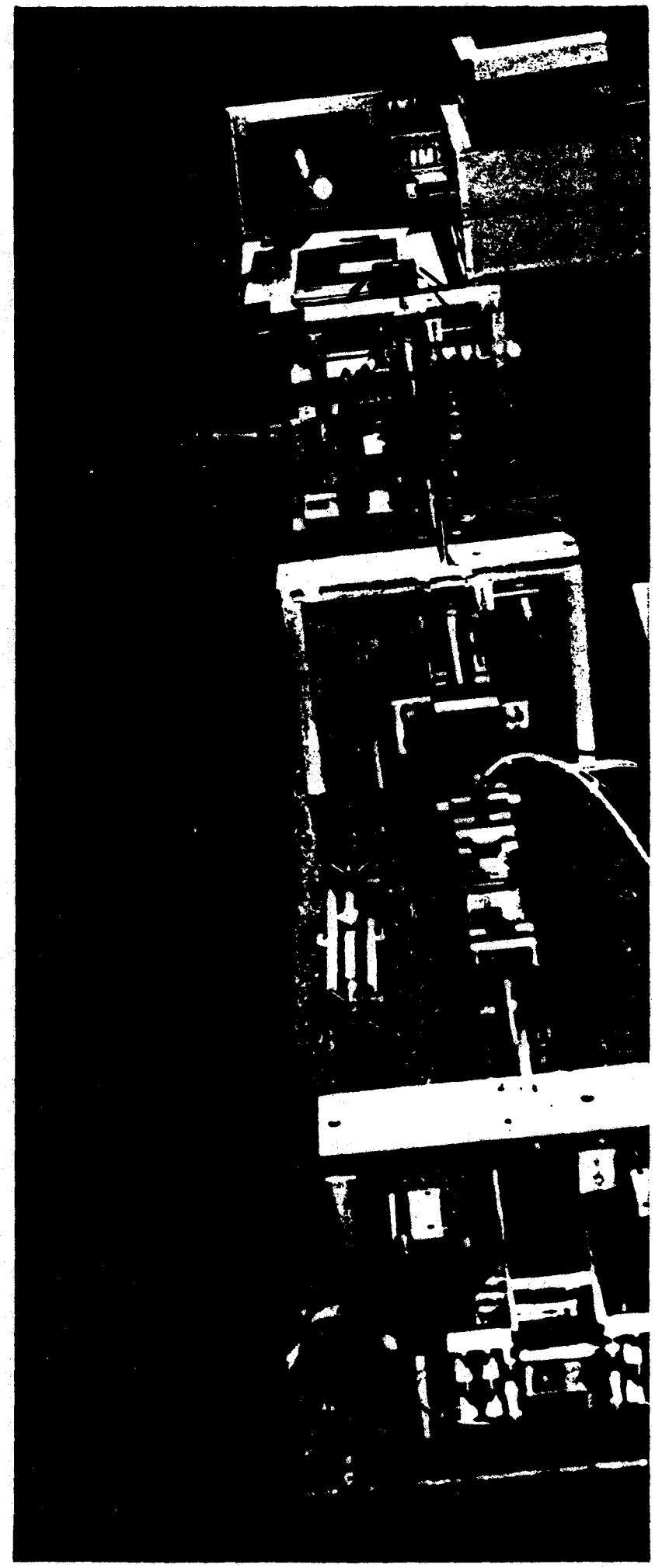

3M

3M Flip-Frame
Transparency Protector

Layout of measurements

- La partie centrale inclut toutes les quad. low Beta et l'expérience.
- Méthode optique pour la partie centrale. (minimum 4 zone plates pour les quad.) + 2 zone plates pour l'expérience.
- Recouvrement de la zone des quadrupoles par des fils.
- Positionnement des fils par rapport aux zone plates.
- Mesure des low Beta quad. par rapport aux fils.
- ~~Traitement des mesures~~ Possibilité de mesures horiz et verticales.
- Installation à demeure.
- Commande à distance.

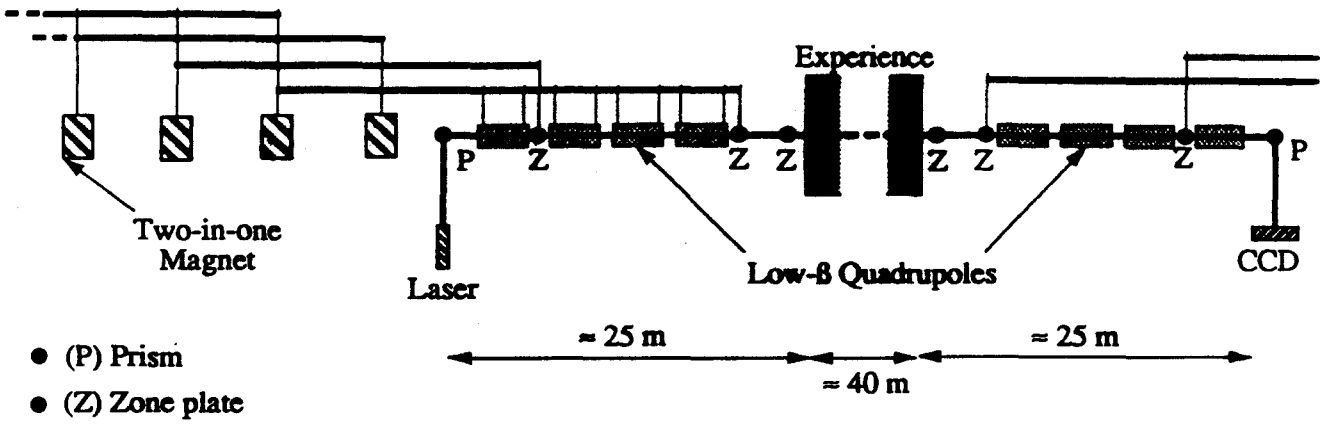

LAYOUT OF MEASUREMENTS

On connait parfaitement la position du Zéro de la vis de la lentille diffractive par rapport :

- au faisceau de protons
- au zéro des capteurs de fils et à la mire externe.

- La lentille diffractive (Zone plate), est escamotable. Positionnement à distance.

- Ensemble à inserrer dans le layout de la machine.

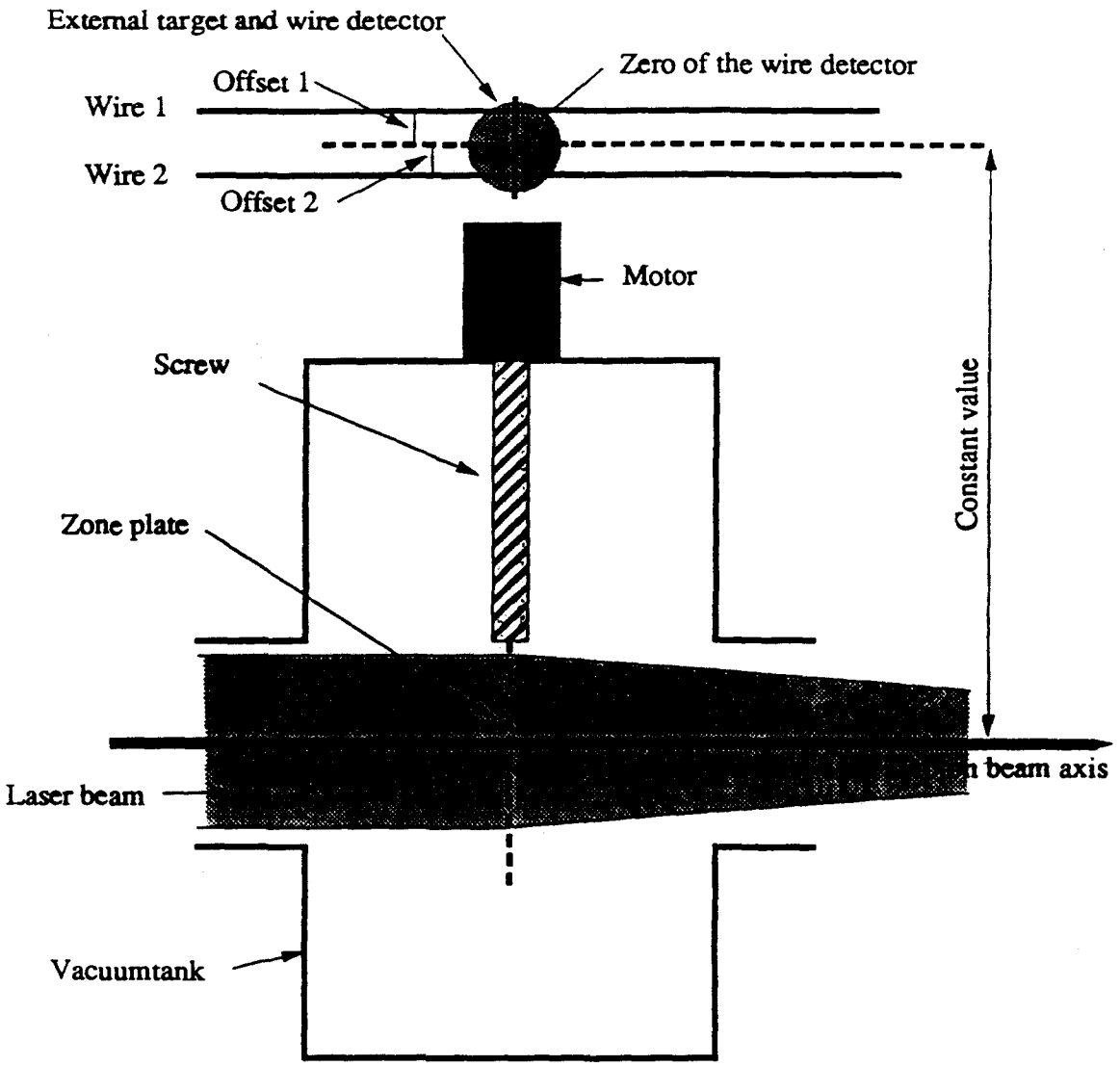

LASER AND WIRE DETECTOR

300mm
300mm
100mm
300mm

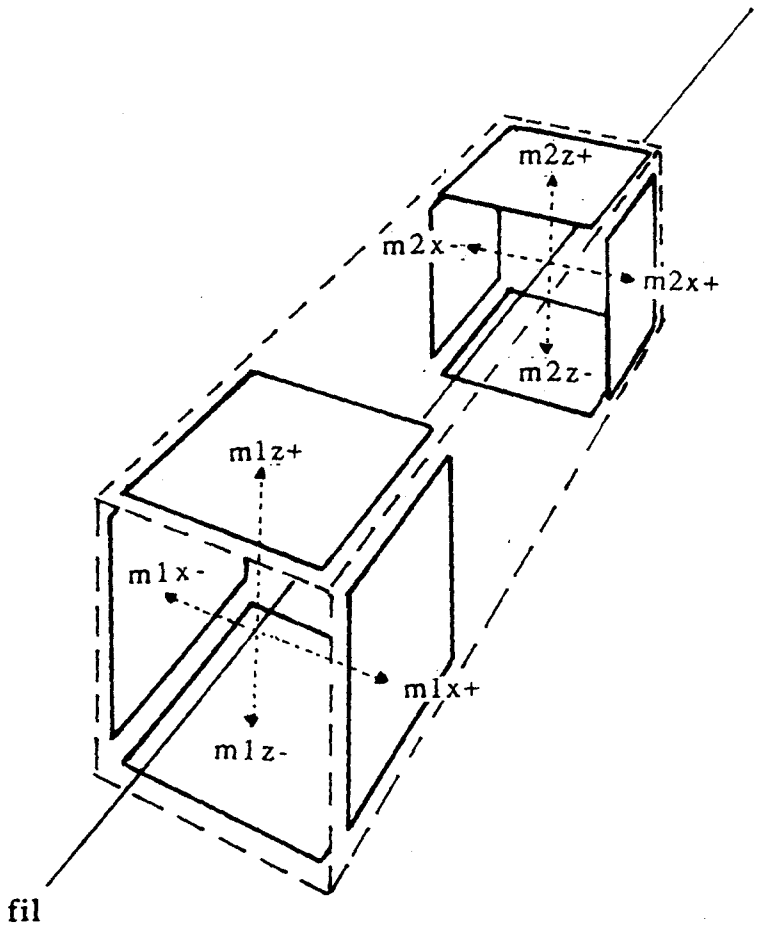
m2z+
m2x-
m2x+
m2z-
m1z+
m1x-
m1x+
m1z-
fil

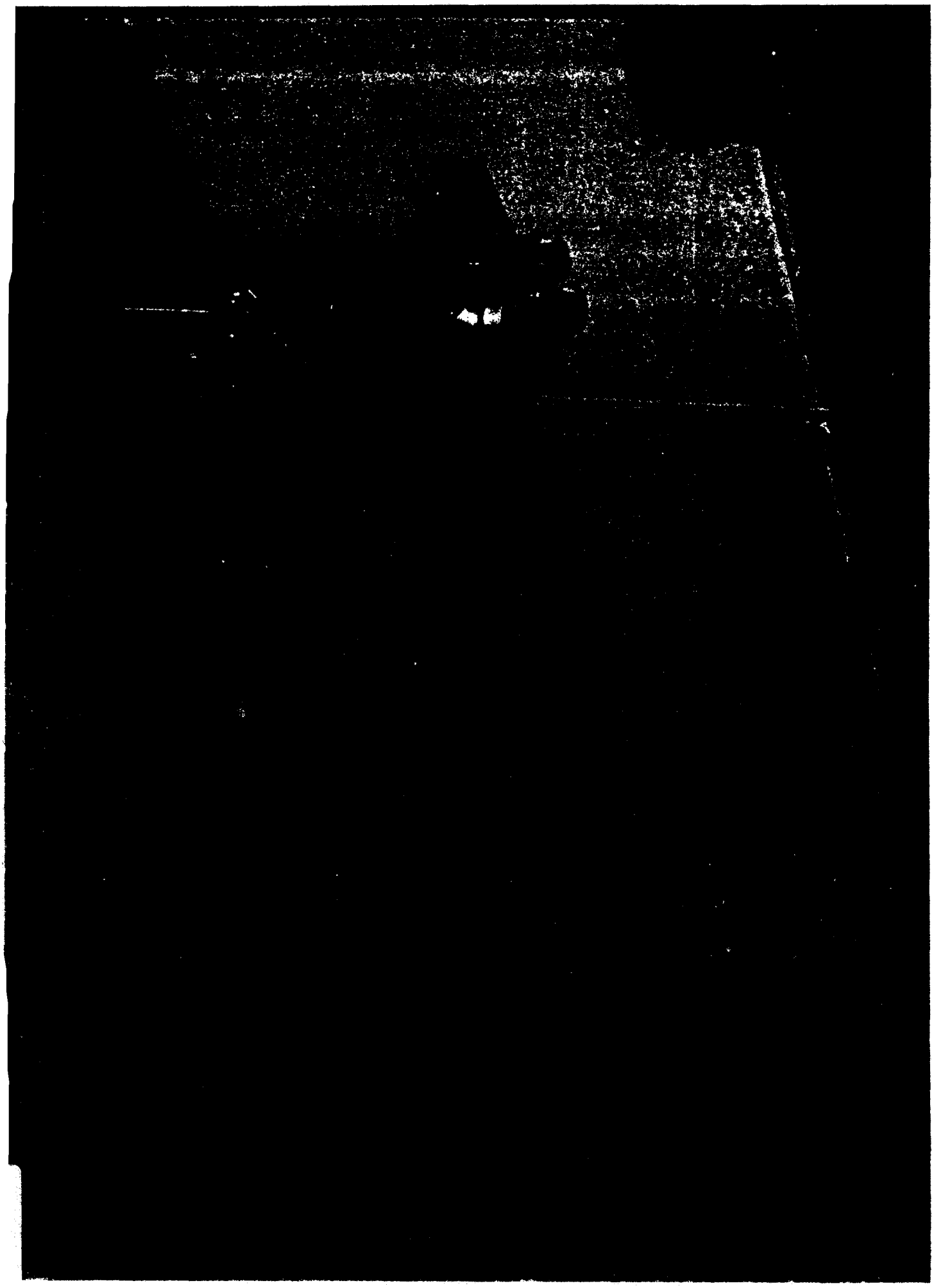

FOGALE nanotech

La mesure SANS CONTACT, précise et rapide

HYDROSTATIC LEVELLING SYSTEM (H.L.S.)

H.L.S. are designed for continously measuring - without contact - vertical positions of each sensor with respect to the horizontal place defined by the water surface : vessels are communicating and water levels are equal because air pressure is the same for all vessels, whatever the local atmospheric pressure (vessels can be several km apart).

Water surface is very well sensed by capacitance-based sensing because water is a good enough electrical conductor.

Sensors have an excellent long term dimensional stability because they useglass-metal sealing technology ; sensors also are fully waterproof.

SPECIFICATIONS OF H.L.S. SENSOR

	ESRF Specs.	other possible sets of specs.	
- range of measurement :	2,5 mm	7 mm	15 mm
- frontal distance between sensor and water level :	6 at 8,5 mm	5 to 12 mm	5 to 20 mm
- output voltage (differential output) :	0 V. at 6 mm 10 V. at 8,5 mm	0 V. at 5 mm 10 V. at12 mm	0 V. at 5 mm 10 V. at 20 mm
- band width :	0 - 10 Hz	0 - 1 Hz	
- resolution :	0,1 µm	0,1 µm	± 0,3 µm
- analogic linearity :	± 3 µm	± 4 µm	± 10 µm
- linearity after numerical correction :	± 0,2 µm	± 0,5 µm	± 1 µm

SPECIFICATIONS OF THE PT 100 THERMOMETER

- range of measurement : 25° C, with output voltages (non differential) : 0 Volt for 10° C ; 10 V for 35° C
- sensitivity of measure : 40 mV for 0,1° C
- absolute error : ≤ ± 0,5° C
- relative error : ≤ ± 0,1° C

SCHEMATIC DRAWING OF H.L.S.

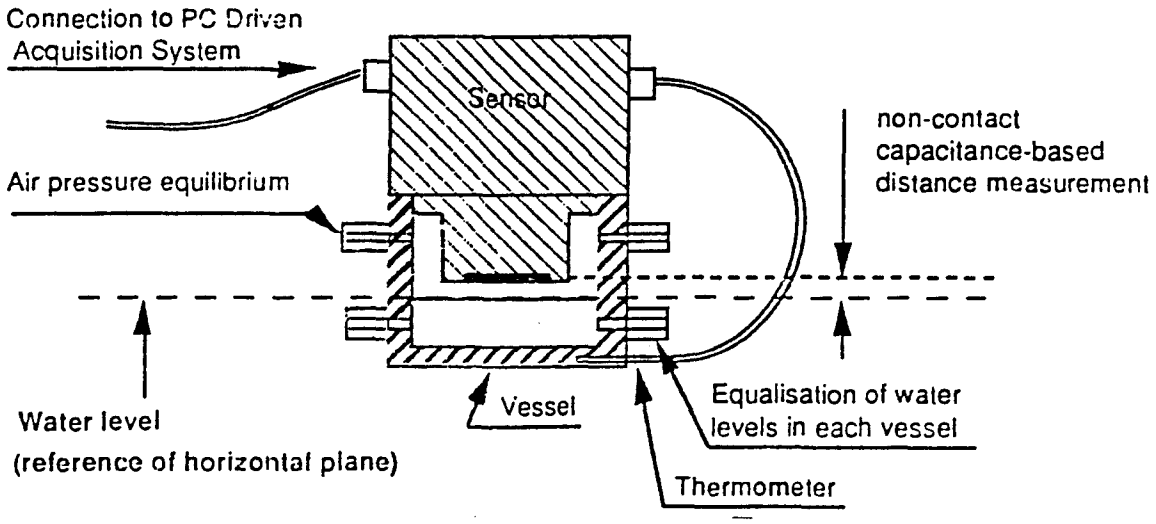

Index 08. représentation 1

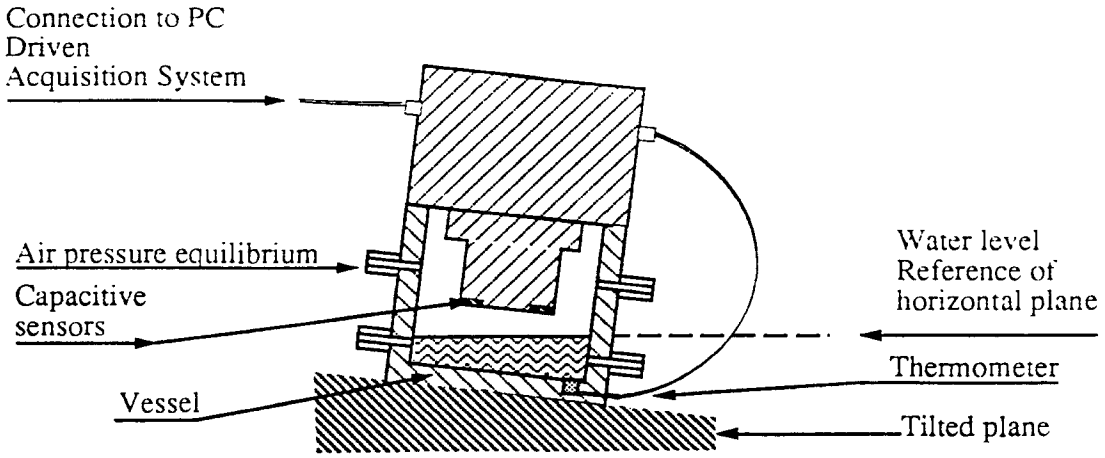

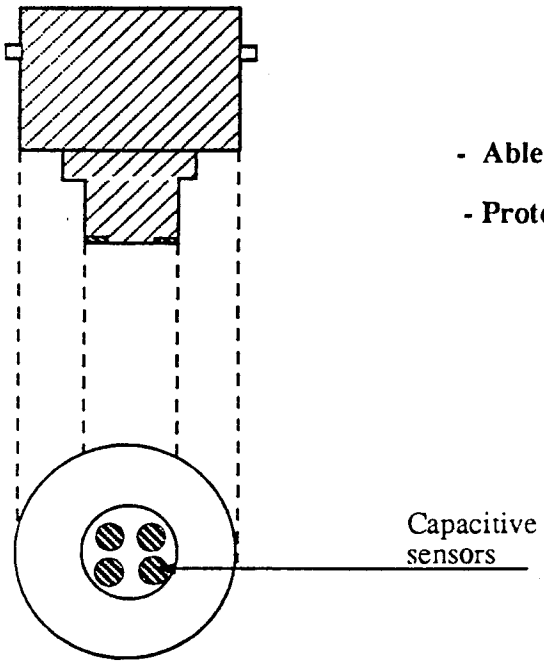

- **Able to measure heights and angular parameters (tilt, slope)**
- **Prototype with 5 sensors, to be tested soon**

CERN / FOGALE NANOTECH "ALTICLINOMETER"

ECARTOMETRE CAPACITIF

- dimensions 9 x 4 x 4 cm
  capteur = 1 cm x 1 cm
  résolution = 1 µm = 1.3 mV ⇒
  fait pour qq 1/100e
  ≤ 0.1 µm dans autres contextes (jusqu'à 0.0
- sur 15 cm = RAS (ni dérive, ni fluctuation)
- capteur capacitif – passif, sans électronique
  sans courant – fil à la masse

fil =
- 132 m r = 0.1 mm d = 7.65 ⇒ pV = 7.65 kg
- tension 4 kg E ≈ 18000 (au lieu de 21000)
- A = 0.0342 mm² p.l = 0.240 g/m
- allong° 4 kg ⇒ 0.96 m (96 cm)
- fréquence propre ≈ 1.2 Hz
- flèche = 0.128 m

acier
tungstène
trop rigide !
nivaflex ?
beryllium ?

idée =
- fixer sous tension
- contrôler tension par mesure fréquence
- mesurer température et calculer variation
- vérifier cohérence

Kinematic Cam Positioning Mounts

Gordon Bowden, SLAC

SLC - The first 2 beam high energy physics accelerator to collide 5μ beams required remote positioning mounts for the final focusing quadrupole triplets.

Desirable Features

- Micron positioning resolution.
- Distortion free support - no bending moments, tensions or compressions transmitted to the pre-aligned triplet of quadrupoles.
- High stiffness to avoid μseismic amplification - no long struts.
- Heavy load positioning capabilties - 6 tons.
- Fail safe - bounded excursions, no limit switches required.
- Power off position stability - no holding voltages or currents required.
- Compact and cheap.

Features **Not** Required

- Fast dynamic response - minutes are good enough for adjustment of magnet position.
- Precise linear orthogonal response - beam guided iterative adjustment requires only simple relative shifts in position. Lack of orthogonal motions is no problem for computer control.
- Large ratio of $\frac{range}{resolution}$ not needed - $\frac{1\ \mathrm{mm}}{1\ \mu\mathrm{m}}$ is sufficient to bridge the gap between installation alignment and operation.

Kinematic Mounts -Lord Kelvin, 1880's

Standard Static Layout

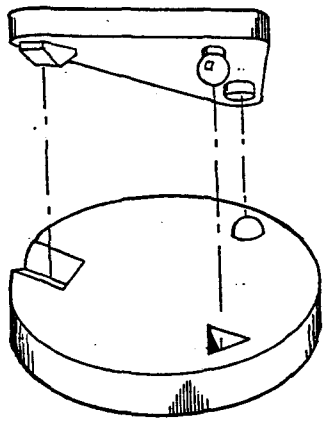

- $x, y, x, \phi, \theta, \psi$
- 6 degrees of freedom
- 6 contact points
- distortion free - no over constraint

Adjustable Cam Support

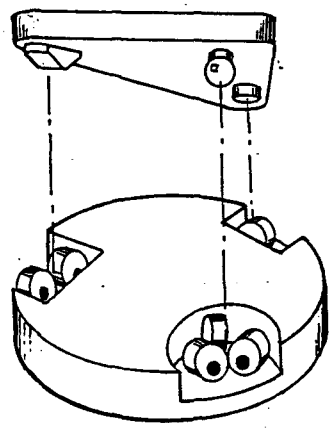

- 6 rotatable cams
- limited positioning
- backlash loaded out by gravity

Cam Roller Bearing Support

backlash free pure rolling motion

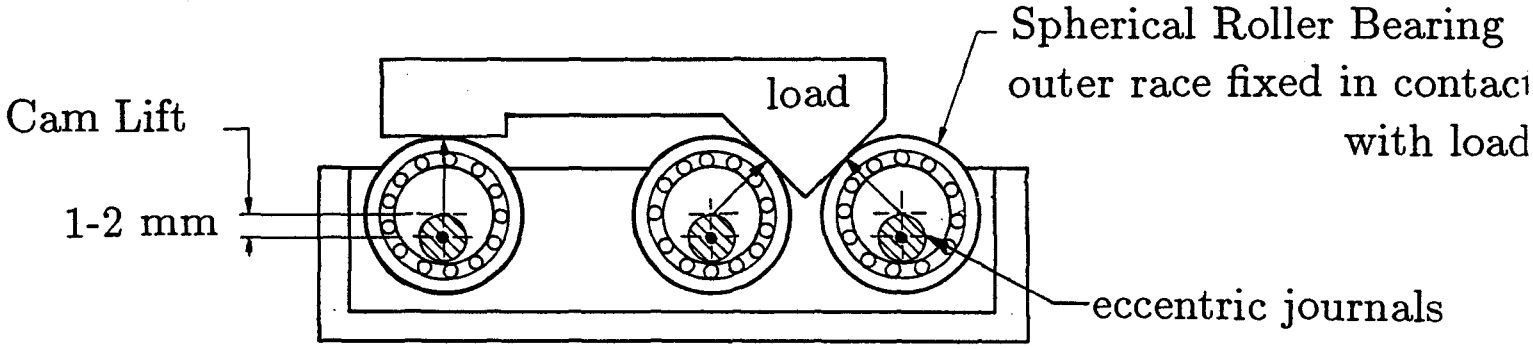

SLC Final Triplets

1985

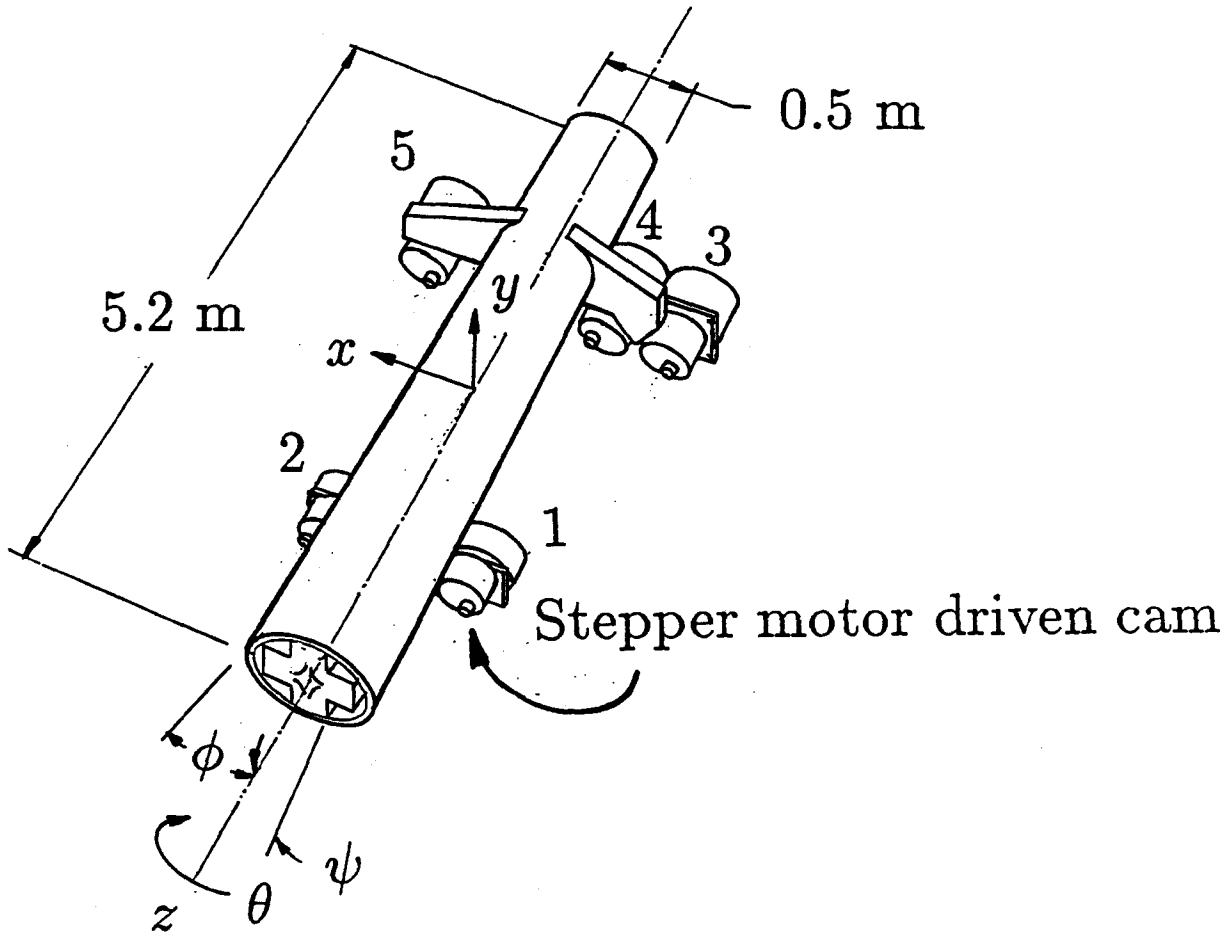

- Length 17 ft, weight 6 tons.
- 5 axis positioning in x, y, roll, pitch and yaw.
- Z position restrained by shoe grip on cam #3.
- Cam lift 1.5 mm (.062 in)
- Positioning drive by 18°,10 in-lb steppers through 650:1 planet and worm reduction.
- Position resolution better than 5 μm using cam shaft potentiometers.

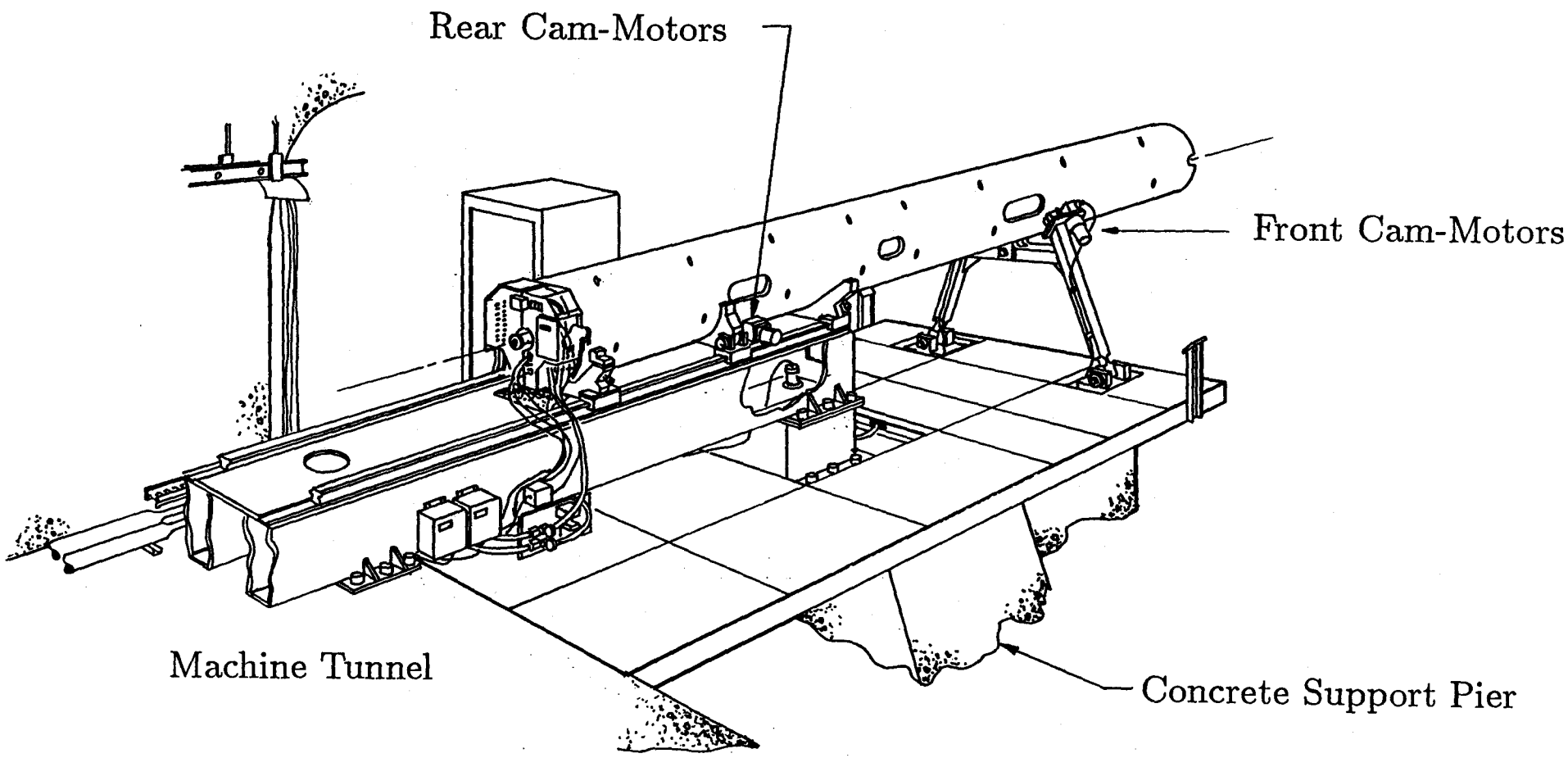

SLC Quad Triplet Support

1987

FRONT

FRONT

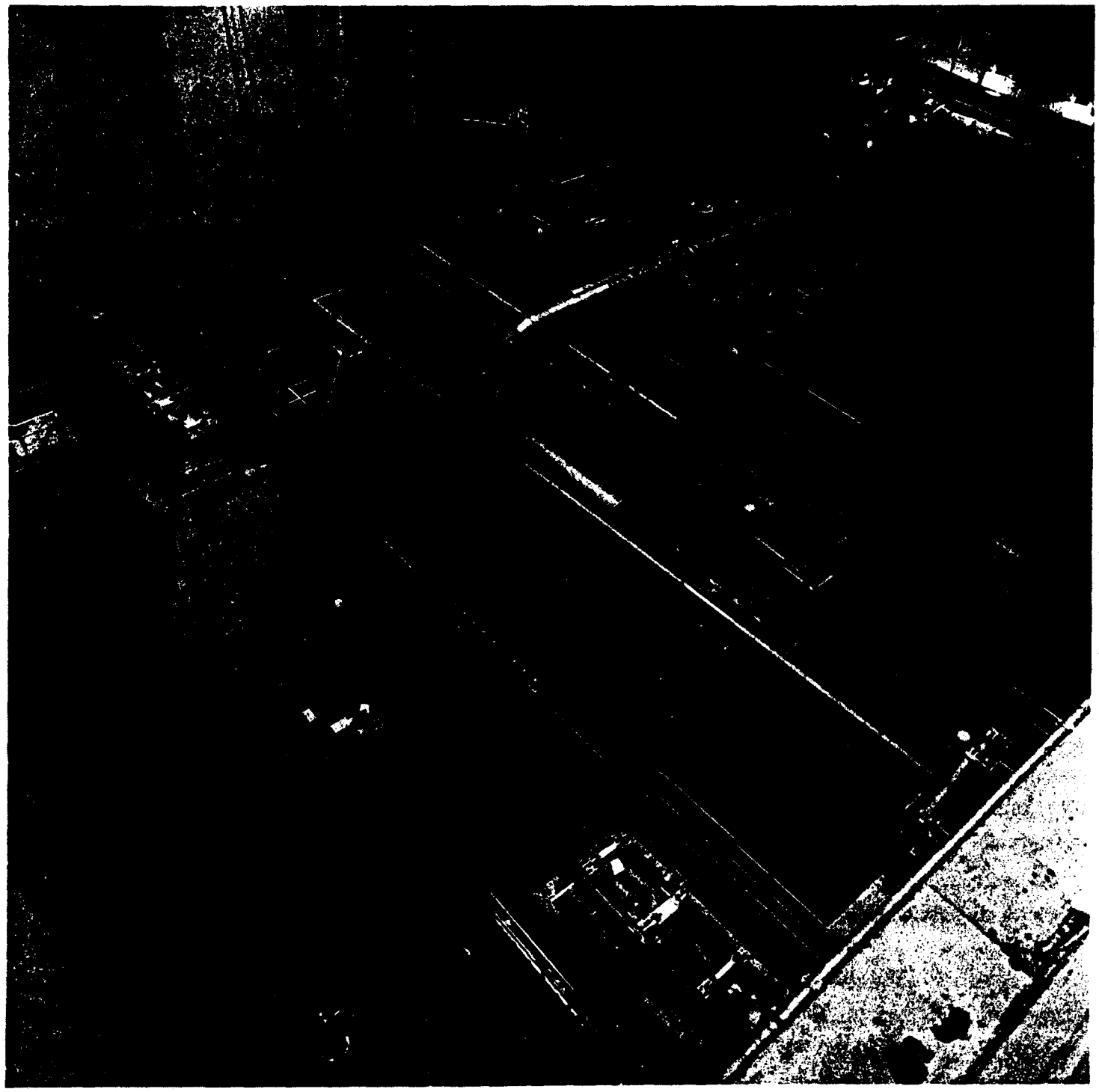

FRONT

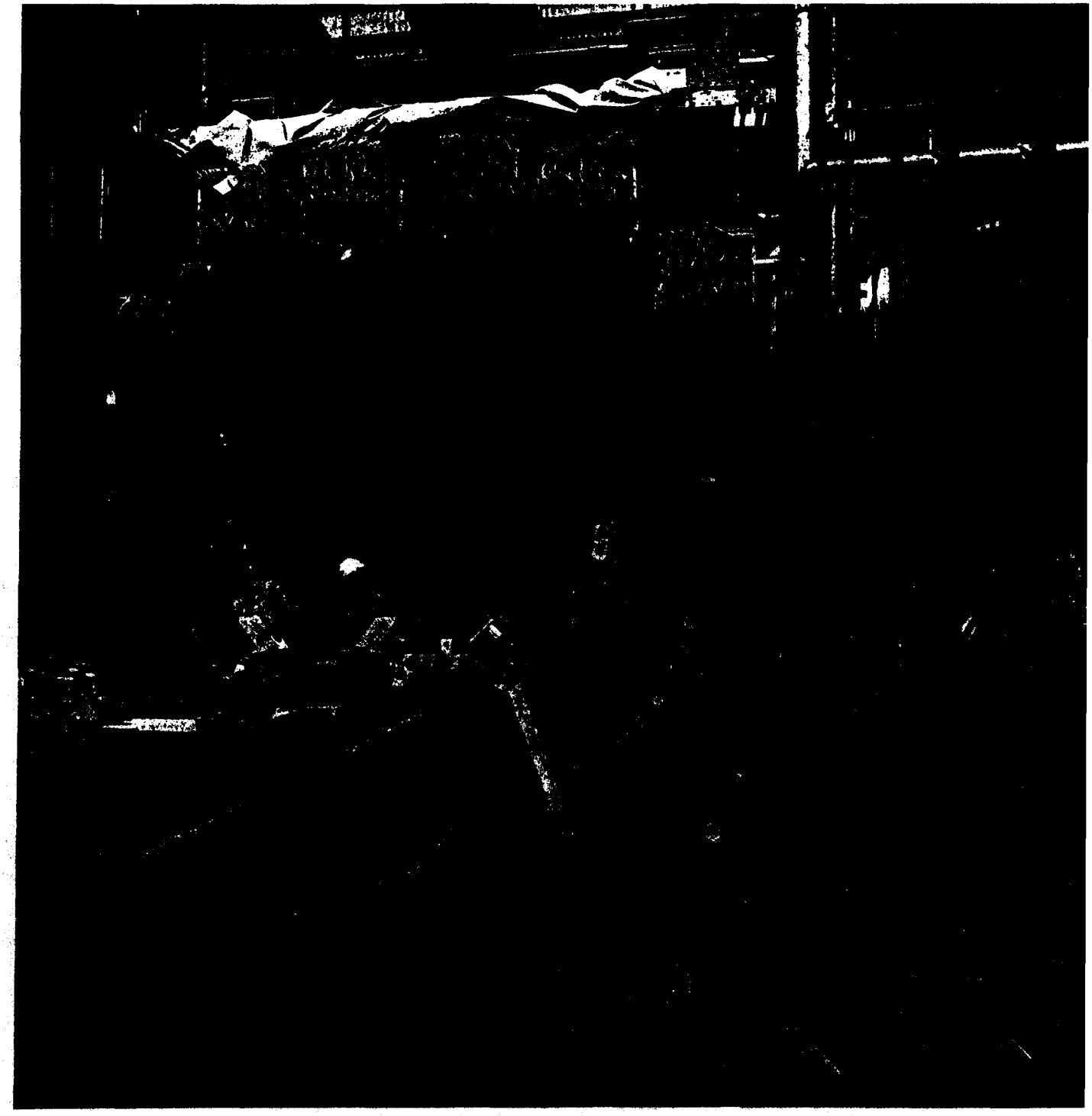

Position Algorithms

- Transform from position to desired cam angles is a a 3 step process.

$$\begin{bmatrix} x \\ y \\ \phi \\ \theta \\ \alpha \end{bmatrix} \xrightarrow{A} \begin{bmatrix} x_1 \\ y_1 \\ x_2 \\ y_2 \\ \alpha \end{bmatrix} \xrightarrow{B} \begin{bmatrix} x_1' \\ y_1' \\ x_3 \\ y_3 \\ \alpha \end{bmatrix} \xrightarrow{C} \begin{bmatrix} \theta_1 \\ \theta_2 \\ \theta_3 \\ \theta_4 \\ \theta_5 \end{bmatrix}$$

- Transformation is neither linear or orthogonal
- Simple 2 dimenstional projections of the triplet axis through support planes reduces problem to 2 dimensional trigonometry - an accurate approximation for long support barrels with small pitch and yaw.

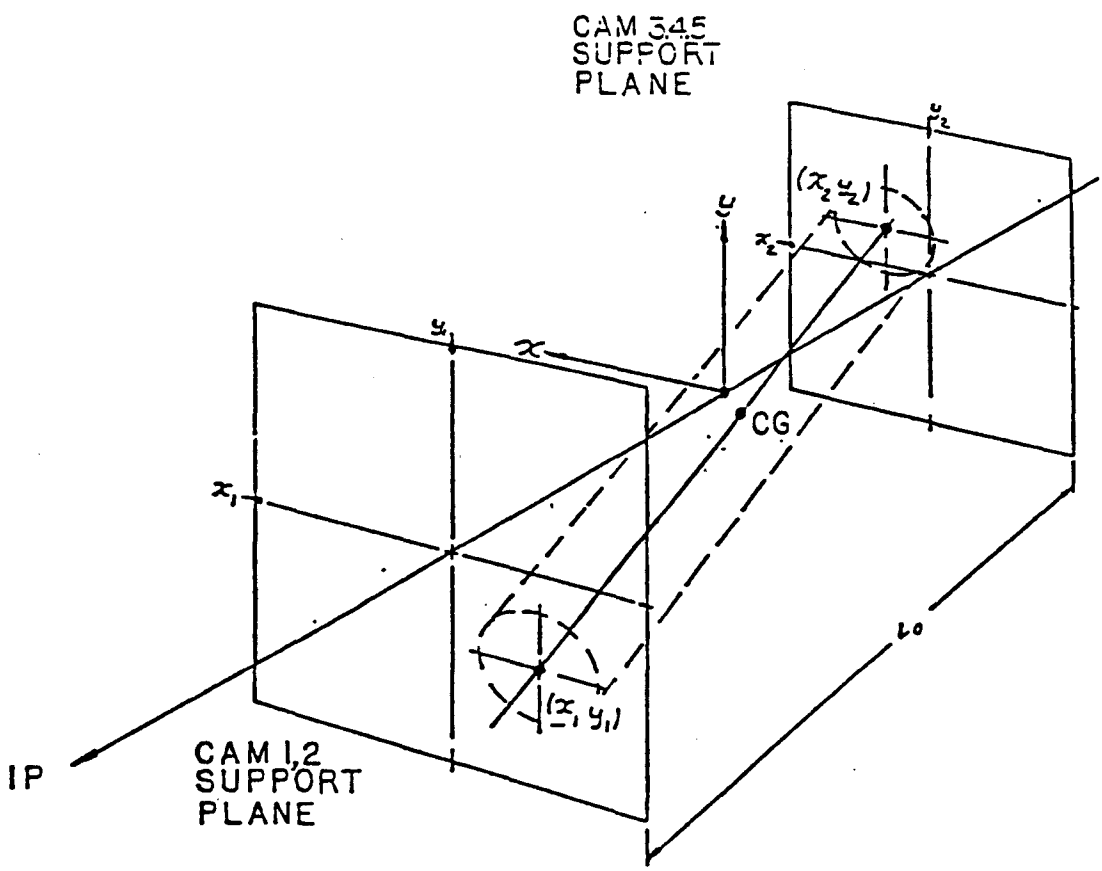

Cam Positioning Geometry

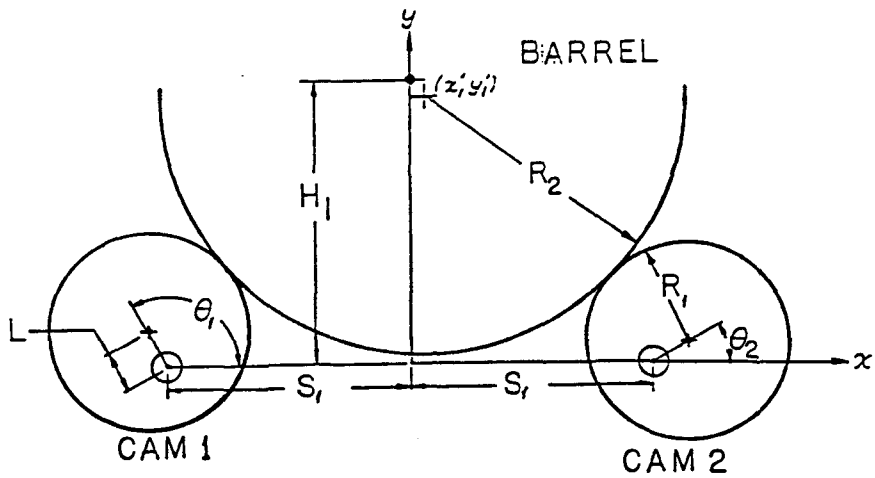

Front Support Geometry

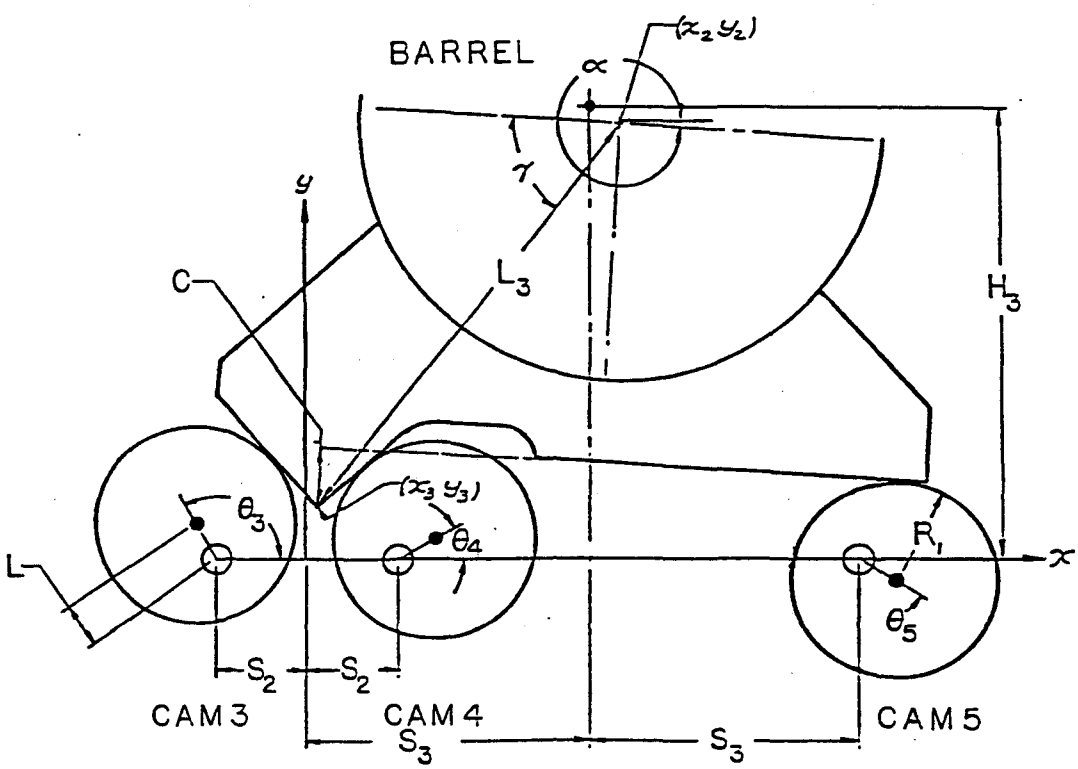

Rear Support Geometry

Shaft Angle Equations

$$\theta_i = \sin^{-1}\left(\frac{c_i}{d_i}\right) - \tan^{-1}\left(\frac{a_i}{b_i}\right)$$

$$\text{where} \qquad d_i = \sqrt{a_i^2 + b_i^2}$$

	a_i	b_i	c_i
θ_1	$-2L(S_1 + x_1')$	$-2y_1'L$	$(R_1+R_2)^2 - L^2 - S_1^2 - 2x_1'S_1 - x_i'^2 - y_1'^2$
θ_2	$2L(S_1 - x_1')$	$-2y_1'L$	$(R_1+R_2)^2 - L^2 - S_1^2 + 2x_1'S_1 - x_1'^2 - y_1'^2$
θ_3	$\sin(\alpha + \frac{3\pi}{4})$	$-\cos(\alpha + \frac{3\pi}{4})$	$\frac{1}{L}\left[(S_2 + x_3 - \frac{y_3}{m_3})\sin(\frac{\pi}{4} - \alpha) - R_1\right]$
θ_4	$-\sin(\alpha + \frac{\pi}{4})$	$\cos(\alpha + \frac{\pi}{4})$	$\frac{1}{L}\left[(S_2 - x_3 + \frac{y_3}{m_3})\sin(\alpha + \frac{\pi}{4}) - R_1\right]$
θ_5	$-\sin\alpha$	$\cos\alpha$	$\frac{1}{L}\left[H_4\sin(\alpha+\beta) - R_1\right]$

$$m_4 = \tan(\alpha + \tfrac{\pi}{4}) \tag{10}$$

$$m_3 = \tan(\alpha - \tfrac{\pi}{4}) \tag{11}$$

$$\beta = Arc\tan\left(\frac{y_3 + C\cos\alpha}{2S_3 - x_3 + C\sin\alpha}\right) \tag{12}$$

$$H_4 = \left[(y_3 + C\cos\alpha)^2 + (2S_3 - x_3 + C\sin\alpha)^2\right]^{1/2} \tag{13}$$

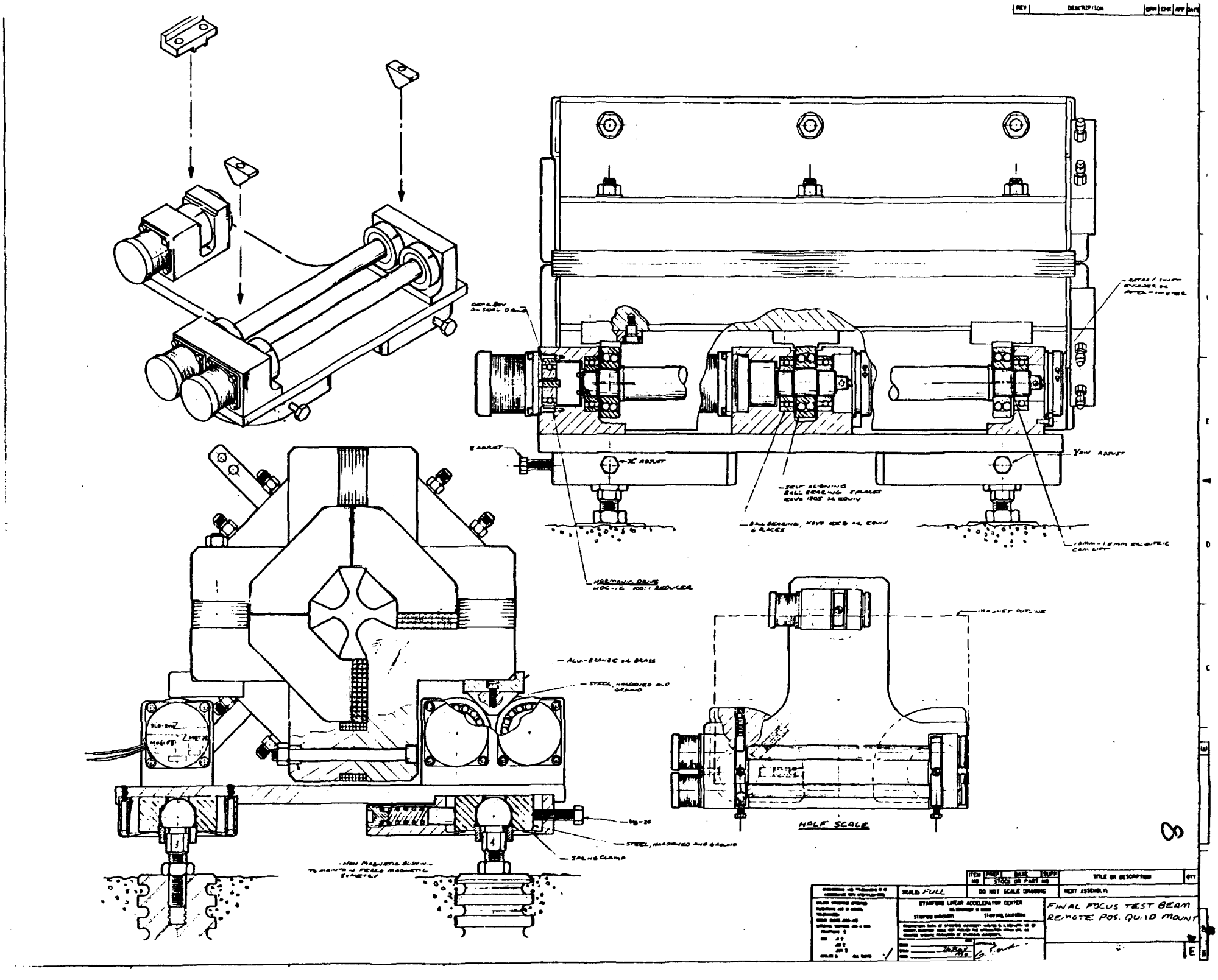
REV
DESCRIPTION
Y ADJUST
X ADJUST
YAW ADJUST
SELF ALIGNING BALL BEARING FRAMES
BALL BEARING, KEYS
HARMONIC DRIVE
ALU-BRONZE VS BRASS
STEEL, HARDENED AND GROUND
STEEL, HARDENED AND GROUND
SPLINE CLAMP
HALF SCALE
ITEM NO
PART NO
STOCK OR PART NO
TITLE OR DESCRIPTION
QTY
SCALE FULL
DO NOT SCALE DRAWING
NEXT ASSEMBLY
STANFORD LINEAR ACCELERATOR CENTER
STANFORD UNIVERSITY
STANFORD, CALIFORNIA
FINAL FOCUS TEST BEAM
REMOTE POS. QUAD MOUNT
8

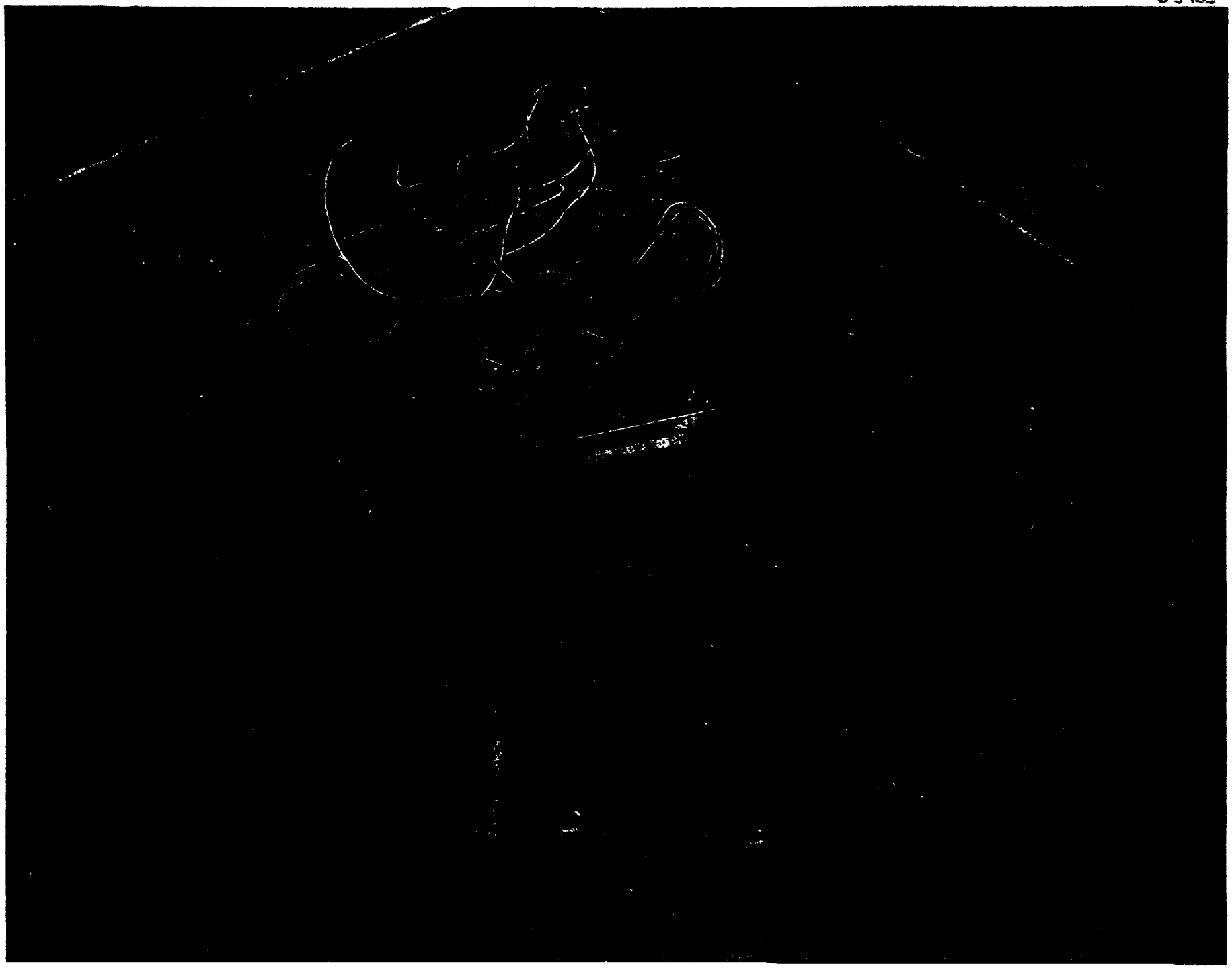

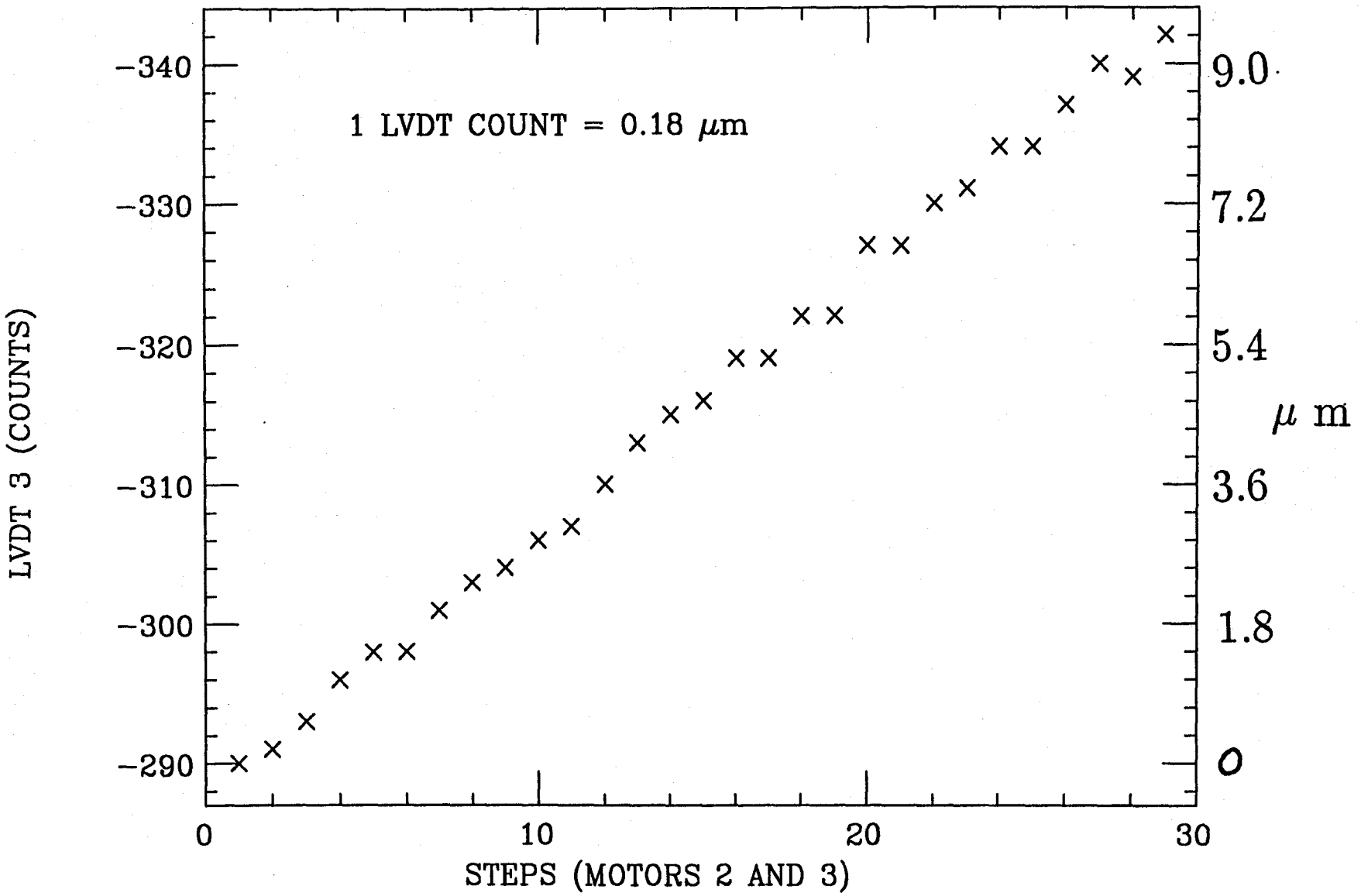
1 LVDT COUNT = 0.18 μm
LVDT 3 (COUNTS)
−340
−330
−320
−310
−300
−290
9.0
7.2
5.4
3.6
1.8
0
μ m
0
10
20
30
STEPS (MOTORS 2 AND 3)

Summary

- Design is fully kinematic and free from play.
- No backlash- all drives are gravity loaded.
- Cam's cyclic motion has natural limits. No stops are needed.
- Design easily carries heavy loads
- Loads are translated by pure rolling motion with low hysteresis. Resolution is better than 1μ m in 1 mm.
- Concept is easily adapted to a broad range of magnet dimensions and positioning requirements.
- Standard roller bearings are precision components at a low price.
- The required control programs are easily integrated into a modern accelerator control system.

ILSE Alignment

Induction Systems Experiments
Conceptual Design Report Engineering Review
Lawrence Berkeley Laboratory

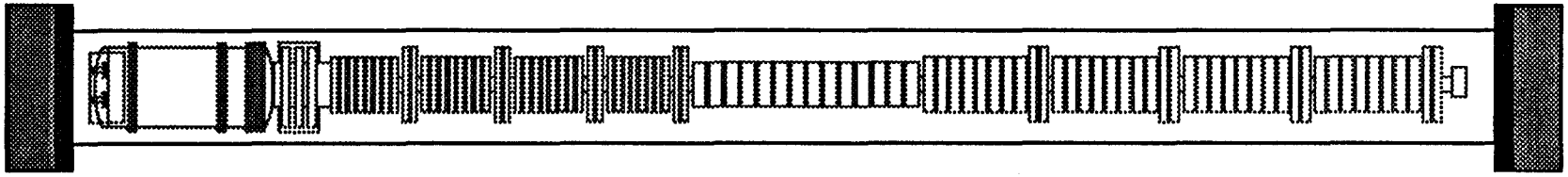

presented February 12, 1992 at the

Workshop on
Vibrational Control and Dynamic
Alignment Issues at the SSC

Lee Griffith
Lawrence Livermore National Laboratory

with major contributions from
Fred Deadrick LLNL
Martin Fong LBL
and Craig Peters LBL

The purpose of this talk is to explain the alignment concept and describe the key operative features

- What is the concept
- How do we identify the field axes
- How is the field axis related to the reference axis
- What are the key features of the calibration table
- How are electrostatic components aligned
- How are magnetic components aligned
- How are diagnostics aligned
- Can we achieve the tolerances
- What will it cost

The parallel wire alignment scheme will interface with a similar system for the bend and drift section

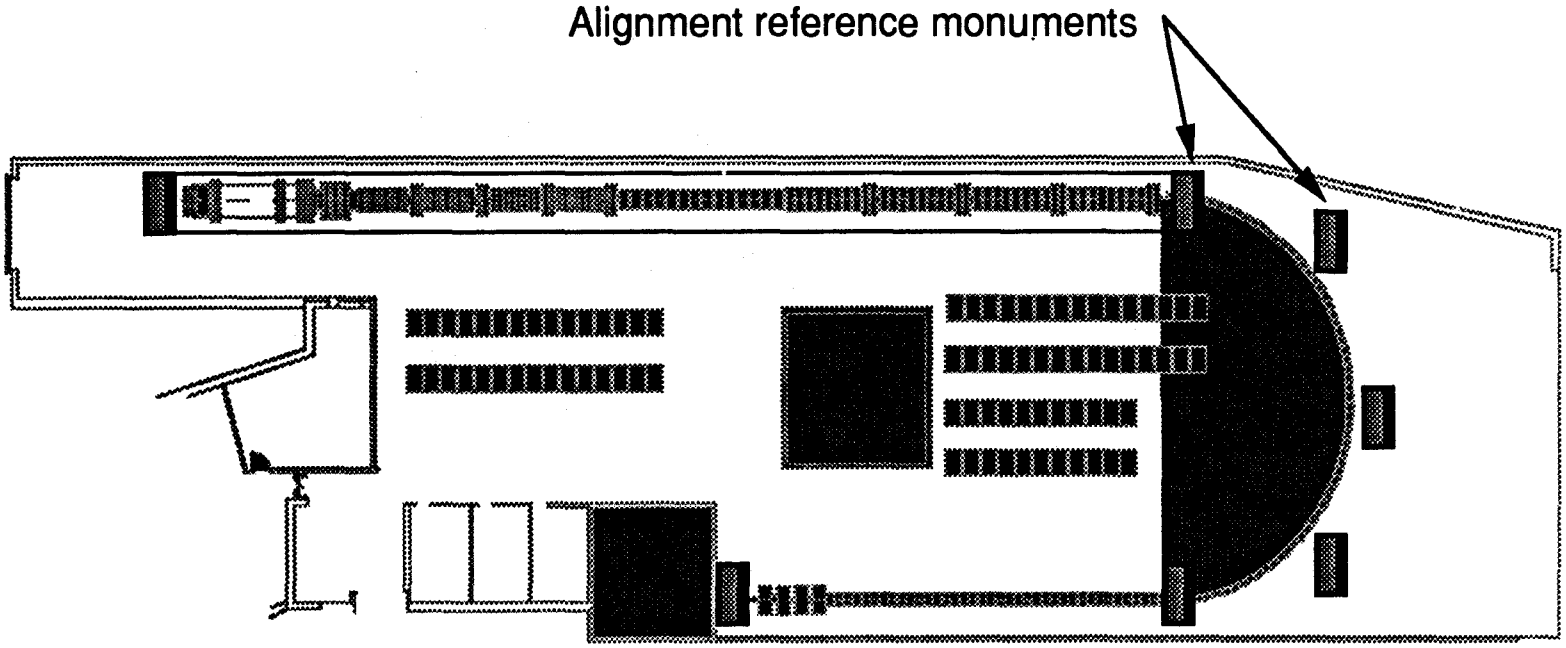

Offset measurements from the fiducials to the field axis are crucial

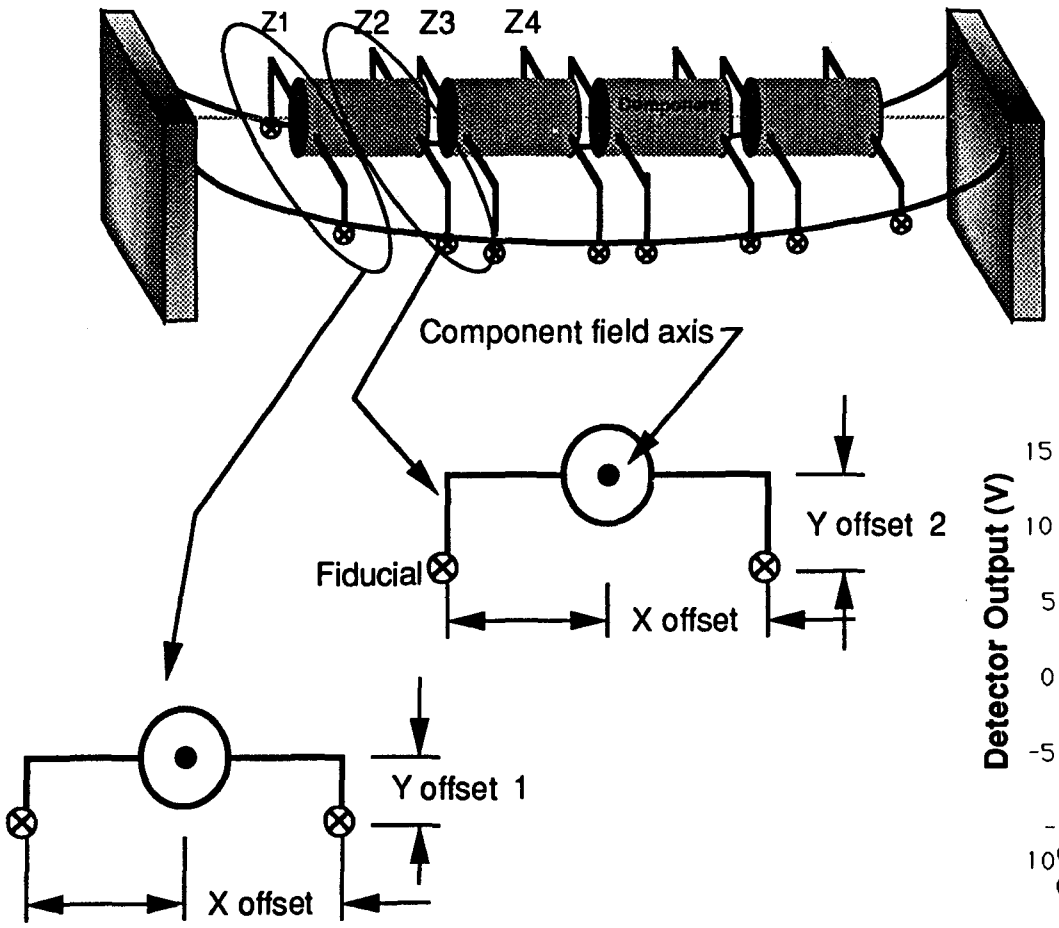

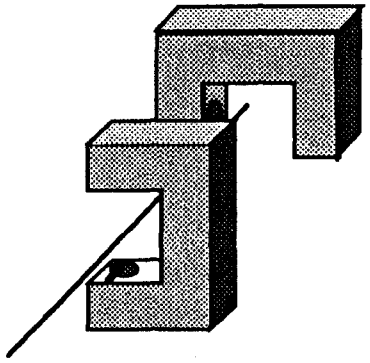

Fiducials are photoelectric proximity switches (PEPS)

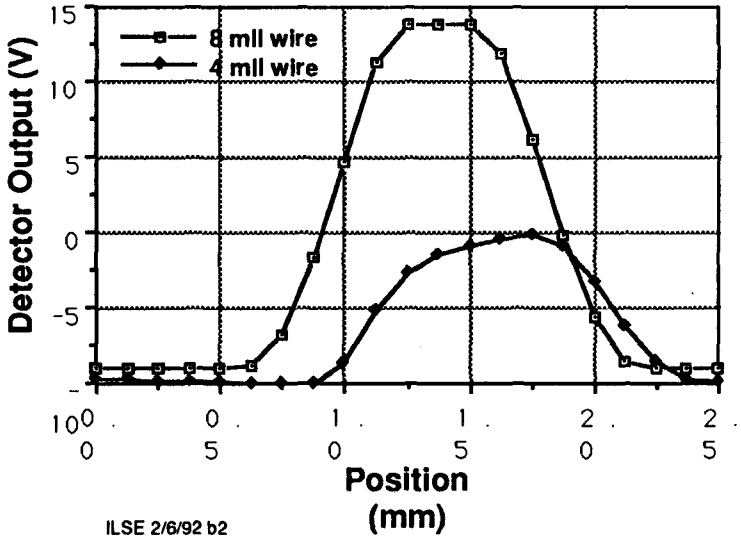

ILSE 2/6/92 b2

Each accelerator component, as well as modules of components, is aligned relative to two parallel wires

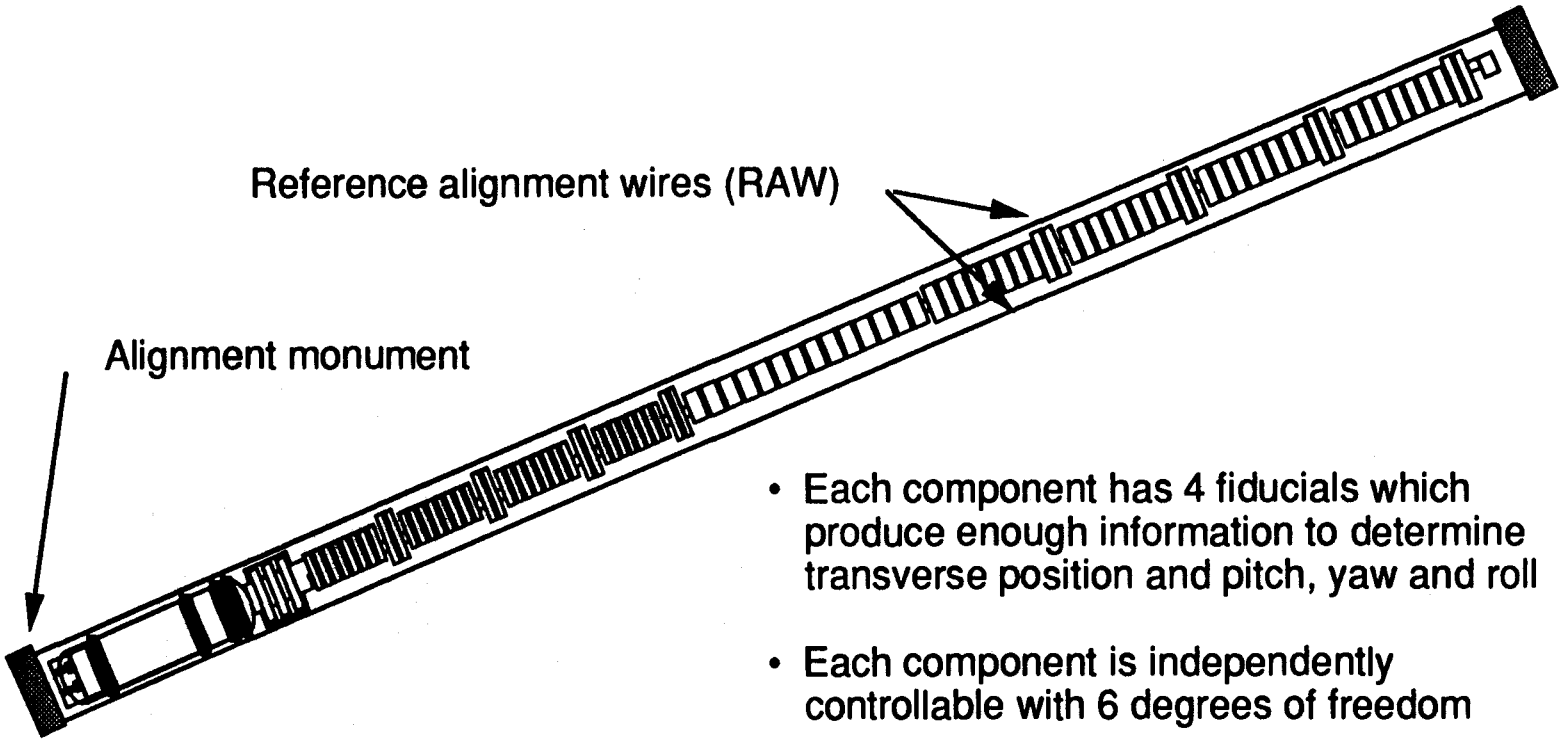

- Each component has 4 fiducials which produce enough information to determine transverse position and pitch, yaw and roll
- Each component is independently controllable with 6 degrees of freedom
- Each module of components is automatically controlled on 5 axes with feedback from 4 fiducials

The injector is internally aligned via mechanical tolerances and the beam axis is optically identified with the aid of a template

- The injector alignment is determined by the machining tolerances of the field plates.
- The field plates are assembled on steel rods, which protrude from each end.
- Templates, with optical fiducials, are fitted onto the steel rods at the beginning and end

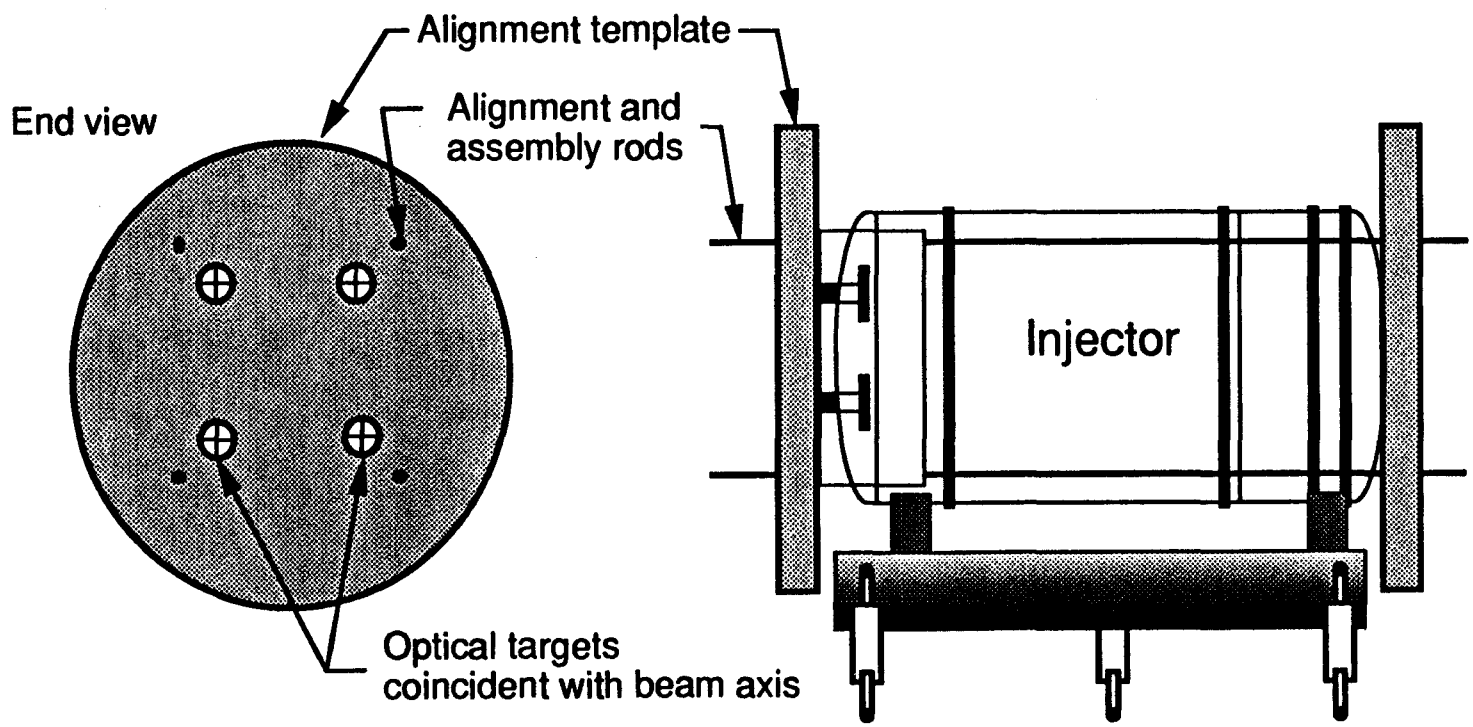

ILSE 1/25/92 f

A calibration and assembly table allows the field centerline to be related to external fiducials

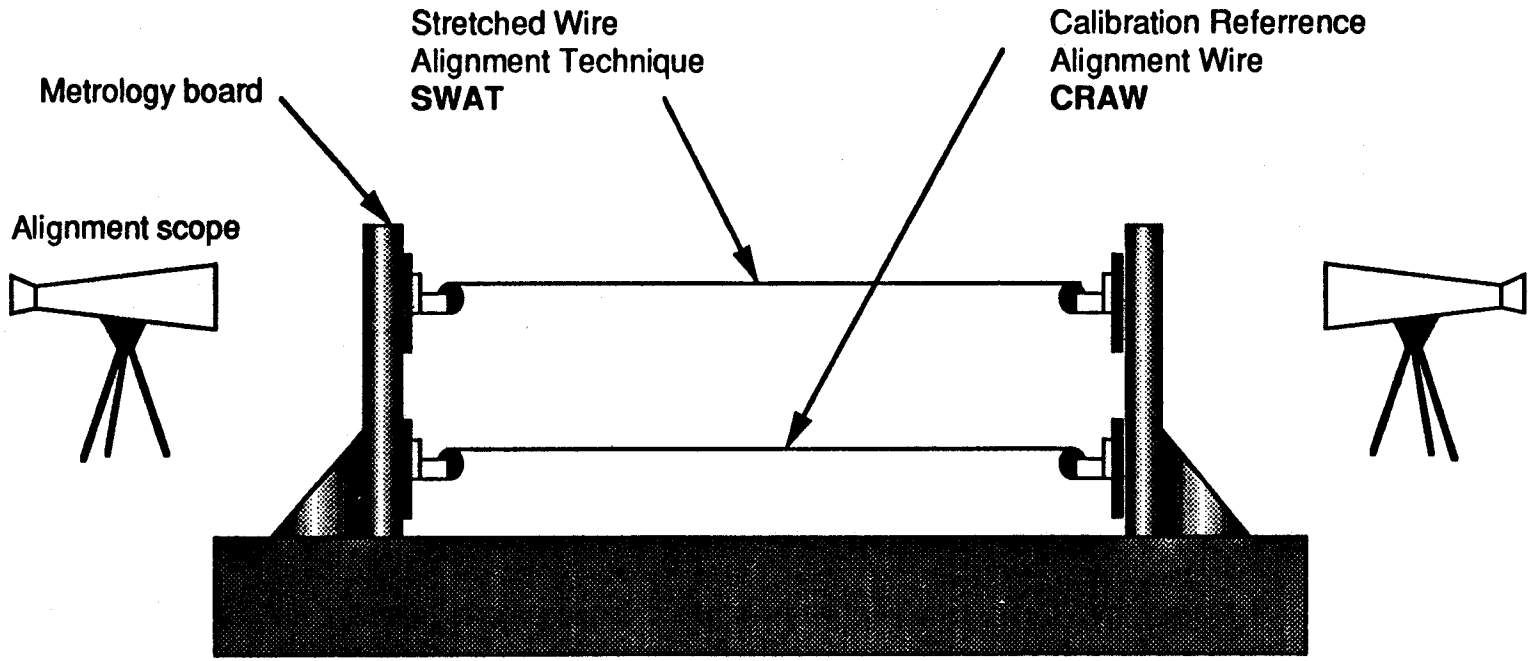

The metrology board has several measurement features to relate field axis to the external reference axis

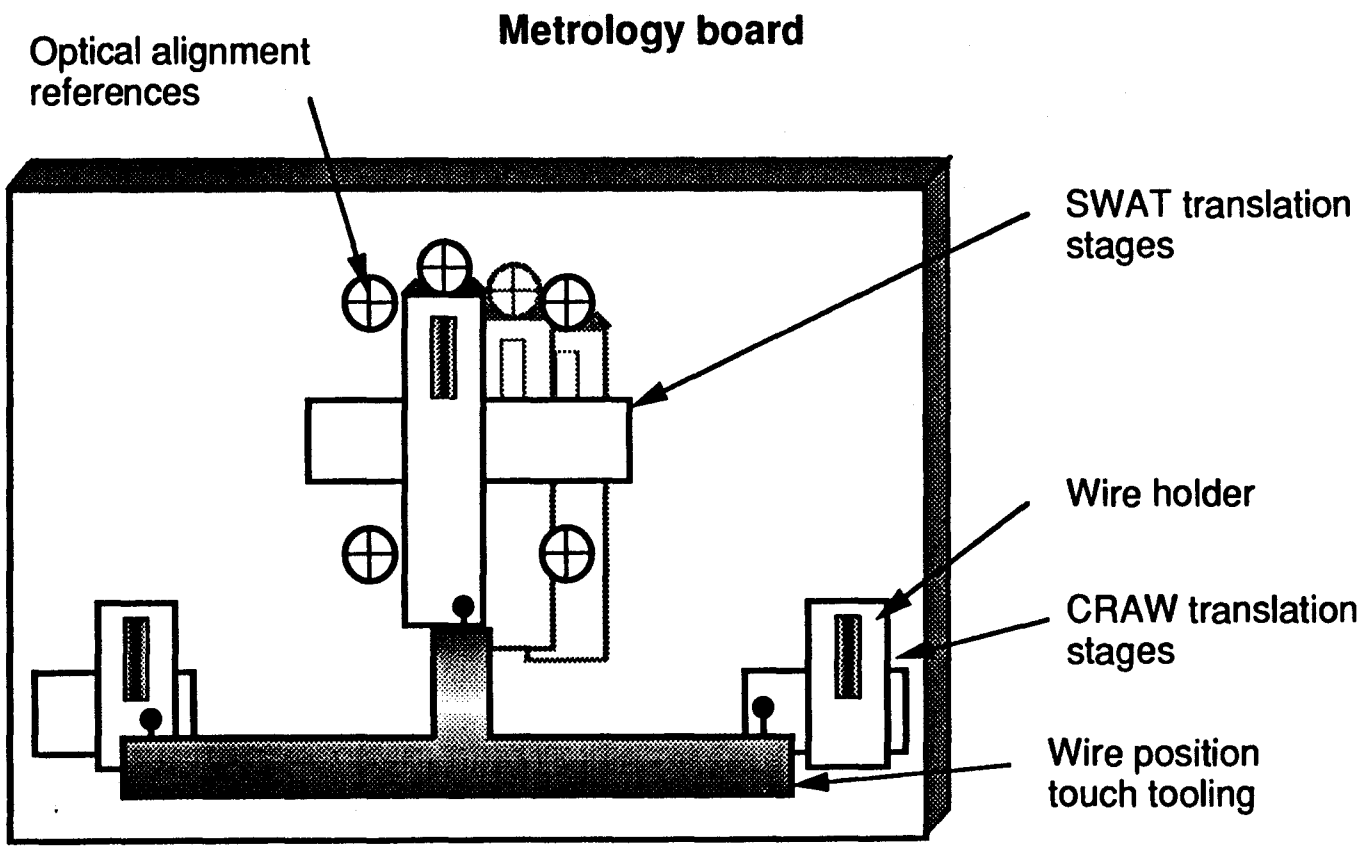

ILSE 1/27/92 h

Each section of ILSE is initially aligned on the calibration table

The injector is moved on the calibration table until the optical fiducials in the alignment templates are aligned with the optical references of the metrology boards

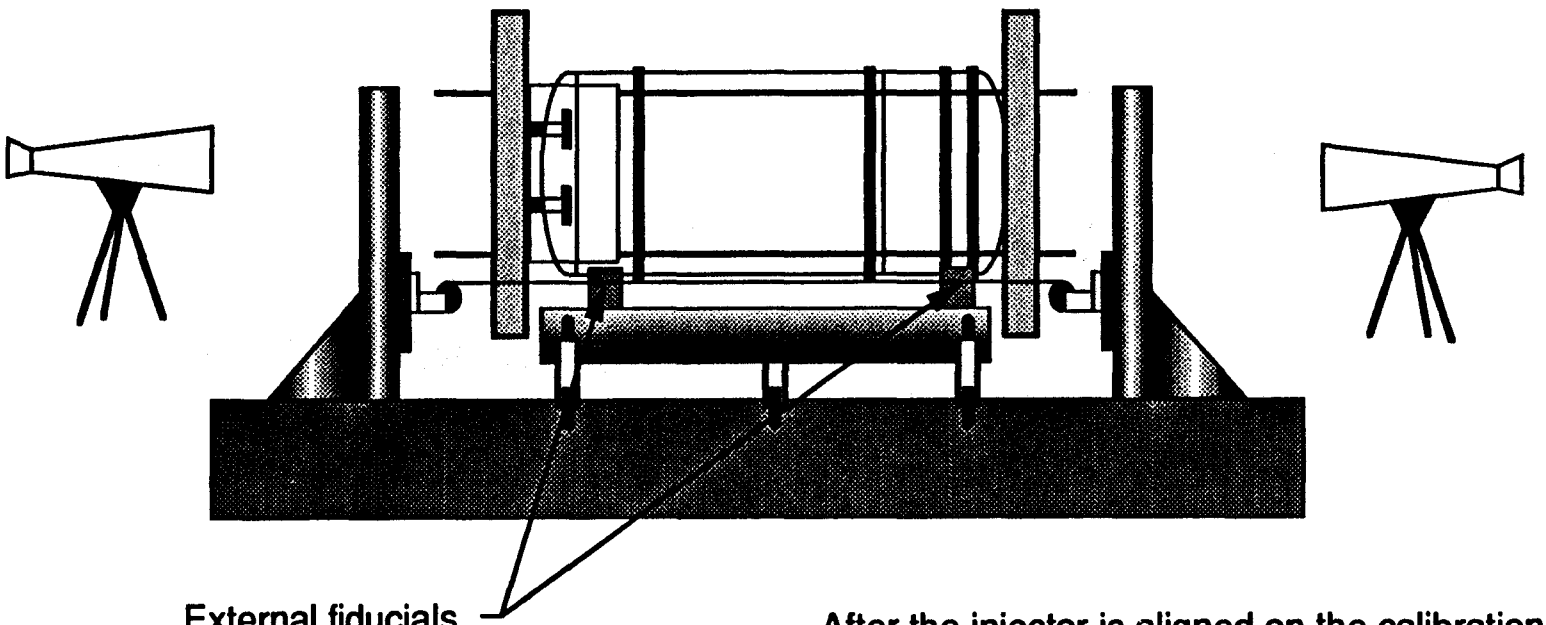

After the injector is aligned on the calibration table, the external fiducials are set relative to the CRAW

The accelerator reference alignment wires (RAW) are separated by the same distance as the CRAW

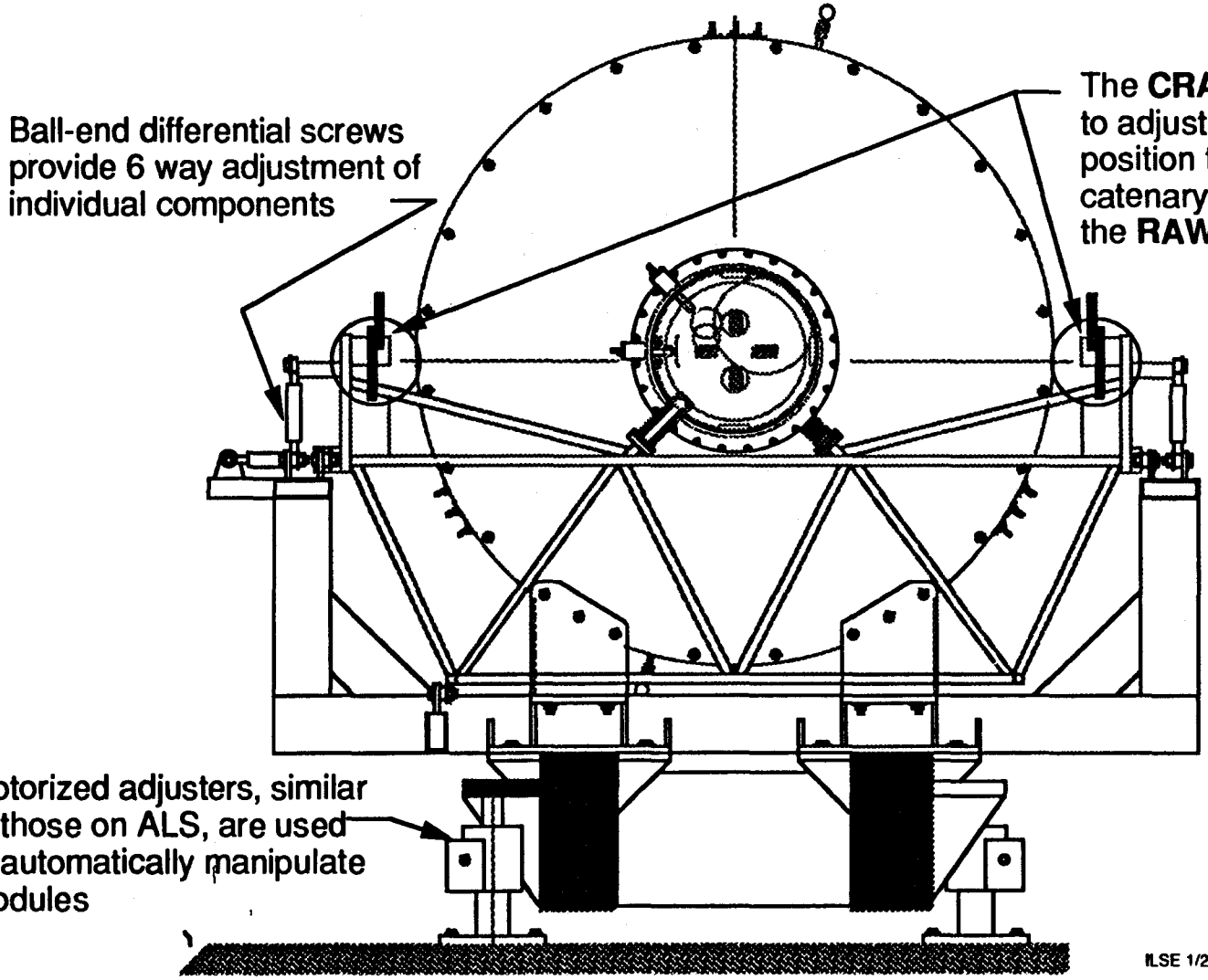

The electrostatic quadrupoles are first aligned in pairs using tight mechanical tolerances

Alignment of quadrupole pairs is checked with a coordinate measuring machine

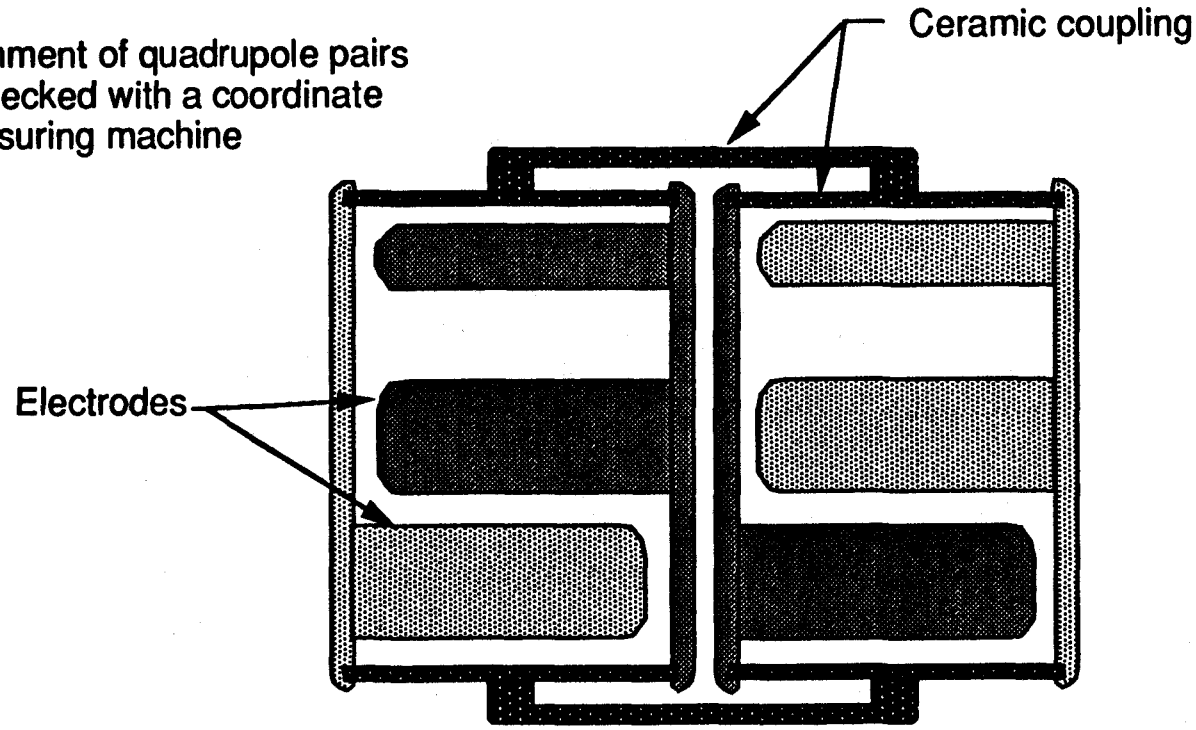

The electrostatic quadrupole pairs are aligned on a strong back using optical targets that are supported on the electrodes

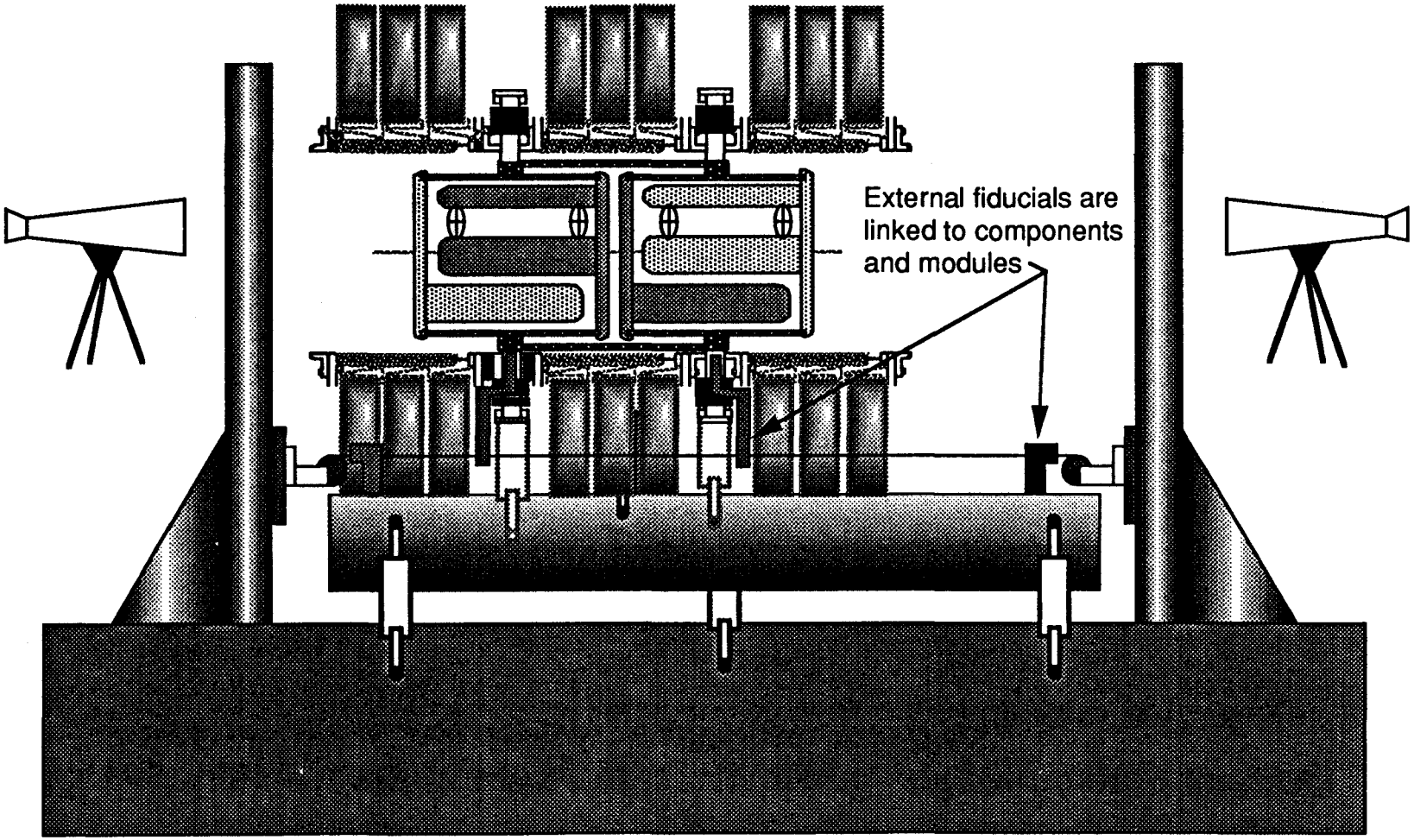

ILSE 1/28/92 m

The field axes of the magnetic quadrupoles are located with the Stretched Wire Alignment Technique (SWAT)

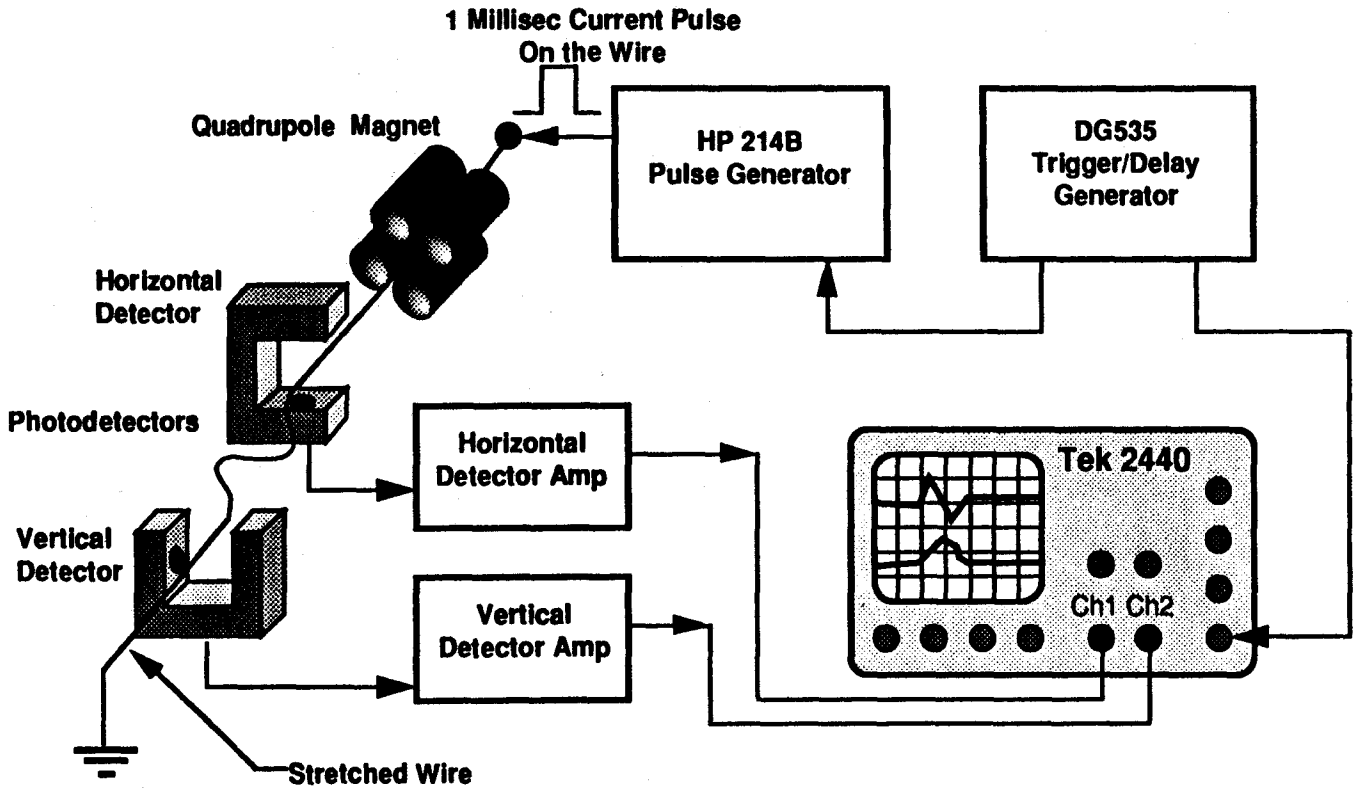

Graphic from document by Fred Deadrick

ILSE 2/3/92

The field axis changes between the electrostatic and magnetic focus sections

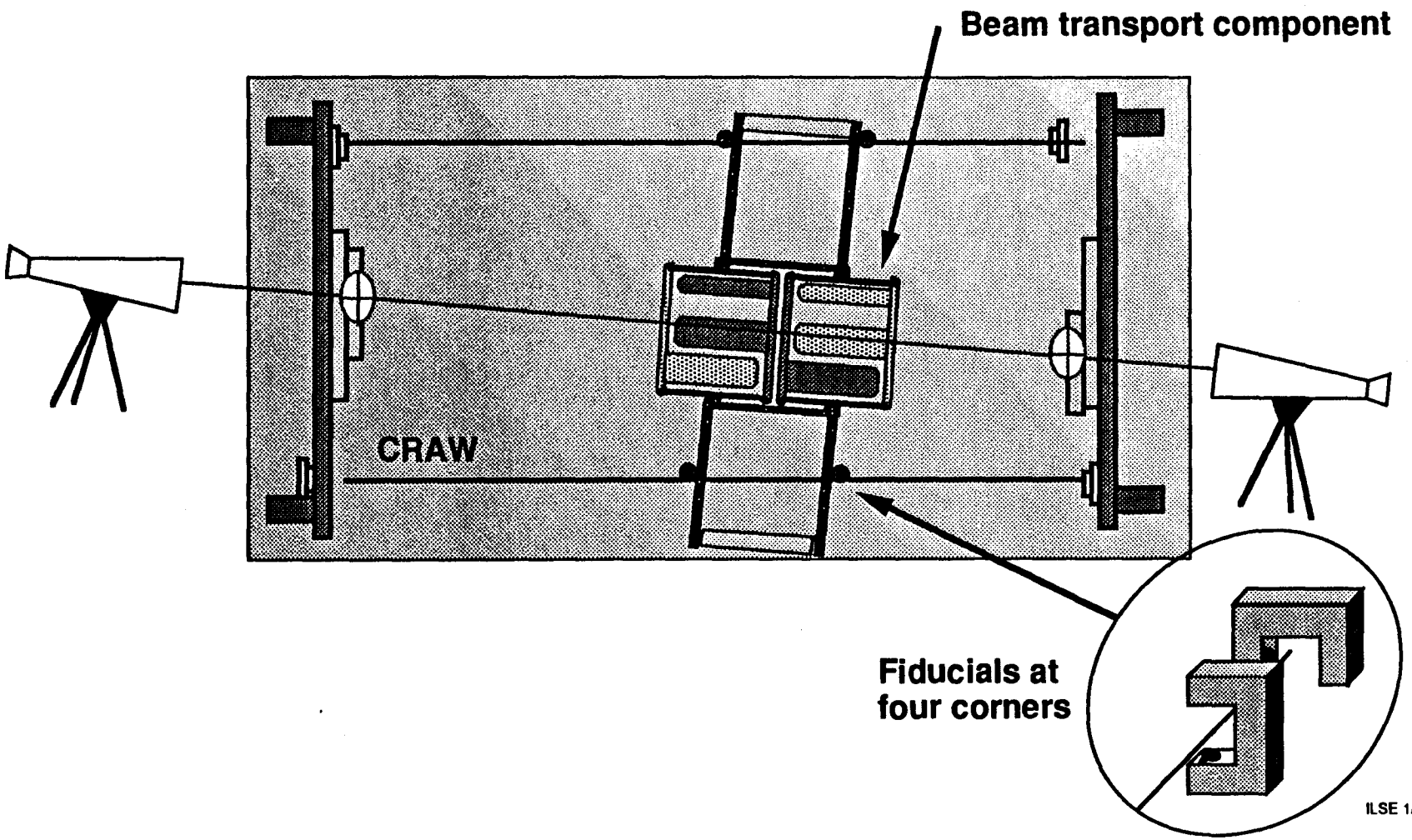

ILSE 1/28/92 o

Beam diagnostics are aligned and calibrated as they are assembled in the module

Noninvasive beam diagnostics

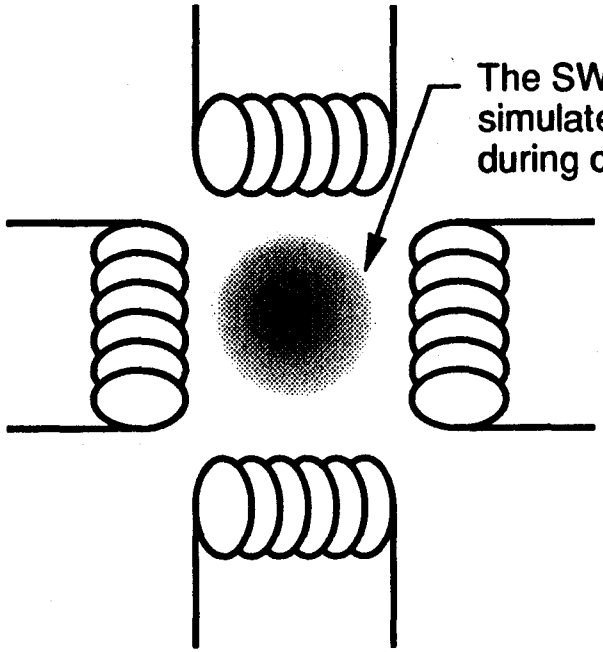

The SWAT wire simulates the beam during calibration

Invasive beam diagnostics

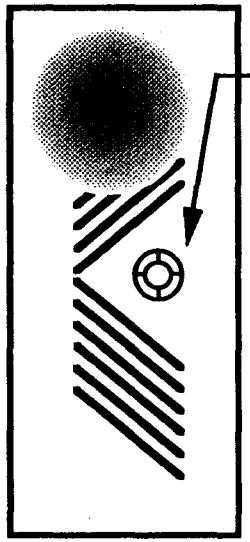

Optical targets permit alignment of insertable diagnostics

What are the tolerances and how is the tolerance budget distributed

Transverse positional tolerance	100μm
Longitudinal tolerance	fit
Angular (tilt) tolerance	1 mrad

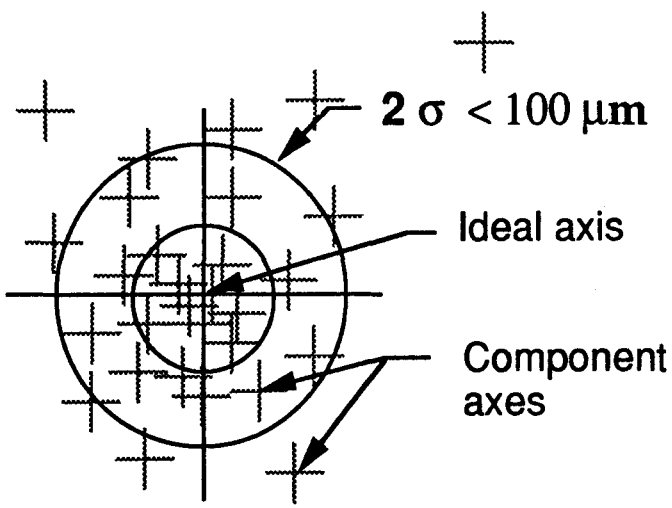

Error Budget

	δ
Catenary	5 μm
PEPS fiducial resolution	2 μm
PEPS temporal drift	10 μm
PEPS temperature drift	10 μm
Fiducial offset creep	30 μm
Offset thermal expansion	20 μm
CMM	1 μm
Individual quad center to array center	25 μm
Optical target	25 μm
Alignment scope	50 μm
Alignment correction threshold	20 μm
$[\Sigma \delta^2]^{1/2}$	= 75 μm

Ground Motion due to CHL

Central Helium Liquifier

Worthington Compressor
4000 horsepower Elliot electric motor

Source

approximately 250 microns @ 277 rpm = 4.62 Hz

Distance

approximately 200 meters

Main Ring

Stand magnet resonance
Apocryphal 1/16" to1/8"
definitley feel the motion

fix was simply to change the spring constant of the system

Tevatron

Magnitude of motion = 20 microns
Modulation of the spill at 4.62 Hz
Fix: run cycle time at a multiple of 13/15 seconds

Numerology : $13/15 = \frac{.8666}{1/4.616 = .2166} = 4.001$

Oscillations repeatable on cycle to cycle basis and extraction learning algorithm was able to substantially reduce the effect.

TABLE III

Vibration Measurement Results

	Location	Orientation	Frequency, HZ	Amplitude, Mils
1.	Northend, west side on foundation	Vertical	4,6	13.1, 1.9
	Northend, west side on foundation	North-South	4,6	6.9, 1.6
	Northend, west side on foundation	East-West	4,6	14.7, 2.4
2.	Northend, west side on floor slab	Vertical	4,6	6.0, 1.4
	Northend, west side on floor slab	North-South	4,6	4.3, 1.8
	Northend, west side on floor slab	East-West	4,6	16.4, 1.0
3.	Southend, west side on foundation	Vertical	4,6	5.4, 0.7
	Southend, west side on foundation	North-South	4,6	9.3, 1.9
	Southend, west side on foundation	East-West	4,6	3.2, 1.7
4.	Southend, west side on floor slab	Vertical	4,6	14.9, 1.5
	Southend, west side on floor slab	North-south	4,6	12.7, 1.3
	Southend, west side on floor slab	East-West	4,6	9.9, 2.3

Because the long axis of the foundation is north-south, it would be expected to see the east-west component larger than the north-south at the operating frequency. This is not, however, consistant suggesting that other vibration interference may be occuring.

TABLE II
Dynamic Soil Properties
From Cross Borehole Testing
Helium Liquefier Addition

Depth	Insitu Density Pcf	Compression Wave Velocity Vp,fps	Shear Wave Velocity Vs,fps	Shear Modulus G,psf	Poisson's Ratio γ
6'	128.1	3457	479	9.1×10^5	.49
9'	130.7	2940	551	12.3×10^5	.48
14'	130.5	2800	794	25.6×10^5	.46
19'	141.4	2681	825	29.9×10^5	.45
24'	141.5	5433	1025	48×10^5	.48
28'	139.2	6863	1076	50×10^5	.49

ANL Jendrzejczyk

3 holes Seismograph + 2 geophones + hammer

CONSOLE LOCATION 36; MCRLib 30-DEC-1991 09:36
None

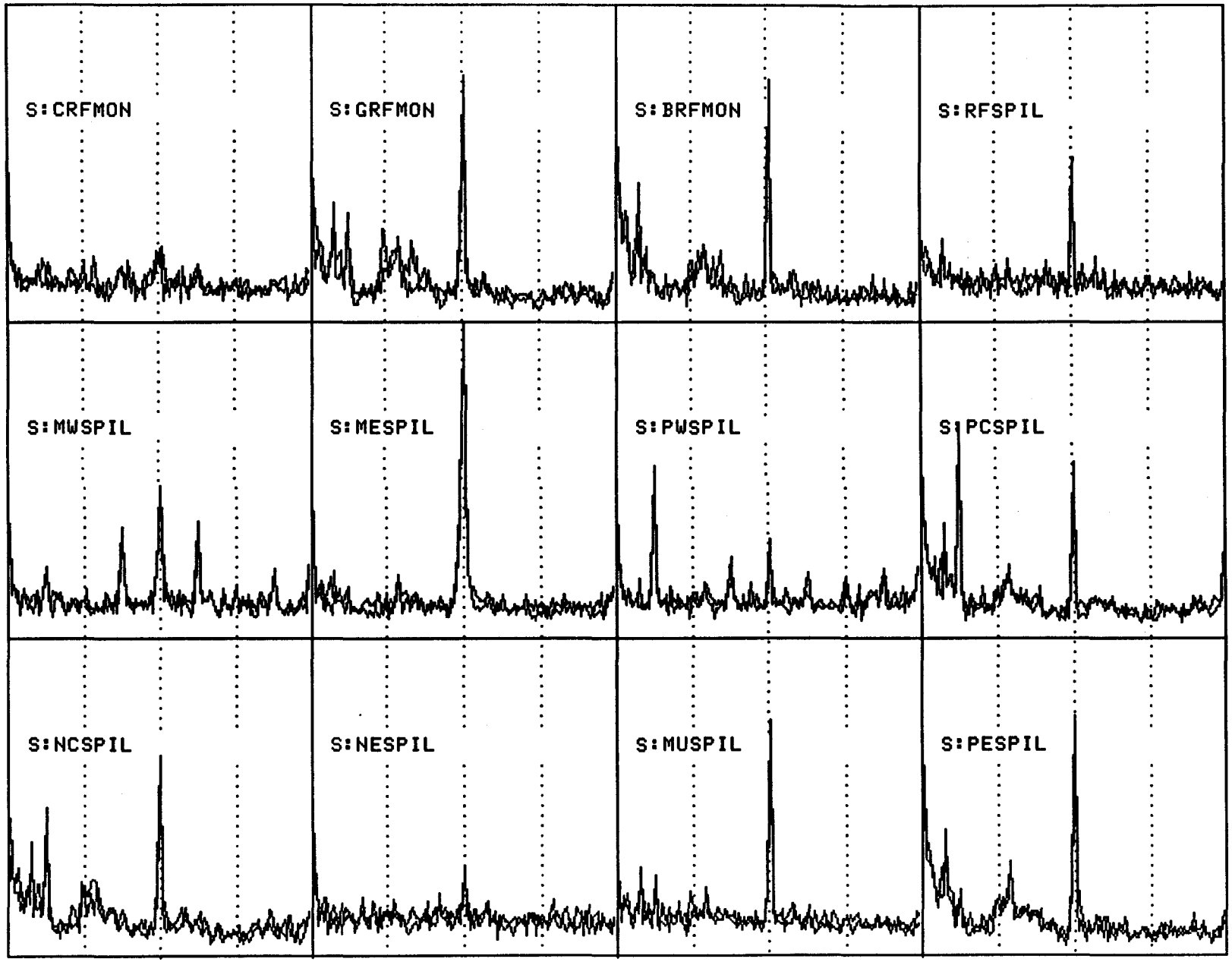

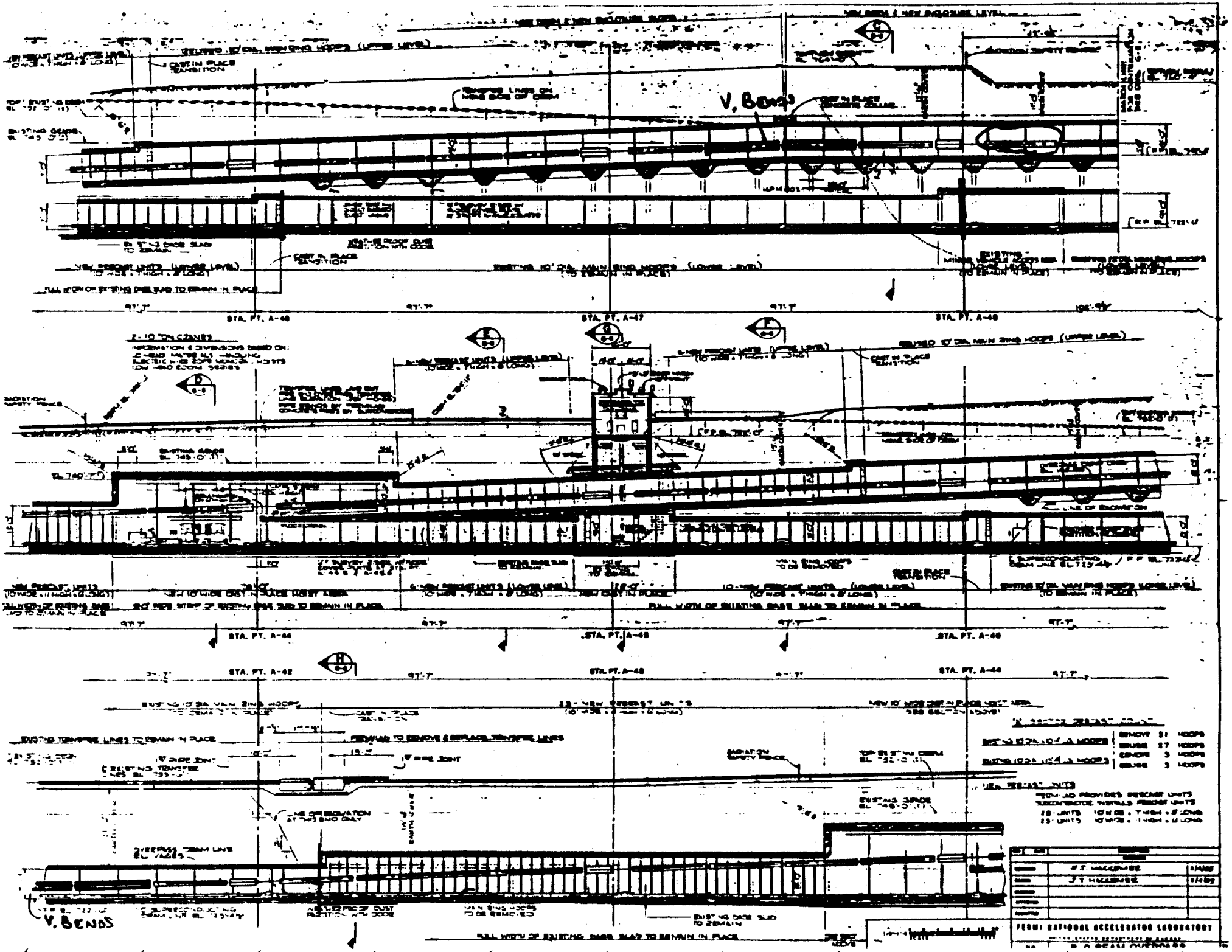
V. Bends
STA. PT. A-46
STA. PT. A-47
STA. PT. A-48
STA. PT. A-44
STA. PT. A-42
V. BENDS
FERMI NATIONAL ACCELERATOR LABORATORY

BIP NEXT

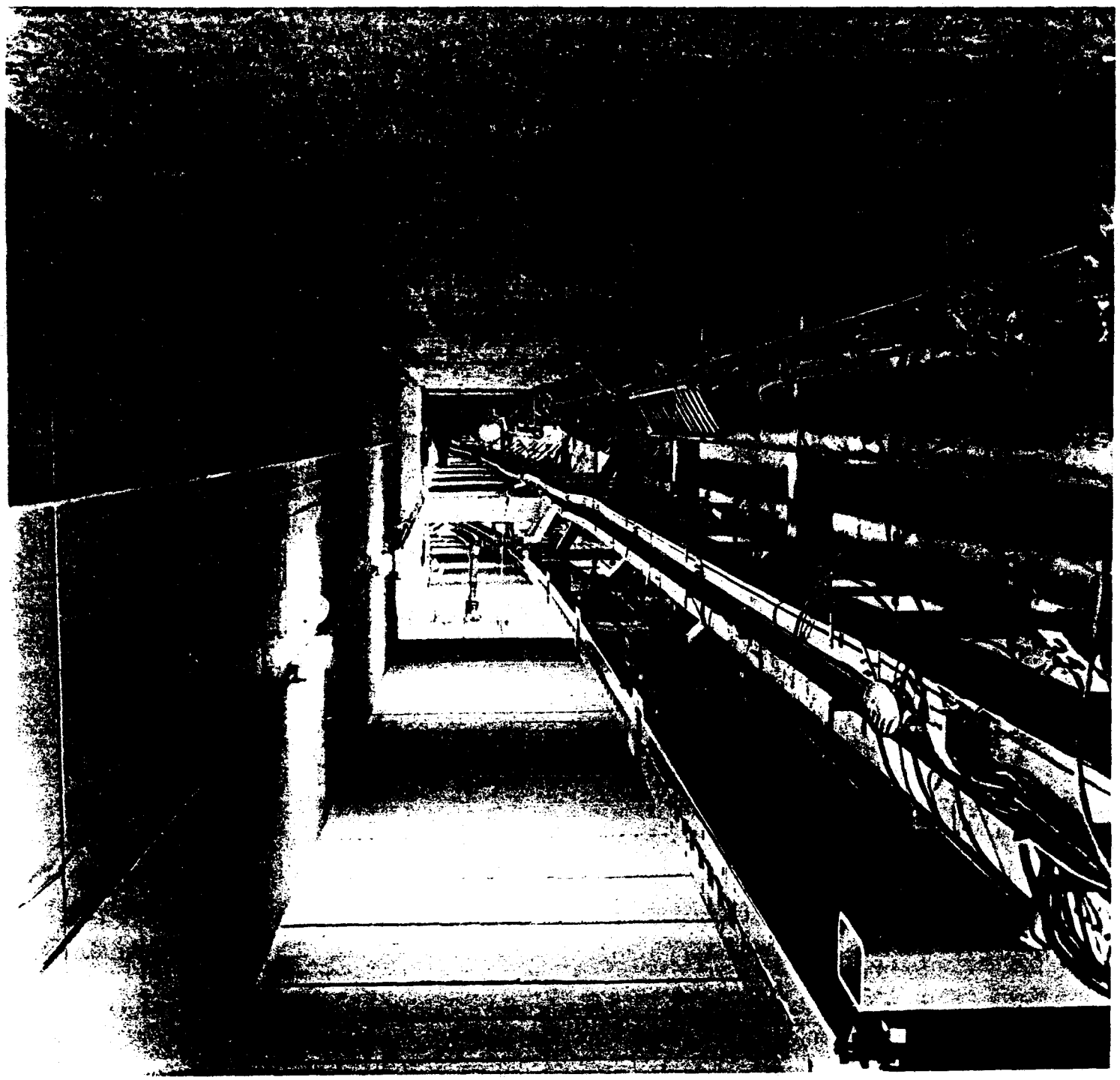

E-619-92

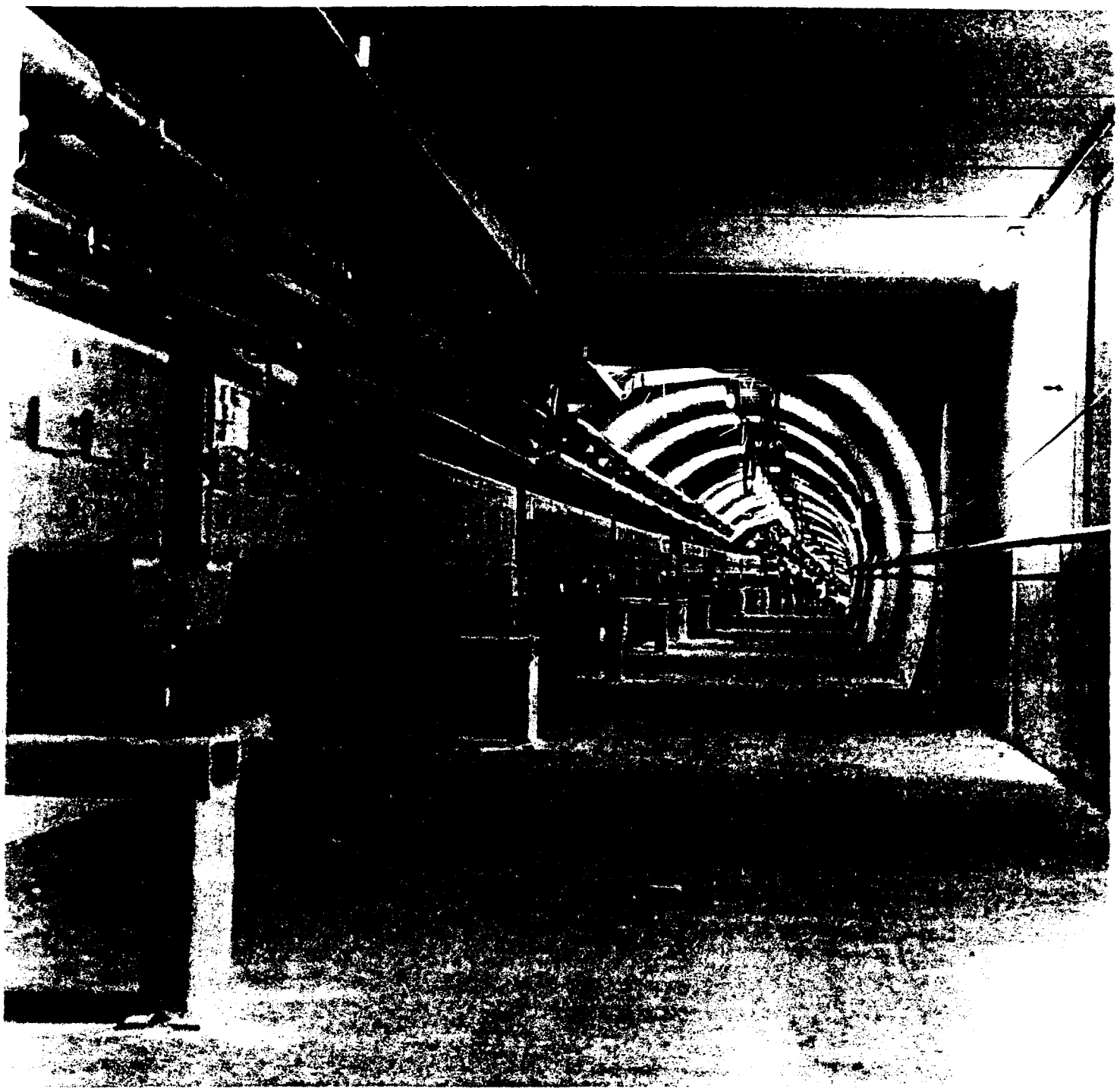

86-522-10

86-522-3

VIBRATION SUPPRESSION IN STRUCTURES

Beam Steering Concepts and Capabilities
Mike Syphers (SSCL)

A Potential Feedback Signal-Luminosity Measurement
Tony Liss (U of Illinois)

Robust Vibration Suppression and Disturbance Rejection
Andrew Krudila (Texas A&M)

Dynamic Control of Large Structures
J. J. Allen (SNL)

Passive and Active Vibration Suppression in Space Structures
Bill Witt (CORE)

Sensors, Actuators, and Systems Issues for Modern Control
W. K. Tucker (SNL)

Application of Base Isolation to Large Structures
R. F. Kulak (ANL)

File Edit Print Mail

Prt Closed Orbit

Theta = ? .01

xo,x'o = ? 0,0

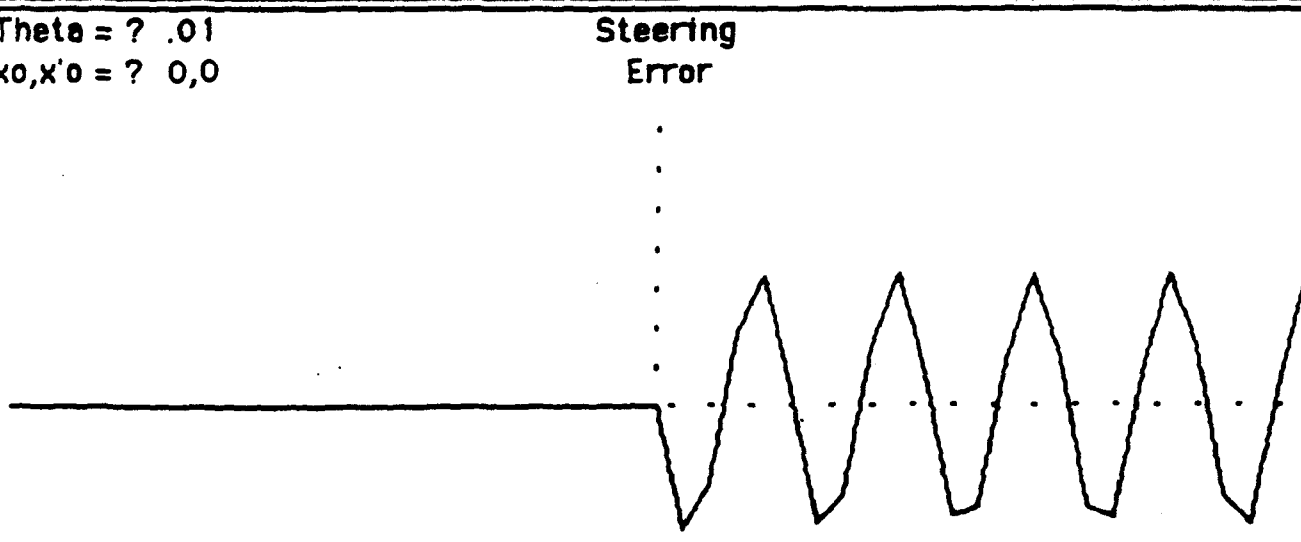

File Edit Print Mail

Prt Closed Orbit

Theta = ? .01

xo,x'o = ? 0,0

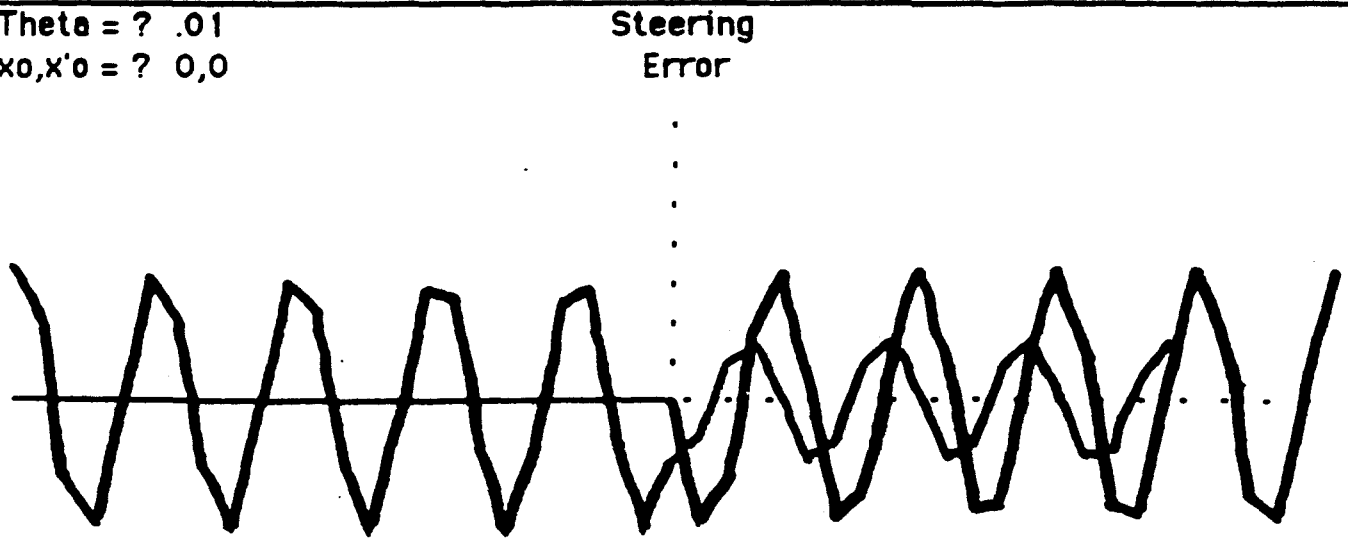

File Edit Print Mail

Prt Closed Orbit

Theta = ? .01

Xo,X'o = ? 0,0

Steering Error

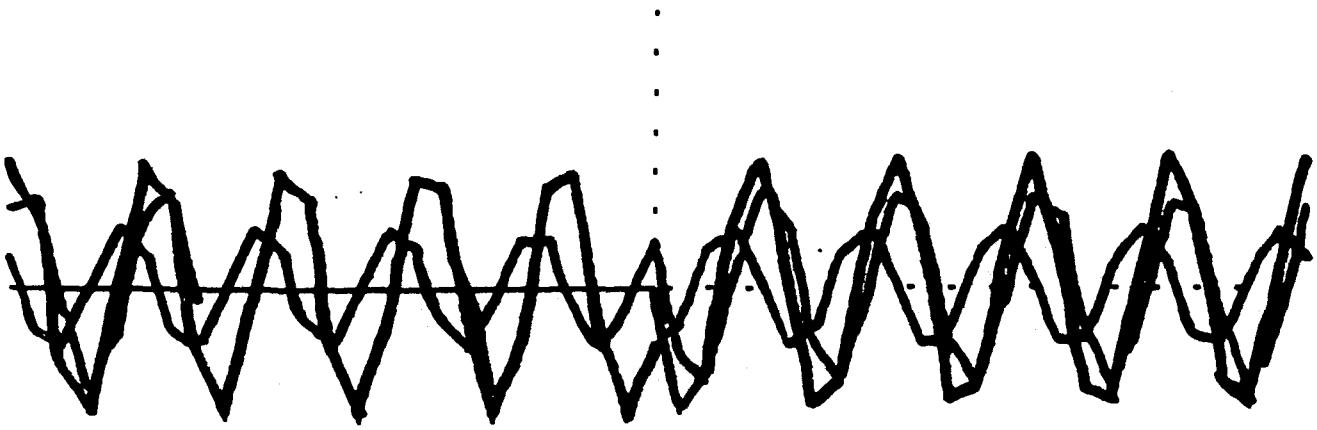

File Edit Print Mail

Prt Closed Orbit

Theta = ? .01

xo,x'o = ? 0,0

Steering
Error

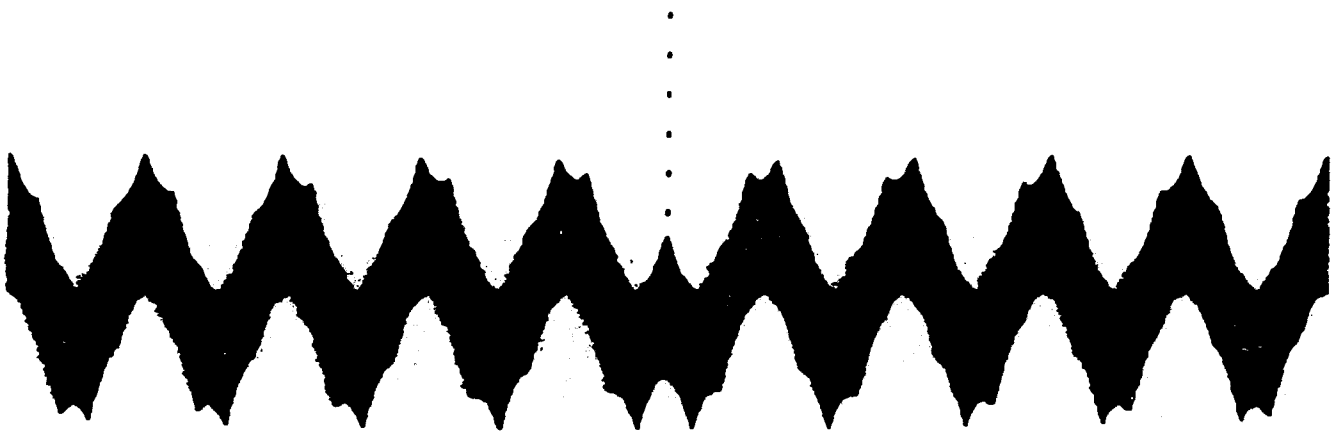

Figure 6 Lattice and orbit functions of low-β IR in collision optics

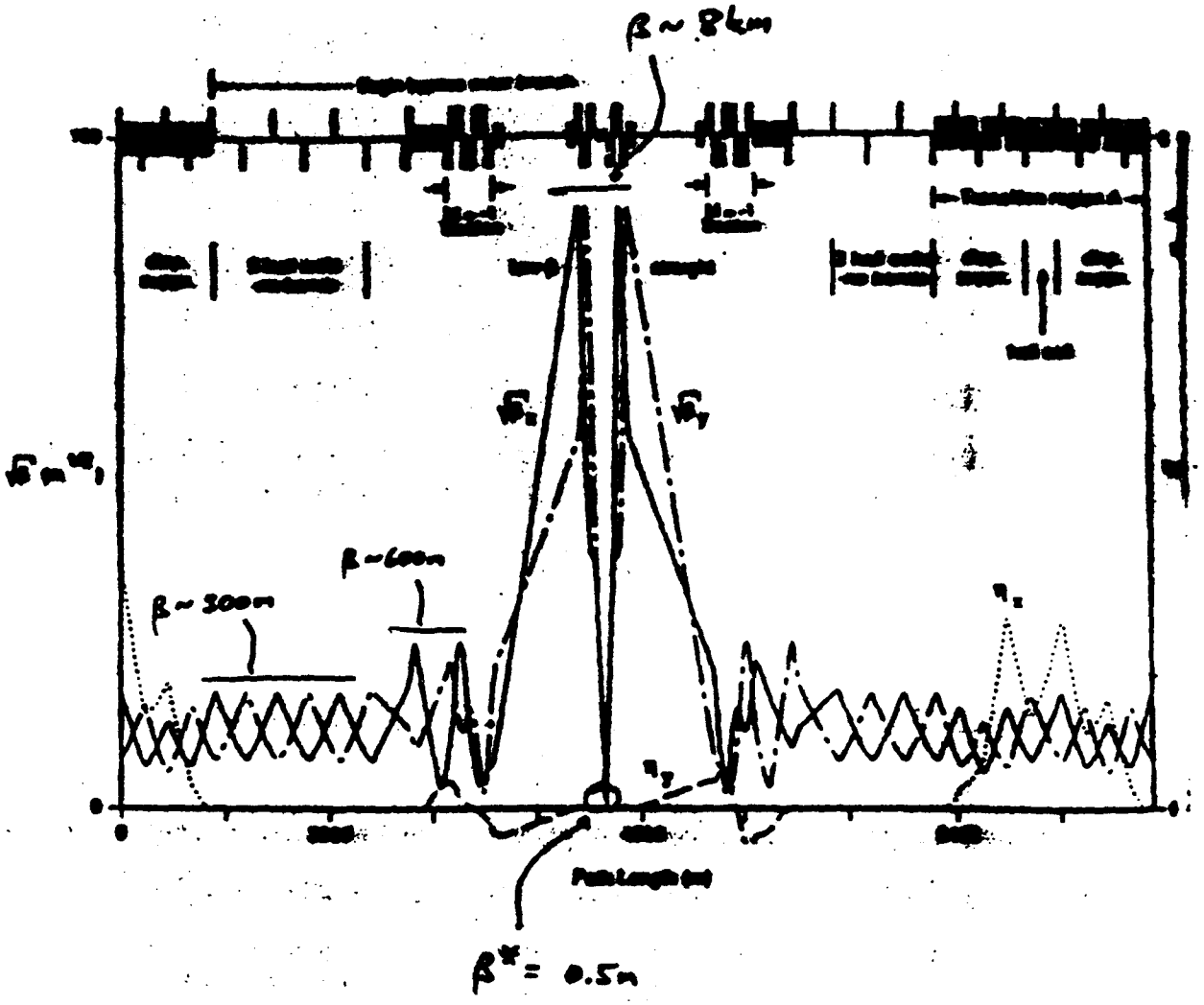

Vibration - related issues : amplitude + frequency

* if f_{vib} small enough, perturbs orbit adiabatically; moves beam around, but no significant emittance growth

if too large, non-adiabatic ; leads to emittance growth.

Common triplet quads :

quad offset d causes $\Delta\theta = \frac{d}{f}$

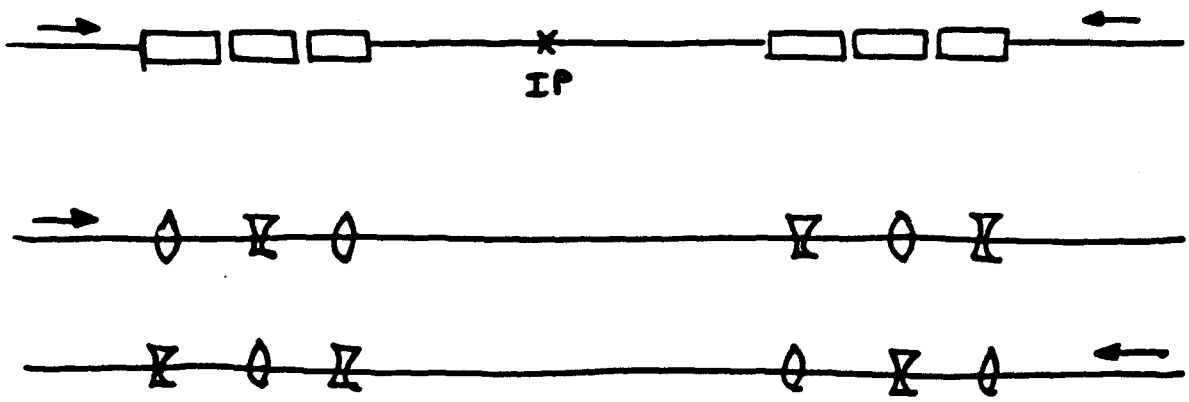

deflection of a single quad steers the two counter-rotating beams in the opposite sense ; i.e, one beam sees "+" deflection, the other sees "−"

Antisymmetric optics may help, especially if ground vibrations are long wavelengths and IR quads move coherently:

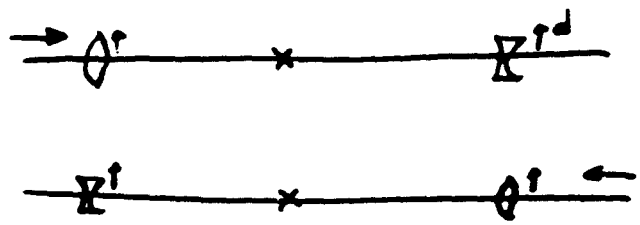

due to displaced quads:

$$\Delta X^*_{LR} = - \Delta X^*_{RL}$$

but, superposition:

$$\Delta X^* = \frac{\theta_1 \sqrt{\beta_1 \beta^*} \cos(\Delta\psi_1 - \pi\nu)}{2 \sin \pi\nu} + \frac{\theta_2 \sqrt{\beta_2 \beta^*} \cos(\Delta\psi_2 - \pi\nu)}{2 \sin \pi\nu}$$

$$= \frac{\beta^* d}{2 \sin \pi\nu} \left\{ \int_{left} \sqrt{\frac{\beta(s)}{\beta^*}} K(s) \cos(\Delta\psi - \pi\nu) ds + \int_{right} \sqrt{\frac{\beta(s)}{\beta^*}} K(s) \cos(\Delta\psi - \pi\nu) ds \right\}$$

$$\left(= \frac{eB'}{p} \right)$$

$$K(s)_{left} = - K(s)_{right}$$

$$(\beta, \Delta\psi)_{left} \approx (\beta, \Delta\psi)_{right} \implies \Delta X^* \approx 0$$

will not be zero, but may not be as large as one might first suspect

Steering capabilities:

mm-scale perturbations

$\Delta x = 1\,\text{mm} \sim \theta_0 \sqrt{\beta_0 \beta^*}$ $\qquad \beta^* = \frac{1}{2}\,\text{m}$

$\beta_0 = 8000\,\text{m} \rightarrow \theta_0 = 16\,\mu\text{rad}$

$\beta_0 = 600\,\text{m} \rightarrow \theta_0 = 67\,\mu\text{rad}$

μm-scale perturbations

$\Delta x = 1\,\mu\text{m} \rightarrow \theta_0 \lesssim 100$ nrad

@ 20 TeV:

$\theta = 100\,\mu\text{rad} \rightarrow B \cdot \ell = 6.6$ T·m

$15\,\mu\text{rad} \rightarrow 1$ T·m

100 nrad $\rightarrow 0.01$ T·m ★

Damping system?

Note $0.5\,\mu\text{m}$ ($\frac{1}{10}\sigma$) free oscillation at IP $\rightarrow$ $10\,\mu\text{m}$ amplitude in arcs; barely within reach of standard BPM (?)

Beam Steering

MIKE SYPHERS
SSC LABORATORY
VIBRATION WORKSHOP
FEB 1992

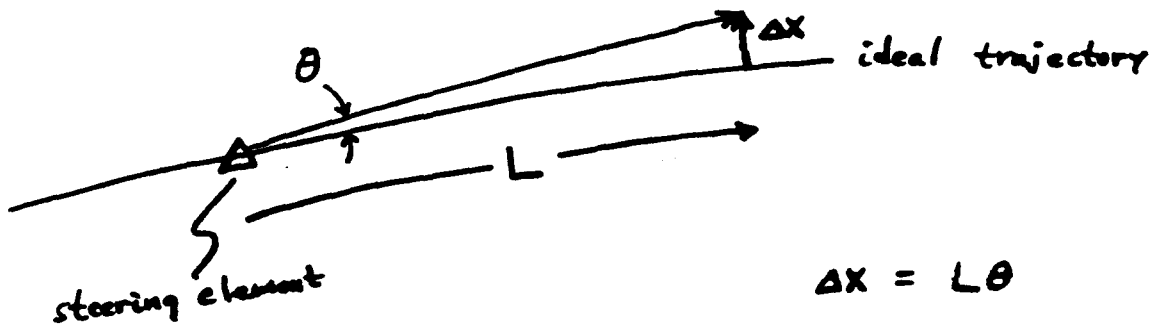

$$\Delta X = L\theta$$

with quadrupole present:

$$\Delta X' = \frac{\ell_1 \theta}{f}$$

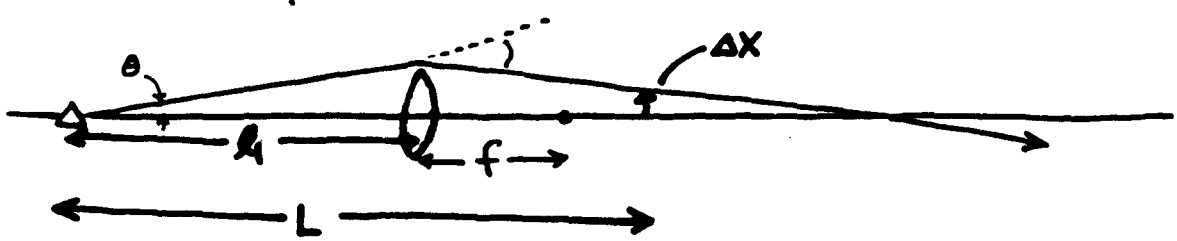

$$\Delta X = L\theta \left[1 - \frac{\ell_1}{f} + \frac{\ell_1^2}{Lf} \right]$$

System of lenses straightforward, but tedious...

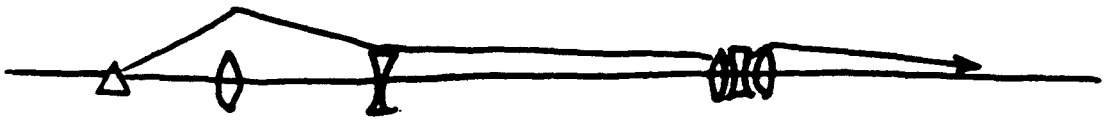

And circular accelerators are closed systems of lenses:

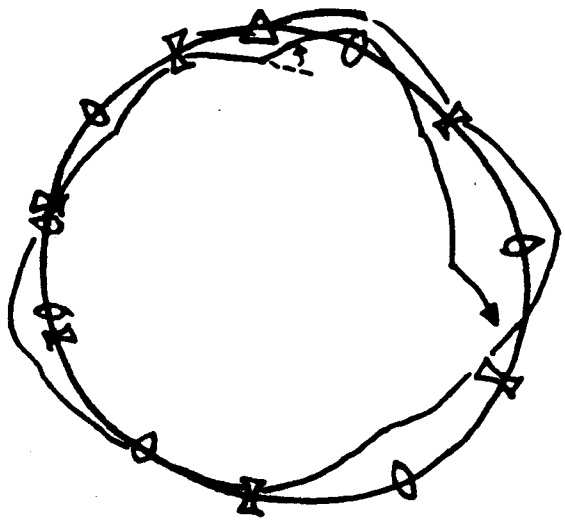

Analysis can be simplified by introducing "lattice functions"

define amplitude function and phase advance β, ψ by

$$\Delta x(s) = A \sqrt{\beta(s)} \sin[\psi(s) + \delta]$$

constants; depend upon particle's initial conditions

File Edit Print

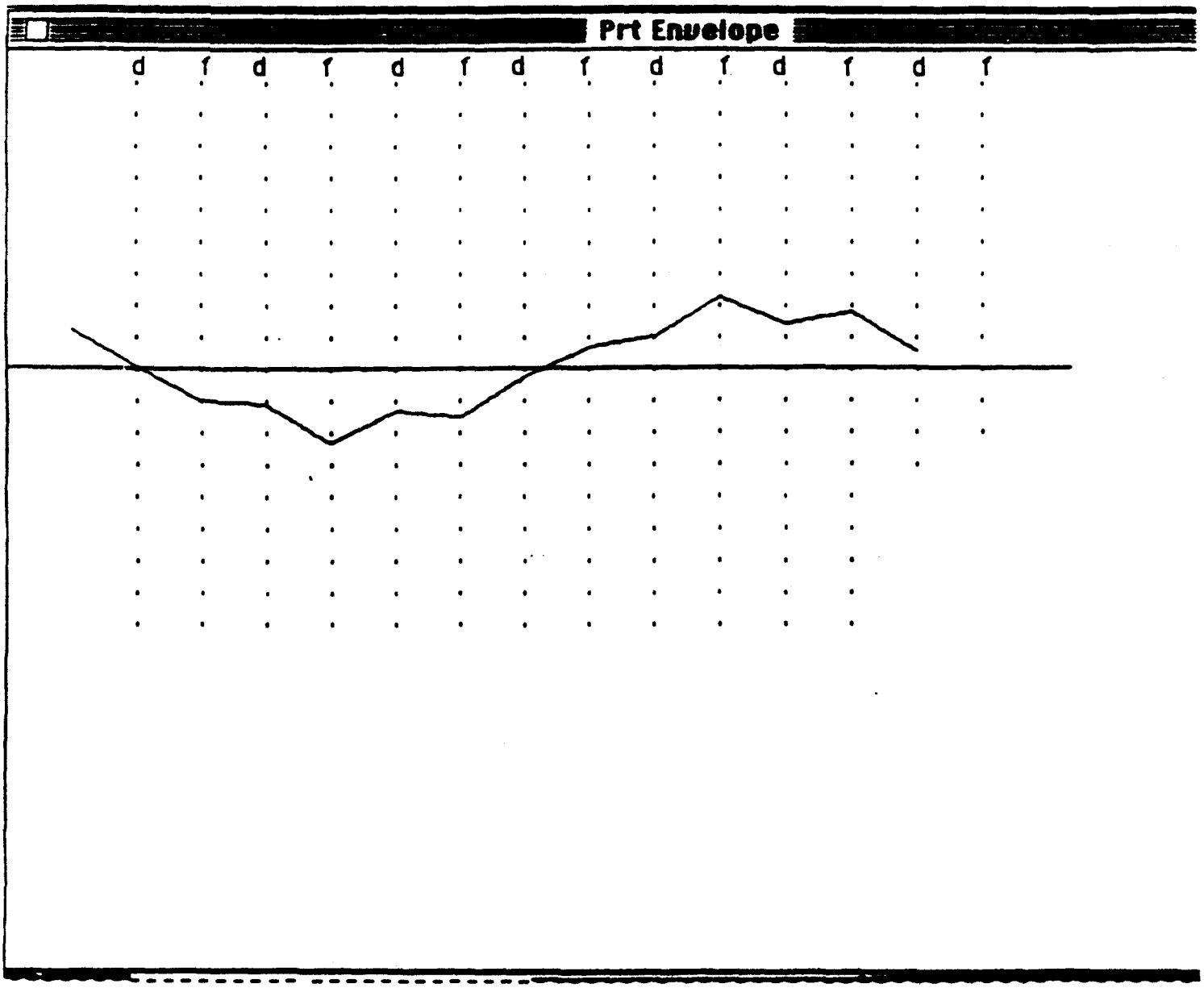

File Edit Print

Prt Envelope

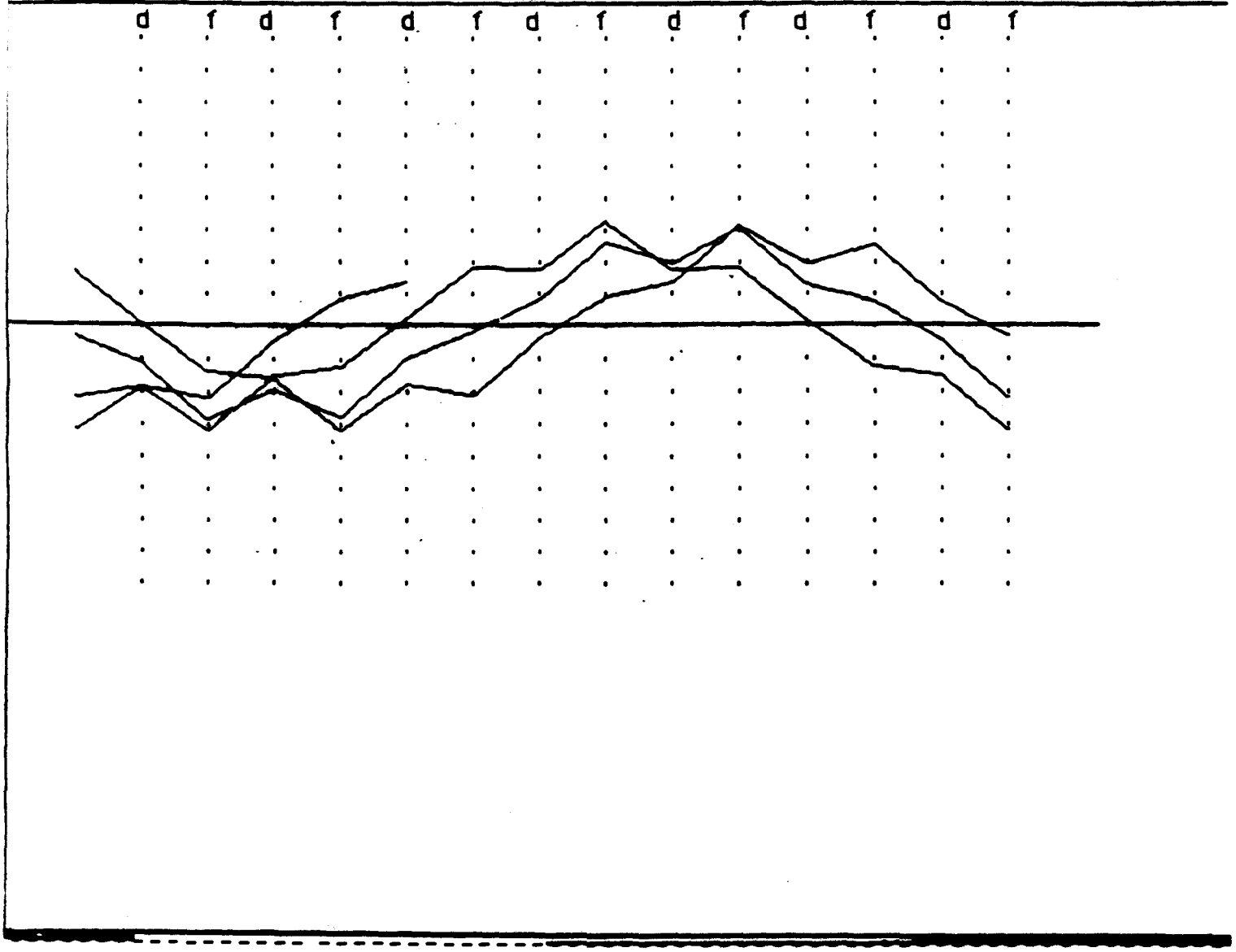

File Edit Print

Prt Envelope

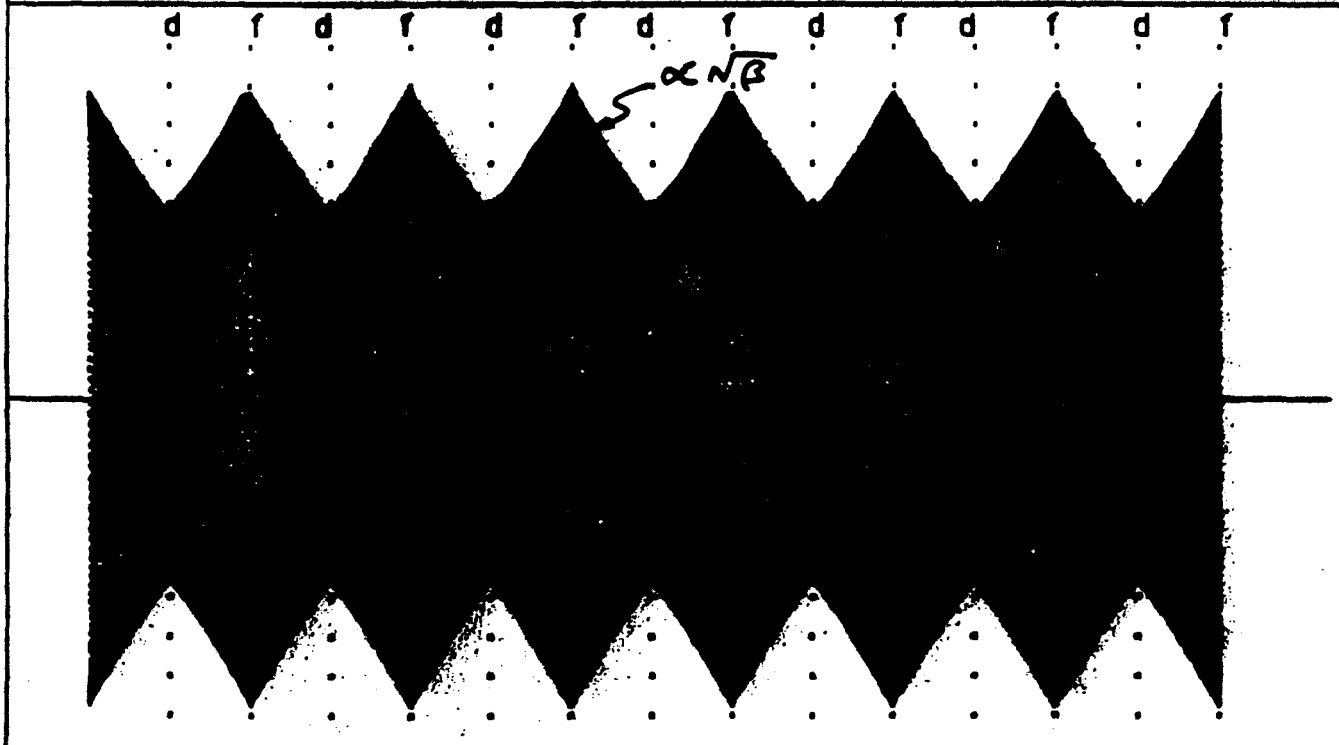

β and ψ can be computed and tabulated for arrangement of focusing elements in accelerator.

then,

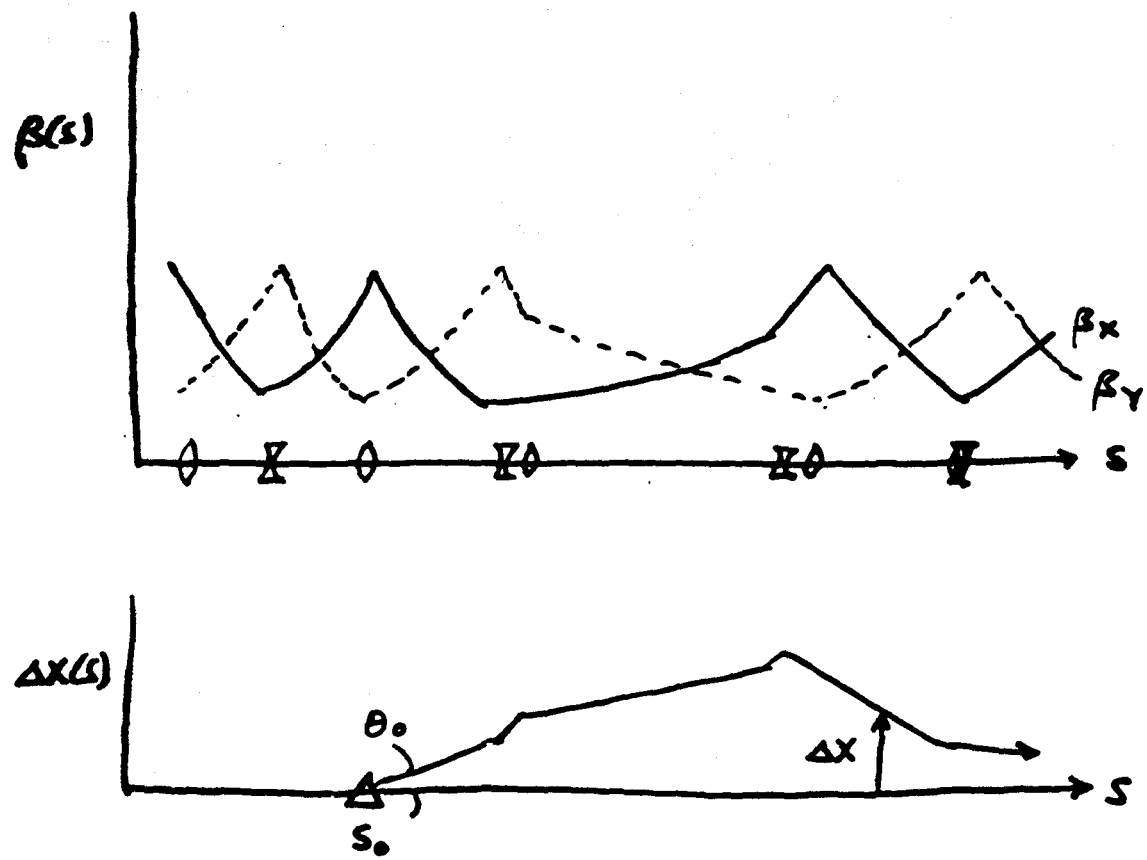

$$\Delta X(s) = \theta_0 \sqrt{\beta(s_0)\beta(s)}\ \sin\left(\psi(s) - \psi(s_0)\right)$$

Steering error will alter the "closed orbit" of the accelerator:

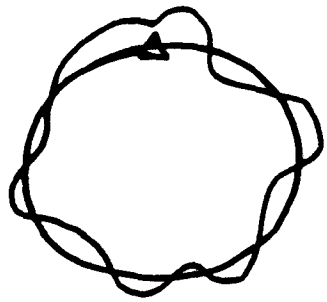

$$\Delta x_{c.o.} = \frac{\theta_0 \sqrt{\beta_0 \beta(s)}}{2 \sin \pi \nu} \cos\left(|\psi - \psi_0| - \pi \nu\right)$$

ν = "tune" = # of oscillations around circumference

Thus, single steering error will distort orbit about entire accelerator. Thus, to perform beam manipulations in a local manner, must use combinations of steering elements:

"3-bump"

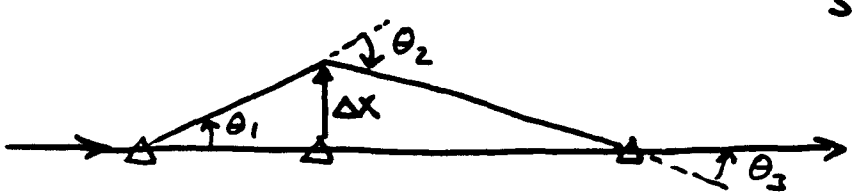

$$\Delta x = \theta_1 \sqrt{\beta_1 \beta_2} \sin \psi_{12}$$

$$\theta_2 = -\theta_1 \sqrt{\frac{\beta_1}{\beta_2}} \frac{\sin \psi_{12}}{\sin \psi_{23}} \qquad \theta_3 = \theta_1 \sqrt{\frac{\beta_1}{\beta_3}} \frac{\sin \psi_{12}}{\sin \psi_{23}}$$

Luminosity Monitoring As a Feedback Signal

Tony Liss
University of Illinois
Feb. 12, 1991

CDF Beam-Beam Counters:

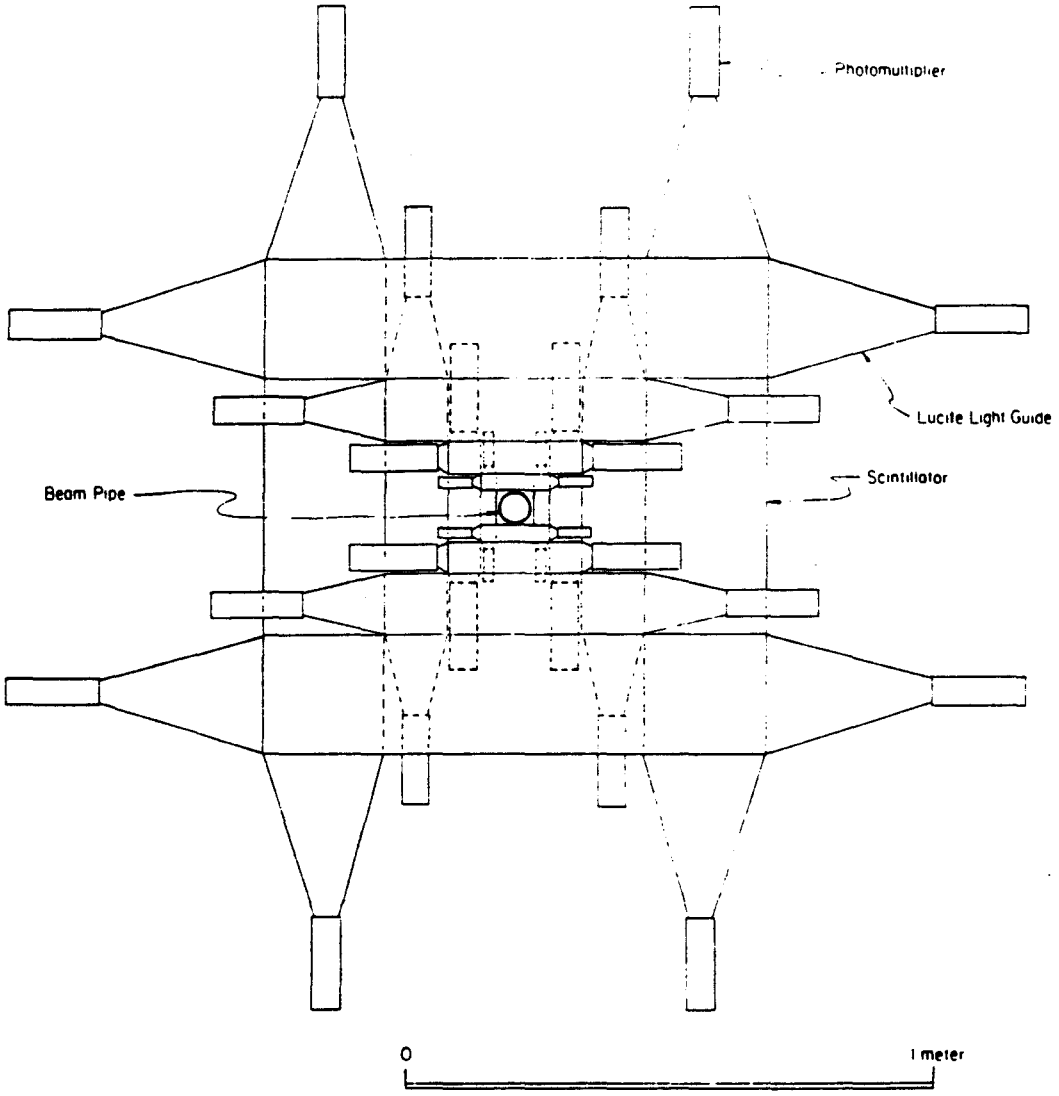

16 counters on each side of the nominal interaction point (about 20ft downstream) covering from 0.32° to 4.47° with respect to the beam.

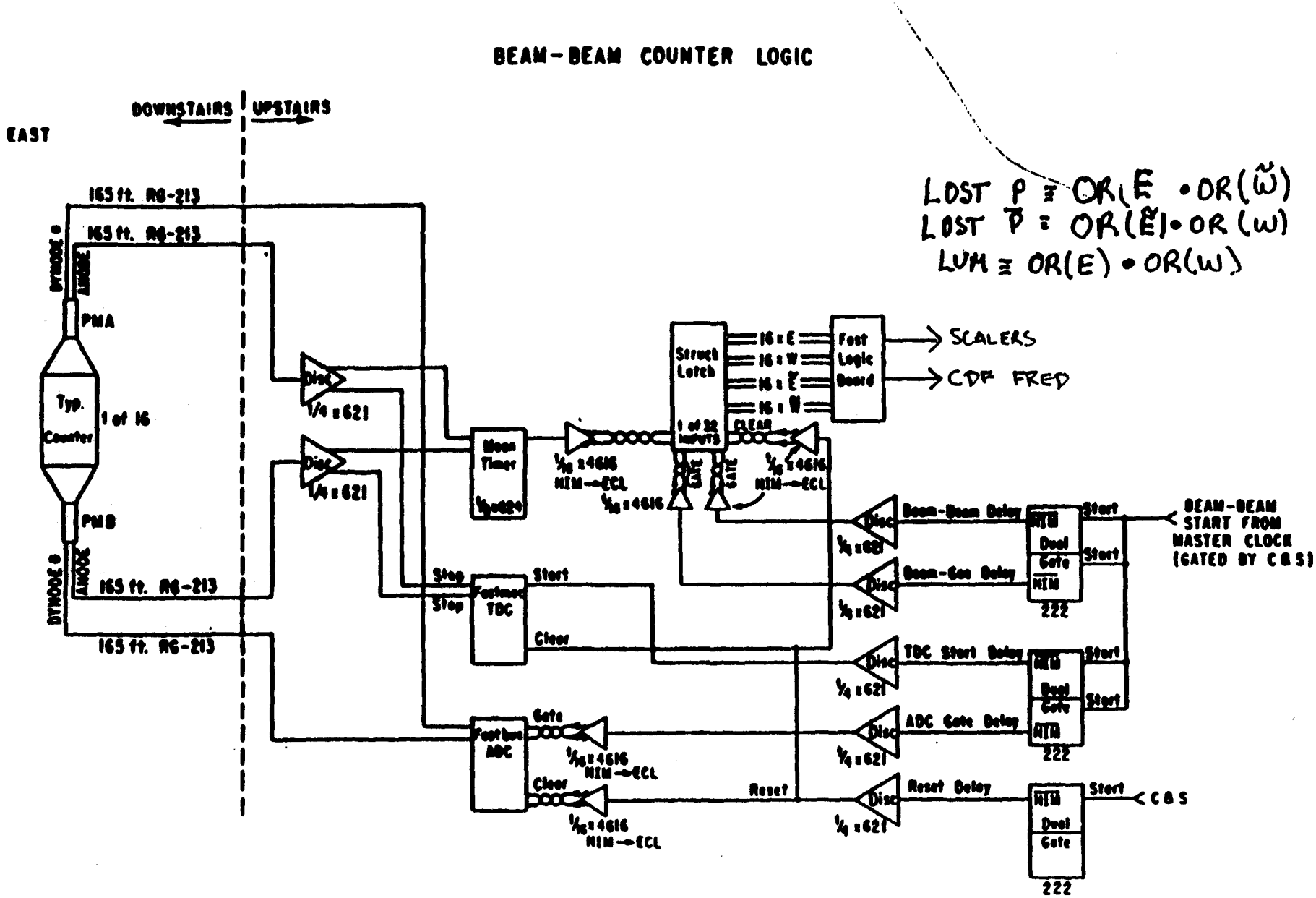

LOST $P \equiv OR(E) \cdot OR(\tilde{W})$
LOST $\bar{P} = OR(\tilde{E}) \cdot OR(W)$
$LUM \equiv OR(E) \cdot OR(W)$

Fig. 1

BBC luminosity was used as an accelerator monitor during squeeze and after in order to measure luminosity lifetime (and try to understand emittance growth). As a monitor of accelerator conditions it was *not* very sensitive (except when the luminosity was *very* low). The sensitive monitors were lost p and to a lesser extent lost pbar.

Lost P:

6 proton bunches per 21 μs with typically 10^{10} protons/bunch ⇒ 2.86×10^{15} protons/sec.

Lost P rates of 2-3 kHz ⇒ loss sensitivity of ~ $1/10^{12}$ of proton beam.

The rates of lost P are not understood in any kind of fundamental way. It has been noted that if *anything* is changed with regard to accelerator tuning lost P increases.

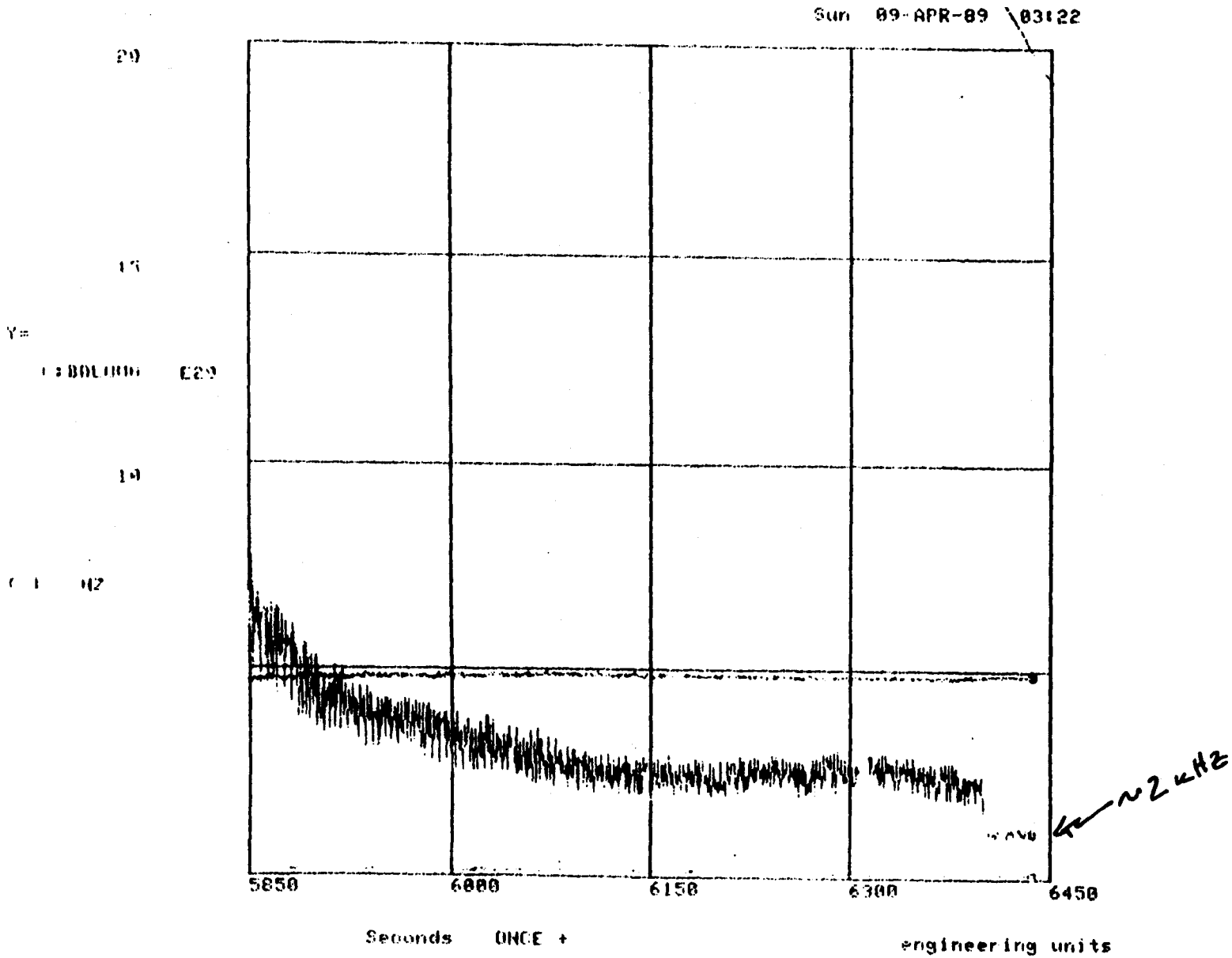
Sun 09-APR-89 03:22
20
10
Y=
10
5850
6000
6150
6300
6450
Seconds ONCE +
engineering units
~2 kHz

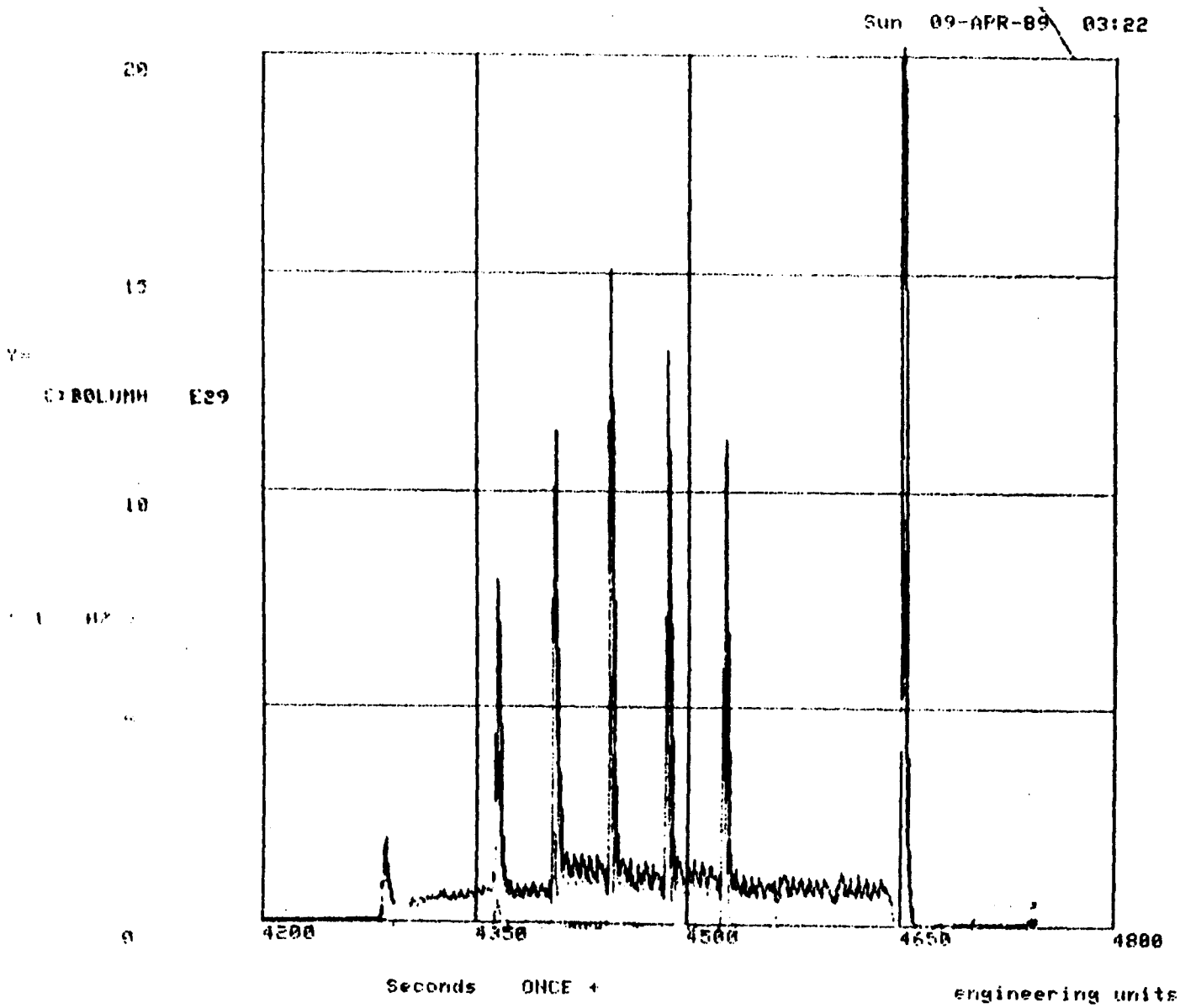
Sun 09-APR-89 03:22
20
15
10
0
4200
4350
4500
4650
4800
Seconds ONCE +
engineering units

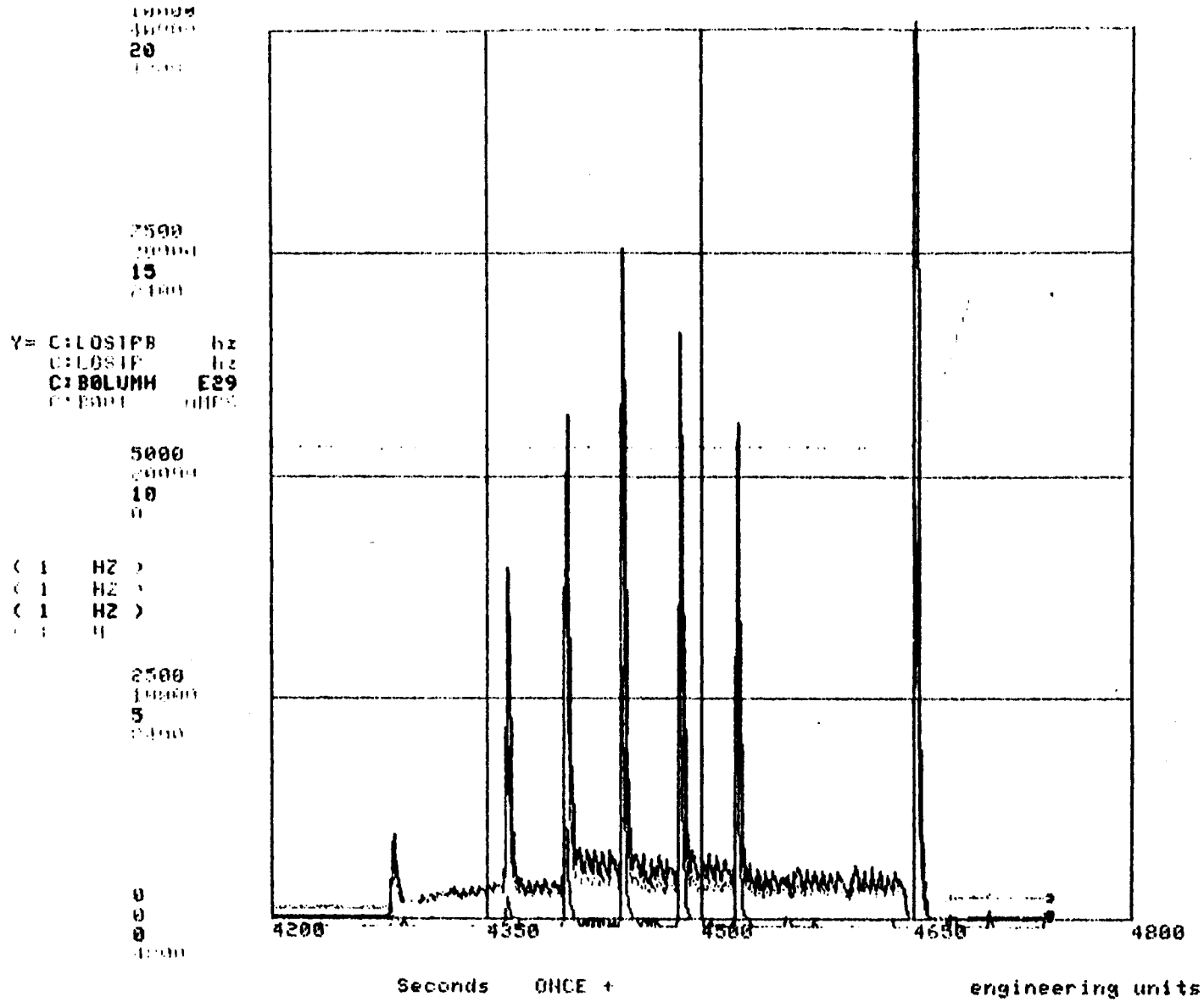
20
7500
15
Y= C:LOSIPB hz
C:LOSIP hz
C:B0LUMH E29
5000
10
(1 HZ)
(1 HZ)
(1 HZ)
2500
5
0
0
0
4200
4350
4500
4650
4800
Seconds ONCE +
engineering units

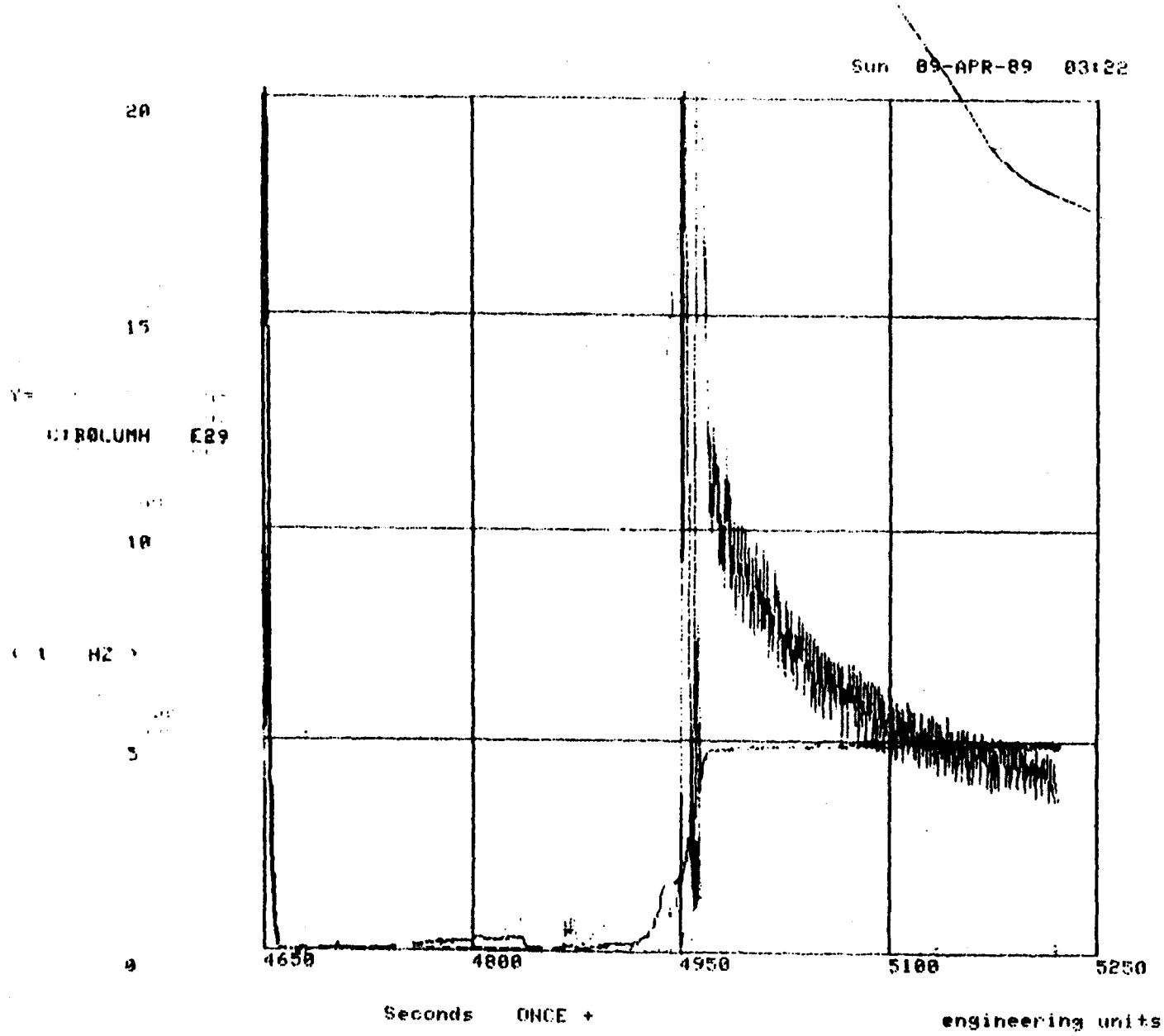
Sun 09-APR-89 03:22
20
15
10
5
0
4650
4800
4950
5100
5250
Seconds ONCE +
engineering units

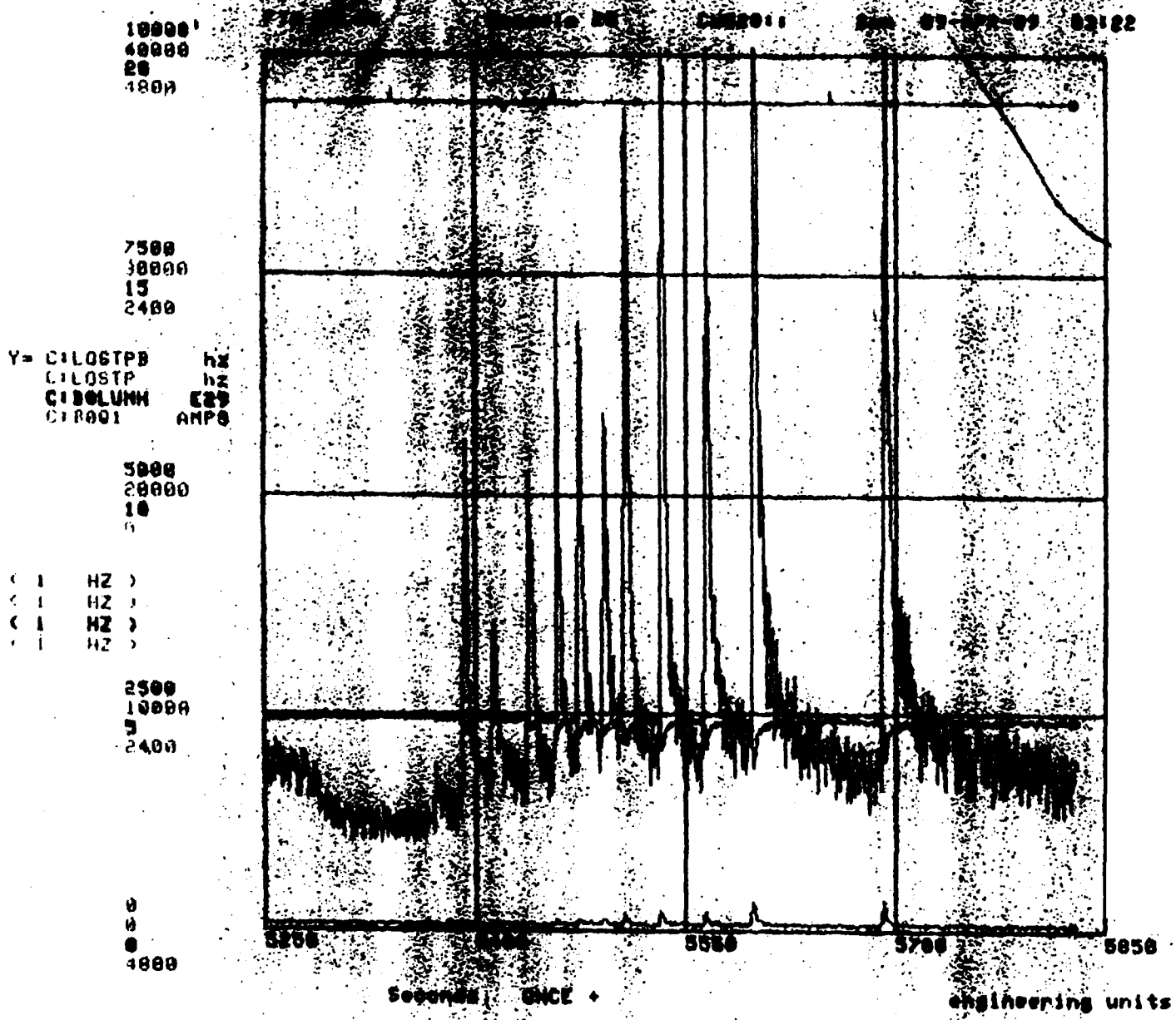
10000
40000
20
4800
7500
30000
15
2400
Y= C:LOGTPB hz
C:LOSTP hz
C:BOLUNH E29
C:B001 AMPS
5000
20000
10
0
(1 HZ)
(1 HZ)
(1 HZ)
(1 HZ)
2500
10000
5
2400
0
0
0
4800
5550
5600
5700
5850
Seconds, ONCE +
engineering units

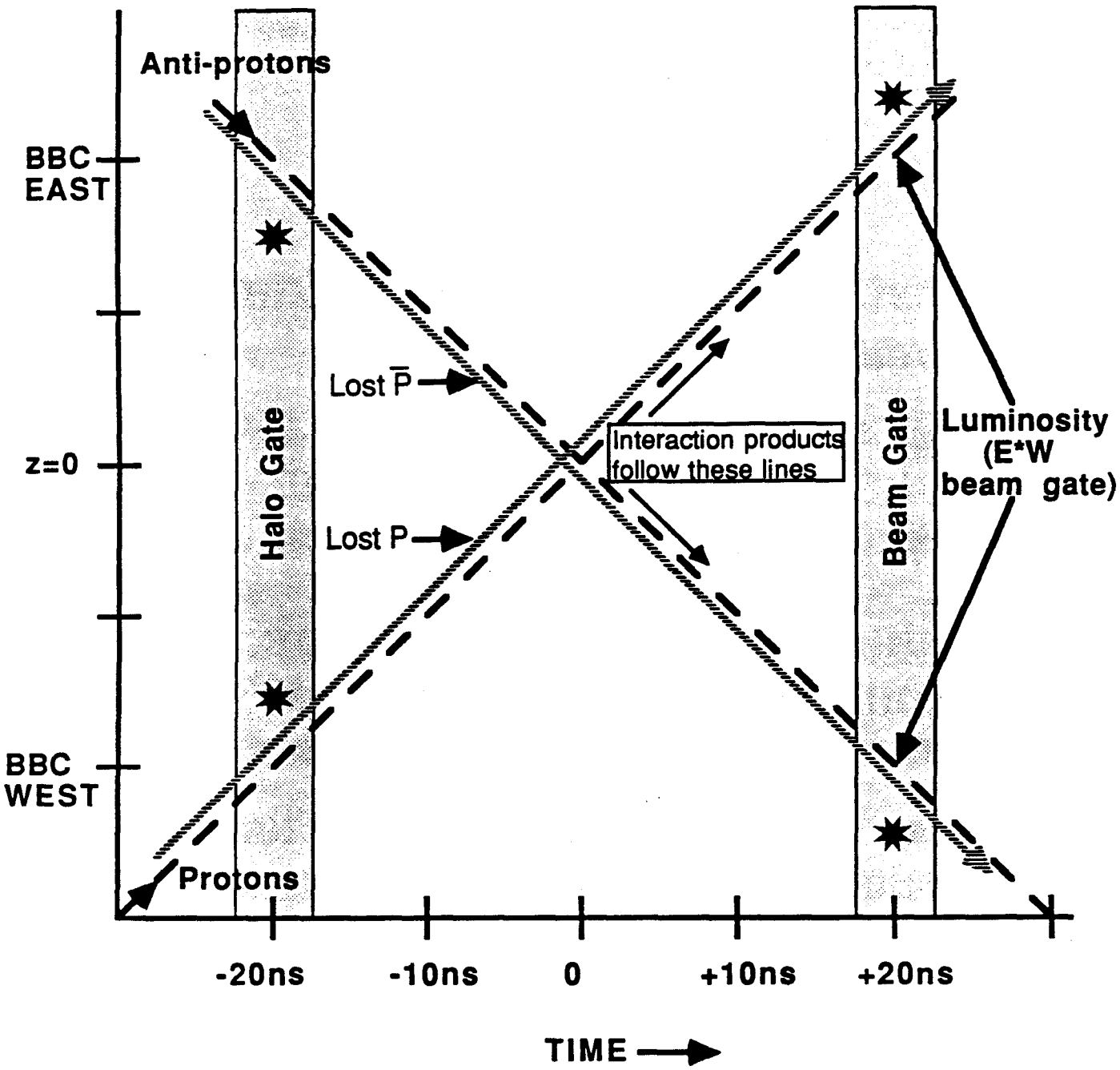
Anti-protons
BBC EAST
z=0
BBC WEST
Protons
Halo Gate
Lost $\bar{P}$
Lost P
Interaction products follow these lines
Beam Gate
Luminosity (E*W beam gate)
-20ns
-10ns
0
+10ns
+20ns
TIME

What To Do At SSC?

- **Need Lost P like signal for best sensitivity**

  - But careful placement is necessary to reduce backgrounds from beam-beam and halo from other direction.

- **With 16ns bunch spacing optimum monitor plane position is N(16)+4ns from nominal interaction point.**

  - *Very* fast gating is needed so that hits from opposite beam and interactions are not counted in the halo gate. Yet another SSC challenge in fast electronics.

- **Lost P monitor need not be at an interaction point**

  - In fact it's better if it's not since downstream side is always hit at interaction time (by definition).

Conclusions:

- Luminosity Monitoring as such is probably not a sensitive enough monitor.

- A loss monitor which detects particles travelling with the incoming beam but outside the pipe has been used at the TeVatron with a sensitivity of 1 part in 10^{12}. If optimized for the task it could probably be made at least an order of magnitude more sensitive.

- Implementation at the SSC requires scintillator planes (N+0.5) bunch spacings apart. This in turn requires very fast gating.

ROBUST VIBRATION SUPPRESSION AND DISTURBANCE REJECTION

Rich Fabiano, Andy Kurdila, Michael Pilant
Texas A&M University
College Station, Texas

presented at

Workshop on Vibrational Control and Dynamic Alignment Issues at the SSC

Superconducting Super Collider Laboratory
Dallas, Texas
February 11-14, 1992

OVERVIEW

(I) ONGOING RESEARCH

- ASTREX - PHILLIPS LABORATORY, EDWARDS AFB
- CSI EVOLUTIONARY MODEL - NASA LANGLEY

(II) FUTURE RESEARCH EFFORTS

- SPACE STATION - NASA JOHNSON SPACE CENTER
- SMART STRUCTURES

(III) ROBUST IDENTIFICATION AND CONTROL

- DISTRIBUTED PARAMETER SYSTEMS (PDE)
- DIFFERENTIAL GAMES ON HILBERT SPACES

  H^∞ ROBUSTNESS
  H^∞ DISTURBANCE REJECTION

ROLE OF IDENTIFICATION

(I) ONGOING RESEARCH

- ***ASTREX - PHILLIPS LABORATORY, EDWARDS AFB***

  Advanced Space Structures Technology Research Experiment

- ***Researchers***

  Dr. Rao Vadali
  Dr. John Junkins
  Dr. Tom Pollock
  Dr. Tarunj Singh

- ***PROJECT GOALS***

  NEAR MINIMUM TIME SLEW MANEUVER

  RAPID RETARGETTING

- ***DESIGN CONSTRAINTS***

  RAPID VIBRATION SUPPRESSION

  STINGENT LINE OF SIGHT / POINTING CRITERIA

- ***STRATEGY***

  LIAPUNOV STABLE FEEDBACK CONTROL LAW DESIGN

  TORQUE SHAPING / OPTIMAL REFERENCE INPUT

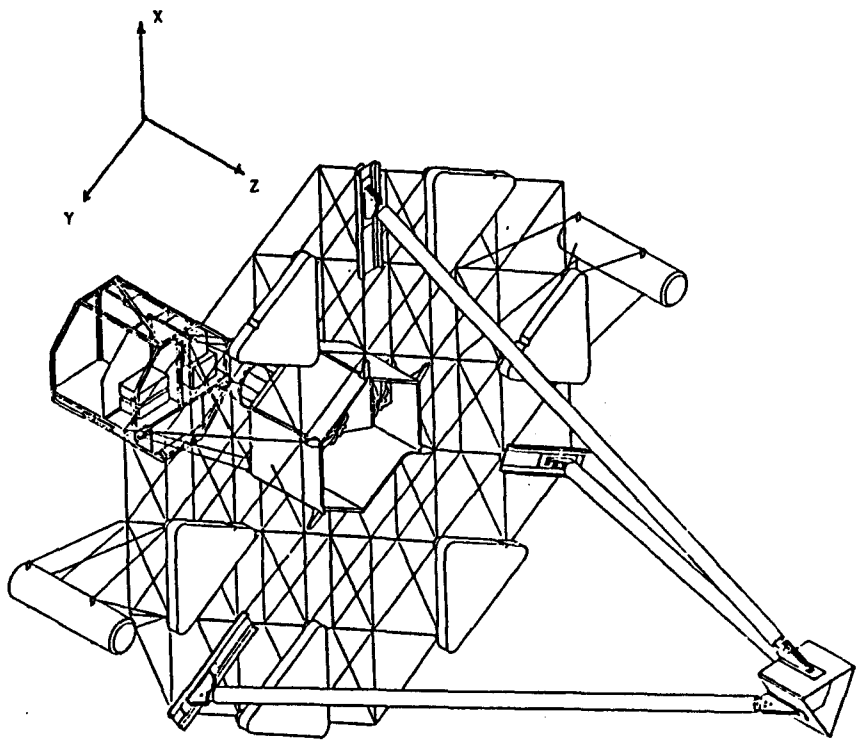
X
Y
Z

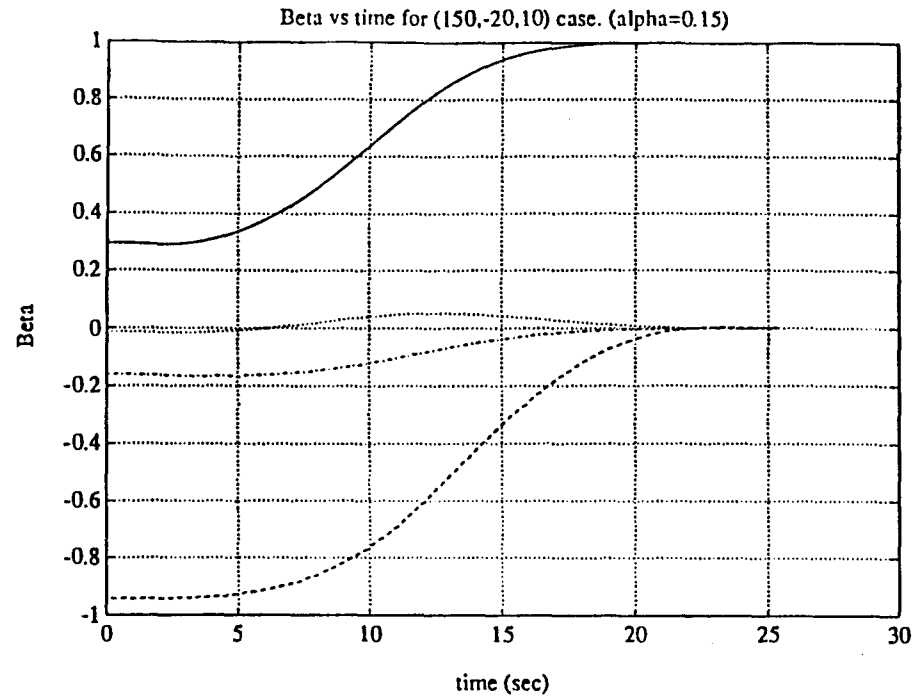
Beta vs time for (150,-20,10) case. (alpha=0.15)
Beta
time (sec)
1
0.8
0.6
0.4
0.2
0
-0.2
-0.4
-0.6
-0.8
-1
0
5
10
15
20
25
30

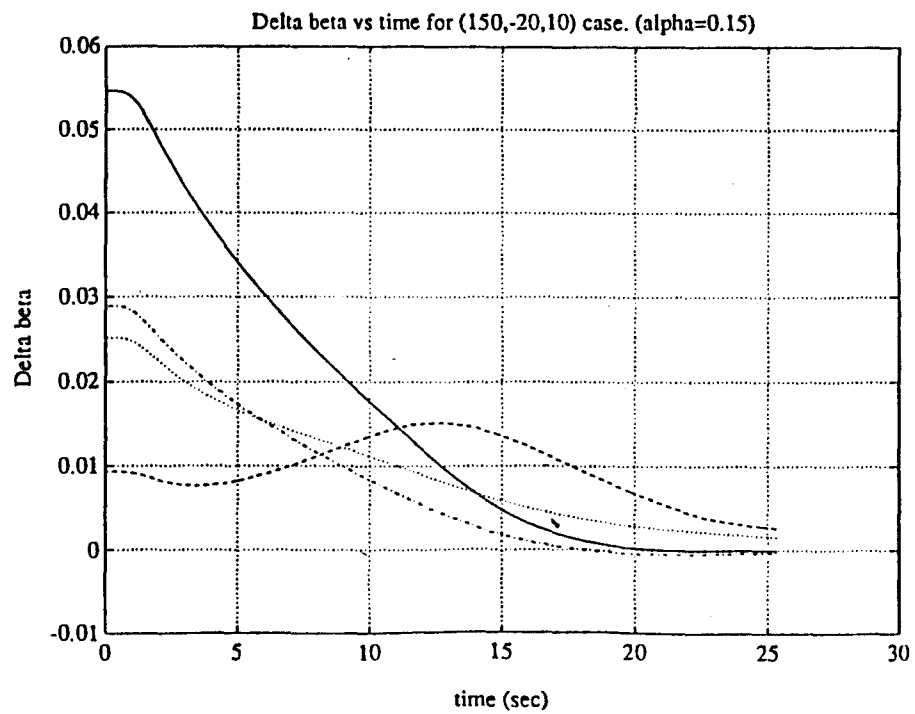
Delta beta vs time for (150,-20,10) case. (alpha=0.15)
Delta beta
time (sec)
0.06
0.05
0.04
0.03
0.02
0.01
0
-0.01
0
5
10
15
20
25
30

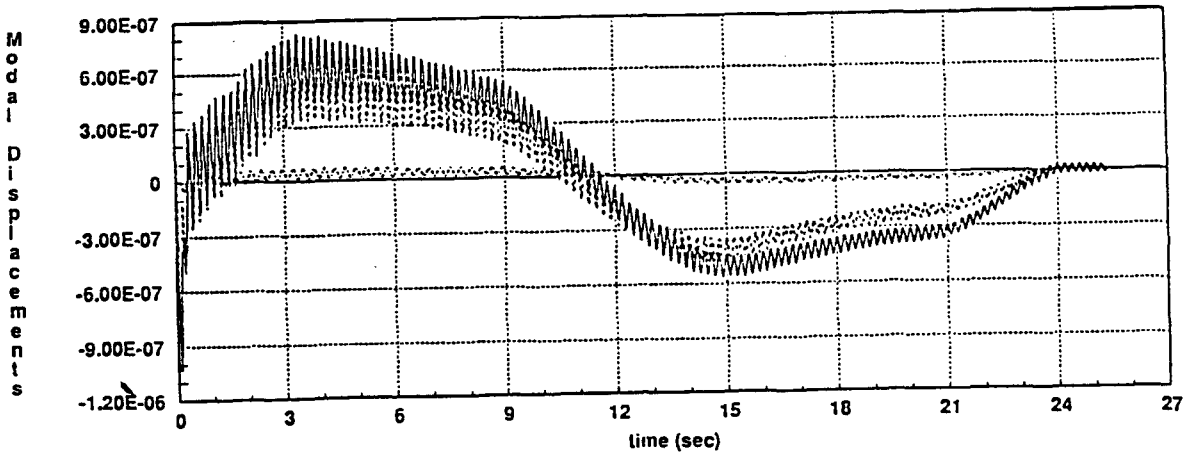
Modal Displacements
9.00E-07
6.00E-07
3.00E-07
0
-3.00E-07
-6.00E-07
-9.00E-07
-1.20E-06
0
3
6
9
12
15
18
21
24
27
time (sec)

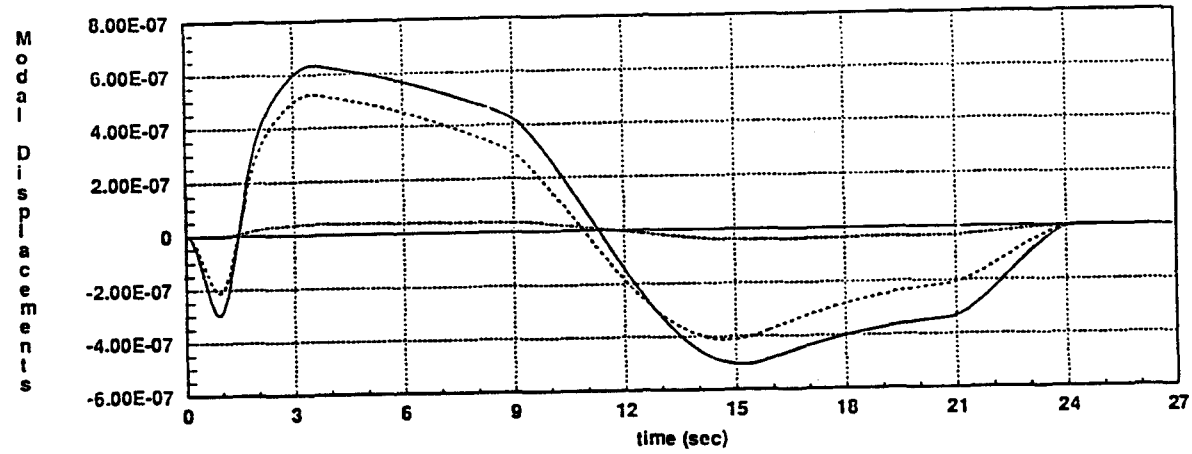
Modal Displacements
8.00E-07
6.00E-07
4.00E-07
2.00E-07
0
-2.00E-07
-4.00E-07
-6.00E-07
0
3
6
9
12
15
18
21
24
27
time (sec)

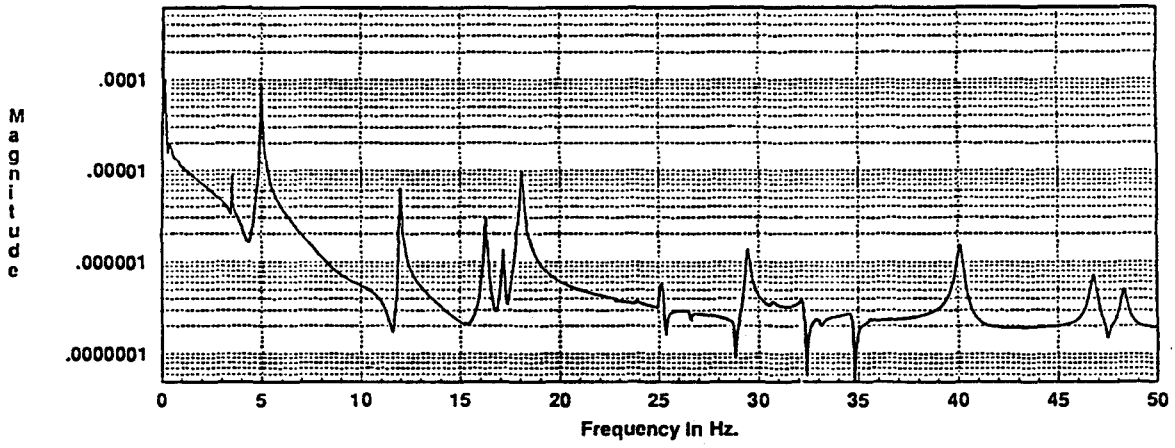
Magnitude
.0001
.00001
.000001
.0000001
0
5
10
15
20
25
30
35
40
45
50
Frequency in Hz.

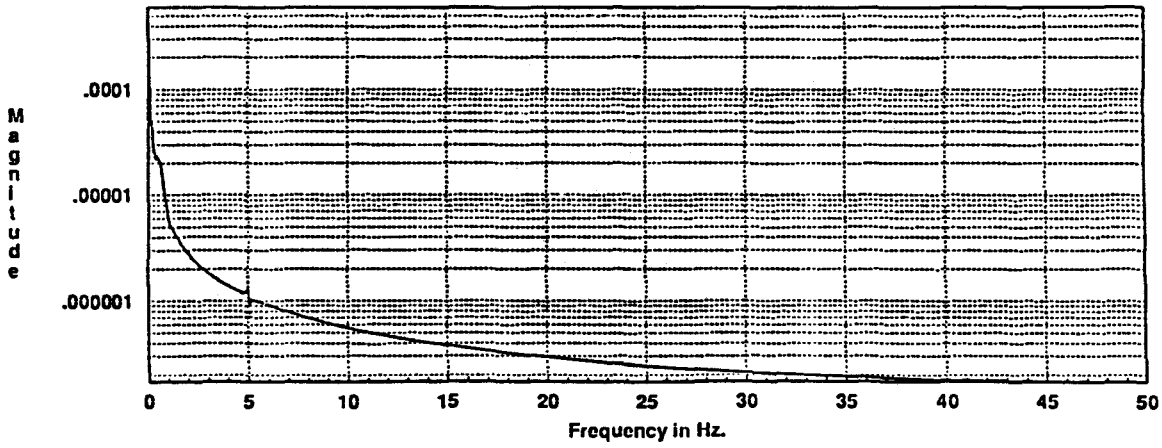
Magnitude
.0001
.00001
.000001
0
5
10
15
20
25
30
35
40
45
50
Frequency in Hz.

(I) ONGOING RESEARCH

- *CSI EVOLUTIONARY MODEL - NASA LANGLEY, HAMPTON VIRGINIA*

  CONTROL STRUCTURE INTERACTION MODEL

- *Researchers*

  Dr. Andrew Kurdila
  Dr. Michael Pilant
  Dr. John Junkins
  Dr. Tarunj Singh

- *PROJECT GOALS*

  LARGE SCALE OPEN / CLOSED LOOP SIMULATION

  (NEAR) REAL TIME SIMULATION AND CONTROL

  STRUCTURAL / CONTROL OPTIMIZATION

- *DESIGN CONSTRAINTS*

  CONTROL STRUCTURE INTERACTION EFFECTS

  STRINGENT LINE OF SIGHT / POINTING CRITERIA

  STRINGENT LASER FOCUSSING REQUIREMENTS

- *STRATEGY*

  CONCURRENT MULTIPROCESSING OPEN/CLOSED LOOP SIM

  ROBUST DECENTRALIZED CONTROL

  ROBUST ADAPTIVE CONTROL

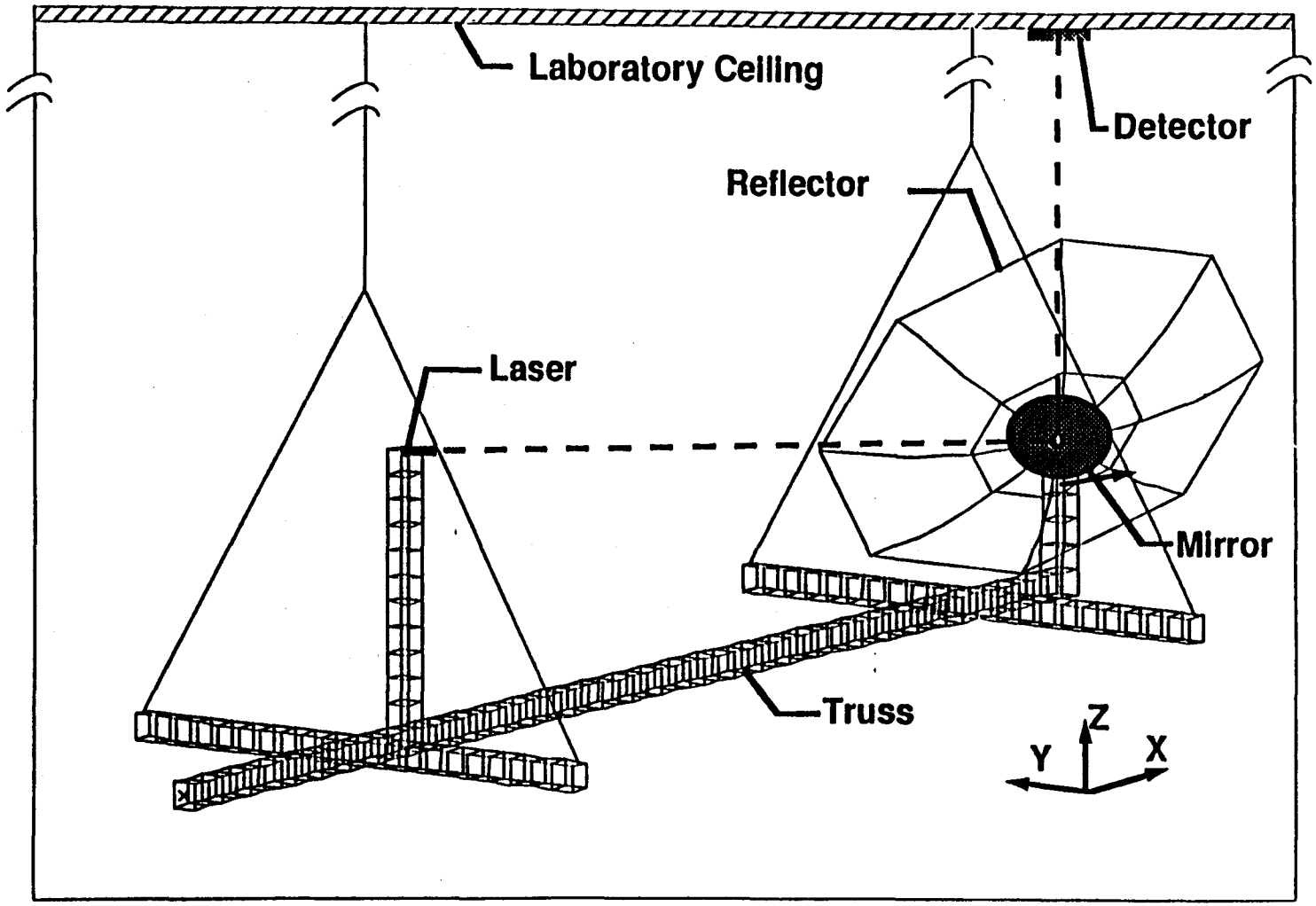

Figure 1. Schematic of CEM testbed

Phase 2 CSI Evolutionary Model

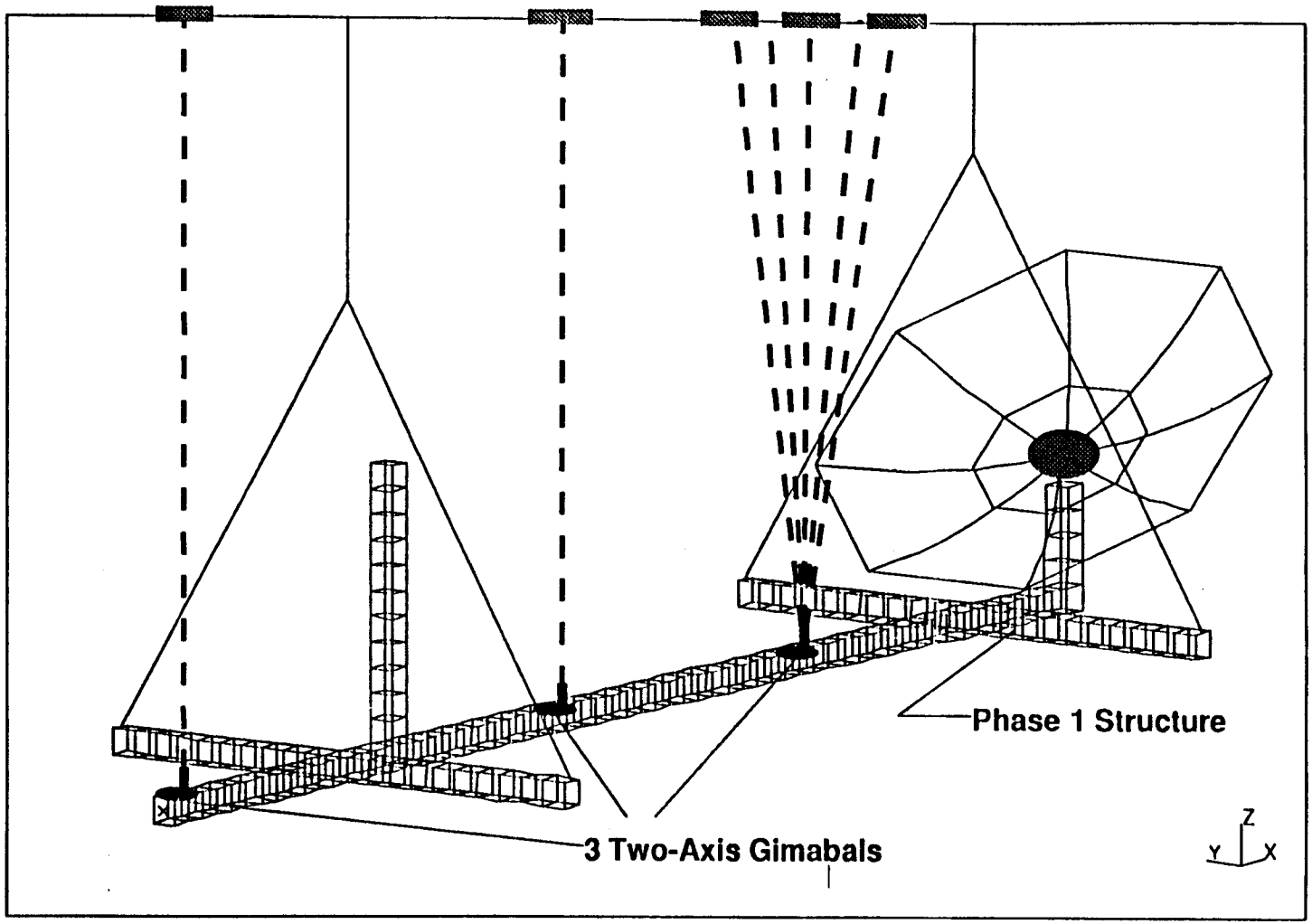

Multi-Payload Platform Control

- O Pointing and Scan
- O Retargeting
- O Decentralized, Centralized and Hierarchical Control

NASA LANGLEY
CONTROL STRUCTURE INTERACTION
EVOLUTIONARY MODEL

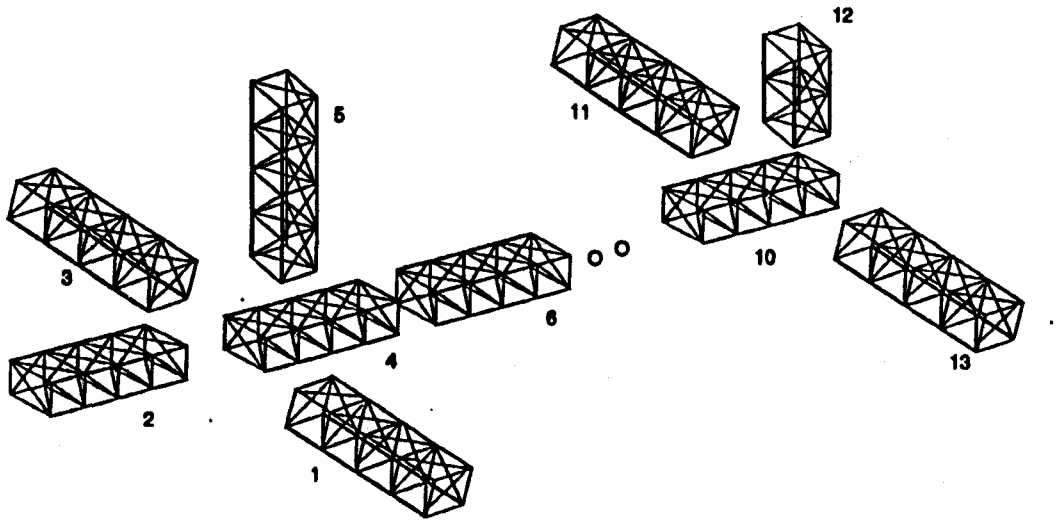

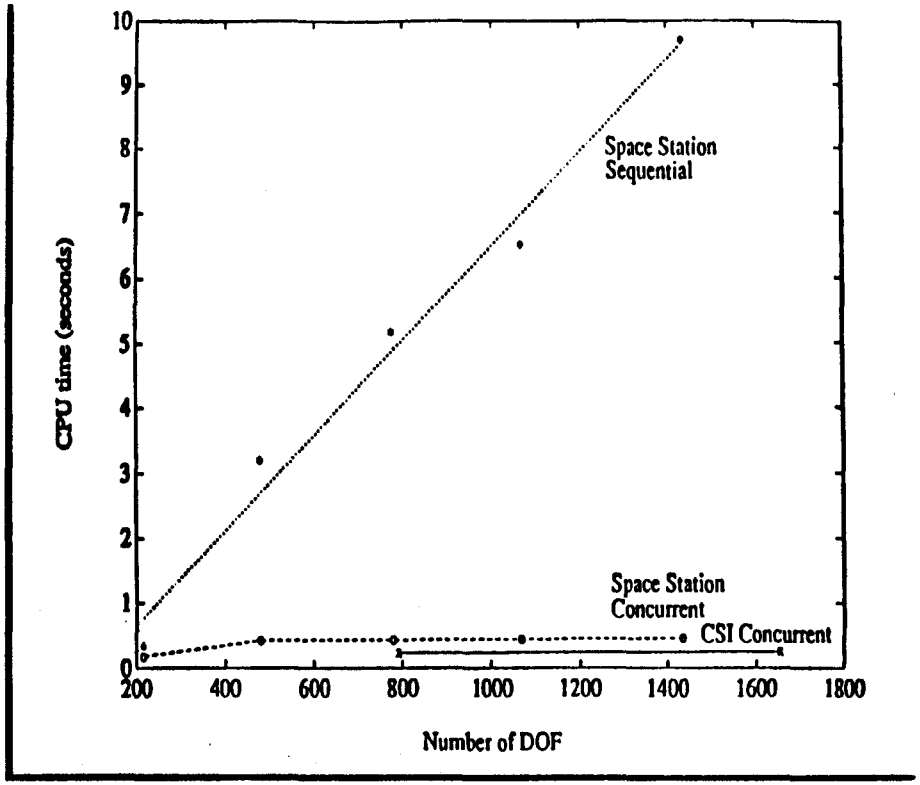

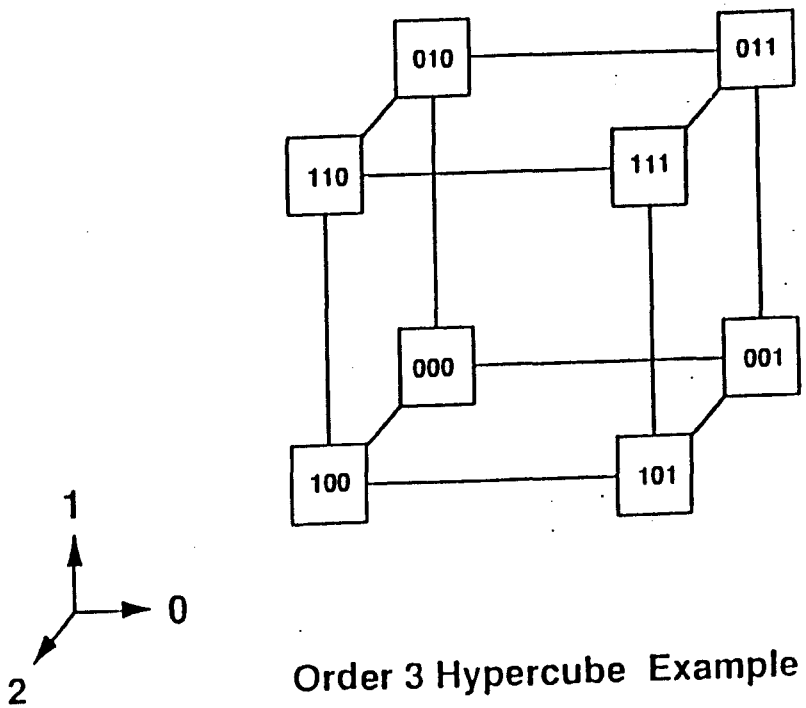

Order 3 Hypercube Example

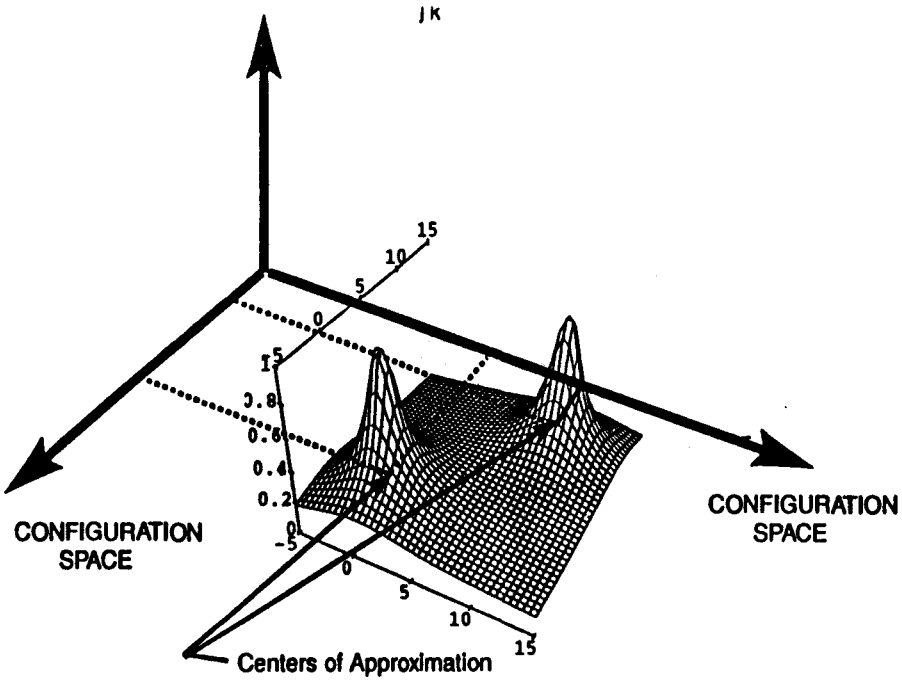

GEOMETRIC REALIZATION OF RBF APPROXIMANT

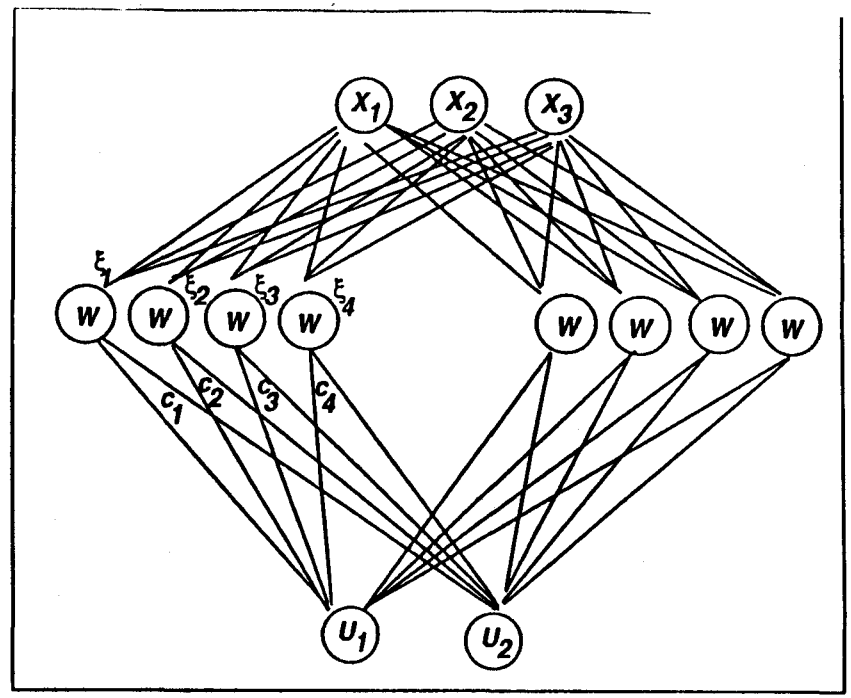

NEURAL NETWORK OF RBF APPROXIMANT

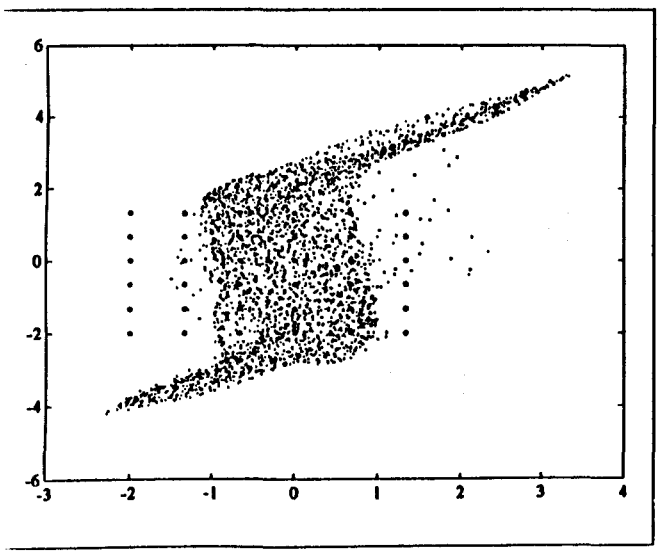

TRAJECTORY DYNAMICS VERSUS FIXED CENTERS OF APPROXIMATION

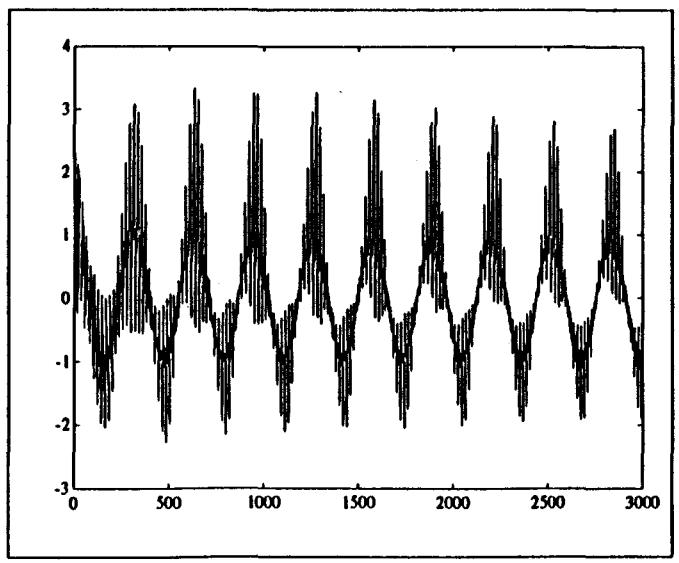

TRACKING PERFORMANCE WITHOUT CENTER ADAPTATION

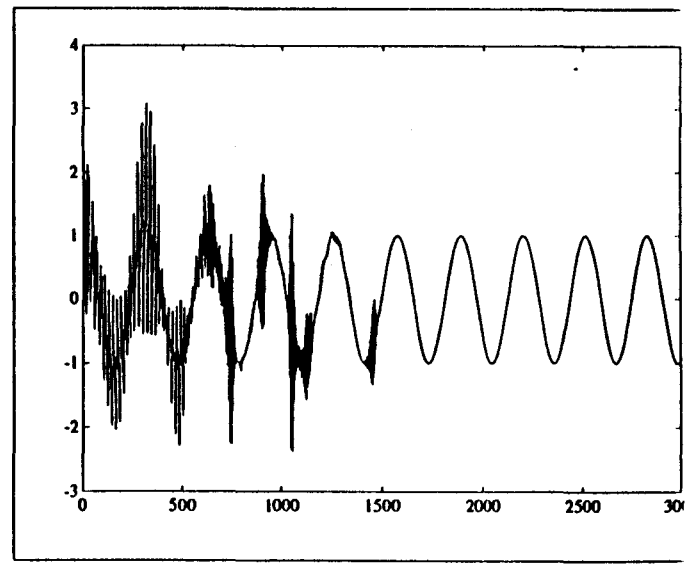

TRACKING PERFORMANCE WITH CENTER ADAPTATION

EVOLUTION OF CENTERS OF APPROXIMATION IN ADAPTIVE TRACKING CONTROL

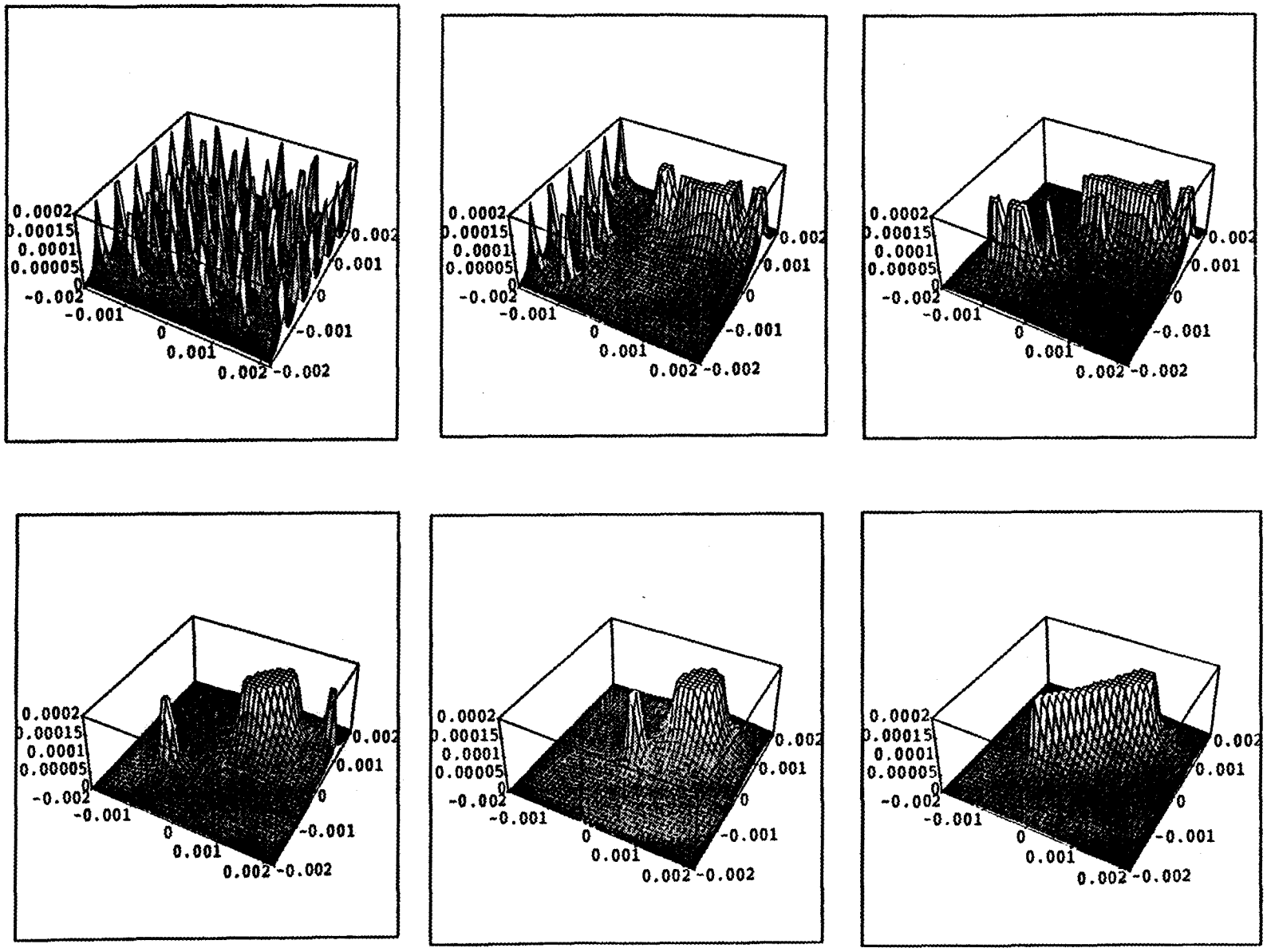

(II) FUTURE RESEARCH : PENDING AEROSPACE PROJECTS

SPACE STATION

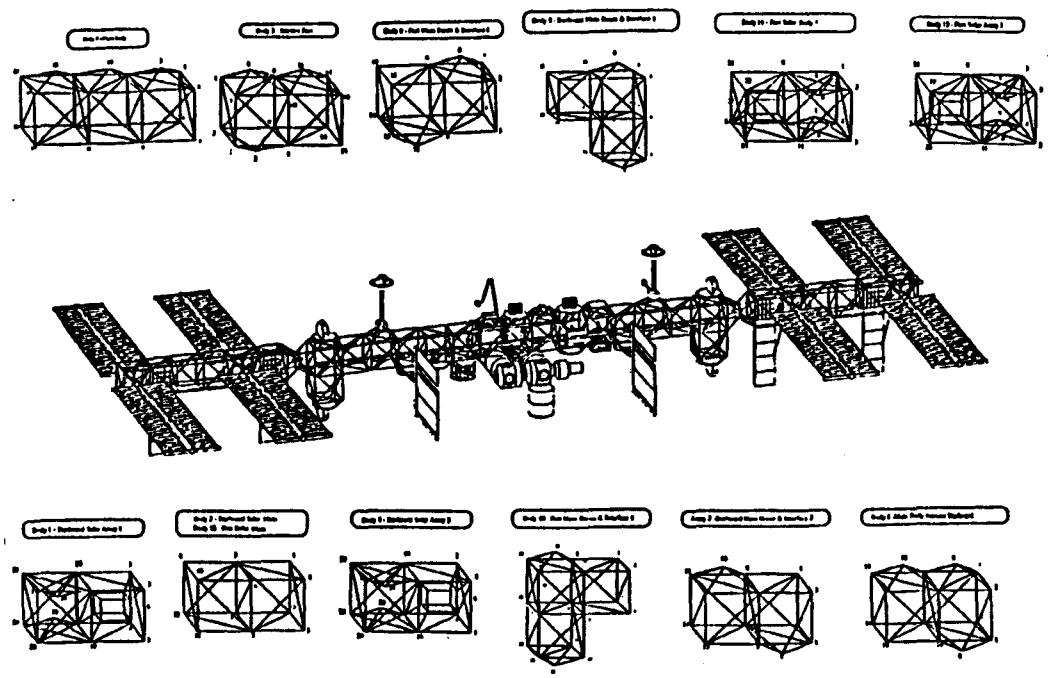

- BERTHING / DOCKING/ CONSTRUCTION
- DAMAGE / CONSTITUTIVE LAW EVOLUTION
- FAULT TOLERANT CONTROL
- MODEL UNCERTAINTY

SMART STRUCTURES (ADAPTIVE MATERIALS)

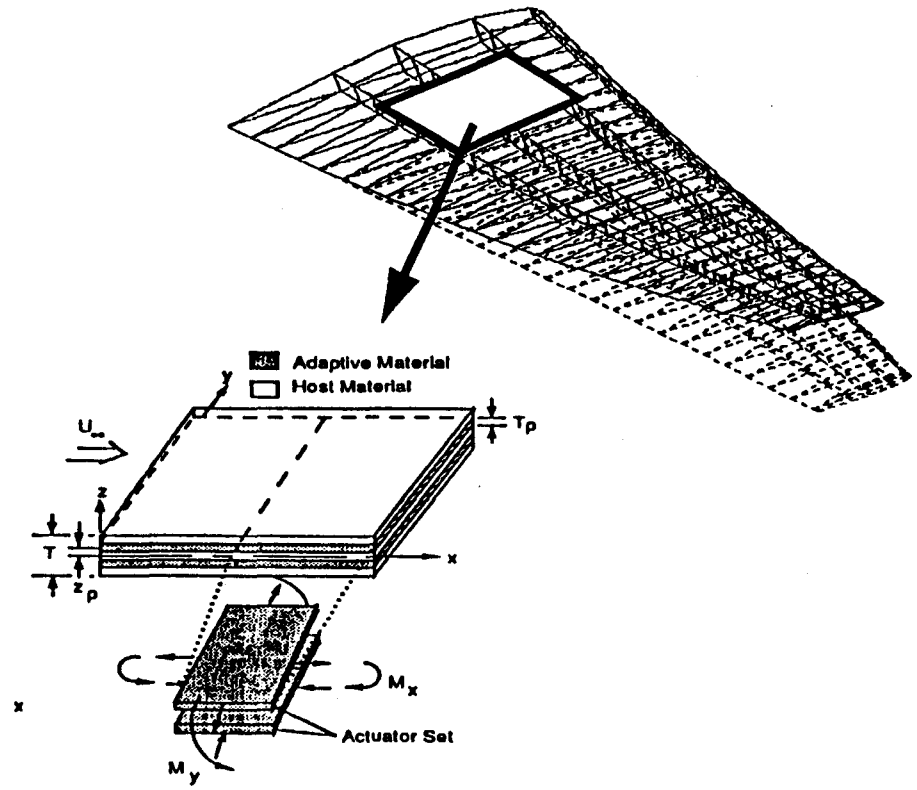

- NONLINEAR AEROELASTICITY
- DAMAGE / CONSTITUTIVE LAW EVOLUTION
- MODEL UNCERTAINTY

(III) ROBUST IDENTIFICATION AND CONTROL OF DPS

- *RESEARCHERS*

  Dr. Rich Fabiano
  Dr. Andy Kurdila
  Dr. Mike Pilant

- *PROBLEM CLASS*

  DISTRIBUTED PARAMETER SYSTEMS IN MECHANICS

  APPROXIMATION (ID) OF MATERIAL PROPERTIES

  CONTROL DESIGN OF UNCERTAIN SYSTEMS

- *STRATEGY*

  DIRECT TREATMENT OF GOVERNING PDE'S

  GAME THEORETIC CONTROL DESIGN IN HILBERT SPACE

  EIGENFUNCTION PROJECTION FOR DPS IDENTIFICATION

- *POTENTIAL ADVANTAGES*

  CONVERGENCE AND STABILITY OF "ORIGINAL SYSTEM"

  STABILITY /ROBUSTNESS OF "ORIGINAL SYSTEM"

  IDENTIFICATION ERROR - ESTIMATES AND APPROXIMATION

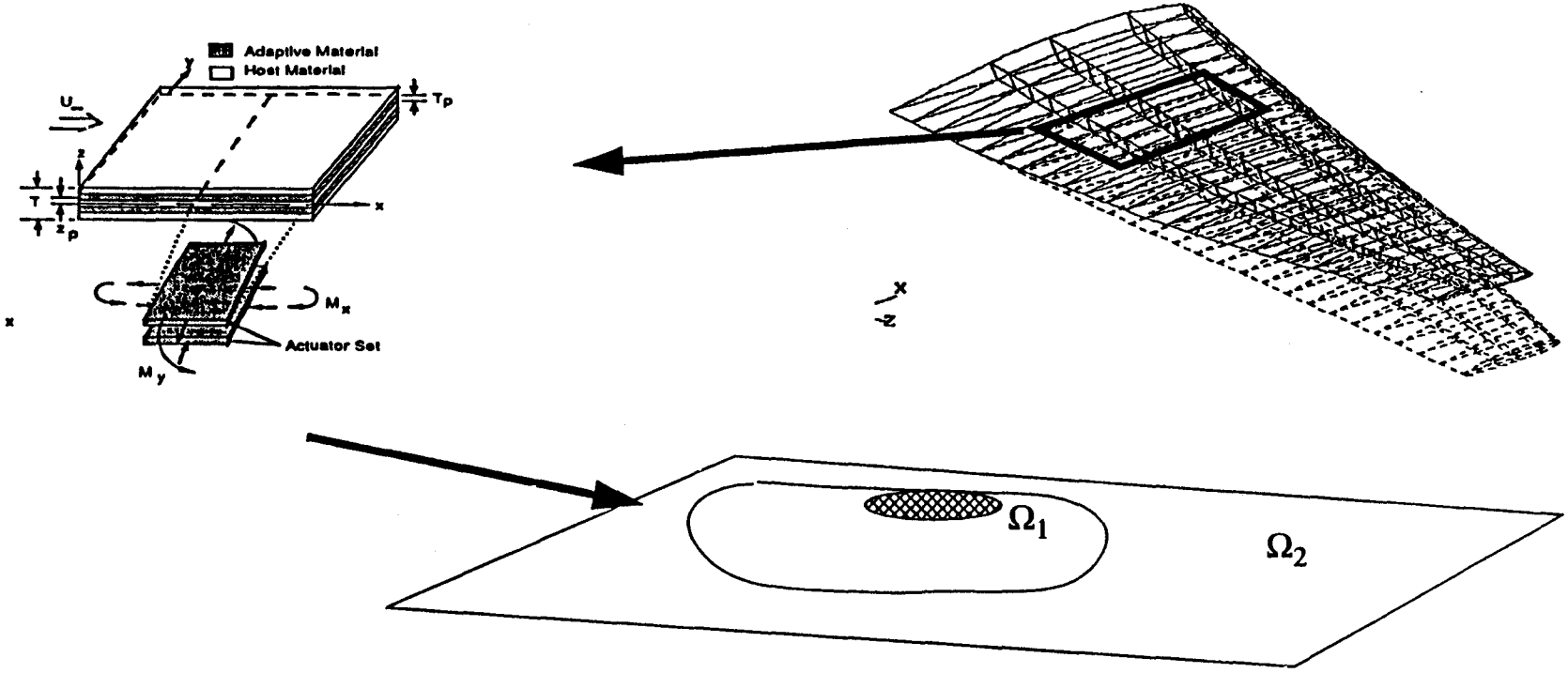

Prototype Equations

$$D_{11}\frac{\partial^4 w}{\partial x^4} + \rho h \frac{\partial^2 w}{\partial t^2} = \frac{\rho_\infty U_\infty}{M_\infty}\left(\frac{\partial w}{\partial x} + \frac{1}{U_\infty}\frac{\partial w}{\partial t}\right) - 2h_p z_p G(t)\, e_{31}^0 \int_{-b/2}^{b/2} F(x,y)\, P_0(x,y)\, dy$$

Robust Stabilization via *Distributed Min-Max Approach*

(i) Damage / Evolution $\quad F(x,y) = F_0(x,y) + \Delta F(x,y)$

(ii) Damage / Evolution $\quad e_{31} = e_{31}^0 + \Delta e_{31}(t)$

(iii) Nonlinear Aeroelasticity $\quad p = p_0 + \Delta p(w)$

(iv) Damage Accumulation $\quad D_{11} = D_{11}(w)$

RELATED WORK

LQR/LQG ON BANACH SPACES

BANKS [84,91]
GIBSON [79,81,89]
ITO [89,90]
KAPPEL [90]
ROSEN [90]
BURNS [91]

ROBUST STABILIZATION ON BANACH SPACES

CURTAIN [90]
CURTAIN [90]
BONTSEMA [91]

GAME THEORY

BENSOUSSAN [71]
BASAR [90]
RHEE, SPEYER [89,90]

PROBLEM STATEMENT

$$\begin{aligned} \dot{x}(t) &= Ax(t) + \beta u(t) + \varphi w(t) \\ y(t) &= Cx(t) \\ x(0) &= x_0 \in H \quad \textit{is given} \end{aligned} \tag{2.1}$$

$$C \in L(H,H) \qquad \beta \in L(U,H) \qquad \varphi \in L(W,H)$$

MILD SOLUTION

$$x = \Lambda Bu + \Lambda \Phi w + f \tag{2.3}$$

$$\mathbf{H} = L^2(0,\infty;H) \qquad \mathbf{U} = L^2(0,\infty;U) \qquad \mathbf{W} = L^2(0,\infty;W)$$

INTEGRAL OPERATOR

$$(\Lambda x)(t) = \int_0^t S(t-s)\,x(s)\,ds$$

MULTIPLICATION OPERATORS

$$\begin{aligned} (Bu)(t) &= \beta u(t) \\ (\Phi w)(t) &= \varphi w(t) \end{aligned}$$

"DISTURBANCE-AUGMENTED" COST FUNCTIONAL

$$J(u,w) = \frac{1}{2}\|y(u,w)\|^2_{\mathbf{H}} + \frac{1}{2}(Nu,u)_{\mathbf{U}} - \frac{1}{2\theta}(Mw,w)_{\mathbf{W}} \tag{2.4}$$

MULTIPLICATION OPERATORS

$$(Nu)(t) = Nu(t)$$
$$(Mu)(t) = Mu(t)$$

where

$$N \in L(U,U)$$
$$M \in L(W,W)$$

UPPER VALUE OF DIFFERENTIAL GAME

$$J_0 = \inf_{u \in \mathbf{U}} \sup_{w \in \mathbf{W}} J(u,w) \tag{2.5}$$

(P1) Find

$$(u^0, w^0) \in \mathbf{U} \times \mathbf{W}$$

such that

$$J_0 = \inf_{u \in \mathbf{U}} \sup_{w \in \mathbf{W}} J(u, w) = J(u^0, w^0) \qquad (2.6)$$

SATISFYING THE GOVERNING EQUATIONS

$$x^0 = \Lambda B u^0 + \Lambda \Phi w^0 + f \qquad (2.3)$$

(P2) FIND CONVERGENT APPROXIMATIONS

$$(u_n, w_n) \to (u^0, w^0)$$

EXISTENCE

$$(H1) \qquad (Nu,u)_{\mathbf{U}} \geq d_1 \|u\|^2_{\mathbf{U}}$$

$$(H2) \qquad (Mw,w)_{\mathbf{W}} \geq d_2 \|w\|^2_{\mathbf{W}}$$

$$(H3) \qquad BN^{-1}B^* - \theta\Phi M^{-1}\Phi^* \geq 0$$

Theorem (3.1) : Suppose that conditions (H1), (H2) and (H3) hold. Then there exists a unique

$$(u^0, w^0) \in \mathbf{U} \times \mathbf{W}$$

such that

$$J_0 = \inf_{u \in \mathbf{U}} \sup_{w \in \mathbf{W}} J(u, w) = J(u^0, w^0)$$

$$x^0 = \Lambda B u^0 + \Lambda \Phi w^0 + f$$

Moreover, (u^0,w^0) is given by

$$w^0(t) = \theta M^{-1}\Phi\Pi x^0(t) \qquad (3.1)$$

$$u^0(t) = -N^{-1}B\Pi x^0(t) \qquad (3.2)$$

and Π solves the Algebraic Riccati equation

$$(\Pi x, Ay)_H + (Ax, \Pi y)_H + (C^*Cx, y)_H - (\Pi\Omega\Omega\Pi x, y)_H = 0$$

for any $y \in D(A) \subset H$ where

$$\Omega \equiv [BN^{-1}B^* - \theta\Phi M^{-1}\Phi^*]^{1/2} \geq 0$$

APPROXIMATION

$$H = \overline{\bigcup_{n=1}^{\infty} H_n}$$

Assume

$$A_n | H_n \to H_n$$
$$\Omega_n | H \to H_n$$
$$C_n | H_n \to H$$

FINITE DIMENSIONAL ARE.

$$A_n^* \Pi_n + \Pi_n A_n - \Pi_n \Omega_n \Omega_n \Pi_n + C_n^* C_n = 0$$

APPROXIMATION HYPOTHESES

(H4) For each $x \in H$, one has

(i) $S_n(t) P_n x \to S(t) x$ (ii) $S^*_n(t) P_n x \to S^*(t) x$

where the convergence is uniform in t on bounded subsets of $(0, \infty)$.

(H5) For each $x \in H$, one has

(i) $\Omega_n x \to \Omega x$ ii) $C_n P_n x \to Cx$

$\Omega_n^* P_n x \to \Omega^* x$ $C_n^* x \to C^* x$

(H6) The family of pairs (A_n, Ω_n) and (A_n, C_n) are uniformly stabilizable and uniformly detectable, respectively. In other words,

(i) there exists a sequence of operators $K_n \in L(H_n, H)$ such that

$$sup\|K_n\| \leq \infty$$

$$\left\| e^{(A_n - \Omega_n K_n)t} P_n \right\| \leq M_1 e^{-\omega_1 t} \qquad t \geq 0$$

for some positive constants M_1 and ω_1, and

(ii)there exists a sequence of operators $G_n \in L(H_n, H)$ such that

$$sup\|G_n\| \leq \infty$$

$$\left\| e^{(A_n - G_n C_n)t} P_n \right\| \leq M_2 e^{-\omega_2 t} \qquad t \geq 0$$

for some positive constants $M_2 > 1$ and ω_2.

Theorem 2 : Under the assumptions (H4)-(H6),

(i) the solution Π_n of the finite dimensional ***approximating Algebraic Riccati Equation converges strongly*** *to Π, the unique solution of the infinite dimensional Riccati Equation.*

$$\lim_{n \to \infty} \| \Pi x - \Pi_n P_n x \| \to 0$$

(ii) ***the approximate closed loop semigroups converge*** to the closed loop semigroup

$$S_n(t) P_n x \to S(t) P x$$

where $S_n(t)$ and $S(t)$ are the C0 semigroups generated by

$$A_n - P_n \Omega^2 P_n \Pi_n = A_n - P_n (BN^{-1}B^* - \theta \Gamma M^{-1} \Gamma^*) P_n \Pi_n$$

and

$$A - \Omega^2 \Pi = A - (BN^{-1}B^* - \theta \Gamma M^{-1} \Gamma^*) \Pi$$

respectively,

(iii) ***the closed loop semigroup*** $S(t)$ ***is exponentially stable***

$$\| S(t) \| \leq k e^{-\omega t}$$

for some w>0.

(iv) Finally, the closed loop transfer funtion satisfies ***the disturbance attenuation bound***

$$\| T_{cl} \|_\infty < \frac{1}{\sqrt{\theta}} \qquad \textit{where} \qquad T_{cl} \left| \left(d \to \left\{ \begin{matrix} x \\ u \end{matrix} \right\} \right) \right.$$

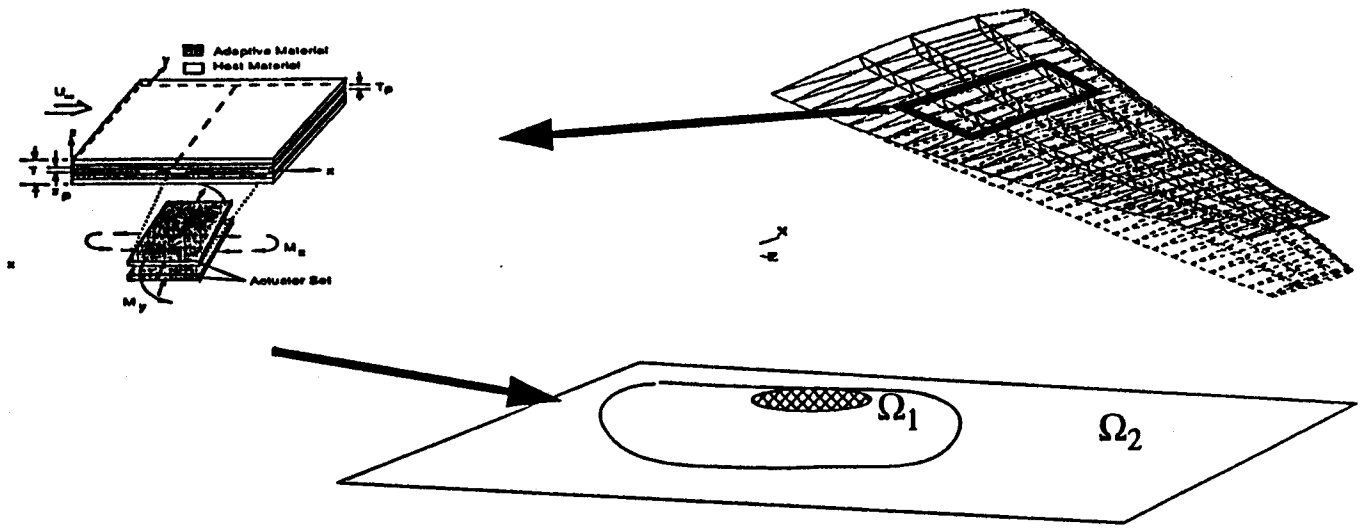

Prototype Equations

$$\frac{\partial^2}{\partial x^2}\left(D\frac{\partial^2 w}{\partial x^2}\right)+2\frac{\partial^2}{\partial y^2}\left(D\frac{\partial^2 w}{\partial x^2}\right)+\frac{\partial^2}{\partial y^2}\left(D\frac{\partial^2 w}{\partial y^2}\right)+\rho h\frac{\partial^2 w}{\partial t^2} = 0 \qquad (plate) \qquad (x,y)\in\Omega$$

$$\frac{\partial^2}{\partial x^2}\left(D\frac{\partial^2 w}{\partial x^2}\right)+\rho h\frac{\partial^2 w}{\partial t^2} = 0 \qquad (beam) \qquad x\in\Omega$$

$$w = 0 \quad or \quad \frac{\partial w}{\partial n} = 0 \qquad (x,y)\in\partial\Omega$$

Identify/Estimate the Change in Material Properties

(i) Given

$$\rho = \rho(x,y)$$

$$D = D_0(x,y)$$

(ii) Find

$$D(x,y) = D_0(x,y) + \Delta D(x,y)$$

IDENTIFICATION OF DISTRIBUTED PARAMETER SYSTEMS

Strategy - Iterative Projection

$$\lambda_k(D) = eigenvalue$$

$$w_k(x, y; D) = eigenfunction \qquad (normalized \quad)$$

$$\Delta\lambda_k = \lambda_k(D) - \lambda_k(D_0)$$

$$\Delta D = D - D_0$$

Fundamental Identity

$$\Delta\lambda_k = \frac{\iint \Delta D \, \{ \nabla w_k(D) \bullet \nabla w_k(D_0) \} \, dV}{\iint \{ w_k(D) \bullet w_k(D_0) \} \, dV}$$

$$= \frac{\iint \Delta D \| \nabla w_k(D_0) \|^2 dV}{\iint \| \nabla w_k(D_0) \|^2 dV} + O(\Delta D^2)$$

$$= \iint \Delta D \| \nabla w_k(D_0) \|^2 dV + O(\Delta D^2)$$

IDENTIFICATION OF DISTRIBUTED PARAMETER SYSTEMS

Basis for Approximation - ,

$$w_k(x, y; D_0)$$

$$\Delta D(x, y) = \sum_{k \in K} D_k \bullet w_k(x, y; D_0)$$

$$\tilde{D}(x, y) = D_0(x, y) + \Delta D(x, y)$$

Projection Onto Finite Dimensions

$$P_K[f] = \sum_{k \in K} (f, w_k(x, y; D_0)) \bullet w_k(x, y; D_0)$$

One can show

$$\|\tilde{D} - P_K[D]\|_{L_2} \leq (1 + c\|D - D_0\|_{L_2}) \|D - P_K[D]\|_{L_2}$$

$$\|\tilde{D} - D\|_{L_2} \leq (2 + c\|D - D_0\|_{L_2}) \|D - P_K[D]\|_{L_2}$$

provided that

$$\frac{\|D - P_K[D]\|_{L_2}}{\|D\|_{L_2}}$$

is small enough

Roughly Speaking,

$$\underbrace{\frac{\|\tilde{D}-D\|_{L_2}}{\|D\|_{L_2}}}_{\textit{reconstruction error}} \leq \underbrace{2\frac{\|D-P_K[D]\|_{L_2}}{\|D\|_{L_2}}}_{\textit{optimal } L_2 \textit{ approximation error}}$$

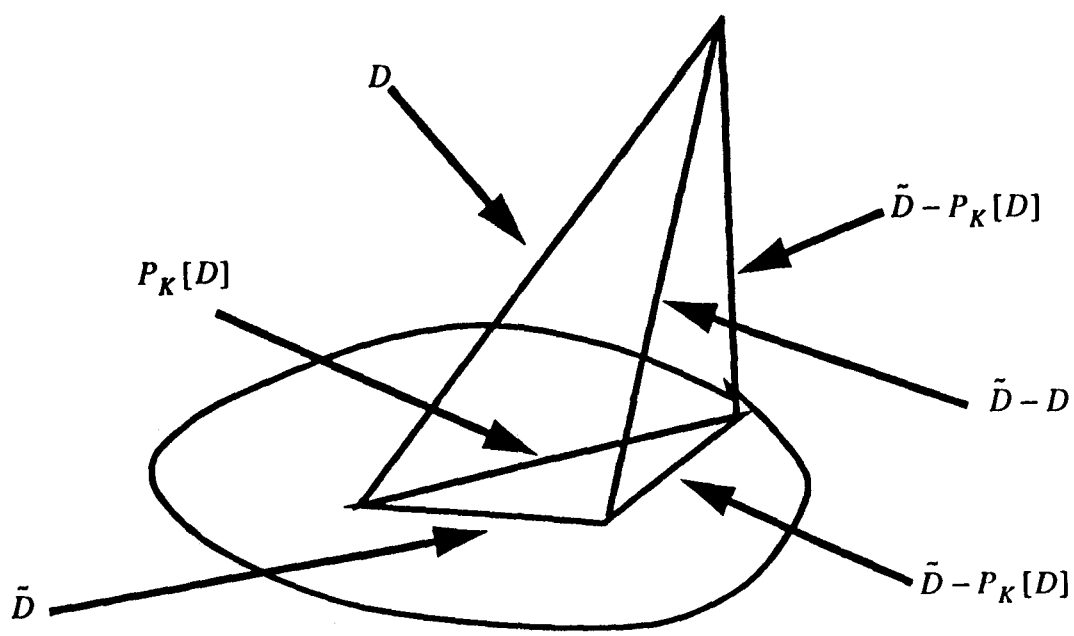

Dynamic Control of Large Structures

James J. Allen

Structural Dynamics Division

Sandia National Laboratories

Albuquerque, NM 87111

Active Control of Large Structures

Structural Analysis

1. Preliminary Design and Analysis
2. Plant Modeling

Structural Testing

1. Disturbance Requirements
2. Plant Model Identification
3. Component Testing

Controller Design

1. Design Methodology
2. Implementation

Components

1. Sensors
2. Actuators
3. Processors

Approaches to Vibration Suppression of Large Structures

1. System Design
2. Passive Damping
3. Active Damping
4. Active Control

System Design

Design Considerations for Vibration Suppression:

1. Structural Stiffness
2. Isolation Mass
3. Weight, Space and Geometry Constraints

Considerations if Active Control is to be considered:

1. Nonlinearity
2. Hysteresis
3. Repeatability
4. System Variability

System Design: Adaptive Mirror (Initial Design)

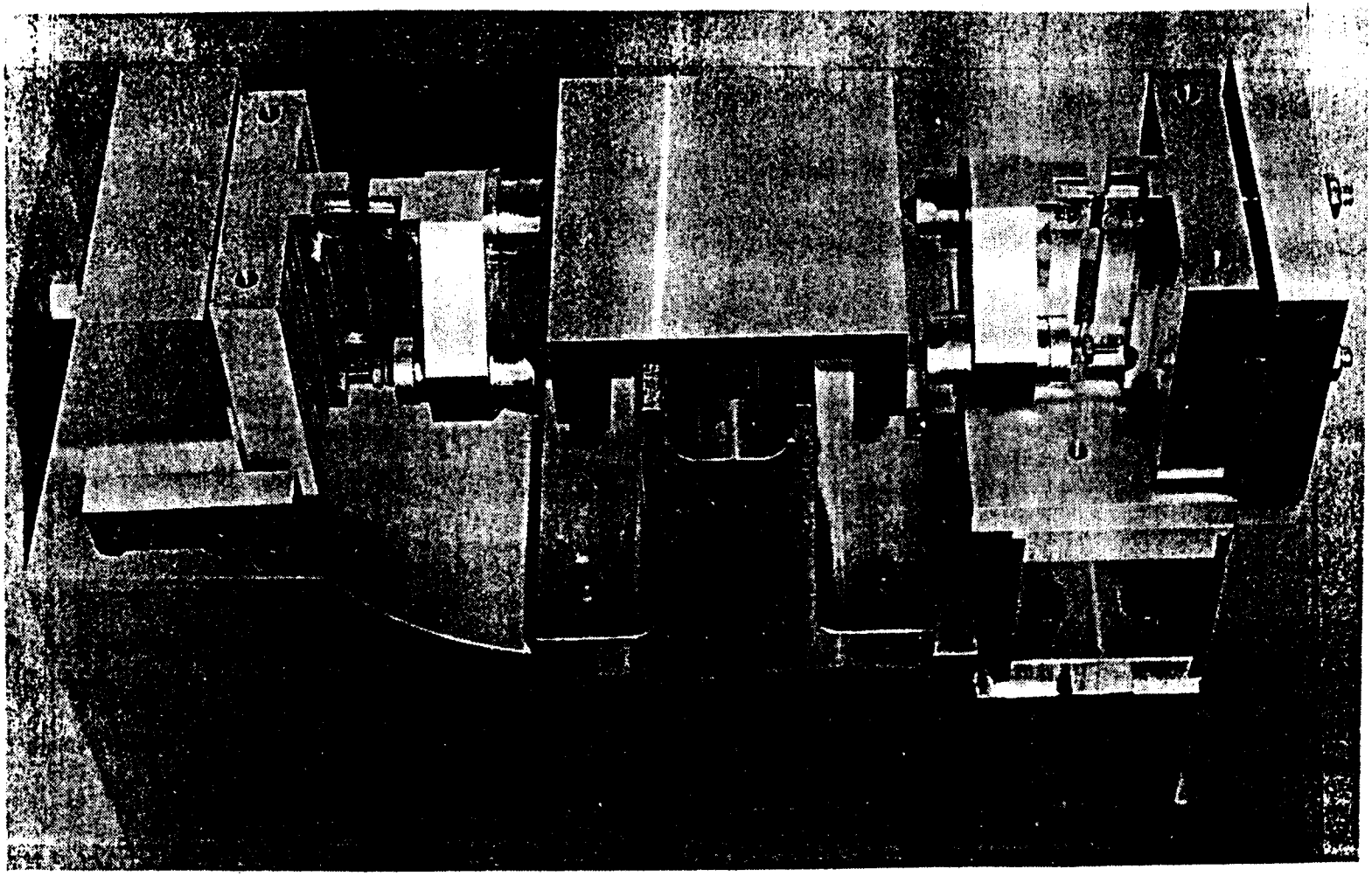

System Design: Adaptive Mirror (Redesign)

Design Constraints

- Control System
  - Linear and Repeatable
  - High modal frequencies
  - Actuator Authority
  - Rigid Body Control
- System Performance
  - Maximum Stress
  - Poisson's Effect
  - Flattening Effect
  - Thermal Isolation
  - Vibration Isolation

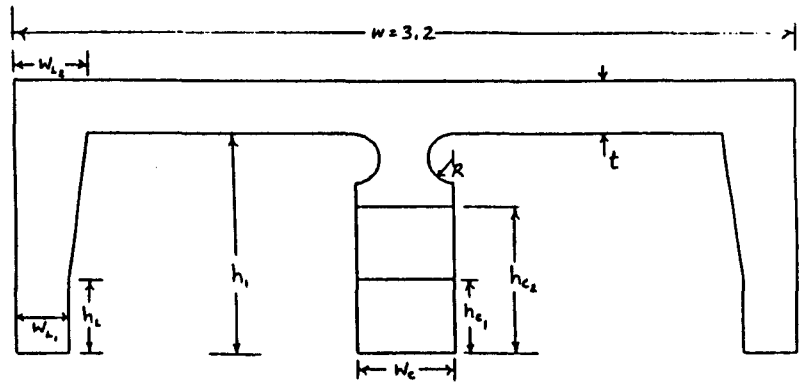

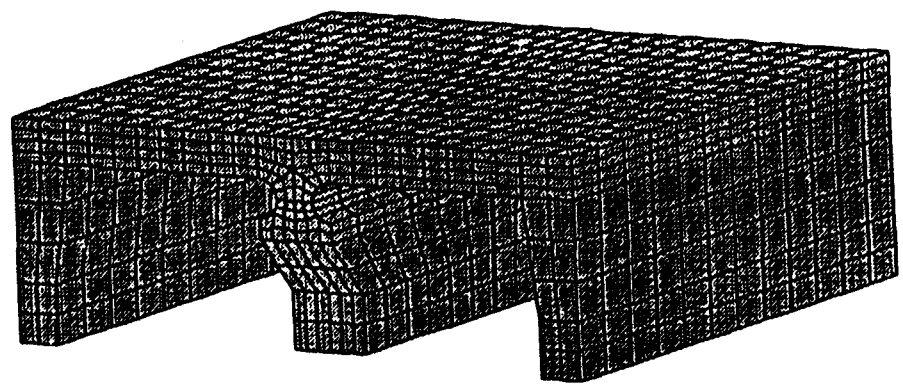

Passive Damping

Purpose:

Induce damping in the system dynamics that are:

- significant in the system response
- detrimental to the dynamics of an active control system

Approaches:

- Lumped damping elements (i.e. damping struts, tuned masses)
- Coatings and Constrained Layer Damping

Pro:

- Guaranteed Stable.
- No peripheral equipment necessary

Con:

- Frequency range and performance frequently limited.
- Difficult to predict the damping apriori

Passive Damping

Developed a rigorous method for calculation of damping matrices of linearly viscoelastic structures:

- D. J. Segalman, "Calculation of Damping Matrices for Linearly Viscoelastic Structures", *J. App. Mech.*, Sept. 1987, Vol. 109, pp. 585-588.

Applied to the *"CSA Beam"* at Phillips Laboratory:

Mode	Test		Prediction	
	Frequency	Damping	Frequency	Damping
1st Bending	15.7 Hz	5.8 %	15.1 Hz	6.1 %
2nd Bending	39.8 Hz	8.1 %	38.0 Hz	11.3 %
3rd Bending	73.8 Hz	8.5 %	70.6 Hz	12.0 %
1st Torsional	91.8 Hz	2.4 %	87.2 Hz	1.7 %
4th Bending	116.5 Hz	8.4 %	113.4 Hz	10.2 %
5th Bending	169.6 Hz	7.1 %	166.8 Hz	9.2 %
2nd Torsional	190.0 Hz	-	177.5 Hz	2.6 %

Active Damping

Purpose:

Induce Damping in structural modes that are:

- decoupled and highly significant in the system response
- detrimental to the dynamics of a coordinated active control system

Approach:

Use control techniques that are highly stable:

- Colocated Sensor - Actuators
- Single Input - Single Output (SISO)
- Velocity Feedback
- Impedance Matching

Active Control of Large Structures

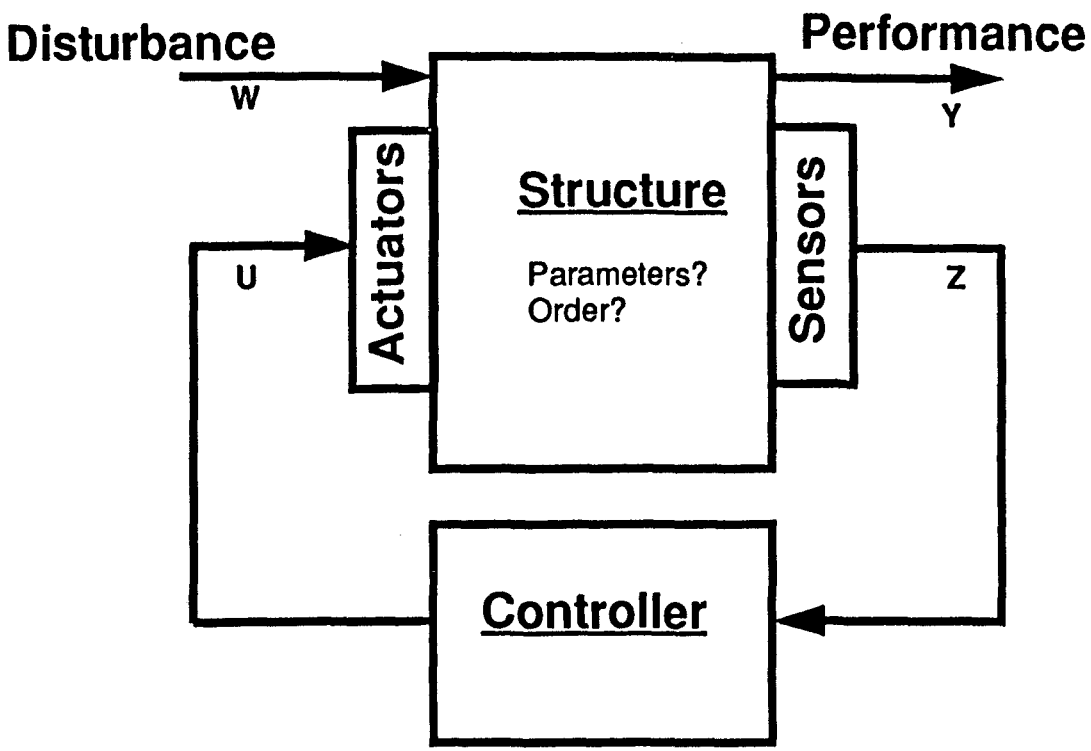

Active Control of Large Structures (Issues)

- Large Order Systems
- Imperfect Models
- Multiple Highly Coupled Feedback Loops (MIMO)
- Precision Performance Requirements
- Limited Actuator Power
- Limited Processor Capacity

Active Control of Large Structures (basic problem)

Given a Linear Model of the system:

$$\dot{x} = \mathbf{A}x + \mathbf{B}u + \mathbf{D}u$$
$$z = \mathbf{M}x + v$$
$$y = \mathbf{C}x$$

Design a Linear Feedback Control System:

$$\dot{x}_c = \mathbf{A}_c x_c + \mathbf{B}_c z$$
$$u = \mathbf{C}_c x_c + \mathbf{D}_c z$$

Designed to minimize some criteria or satisfy some constraints:

Active Control of Large Structures (basic problem)

This is a very general and broad problem statement. When the criteria and constraints are specified a large number of control design techniques result.

- **Linear Quadratic Gaussian (LQG)**
  - Cost Function:

$$V = \lim_{t \to \infty} E\left[y(t)^T Q y(t) + u(t)^T R u(t)\right]$$

  - Many variations on this basic theme:
    - Reduced Order LQG
    - Frequency Weighted LQG (gain stabilize uncertain dynamics)
    - Optimal Projection (Fixed order control design to minimize spillover)

- **H_∞:**
  - Cost Function: $V = \left\| \begin{matrix} W_1 S \\ W_2 T \end{matrix} \right\|_\infty$

Active Control

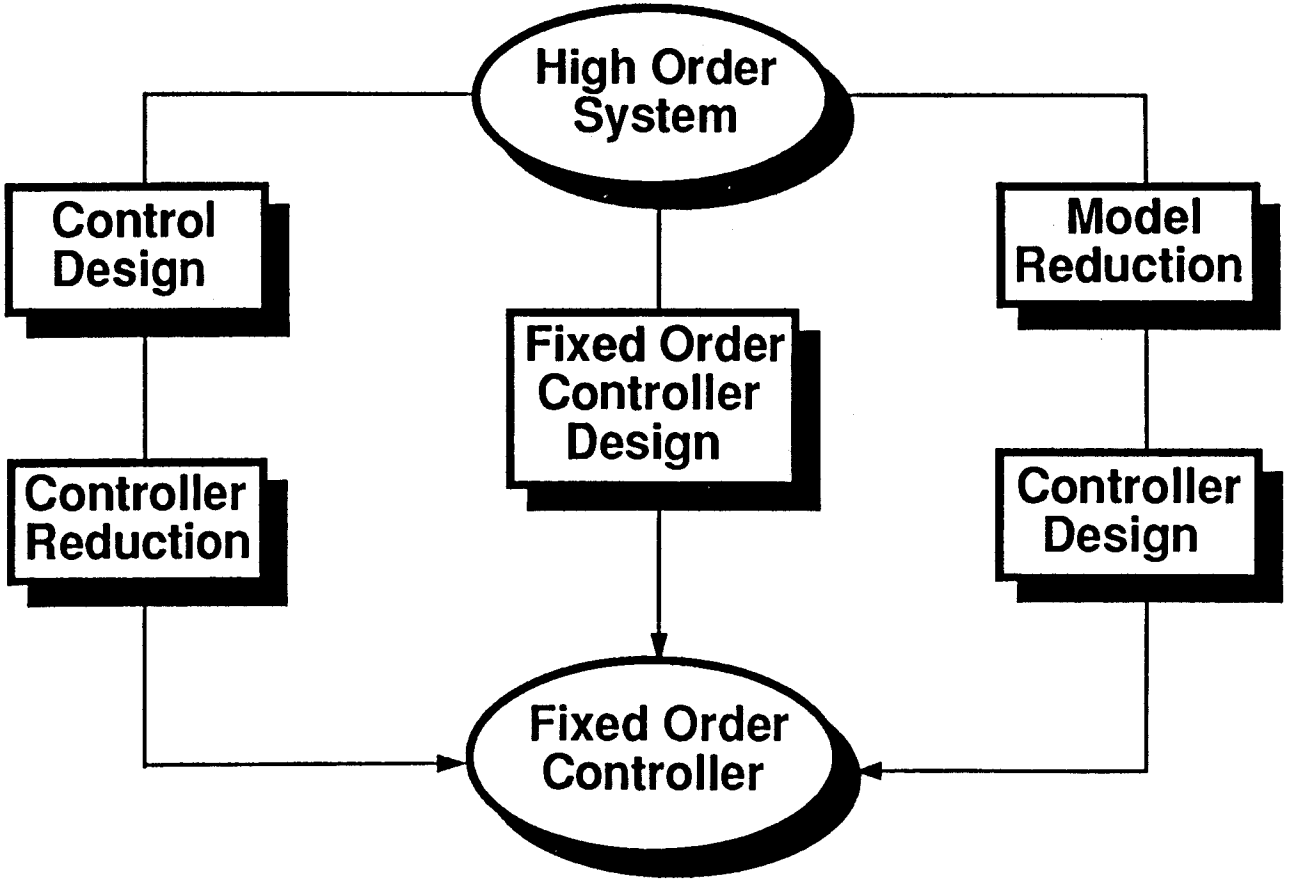

Active Control of Large Structures (Design Process)

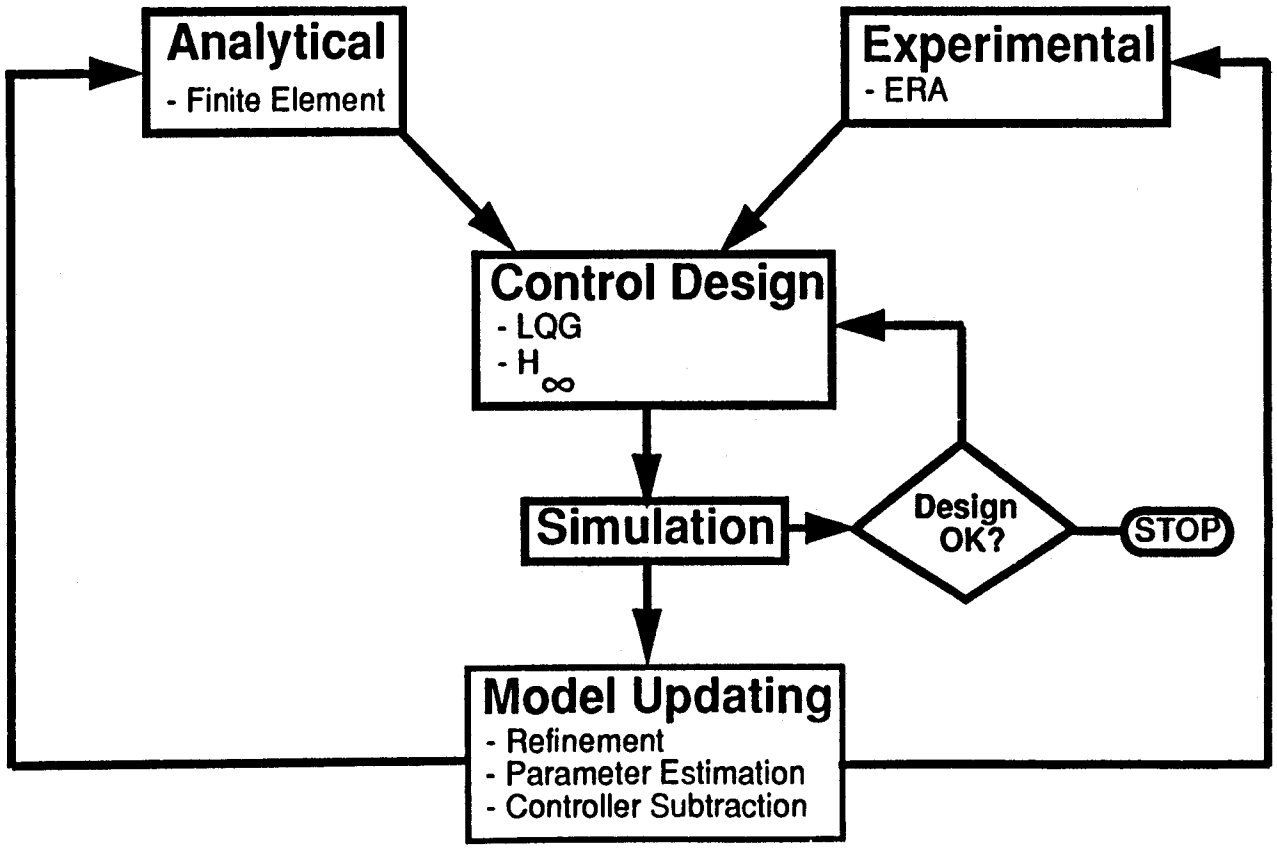

Active Control (Sandia Truss)

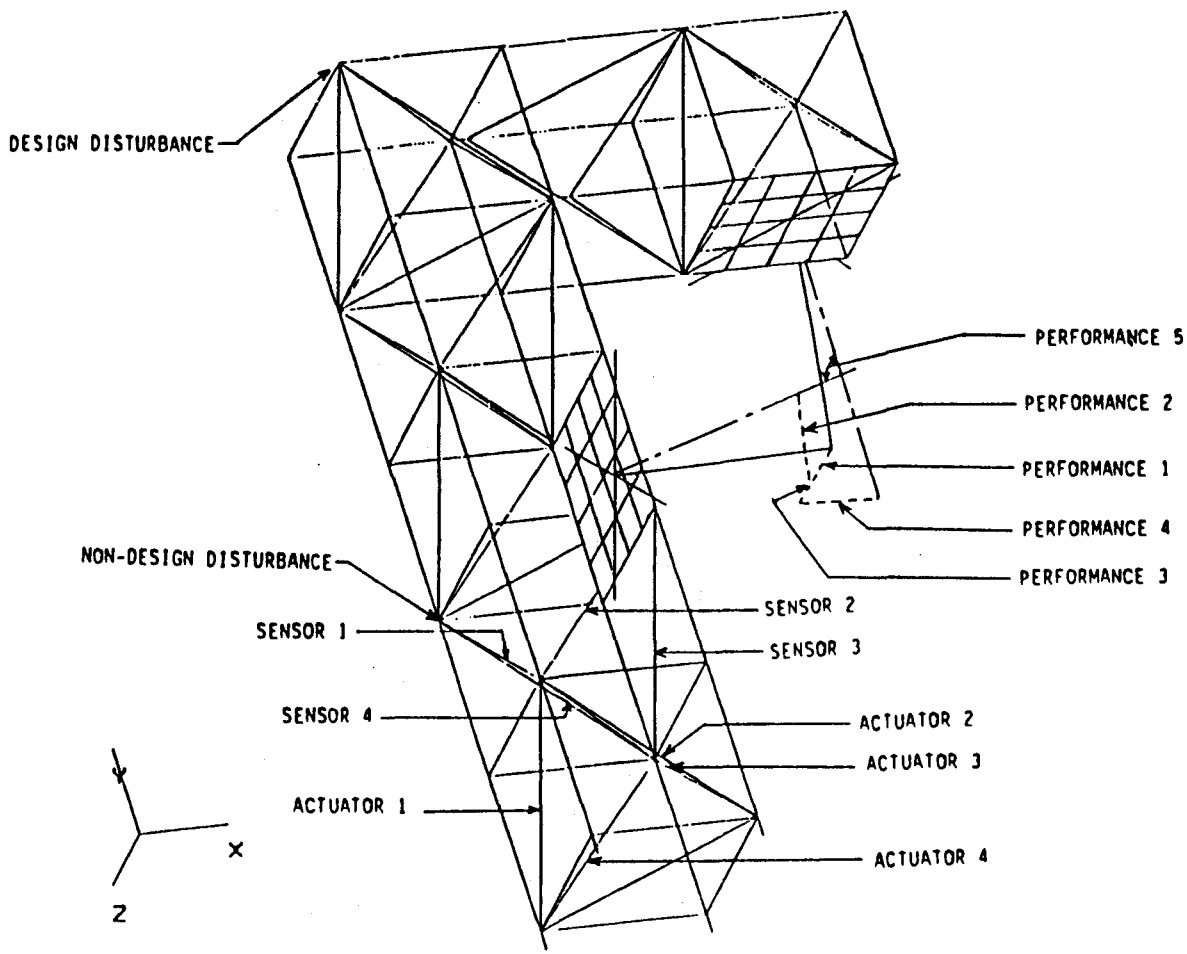

Active Control (Sandia Truss)

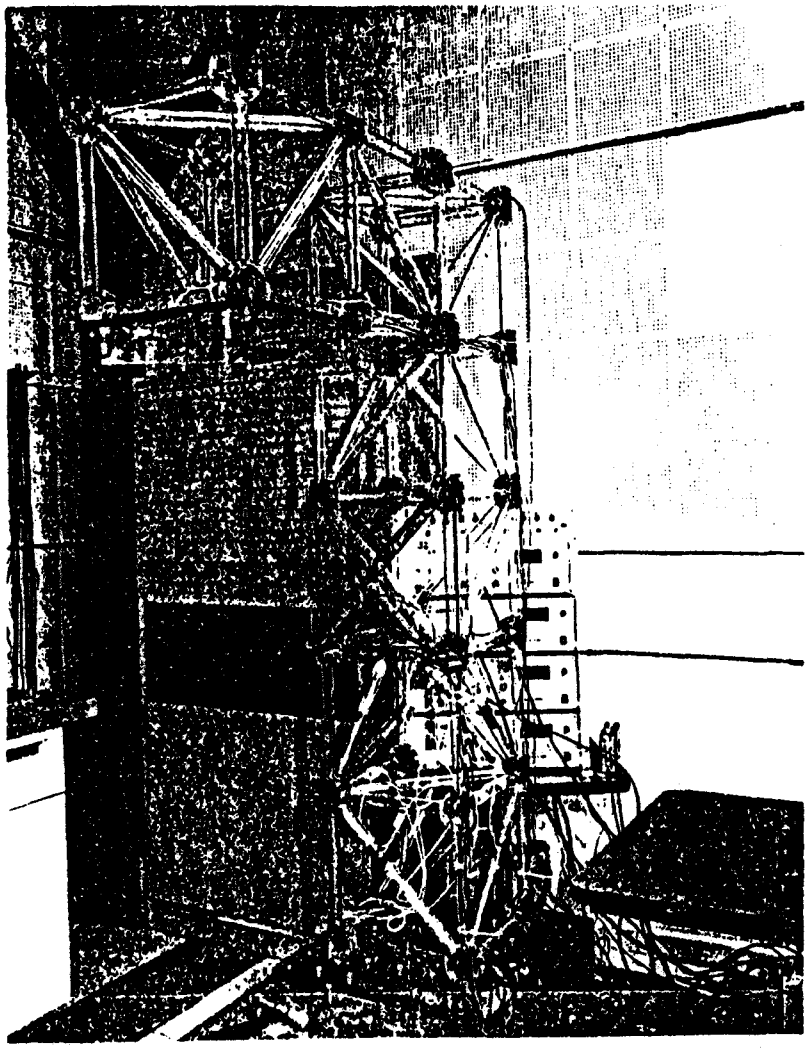

Active Control (Sandia Truss)

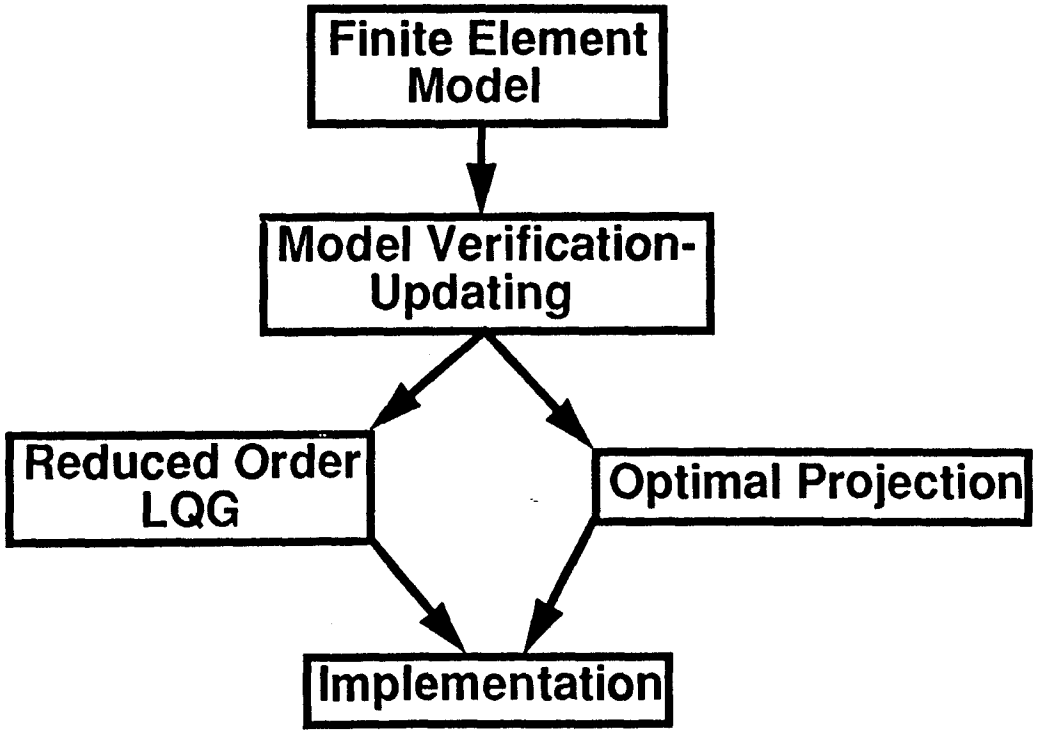

Active Control (Model Verification and Updating)

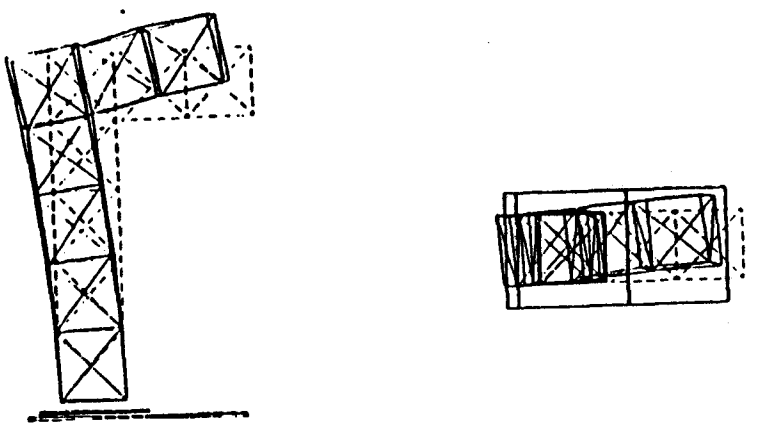

(a) Experimental (10.28 Hz)

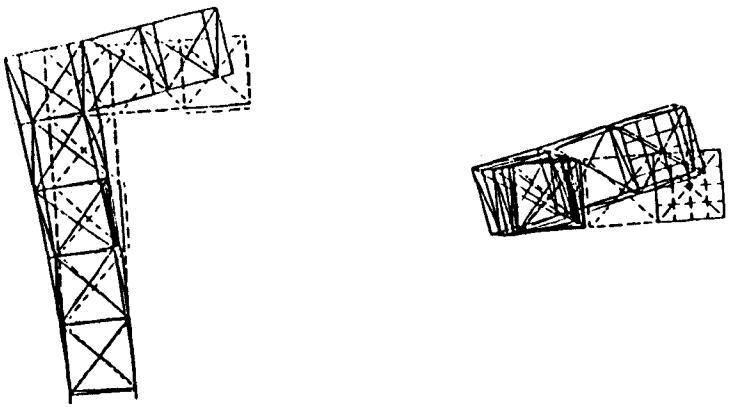

(b) Structural Model with Updated E (10.25 Hz)

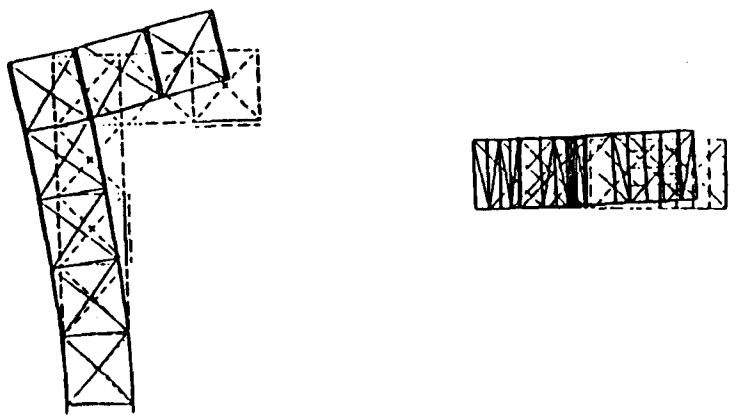

(c) Structural Model with Updated E and K (10.28 Hz)

Active Control (Closed Loop Results)

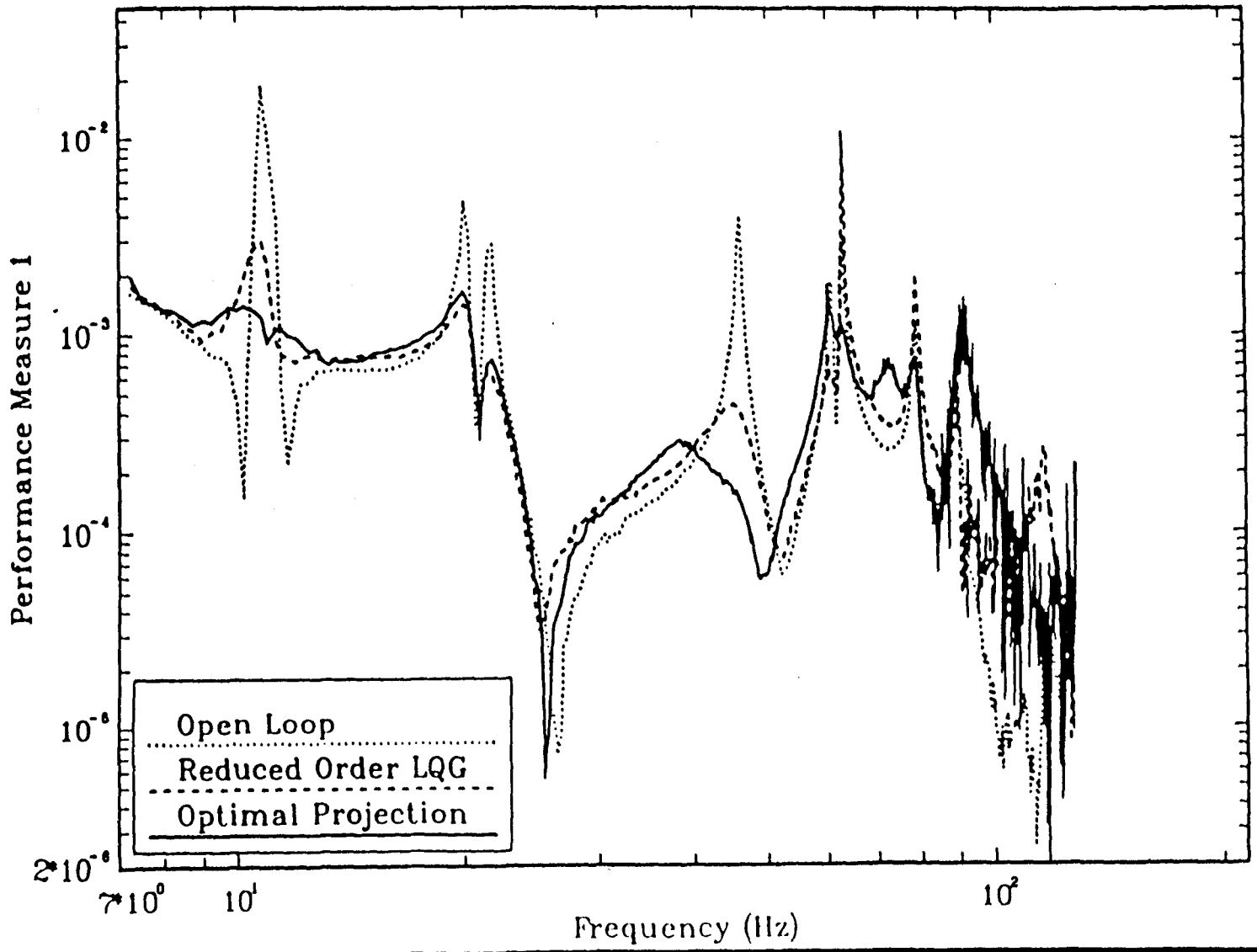

Active Control (Closed Loop Results)

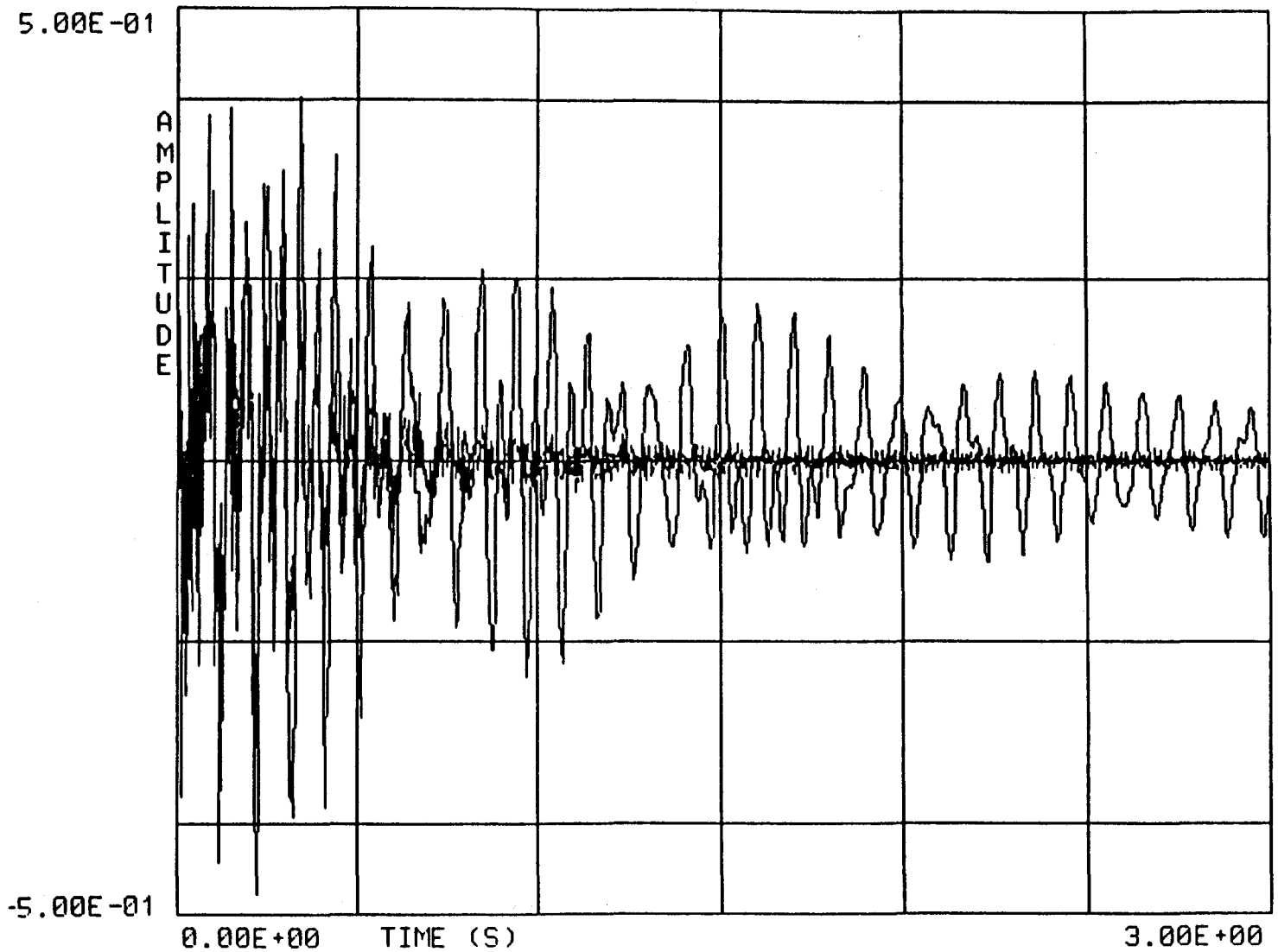

Ongoing Work

- Robust Control of Flexible Structures
- Control of Flexible Robots.
- Development, characterization and modeling of electromechanical gels.
- Parameter estimation in finite element models
    - Currently being applied to the JPL Micro Precision Interferometer Phase I.
- Completing development of Control Design Software:
    - Integrated Modeling and Control (Purdue)
    - Optimal Projection - Maximum Entropy (Harris)
- Optimization applied to:
    - Shape optimization of a nuclear fuel cask
    - Application of genetic algorithms to design of gas guns
- Active Noise Control.

Summary

To the extent possible, design of a large system for vibration suppression should consider the following:

- System Design
- Passive Damping
- Active Damping
- Active Control

The various approaches are all interrelated and not mutually exclusive.

THE CORE GROUP

DE SYSTEMS

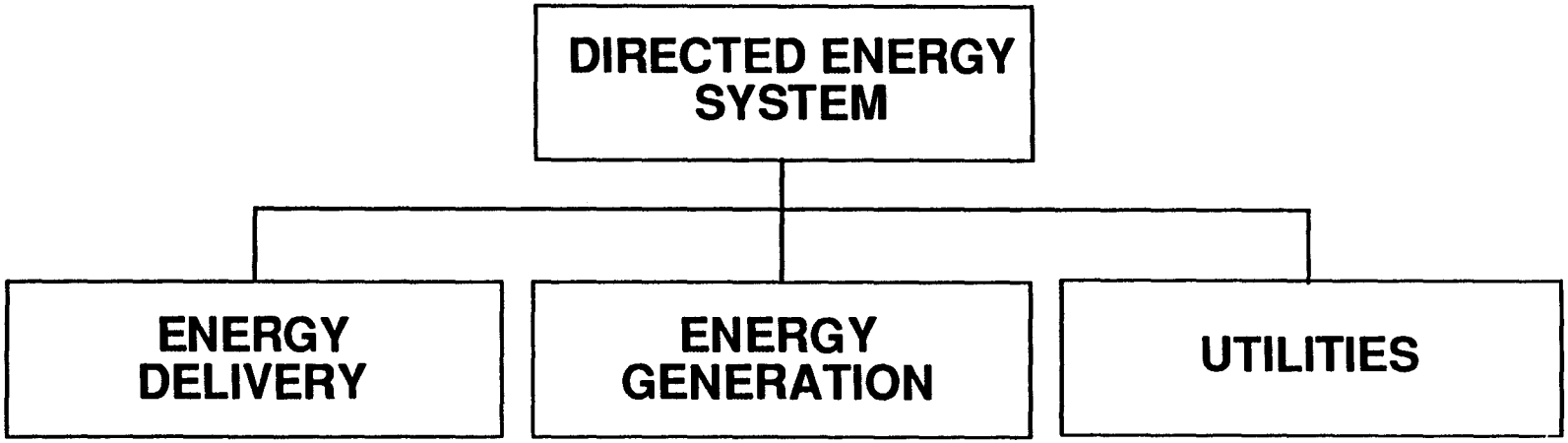

THE CORE GROUP

ENERGY DELIVERY SUBSYSTEM

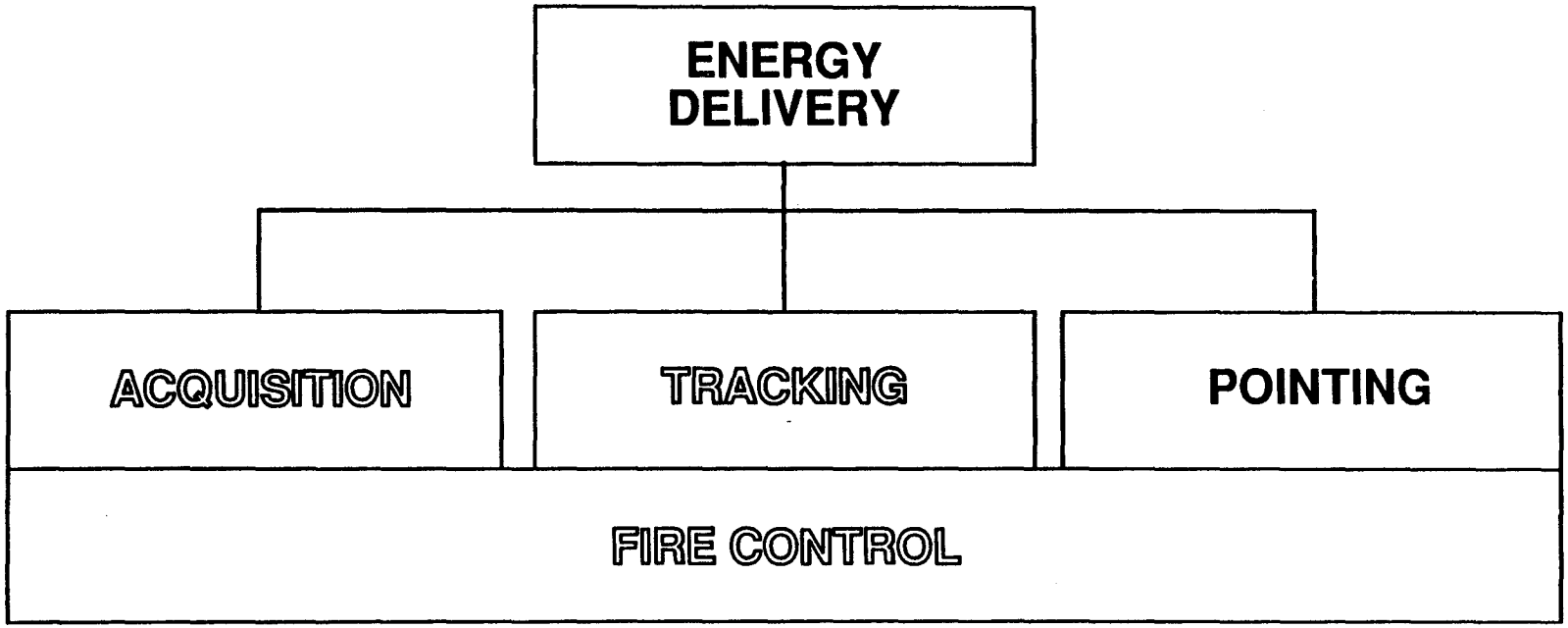

THE CORE GROUP

POINTING-BEAM CONTROL

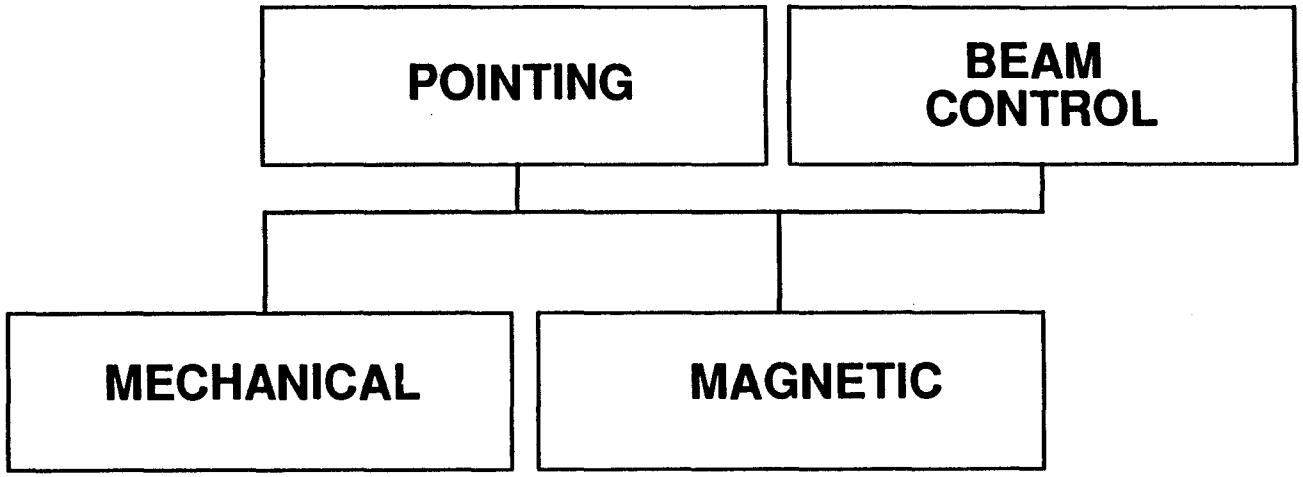

THE CORE GROUP

MECHANICAL OPTIONS

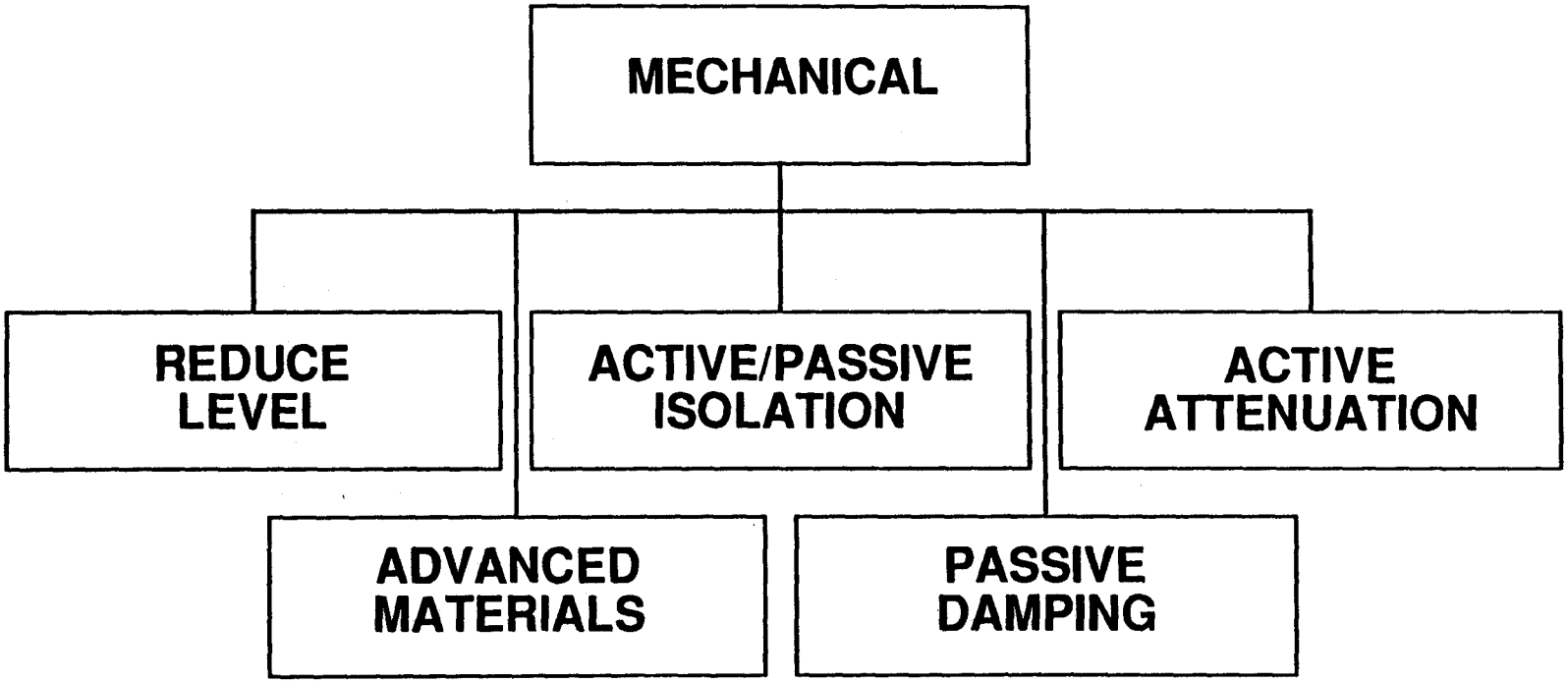

POINTING PROBLEM

PROBLEM: Place the beam on the target for sufficient time within required jitter and dispersion.

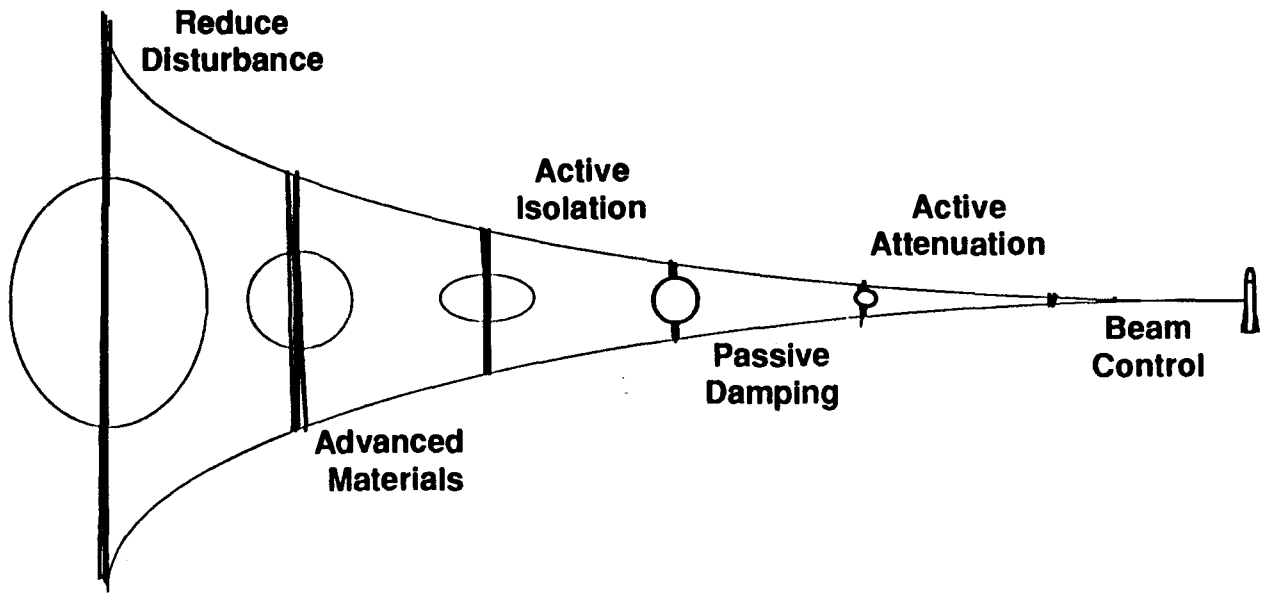

DESIGNER'S PROBLEM: What combination of techniques achieves the required jitter and dispersion for minimum cost and weight with the most reliability.

THE CORE GROUP

VIBRATION SUPPRESSION EQN

$$m\,\ddot{x}(t) + c\,\dot{x}(t) + k\,x(t) = F(t)$$

$$x(t) = \frac{1}{\sqrt{m\,k\,(1-\zeta^2)}} \int_0^t F(\tau)\, e^{-\zeta\omega_n(t-\tau)} \sin\omega_d(t-\tau)\, d\tau \;+$$

$$\frac{x_0}{\sqrt{(1-\zeta^2)}}\, e^{-\zeta\omega_n t}\cos(\omega_d t-\psi) + \frac{v_0}{\omega_d} e^{-\zeta\omega_n t}\sin\omega_d t$$

$$\omega_n^2 = \frac{k}{m}$$

$$\zeta = \frac{c}{2m\omega_n}$$

$$\omega_d = \omega_n\sqrt{1-\zeta^2}$$

$$\psi = \tan^{-1}\frac{\zeta}{\sqrt{1-\zeta^2}}$$

THE CORE GROUP

SOLUTION OPTIONS

REDUCE THE DISTURBANCE LEVELS

USE ADVANCED MATERIALS

ACTIVE/PASSIVE ISOLATION OF CRITICAL COMPONENTS

USE PASSIVE DAMPING TREATMENTS

USE ACTIVE STRUCTURAL CONTROL

USE BEAM CONTROL

COMBINED USE TO ACHIEVE BEST SYSTEM

THE CORE GROUP

PREVENT OR CORRECT?

"AN OUNCE OF PREVENTION IS WORTH A POUND OF CURE."

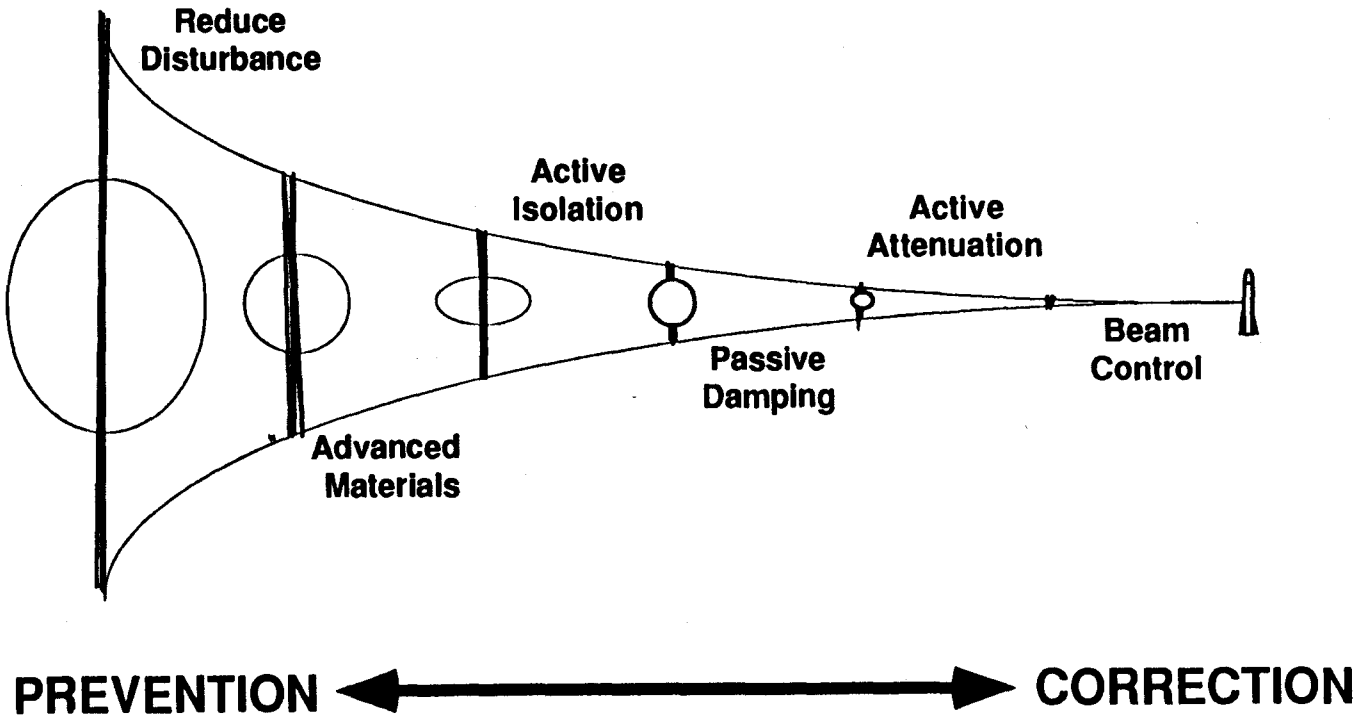

THE CORE GROUP

REDUCE LEVELS

PRO	CON
EXISTING PROGRAMS	CANNOT BEAT THERMODYNAMICS
MAYBE EASIER THAN CORRECTING	CANNOT GET AT CAUSES
HIGH POWER ENVIRONMENT DOES NOT AFFECT APPLICATION	NO ATTENUATION OF ABERRATIONS ON THE BEAM

THE CORE GROUP

ADVANCED MATERIALS

PRO	CON
RELIABLE	ONLY ATTENUATES BY 2 OR 3
TECHNOLOGY AVAILABLE	OUTGASSING AND ENVIRONMENTAL EFFECTS
PREDICTABLE RESULTS	MANUFACTURING WITH MULTIPLE MATERIALS
DECREASES DISTURBANCE MAGNITUDE & INCREASES FREQUENCY	
HIGH POWER ENVIRONMENT DOES NOT AFFECT APPLICATION	NO ATTENUATION OF ABERRATIONS ON THE BEAM

THE CORE GROUP

ACTIVE ISOLATION

PRO	CON
SEVERAL ORDERS OF MAGNITUDE ATTENUATION	COMPLICATED CONTROL SYSTEM
PREVENTS DISTURBANCES FROM REACHING CRITICAL OPTICS	WEIGHT PENALTY
HIGH POWER ENVIRONMENT DOES NOT AFFECT APPLICATION	FORWARD BODY ON SOFT SPRING
	NO ATTENUATION OF DISTURB-ANCES GENERATED IN CRITICAL OPTICS
	NO ATTENUATION OF ABERRATIONS ON THE BEAM

THE CORE GROUP

PASSIVE DAMPING

PRO	CON
RELIABLE	TEMPERATURE DEPENDENCE
ORDER OF MAGNITUDE ATTENUATION	OUTGASSING AND ENVIRONMENTAL EFFECTS
DEVELOPED TECHNOLOGY	WEIGHT PENALTY IF NOT DESIGNED CORRECTLY
POSSIBLE DECREASED GROUND TESTING REQUIREMENT	ATTENUATION LEVEL LIMITED
HIGH POWER ENVIRONMENT DOES NOT AFFECT APPLICATION	NO ATTENUATION OF ABERRATIONS ON THE BEAM

THE CORE GROUP

ACTIVE CONTROL

PRO	CON
SEVERAL ORDERS OF MAGNITUDE ATTENUATION	COMPLICATED CONTROL SYSTEM
CAN BE APPLIED IN PROBLEM AREAS	WEIGHT PENALTY
GRACEFUL DEGRADATION	TECHNOLOGY HAS NOT BEEN APPLIED ON LARGE SYSTEM
HIGH POWER ENVIRONMENT DOES NOT AFFECT APPLICATION	NO ATTENUATION OF ABERRATIONS ON THE BEAM

THE CORE GROUP

ACTIVE BEAM CONTROL

PRO	CON
CAN CORRECT ABERRATIONS ON THE BEAM	COMPLICATED CONTROL SYSTEM
SEVERAL ORDERS OF MAGNITUDE CORRECTION	WEIGHT PENALTY
THEORETICALLY STRAIGHT FORWARD	CATASTROPHIC DEGRADATION
	HIGH POWER AFFECTS APPLICATION
	EXPENSIVE
	CANNOT ATTENUATE ALL MECHANICALLY INDUCED EFFECTS

THE CORE GROUP

CONCLUSIONS

THE ANALYTICAL SIMULATION CAPABILITY TO DO QUICK COMPARISONS OF DIFFERENT ENGINEERING APPROACHES IS NOT YET AVAILABLE.

ACTIVE STRUCTURAL CONTROL VERSUS ACTIVE BEAM CONTROL:

1. WEIGHT EFFECTS ARE AN EVEN TRADE,
2. BEAM CONTROL MUST BE USED TO CORRECT ABERRATIONS ON THE BEAM,
3. STRUCTURAL CONTROL IS MORE RELIABLE,
4. NEITHER METHOD CAN PREVENT OR CORRECT ALL ABERRATIONS,
5. PREVENTION IS PREFERABLE TO CORRECTION.

<u>AN INTEGRATED SYSTEMS APPROACH IS PREFERABLE TO DEPENDING ON ONLY ONE TECHNOLOGY.</u>

Sensors, Actuators, and Processors for Modern Control

W. K. Tucker

Sandia National Laboratories

Albuquerque, New Mexico

Workshop on Vibration Control and Dynamic Alignment Issues
at the Superconducting Super Collider

February 11-14, 1992

Sensors, Actuators, and Processors For Modern Control

- System and Component Issues
- Sensor and Actuator Materials
- Sensor and Actuator Designs
- Processor Designs for Large Structure Control

An actively controlled structure consists of several components

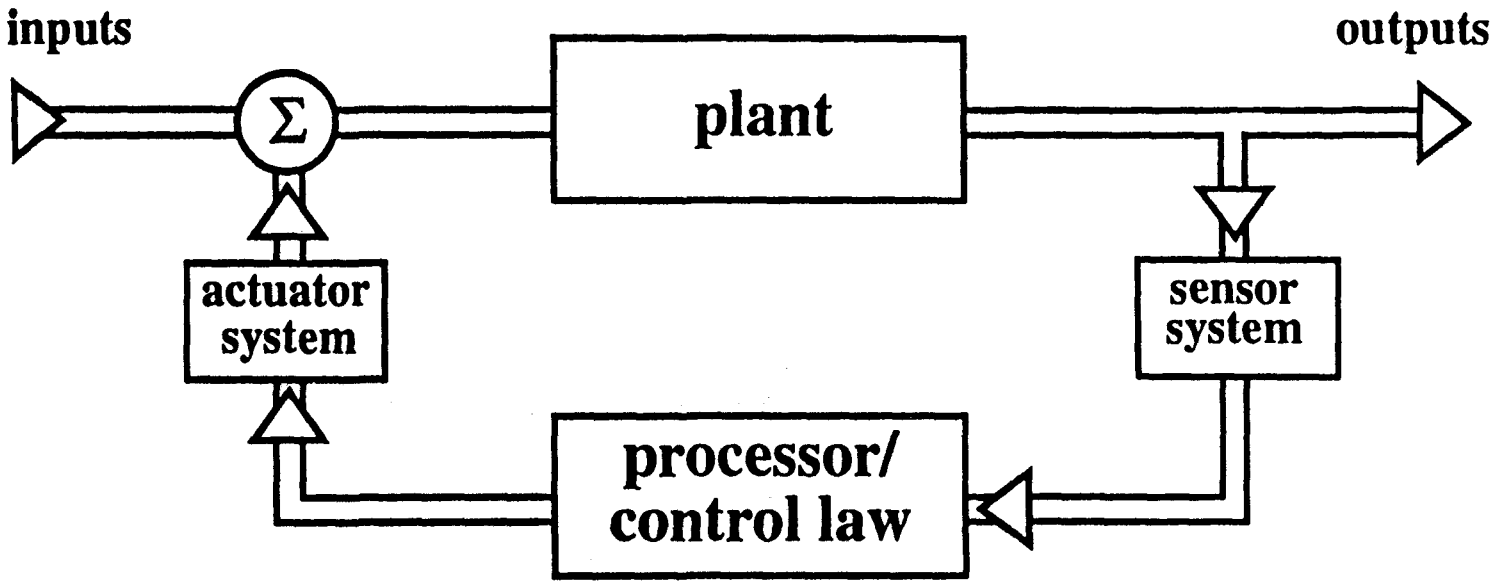

Each system can be represented by a state space equation

$$\dot{X}=AX + BU$$
$$Y=CX + DU$$

Sandia National Laboratories

We can divide active control into four core technologies

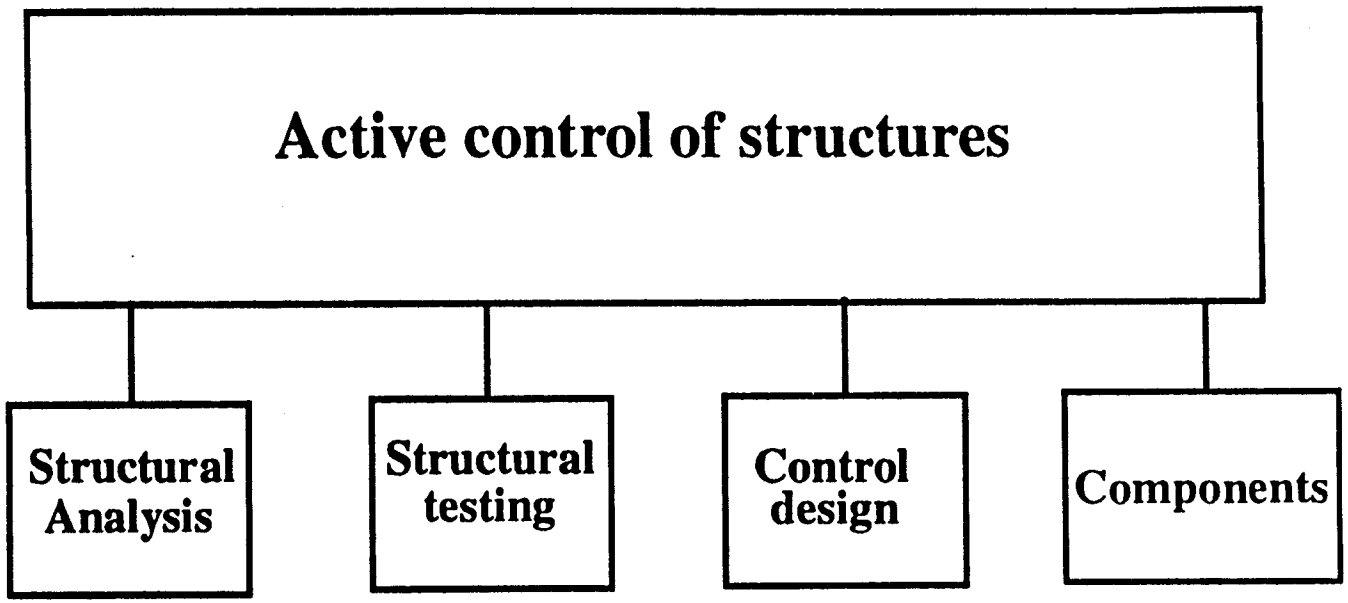

Structural Analysis

1) preliminary design and analysis
2) plant modeling

Structural testing

1) disturbance requirements
2) plant model identification
3) component testing
4) implementation

Control design

1) design methods
2) implementation

Components

1) sensors
2) actuators
3) processors

Filename:SNLA_2743_02_HD:FrameMaker 3.0:JPLauffer_Documents:scsi_Feb:scsi_presentation

System Issues for Sensors, Actuators, and Processors

- Sensor Issues - Is the plant observable?
  - Signal to noise ratio
  - Dynamic range
  - Linearity
  - Sensitivity
  - Environmental effects

- Actuator Issues - Is the plant controllable?
  - Resulting mechanical effect
  - Electrical power/energy required
  - Dynamic range
  - Linearity
  - Electrical noise produced
  - Environmental effects

System Issues for Sensors, Actuators, and Processors
(continued)

- Processor Issues - Is the required performance obtained?
  - Control algorithm implementation
  - Number of inputs and outputs
  - State-space or filter implementation
    Number of states, FIR filter length, IIR filter order
  - Computation efficiency versus sample time
  - Latency

- Control Algorithm Issues - Is the required performance obtained, and is the controller robust?

SANDIA IS DEVELOPING PIEZOELECTRIC SENSORS FOR LOW-LEVEL STRAIN MEASUREMENTS

- PVF_2 FILMS - DEVICES UNDER DEVELOPMENT AT SANDIA, MATERIALS AT ATOCHEM, INC.
- PVF_2 COPOLYMER FILMS - DEVICES UNDER DEVELOPMENT AT SANDIA, MATERIALS AT ATOCHEM, INC.
- PZT COMPOSITES - DEVICES UNDER DEVELOPMENT AT SANDIA, MATERIALS AT FIBER MATERIALS INC., NTK, PENN STATE

SANDIA IS DEVELOPING ACTUATORS USING PIEZOELECTRIC AND POLYMERIC GEL MATERIALS

- PVF_2 FILMS - DEVICES UNDER DEVELOPMENT AT SANDIA, MATERIALS AT ATOCHEM, INC.
- PVF_2 COPOLYMER FILMS - DEVICES UNDER DEVELOPMENT AT SANDIA, MATERIALS AT ATOCHEM, INC.
- PZT COMPOSITES - DEVICES UNDER DEVELOPMENT AT SANDIA, MATERIALS AT FIBER MATERIALS INC., NTK, PENN STATE
- ELECTROMAGNETIC/POLYMERIC GELS - MATERIALS AND DEVICES UNDER DEVELOPMENT AT SANDIA

PIEZOELECTRIC SENSORS AND ACTUATORS

- DIFFERENTIAL SENSOR DESIGN FOR REDUCTION OF COMMON-MODE ELECTROMAGNETIC NOISE OR SENSITIVITY TO EXTERNAL PRESSURE

- DIFFERENTIAL ACTUATORS FOR REDUCTION OF RADIATED ELECTROMAGNETIC NOISE

- SENSOR/ACTUATOR DESIGNS FOR MEASURING/GENERATING HOOP OR AXIAL STRAIN IN CYLINDERS TO CANCEL STRUCTURAL VIBRATION

Piezoelectric Films - Sensors and Actuators

Polarization Constant

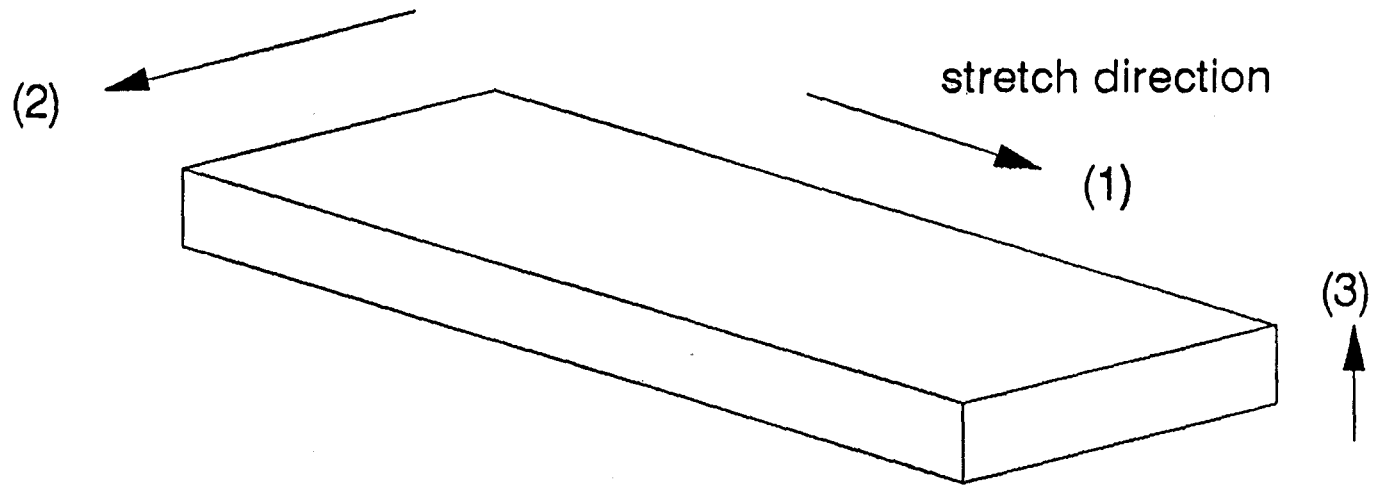

d_{ij} = polarization constant ((m/m)/(V/m) or (C/m)/(N/m))
i = electric field direction
j = stress/strain direction
(Electric field is applied in direction (3))

wkt 7/3/90

PZT Composites

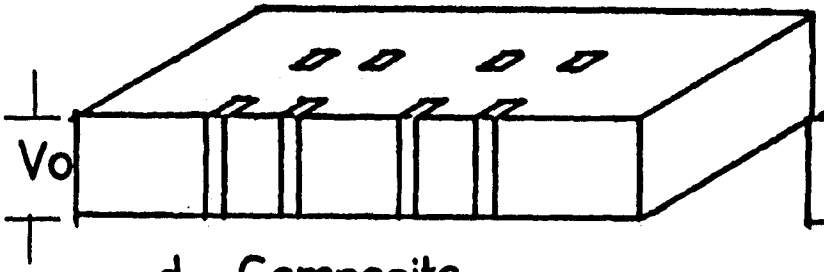

d_{33} Composite
(uses d_{33} of PZT)

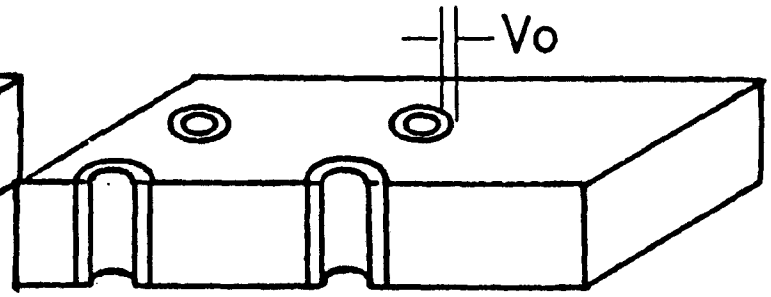

d_{33} Hybrid
(uses d_{31} of PZT)

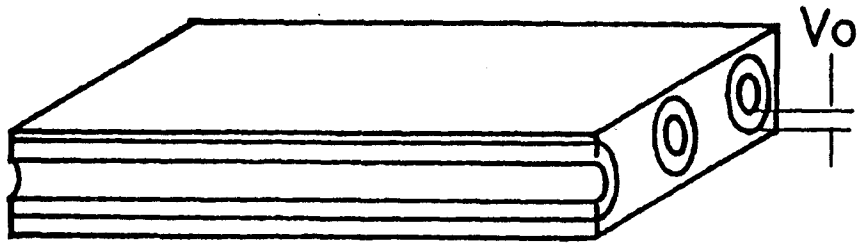

d_{31} Composite
(uses d_{31} of PZT)

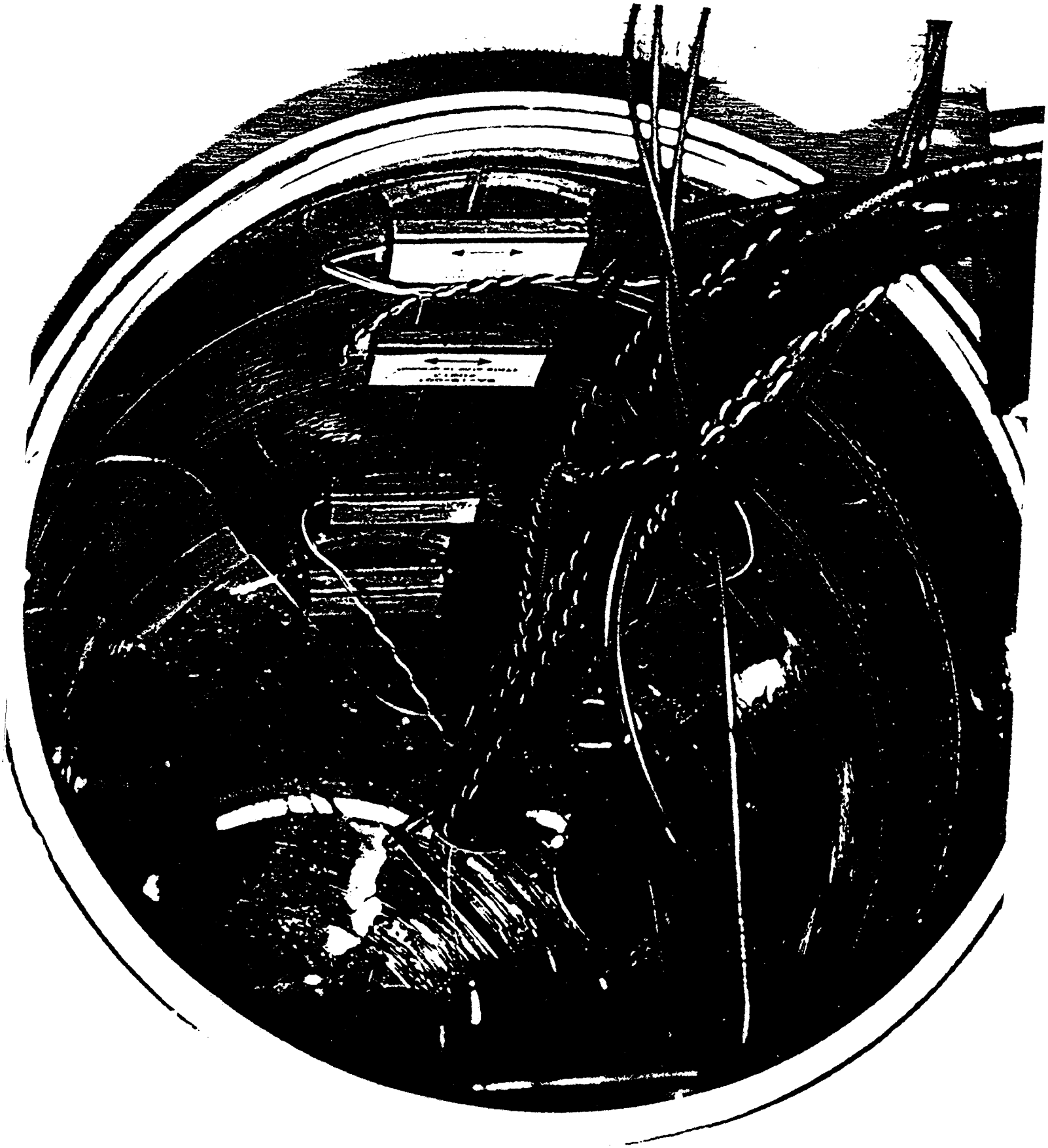

WHAT IS A SMART GEL?

- A SMART GEL IS AN IONIZED POLYMERIC NETWORK THAT IS SWOLLEN WITH A SOLVENT.
  - MOLECULAR SPONGE
  - REVERSIBLE PHASE TRANSITION
  - CHEMICALLY OR ELECTRICALLY ACTIVATED
  - VOLUME CHANGE OF SEVERAL MAGNITUDES CONTROLLED BY MATERIAL FORMULATION

SANDIA RESEARCH INTO GELS HAVE PRODUCED INTERESTING RESULTS

- POLYMERIC GELS HAVE PROPERTIES THAT HAVE NOT BEEN FOUND WITH CONVENTIONAL ACTUATOR MATERIALS.
- GEL ACTUATORS HAVE THE CAPABILITY OF PERFORMING LARGE DEFORMATION WHERE WEIGHT IS OF PREMIUM AND ELECTRIC POWER IS AVAILABLE.
- A COMPLETE MATHEMATICAL DESCRIPTION THAT LENDS ITSELF TO A NUMERICAL SOLUTION HAS BEEN FORMULATED.
- DYNAMIC BEHAVIOR CAN BE PREDICTED THROUGH FEM COMPUTATIONS.
- ELECTRIC POWER REQUIREMENTS ARE LOW - LESS THAN SEVERAL HUNDRED WATTS.
- WE HAVE INITIATED DESIGN AND CONSTRUCTION OF A LINEAR ACTUATOR.

SANDIA IS DEVELOPING HIGH-SPEED, PARALLEL PROCESSORS FOR STRUCTURAL CONTROL OF LARGE STRUCTURES

- DESIGNED, FABRICATED, AND TESTED A STATE-SPACE PROCESSOR
  - 8 INPUTS, 8 OUTPUTS, AND 32 STATES
  - CUSTOM ADC AND DAC BOARDS, OFF-SHELF PROCESSOR BOARDS
  - VME BUS ARCHITECTURE WITH A CUSTOM DATA BUS
  - 50 kHz SAMPLE RATE AND ALL CALCULATIONS COMPLETED WITHIN 20 μs
  - SUN WORKSTATION HOST

- DESIGNED AND INITIATED FABRICATION OF AN ADVANCED PROCESSOR
  - 64 INPUTS, 16 OUTPUTS, AND 64 STATES
  - ALL CUSTOM BOARDS USING OFF-SHELF ICs
  - VME BUS ARCHITECTURE WITH TWO CUSTOM DATA BUSES
  - SELECTABLE SAMPLE RATE (64/16/64 CONFIGURATION REQUIRES 18 μs)
  - SUN WORKSTATION OR EQUIVALENT VME HOST

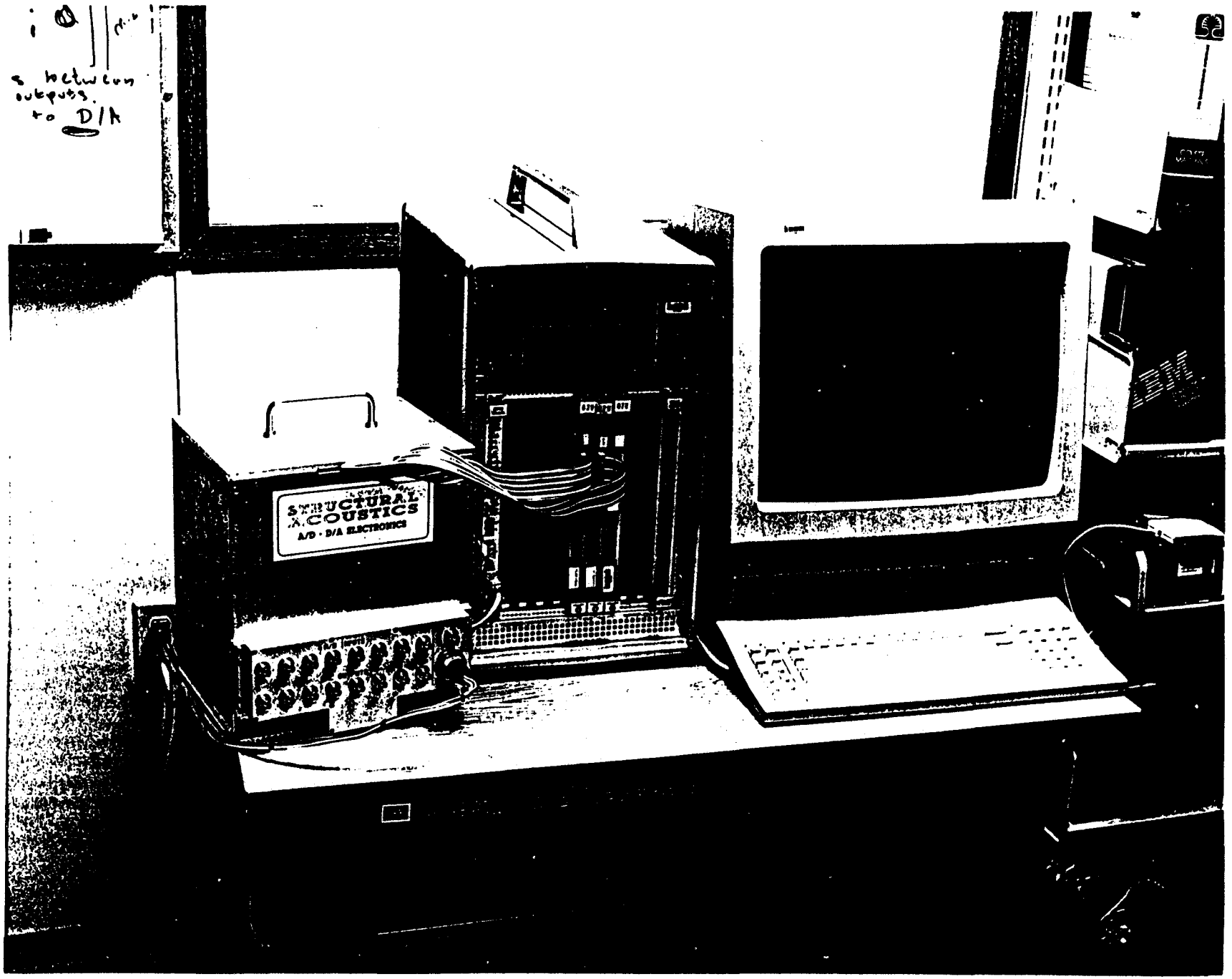
STRUCTURAL ACOUSTICS
A/D · D/A ELECTRONICS

Real-Time Control Processor

- The Control Processor is a real-time processor for implementing digital state-space controllers and FIR and IIR digital filters.
- Receives conditioned analog inputs from strain sensors.
- Outputs analog signals for driving actuator power amplifiers.
- Digital processor implements a variety of state-space control algorithms and filters.

Real-Time Control Processor

- **Flexible Architecture Suitable for Variety of Matrix Processing Applications.**

  Efficiently Supports Control Equations in the Matrix Form:

$$\begin{bmatrix} x(n+1) \\ \hdashline u(n) \end{bmatrix} = \left[\begin{array}{c:c} A & B \\ \hdashline C & D \end{array}\right] \times \begin{bmatrix} x(n) \\ \hdashline y(n) \end{bmatrix}$$

where:

$A, B, C, \& D$ are control matrices

$x(n)$ = current state vector

$y(n)$ = input vector

$x(n+1)$ = estimate of next state vector

$u(n)$ = output vector

Sandia National Laboratories

Real-Time Control Processor

- Sequence of Computation During a Sample Interval:
  1. Computation of Output Vector $u(n)$

$$[u(n)] = [C] \times [x(n)] + [D] \times [y(n)]$$

  2. Computation of Next State

$$[x(n+1)] = [A] \times [x(n)] + [B] \times [y(n)]$$

  3. Computation of Partial $u(n)$ Result

$$[C] \times [x(n+1)]$$

Note: Computation of $[C]\times[x(n)]$ has already been done during the previous cycle. Thus, the output of $[u(n)]$ can be done as soon as $[D]\times[y(n)]$ is computed and added to $[C]\times[x(n)]$.

Sandia National Laboratories

Processing Timeline Example

TIME IN MICROSECONDS

0.00		SAMPLE AND HOLD ANALOG INPUT
0.30	$D \cdot y(n) + [C \cdot x(n)]$	A/D CONVERSION FINISHED
2.65		DIGITAL OUTPUTS AVAILABLE
3.10	$A \cdot x(n) + B \cdot y(n)$	ANALOG RESULTS AVAILABLE AT D/A OUTPUT
6.25	$A \cdot x(n) + B \cdot y(n)$	NEXT STATE CALCULATION FINISHED, PASS 1
9.85	$A \cdot x(n) + B \cdot y(n)$	NEXT STATE CALCULATION FINISHED, PASS 2
13.45	$A \cdot x(n) + B \cdot y(n)$	NEXT STATE CALCULATION FINISHED, PASS 3
17.05	$A \cdot x(n) + B \cdot y(n)$	NEXT STATE CALCULATION FINISHED, PASS 4
19.05	$C \cdot x(n+1)$	C MATRIX * NEXT STATE CALCULATION FINISHED

SAMPLE PERIOD:
20.0 MICROSECONDS

HARDWARE:

- 4 A/D MODULES
- 2 D/A MODULES
- 4 MAT. PROC. MODULES

CONFIGURATION:

- 64 INPUTS
- 16 OUTPUTS
- 64 STATES

Sandia National Laboratories

Control Processor System Architecture

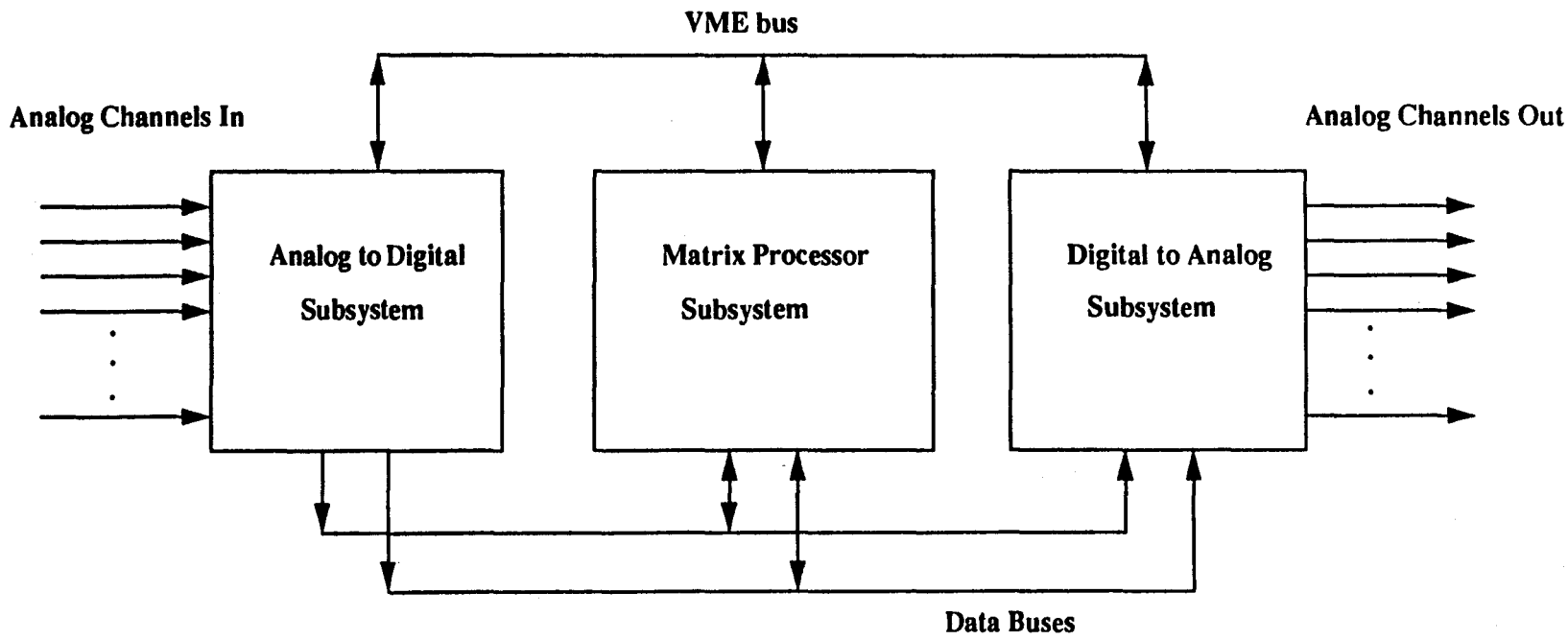

Each subsystem is composed of one or more modules.

Sandia National Laboratories

Control Processor - System Features

- Communicates with host (Sun workstation) via industry-standard VMEbus.
- All matrix operations performed in 32-bit floating point.
- Modular implementation:
  Analog-to-Digital (A/D) module: 16 channels, 14 bit precision
  Digital-to-Analog (D/A) module: 16 channels, 14 bit precision
  Matrix Processor (MP) module: 320 MFLOPS
  Interface/Control (I/C) module: interfaces A/D and D/A to MP
- Double-buffered matrix stores to accommodate real-time updates.
- Design optimized for low input to output latency.
- Maximum computational rate of 3.84 GFLOPS in one VME chassis.
- Hardware support for zero-skipping reduces computation for sparse matrices.

Control Processor - System Features (cont'd)

- Diagnostic mode:
  Insert and capture data from host computer.
  64K words for storage of past inputs and outputs.
  128K words for storage of past states and intermediate results.
  Aids in system identification and controller debugging.
- Programmable sample clock frequency:
  38 Hz to 625 kHz
- Automatic shutdown on detection of output overload conditions.
- Hardware look-up-tables for linearizing sensors and actuators.

Summary and Conclusions

- Selection of sensors, actuators, and processor for control of large structures is critical for performance requirements.
- Piezoelectric sensors offer high sensitivity, wide dynamic range, and EM noise rejection with differential construction.
- Piezoelectric actuators offer wide dynamic range, low real power requirements, and EM noise cancellation with differential construction.
- Gel actuators offer large volume changes for low electric fields and light weight.
- High-speed, parallel processors offer choice of solution method (SS, FIR, or IIR), small latency, and easy expansion for additional inputs, output, or states.

Application of Base Isolation to Large Structures

R. F. Kulak
Reactor Engineering Division
Argonne National Laboratory
USA

Holiday Inn
DeSoto, Texas
February 11-14, 1992

WHAT IS BASE ISOLATION

- A system installed between a structure and its surrounding foundation to isolate it from damaging ground motions.
- Accelerations of the structure and equipment are significantly reduced.
- The structure moves without upper story amplification.

EFFECT OF SEISMIC ISOLATION

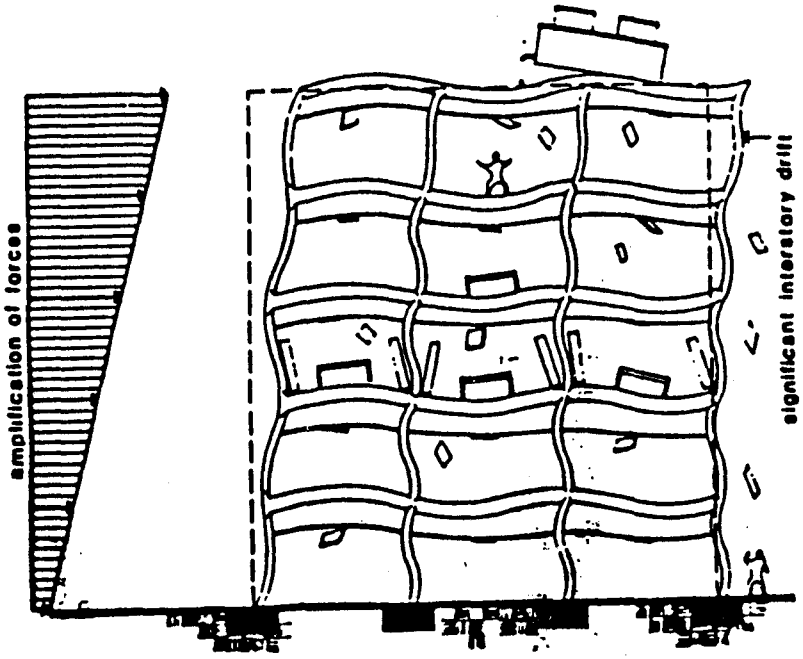

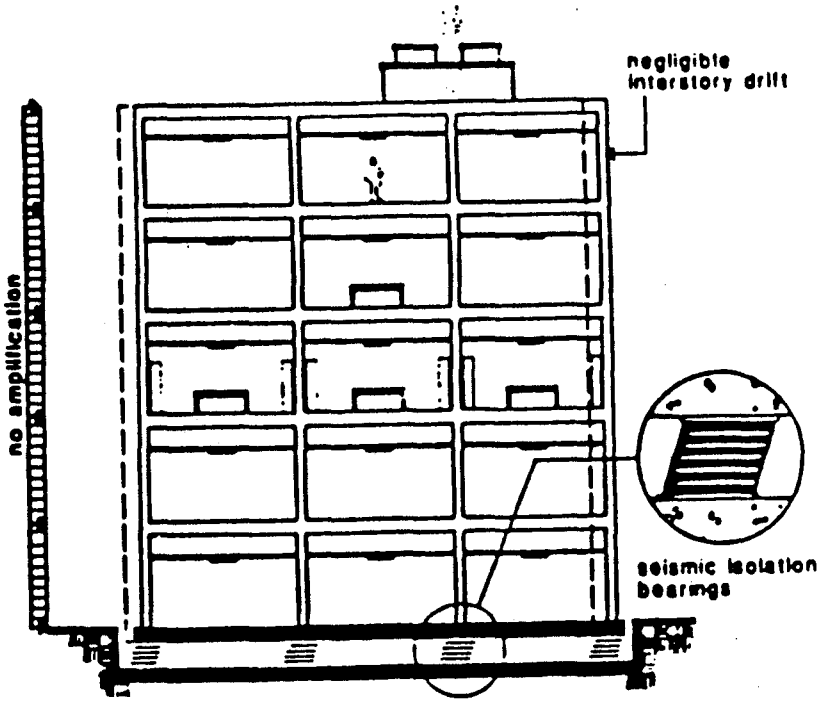

RESPONSE SPECTRUM (TOP OF BUILDING)

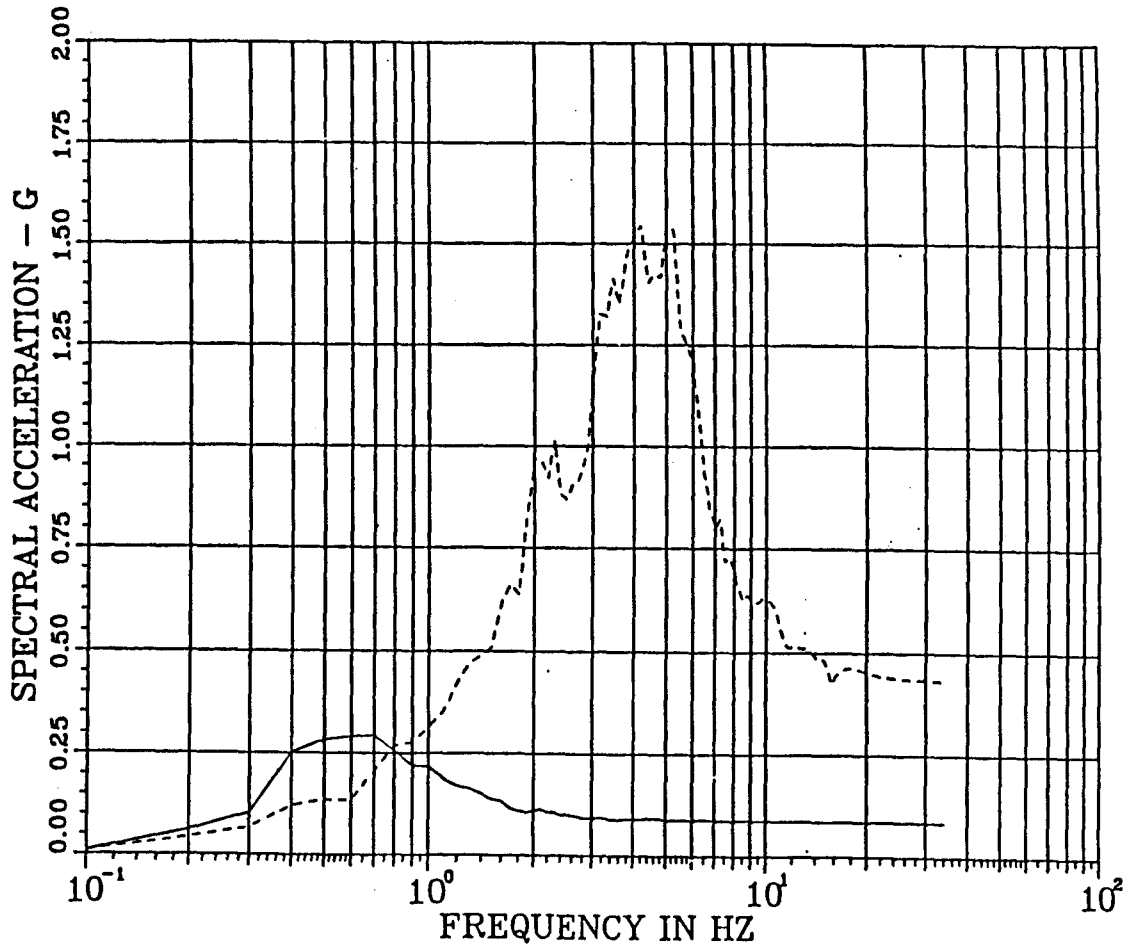

Applications

- Civil Structures
  - Buildings
  - Bridges
  - Nuclear Power Plants
  - Elevated Water Tanks
- Electrical Breakers
- Museum Sculptures
- Retrofit
  - Salt Lake City and County Building
  - St. Peter, Historical Church in Frigento, Italy

ANL/RE INVOLVEMENT

- Bearing Design
- Bearing Procurement Specifications
- Testing Program
  - Individual Bearings
  - In-Situ (Sendai, Japan)
- Computer Code Development
  - System Response
  - Individual Bearing Response

Seismic Isolation Systems

- Steel Laminated High Damping Rubber Bearings
- Steel Laminated Rubber with Lead Plug
- Steel Laminated Rubber with Teflon Slider
- Steel Springs and Viscous Dampers
- Friction Pendulum System
- Alexisismon System

ALEXISISMON SYSTEM (GREECE)

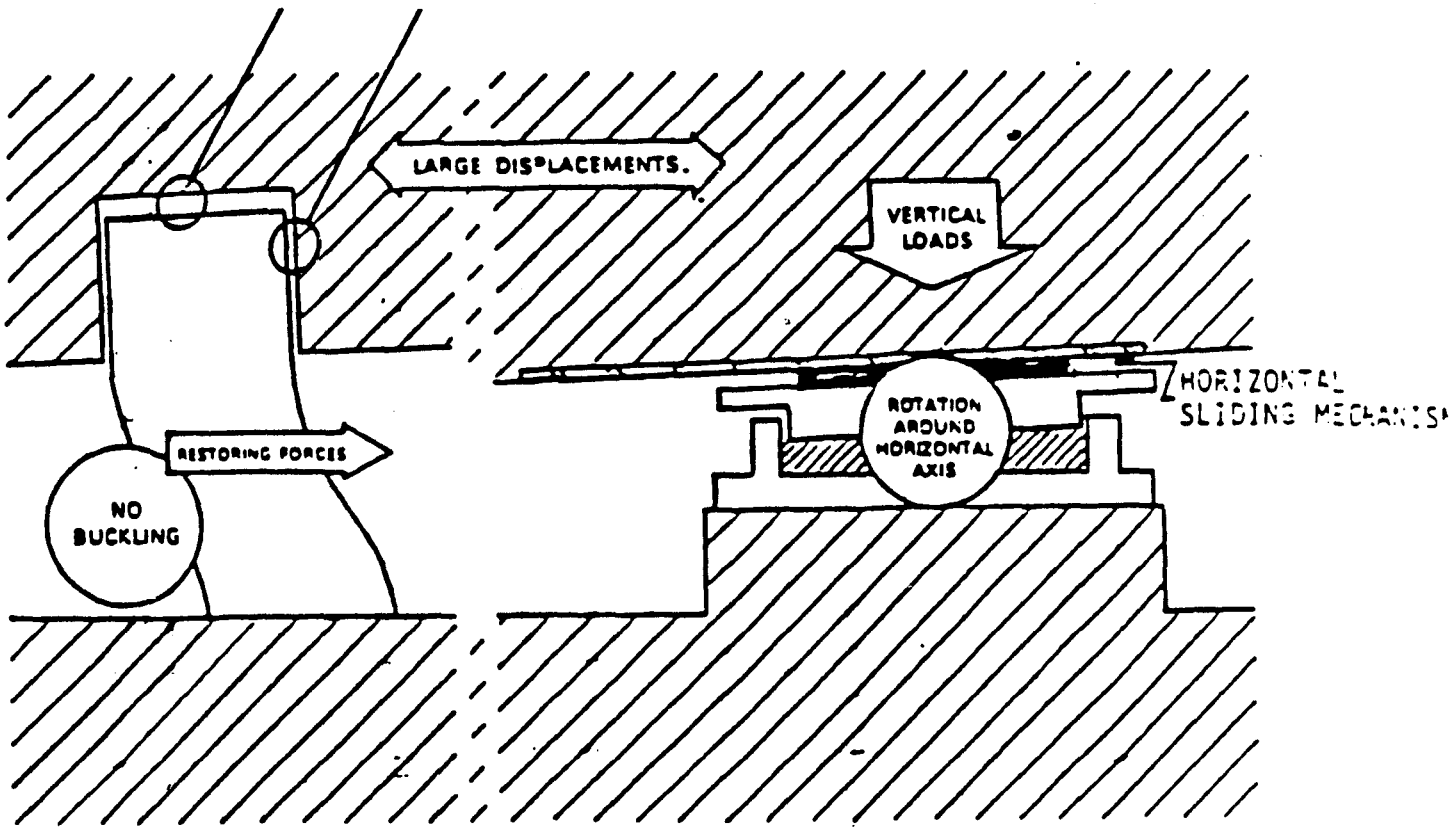

SOFT SPRING COMPONENT

VERTICAL LOAD SUPPORT

LEAD RUBBER BEARING (NEW ZEALAND)

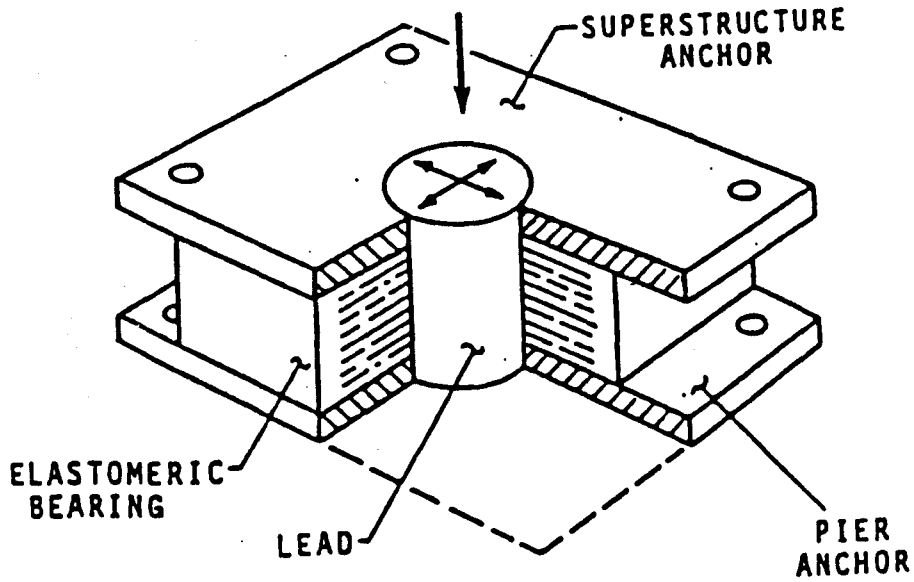

FRICTION PENDULUM SYSTEM (EPS)

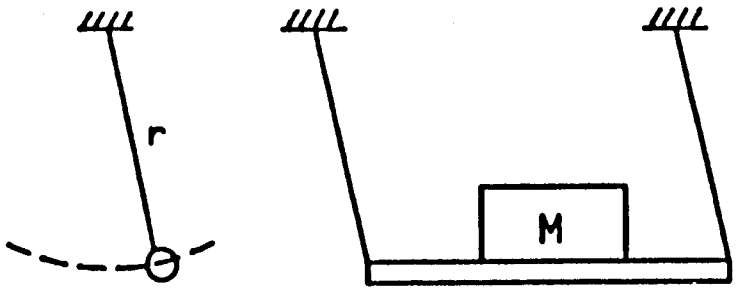

PENDULUM MOTION

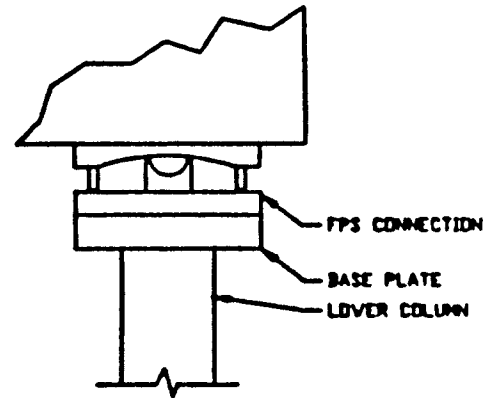

CENTERED POSITION

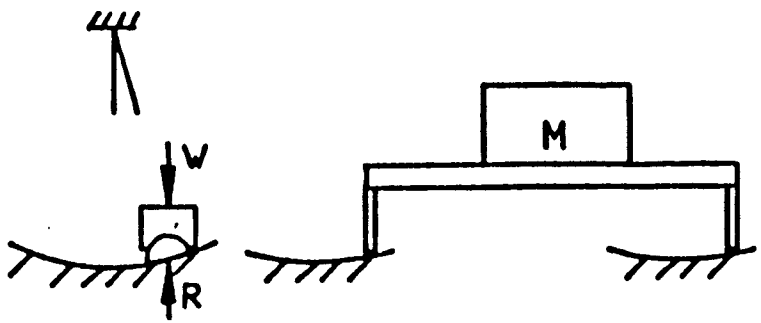

SLIDING PENDULUM MOTION

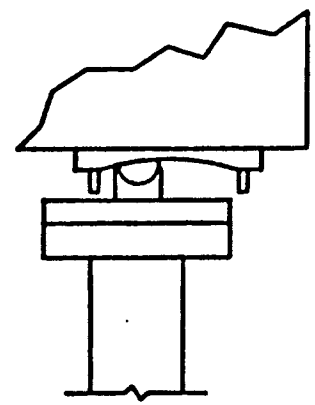

DISPLACED POSITION

EQUATIONS PERIOD $T=2\pi\sqrt{r/g}$

STIFFNESS $k = W/r$

STEEL LAMINATED HIGH DAMPING RUBBER BEARING

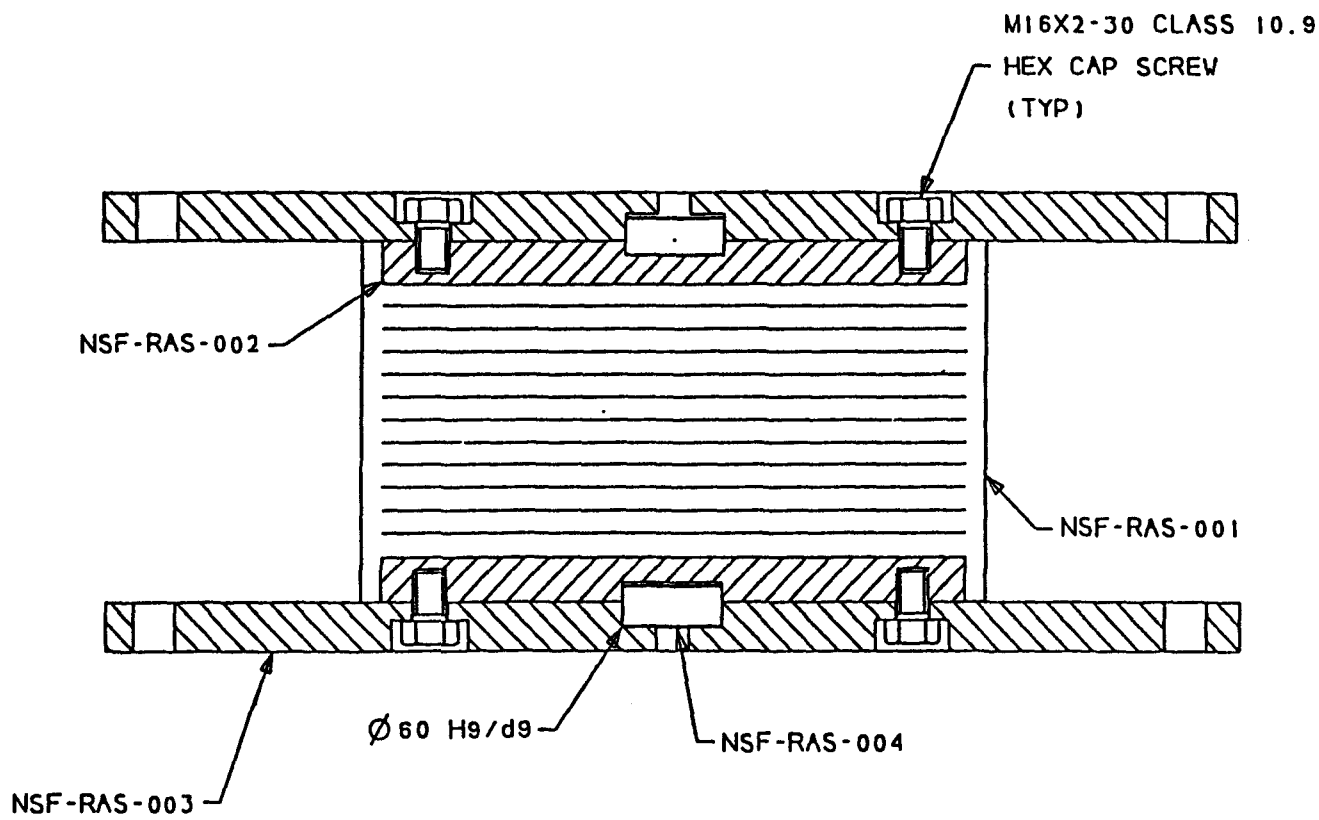

HYSTERESIS LOOP

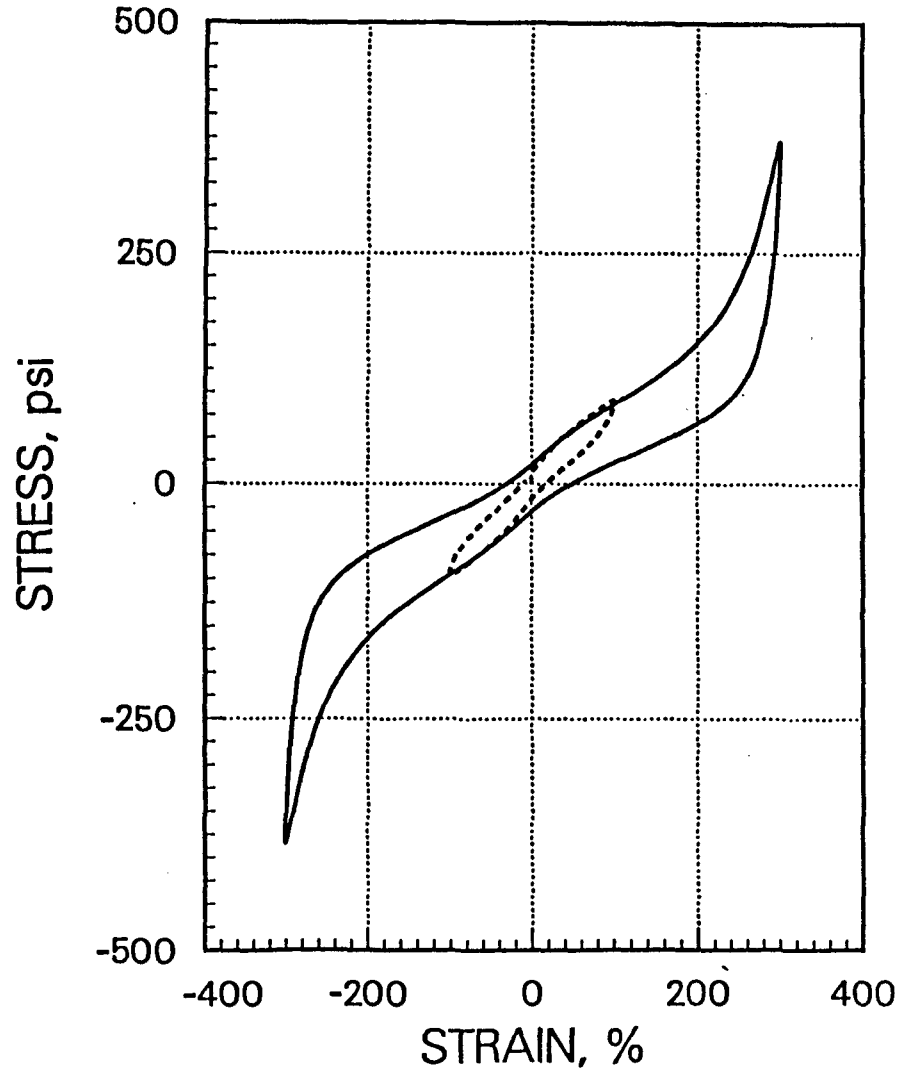

VARIATION OF STIFFNESS WITH SHEAR STRAIN

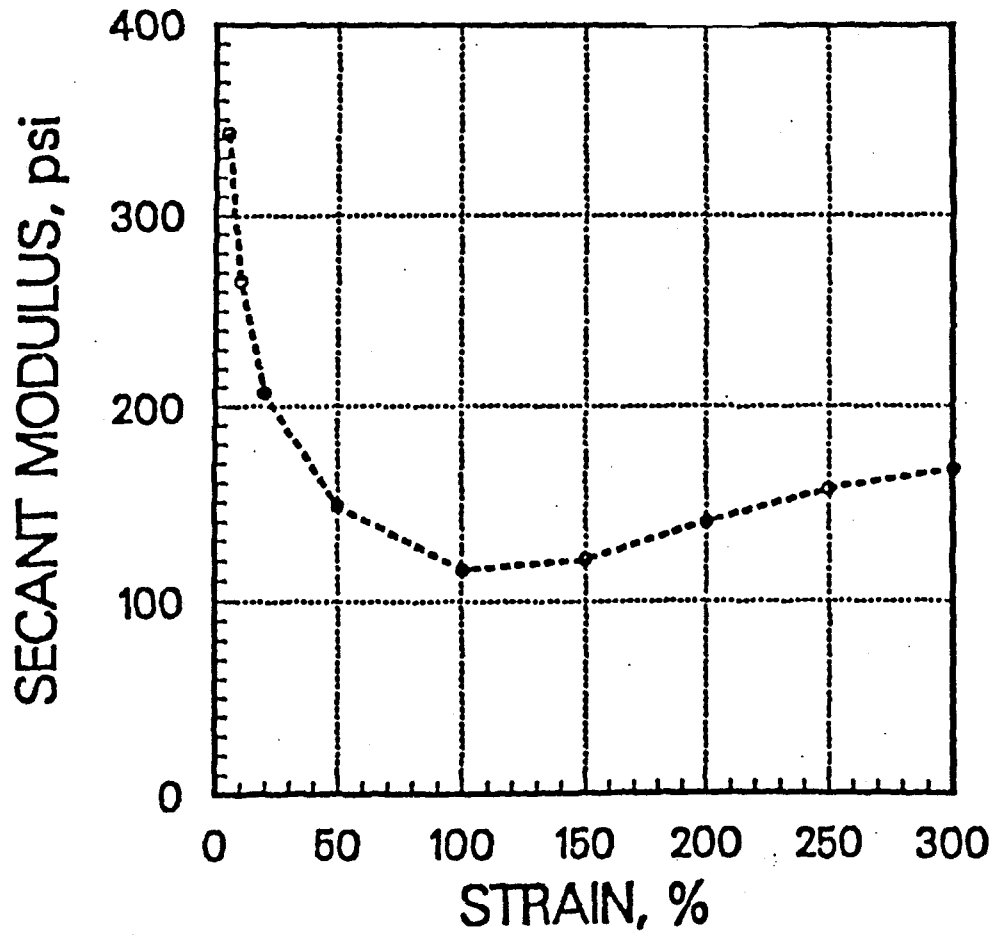

VARIATION OF DAMPING WITH SHEAR STRAIN

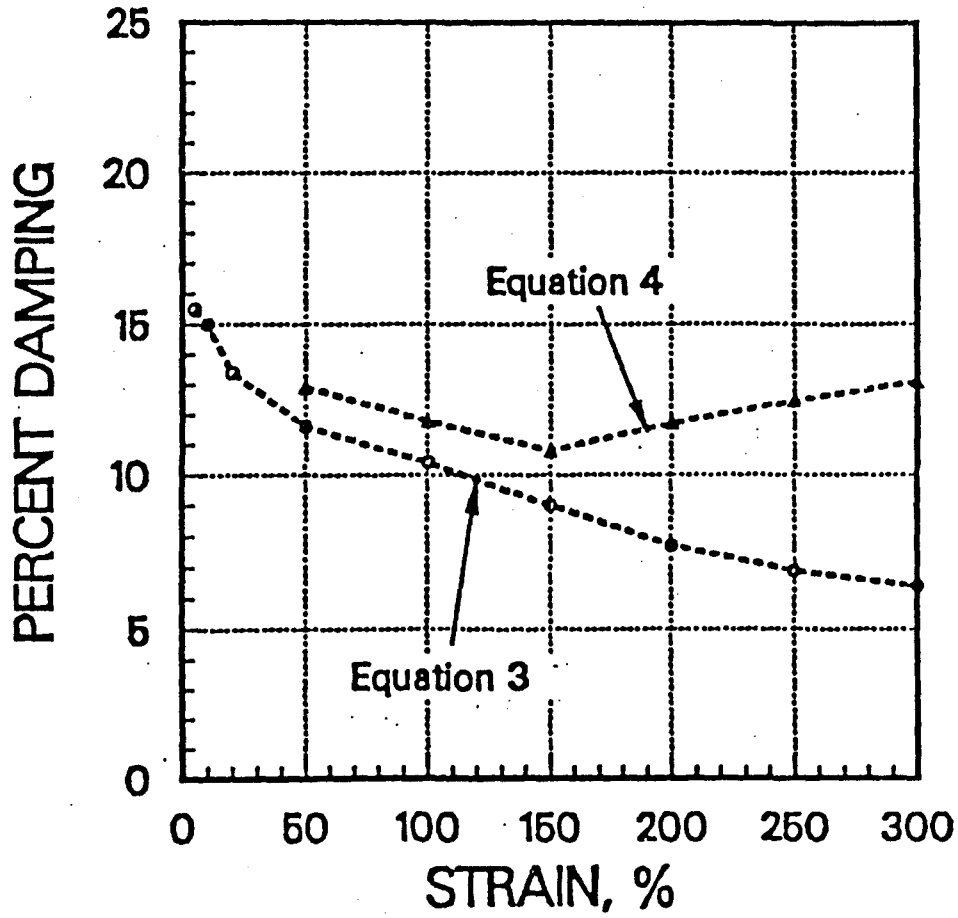

Bearing Manufactures

- FURON (Athens, TX)
- LTV (Arlington, TX)
- Rubber Consultants (UK)
- Bridgestone (Japan)

FOOTHILL LAW AND JUSTICE CENTER
MEASURED RESPONSE TO UPLAND EARTHQUAKE
(2/28/90; M=6)

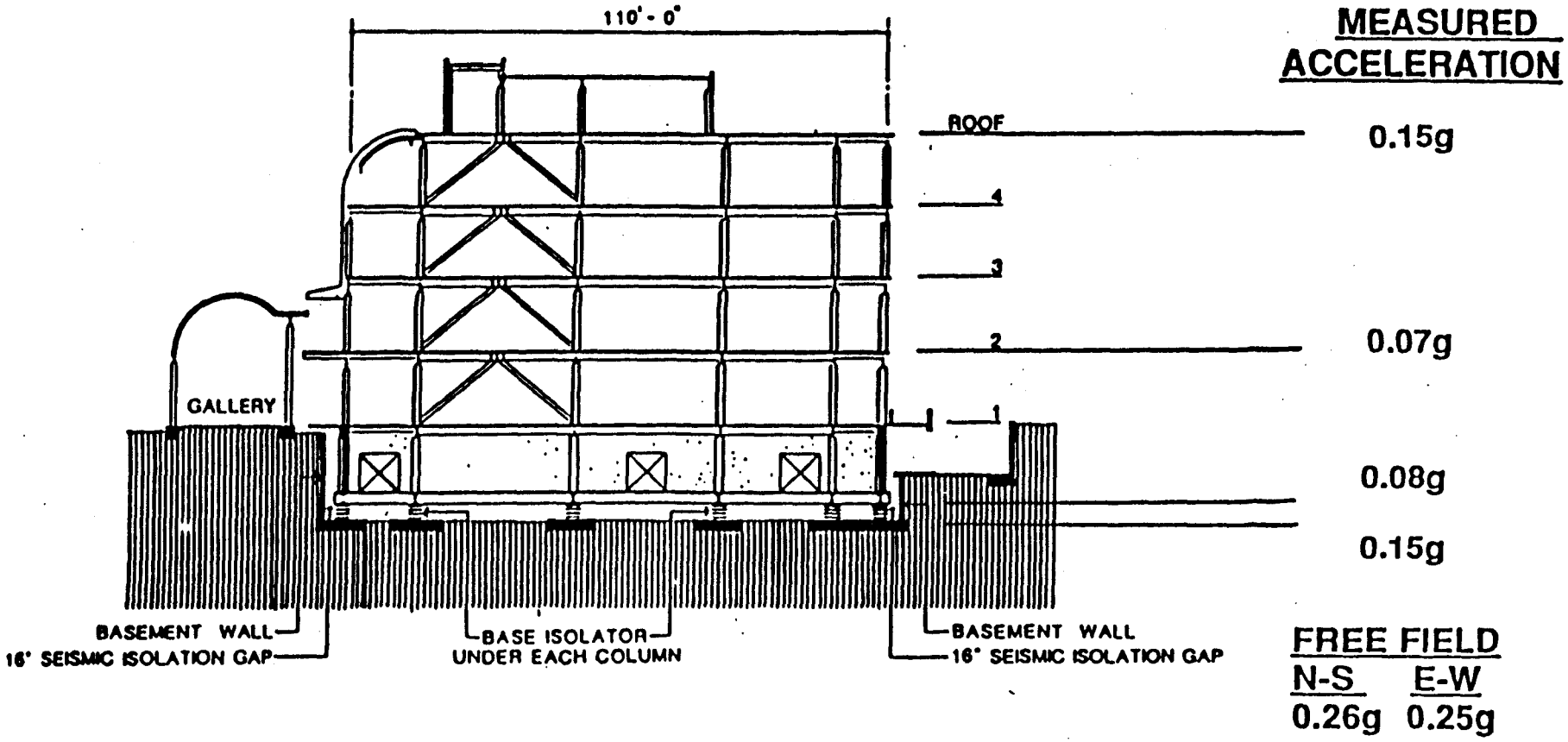

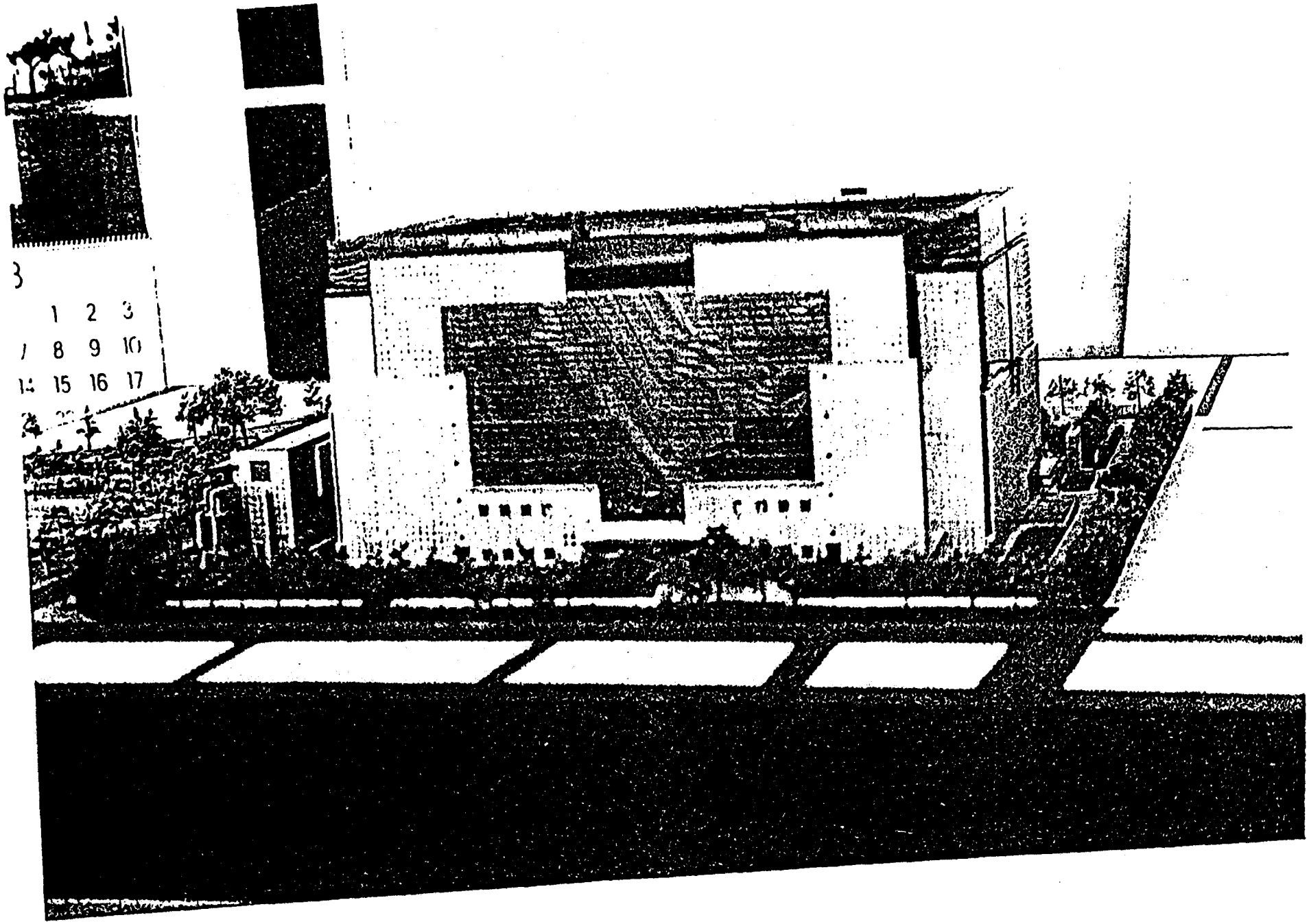
1 2 3
8 9 10
15 16 17

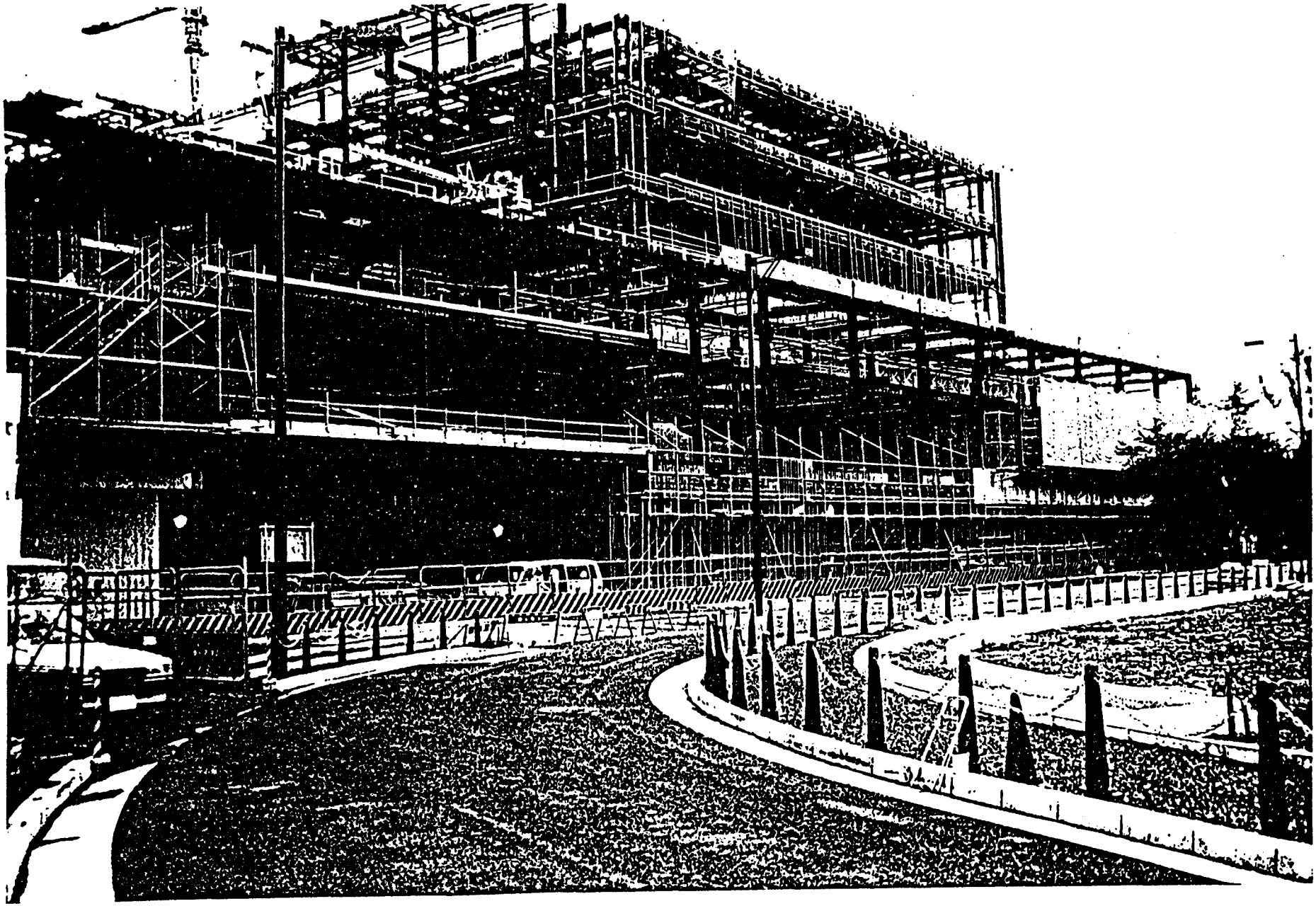

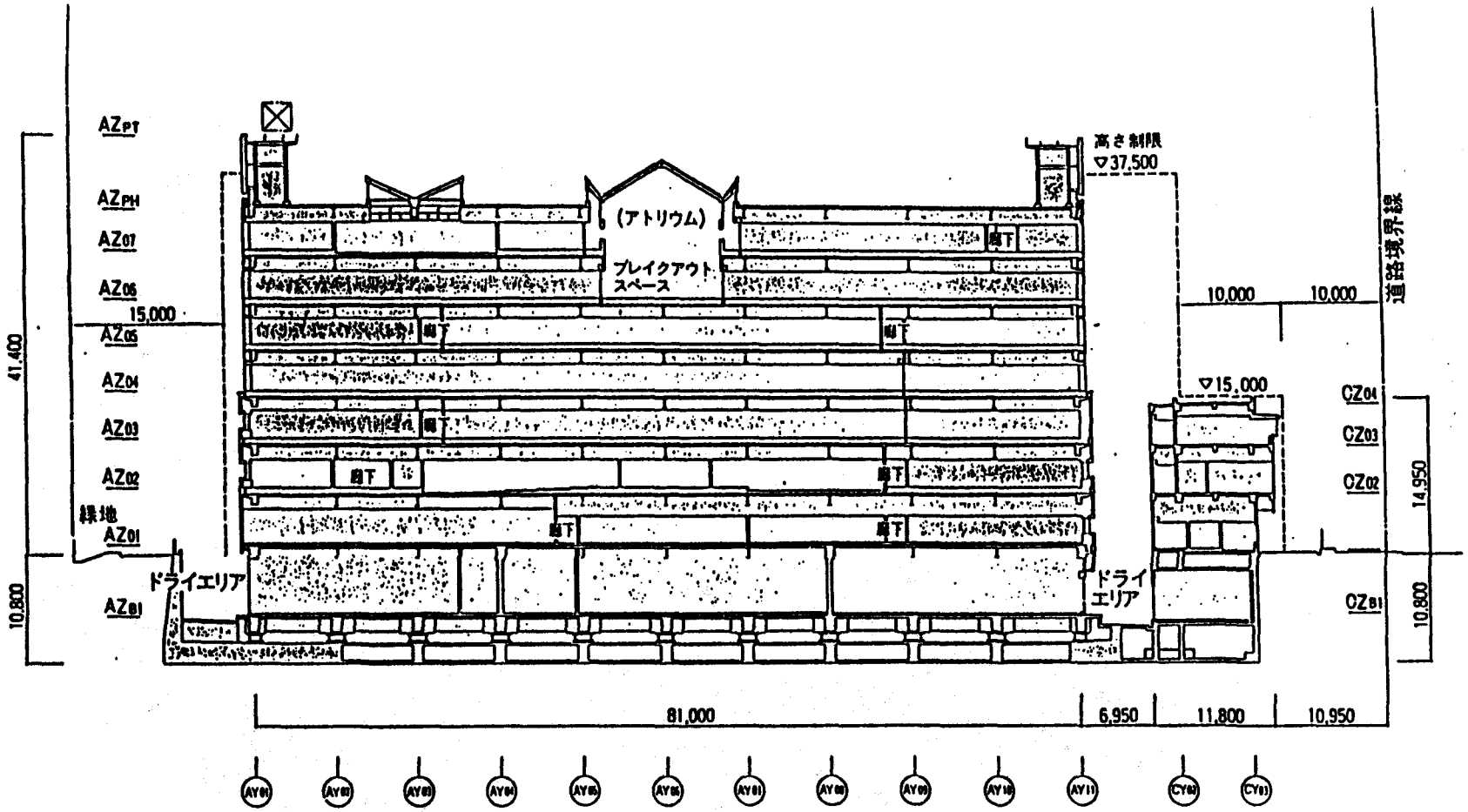

C-1 Building: World's Largest Isolated Building

Fucha City Tokyo	Lead Rubber Bearings
7-Floor Superstructure	ϕ = 1.1, 1.2, 1.3, 1.5 m
1-Floor Basement	T_h = 3.0 sec
Total Weight = 62,800 tons	f_v = 12 Hz

CONCLUDING REMARKS

- The technology for base isolation that now exist can be use to isolate large structures.
- Base isolation is being used as a strategy to protect large structures from earthquake damage.
- Reinforced rubber base-isolation bearings have been used in the United States in non-seismic applications (bridge bearings and anti-vibration mounts) for over 50 years.
- Worldwide over 100 structures (bridges, buildings, nuclear power plants) are protected by seismic isolation bearings.

SUMMARY / RECOMMENDATIONS, Joe Weaver, Chairman

Vibrational Concerns Working Group Report
by Jack Peterson, Chairman

Design of Stable Structures Working Group Report
by Chuck Hurley, Chairman

Dynamic Alignment Working Group Report
Larry Ketcham, Chairman

Control Issues Working Group Report
Jim Lauffer, Chairman

Adjournment

REPORT OF THE BEAM-EFFECTS WORKING GROUP

Members:

Gerry Fischer	SLAC
Dave Goss	SSC
Joe Jendrzejcsyk	ANL
Bill Ng	FNAL
Vasily Parchomchuk	Novosibirsk
Jack Peterson (chair)	SSC
Dave Ritson	SLAC
Gena Stupakov	SSC/Novosibirsk

Introduction

The Beam-Effects Working Group had two concerns regarding ground motion and vibration effects on the beam of the SSC:

1. Closed-Orbit Effects--mainly beam separation (s) at the beam crossings, which degrades the luminosity (Lu) as:

$$Lu = L_o \exp(-s^2/2\sigma^2)$$

2. Emittance (ε) Growth, which degrades the luminosity as:

$$Lu = N_b^2 f_{coll}/4\pi \text{ beta}^* \varepsilon$$

This report is a review of our assessment of these problems--that is, what is known and understood and what is unknown or uncertain. Finally, we recommend a program for clarifying the issues and ensuring satisfactory collider operation.

A) Closed orbit effects:

Closed orbit distortions are due to slow, adiabatic motion of the quadrupole magnets. The IR quads are the principal sources of these distortions, but the arc quads also are significant contributors to this effect.

Principal Sources:

1. Train crossings: Vibration measurements in boreholes at tunnel depth by Earth Technology Corp in 1989 have been translated to the consequent beam separations at the four beam crossings.

Result: Luminosity degradation of less than 1 % in the worst case. (Assuming quad support magnification of 5 in the frequency range 1 to 10 Hz.)

Caveat: Data are needed at the Midlothian Crossing because the RR bridge at that location is believed to couple the Austin Chalk stratum much better than through the alluvial soil at the bore hole used for the measurement in 1989 located now about 1 KM away. (Dave Goss)

2. Quarry Blasts:

Similar measurements and calculations indicate possible luminosity degradation of up to 67% for a period of several seconds two or three time a week(again assuming quad-support magnification of 5)

3: Freeway traffic noise: Negligible effects.

4: Ground Diffusion Model:

According to a phenomenological fit to a number of ground motion measurements by the Russian group, relative quad positions will diffuse according to the relation:

$$[\langle \delta x^2 \rangle]^{1/2} = 10^{-2} [L T]^{1/2} \quad \text{microns}$$

in which L is the inter-quad spacing (meters) and T the time (seconds). This formula yields for L=90m (SSC) an rms quad motion of:

6 microns	in	1 hour
0.5 mm	in	1 year
2.3 mm	in	20 years

(Random quad motions of 1 micron (rms) produce 1-sigma beam separations at the crossings.)

If this expression is a valid representation of how the tunnel floor will behave at the SSC, these estimates suggest that the Jostlein method of keeping the beams in proper collision will be essential in the interaction regions and periodic updating the operating closed orbit throughout the rest of the machine. It also calls for a survey and repositioning after a year or so.

The working group did not come to a consensus regarding the derivation of such a diffusion model, but it did note that its estimates for typical inter-quad spacing (such as 90 meters for the SSC in the example above) are not inconsistent with observations at number of machines. However, the application of this formula for interquad spacings of up to the diameter of an accelerator ring can predict relative displacements that are an order of magnitude larger. These larger estimates do not seem to be supported by observations at SLAC, CERN, and FNAL.

Regarding other closed orbit considerations, there was general agreement on the following matters:

1. Diagnosis of beam separation at the beam crossings: The Jostlein method is effective and should not cause emittance growth.

2. Control of beam separation should be readily accomplished by half-wave bumps produced by corrector dipoles just outboard of the inner triplets.

3. Quad-support amplification is an important factor.

B) Emittance growth:

B1. Low Frequencies:

Emittance growth due to vibrations at low frequencies do not cause significant emittance growth, according to several analytic and simulation calculations. That is, vibrations due to train crossing, quarry blasts and freeway traffic and the low frequency ambient should not be troublesome in this regard.

A caveat on this statement is the theoretical possibility that non-linear effects could excite a high order resonance with a difference frequency in the region of a few Hz. This possibility has not been analyzed in any detail.

B2. High Frequencies:

The work of the Russian groups (Parchomchuk, Skrinsky, Stupakov, and co-workers) has pointed out that significant emittance growth can occur when the quadrupole motion is in resonance with the betatron motion of the beam. Such resonances occur at vibration frequencies that are harmonically related to the betatron frequency --i.e., at the frequencies $(n-\nu)f_o$, where n is a harmonic close to the integer part of the betatron tune ν, and fo is the revolution frequency. For the SSC at the nominal tune of 123.28, the lowest resonant vibration frequency is 960 Hz, a vibration frequency so high that it was not considered a possible source of trouble by previous authors because the spectral content of ground motion is well known to fall rapidly with increasing frequency. Note that this resonant frequency varies inversely with the accelerator radius, so that the SSC is undoubtedly the first machine to be so threatened.

Using a vibration power density of 10^{-9} micron^2/Hz, which is a typical level from one set of measurements in the UNK tunnel in the few-hundred herz region, Stupakov calculated an emittance doubling time for the SSC of about 2 minutes. The theory for the assumptions used is not in question. However, there are three or four further important questions: (a) Are there sufficient amplitudes near 1 kHz in the SSC tunnel? (b) Can these vibrations be transmitted through the quadrupole cryogenic supports? (c) What is the average quadrupole displacement relative to the vibration amplitude at these frequencies? and (d) Can the emittance growth be controlled through feedback on the beam? (The theory used assumed that the amplitude of the quad motion was equal to the vibration amplitude in the floor and that the quads had negligible length.)

(a)Ground motion levels:

Very few data exist on ground motion in the range 100 to 1000 Hz because ground waves at these frequencies are generally easily absorbed in the medium of transmission and are therefore of little interest to the seismological community. They have been studied and used in local seismic exploration work, however. Disturbances at these frequencies generally result from cultural activity.

One set of measurements in the UNK tunnel gave the power density of 10^{-9} micron^2/Hz at frequencies of several hundred herz, as used above. A later measurement with another instrument gave 10^{-10}. Similar measurements on a VEPP magnet in Novosibirsk gave 10^{-10} during a period of normal operation, and 2×10^{-12} during a "quiet" period.

Extensive ground-noise investigations have been carried out by seismologists interested in nuclear-test-ban-treaty verification. These studies include work at quiet sites in Nevada, in Kazakhstan, and in Russia. The investigators point out that the very low level noise at these frequencies is often contaminated by instrumental noise at the higher frequencies and must be carefully analyzed. They point out that there are often 20 db lower values found in bore holes (underground tunnels) than in surface measurements, as well as daytime/night-time and winter/summer differences. One thing they maintain, however, is that the acceleration power spectral density is nearly flat with frequency at a level of -160 db, referenced to $1(m/s^2)^2$/Hz, at a quiet site. This level translates to an amplitude power spectral density at 100 Hz of about 10^{-15} micron^2/Hz. A site near Lajitas, Texas, is reported to be about one order of magnitude more quiet; it is thought to be the quietest seismological site in the United States.

An extrapolation of ambient noise measurements made in the range 1 to 50 Hz in bore holes at the SSC site at a 80-meter tunnel depth extrapolate to a few times 10^{-12} μ^2/Hz near 1 kHz, but such an extrapolation is not very convincing.

The key question, of course, is what will be the average and the range of the spectral power density in the SSC tunnel? Different sites and different conditions have produced values that vary over a range of 10^6 or more in the band near 1 kHz. It is clear that the principal noise sources will be cultural and that local sources must be monitored and possibly controlled.

(b)Transmissibility of Quadrupole Supports:

The very nature of cryogenic supports makes them rather fragile. This means that by general mechanical considerations their horizontal and vertical spring constants will be weak and that their lowest-order resonances will be in the perhaps a few to tens-of-herz frequency range. If they had no other modes, the transmissibility (i.e., the magnitude of their ground-to-cold-mass transfer coefficient) should be quite small--of order 10^{-3} to 10^{-4}. In real life this is probably not true, and they will no doubt exhibit higher-order resonances whose properties cannot be predicted. We need an order of magnitude measurement to assess this matter. It was pointed out that the adjacent spool pieces suffer from even more questionable mechanical resonances, since they contain not only all the corrector elements but all the in-and-out piping and wiring, which will affect the transfer coefficient.

(c) Average Quad Displacement at the Higher Frequencies

At a vibration frequency of 1 kHz, the transverse wavelength in the quadrupole cold mass may be in the 10 to 20 cm range. Thus, the length of the arc quads may be 25 acoustic wavelengths, and the triplet quads up to 70 acoustic wavelengths. In this case the average quad displacement could be at most only a few percent of the vibration amplitude. This feature was not taken into account in the emittance-growth estimates, where the quads were treated like point objects.

(d)Beam Feedback Correction:

Correction of collective beam oscillations in times short compared to the smearing time (about 0.4 sec) could greatly lengthen the emittance-growth time. Such a beam-feedback correction system appears to be feasible, according to the Novosibirsk workers. The working group was not able to address this subject adequately but recommends that it be analyzed more fully.

Power spectrum (micron**2/Hz)

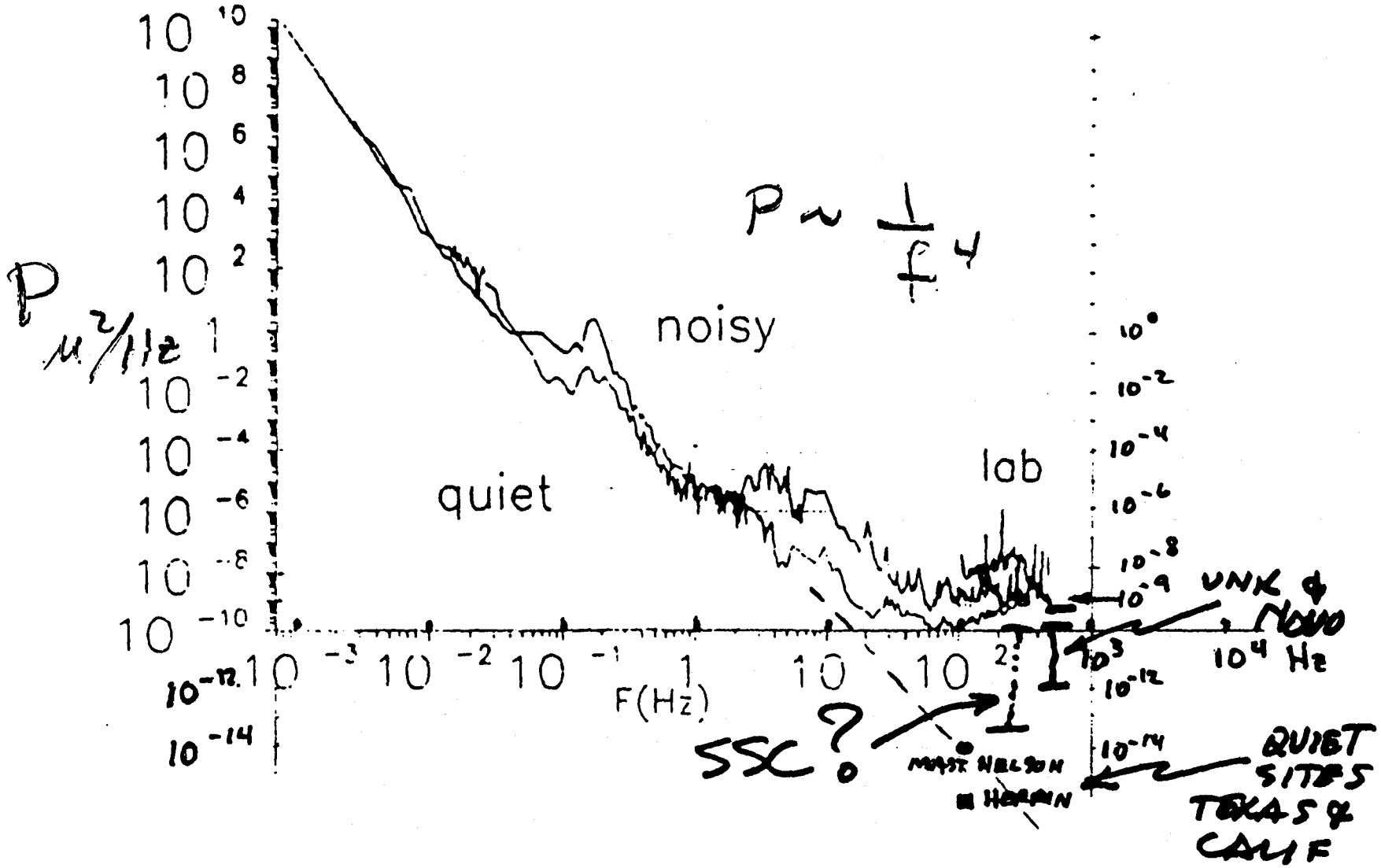

Recommendations

Since the pristine SSC site has not yet been contaminated by construction activity and the cultural noise endemic of a larger population, we suggest that a two pronged seismic measurement program be adopted to help answer the question raised above

1. An instrument station be set up to monitor the seismic activity of the site on a permanent basis. This station might measure the rms average magnitude of the vertical and horizontal components at a location removed from heavy construction that might be representative of conditions obtaining when the collider begins to operate.

2. A measurement of the difficult high frequency band at tunnel depth at two locations that might be sensitive to ongoing cultural noise. (Trains etc.) We note that the Midlothian train crossing may be subject to increased levels since the train bridge piers are believed anchored in the Austin Chalk formation directly coupling to the tunnel.

3. The quad support transfer functions to at least one order of magnitude at frequencies of interest.

4. Vibration measurements of the quadrupoles during a cryogenic string test is highly desirable to experimental determine that no appreciable acoustic noise is generated by flow of the cryogens.

5. Beam feedback to control emittance dilution needs further analysis.

Larry

Dynamic Alignment Working Group

Task: Understand & comment on alignment Issues related to final focus Quads at IR.

Delineate between alignment by mechanical moves and by electrical corrections.

Consider dynamic corrections for random movement and freq. $\geq$ mins.

Vibrations / suppression diff. group.

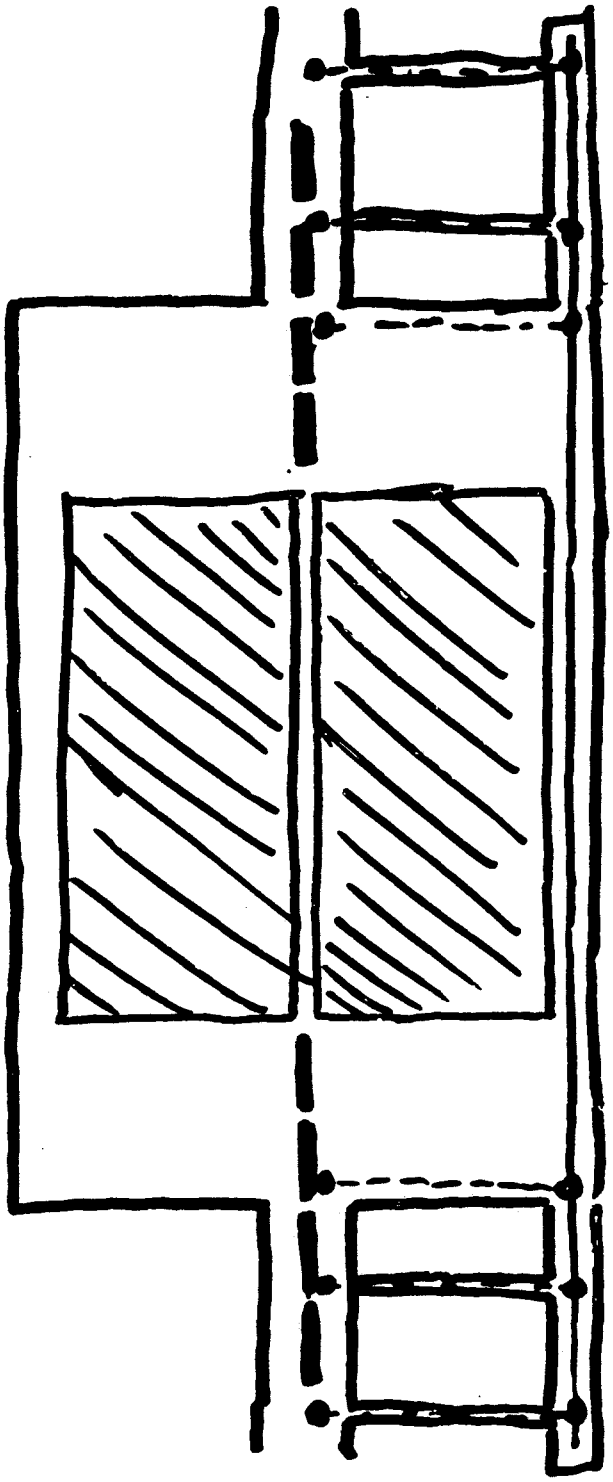

CELL (barrel) to CELL Requirements:

1. <u>at</u> <u>startup</u> no electrical Corr.

≈ 1mm offset -
no comment on direction require.
marginially achievable via traverse.
around detector.

< 1mm

1. through beamtube
   optically -
   mechanically -
2. Special Survey tube
3. Special Survey tunnel.

Clear impact on procedure, costs,
and <u>early</u> <u>design</u>.

during Startup (large beam dia)

Electrical Corr limit

- Arc orbit distortion < 1mm
- Quad cell correction ~ 50 μm

* NOTE THAT Quad cell cannot be moved as a rigid package.

- range of mechanical moves must be coordinated with operations design.
- mechanical moves / micron resolution

  ≤ 50 μm = electrical Corr.

  > 50 μm =

  1. add correctors
  2. Mech. re-align magnets.

Technology exist

must combine groups to optimize procedure.

NEED FOR REQUIRMENTS EARLY ☆

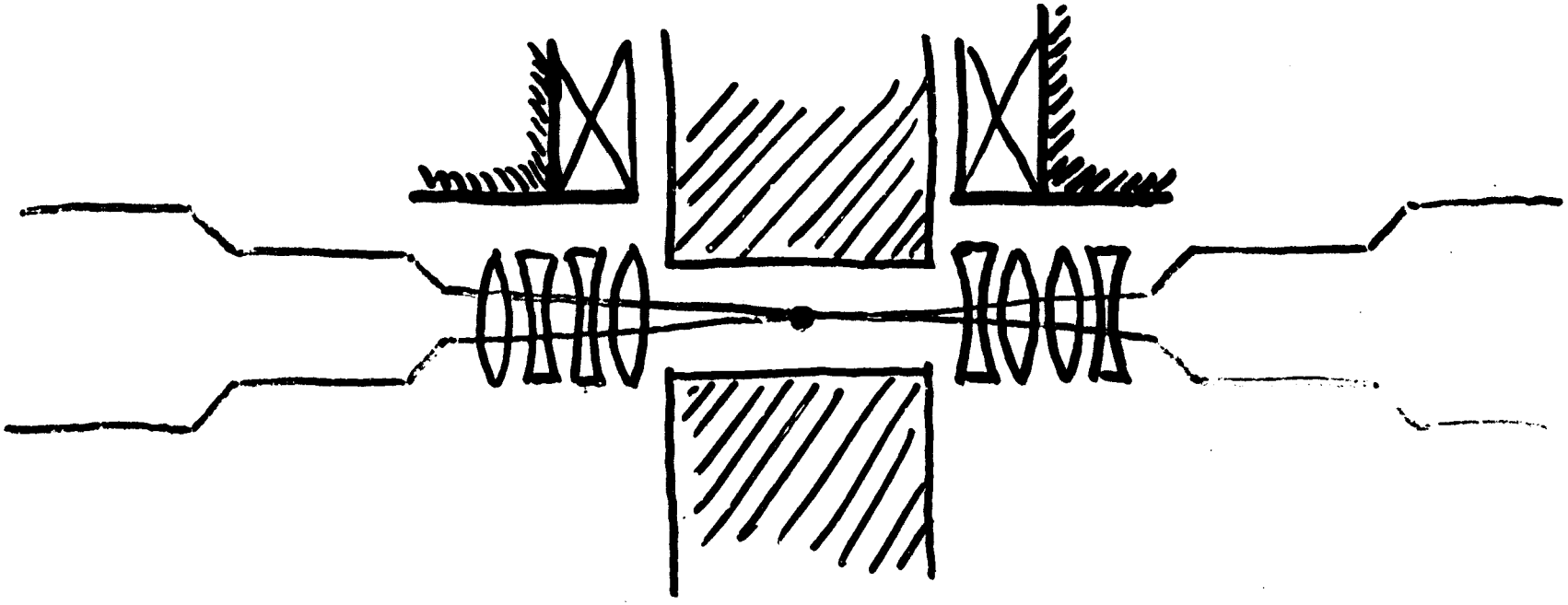

3 MODES OF operation equal
3 sets of alignment requirements:

1.) at startup

2.) during startup (med beta)

3.) during operation (high beta)

INDIVIDUAL MAGNET VS QUAD CELL

During Operation (high beta)
Electrical Corrections only!

Individual Quads -

1. Sensitive to movements @ micron level.

2. Alignment by beam has different concerns at SSC.
   - two beam tracks (SLC)
   - not colinear at I.P. (new)

micron level initial and dynamic alignment achievable but has SERIOUS costs and magnet design & installation requirements.

Workshop on Vibrational Control and Dynamic Alignment Issues at the SSC.

Vibration Suppression Working Group

J. P. Lauffer
Sandia National Lab.

Vibration Suppression Group

Objectives:

1. Review existing information

2. Determine if vibration problem exists.

3. Recommend Approaches to attacking the vibration problem.

Is Vibration Suppression Required

1. Determine existing source levels
   a. Review existing data.
   b. Gather data from similiar sites.
   c. Perform scoping Calculations
   d. Measure as needed.

2. Characterize System
   a. Perform scoping calculations
   b. Do detailed numerical modeling
   c. Experimental Model Qualification

3. Perform response analysis

4. Compare results with system requirements.

5. Determine need for vibration suppression.

Inputs to Vibration Suppression Group

* Final Focus Quad motion has maximum effect on beam position.

* Two frequency regimes of concern.
  - 1-30 Hz
    Ground motions of 1 μm indicate vibration suppression needed.
  - 600-1200 Hz
    Motion in this band will cause emittance growth and loss of luminosity.

* Flow induced vibrations - amplitudes and frequency not known.

* Relative motion between quads should be less than 0.05 μm

THE CORE GROUP

PREVENT OR CORRECT?

"AN OUNCE OF PREVENTION IS WORTH A POUND OF CURE."

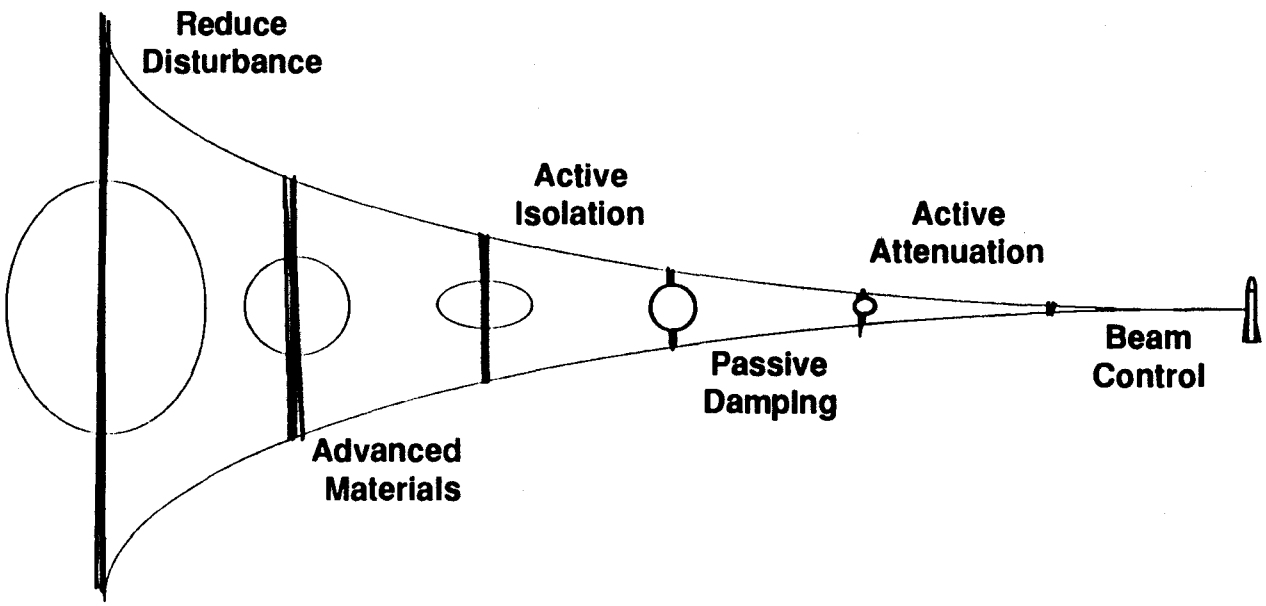

PREVENTION ⟷ CORRECTION

Method	PRO	CON	Sources: External	Sources: Internal
Damping (Passive)	* Stable * Add on * Compatible with Active Control	* Hard to Predict * Limited Dynamic Range * Environmental Dep.	* Compatible with Active Control * Limit Excursions (5-30Hz)	N/A
Damping (Active)	* Tunable	* Stability * Complicated (Sensor/Actuator * Does Not Directly Control Beam	* Of questionable use maybe for a specific problem	* Difficult
Active Structural Control	* Tailor Freq. Resp. * Hi Precision * Specific Design Objectives	* Does not Directly control beam motion * Complex * Stability * Technically Immature	In order to achieve hi attenuation at hi. frequency. and/or correct errors due to internal sources: A coordinated active control system may be necessary	
Beam Control	* Specific Design Objective * Existing BPM (Accurracy?) * Control Effort Low	* Freq. Resp. (Actuator Limited) * Dynamic Range? * Sensor Motion Errors	See Above	* Adequate BPM is needed * Luminosity Measurements

Method	PRO	CON	Sources: External	Sources: Internal
Conventional Construction (stiffness-mass)	* Simple, Reliable * Tailor Response	* Limited Dyn. Range * Hard to Change * Thermal Effects (mag. support)	* Stiff as possible (Alignment an Issue)	N/A
Isolation (passive)	* Cheap * Isolates Inputs from structure	* Increase Low Freq. Response * Passes Discrete Freq. * Environmental Dep. * Aging, Creep	* Alignment an Issue * Induce Low Freq. Modes	* Inc. Freq. & Damping of cold mass
Isolation (Active)	* Tailor Freq. Resp * Adaptable	* Complicated * Actuator Req'mt * Requires Failsafing * Immature Tech.	* use to Isolate cold mass (low freq)	N/A
Dynamic Absorber	* Narrow Band * Possible use during troubleshooting		N/A	N/A

— Recommendations of VSG

1. Systems engineering approach to vibration suppression.
2. Accurate Beam Position monitor is needed to implement beam control.
3. Additional testing to determine if 600-1200 Hz frequency band is a problem.
4. Testing to determine if He flow and boiling is a problem for spool and or quads.
5. Isolate/remove vibration sources.

Working group attendees

• Patricia Manning	LLNL
• Brad Burdick	LLNL
• Bob Viola	SSCL
• Walter Bauke	SSCL
• Anthony Passi	ANL-APS
• Danny J. Mangra	ANL-APS
• Marty Wamsganss	ANL-MCT
• M.G. Srinivasan	ANL-RE
• Joe Jendrzejczyk	ANL-MCT
• Juan Barraza	ANL-APS
• Joel Bowers	LLNL GEM
• Bui Dao	SSCL-ASD
• Steve Lesser	SSCL-ASD
• Linda Karanian	MMES Denver
• C.A. HURLEY	LLNL

General comments by working group
Design of stable structures

- Recommendation: establishing in house design reviews
  - preliminary
  - concept
  - final

- Design criteria needed: vibration, deflection , radiation, seismic

Workshop on design of stable structures

- Charter

  To come to a consensus on a clear understanding and description of the issues and problems

  recommend a design philosophy or a course of action

- Prepare recommendations on:

  design philosophy
  description of the problems
  list of the issues
  list of the studies to be made
  list of options and tradeoffs

Workshop on design of stable structures

- Things to consider during discussion
  - operational efficiency
  - maintenance
  - analysis
  - design for thermal, earthquake, vibration
  - foundation
  - isolation
  - radiation
  - safety
  - testing
  - material
    - method of fabrication
    - stiffness
    - shapes
    - construction
  - residual stresses
  - measurements
  - cleanliness
  - vendor survey
  - QA
  - cost
  - schedule
  - compatibility with alignment system

We discussed four topics

- Vibration problems associated with the spool piece
- Dipole/ quadpole support in the experimental hall
- Support of large detector assemblies
- Dipole/ quadpole support in the tunnel

Vibration problems associated with the spool piece

- Flow of coolant will cause assembly to vibrate
- These vibrations may disturb other magnets
- Sources:
  Flow in cold mass
  flow in pipes
  accoustic oscillation from natural convection
  boiling in the heater
- Recommendations:
  modeled and tested
  accurate analysis is impossble

Dipole/ quadpole support in the experimental hall

- Move tank sideways into another hall Fermi Lab approach
- Use concrete blocks under magnets
- Use a steel space frame

Concrete support approach

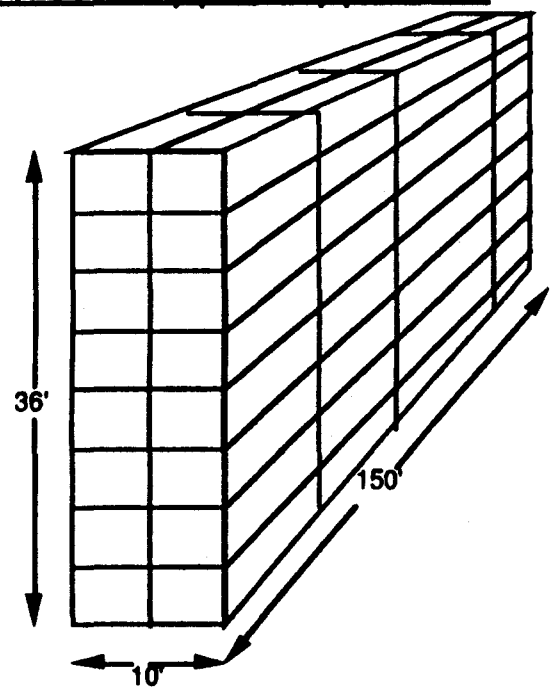

Pro: High frequency, good damping

Con:

- 80 blocks requiredcrane limitation
- creep
- thermal cracks
- high floor loads
- requires long tie rods to floor
- needs grouting

Steel approach

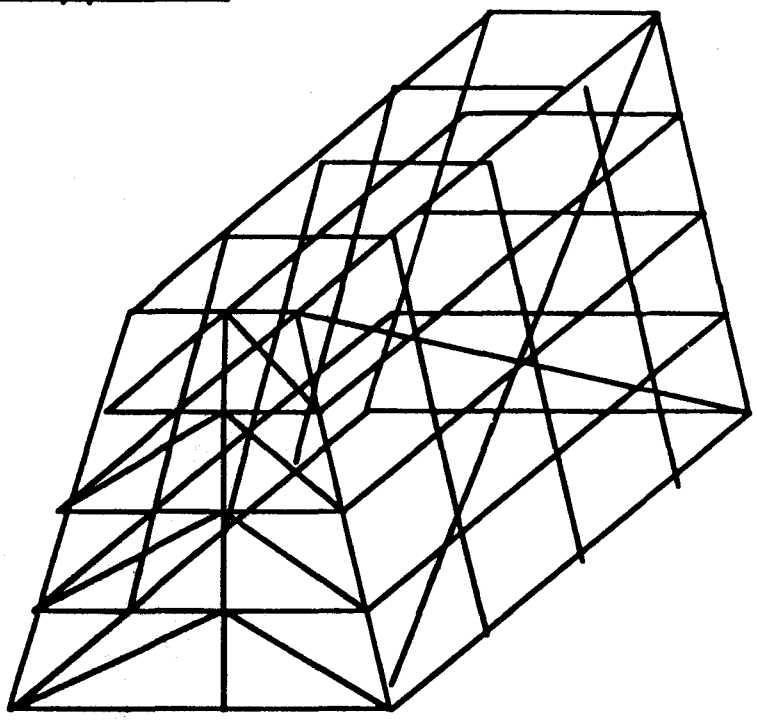

- frequency 20-40 hz
- welded and bolted assy (damping 2-5%)
- easy to model
- inexpensive

recommendation: space frame instead of columns

Dipole/ quadpole support in the tunnel

- Recommend six strut system on C-frame support

- Issues:
  - design of C-frame, stiffness
  - removing one set of magnets will disturb alignment of other set
  - should be modeled and tested
  - resonances can be transmitted between adjacent magnet sets

because of symmetry.... could vary fundamental frequency of adjacent assembles

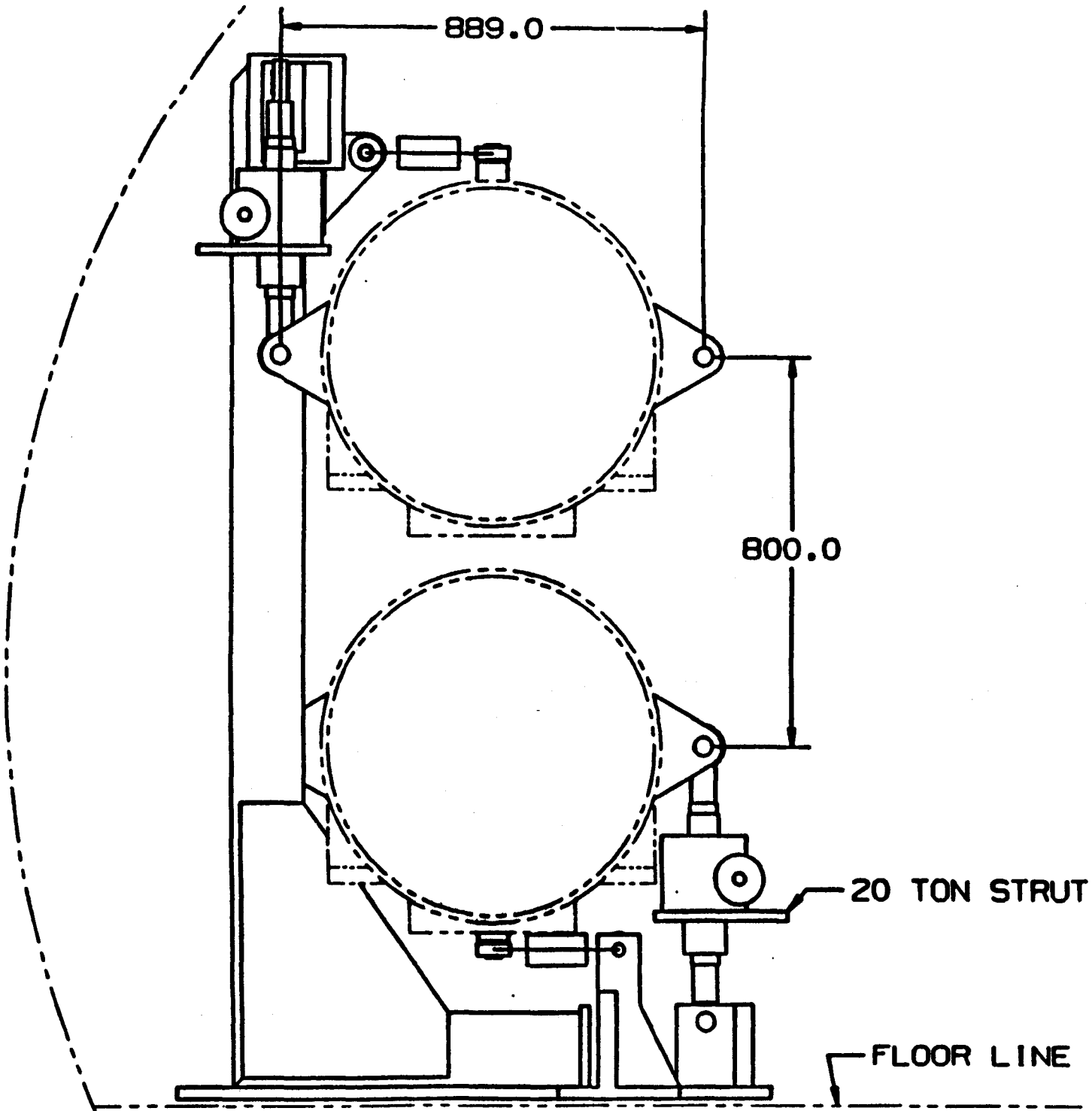

LEAD END SUPPORT

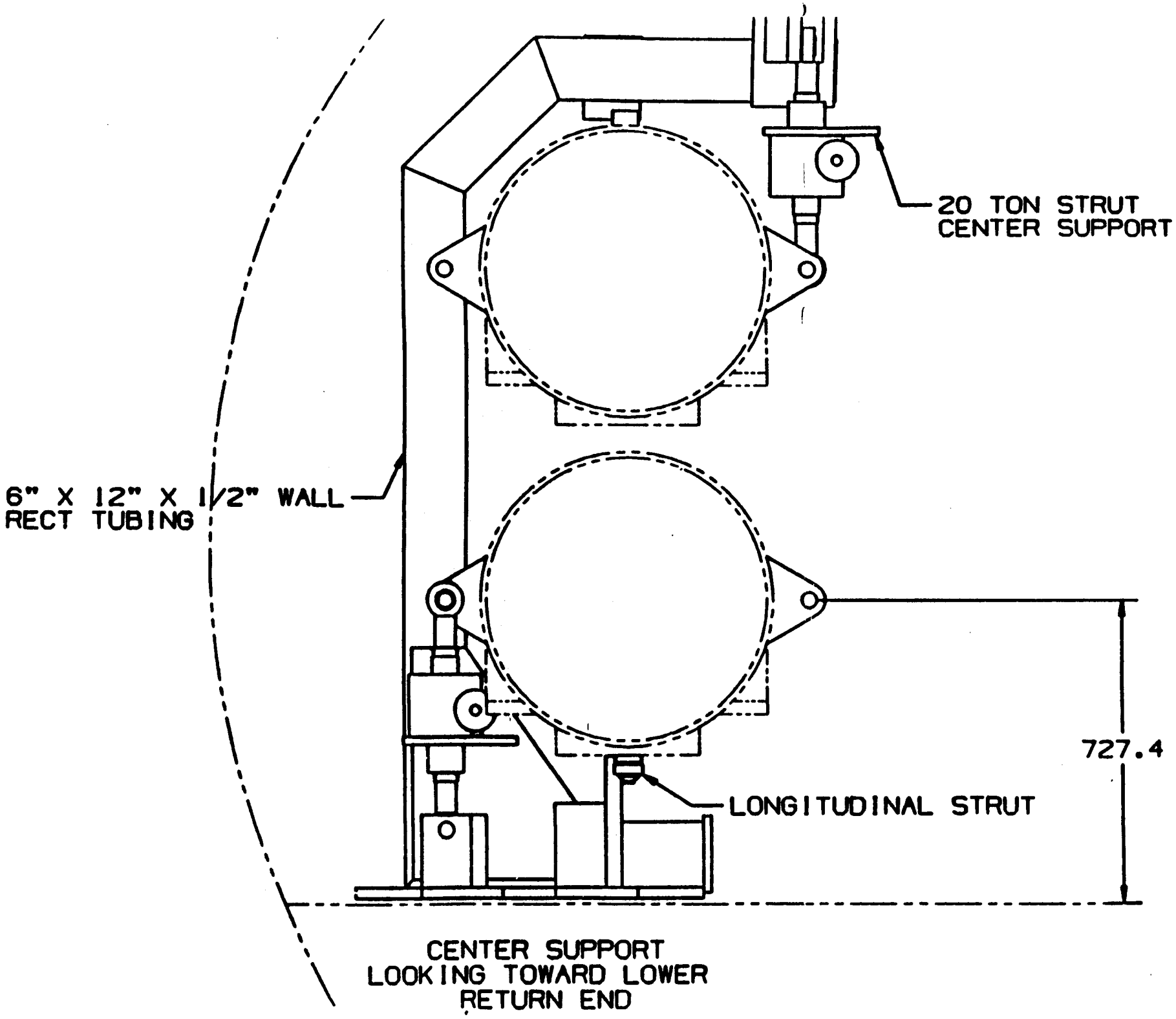
20 TON STRUT
CENTER SUPPORT
6" X 12" X 1/2" WALL
RECT TUBING
727.4
LONGITUDINAL STRUT
CENTER SUPPORT
LOOKING TOWARD LOWER
RETURN END

Support of large detector assemblies

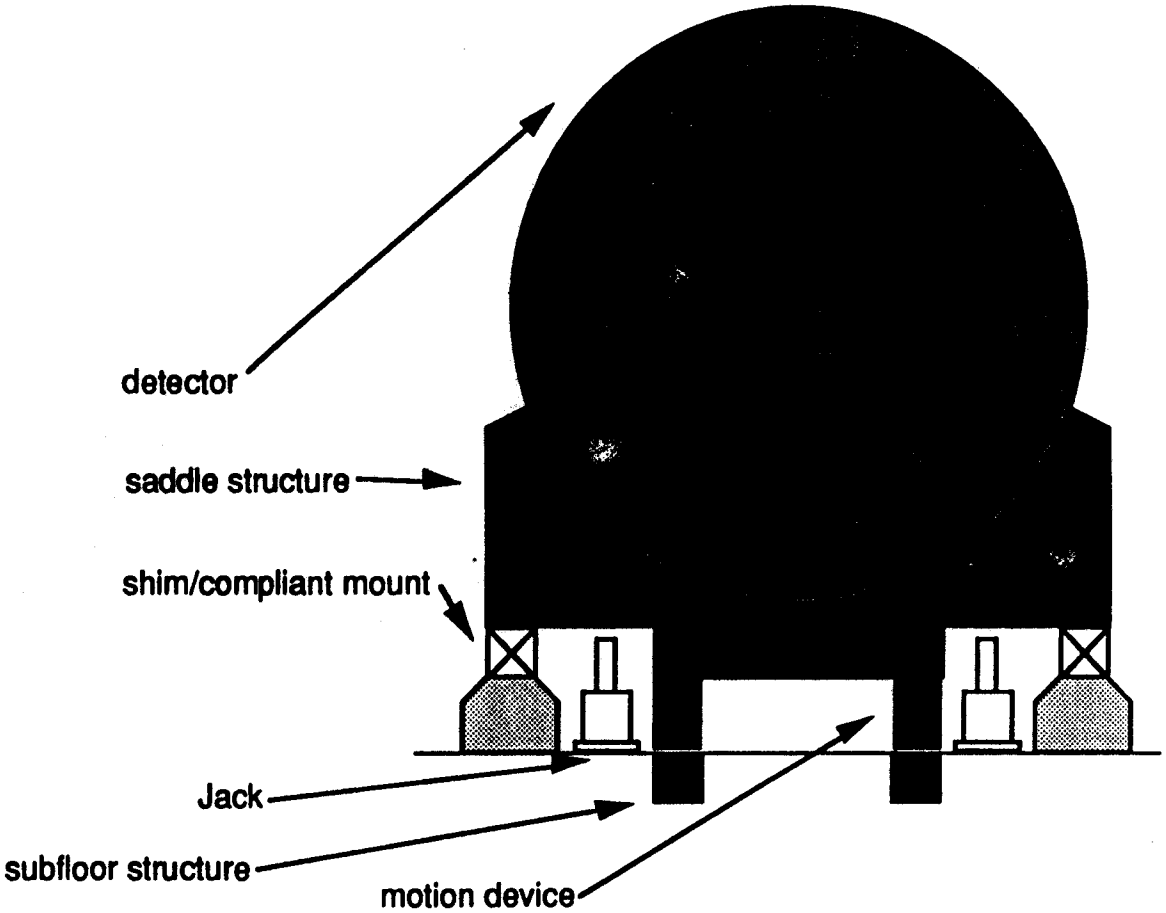

Support of large detector assemblies

- Three main features
  1) Track system for disassembly/assembly
     hard rail / Hillman roller, single direction motion
     Grease bearing, XY direction (used in CERN)
     Air bearing, XY motion

  2) Jacking system for lifting load
     Hydraulic jacks with controls

  3) Support and alignment system
     Simplest form : shims
     motor driven wedge

- Issues
  oil and grease in the hall, cleanliness spec needed
  radiation damage to o-rings
  long term support on hydraulic jacks